THE UNIVERSITY OF QUEENSLAND

AUSTRALIA

Synthetic Strategies to Build Macromolecular Architectures

Derong Lu

BSc, MSc

A thesis submitted for the degree of Doctor of Philosophy at

The University of Queensland in 2015

Australian Institute for Bioengineering and Nanotechnology

Abstract

The ability to build complex macromolecular architectures from linear polymer building blocks through a combination of 'living' radical polymerization (LRP) and 'click' chemistries has opened the way for tailor-made polymers. We have only started on our journey to discover the types of designer polymers this versatile methodology will produce. The great advantage of LRP is the production of polymers with high chain-end fidelity, and in combination with orthogonal 'click' reactions allows precise coupling of building blocks into a desired architecture. It further opens the opportunity to mimic natural proteins and peptides, which have become a growing area as therapeutic agents. Many proteins and peptides are unstable in the body, and breakdown rapidly with loss of function. Through coupling these peptides onto the periphery of polymer architectures, stability can be significantly increased leading to an enhanced therapeutic efficacy. The main focus of this thesis was to develop new chemical strategies, through LRP and 'click' reactions, to produce polymers with diverse architectures, including macrocycles, miktoarm star, and dendrimers. Further, these will be coupled to amino acids and peptides to mimic the properties of natural peptides and proteins.

First, the Reversible Addition Fragmentation Chain Transfer (RAFT) polymerization and the metal-free thiol-ene Michael addition reaction were used to build a variety of alkyne-functional cyclic polymers *via* ring-closure strategy in a one-pot system. A library of well-defined alkyne-terminated linear RAFT polymers were successfully made followed by post-modification to introduce an acrylate functionality on polymer chain-end. The concentration-dependent aminolysis of trithocarbonate group on the polymer afforded the slow and *in-situ* generation of thiol-terminal polymer. The resulting thiol-polymers readily deprotonated to form the corresponding thiolate anion in the presence of base (hexylamine) followed by rapid intramolecular coupling with the activated double bond on the other side of the polymer chain to generate a cyclic polymer.

Next, a new strategy was derived to make an ABCD 4-arm miktoarm star copolymers *via* another combination of LRP and Copper-catalyzed Azide-Alkyne Cycloaddition (CuAAC) 'click' reaction. The Atom Transfer Radical Polymerization (ATRP) and Single Electron Transfer-Living Radical Polymerization (SET-LRP) techniques were utilized to prepare well-defined polymer chains with high chain-end bromine functionality. By efficient post-modification, alkyne-terminated polymer building blocks, including poly(styrene) (PSTY), poly(ethylene glycol) (PEG), poly(*N*-isopropylacrylamide) (PNIPAm), and poly(*tert*-butyl acrylate) (P^{t}BA) were successfully prepared. Selective and sequential 'click' reactions between the alkyne-terminated building blocks and a

trifunctional linker bearing two azide and one Tips-protected alkyne groups give alkyne-protected 2-arm diblocks. Subsequent deprotection of the Tips protecting group followed by modification using another diazide linker generated both the alkyne and aizde functional 2-arm copolymers. These polymers were then coupled *via* CuAAC to form 4-arm star polymer. Our new strategy was first employed to make 4-arm PSTY star as a proof-of-concept and then used to synthesise a rare ABCD miktoarm star.

3rd or 4th generation polymeric dendritic peptidomimetics attached with amino acids or tripeptide at the periphery were prepared *via* a combination of ATRP and two orthogonal 'click' reactions (CuAAC and Nitroxide Radical Coupling (NRC)) in one-pot. Pre-synthesized building blocks (including PSTY, Lysine, Lysine dendron) containing nitorxide, bromine, azide, and alkyne functionalities, respectively, allowed further CuAAC and NRC coupling reactions in one-pot. By using a mixture of toluene and DMSO (50:50, v:v) as solvent and Cu(I)Br and PMDETA as catalyst, the CuAAC and NRC reactions could be carried out in a parallel pathway to couple building blocks in each generation that resulted in 3 different polymeric dendrimers with high purity (> 94 %). Moreover, the size and both the type and density of the peripheral groups were able to be controllable and adjustable. After deprotection of the Boc group on the lysine units, the resulting amphiphilic dendrimers were able to self-assemble in water to form micelles with low aggregation number, and possibly form the unimolecular micelles.

Finally, the CuAAC 'click' reaction was extended to prepare 4-arm small molecular dendritic peptidomimetics that consisted of a 4-arm core, second generational ethylene glycol (EG) spacer, and Lysine or tripeptide (MKF) peripheral moiety. The EG backbones with different units were conjugated with either lysine or MKF peptide *via* 'click' reaction to give alkyne-terminal EG-Lysine or EG-MKF conjugates. At the final step, alkyne-functionalized conjugates were coupled onto a tetra-azide core *via* CuAAC reaction to form 4-arm dendritic peptidomimetics. By elaborating on the synthetic approach, the size, peripheral charge and molecules of dendrimers were also adjustable. These structures will be tested in the future as ion channel blockers.

Declaration by author

This thesis is composed of my original work, and contains no material previously published or written by another person except where due reference has been made in the text. I have clearly stated the contribution by others to jointly-authored works that I have included in my thesis.

I have clearly stated the contribution of others to my thesis as a whole, including statistical assistance, survey design, data analysis, significant technical procedures, professional editorial advice, and any other original research work used or reported in my thesis. The content of my thesis is the result of work I have carried out since the commencement of my research higher degree candidature and does not include a substantial part of work that has been submitted to qualify for the award of any other degree or diploma in any university or other tertiary institution. I have clearly stated which parts of my thesis, if any, have been submitted to qualify for another award.

I acknowledge that an electronic copy of my thesis must be lodged with the University Library and, subject to the policy and procedures of The University of Queensland, the thesis be made available for research and study in accordance with the Copyright Act 1968 unless a period of embargo has been approved by the Dean of the Graduate School.

I acknowledge that copyright of all material contained in my thesis resides with the copyright holder(s) of that material. Where appropriate I have obtained copyright permission from the copyright holder to reproduce material in this thesis.

Publications during candidature

1) Lu, D. R.; Jia, Z. F.; Monteiro, M. J. *Polym Chem-Uk* **2013,** 4, (6), 2080-2089

2) Lu, D. R.; Hossain, M. D.; Jia, Z. F.; Monteiro, M. J. *Macromolecules* **2015,** 48, (6), 1688-1702.

3) Hossain, M. D.; Lu, D. R.; Jia, Z. F.; Monteiro, M. J. *ACS Macro Lett* **2014,** 3, (12), 1254-1257.

4) Rong Chen, Derong Lu, Zili Xie, Jing Feng, Zhongfan Jia, Junming Ho, Michelle L. Coote, Yingliang Wu, Michael J. Monteiro, Shin-Ho Chung. Peptidomimetic Star Polymers for Targeting Biological Ion Channels. Submitted to *elife*.

Publications included in this thesis

1. Lu, D. R.; Jia, Z. F.; Monteiro, M. J. *Polym Chem-Uk* **2013,** 4, (6), 2080-2089. – Incorporated as Chapter 2.

Lu, D. R.was responsible for 40 % of analysis and interpretation of data, 30 % of drafting and writing and 30% of conception and design. Zhongfan Jia was responsible for 20 % of analysis and interpretation of data, 10 % of drafting and writing, and 20 % of conception and design. Monteiro, M. J was responsible for 40% of analysis and interpretation of data, 60 % of drafting and writing and 50 % of conception and design.

2. Lu, D. R.; Hossain, M. D.; Jia, Z. F.; Monteiro, M. J. *Macromolecules* **2015,** 48, (6), 1688-1702. – Incorporated as Chapter 4.

Lu, D. R. was responsible for 45 % of analysis and interpretation of data, 30 % of drafting and writing and 30 % of conception and design. Hossain, M. D was responsible for 15 % of analysis and interpretation of data and 10 % of conception and design. Zhongfan Jia was responsible for 10 % of analysis and interpretation of data and 10 % of conception and design. Monteiro, M. J was responsible for 30 % of analysis and interpretation of data, 60% of drafting and writing and 50 % of conception and design.

Contributions by others to the thesis

The author acknowledges the following individuals who have contributed to this thesis:

Prof. Michael J. Monteiro for contributing to the conception, design, analysis and interpretation of the research detailed in this thesis.

Dr. Zhongfan Jia for contributing to the later parts of the conception, design, analysis and interpretation of the research detailed in this thesis.

Statement of parts of the thesis submitted to qualify for the award of another degree

None

Acknowledgements

First and foremost, I would like to express my gratitude and appreciation to my supervisor, Professor Michael Monteiro for offering me an opportunity to do my PhD in the University of Queensland. He has guided me throughout the years, and has always been available for support. He has exerted tremendous patience and efforts on me, and has been more than willing to provide one-on-one mentoring so I could achieve to current standard. I would also like to express my entire gratitude to Dr. Zhongfan Jia, who has shared his wealth of knowledge and experience for my research projects, as well as a large amounts of help in the lab. I am grateful for his time for me and have enjoyed his company throughout my PhD career. In addition, I would like to appreciate my previous supervisor, Professor Congming Xiao, who tried his best to offer me a good condition to do research during my master career. The same appreciation would also go to Associate Professor Conghui Yuan, who had great contribution for the characterization of my products during my master. Without Professor Xiao and Yuan, I could not open the door to University of Queensland to continue my academic career.

My appreciation also goes to the past and present members of our group, who have all contributed in one way or another to the success and enjoyment of my PhD. Firstly I would like to appreciate Dr. Jakov Kulis who was very patient in answering my questions in experiments. Also, I would like to thanks Dr. Md. D. Hossain who taught me to do the first silica gel column in my life, after that I started my career of organic synthesis. Furthermore, I would like to appreciate Jennifer for her sincere help for the correction of thesis.

In addition, I would like to mention my colleagues Faheem, Valentin, Guanghui and Yangyang for their friendship and help. I thank them for all the fun over the years. Particularly, I have to thank my previous housemates Hongwei, Yanfen, Zhilin, Yanle, and Zhonglian, who lived in 254 Sir Fred Schonell Drive together. I really enjoyed the happy time in that house. My appreciation should also be expressed to Yanshuang and Suoying, who also gave me tremendous help during my PhD.

I would appreciate receipt of International Postgraduate Research Scholarship from Australia Government and also express my gratitude to the Australian Institute for Bioengineering and Nanotechnology for their state-of-the-art facilities.

Finally, I would like to thank my family and my parents, especially my father who supported me and made it possible for me to be able to finish my university degree and PhD. Particularly, I have to thank my wife who has been waiting for me for a couple years. Thank you.

Keywords

living radical polymerization, click chemistry, cyclic polymer, miktoarm star, dendrimer

Australian and New Zealand Standard Research Classifications (ANZSRC)

030306 Synthesis of Materials, 60%

030503 Organic Chemical Synthesis, 30%

030301 Chemical Characterisation of Materials, 10%

Fields of Research (FoR) Classification

0303 Macromolecular and Materials Chemistry, 70%

0305 Organic Chemistry, 30%

Table of Content

Chapter 2

Chapter 3

List of Figures

List of Schemes

List of Tables

List of Abbreviations

AIBN – 2,2-Azobis(2-methylpropionitrile)

ATNRC – Atom Transfer Nitroxide Radical Coupling

ATR-FTIR – Attenuated Total Reflectance Fourier Transform Infra-Red

ATRP – Atom Transfer Radical Polymerization

BiB – 2-Bromoisobutyryl Bromide

BPB – 2-Bromopropionyl Bromide

$CHCl_3$ – Chloroform

CuAAC – Copper-Catalyzed Azide-Alkyne Cycloaddition

CuBr – Copper(I) Bromide

$CuBr_2$ – Copper(II) Bromide

DBU – 1,8-Diazabicycloundec-7-ene

DCC – *N*,*N*-dicyclohexylcarbodiimide

DCM – Dichloromethane

DLS – Dynamic Light Scattering

DMA. –. *N*,*N*-dimethylacrylamide

DMAP. –. 4-(dimethylamino) pyridine

DMF – N,N-Dimethylformamide

DMSO – Dimethylsulfoxide

DPPA – Diphenylphosphoryl azide

EBiB – Ethyl-2-bromo Isobutyrate

EtOAc – Ethyl Acetate

FRP. –. Free radical polymerization

G1 – Generation 1

G2 – Generation 2

G3 – Generation 3

LND – Log Normal Distribution

LRP – Living Radical Polymerization

MALDI-ToF – Matrix-Assisted Laser Desorption Ionization – Time-of-Flight

Me_6TREN – Tris[2-dimethylamino)ethyl]amine

MeOH – Methanol

$MgSO_4$ – Magnesium Sulfate Anhydrous

MWD – Molecular Weight Distribution

NaN_3 – Sodium Azide

NIPAm – *N*-Isopropylacrylamide

NMP – Nitroxide-Mediated Polymerization

NMR – Nuclear Magnetic Resonance

NRC – Nitroxide Radical Coupling

PAA – Poly(acrylic acid)

PDI – Polydispersity Index

PDMA. –. Poly(N,N-dimethylacrylamide)

PEG – Poly(ethylene glycol)

PMDETA – N,N,N',N'',N''-Pentamethyldiethylenetriamine

PNIPAm – Poly(N-isopropylacrylamide)

PREP-SEC – Preparative Size Exclusion Chromatography

PSTY – Polystyrene

P^{t}BA – Poly(tert-butyl acrylate)

RAFT – Reversible Addition-Fragmentation Chain Transfer

RI – Refractive Index

RT – Room Temperature

SEC – Size Exclusion Chromatography

SET – Single-Electron Transfer

STY – Styrene

tBA – *tert*-Butyl Acrylate

TBAF – Tetrabutyl Ammonium Fluoride

TCEP – Tris (2-carboxyethyl) Phosphine hydrochloride

TEA – Triethylamine

TEM – Transmission Electron Microscopy

THF – Tetrahydrofuran

UV-Vis – Ultraviolet-Visible

Chapter 1
Introduction

Free-radical polymerization (FRP) is one of the most used polymerization methods to produce synthetic polymers.[1, 2] Nearly 50 % of all commercially available synthetic polymers are prepared by FRP. [1, 3-8] However, FRP usually generates polymers with broad molecular weight distributions (MWDs) and little control over end-group functionalities. Tremendous research effort has focused on developing techniques to prepare well-defined synthetic polymers.

Over the past few decades, 'living' radical polymerization (LRP) has emerged as a powerful tool to make polymers with a narrow MWD and near quantitative end-group functionality.[7-9] 'Living' radical polymerization can be categorised into several classes, including Nitroxide-Mediated Polymerization (NMP),[10-12] Atom-Transfer Radical Polymerization(ATRP),[13-20] Reversible Addition-Fragmentation Transfer (RAFT) polymerization,[21-27] and Single-Electron Transfer Living Radical Polymerization (SET-LRP).[28-31] LRP opens an avenue to produce a wide range of well-defined polymers with pre-determined molecular weight, a narrow molecular weight distribution, and with near quantitative end-group functionality. These end-group functionalities can be further converted to other moieties for the subsequent construction of complex polymeric architectures *via* a family of robust and efficient coupling reactions termed as 'click' chemistries. Examples of these reactions include Copper-Catalysed Azide-Alkyne Cycloaddition (CuAAC),[32-37] Nitroxide Radical Coupling (NRC), [38-42] and base-catalysed thiol-ene Michael addition. [43-49] The utilization of LRP and 'click' techniques enables the synthesis of a wide diversity of complex polymer architectures with controllable composition, topology, and functionality; all of which are key factors in determining the properties of polymeric materials.

1.1 'Living' Radical Polymerization

Free-radical polymerizations that have negligible chain-breaking reactions (i.e. bimolecular termination or chain transfer) are termed 'living' radical polymerizations. [50] The regeneration of the propagation centre (active site) in LRP enables continuous propagation and growth of monomer to the polymer chain. The molecular weight can be controlled

through the ratio of monomer to 'living' agent (e.g. RAFT agent or ATRP initiator) concentrations and monomer conversion.[3, 8] Addition of identical monomers generates homopolymers, which can be chain extended with another monomer-type to form block copolymers. Compared to living ionic polymerization, LRP possesses the following advantages; access to a wide choice of monomers, can be conducted in bulk and in a variety of solvents (even water) under mild conditions, and has a high tolerance for a wide variety of chemical functionalities. [7, 8, 51] Among the family of 'living' radical polymerizations, ATRP, SET-LRP and RAFT polymerization have differing mechanisms that allow control over several features of the polymerization. For example, RAFT allows a wide range of monomers to be polymerized, ATRP produces a bromine end-group which can readily be converted to an azide (for the CuAAC 'click' reaction) or other functional groups, and SET-LRP allows the rapid polymerization of monomers with near quantitative end-groups. Therefore, in this thesis, these LRP techniques will be used on a case-by-case basis for the synthesis of complex polymer architectures.

1.1.1 Atom-Transfer Radical Polymerization (ATRP)

ATRP is a method derived from the study of atom transfer radical addition (ATRA).[13] Since its inception in 1995, ATRP has been a common tool used to synthesize well-defined polymers with diverse functionalities, narrow molecular weight distributions, and pre-determined molecular weights. [13]

Scheme 1.1 General mechanism for atom transfer radical polymerization (ATRP)[13]

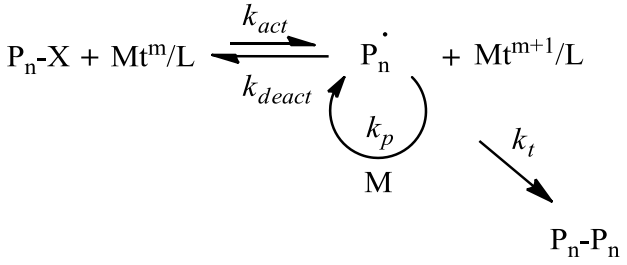

In a typical ATRP polymerization (Scheme 1.1), the transition metal (Mt), commonly Cu(I) in a halide salt form, is complexed with a ligand (L), often a nitrogen containing compound to improve its solubility in organic solvents and monomers. During the ATRP

process, the Mt and ligand complex (Mt^m/L) serve as catalysts (activators) while alkyl halides (R-X) serve as the initiator.[52] The ATRP mechanism involves a transfer reaction between the alkyl halide bond R-X and the transition metal complex (typically CuBr/PMDETA) to form the corresponding higher oxidation state metal halide complex and a carbon-centered radical $R^{\cdot}$ which initiates polymerization.[14] The equilibrium is maintained by the reverse process in which the higher oxidized transition metal complex transfers a halogen atom to the propagating radical resulting in deactivation of the chain radical through formation a new C-X bond at the chain end and regeneration of Mt^m.[13, 52, 53] Bimolecular termination of radicals increases the concentration of Mt^{m+1}/L (deactivator, e.g., Cu(II)Br_2/PMDETA complex) and thus minimizes further termination of polymeric radicals.[51, 52, 54, 55] This is known as the persistent radical effect (PRE). Therefore, employing a catalyst containing a certain initial amount of deactivator affords better control over the ATRP, leading to a higher chain-end functionality on the resulting polymer.

A common pathway to utilize ATRP-made polymers is to convert the halide atom to an azide group *via* nucleophilic substitution with sodium azide in near quantitative yields. This azide group can now be coupled with a wide range of alkyne functional compounds , via the copper catalysed alkyne-azide cycloaddition (CuAAC) 'click' reaction.[56] Alternatively, the halide-functional polymers can also be directly coupled with a variety of small molecules to modify the chain-end. These polymers can also be terminated with nitroxide- polymers to construct complex polymer structures *via* copper catalysed nitroxide radical coupling (NRC) reaction.[57]

1.1.2 Single-Electron Transfer living radical polymerization (SET-LRP)

In 2002, Percec and colleagues reported a novel metal-catalysed 'living' radical polymerization, the so-called SET-LRP. [28] The method used an extremely reactive Cu(0) generated through disproportionation of Cu(I) species to initiate polymerization of vinyl chloride monomer in an aqueous medium at room temperature . This overcomes the drawback of ATRP that undergoes an inner-sphere radical process to activate halide initiator,[53] and therefore difficult to polymerize nonactivated monomers (e.g, vinyl acetate, vinyl chloride) due to the formation of stable alkyl-halide dormant species.[58, 59] However, in the case of SET-LRP, the equilibrium between dormant and active chains is mediated by an outer-sphere heterogeneous single-electron transfer activation process *via* Cu(0) and deactivation with Cu(II)X_2/*N*-ligand.[60, 61] Subsequent studies have expanded this

methodology to polymerize a wide range of monomers, including acrylates,[29, 30, 62-64] acrylamides,[65-67] and methacrylates.[68, 69]

Scheme 1.2 General mechanism of SET-LRP[28]

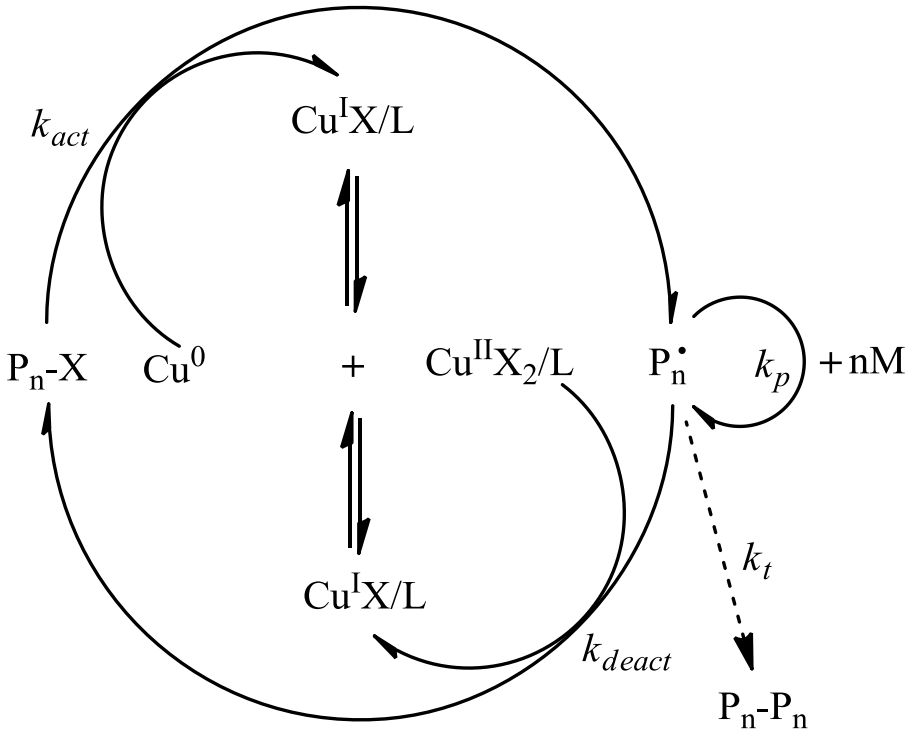

Scheme 1.2 shows the proposed mechanism of SET-LRP. In SET-LRP, Cu(0) is the catalyst which can be introduced into the reaction by directly adding Cu(0) source (e.g., Cu wire or Cu powder). Alternatively, it could be generated *in-situ* by disproportionation from various Cu(I) species. Cu(0) acts as electron donor to activate the electron acceptor alkyl halide initiator or dormant propagating specie through single electron transfer giving Cu(I)X and propagating radicals.[28-30] The generated Cu(I)X then undergoes disproportionation to regenerate the Cu(0) activator and Cu(II)X_2 deactivator required for the deactivation of propagation macroradicals with Cu(II)X_2/*N*-Ligand (reversible termination step). Such a self-regulated disproportionation mechanism eliminates bimolecular termination required to obtain the persistent radical effect as found in ATRP. [14, 55] In addition, *N*-ligands (i.e., Me_6TREN) in combination with polar solvents, such as DMSO, alcohols, and water, allow the rapid disproportionation of Cu(I)X to *nascent* Cu(0) and Cu(II)X_2 species. [70-72]

SET-LRP is able to produce acrylamide polymers (PDMA, PNIPAm) with narrow molecular weight distribution and high chain-end functionality which are difficult to be achieved by using ATRP. [73-75] It was suggested that the amido group at the chain end

stabilized propagation radicals during the ATRP of acrylamide monomers, leading to a high instant concentration of polymeric radicals in the system. The relative high concentration of radicals consequently promotes bimolecular radical coupling to give polymers with a broad MWD. Furthermore, the Br group of polymer is readily transformed to hydroxyl group by hydrolysis during the ATRP, which also limits the further construction of complex architectures due to the low chain-end fidelity.[70, 73, 76]

It should be noted that, there is an ongoing argument on the mechanism of SET-LRP. Matyjaszewski group proposed that SET-LRP is a subset of ATRP known as "SARA-ATRP" (Supplemental Activator and Reducing Agent-Atom Transfer Radical Polymerization).[52,53] In the mechanism of SARA-ATRP, alk halides were primarily primarily activated by Cu(I), while in proposed mechanism of SET-LRP, Cu(0) is the exculsive activator.[76]

1.1.3 Reversible Addition-Fragmentation Transfer (RAFT) polymerization

RAFT polymerization is another most effective and common 'controlled' radical polymerizations. It was developed by Rizzardo, Moad, Thang and coworkers from the Commonwealth Scientific and Industrial Research Organization (CSIRO) in 1998. [21]

The RAFT process distinguishes itself from ATRP and SET-LRP by its close relationship to conventional free-radical polymerization. RAFT polymerization is mediated by a highly active chain transfer agent (CTA), also referred to as a RAFT agent. The CTA is readily fragmented during the chain-transfer process to generate a new radical and a new thiocarbonylthio (thioester) specie through an addition-fragmentation mechanism (Scheme 1.3). [21, 27]

Scheme 1.3 General mechanism of RAFT polymerization[27]

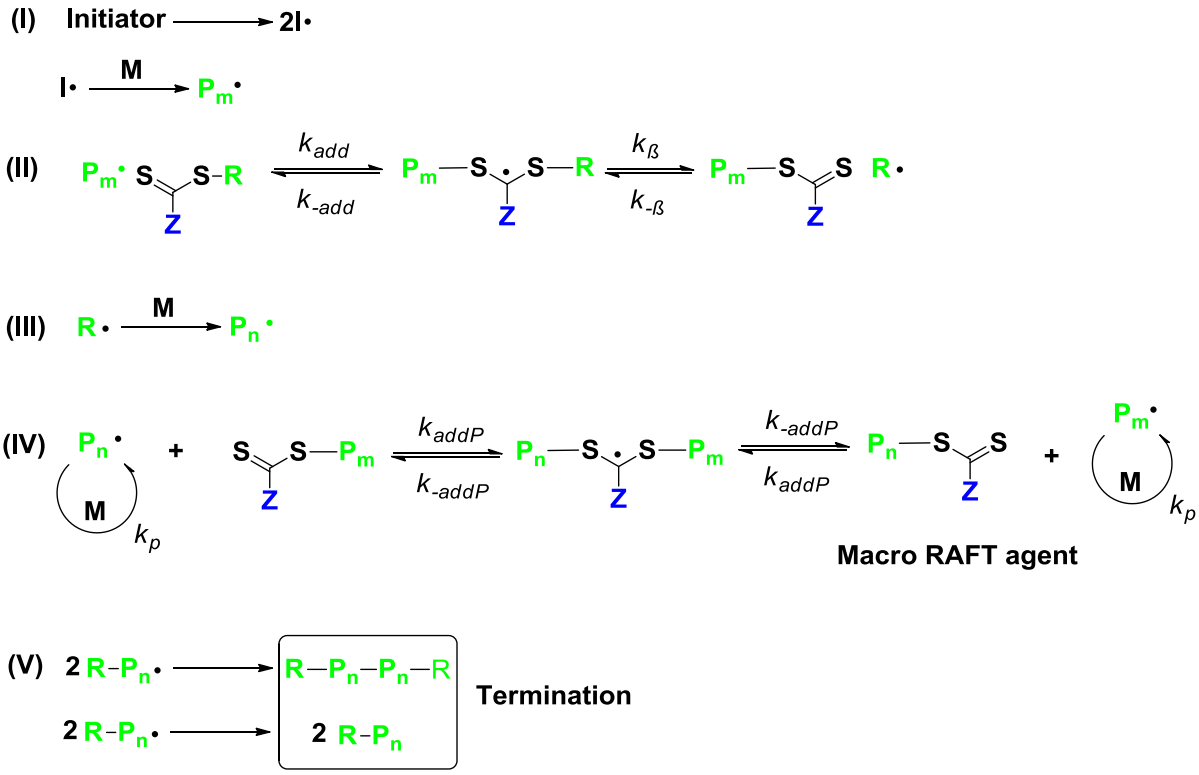

This thiocarbonylthio is the key component that provides the living characteristics of RAFT process. RAFT agents generally belong to one of the following main classes; dithioesters, [77-79] xanthates, [25, 80] dithiocarbamates, [81-83] and trithiocarbonates (Scheme 1.4).[84-91] It is crucial for achieving 'living' radical polymerization to choose the correct RAFT agent by matching the reactivity of the monomer to the RAFT agent. For example, the more reactive RAFT agents (e.g., trithiocarbonates) are suitable for maintaining 'living'-type radical polymerization of the more reactive monomers such as styrene, acrylates, and acrylamides (which generates corresponding polymeric radicals with low reactivity).[27]

Scheme 1.4 General structure of common RAFT agents

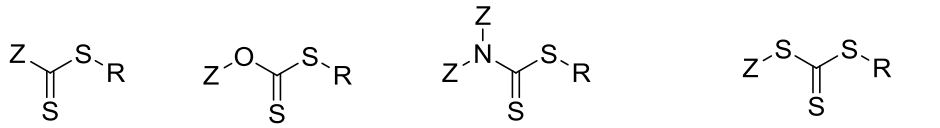

Dithioester **Xanthates** **Dithiocarbamates** **Trithiocarbonates**

Z = aryl, alkyl

The reactivity of RAFT chain transfer agents can be adjusted by changing the Z and R group on the RAFT agents.[27] The RAFT technique allows the polymerization of a wide range of monomers, including styrene derivatives, acrylamides, acrylates, acrylonitrile, vinyl

acetates, vinyl formamide, vinyl chlorides as well as a range of other vinyl monomers [92-95] *via* a range of initiation methods and at a varying reaction temperatures.[27, 96, 97] Owing to its similarity to the conventional free-radical polymerization procedure, the RAFT process is able to mediate polymerizations in bulk, solution, emulsion and dispersion conditions, [23, 98-106] using either aqueous or/and organic solvent medias. [99, 102, 107-109] RAFT polymerization generates control over molecular weight and molecular weight distribution with the retention of high end group fidelity.[110-114]

The generally accepted mechanism of synthesis of homopolymer *via* the RAFT process is described in Scheme 1.3, and involves five general steps: initiation, pre-equilibrium, reinitiation, main-equilibrium, and termination. [21, 27]

Initiation (I): Generation of free radicals from the homolysis of the initiator (e.g., AIBN) to form corresponding chain radicals.

Pre-equilibrium (II):The propagating polymeric radicals are captured by the addition to the reactive C=S bond of the chain transfer agent (CTA) to form intermediate radicals which are able to fragment reversibly to produce a polymeric RAFT-capped species (macro-CTA) and a re-initiating radical R·.

Reinitiation (III): The released R· radical can reinitiate a new polymer chain. When the initial RAFT agent has been completely consumed, the polymerization system is controlled by the presence of macro-CTA.

Main-equilibrium (IV): This step involves the rapid exchange of thiocarbonylthio groups between dormant polymeric thiocarbonylthio compounds and active propagating radicals. Each generated macro-radical has an equal probability of undergoing chain growth, promoting homogenous chain growth which leads to a low polymer dispersity.

Termination (V): The polymerization is terminated *via* combination or disproportionation inherent to the free radical polymerization processes.

The RAFT technique has not only been extensively employed to synthesize well-defined functional homopolymers but also employed in constructing a variety of complex polymer architectures, ranging from copolymers, graft-polymers, star-like polymers, and dendrimers. These structures can be obtained *via* either sequential addition of monomer or combining RAFT with 'click' chemistries. This makes RAFT a promising and powerful tool for the synthesis of advanced polymers. [115-117]

1.2 'Click' Chemistries

'Click' chemistry, the term identifying a new approach to old organic coupling reactions, was first coined by Sharpless and co-wokers.[32] The typical 'click' reaction is defined as having mild reaction conditions, quantitative yields, stereospecific products, inoffensive by-products, simple purification (using non-chromatographic methods), readily available starting materials and reagents, and a high tolerance of functionalities.[32, 33]

In the polymer field, the 'click' reaction provides access to an enormous diversity of complex polymeric architectures incorporating desired functions, which has greatly expanded the application area of polymeric materials. Below we discuss three reactions that fulfil the criteria of 'click' chemistry, which have been extensively used in the construction of a variety of complex macromolecular structure such as cyclic polymers,[118-125] miktoarm star copolymers,[126-132] and dendrimers. [56, 133-138]

1.2.1 Thiol-ene Michael Addition

Thiol-ene Michael addition has been demonstrated as a robust organic 'click' reaction that forms complex polymer architectures.[46-48, 139] It represents a common route to quantitatively convert RAFT-end groups on polymer chains into a variety of desired functional groups by an *in-situ* aminolysis/thiol-ene Michael addition sequence.[140] Thiol-ene 'click' chemistry is actually enjoying much research interest due to its metal-free catalyst system and efficiency of thiol-click reaction.[45]

The mechanism of base-catalysed thiol-ene raction *via* Michael-addition is illustrated in Scheme 1.5. In a polar solvent, the proton on the thiol group is readily removed by a stronger base (e.g., primary amine) to form corresponding thiolate anions, which are potent nucleophiles. The resulting thiolate anion can easily attack the activated ene (electron-deficient double bond), giving an intermediate carbanion. Finally, the enolate is protonated at the α-carbon of the original double bond. [141, 142] The primary amine (e.g, hexylamine) is an efficient catalyst for the thiol-ene reaction and the aminolysis of the RAFT end-group on the polymer. Primary amines are therefore widely used for the *in-situ* formation of free thiol groups from the RAFT-polymer chain-end followed by the addition of a second moiety (either small molecular or polymer-based bearing the activated double bond) in a nearly quantitative conversion. [47, 140, 143, 144]

Scheme 1.5 General mechanism of Base-catalysed Thiol-Michael addition reaction[141]

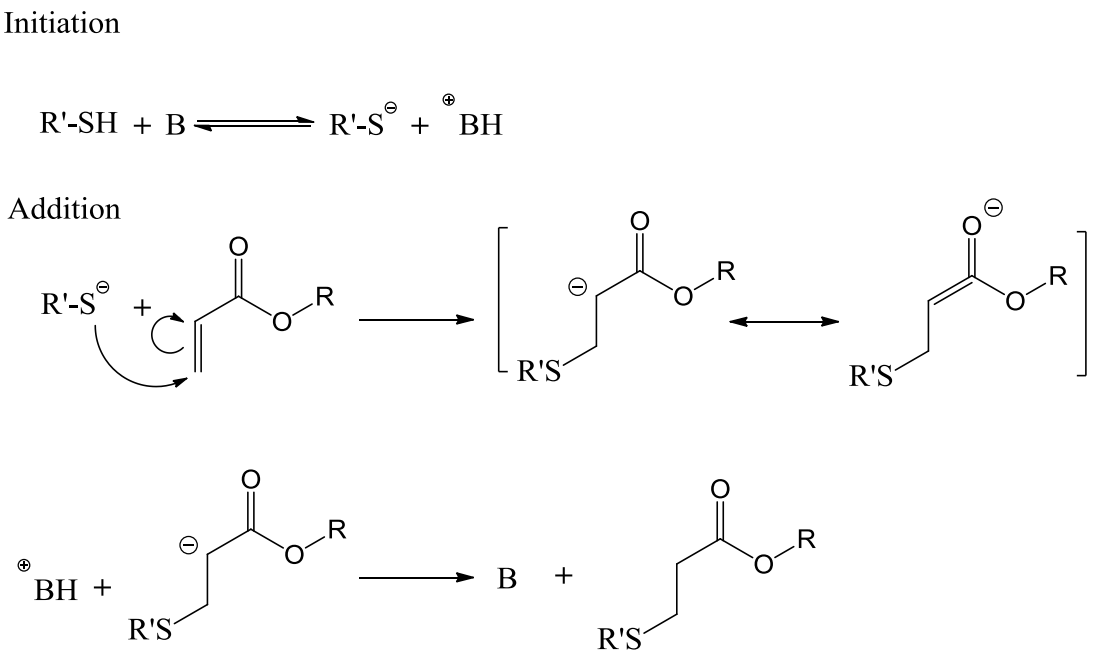

1.2.2 Copper Catalysed Azide-Alkyne Cycloaddition (CuAAC)

One of the most popular reactions within the 'click' chemistry concept is the 1,3-substituted azide alkyne Huisgen cycloaddition (also called copper catalysed Azide-alkyne cycloaddition) using a Copper (Cu) catalyst at room temperature.[33] It fulfils all of the criteria of 'click' chemistry, and is therefore one of the most used over the other 'click' reactions in polymer chemistry (Scheme 1.6).

Scheme 1.6 General outline of the 1,3-substituted azide-alkyne Huisgen 'click' reaction[145]

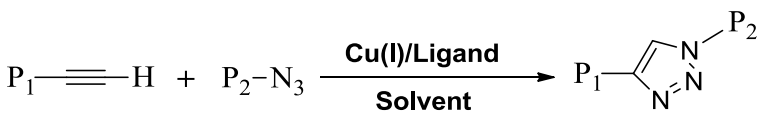

The reaction is regiospecific due to the exclusion of 1,4-substituted side products.[145] It typically does not require elevated temperatures but can be performed over a wide range of

temperatures (0-160°C), in a variety of solvents (including water), and over a wide range of pH values (5 to 12). [146] Furthermore, it is normally unaffected by steric factors and is therefore an ideal chemistry for making giant polymeric molecules with considerable steric hindrance in the structure (i.e. dendrimers). An additional reason for using the CuAAC 'click' reaction is that the precursor azide or alkyne terminal polymers are easily obtained *via* post-modification of LRP polymer end-groups. For example, one-step azidation of ATRP polymers or *in-situ* aminolysis/thiol-ene modification of RAFT-made polymers.

1.2.3 Nitroxide-Radical coupling(NRC)

In 1998, the Matyjaszewski group reported the synthesis of several alkoxyamines derived from organic halides and 2,2,6,6-tetram-ethylpiperidine-1-oxyl (TEMPO) or TEMPO derivatives using a copper catalyst.[147] Halogen transfer between organic halides and Cu(I) salts gave Cu(II) complexes followed by instant trapping by nitroxide radicals to form corresponding alkoxyamines, which is, in this case, called atom transfer nitroxide radical coupling (ATNRC).

Scheme 1.7 General outline of the Nitroxide-Radical coupling reaction[147]

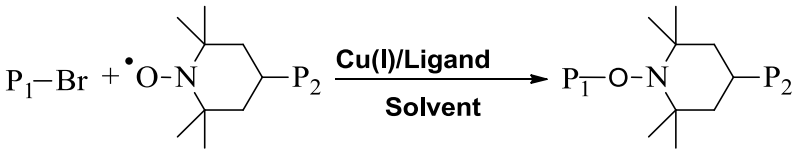

Huang et al extended this reaction to the polymer field, in order to tether two polymer segments containing TEMPO and a halide group, to form graft copolymers[148]. Triblock copolymer[38] and star copolymer[149] were also made by using ATNRC technique. During the reaction, Cu(I)Br was used to remove the halide to generate corresponding polymer radicals, which were rapidly trapped by the TEMPO group, linking the two building blocks *via* a stable alkoxyamine bond. [38, 147-149] Due to the rapid nitroxide trapping, the concentration of radicals in the reaction was low enough to eliminate almost all the bimolecular radical termination and gave a nearly quantitative conversion.

In contrast to the activation by atom transfer, another family of NRC coupling reactions, single electron transfer nitroxide radical coupling (SET-NRC), has been developed by the Monteiro group and used in the polymer science.[41] In SET-NRC, high-activating *nascent* Cu(0) was generated *in-situ* by Cu(I)Br in the presence of DMSO and tris-[2-(dimethylamino)ethyl]amine (Me_6TREN) ligand, and subsequently activated with R-X to form corresponding incipient radicals (Scheme 1.8). A detailed kinetic study of both ATNRC and SET-NRC was carried out by Kulis et al.[42] The two NRC reactions differ in the manner of the activation of R-X to its incipient radical ($R^{\cdot}$) (Scheme 1.8). In ATNRC, R-X is activated by Cu(I)Br, while in SET-NRC Cu(0) is employed. SET-NRC coupling is also a powerful tool for modifying the chain end of ATRP-generated polymers. A wide range of functionalities on polymer backbones including glycidyl ether, styryl, acrylate, methacrylate, alkyne, dialkyne, tosylate, active ester, biotin, and pyrene groups could be introduced at the chain-end of polymer *via* a universal and efficient one-step post-polymerization method using SET-NRC. [57]

Scheme 1.8 Proposed mechanisms for ATNRC and SET-NRC[42]

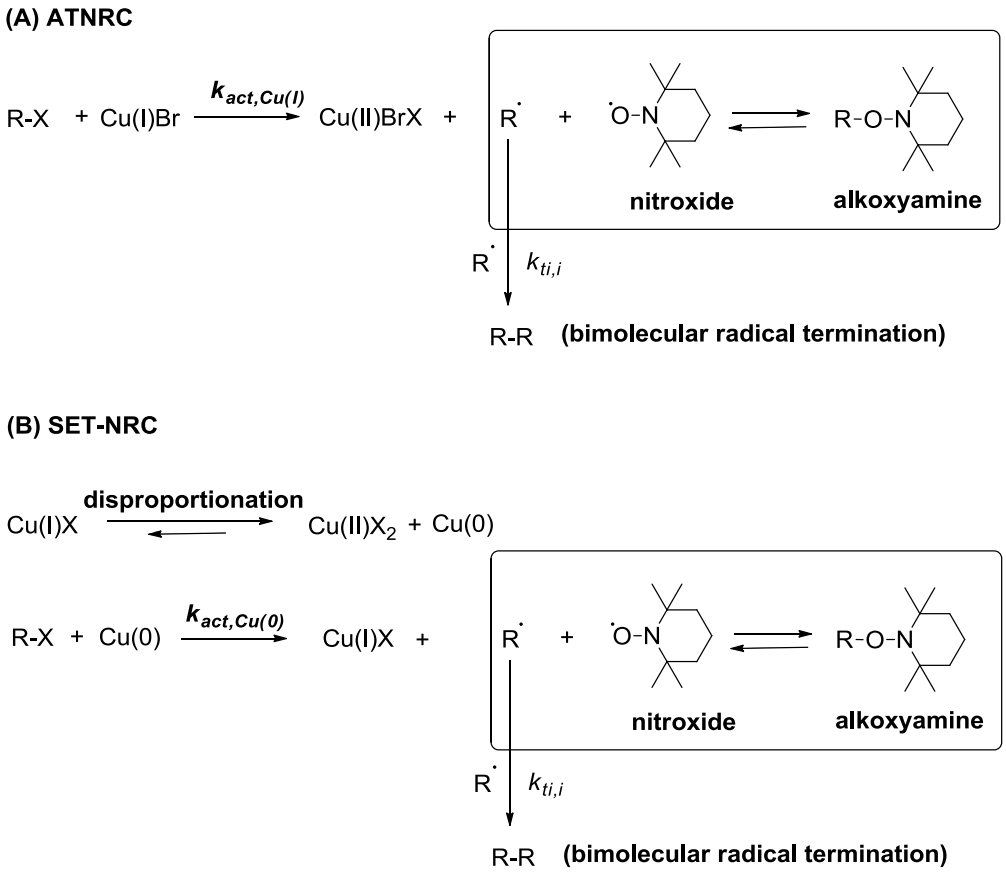

1.2.4 Combination of CuAAC and NRC

Construction of sophisticated polymer architectures is still a synthetic challenge for polymer chemists. This is because it normally involves a multi-step synthetic protocol due to the utilization of two or more 'click' reactions, for which the catalyst system or functionalities are not compatible in one-pot system. To accelerate and simplify the synthetic procedure, there is an emphasis on developing a synthetic methodology that can reduce the number of reaction and purification steps involved. Overcoming these non-compatible interactions will lead to more eco-friendly polymer products.

CuAAC and NRC are both copper-catalysed 'click' reactions. The similar catalyst system (i.e., Cu(I) and *N*-containing ligand), and the compatibility of azide, alkyne, and bromide functionalities, allow CuAAC and NRC to be carried out in a one-pot reaction system. Based on the synthesis of diblock polymers *via* NRC coupling, Huang et. al. further developed a new strategy to prepare ABC triblock copolymers using a combination of CuAAC and NRC

in one-pot reaction in 2008 (Scheme 1.9).[38] The ease and efficiency of the aforementioned strategy opens an avenue to construct more complex polymer structures through a mild, rapid, and efficient approach. This strategy was also applied in the construction of more complex macromolecular derivatives, including AB-type block-graft copolymers, [150] mikto three arm AB_2 stars,[151] and tricyclic miktoarm stars.[152] These achievements have a broad synthetic appeal as they reduced the steps of chemical protection, synthetic and purification, meanwhile diminishing the necessity for large excess of starting reactants.

Scheme 1.9 Synthesis of ABC type linear copolymers *via*combining CuAAC and NRC 'click' reactions in a one-pot system.[38]

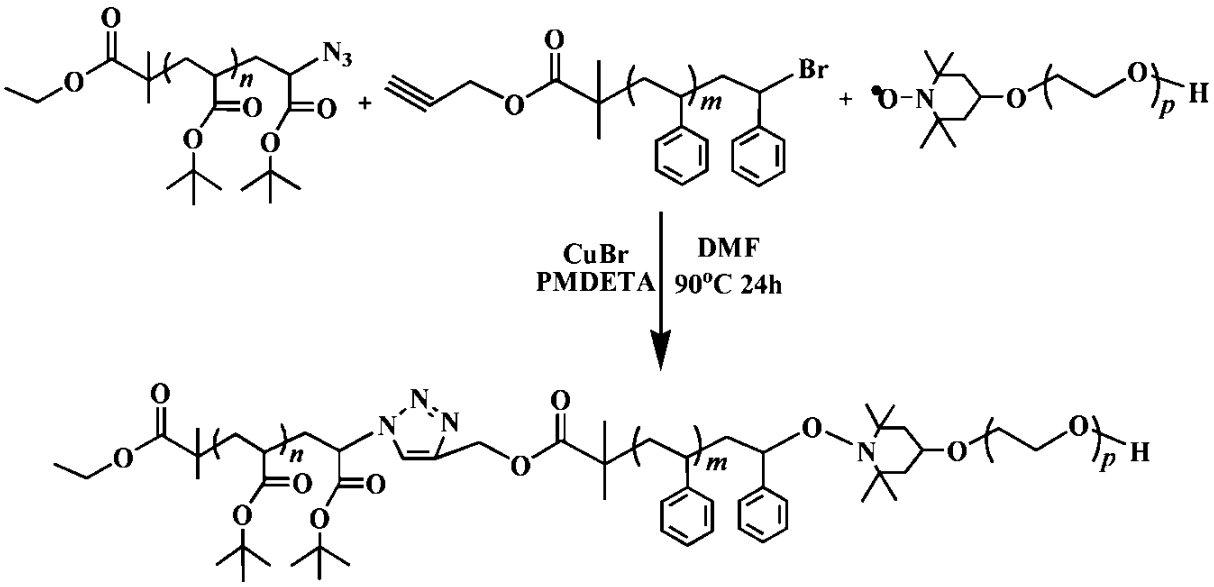

1.3 Dendrimers

Dendrimers are a tree-like cascade molecules with hyperbranched, monodisperse, three-dimensional, and well-defined structures [153, 154] A typical dendrimer structure consists of a multifunctional core, branched units and many peripheral groups. The inner branched units that exist as layers are called 'generations', which are the repeating monomeric units of dendrimers.[155] Due to the dendritic topology, dendrimers exhibit distinct physical and chemical properties compared to their linear polymer analogs. For example, as molecular weight increases, the viscosity of the dendrimer will reach a maximum plateau and then begin to decline, while the viscosity of linear polymers follows logarithmic increase with molecular weight [156, 157]. The glass transition temperature of a dendrimer follows a similar trend[158]. Dendrimers also show better solubility than linear polymers counterparts.[159] Moreover, dendrimers also possess predictable shape changes as a function of their molecular weight and core confirmation-restricted surface area. [160, 161] The unique physical and chemical properties of dendrimers make them ideal candidates for applications in biological and materials engineering, including being used as adhesives, coatings, chemical sensors, drug delivery systems, catalysts and medical diagnostic tools. [155, 162, 163]

1.3.1 Synthesis of dendrimers

The synthetic strategy for constructing dendrimers are completely different from that for making classical polymers. The synthesis of dendrimers is normally well controlled and results in macromolecules with exact molecular weights, and monodisperse and regular branched structures. Therefore, by regulating dendrimer synthesis, a couple of key structural factors of dendrimers, such as size, shape, surface chemistry, flexibility/rigidity, architecture, and composition can be controlled and adjusted.[155, 164, 165]

Dendrimer formation can typically be categorized into two primary methods, namely, convergent and divergent synthesis. The first work prepared 10^{th} generation PAMAM dendrimers by a divergent method was presented by Tomalia and coworkers in 1985.[166] Five years later, another paper published by Hawker and Frechet in 1990 reported a synthetic approach termed convergent method to make poly (aryl ether) dendrimers. [167]

1.3.1.1 Divergent synthesis of dendrimers

In the divergent approach (Scheme 1.10), synthesis begins at a mutilfunctional core and construction proceeds layer by layer (generation by generation), growing at the periphery. This occurs *via* sequential addition of AB_n type of monomers (n≥2). The most commonly used monomer is AB_2, where A is the reactive group enabling the coupling reaction with the core, while group B is protected. After the formation of first generation (G1), the G1 dendrimer undergoes an activation process to activate the B functionality, resulting in new peripheral reactive sites, which allows the coupling of a new generation of monomer. By repeating the coupling and activation procedure, a desired number of generation of dendrimer can be obtained.

Scheme 1.10 Synthesis of dendrimers *via* divergent method.[164]

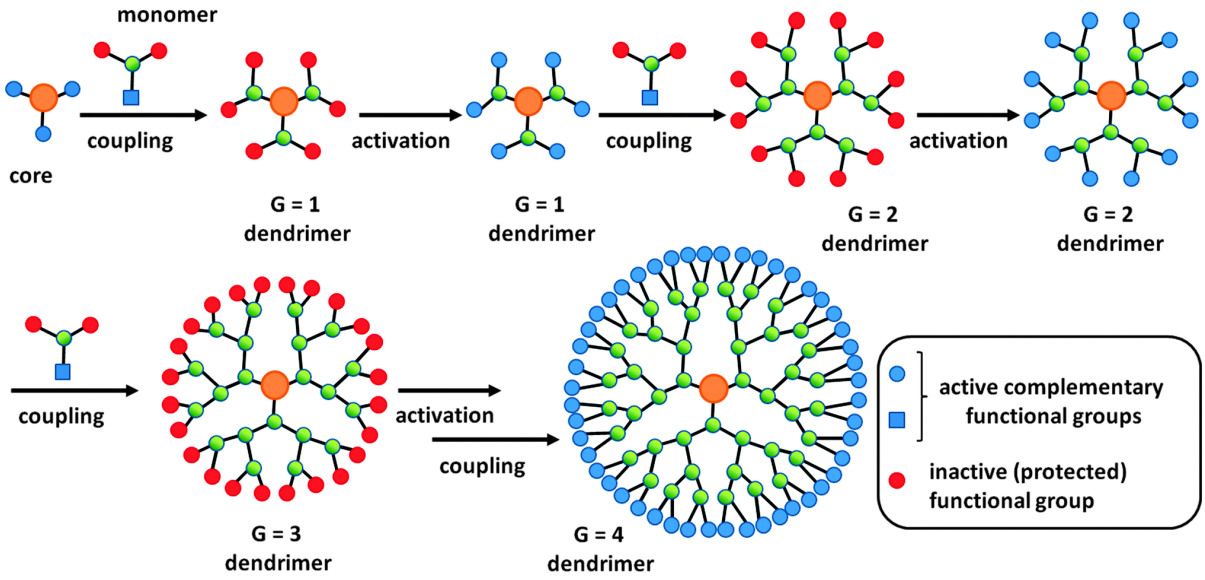

In the divergent synthesis approach, the growth of the dendrimer is based on the reactive sites at the outmost layer, therefore, the fidelity of functionality at the periphery is crucial for achieving high purity of dendrimer with minimal structural defects. Moreover, the exponentially increase of terminal groups with each generation will lead to a densely-packed effect and increased steric hindrance at higher generations. As a result, the surface reactive sites are less accessible for each further coupling reaction. Moreover, dendrimers obtained from the divergent approach also suffer from the difficulty of purification due to the similar chemical properties(e.g, molecular weight, size, and solubility) of defective and defect-free

dendrimers. This shortcoming is one of the main reasons why dendrimer synthesis is considered tedious and time-consuming.

It should also be noted that the modification of surface area of dendrimers synthesized by the divergent strategy is relatively simple (normally in one step), which provides the flexibility of the application in different fields achieved by changing dendrimer peripheral groups. For this reason, all commercially available dendrimers (e.g., PAMAM and PPI) were made by this strategy.[168, 169]

1.3.1.2 Convergent synthesis of dendrimers

In the convergent method (Scheme 1.11), individual 'wedges' of dendrimer, so-called dendrons, are made first and then coupled with a multifunctional core. Similar to divergent growth, convergent synthesis also uses AB_2 monomers, however the terminal group A is protected while groups B are reactive and readily coupled with the outmost units to generate the first generation dendron. The new reactive site is then created through the deprotection of the A functionality, which is subsequently coupled with AB_2 monomer to give the G2 dendron. Each repetition of the two steps above results in the addition of one more generation. The synthesis of the dendrimer is accomplished *via* attaching dendrons or 'wedges' to the core in the final step.

Scheme 1.11 Synthesis of dendrimers *via* convergent method.[164]

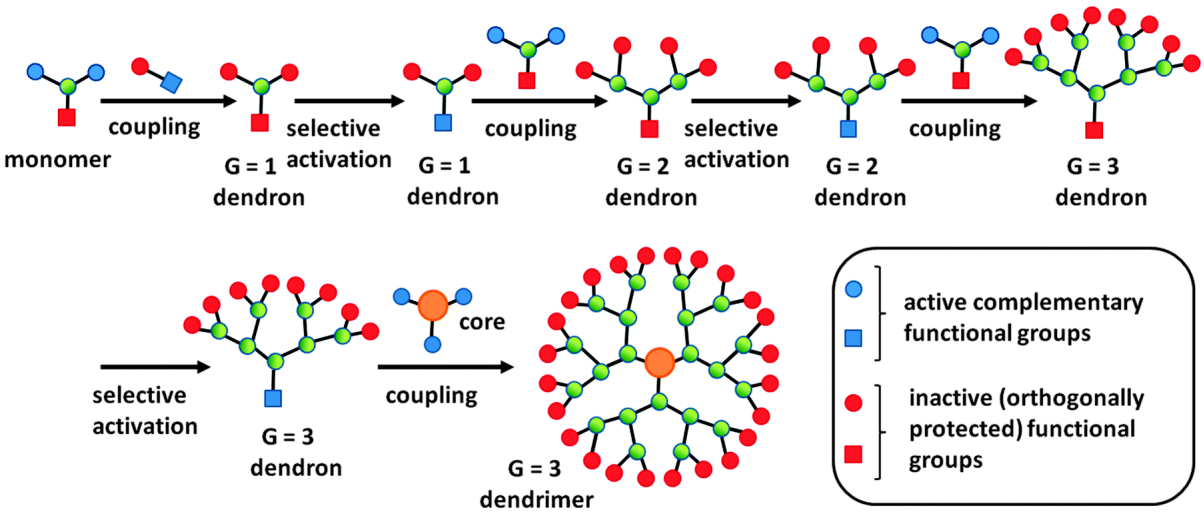

Generally, convergent synthesis involves more synthetic steps than divergent synthesis. Nonetheless, it does provide more structural diversity and types of dendrimers with respect to

synthesis. For example, the convergent approach allows incorporation of different types of pre-synthesized dendrons with different compositions, surface functional groups, and/or generations, resulting in structural variations in the final dendrimer.[155] Another advantage of this strategy is that purification is easier than that of divergent method. After each step of growth, the resulted dendron is over two fold molecular weight than that of starting dendron, and therefore, the unreacted starting reactants or defective dendrons are easily removed by chromatographic techniques (e.g, preparative-SEC), yielding a dendrimer with high purity. [155]

However, with the increasing dendron generation, the reactivity and availability of focal point decreases, which causes a coupling reaction with lower efficiency. As a result, only lower generation dendrimers can be prepared using convergent method.[170]

1.3.1.3 Accelerated synthesis of dendrimer *via* orthogonal coupling reactions

The protocols utilized to synthesize dendrimers are tedious and time-consuming by either divergent or convergent approach. By taking advantage of 'click'-type reactions (e.g., CuAAC, NRC, and thiol-ene), their synthesis could be simplified, especially by employing orthogonal 'click' reactions. For example, a divergent approach using AB_2 and CD_2 type monomers was used to prepare a 6^{th} generation dendrimer by combing the orthogonal CuAAC and thiol-ene click chemistries in sequence.[137] Another advantage of using orthogonal 'click' reactions is that it is possible to synthesize dendrimers in a one-pot system using two or more orthogonal coupling reactions. Although the orthogonal coupling reactions allow the rapid and efficient synthesis of dendrimers, only few syntheses using this strategy have been reported. It is because the compatible functionalities onto the monomers (or building blocks) for the coupling reactions are limited.

The success of using CuAAC and NRC coupling reactions to make ABC triblock copolymers and ABC miktoarm structures was further expanded to synthesize dendrimers. Jia et al[171] developed an elegant method to construct second generation dendritic architectures in a one-pot system with high yield using orthogonal CuAAC and NRC (ATNRC or SET-NRC) 'click' reactions (Scheme 1.12). Interestingly, the pathway of dendrimer formation could be controlled *via* a divergent, convergent or parallel sequence by modulating the copper (e.g., Cu(0) and Cu(I)) catalyst activity, and consequently, changing the rates of the two 'click' reactions.

Scheme 1.12 Synthetic pathways for divergent, parallel and convergent formation of a highly branched G2 architecture in one-pot.[57]

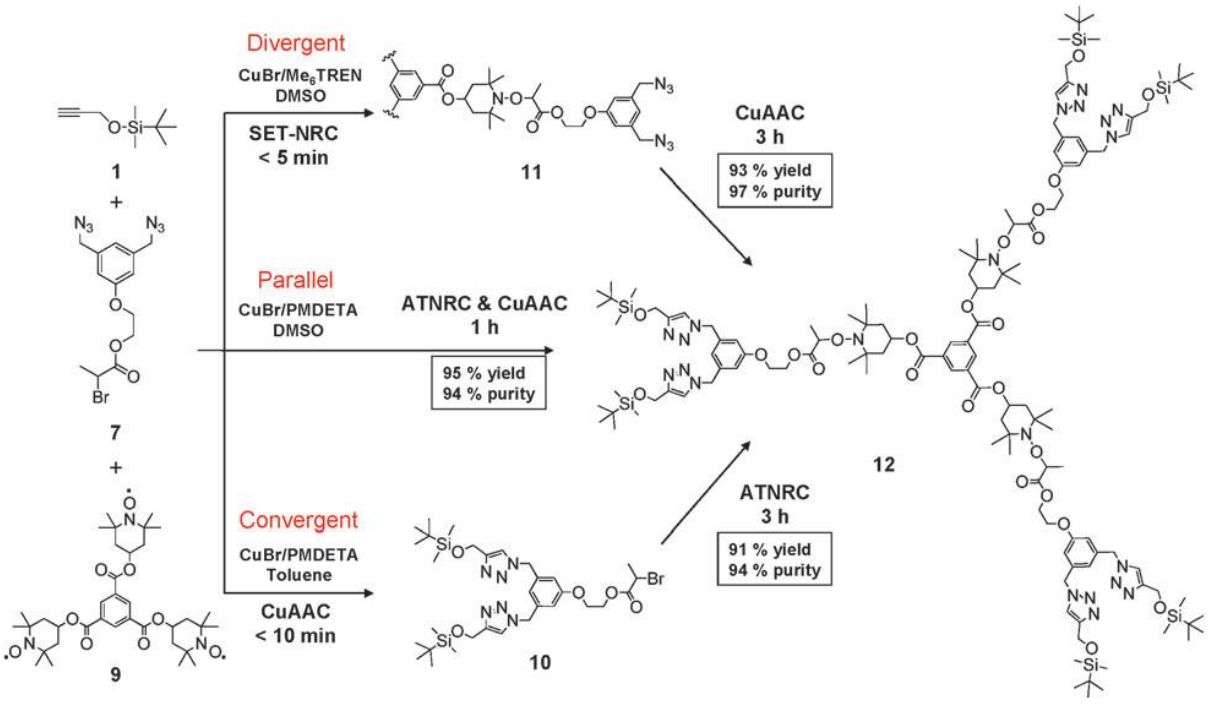

Based on this work, a third generation dendrimer was prepared by applying three different 'click' reactions (CuAAC, SET-NRC or ATNRC, and thiol-ene Michael additions) with a one-pot, two-step approach. This work demonstrated the possibility to carry out three orthogonal 'click' reactions in a one-pot system, representing a significant advance in the chemistry of dendrimer synthesis.

Soon after, Bell et al[138] combined CuAAC and NRC reactions to make 3rd generation of polymeric dendrimers in a one-pot system. Moreover, a range of polymers (e.g., PSTY, P^{t}BA, PEG, PNIPAm) can be used as the building blocks for the construction of dendrimers, which permits the synthesis of a diverse range of dendrimers with different compositions.

Scheme 1.13 General Schematic for the Synthesis of G3 Polymeric dendrimers in One-Pot synthesis by NRC and CuAAC[138]

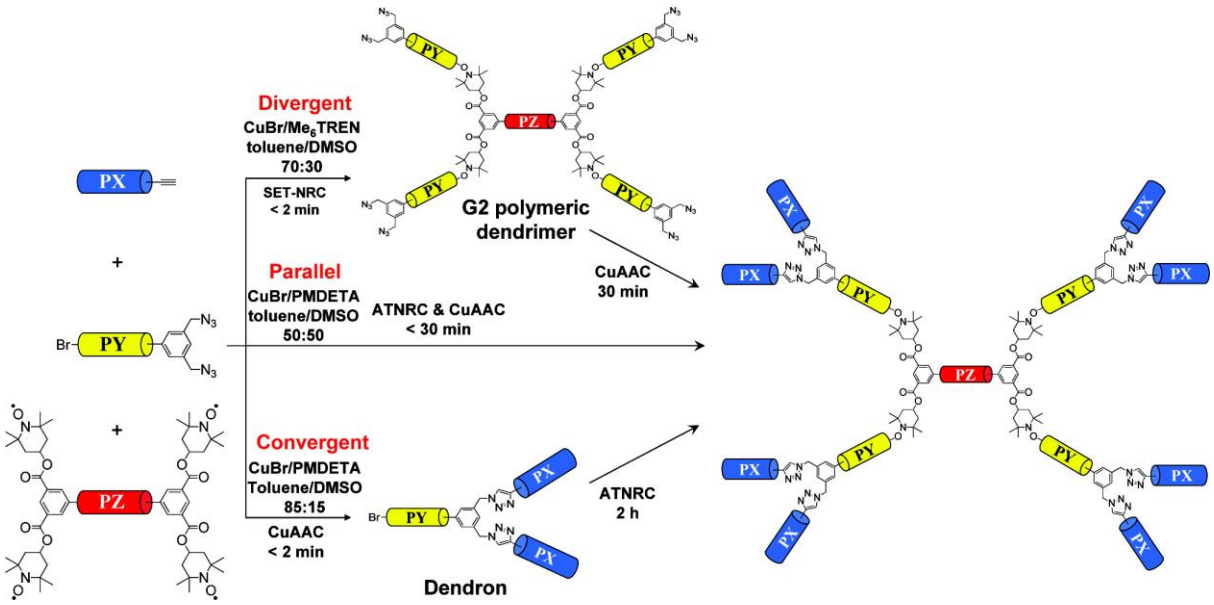

The successful utilization of the combination of CuAAC and NRC to form complex molecular structures in both small molecular and polymeric systems has a broad synthetic appeal as they reduced the number of chemical protection, synthetic and purification steps.

1.4 Peptidomimetics and Dendritic Peptidomimetics

Peptidomimetics are the compounds have similar biological activity as native peptides. [172-174] Peptidomimetics are purposely designed to overcome some of the problems associated with natural peptides, such as low stability in plasma, rapid degradation by proteases, short circulation time, and highly mobile conformation. [175] Peptidomimetics were firstly described as the molecules that were derived from existing peptides by structural modification, [173, 176] including cyclization of linear peptides,[177, 178] or/and attached stable unnatural amino acids which obtained from their native analogs *via* modification of side chain or backbone. [179, 180] Alternatively, peptidomimetics are also referred to unnatural synthetic peptides which have secondary structures (i.e., helical and turn) analogous to that of the original peptide.[181-183] Today, the definition is more biased towards the similar function rather than similar structure. And therefore, the term is by far more generally understood as "a compound which mimics the function of the native peptide".[184]

Native peptides are normally conformationally flexible, leading to a decrease in chemical interactions with corresponding biological targets.[185] Peptidomimetics can be developed to be conformationally restricted, in which the peptide conformation is constrained to obtain an improvement of biological activities.[186] Dendrimers with amino acids or peptides attached to the periphery represent one form of conformationally restricted peptidomimetics.[187, 188] Due to the hyperbranched structure of dendrimers, the mobility of the terminal groups at the periphery is restricted as a consequence of steric hindrance.[153] This property is similar with the preparation of conformationally restricted peptides (e.g., cyclic peptides).[183] Another advantage associated with dendritic structures is that it contains many surface functional groups, which provides multiple binding interactions, resulting in a potent levels of affinity due to the multivalent bonding.[186, 187, 189] For example dendrimers with antigen peptides at the periphery have an increased half-life, higher resistance to protease, and are also more efficient than monomeric peptides in diagnostic applications. [190]

Dendritic peptidomimetics have been widely investigated for many biological applications.[186, 187, 191, 192] For example, polycationic small molecular dendrimers Polyamidoamine (PAMAM) and Poly(lysine) (PLL) have been used as anti-HIV microbicides, or anti-viral agents based on the electrostatic interactions,[186, 187, 193, 194] which indicates that dendrimers conjugated with amino acids or peptides can serve as peptidomimetics.

However small molecular dendrimers (<15 nm) are limited in their applications, with extended applications requiring larger sizes (> 15 nm), especially for some biological target sites with large surface areas. To reach a diameter above 10 nm, dendrimers made from small molecules must have up to 10 generational layers.[195] The synthesis involves multiple steps, with each step requiring a highly time-consuming purification processes (over 2 months in some cases).[195]

Recent advances in 'living' radical polymerization techniques and 'click'-type reactions offer a powerful tool to build polymeric dendrimers with adjustable sizes simply by changing the degree of polymerization for the building blocks. The ease of chain end modification also allows attachment of a variety of biological molecules (i.e., amino acids or peptides). Recently, a polymeric dendritic peptidomimetic, which consisted of star-like hydrophobic poly(*tert*-butyl-acrylate) core and hydrophilic peptide vaccine peripheral molecules, has been used as a self-adjuvanting vaccine. [136] A further advantage of 'living' radical polymerization techniques and 'click'-type reactions for dendrimer synthesis is that the confirmation of attached peptides can be changed from random to an α-helix secondary structure after self-

assembly.[136] Thus, polymeric dendritic peptidomimetics combine the attributes of hyperbranched structure, consisting of well-defined functionality within the generational layers and periphery, with the advantages of size and shape associated with nanoparticles.

1.5 Objectives and Outlines of Thesis

The main objective of this thesis was to develop new synthetic strategies based on the LRP and 'click' chemistry to construct complex polymeric architectures. At the beginning, we synthesized a variety of novel trithiocarbonates as chain transfer agents and halide compounds as ATRP or SET-LRP initiators with desired functionalities. The resulting multifunctional RAFT agent and initiators were then further used to mediate the 'living' radical polymerizations (LRP), such as RAFT polymerization, ATRP, and SET-LRP to prepare a library of well-defined polymeric building blocks with pendant and built-in functionalities. Subsequently, three robust and efficient 'click' reactions (e.g., thiol-ene Michael addition, CuAAC, and NRC) were employed to couple pre-synthesized functional building blocks to complex polymer architectures, including cyclic polymers, miktoarm star copolymers, and polymeric dendrimers. The versatile CuAAC 'click' reaction also permitted the construction of sophisticated macromolecules (e.g., dendritic peptidomimetic) by conjugating biocompatible small molecular compounds and biological molecules. Taking both the advantages of LRP and 'click' chemistries, we were able to construct macromolecular structures such as cyclic polymers, miktoarm star polymers, and dendrimers, with predicted and controllable compositions, topologies and properties. This work and the resulting structures provide new insights into polymer chemistry and physics, and has potential use in biological applications.

Chapter 2 of this thesis details a new synthetic approach to cyclic polymers. The combination of RAFT polymerization and thiol-ene Michael addition enables the one-pot rapid synthesis of a variety of alkyne-functional cyclic polymers with high purities, including cyclic PSTY, P^{t}BA, PDMA and PNIPAm. Compared to ATRP, RAFT polymerization permits the use of a wider range of water soluble polymers. This work was also the first report of the synthesis of cyclic PDMA. The in-chain alkyne functionality avoid the further post-polymerization modification to introduce functional group which is essential for constructing more complex architectures (e.g., dendritic cyclic macromolecules, nuimolecular

micelles). Studies on the complex polymers strucutre have not only offered new insight into polymer physical properties (i.e, viscoelasticity and their diffusion, self-assembly of unimolecular micelles) but have provided insight into mechanisms for biological field (e.g, DNA packing and replication) that is governed largely by polymer-polymer interactions based on a cyclic polymer model system.

Chapter 3 details a novel synthetic strategy to make miktoarm star copolymers consisting of four different arm segments. The ATRP and SET-LRP techniques provide the possibilities to make a wide range of hydrophobic and hydrophilic polymers. Subsequent post-functionalization introduces alkyne functionalities onto polymer building blocks, therefore enabling further CuAAC click reactions with azide-functionalized cores, yielding ABCD miktoarm star copolymers. The synthetic strategy developed in this chapter presents an approach for generating asymmetric star-like copolymers with more than four chemically-distinct arm segments, which enriches the family of miktoarm star polymers Furthermore, this strategy could be used as a proof concept to prepare more complex polymeric structure, for example, asymmetric dendrimer, which expands the scope of their applications.

Chapter 4 elaborates on a new process of using two copper-catalyzed orthogonal 'click'-type reactions (i.e. nitroxide radical coupling (NRC) and CuAAC) to produce polymer dendrimers that are densely coated with L-lysine groups in a one-pot reaction at 25 ^{o}C with high purity and yield. The synthetic methodology developed in this chapter provides a rapid and efficient pathway for synthesis of polymeric dendrimers decorated with biological molecules at the periphery with controllable composition, size and surface density. These dendritic macromolecular peptidomimetics has potential use as anti-virus materials, gene delivery and vaccine delivery platforms.

Chapter 5 describes the synthesis of four 4-arm star-like dendrimers with single amino acid or peptides attached to the ethylene glycol chain-ends *via* a CuAAC 'click' reaction. The resulting star dendrimers are presented as possible peptidomimeticsfor use in mimicking the action of scorpion toxins on voltage-activated K^+ channels.

1.6 References

1. Prane, J. R. *J Coating Technol* **1996,** 68, (860), 74-79.
2. Pearce, E. M. *J Am Chem Soc* **1984,** 106, (12), 3708-3708.
3. Matyjaszewski, K.; Spanswick, J. *Mater Today* **2005,** 8, (3), 26-33.
4. North, A. M. *J Chem Soc Farad T 1* **1983,** 79, 1676-1677.
5. McKeen, L. *Permeability Properties of Plastics and Elastomers, 3rd Edition* **2012**, 21-37.
6. Noble, B. B.; Coote, M. L. *Int Rev Phys Chem* **2013,** 32, (3), 467-513.
7. Moad, G.; Rizzardo, E.; Thang, S. H. *Accounts Chem Res* **2008,** 41, (9), 1133-1142.
8. Goto, A.; Fukuda, T. *Prog Polym Sci* **2004,** 29, (4), 329-385.
9. Braunecker, W. A.; Matyjaszewski, K. *Prog Polym Sci* **2007,** 32, (1), 93-146.
10. Hawker, C. J.; Bosman, A. W.; Harth, E. *Chem Rev* **2001,** 101, (12), 3661-3688.
11. Hawker, C. J.; Barclay, G. G.; Orellana, A.; Dao, J.; Devonport, W. *Macromolecules* **1996,** 29, (16), 5245-5254.
12. Fukuda, T.; Terauchi, T.; Goto, A.; Ohno, K.; Tsujii, Y.; Miyamoto, T.; Kobatake, S.; Yamada, B. *Macromolecules* **1996,** 29, (20), 6393-6398.
13. Wang, J. S.; Matyjaszewski, K. *Macromolecules* **1995,** 28, (22), 7572-7573.
14. Kajiwara, A.; Matyjaszewski, K. *Macromol Rapid Comm* **1998,** 19, (6), 319-321.
15. Patten, T. E.; Matyjaszewski, K. *Adv Mater* **1998,** 10, (12), 901-915.
16. Matyjaszewski, K.; Tsarevsky, N. V. *Nat Chem* **2009,** 1, (4), 276-288.
17. Gao, H. F.; Matyjaszewski, K. *Macromolecules* **2006,** 39, (15), 4960-4965.
18. Matyjaszewski, K. *Macromolecules* **2012,** 45, (10), 4015-4039.
19. Averick, S.; Simakova, A.; Park, S.; Konkolewicz, D.; Magenau, A. J. D.; Mehl, R. A.; Matyjaszewski, K. *Acs Macro Lett* **2012,** 1, (1), 6-10.
20. Li, Y. T.; Armes, S. P. *Macromolecules* **2005,** 38, (20), 8155-8162.
21. Chiefari, J.; Chong, Y. K.; Ercole, F.; Krstina, J.; Jeffery, J.; Le, T. P. T.; Mayadunne, R. T. A.; Meijs, G. F.; Moad, C. L.; Moad, G.; Rizzardo, E.; Thang, S. H. *Macromolecules* **1998,** 31, (16), 5559-5562.
22. Chong, Y. K.; Le, T. P. T.; Moad, G.; Rizzardo, E.; Thang, S. H. *Macromolecules* **1999,** 32, (6), 2071-2074.
23. Smulders, W.; Monteiro, M. J. *Macromolecules* **2004,** 37, (12), 4474-4483.
24. Moad, G.; Chong, Y. K.; Postma, A.; Rizzardo, E.; Thang, S. H. *Polymer* **2005,** 46, (19), 8458-8468.
25. Perrier, S.; Takolpuckdee, P. *J Polym Sci Pol Chem* **2005,** 43, (22), 5347-5393.

26. Boyer, C.; Bulmus, V.; Davis, T. P.; Ladmiral, V.; Liu, J. Q.; Perrier, S. *Chem Rev* **2009,** 109, (11), 5402-5436.

27. Moad, G.; Rizzardo, E.; Thang, S. H. *Aust J Chem* **2012,** 65, (8), 985-1076.

28. Percec, V.; Popov, A. V.; Ramirez-Castillo, E.; Monteiro, M.; Barboiu, B.; Weichold, O.; Asandei, A. D.; Mitchell, C. M. *J Am Chem Soc* **2002,** 124, (18), 4940-4941.

29. Rosen, B. M.; Percec, V. *Chem Rev* **2009,** 109, (11), 5069-5119.

30. Percec, V.; Guliashvili, T.; Ladislaw, J. S.; Wistrand, A.; Stjerndahl, A.; Sienkowska, M. J.; Monteiro, M. J.; Sahoo, S. *J Am Chem Soc* **2006,** 128, (43), 14156-14165.

31. Alsubaie, F.; Anastasaki, A.; Wilson, P.; Haddleton, D. M. *Polym Chem-Uk* **2015,** 6, (3), 406-417.

32. Kolb, H. C.; Finn, M. G.; Sharpless, K. B. *Angew Chem Int Edit* **2001,** 40, (11), 2004-2021.

33. Rostovtsev, V. V.; Green, L. G.; Fokin, V. V.; Sharpless, K. B. *Angew Chem Int Edit* **2002,** 41, (14), 2596-2599.

34. Geng, J.; Lindqvist, J.; Mantovani, G.; Haddleton, D. M. *Angew Chem Int Edit* **2008,** 47, (22), 4180-4183.

35. Lutz, J. F.; Zarafshani, Z. *Adv Drug Deliver Rev* **2008,** 60, (9), 958-970.

36. Hein, J. E.; Fokin, V. V. *Chem Soc Rev* **2010,** 39, (4), 1302-1315.

37. Liang, L. Y.; Astruc, D. *Coordin Chem Rev* **2011,** 255, (23-24), 2933-2945.

38. Lin, W. C.; Fu, Q.; Zhang, Y.; Huang, J. L. *Macromolecules* **2008,** 41, (12), 4127-4135.

39. Fu, Q.; Wang, G. W.; Lin, W. C.; Huang, J. L. *J Polym Sci Pol Chem* **2009,** 47, (3), 986-990.

40. Fu, Q.; Zhang, Z. N.; Lin, W. C.; Huang, J. L. *Macromolecules* **2009,** 42, (13), 4381-4383.

41. Kulis, J.; Bell, C. A.; Micallef, A. S.; Jia, Z. F.; Monteiro, M. J. *Macromolecules* **2009,** 42, (21), 8218-8227.

42. Kulis, J.; Bell, C. A.; Micallef, A. S.; Monteiro, M. J. *J Polym Sci Pol Chem* **2010,** 48, (10), 2214-2223.

43. Hoyle, C. E.; Lee, T. Y.; Roper, T. *J Polym Sci Pol Chem* **2004,** 42, (21), 5301-5338.

44. Campos, L. M.; Killops, K. L.; Sakai, R.; Paulusse, J. M. J.; Damiron, D.; Drockenmuller, E.; Messmore, B. W.; Hawker, C. J. *Macromolecules* **2008,** 41, (19), 7063-7070.

45. Dondoni, A. *Angew Chem Int Edit* **2008,** 47, (47), 8995-8997.

46. Hoyle, C. E.; Bowman, C. N. *Angew Chem Int Edit* **2010,** 49, (9), 1540-1573.

47. Hoyle, C. E.; Lowe, A. B.; Bowman, C. N. *Chem Soc Rev* **2010,** 39, (4), 1355-1387.

48. Kade, M. J.; Burke, D. J.; Hawker, C. J. *J Polym Sci Pol Chem* **2010,** 48, (4), 743-750.

49. Lowe, A. B. *Polym Chem-Uk* **2014,** 5, (17), 4820-4870.

50. Otsu, T.; Matsunaga, T.; Kuriyama, A.; Yoshioka, M. *Eur Polym J* **1989,** 25, (7-8), 643-650.

51. Matyjaszewski, K. *Abstr Pap Am Chem S* **2010,** 240.

52. Zhang, Y. Z.; Wang, Y.; Peng, C. H.; Zhong, M. J.; Zhu, W. P.; Konkolewicz, D.; Matyjaszewski, K. *Macromolecules* **2012,** 45, (1), 78-86.

53. Konkolewicz, D.; Wang, Y.; Zhong, M. J.; Krys, P.; Isse, A. A.; Gennaro, A.; Matyjaszewski, K. *Macromolecules* **2013,** 46, (22), 8749-8772.

54. Zhang, H. Q.; Klumperman, B.; Ming, W. H.; Fischer, H.; van der Linde, R. *Macromolecules* **2001,** 34, (18), 6169-6173.

55. Fischer, H. *J Polym Sci Pol Chem* **1999,** 37, (13), 1885-1901.

56. Whittaker, M. R.; Urbani, C. N.; Monteiro, M. J. *J Am Chem Soc* **2006,** 128, (35), 11360-11361.

57. Jia, Z. F.; Bell, C. A.; Monteiro, M. J. *Macromolecules* **2011,** 44, (7), 1747-1751.

58. Queffelec, J.; Gaynor, S. G.; Matyjaszewski, K. *Macromolecules* **2000,** 33, (23), 8629-8639.

59. Stockland, R. A.; Jordan, R. F. *J Am Chem Soc* **2000,** 122, (26), 6315-6316.

60. Guliashvili, T.; Percec, V. *J Polym Sci Pol Chem* **2007,** 45, (9), 1607-1618.

61. Rosen, B. M.; Percec, V. *J Polym Sci Pol Chem* **2008,** 46, (16), 5663-5697.

62. Lligadas, G.; Percec, V. *J Polym Sci Pol Chem* **2007,** 45, (20), 4684-4695.

63. Nicol, E.; Derouineau, T.; Puaud, F.; Zaitsev, A. *J Polym Sci Pol Chem* **2012,** 50, (18), 3885-3894.

64. Nguyen, N. H.; Kulis, J.; Sun, H. J.; Jia, Z. F.; Van Beusekom, B.; Levere, M. E.; Wilson, D. A.; Monteiro, M. J.; Percec, V. *Polym Chem-Uk* **2013,** 4, (1), 144-155.

65. Feng, C.; Shen, Z.; Gu, L. N.; Zhang, S.; Li, L. T.; Lu, G. L.; Huang, X. Y. *J Polym Sci Pol Chem* **2008,** 46, (16), 5638-5651.

66. Feng, C.; Shen, Z.; Li, Y. G.; Gu, L. N.; Zhang, Y. Q.; Lu, G. L.; Huang, X. Y. *J Polym Sci Pol Chem* **2009,** 47, (7), 1811-1824.

67. Nguyen, N. H.; Rosen, B. M.; Percec, V. *J Polym Sci Pol Chem* **2010,** 48, (8), 1752-1763.

68. Fleischmann, S.; Percec, V. *J Polym Sci Pol Chem* **2010,** 48, (10), 2251-2255.

69. Fleischmann, S.; Percec, V. *J Polym Sci Pol Chem* **2010,** 48, (21), 4884-4888.

70. Zhang, Q.; Wilson, P.; Li, Z. D.; McHale, R.; Godfrey, J.; Anastasaki, A.; Waldron, C.; Haddleton, D. M. *J Am Chem Soc* **2013,** 135, (19), 7355-7363.

71. Levere, M. E.; Nguyen, N. H.; Leng, X. F.; Percec, V. *Polym Chem-Uk* **2013,** 4, (5), 1635-1647.

72. Lligadas, G.; Rosen, B. M.; Monteiro, M. J.; Percec, V. *Macromolecules* **2008,** 41, (22), 8360-8364.

73. Rademacher, J. T.; Baum, R.; Pallack, M. E.; Brittain, W. J.; Simonsick, W. J. *Macromolecules* **2000,** 33, (2), 284-288.

74. Teodorescu, M.; Matyjaszewski, K. *Macromolecules* **1999,** 32, (15), 4826-4831.

75. Ding, S. J.; Radosz, M.; Shen, Y. Q. *Macromol Rapid Comm* **2004,** 25, (5), 632-636.

76. Konkolewicz, D.; Wang, Y.; Krys, P.; Zhong, M. J.; Isse, A. A.; Gennaro, A.; Matyjaszewski, K. *Polym Chem-Uk* **2014,** 5, (15), 4396-4417.

77. Hua, D. B.; Ge, X. P.; Bai, R. K.; Lu, W. Q.; Pan, C. Y. *Polymer* **2005,** 46, (26), 12696-12702.

78. Salami-Kalajahi, M.; Haddadi-Asl, V.; Ganjeh-Anzabi, P.; Najafi, M. *Iran Polym J* **2011,** 20, (6), 459-478.

79. Zhou, N. C.; Zhu, J.; Zhang, Z. B.; Zhu, X. L. *E-Polymers* **2007**.

80. Johnson, I. J.; Khosravi, E.; Musa, O. M.; Simnett, R. E.; Eissa, A. M. *J Polym Sci Pol Chem* **2015,** 53, (6), 775-786.

81. Mayadunne, R. T. A.; Rizzardo, E.; Chiefari, J.; Chong, Y. K.; Moad, G.; Thang, S. H. *Macromolecules* **1999,** 32, (21), 6977-6980.

82. Schilli, C.; Lanzendorfer, M. G.; Muller, A. H. E. *Macromolecules* **2002,** 35, (18), 6819-6827.

83. Malepu, V.; Petruczok, C. D.; TuTrinh, T.; Zhang, T. X.; Thopasridharan, M.; Shipp, D. A. *Controlled/Living Radical Polymerization: Progress in Raft, Dt, Nmp & Omrp* **2009,** 1024, 37-47.

84. Mayadunne, R. T. A.; Rizzardo, E.; Chiefari, J.; Krstina, J.; Moad, G.; Postma, A.; Thang, S. H. *Macromolecules* **2000,** 33, (2), 243-245.

85. Lai, J. T.; Filla, D.; Shea, R. *Macromolecules* **2002,** 35, (18), 6754-6756.

86. Wang, R.; McCormick, C. L.; Lowe, A. B. *Macromolecules* **2005,** 38, (23), 9518-9525.

87. Rotzoll, R.; Nguyen, D. H.; Vana, P. *Macromol Symp* **2008,** 275, 1-12.

88. Fu, J. W.; Cheng, Z. P.; Zhou, N. C.; Zhu, J.; Zhang, W.; Zhu, X. L. *Polymer* **2008,** 49, (25), 5431-5438.

89. Ohno, K.; Ma, Y.; Huang, Y.; Mori, C.; Yahata, Y.; Tsujii, Y.; Maschmeyer, T.; Moraes, J.; Perrier, S. *Macromolecules* **2011,** 44, (22), 8944-8953.

90. Ponnusamy, K.; Babu, R. P.; Dhamodharan, R. *J Polym Sci Pol Chem* **2013,** 51, (5), 1066-1078.

91. Keddie, D. J.; Guerrero-Sanchez, C.; Moad, G. *Polym Chem-Uk* **2013,** 4, (12), 3591-3601.

92. Theis, A.; Feldermann, A.; Charton, N.; Davis, T. P.; Stenzel, M. H.; Barner-Kowollik, C. *Polymer* **2005,** 46, (18), 6797-6809.

93. Zhang, Q. H.; Wang, Q. Y.; Luo, Z. H.; Zhan, X. L.; Chen, F. Q. *Polym Eng Sci* **2009,** 49, (9), 1818-1824.

94. Huang, Z. C.; Peng, Y.; Chen, H. B.; Xue, Q.; Li, H. M. *Des Monomers Polym* **2014,** 17, (7), 601-609.

95. Gao, J.; Luo, Y. W.; Wang, R.; Zhang, X. J.; Li, B. G.; Zhu, S. P. *Polymer* **2009,** 50, (3), 802-809.

96. Moad, G.; Rizzardo, E.; Thang, S. H. *Aust J Chem* **2009,** 62, (11), 1402-1472.

97. Moad, G.; Rizzardo, E.; Thang, S. H. *Polymer* **2008,** 49, (5), 1079-1131.

98. Butte, A.; Peklak, A. D.; Storti, G.; Morbidelli, M. *Macromol Symp* **2007,** 248, 168-181.

99. Ji, J.; Jia, L.; Yan, L. F.; Bangal, P. R. *J Macromol Sci A* **2010,** 47, (5), 445-451.

100. Shi, X. F.; Zhou, W.; Qiu, Q.; An, Z. S. *Chem Commun* **2012,** 48, (59), 7389-7391.

101. Yang, L.; Sun, P.; Qi, D. M.; Shen, Y. F. *Acta Polym Sin* **2014**, (3), 316-325.

102. Velasquez, E.; Rieger, J.; Stoffelbach, F.; Charleux, B.; D'Agosto, F.; Lansalot, M.; Dufils, P. E.; Vinas, J. *Polymer* **2013,** 54, (24), 6547-6554.

103. Smulders, W.; Gilbert, R. G.; Monteiro, M. J. *Macromolecules* **2003,** 36, (12), 4309-4318.

104. Monteiro, M. J.; Charleux, B. *Chemistry and Technology of Emulsion Polymerisation* **2005**, 111-139.

105. Urbani, C. N.; Monteiro, M. J. *Aust J Chem* **2009,** 62, (11), 1528-1532.

106. Jia, Z. F.; Bobrin, V. A.; Truong, N. P.; Gillard, M.; Monteiro, M. J. *J Am Chem Soc* **2014,** 136, (16), 5824-5827.

107. Pepels, M. P. F.; Holdsworth, C. I.; Pascual, S.; Monteiro, M. J. *Macromolecules* **2010,** 43, (18), 7565-7576.

108. Zeng, J. G.; Shi, K. Y.; Zhang, Y. Y.; Sun, X. H.; Deng, L.; Guo, X. Z.; Du, Z. J.; Zhang, B. *J Colloid Interf Sci* **2008,** 322, (2), 654-659.

109. Lowe, A. B.; McCormick, C. L. *Prog Polym Sci* **2007,** 32, (3), 283-351.

110. Shipp, D. A. *J Macromol Sci-Pol R* **2005,** C45, (2), 171-194.

111. Moad, G.; Rizzardo, E.; Thang, S. H. *Aust J Chem* **2005,** 58, (6), 379-410.

112. Tobita, H. *Macromol React Eng* **2008,** 2, (5), 371-381.

113. Qin, J.; Zhang, L. F.; Jiang, H. J.; Zhu, J.; Zhang, Z. B.; Zhang, W.; Zhou, N. C.; Cheng, Z. P.; Zhu, X. L. *Chem-Eur J* **2012,** 18, (19), 6015-6021.

114. Johnston-Hall, G.; Monteiro, M. J. *Controlled/Living Radical Polymerization: Progress in Raft, Dt, Nmp & Omrp* **2009,** 1024, 19-35.

115. Gregory, A.; Stenzel, M. H. *Prog Polym Sci* **2012,** 37, (1), 38-105.

116. Barner, L.; Davis, T. P.; Stenzel, M. H.; Barner-Kowollik, C. *Macromol Rapid Comm* **2007,** 28, (5), 539-559.

117. Barner, L.; Barner-Kowollik, C.; Davis, T. P.; Stenzel, M. H. *Aust J Chem* **2004,** 57, (1), 19-24.

118. Hayashi, S.; Adachi, K.; Tezuka, Y. *Chem Lett* **2007,** 36, (8), 982-983.

119. Lonsdale, D. E.; Monteiro, M. J. *Chem Commun* **2010,** 46, (42), 7945-7947.

120. Wu, Y. S.; Wang, Q. *J Polym Sci Pol Chem* **2010,** 48, (11), 2425-2429.

121. Baba, E.; Honda, S.; Yamamoto, T.; Tezuka, Y. *Polym Chem-Uk* **2012,** 3, (7), 1903-1909.

122. Chen, H. J.; Yan, T.; Shi, X. H.; Yu, R. W. *J Polym Res* **2012,** 19, (10).

123. Hossain, M. D.; Valade, D.; Jia, Z. F.; Monteiro, M. J. *Polym Chem-Uk* **2012,** 3, (10), 2986-2995.

124. Lu, D. R.; Jia, Z. F.; Monteiro, M. J. *Polym Chem-Uk* **2013,** 4, (6), 2080-2089.

125. Hossain, M. D.; Jia, Z. F.; Monteiro, M. J. *Macromolecules* **2014,** 47, (15), 4955-4970.

126. Deng, G. H.; Ma, D. Y.; Xu, Z. Z. *Eur Polym J* **2007,** 43, (4), 1179-1187.

127. Dong, Y. Q.; Dong, B. T.; Du, F. S.; Meng, J. Q.; Li, Z. C. *Polymer* **2009,** 50, (1), 125-132.

128. Yuan, Y. Y.; Wang, Y. C.; Du, J. Z.; Wang, J. *Macromolecules* **2008,** 41, (22), 8620-8625.

129. Iskin, B.; Yilmaz, G.; Yagci, Y. *Polym Chem-Uk* **2011,** 2, (12), 2865-2871.

130. Bai, Y.; Fan, X. D.; Tian, W.; Yao, H.; Fan, W. W.; Liu, T. T.; Dang, J.; Zhu, X. Z. *Acta Polym Sin* **2014**, (6), 851-859.

131. Altintas, O.; Schulze-Suenninghausen, D.; Luy, B.; Barner-Kowollik, C. *Eur Polym J* **2015,** 62, 409-417.

132. Alizadeh, R.; Ghaemy, M. *Polymer* **2015,** 66, 179-191.

133. Lee, J. W.; Kim, J. H.; Kim, B. K.; Shin, W. S.; Jin, S. H. *Tetrahedron* **2006,** 62, (5), 894-900.

134. Urbani, C. N.; Bell, C. A.; Lonsdale, D.; Whittaker, M. R.; Monteiro, M. J. *Macromolecules* **2008,** 41, (1), 76-86.

135. Franc, G.; Kakkar, A. *Chem Commun* **2008**, (42), 5267-5276.

136. Skwarczynski, M.; Zaman, M.; Urbani, C. N.; Lin, I. C.; Jia, Z. F.; Batzloff, M. R.; Good, M. F.; Monteiro, M. F.; Toth, I. *Angew Chem Int Edit* **2010,** 49, (33), 5742-5745.

137. Antoni, P.; Robb, M. J.; Campos, L.; Montanez, M.; Hult, A.; Malmstrom, E.; Malkoch, M.; Hawker, C. J. *Macromolecules* **2010,** 43, (16), 6625-6631.

138. Bell, C. A.; Jia, Z. F.; Kulis, J.; Monteiro, M. J. *Macromolecules* **2011,** 44, (12), 4814-4827.

139. Killops, K. L.; Campos, L. M.; Hawker, C. J. *J Am Chem Soc* **2008,** 130, (15), 5062-+.

140. Boyer, C.; Granville, A.; Davis, T. P.; Bulmus, V. *J Polym Sci Pol Chem* **2009,** 47, (15), 3773-3794.

141. Chan, J. W.; Hoyle, C. E.; Lowe, A. B.; Bowman, M. *Macromolecules* **2010,** 43, (15), 6381-6388.

142. Li, G. Z.; Randev, R. K.; Soeriyadi, A. H.; Rees, G.; Boyer, C.; Tong, Z.; Davis, T. P.; Becer, C. R.; Haddleton, D. M. *Polym Chem-Uk* **2010,** 1, (8), 1196-1204.

143. Willcock, H.; O'Reilly, R. K. *Polym Chem-Uk* **2010,** 1, (2), 149-157.

144. Li, M.; De, P.; Li, H. M.; Sumerlin, B. S. *Polym Chem-Uk* **2010,** 1, (6), 854-859.

145. Mespouille, L.; Coulembier, O.; Paneva, D.; Degee, P.; Rashkov, I.; Dubois, P. *J Polym Sci Pol Chem* **2008,** 46, (15), 4997-5013.

146. Bock, V. D.; Hiemstra, H.; van Maarseveen, J. H. *Eur J Org Chem* **2006**, (1), 51-68.

147. Matyjaszewski, K.; Woodworth, B. E.; Zhang, X.; Gaynor, S. G.; Metzner, Z. *Macromolecules* **1998,** 31, (17), 5955-5957.

148. Fu, Q.; Lin, W. C.; Huang, J. L. *Macromolecules* **2008,** 41, (7), 2381-2387.

149. Liu, C.; Pan, M. G.; Zhang, Y.; Huang, J. L. *J Polym Sci Pol Chem* **2008,** 46, (20), 6754-6761.

150. Jing, R. K.; Wang, G. W.; Huang, J. L. *J Polym Sci Pol Chem* **2010,** 48, (23), 5430-5438.

151. Kulis, J.; Jia, Z. F.; Monteiro, M. J. *Macromolecules* **2012,** 45, (15), 5956-5966.

152. Jia, Z. F.; Lonsdale, D. E.; Kulis, J.; Monteiro, M. J. *Acs Macro Lett* **2012,** 1, (6), 780-783.

153. Tomalia, D. A.; Frechet, J. M. *Prog Polym Sci* **2005,** 30, (3-4), 217-219.

154. Tomalia, D. A. *Prog Polym Sci* **2005,** 30, (3-4), 294-324.

155. Fischer, M.; Vogtle, F. *Angew Chem Int Edit* **1999,** 38, (7), 885-905.

156. Mourey, T. H.; Turner, S. R.; Rubinstein, M.; Frechet, J. M. J.; Hawker, C. J.; Wooley, K. L. *Macromolecules* **1992,** 25, (9), 2401-2406.

157. Jeong, M.; Mackay, M. E.; Vestberg, R.; Hawker, C. J. *Macromolecules* **2001,** 34, (14), 4927-4936.

158. Wooley, K. L.; Hawker, C. J.; Pochan, J. M.; Frechet, J. M. J. *Macromolecules* **1993,** 26, (7), 1514-1519.

159. Gupta, U.; Agashe, H. B.; Asthana, A.; Jain, N. K. *Biomacromolecules* **2006,** 7, (3), 649-658.

160. Uppuluri, S.; Keinath, S. E.; Tomalia, D. A.; Dvornic, P. R. *Macromolecules* **1998,** 31, (14), 4498-4510.

161. Chai, M. H.; Niu, Y. H.; Youngs, W. J.; Rinaldi, P. L. *J Am Chem Soc* **2001,** 123, (20), 4670-4678.

162. Menjoge, A. R.; Kannan, R. M.; Tomalia, D. A. *Drug Discov Today* **2010,** 15, (5-6), 171-185.

163. Bosman, A. W.; Janssen, H. M.; Meijer, E. W. *Chem Rev* **1999,** 99, (7), 1665-1688.

164. Sowinska, M.; Urbanczyk-Lipkowska, Z. *New J Chem* **2014,** 38, (6), 2168-2203.

165. Hourani, R.; Kakkar, A. *Macromol Rapid Comm* **2010,** 31, (11), 947-974.

166. Tomalia, D. A.; Baker, H.; Dewald, J.; Hall, M.; Kallos, G.; Martin, S.; Roeck, J.; Ryder, J.; Smith, P. *Polym J* **1985,** 17, (1), 117-132.

167. Hawker, C. J.; Frechet, J. M. J. *J Am Chem Soc* **1990,** 112, (21), 7638-7647.

168. Worner, C.; Mulhaupt, R. *Angew Chem Int Edit* **1993,** 32, (9), 1306-1308.

169. Debrabander-van den Berg, E. M. M.; Meijer, E. W. *Angew Chem Int Edit* **1993,** 32, (9), 1308-1311.

170. Brauge, L.; Magro, G.; Caminade, A. M.; Majoral, J. P. *J Am Chem Soc* **2001,** 123, (27), 6698-6699.

171. Jia, Z. F.; Bell, C. A.; Monteiro, M. J. *Chem Commun* **2011,** 47, (14), 4165-4167.

172. Angell, Y. L.; Burgess, K. *Chem Soc Rev* **2007,** 36, (10), 1674-1689.

173. Avan, I.; Hall, C. D.; Katritzky, A. R. *Chem Soc Rev* **2014,** 43, (10), 3575-3594.

174. Vagner, J.; Qu, H. C.; Hruby, V. J. *Curr Opin Chem Biol* **2008,** 12, (3), 292-296.

175. Vlieghe, P.; Lisowski, V.; Martinez, J.; Khrestchatisky, M. *Drug Discov Today* **2010,** 15, (1-2), 40-56.

176. Ahn, J. M.; Boyle, N. A.; MacDonald, M. T.; Janda, K. D. *Mini-Rev Med Chem* **2002,** 2, (5), 463-473.

177. White, C. J.; Yudin, A. K. *Nat Chem* **2011,** 3, (7), 509-524.

178. Marsault, E.; Peterson, M. L. *J Med Chem* **2011,** 54, (7), 1961-2004.

179. Moure, A.; Sanclimens, G.; Bujons, J.; Masip, I.; Alvarez-Larena, A.; Perez-Paya, E.; Alfonso, I.; Messeguer, A. *Chem-Eur J* **2011,** 17, (28), 7927-7939.

180. Sharma, G. V. M.; Babu, B. S.; Ramakrishna, K. V. S.; Nagendar, P.; Kunwar, A. C.; Schramm, P.; Baldauf, C.; Hofmann, H. J. *Chem-Eur J* **2009,** 15, (22), 5552-5566.

181. Gademann, K.; Hane, A.; Rueping, M.; Jaun, B.; Seebach, D. *Angew Chem Int Edit* **2003,** 42, (13), 1534-1537.

182. Patgiri, A.; Jochim, A. L.; Arora, P. S. *Accounts Chem Res* **2008,** 41, (10), 1289-1300.

183. Gierasch, L. M.; Deber, C. M.; Madison, V.; Niu, C. H.; Blout, E. R. *Biochemistry-Us* **1981,** 20, (16), 4730-4738.

184. Patch, J. A.; Barron, A. E. *Curr Opin Chem Biol* **2002,** 6, (6), 872-877.

185. Huang, F.; Nau, W. M. *Angew Chem Int Edit* **2003,** 42, (20), 2269-2272.

186. Kojima, C.; Fukada, H.; Inui, T. *Polym J* **2013,** 45, (3), 339-345.

187. Majoros, I. J.; Myc, A.; Thomas, T.; Mehta, C. B.; Baker, J. R. *Biomacromolecules* **2006,** 7, (2), 572-579.

188. Le, T.; Cheah, W. C.; Wood, K.; Black, D. S.; Willcox, M. D.; Kumar, N. *Tetrahedron Lett* **2011,** 52, (28), 3645-3647.

189. Roy, R.; Baek, M. G.; Rittenhouse-Olson, K. *J Am Chem Soc* **2001,** 123, (9), 1809-1816.

190. Bracci, L.; Falciani, C.; Lelli, B.; Lozzi, L.; Runci, Y.; Pini, A.; De Montis, M. G.; Tagliamonte, A.; Neri, P. *J Biol Chem* **2003,** 278, (47), 46590-46595.

191. Waite, C. L.; Roth, C. M. *Bioconjugate Chem* **2009,** 20, (10), 1908-1916.

192. Yang, X.; Shang, H.; Ding, C. M.; Li, J. S. *Polym Chem-Uk* **2015,** 6, (5), 668-680.

193. Jiang, Y. H.; Emau, P.; Cairns, J. S.; Flanary, L.; Morton, W. R.; McCarthy, T. D.; Tsai, C. C. *Aids Res Hum Retrov* **2005,** 21, (3), 207-213.

194. Bourne, N.; Stanberry, L. R.; Kern, E. R.; Holan, G.; Matthews, B.; Bernstein, D. I. *Antimicrob Agents Ch* **2000,** 44, (9), 2471-2474.

195. Jackson, C. L.; Chanzy, H. D.; Booy, F. P.; Drake, B. J.; Tomalia, D. A.; Bauer, B. J.; Amis, E. J. *Macromolecules* **1998,** 31, (18), 6259-6265.

Chapter 2

Synthesis of alkyne functional cyclic polymers by one-pot thiol-ene cyclization

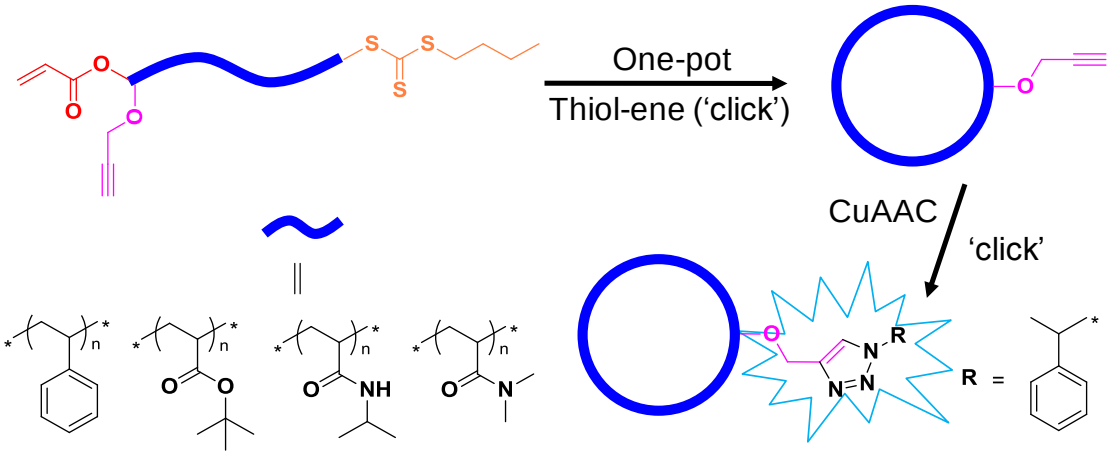

In this chapter, we demonstrate the cyclization of polymers, made by reversible addition-fragmentation chain transfer (RAFT), using a one-pot thiol-ene reaction. Hexylamine converted the RAFT end-group to a free thiol which could then rapidly react with the acrylate on the other chain-end of the polymer to form a cyclic polymer. This procedure allowed a wide range of polymers such as polystyrene (PSTY), poly(tert-butyl acrylate) (PtBA), poly(*N*-isopropylacrylamide) (PNIPAM) and poly(*N*,*N*-dimethylacrylamide) (PDMA) to be cyclized with close to 80 % cyclic formation with an alkyne functional group. Attempts to use the thio-bromo reaction to cyclize PSTY were not as successful as the thiol-ene cyclization reaction produced less than 25 % cyclic.

2.1 Introduction

Cyclic polymers have unique properties due to their "endless" and compact topology compared to their linear counterparts.[1, 2] Considerable effort has been made in developing highly efficient synthetic methods for the preparation of macrocycles.[3-11] Renewed attention in macrocyclics has stemmed from the ability of 'living' radical polymerization (LRP) to control not only the molecular weight and polymer chemical composition but to introduce various functional groups onto monodisperse polymer chain-ends.[12-15] The diversity and reactivity of in-chain functionalities consequently afford intramolecular end-to-end cyclization through highly efficient coupling reactions.[16] The ring-closure approach to

produce monodisperse monocyclic PSTY has been reported using the combination of atom transfer radical polymerization (ATRP) and copper catalyzed azide-alkyne cycloaddition (CuAAC) 'click' reaction[17] and many other combinations of LRP and robust coupling reactions.[9, 11, 18-24]. According to the Jacobson-Stockmayer theory,[25] highly efficient intramolecular ring-closure should be carried out under high dilution or feed conditions, ensuring that intermolecular coupling is negligible.[26-28] The success of the feed reactions relies on extremely rapid coupling reactions. Thus, in the case of the CuAAC coupling reaction very high levels of copper are required to achieve fast coupling rates, making purification of the cyclic polymer difficult. Copper-free 'click' reactions will make the post-reaction purification much easier and allow scale-up of such monodisperse polymer topologies.[18, 22]

Among the tool box of click chemistry,[16, 29] thiol-ene Michael addition has been widely used in combination with reversible addition-fragmentation chain-transfer (RAFT) polymerization to either construct complex polymer architectures or convert the RAFT moiety on the polymer chain to a desired functional group by a simple cascade aminolysis/thiol-ene Michael addition sequence.[30-34] Although thiol-ene chemistry is very versatile, there is only one report using the thiol-ene Michael addition to form cyclic polymer through tethering homodifuntional linear precursor together with a small molecular weight linker.[35] An advantage of RAFT over ATRP is the production of a wider range of water soluble polymers that will provide functional cyclic hydrophilic building blocks in the construction of more complex cyclic architectures.[23, 36-39]

In this work, the cyclization of functional polymers made directly from RAFT polymerization was carried out by using two known coupling reactions: (i) thiol-ene, and (ii) thio-bromo reactions. We designed a heterodifunctional trithiocarbonate RAFT agent to mediate RAFT polymerization of styrene (STY), *t*-butyl acrylate (^{t}BA), *N*-isopropylacrylamide (NIPAm) and *N*,*N*-dimethylacrylamide (DMA), followed by a one-step post-polymerization modification to introduce either an activated acrylate or bromine functionality on one chain-end of the polymer (see Scheme 2.1). The polymer was cyclized in one-pot using a hexylamine-catalyzed cascade aminolysis and thiol-ene Michael or thio-bromo addition sequence at 25 ^{o}C. The percent alkyne functionality on the cyclic polymer was determined by reacting a small molecule azide using the CuAAC coupling reaction.

2.1.1 Aim of Chapter

The aim of the work is to develop a new strategy to make functional cyclic polymers, especially water-soluble polymers (e.g. PNIPAM and PDMA), via combination of RAFT polymerization and base catalysed thiol-based coupling reaction (e.g, thiol-ene and thiolbromo).

Scheme 2.1 Synthetic route of functional macrocycles

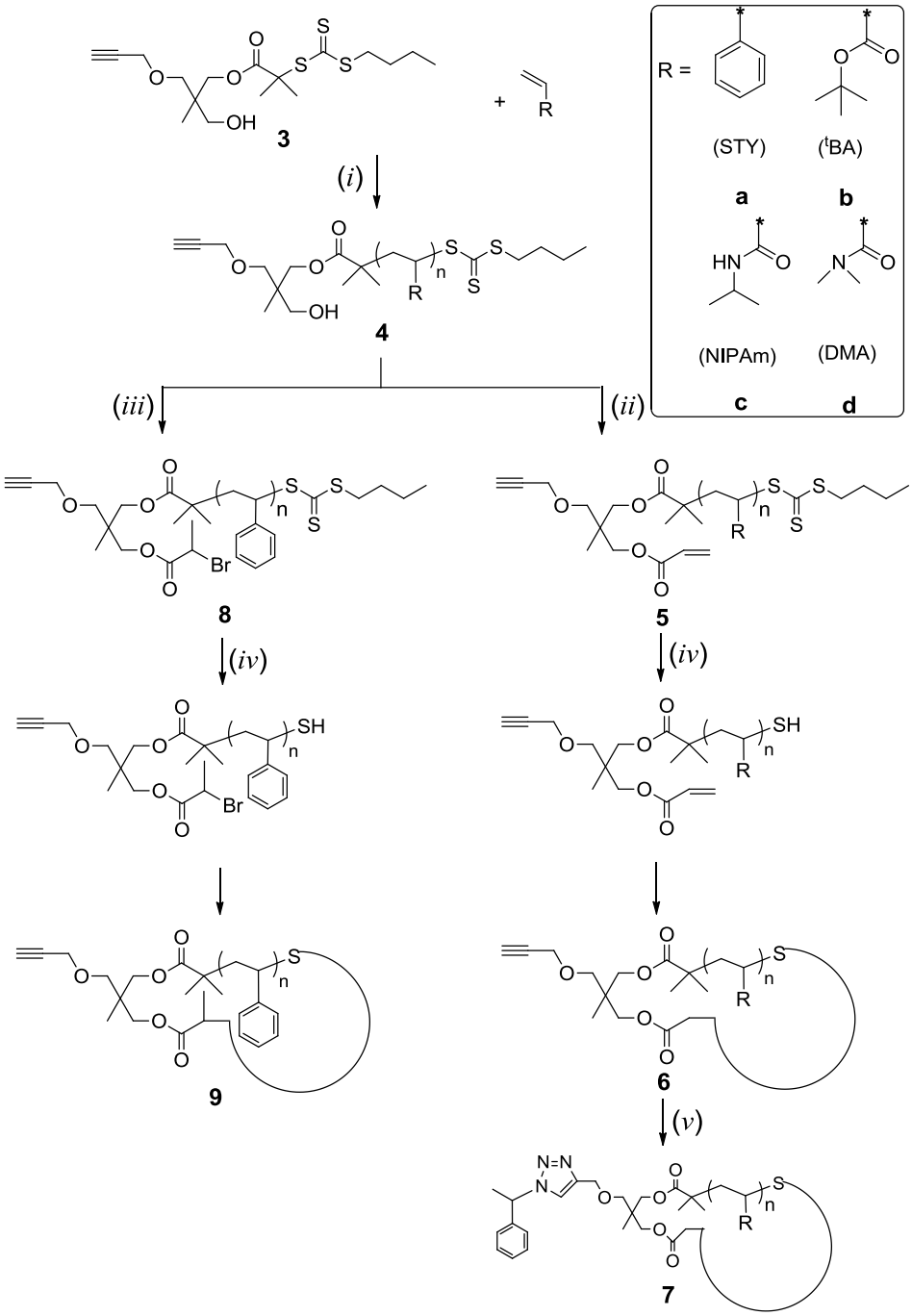

(*i*) Polymerization of monomers initiated with AIBN: STY in bulk at 80 °C for 5 h; ^{t}BA in acetone at 60 °C for 8 h; NIPAm in DMSO at 60 °C for 15 h; and DMA in DMSO at 60 °C for 6 h. (*ii*) Acryloyl chloride, TEA, DCM, 0 °C - R.T., 48 h. (*iii*) 2-Bromopropionyl bromide, TEA, DCM, 0 °C - R.T., 48 h. (*iv*) One-pot, hexylamine, TCEP, DMF, R.T., 2 h or 12 h; (*v*) (1-Azidoethyl)benzene , CuBr, PMDETA, toluene or DMF, R.T., 2 h.

2.2 Experimental

2.2.1 Materials

The following reagents and solvents were used as received: silica gel 60 (230-400mesh) ATM (SDS), TLC plates (silica gel 60 F254), methanol (MeOH, HPLC grade), dichloromethane (DCM, Labscan, AR grade), diethyl ether (Et_2O, Pronalys, AR grade), tetrahydrofuran (THF, HPLC grade, Lichrosolv, 99.8 %), dimethyl sulfoxide (DMSO, Aldrich, 99.8 %), triethylamine (TEA, Fluka, purum), sodium hydride (Aldrich, 60 wt% in mineral oil), *N*,*N*′-dicyclohexylcarbodiimide (DCC, Aldrich, 99 %), 4-(dimethylamino)pyridine (DMAP, Aldrich, >99 %) propargyl bromide (Aldrich, 80 wt % in toluene), acryloyl chloride (Alfa Aesar, 96 %). *N*,*N*-Dimethylformamide (DMF, Aldrich, HPLC grade), Tris (2-carboxyethyl) phosphine hydrochloride (TCEP, Aldrich), hexylamine (Aldrich, 99 %), magnesium sulfate anhydrous ($MgSO_4$), Dowex® 50W X8-200 ion-exchange resin (Aldrich, 200-400 mesh) , *p*-toluenesulfonic acid monohydrate (*p*-TsOH, Aldrich, ≥98.5%), 1,1,1-tris(hydroxymethyl)ethane (Aldrich, 99 %), (1-bromomethyl)-benzene (Aldrich, 97%), 2-bromopropionyl bromide (Aldrich, 98 %), sodium azide (Aldrich, 99.5 %), acetone(repacked), ethyl acetate (repacked) and petroleum spirit (repacked, b.p 40-60 ^{o}C) were obtained from The University of Queensland Chemical Store and used as received. Styrene (Aldrich, 99 %) *tert*-Butyl acrylate (^{t}BA, Aldrich, HPLC grade) and N,N-dimethylacrylamide (DMA, Aldrich, HPLC grade) were purified from inhibitor by passage through a column of activated basic alumina (Aldrich, Brockmann I, standard grade, ~150 mesh, 58Å). *N*-isopropylacrylamide (NIPAm, Aldrich, 99 %) was purified twice by recrystallization in *n*-hexane and toluene (9:1, v:v).

2.2.2 Synthetic procedures

Scheme 2.2 Synthetic route of alkyne functional RAFT agent 3

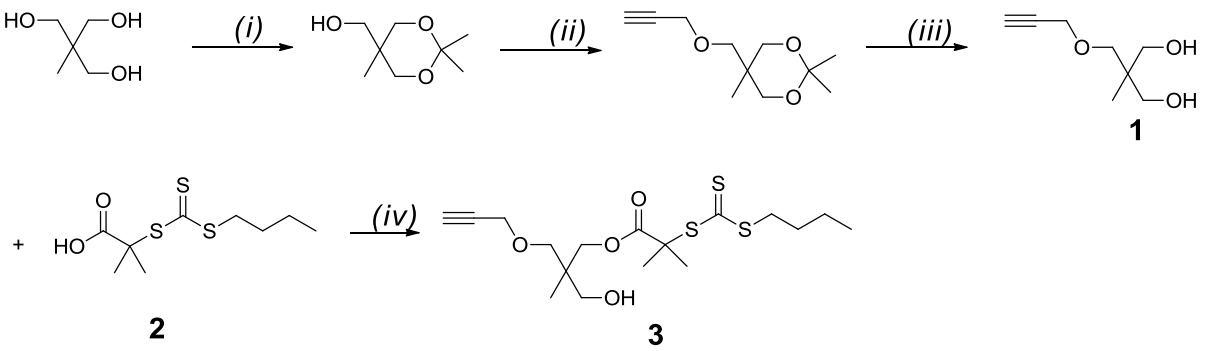

(*i*) Acetone, p-TsOH, RT,16 h; (*ii*) THF, NaH, propargyl bromide, -78 ^{o}C to R.T., 16 h; (*iii*) DOWEX, Methanol, R.T. 16 h; (*iv*) DCC, DMAP, DCM, 0^{o}C-R.T., 16 h.

2.2.2.1 Synthesis of α-hydroxyl- α'-alkyne heterofunctional RAFT agent 3

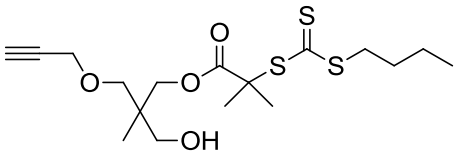

Propargyl diol 1 and RAFT acid 2 were synthesized according previous procedure.[23, 38]

Propargyl diol **1** (3.81 g, 2.41 x 10^{-2} mol), RAFT acid **2** (6.07 g, 7.65 x 10^{-2} mol), and DMAP (0.809 g, 6.63 x 10^{-3} mol) were dissolved in 100 mL dry DCM, the mixture was allowed to stir for 30 min, and then cooled into an ice-bath. To the above solution, the mixture of DCC (13.6 g, 6.63 x 10^{-2} mol) and 50 mL DCM was added dropwise in 30 min. The reaction was stirring for 15 h and warmed up to R.T. The reaction mixture was filtered to remove the solid, concentrated and applied under vacuum at R.T. The orange color crude product was purified by column chromatography with EtOAc/petroleum spirit (2/1, v/v) as eluent. The fraction with R_f as 0.45 was collected. The orange viscous liquid product **3** was obtained with the yield as 46.5 %.

^{1}H NMR ($CDCl_3$, 298K, 300 MHz): δ, ppm, 4.10 (t, 2H; *J*=2.43 Hz; -C*H*$_2$O-), 4.01 (d, 2H; *J*=2.40 Hz; HC≡C*H*$_2$-), 3.48 (s, 2H, -C*H*$_2$OH), 3.42(d, 2H; *J*=1.53 Hz; -OC*H*$_2$C-), 3.26 (t, 3H, *J*=7.40 Hz, -S*CH*$_2$CH$_2$-), 2.40 (t, 1H, *J*=2.39 Hz, *HC*≡CCH$_2$-),1.68 (d, *J*=2.04 Hz, *(CH*$_3$*)*$_2$C-), 1.62 (m, *J*=7.66 Hz, -CH$_2$*CH*$_2$CH$_2$-); 1.39 (m, *J*=7.26 Hz, -CH$_2$-*CH*$_2$-CH$_3$), 0.89

(3H, t, *J*=7.32 Hz, -$CH_2CH_2CH_3$), 0.88 (3H, s, -CCH_3). ^{13}C NMR ($CDCl_3$, 298K, 300MHz): 221.8, 172.9, 79.4, 74.6, 73.6, 68.4, 66.7, 58.7, 56.0, 40.1, 36.6, 29.9, 25.4, 17.0, 13.5.

2.2.2.2 Synthesis of α-hydroxyl- α'-alkyne RAFT polymer 4

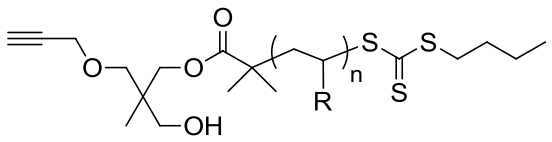

R= STY, ^{t}BA, NIPAm, DMA

For the synthesis of PSTY: styrene (9.324 mL, 8.12 x 10^{-2} mol), **3** (0.318 g, 8.12 x 10^{-4} mol), and AIBN (13.3 mg, 8.12 x 10^{-5} mol) were added into a 100 mL Schlenk flask. The mixture was deoxygenated by purging with argon for 40 min then heated at 80 ^{o}C for 5 h. The reaction was terminated by cooling to 0 ^{o}C and then exposed to air. The mixture was diluted with dichloromethane and precipitated in 10 folds excess of methanol and isolated by filtration. The dissolution and precipitation cycle was repeated three times. The polymer was dried under high vacuum for 48 h at room temperature to yield a yellow solid product **4a** (M_n=3980, PDI=1.08).

For the synthesis of P ^{t}BA: ^{t}BA (12.4 mL, 8.47 x 10^{-2} mol), **3** (0.641 g, 1.62 x 10^{-3} mol), AIBN (26.8 mg, 1.62 x 10^{-4} mol) and acetone (2.2 mL) were added into a 100mL Schlenk flask. The mixture was deoxygenated by purging with argon for 40 min then heated at 60 ^{o}C for 8 h. The reaction was terminated by cooling to 0 ^{o}C and exposure to air. The mixture was diluted with acetone and precipitated in a 10 fold excess a mixture of MeOH and water (v:v=1:1) and then isolated by filtration. The dissolution and precipitation cycle was repeated three times. The polymer was dried under high vacuum for 48 h at room temperature to yield a yellow solid product **4b** (M_n=4180, PDI=1.09).

For the synthesis of PNIPAm: NIPAm (6.0 g, 5.31 x 10^{-2} mol), **3** (0.46 g, 1.17 x 10^{-3} mol), and AIBN (19.2 mg, 1.17 x 10^{-4} mol) were dissolved in DMSO (12 mL). The mixture was deoxygenated by purging with argon for 40 min then heated at 60 ^{o}C for 15 h. The reaction was terminated by cooling to 0 ^{o}C and exposed to air. The mixture was dissolved in a large excess of DCM and twice extracted by distilled water. The organic phase was removed by reduce pressure, and the concentrated mixture was precipitated in 10 folds excess of Et_2O and then isolated by filtration. The dissolution and precipitation cycle was repeated two times.

The polymer was dried under high vacuum for 48 h at room temperature to give a solid yellow product **4c** (M_n=3540, PDI=1.13).

For the synthesis of PDMA: DMA (4.174 mL, 4.06 x 10^{-2} mol), **3** (0.318 g, 8.12 x10^{-4} mol), and AIBN (13.3 mg, 8.12 x 10^{-5} mol) were dissolved in DMSO (8.35 mL). The mixture was deoxygenated by purging with argon for 40 min then heated at 60 ^{o}C for 6 h. The reaction was terminated by cooling to 0 ^{o}C and exposed to air. The mixture was dissolved in a large excess of DCM and twice extracted by distilled water. The organic phase removed by reduce pressure, the concentrated mixture was precipitated in a 10 fold excess of Et_2O and then isolated by filtration. The dissolution and precipitation cycle was repeated two times. The polymer was dried under high vacuum for 48 h at room temperature to give a solid yellow product **4d** (M_n=3620, PDI=1.13).

2.2.2.3 Synthesis of α-acrylyl-α'-alkyne RAFT polymer 5

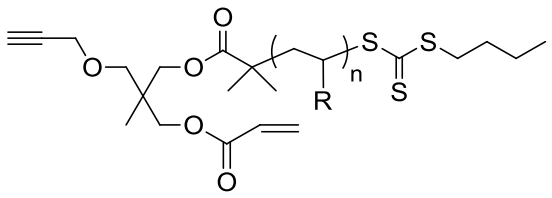

R= STY, ^{t}BA, NIPAm, DMA

4a (PSTY, 1 g, 2.51 x 10^{-4} mol) and TEA (0.524 mL, 3.76 x 10^{-3} mol) were dissolved in DCM (8 mL) and cooled into the ice bath. The mixture of DCM (8 mL) and acryloyl chloride (0.304 mL, 3.76 x 10^{-3} mol) was added drop-wise into the solution above within 30 min under argon atmosphere. The reaction was stirred for 48 h and warmed up to R.T. The reaction mixture was filtered to remove the solid, concentrated and precipitated in a 10 fold excess of MeOH and then isolated by filtration. The dissolution and precipitation cycle was repeated three times. The product was then dried at vacuum at R.T. and obtained light yellow solid **5a** (M_n=4140, PDI=1.07, M_p=4400).

For the acylation of **4b** (P^{t}BA), **4c** (PNIPAm), and **4d** (PDMA). The same mole ratio of reactants and procedure were used to synthesize corresponding **5b**, **5c**, and **5d**. The precipitation of **5b**, **5c**, and **5d** were carried out in a 10 fold excess of a mixture of MeOH and water (v:v=1:1), Et_2O, and Et_2O, respectively, yielding a light yellow solid **5b (**M_n=4260, PDI=1.09, M_p=4490**)**, **5c (**M_n=4010, PDI=1.06, M_p=4170**)**, and **5d (**M_n=3980, PDI=1.14, M_p=4280**)**,respectively.

2.2.2.4 Synthesis of alkyne functional cyclic polymer 6 by thiol-ene reaction

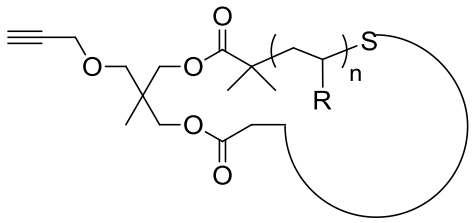

R= STY, ^{t}BA, NIPAm, DMA

Purified **6a** (5.0 mg, 1.21 x 10^{-6} mol) was dissolved in DMF (1 mL) and purging with argon for 5 min, then TCEP (1.03 mg, 3.63 x 10^{-6} mol) was added under positive argon flow. The mixture was allowed to bubble with argon for an additional 5 min. The hexylamine (19.9 µL, 1.51 x 10^{-4} mol) was also dissolved in DMF (1 mL) and purging with argon for 10 min. A hexylamine solution was then transferred into the PSTY solution by using a 1 mL syringe. The reaction was allowed to react for 2 h under an argon atmosphere at room temperature. The product was recovered by precipitation into a 10 fold excess of MeOH. The precipitation was repeated twice and then dried into the vacuum oven, giving a white solid.

The synthesis of **6b**, **6c**, and **6d** followed the same synthetic procedure of **6a** using the same mole ratio of reactants. The resulting products were precipitated in a 10 fold excess of a mixture of MeOH and water (v:v=1:1), Et_2O, and Et_2O, respectively, yielding a white solid **6b** (M_n=3550, PDI=1.11), **6c** (M_n=3050, PDI=1.15), and **6d** (M_n=3350, PDI=1.21), respectively.

Purification of polymers **6a**, **6b** and **6c** were conducted by preparative SEC and **6d** by fractionation precipitation in DCM/Et_2O mixture. The yield for **6a**, **6b**, **6c** and **6d** were 54 %, 51 %, 46 % and 61 %, respectively.

2.2.2.5 Synthesis of polymer 7

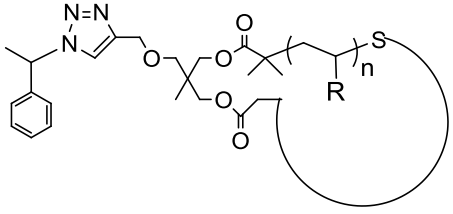

R= STY, ^{t}BA, NIPAm, DMA

6a (100 mg, 3.03 x 10^{-5} mol) and (1-azidoethyl)benzene (35.6 mg, 2.42 x 10^{-4} mol) were placed in a Schlenk tube and dissolved in a mixture of PMDETA (6.3 µL, 3.03 x 10^{-5} mol) and DMF (3 mL). Oxygen was removed from the solution by purging with argon for 15 min. Cu(I)Br (4.33 mg, 3.03 x 10^{-5} mol) was added under a positive argon flow and the reaction vessel was sealed and placed in an oil bath at 25 ^{o}C and stirred for up to 3 h. The mixture was diluted in DCM and passed through activated basic alumina. The solvent was removed under reduced pressure, and the residue was precipitated into a 10 fold excess of MeOH. The precipitation was repeated twice and then dried into the vacuum oven, giving a white solid **7a** (M_n=3390, PDI=1.10).

The synthesis of **7b**, **7c**, and **7d** followed the same synthetic procedure of **7a** using the same mole ratio of reactants. The resulting products were precipitated in a 10 fold excess of MeOH and water (v:v=1:1), Et_2O, and Et_2O, respectively, yielding a white solid **7b** (M_n=3340, PDI=1.16), **7c** (M_n=3030, PDI=1.11), and **7d** (M_n=3430, PDI=1.36), respectively.

2.2.2.6 Synthesis of α-bromo-α'-alkyne RAFT polymer 8

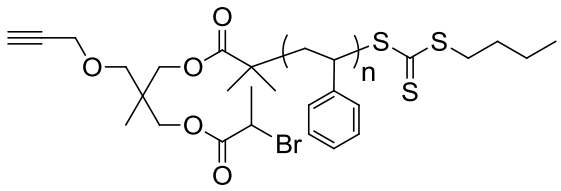

4a (1g, 2.51 x 10^{-4} mol) and TEA (0.524 mL, 3.76 x 10^{-3} mol) were dissolved in dry DCM (8 mL) and cooled into the ice bath. A mixture of DCM (8 mL) and 2-bromopropionyl bromide (0.392 mL, 3.76 x 10^{-3} mol) was added dropwise into the solution above in 30 min under an argon atmosphere. The reaction was kept stirring for 48 h and warmed up to R.T. The reaction content was filtered to remove the solid, concentrated and precipitated in a 10 fold excess of MeOH and then isolated by filtration. The dissolution and precipitation cycle was repeated three times. The product was then dried at vacuum at R.T. to give a light yellow solid **8** (M_n=4230, PDI=1.08, M_p=4460)

Scheme 2.3 Synthetic route of functional monocyclic PSTY by thiol-bromo cyclization.

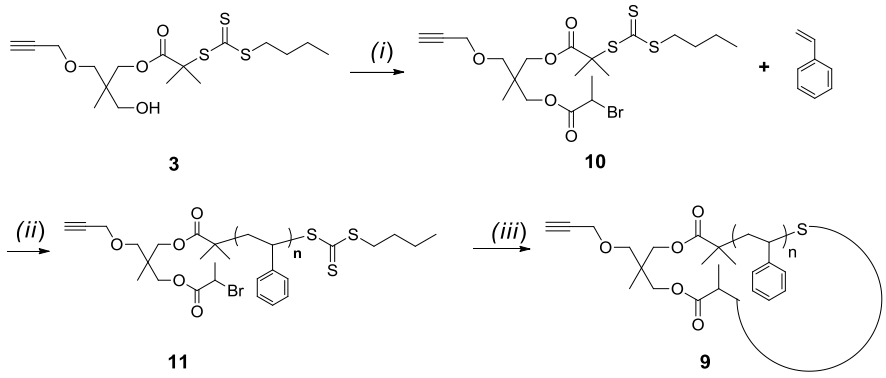

(*i*) 2-Bromopropionyl bromide, TEA, DCM, 0 ^{o}C - R.T., 6 h. (*ii*) AIBN, 80 ^{o}C, 6.5 h in bulk. (*iii*) One-pot, hexylamine, TCEP, DMF, R.T., 12 h.

2.2.2.7 Synthesis of α-hydroxyl- α'-bromo heterofunctional RAFT agent 10

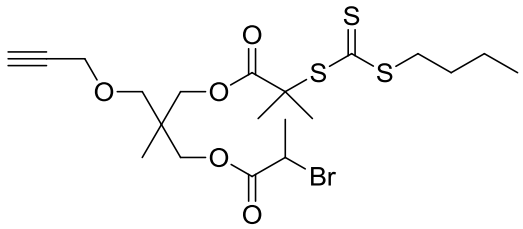

α-Hydroxyl-α'-alkyne heterofunctional RAFT agent **3** (2.0 g, 5.10 x 10^{-3} mol), and TEA (0.773 g, 7.65 x 10^{-3} mol) were dissolved in 50 mL dry DCM, the mixture was allowed to stir for 30 min, and then cooled into an ice-bath. To the above solution, the mixture of 2-bromopropionyl bromide (0.8 mL, 7.65 x 10^{-3} mol) and 50 mL DCM was added dropwise over 30 min. The reaction was stirred for 6 h and then warmed up to R.T. The reaction mixture was filtered to remove the solid, concentrated and dried under vacuum at R.T. The orange color crude product was purified by column chromatography with EtOAc/petroleum spirit (1/6, v/v) as eluent. The fraction with R_f as 0.65 was collected. The orange viscous liquid product **10** was obtained with the yield as 59.6 %.

^{1}H NMR ($CDCl_3$, 298K, 400 MHz): δ, ppm, 4.38 (q, 1H; *J*=2.43 Hz; -CO*CH*(CH_3)Br), 4.12 (t, 2H; *J*=2.40 Hz; -C*CH*$_2$OOC-), 4.04 (dd, 2H; *J*=11.16, 5.00 Hz; -C*CH*$_2$OOC-), 3.99 (d, 2H, HC≡C*CH*$_2$-), 3.42(d, 2H; *J*=1.60 Hz; -OC*H*$_2$C-), 3.28 (t, 3H, *J*=7.40 Hz, -S*CH*$_2$(CH_2)$_2$$CH_3$), 2.42 (t, 1H, *J*=2.38 Hz, *HC*≡CCH_2-), 1.83 (d, 3H; *J*=6.96 Hz; -

COCH(CH_3)Br), 1.65 (d, J=2.04 Hz, $(CH_3)_2$C(C=O)S-), 1.63 (m, J=7.56 Hz, -$CH_2CH_2CH_2$-); 1.41 (m, J=7.56 Hz, -$CH_2CH_2CH_3$), 1.02 (3H, s, CH_3C), 0.93 (3H, t, J=7.36 -$CH_2CH_2CH_3$). ^{13}C NMR ($CDCl_3$, 298K, 400MHz): 172.6, 169.8, 79.5, 74.5, 71.7, 67.7, 67.1, 58.6, 55.9, 40.0, 39.2, 36.6, 29.8, 25.3, 22.0, 21.6, 17.0, 13.6.

2.2.2.8 Synthesis of α-bromo-α'-alkyne RAFT polymer 11

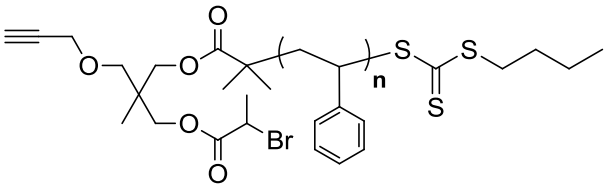

Styrene (9.324 mL, 8.12 x 10^{-2} mol), **10** (0.318 g, 8.12 x 10^{-4} mol), and AIBN (13.3 mg, 8.12 x 10^{-5} mol) were added into a 100 mL Schlenk flask. The mixture was deoxygenated by purging with argon for 40 min then heated at 80 ^{o}C for 6.5 h. The reaction was terminated by cooling to 0 ^{o}C and exposure to air. The mixture was diluted with dichloromethane and precipitated in 10 folds excess of methanol and then isolated by filtration. The dissolution and precipitation cycle was repeated three times. The polymer was dried under high vacuum for 48 h at room temperature to yield a yellow solid product **11** (M_n=4480, PDI=1.10, M_p=4730).

2.2.2.9 Synthesis of alkyne functional cyclic polymer 9 by thiol-bromo reaction

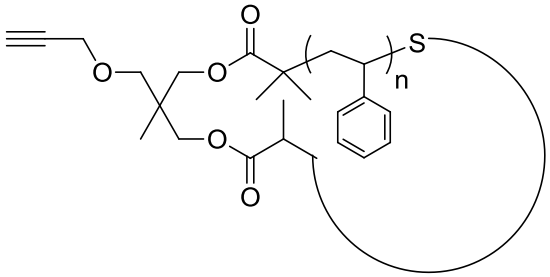

5 mg of **8** (see experiments 22 to 26, Table 2.3) or **11** (see to experiments 27 to 31, Table 2.3) (5.0 mg, 1.12 x 10^{-6} mol) was dissolved in DMF (1 mL) and purged argon for 5 min, then TCEP (1.00 mg, 3.36 x 10^{-6} mol) was added under positive argon flow. The mixture was allowed to bubble argon for additional 5 min. The hexylamine (from 30 equiv. to 200 equiv.) was also dissolved in DMF (1 mL) and purged argon for 10 min. A hexylamine solution was then transferred into the PSTY solution by using a 1 mL syringe. The reaction was allowed to

react for 12 h under an argon atmosphere at room temperature. The product was recovered by precipitation into a 10 fold excess of MeOH. The precipitation was repeated twice and then dried into the vacuum oven, giving a white solid **9**.

2.2.3 Analytical Methodologies

Size Exclusion Chromatography (RI-SEC)

For PSTY, PNIPAm, and P^{t}BA, the dried polymer was dissolved in tetrahydrofuran (THF) to a concentration of 1 mg mL^{-1} and then filtered through a 0.45 μm PTFE syringe filter. Analysis of the molecular weight distributions of the polymers was accomplished using a Waters 2695 separations module, fitted with a Waters 410 refractive index detector maintained at 35 $^{\circ}$C, a Waters 996 photodiode array detector, and two Ultrastyragel linear columns (7.8 x 300 mm) arranged in series. These columns were maintained at 40 ^{o}C for all analyses and are capable of separating polymers in the molecular weight range of 500 to 4 million g mol^{-1} with high resolution. All samples were eluted at a flow rate of 1.0 mL min^{-1}. Calibration was performed using narrow molecular weight PSTY standards (PDI $\leq$ 1.1) ranging from 500 to 2 million g mol^{-1}. Data acquisition was performed using Empower software, and molecular weights were calculated relative to polystyrene standards.

For PDMA, Polymer Laboratories GPC50 Plus equipped with differential refractive index detector was used. HPLC grade *N*,*N*-dimethylacetamide (DMAc, containing 0.03 wt % LiCl) was used as the eluent at a flow rate of 1.0 mL min^{-1}. Separations were achieved using two PL Gel Mixed B (7.8 x 300 mm) SEC columns connected in series and held at a constant temperature of 50 ^{o}C. Calibration was performed using a 2 mg mL^{-1} PSTY standard. Samples were freshly prepared in DMAc+0.03 wt % LiCl and passed through a 0.45 μm PTFE syringe filter prior to injection.

Preparative Size Exclusion Chromatography (Prep-SEC).

Polymer **6a**, **6b** and **6c** were purified using a Varian Pro-Star preparative SEC system equipped with a manual injector, differential refractive index detector, and single wave-length ultra-violet visible detector. Flow rate was maintained 10 mL min^{-1} and HPLC grade tetrahydrofuran was used as the eluent. Separations were achieved using a PLgel 10 μm 1 x 10^{3} Å, 300 mm x 25 mm preparative SEC column held at 25 °C. The dried crude polymer was dissolved in THF at 100 mg mL-1 concentration and filtered through a 0.45 μm PTFE syringe filter prior to inject. Different fractions were collected manually, and the composition

of each was determined using the Polymer Laboratories GPC50 Plus equipped with triple detection as described above.

Matrix Assisted Laser Desorption Ionization – Time of Flight (MALDI-ToF) Mass Spectrometry.

MALDI-ToF MS mass spectra were obtained using a Bruker Autoflex III Smartbeam TOF/TOF 200. All spectra were recorded in reflectron mode. For PSTY polymers *Trans*-2-(3-(4-*tert*-butylphenyl)-2-methyl-propenylidene) malononitrile (DCTB; 20 mg mL^{-1} in THF) was used as the matrix and $Ag(CF_3COO)$ (1 mg mL^{-1} in THF) as the cation source. For P^tBA, PNIPAm and PDMA polymers *Trans*-2-(3-(4-*tert*-butylphenyl)-2-methyl-propenylidene) malononitrile (DCTB; 20 mg mL^{-1} in THF) was used as the matrix and $Na(CF_3COO)$ (1 mg mL^{-1} in THF) as the cation source. All samples were prepared by spotting 1µL of the mixture of the matrix (20 µL), salt (2 µL) and polymer (20 µL, 1 mg mL^{-1} in THF) solutions on the target plate.

^{1}H Nuclear Magnetic Resonance (NMR).

All NMR spectra were recorded on a Bruker DRX 300, 400 or 500 MHz spectrometer at 25 ^oC firstly using an external lock ($CDCl_3$) and referenced to the residual non-deuterated solvent ($CHCl_3$).

2.3 Results and Discussion

The RAFT agent, α-alkyne-α'-hydroxyl trithiocarbonate **3** (Scheme 2.1), used in this work was synthesized by esterification of **1** and **2** (Scheme 2.2) according to the literature procedures.[23, 38] ^{1}H NMR and ^{13}C NMR spectra were used to confirm the structure of **3** (Figure 2.1 and 2.2). This novel trifunctional RAFT agent **3** was subsequently employed to mediate RAFT polymerization of STY, ^{t}BA, NIPAm, and DMA to produce well-defined trifunctional (i.e. RAFT moiety, alkyne and hydroxyl groups) polymers **4** (Scheme 2.1).

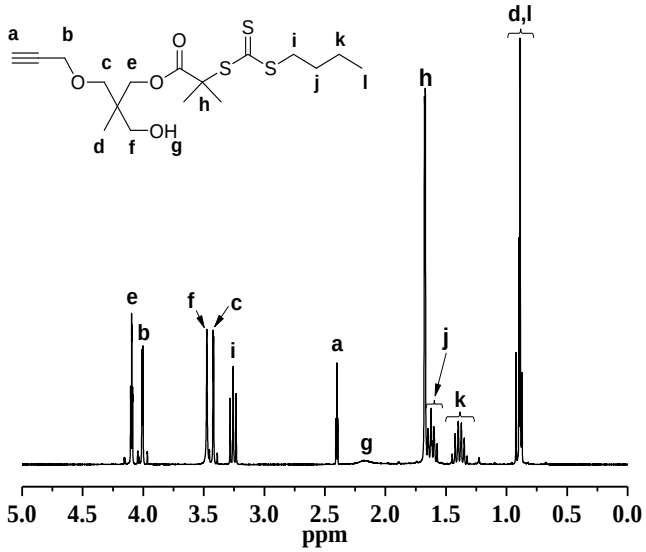

Figure 2.1 ^{1}H NMR spectrum (300 MHz) of α-hydroxyl-α'-alkyne RAFT agent **3** in $CDCl_3$ at 298 K.

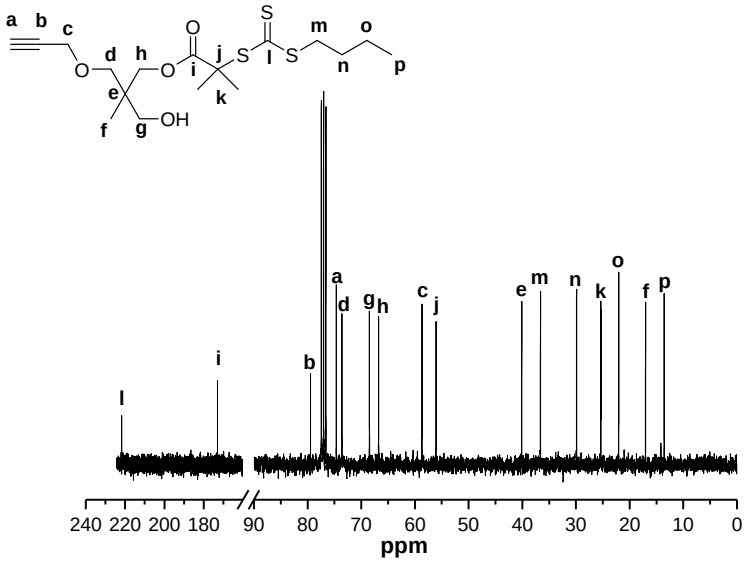

Figure 2.2 ^{13}C NMR spectrum (300 MHz) of **3** in $CDCl_3$ at 298 K.

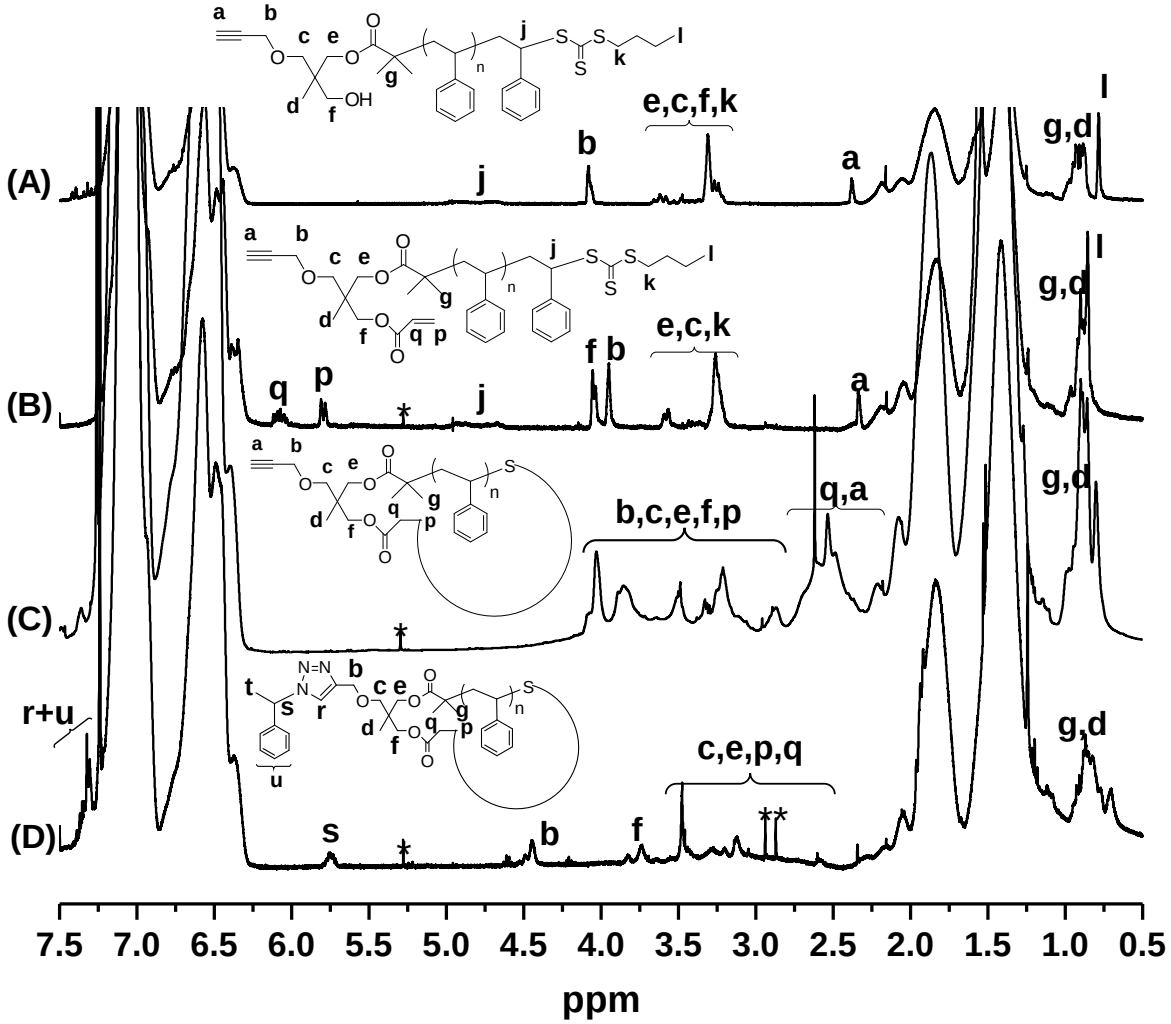

Figure 2.3 ^{1}H NMR spectra (400 MHz) of (A) **4a**, (B) **5a**, (C) **6a** and (D) **7a** in $CDCl_3$ at 298K. *=DCM, **=DMF.

2.3.1. Cyclization through thiol-ene reaction

The first cyclization reaction used the thiol-ene reaction between an acrylate and thiol (after aminolysis of **5**). The hydroxyl groups of polymer **4** were treated with a 15-fold excess of acryloyl chloride to introduce electron-deficient ene functionality and generate α-acrylyl-α'-alkyne polymer **5** (Scheme 2.1). High degrees of the acrylation and the retention of the RAFT moiety on the chain-ends are key requirements to obtain high cyclic purity through the cascade aminolysis and thiol-ene Michael addition reactions. Therefore, the resultant polymer **5** was characterized by ^{1}H NMR and MALDI-ToF mass spectra (Figure 2.3 and Figure 2.4 for PSTY, for ^{1}H NMR and MALDI-ToF mass spectra of PtBA, PNIPAm, and PDMA, see appendix Figure A2.9 to A2.24, and Figure A2.38 to A2.60). Taking the PSTY **5a** as an

example and comparing the ^{1}H NMR with **4a** after acylation, new peaks appeared at 5.60 ppm (**p**) and 6.50 ppm (**q**) ascribed to acrylate protons, and at 4.15 ppm ascribed to methylene protons (**f**) adjacent to the acrylate. This shows the successful functionalization of the acrylate group to the polymer (Figure 2.3B). Moreover, the acrylate functionality of all the resulting polymers were found to be above 95 % as calculated from the ^{1}H NMR spectra based on the integration ratio between one acrylate protons at 5.6 ppm and methine proton at 4.5 ppm. The MALDI-ToF mass spectra of **4a** and **5a** were shown in Figure 2.4A and 2.4B. A major population was observed in both spectra, and their expanded spectra showed the experimental peak values matched with theory. A detailed analysis of all the polymers **4a~4d** and **5a~5d** were given in Appendix. A 54 amu increase from polymer **4a** to **5a** on the MALDI-ToF mass spectra was observed and ascribed to the incorporation of acrylate (Figure A2.65). Moreover, there was no observed population assigned to precursor **4** in the MALDI-ToF mass spectra of **5**, indicating near quantitative end-groups transformation (Figure 2.4B and appendix). Both the ^{1}H NMR and MALDI-TOF mass spectra characterization suggested that through a one-step post-polymerization modification, the heterotrifunctional polymer **5** was easily obtained with very high acrylate functionality and conservation of RAFT moiety.

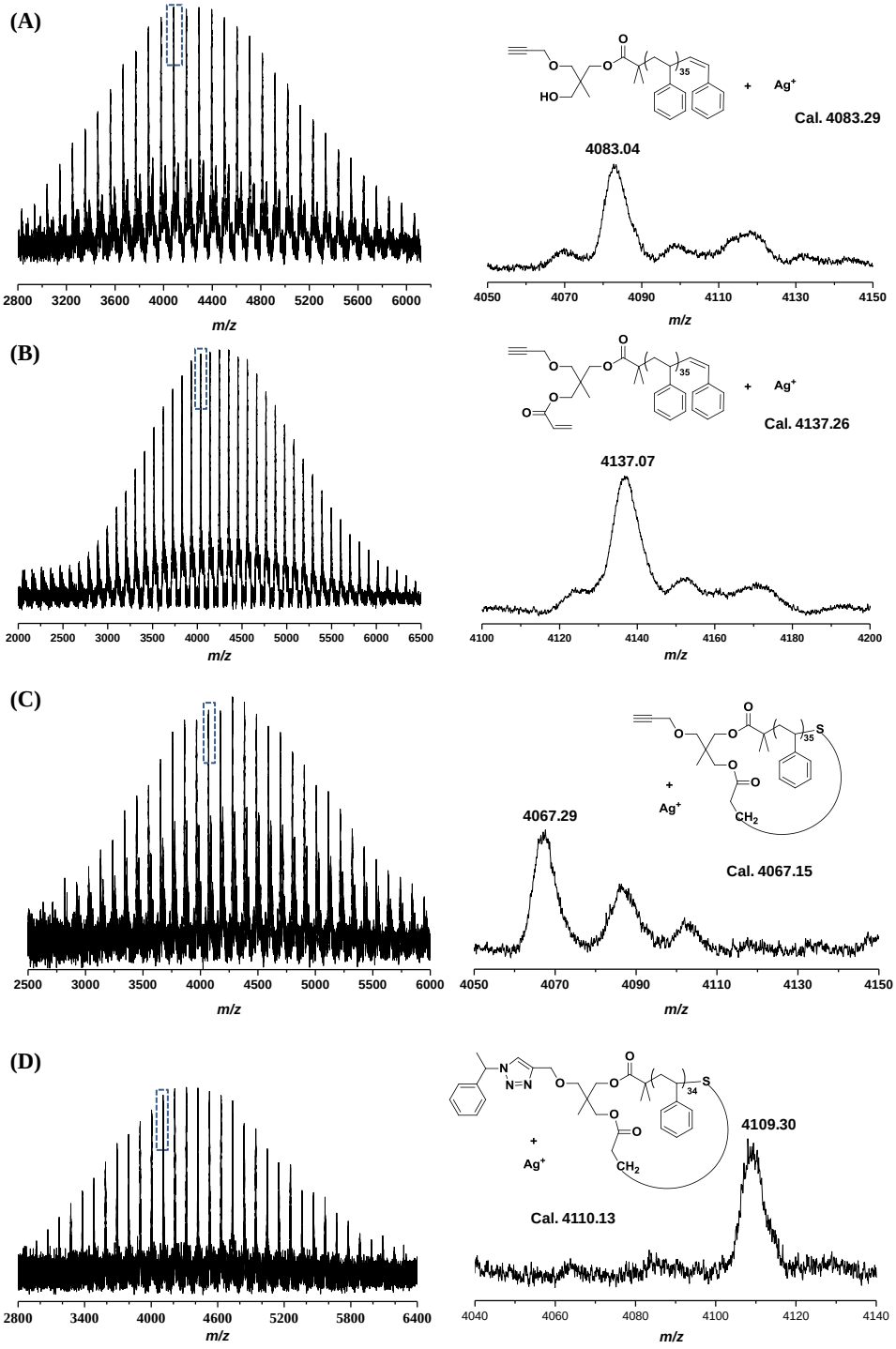

Figure 2.4 MALDI-TOF mass spectra of **4a**, **5a**, **6a** and **7a** with $Ag(CF_3COO)$ as cationization agent and DCTB matrix in reflectron mode. (A) Full spectrum and expanded spectra of **4a**, (B) full spectrum and expanded spectra of **5a**, (C) full spectrum and expanded spectra of **6a**, and (D) full spectrum and expanded spectra of **7a**.

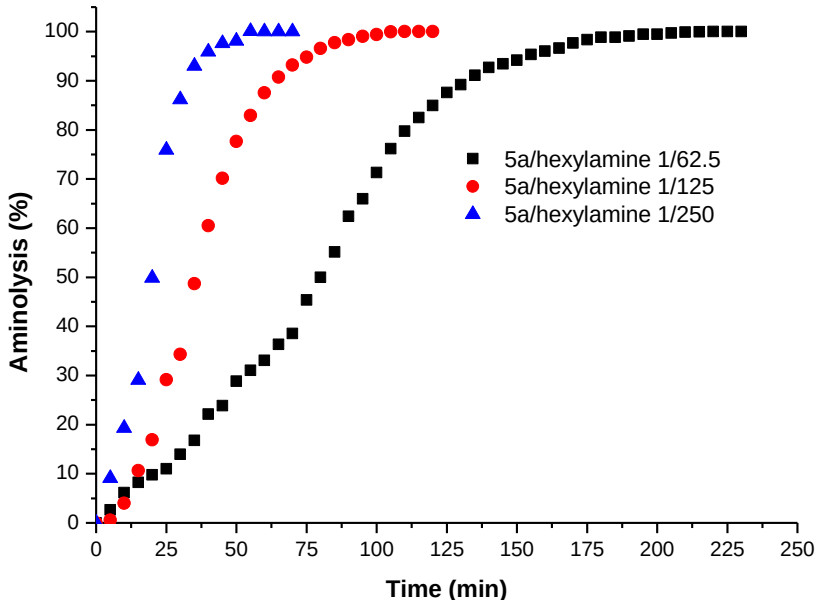

Figure 2.5 Aminolysis kinetics of **5a** varying the concentrations of hexylamine in DMF at room temperature. The aminolysis (%) was calculated from UV-vis absorbance of RAFT moiety according to the equation: aminolysis (%)=(1-A_t/A_0) x 100, where A_t was the absorbance at time t and A_0 was the absorbance before adding the hexylamine. Measurements were recorded every 5 min.

The rate of aminolysis is a critical parameter in obtaining high yields and purity of mono-cyclic polymer. Figure 2.5 shows the effect of hexylamine on the aminolysis rate of **5a**. The higher the amount of hexylamine the more rapid the aminolysis, suggesting that high levels of hexylamine are required to produce rapid intramolecular cyclization. As will be described below, hexylamine can also react with the acrylate via a Michael addition which permanently terminates the acrylate chain-end,[40, 41] and thus an optimal amount of hexylamine will be required to maximize the mono-cyclic product without compromising the rate. We carried out one-pot cyclization reactions of **5a** (5 mg mL^{-1}) in DMF with increasing amounts of hexylamine (from 50 to 200 equivalents to **5a**, Table 2.1, expt. 1-7). The maximum cyclic of 80 % (Figure 2.6A and B) was observed at 125 eq. hexylamine (see expt. 5 in Table 2.1 for experimental conditions). The percentage of cyclization was determined using the Log Normal Distribution (LND) with Gaussian function[27, 42] and using a hydrodynamic volume change (ΔHDV) from linear to cyclic of 0.76.[43] The LND simulation methodology has been demonstrated to be an excellent non-experimental means to predict the % cyclic.[23, 27, 36, 38, 39] This maximum percentage cyclic further correlated with a change in HDV of the main peak close to 0.78, suggesting that this peak has a high purity of monocyclic. Even with slightly lower or higher equivalents of hexylamine the amount of cyclic was high (> 70 %) with low amounts of higher (i.e. double) molecular weight polymer species. Increasing the polymer

amount in solution from 5 to 50 mg mL^{-1} resulted in a loss of % cyclic (Figure 2.6C) and an increase in the amount of double molecular weight polymer (Figure 2.6D) in accordance with the Jacobson-Stockmayer theory. The best cyclization result was at 5 mg mL^{-1} and using 125 eq. of hexylamine. This reaction took approximately 30 min to reach greater than 70 % cyclic (Figure 2.6E), after which the % cyclic increased slowly but more importantly the change in HDV decreased close to 0.78. The SEC chromatograms (Figure 2.6F) showed that the low molecular weight distribution decreased with time due to the production of more cyclic product.

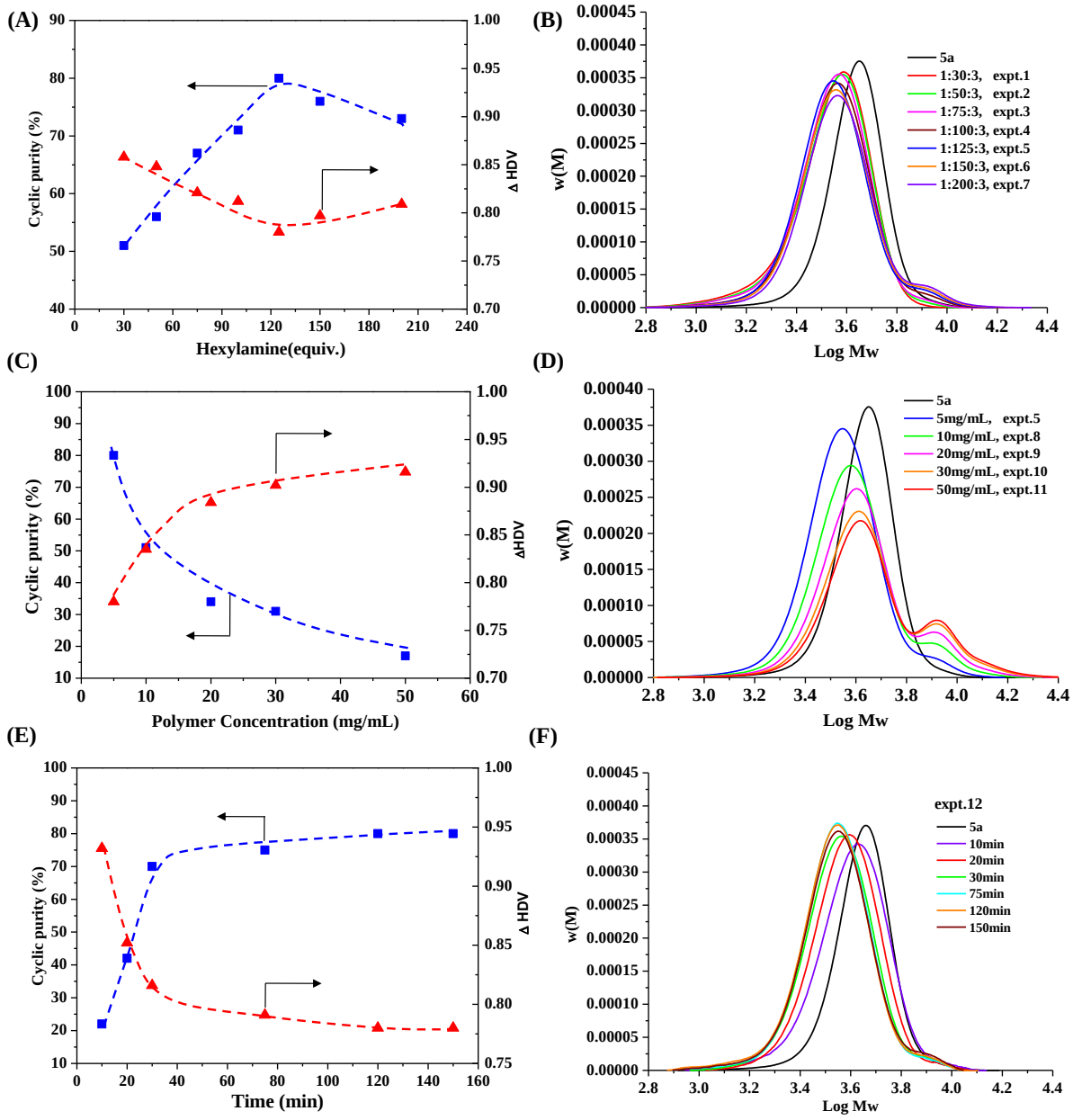

Figure 2.6 One-pot cyclization of **5a** in DMF at room temperature for 12 h. (A) Effect of hexylamine from 1:30:3 to 1:200:3 (PSTY:hexylamine:TCEP) on cyclic purity (%) and hydrodynamic volume change (ΔHDV) using 5 mg mL^{-1} (1.2 x 10^{-3} M) of 5a (expt. 1 to 7 in Table 2.1); (B) SEC traces from (A); (C) Effect of polymer concentration at 1:125:3 (PSTY:hexylamine:TCEP) on cyclic purity (%) and ΔHDV (expt. 5 and 8 to 11 Table 1); (D) SEC traces from (C); (E) Cyclic purity (%) and ΔHDV *vs* time using 5mg mL-1 (1.2 x 10^{-3} M) of **5a** at 1:125:3 (PSTY:hexylamine:TCEP) (expt. 12 in Table 2.1); (F) SEC traces from (E). Molecular weight distributions were determined from RI-SEC using PSTY standards.

Table 2.1 Effect of the thiol-ene cyclization on the hydrodynamic volume changes and purities of the polymer cyclic products (Scheme 2.1).

Expt.[a]	Polymer	Reaction scale		Mole ratio of reactants	Cyclic products		
		Mass(mg)	DMF(mL)	[P]:[Hex.]:[TCEP][b]	Time(h)	ΔHDV[c]	Purity%[d]
1	**5a(PSTY)**	5	1	1:30:3	12	0.858	51
2	**5a(PSTY)**	5	1	1:50:3	12	0.848	56
3	**5a(PSTY)**	5	1	1:75:3	12	0.821	67
4	**5a(PSTY)**	5	1	1:100:3	12	0.812	71
5	**5a(PSTY)**	5	1	1:125:3	12	0.780	80
6	**5a(PSTY)**	5	1	1:150:3	12	0.797	76
7	**5a(PSTY)**	5	1	1:200:3	12	0.809	73
8	**5a(PSTY)**	10	1	1:125:3	12	0.835	51
9	**5a(PSTY)**	20	1	1:125:3	12	0.884	34
10	**5a(PSTY)**	30	1	1:125:3	12	0.902	31
11	**5a(PSTY)**	50	1	1:125:3	12	0.916	17
12	**5a(PSTY)**	20	4	1:125:3	0.17	0.932	22
					0.33	0.852	42
					0.5	0.816	70
					1.25	0.791	75
					2	0.780	80
					2.5	0.780	80
13	**5a(PSTY)**	5	1	1:50:3	5.33	0.859	44
14	**5a(PSTY)**	5	1	1:100:3	5.33	0.852	48
15	**5a(PSTY)**	5	1	1:125:3	5.33	0.849	49
16	**5a(PSTY)**	5	1	1:150:3	5.33	0.822	54
17	**5a(PSTY)**	5	1	1:200:3	5.33	0.846	45
18	**5a(PSTY)**	250	50	1:125:3	2	0.780	80
19	**5b(P^{t}BA)**	250	50	1:125:3	2	0.783	80
20	**5c(PNIPAm)**	250	50	1:125:3	2	0.729	81
21	**5d(PDMA)**	250	50	1:125:3	2	0.790	78

[a]Reaction **1**-**12** and **18**-**21** were conducted in DMF in one-pot under the argon atmosphere at R.T., and reactions **13**-**17** were run in DMF by feeding with 0.0025 mL min^{-1}.

[b]Molar ratio of Polymer:Hexylamine:TCEP.

[c]ΔHDV-hydrodynamic volume change of cyclic polymers **6** to their precursors **5**, calculated from the comparison of peak molecular weight (M_p) of **5** to **6**. The M_p of **5a**, **5b**, **5c**, **6a**, **6b**, and **6c** were determined from THF SEC, RI detector, PSTY standard. The M_p of **5d** and **6d** were determined from DMAc SEC, RI detector, PSTY standard.

[d]Purity of monocyclic products after cyclization determined from the Log Normal Distribution by using Gaussian function.

According to theory,[28] feeding the linear polymer into the reaction mixture will produce very high percentages of cyclic (>98 %). However, when a solution of **5a** (5 mg mL^{-1}) in DMF was fed into a reaction containing increasing amounts of hexylamine (from 50 to 200 equivalents to **5a**), the amount of cyclic only reached a maximum of 54% at 150 eq hexylamine (Figure 2.7A), and with an increased amount of hexylamine to 200 eq. the amount of cyclic dramatically decreased to 45 %. This suggested that hexylamine permanently terminates the acrylate chain-end in competition with the thiol-ene coupling reaction, which is further supported by the SEC (Figure 2.7B) chromatograms that show no excessive amounts of polymer at double the molecular weight of **5a**.

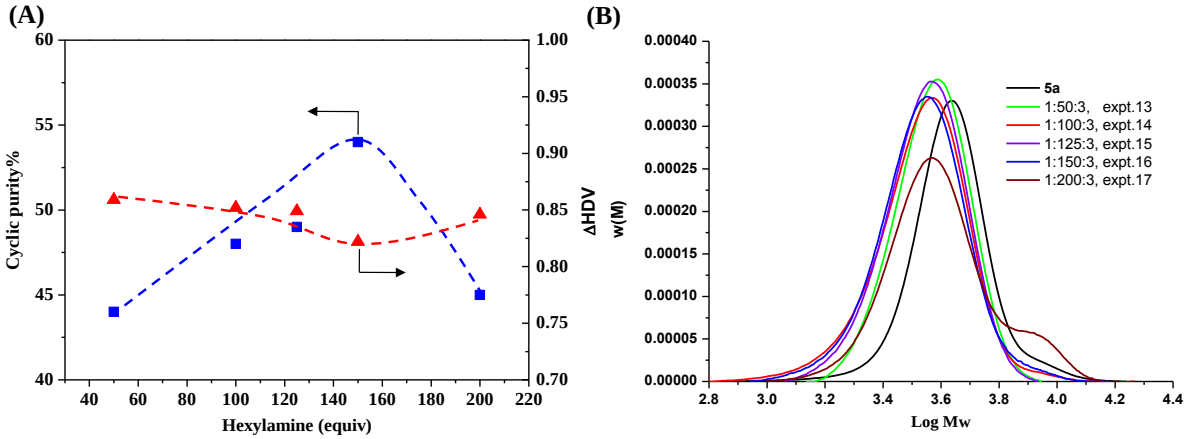

Figure 2.7 Feeding experiments using **5a** (5 mg mL^{-1}; 1.20 x 10^{-3} M) in DMF at room temperature using a feed rate of 0.005 mL min^{-1} over 320 min (expt. 13 to 17 in Table 2.1) using different mole ratios of hexylamine. (A) Cyclic purity (%) and hydrodynamic volume change (ΔHDV) *vs* time; (B) SEC traces determined from RI-SEC using PSTY standards.

2.3.2. Cyclization through thiol-bromo reaction

The thio-bromo coupling cyclization was tested due to its rapid coupling rate.[44, 45] The precursor polymer **8** was prepared according to Scheme 2.1. The characterization of **8** is given in appendix. This cyclization reaction (Figure 2.8A) was not as successful as the thiol-ene cyclization, reaching only as high as 26 % cyclic in a one pot reaction (see expt. 22-26 in Table 2.2). The SEC chromatograms in Figure 2.8B showed both cyclic and high molecular multiblock species, suggesting that side reactions between the hexylamine and bromine played a dominant role. This was a surprise as we expected quite fast coupling as found from other thiol-bromo coupling reactions.[44, 45] To confirm that the lower cyclization efficiency was not caused by post-polymerization chain-end bromination, we also attempted to make a

RAFT agent **10** from RAFT agent **3** by direct bromination of the hydroxyl group with 2-bromopropionyl bromide (Scheme 2.3). Previous studies have shown that the bromo group is stable during the RAFT polymerization.[46, 47] We therefore polymerized STY in the presence of RAFT agent **10** to give the polymer **11** (Scheme 2.3). The characterization of **11** is given in appendix. By using the same cyclization condition as polymer **8**, similar results were obtained (expt. 27-31 in Table 2.2). The cyclic purities were still low (<24 %) and the hydrodynamic volume changes were greater than 0.85 even with an increase of hexylamine to 200 eq. (Figure 2.8C). The SEC chromatograms showed both linear and multiblock species (Figure 2.8D). Again the results suggested the competition reaction of hexylamine with bromine groups thus lowering the effectiveness for the thiol-bromo reaction to cyclize PSTY.

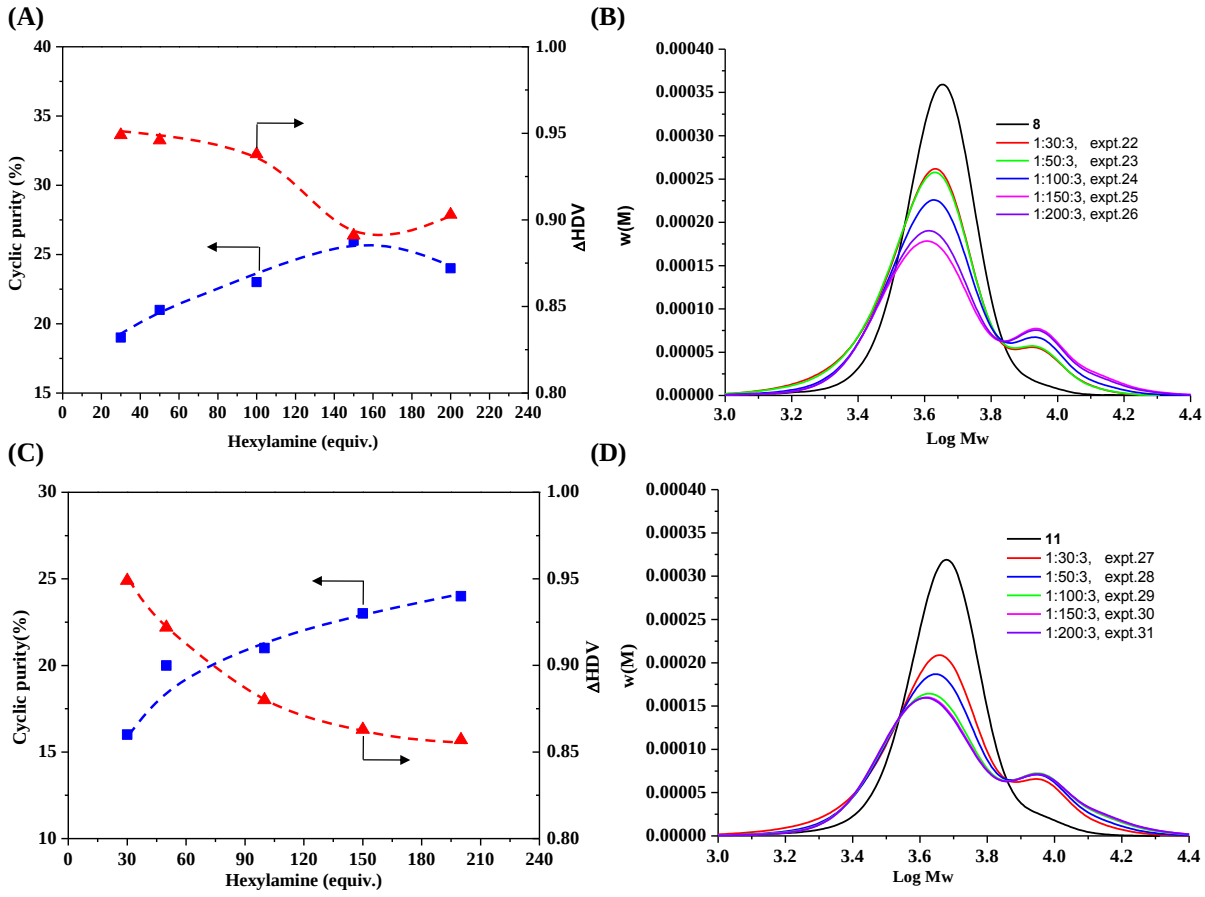

Figure 2.8 Comparison for the one-pot thio-bromo cyclization reaction of 5 mg mL^{-1} PSTY in DMF at R.T. for 12 h: **8** (Scheme 2.1) and **11** (Scheme 2.3). (A) Cyclic purity (%) and hydrodynamic volume change (ΔHDV) from **8** *vs* hexylamine (expt. 22 to 26 in Table 2.2); (B) SEC traces from (A); (C) Cyclic purity (%) and ΔHDV vs hexylamine from **11** (expt. 27 to 31 in Table 2.2); (D) SEC traces from (C). Molecular weight distributions were determined from RI-SEC (THF) using PSTY standard.

Table 2.2 Effect of the thiol-bromo cyclization on the hydrodynamic volume changes and purities of PSTY macrocycles. (Scheme 2.1 for expt. 22-26, and Scheme 2.3 for expt. 27-31).

Expt.[a]	Polymer	Reaction scale		Mole ratio of reactants	Cyclic products		
		Mass(mg)	DMF(mL)	[P]:[Hex.]:[TCEP][b]	Time(h)	ΔHDV[c]	Purity%[d]
22	**8(PSTY)**	5	1	1:30:3	12	0.949	19
23	**8(PSTY)**	5	1	1:50:3	12	0.946	21
24	**8(PSTY)**	5	1	1:100:3	12	0.938	23
25	**8(PSTY)**	5	1	1:150:3	12	0.891	26
26	**8(PSTY)**	5	1	1:200:3	12	0.903	24
27	**11(PSTY)**	5	1	1:30:3	12	0.949	16
28	**11(PSTY)**	5	1	1:50:3	12	0.922	20
29	**11(PSTY)**	5	1	1:100:3	12	0.880	21
30	**11(PSTY)**	5	1	1:150:3	12	0.863	23
31	**11(PSTY)**	5	1	1:200:3	12	0.857	24

[a]All one-pot cyclization reactions of **8** and **11** were conducted in DMF under the argon atmosphere at R.T.

[b]Molar ratio of Polymer:Hexylamine:TCEP.

[c]ΔHDV-hydrodynamic volume change of cyclic polymers **9** to their precursors **8** or **11**, calculated from the comparison of peak molecular weight (M_p) of **8** or **11** to **9**. The M_p of **8, 11** and **9** were determined from THF SEC, RI detector, PSTY standard.

[d]Purities of monocyclic products after cyclization determined from the Log Normal Distribution by using Gaussian function.

The RAFT technique can afford a wider range of polymers, especially those that are water-soluble or thermoresponsive. With the optimized cyclization condition found above for the thiol-ene reaction, we extended this method to synthesized both hydrophobic and hydrophilic alkyne functional cyclic polymers PSTY, P^{t}BA, PNIPAm and PDMA on a much larger scale (from 5 to 250 mg). Table 2.3 shows the molecular weights and polydispersity indexes of all the four starting and final polymer products. In 50 mL of solvent, a batch of 250 mg linear PSTY **5a**, P^{t}BA **5b**, PNIPAm **5c** and PDMA **5d** was added to a DMF solution of hexylamine (125 eq.) and reacted for 2 h. All the four different alkyne functional cyclic polymers **6** were then purified and analyzed by SEC, MALDI-TOF and ^{1}H NMR. Figure 2.9 shows the SEC traces of the linear polymers **5**, crude cyclic products **6** and the corresponding LND Gaussian simulation (Table 1.1, expt. 18 to 21). The hydrodynamic volume change ΔHDV for **5a**, **5b**, **5c** and **5d** to **6a**, **6b**, **6c** and **6d** were 0.78, 0.78, 0.73 and 0.79, and gave cyclic purities of 80 %, 80 %, 81 %, and 78 %, respectively. The cyclic products **6** were characterized by ^{1}H NMR. Figure 2.3C showed the ^{1}H NMR spectra of cyclic PSTY **6a,** the

peaks at 5.60 and 6.50 ppm were not observed compared to Figure 2.3B, suggesting that the acrylate was fully converted to thioester by thiol-ene Michael addition reaction. Figure 2.4C showed the MALDI-TOF of the cyclic PSTY **6a**, all the populations were assigned to **6a** with different metal ions and matched with theoretical isotopic patterns. Compared to **5a**, a 34 amu difference was observed attributed to the change from **5a'** (cleavage from **5a** under laser)[48] to cyclic **6a** as depicted in Figure A2.65. However, for polymers **5b**, **5c** and **5d**, the polymer chains with metal ions were observed from MALDI-TOF mass spectra with no significant cleavage of RAFT moieties due to the laser for polyacrylate or polyacryamide. Taking PNIPAm as an example, (Figure A2.65) showed the MALDI-TOF mass spectra peak shift from **5c** to **6c**. A 132 amu difference was attributed to the formula change caused by the aminolysis of the RAFT chain ends and thio-ene Michael addition reactions. Similar results were observed for cyclic P^{t}BA **5b**, and PDMA **5d** (see appendix Figure A2.53 to 2.54 and Figure A2.55 to 2.56). All the characterization data suggested the monocyclic alkyne functional polymers have very high chain end functionalities and purity. This is the first report for the synthesis of the water soluble cyclic PDMA.

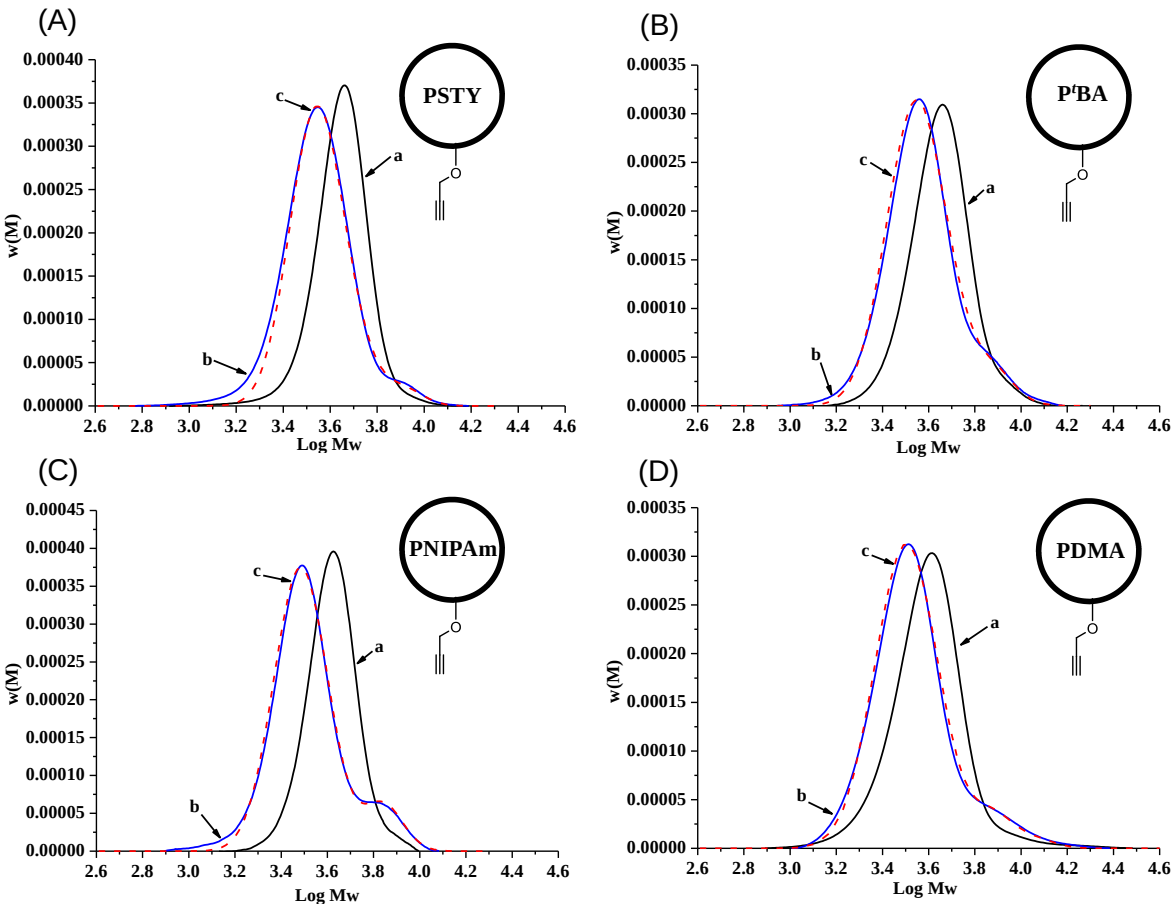

Figure 2.9 Scale-up one-pot cyclization of **5** with the ratio of 5:hexylamine:TCEP as 1:125:3 in DMF at R.T. for 2 h. Curves a (—), b (—) and c (----) represent molecular weight distribution (MWDs) of **5**, **6**, and LND Gaussian simulation, respectively. (A) PSTY; (B) P^{t}BA; (C) PNIPAm and (D) PDMA. See expt. 18, 19, 20, and 21 in Table 2.1 for the cyclization reactions of **5a**, **5b**, **5c**, and **5d** , respectively. SEC analysis based on linear polystyrene calibration curve.

Table 2.3 SEC characterization of alkyne functional cyclic polymers, click product, and their precursors (Scheme 2.1).

Polymer[a]	**4**			**5**			**6**						7[c]		
							Crude			**Purified**[b]					
	M_n	M_p	PDI	M_n	M_p	PDI	M_n	M_p	PDI	M_n	M_p	PDI	M_n	M_p	PDI
a(PSTY)	3980	4220	1.08	4140	4400	1.07	3310	3430	1.08	3300	3320	1.08	3390	3350	1.10
b(P^{t}BA)	4180	4400	1.09	4260	4490	1.09	3550	3450	1.11	3190	3330	1.08	3340	3420	1.16
c(PNIPAm)	3540	3630	1.13	4010	4170	1.06	3050	3040	1.15	2670	2770	1.10	3030	2900	1.11
d(PDMA)	3620	4130	1.13	3980	4280	1.14	3350	3380	1.21	3160	3260	1.16	3430	3510	1.36

[a] The M_n and M_p of polymer **a**, **b**, **c** were determined from THF SEC, RI detector, PSTY standard. The M_n and M_p of **d** were determined from DMAc SEC, RI detector, PSTY standard.

[b] The crude **6a**, **6b**, and **6c** were purified from prep-SEC, and the crude **6d** was purified from fractionation precipitation.

[c] The products of **7** were obtained from CuAAC click reaction between purified **6** and (1-azidoethyl)benzene.

To test the reaction efficiency of the alkyne functionality on the monocyclic polymer **6**, a CuAAC reaction with (1-azidoethyl)benzene (detail of synthesis and NMR characterizations see appendix) as shown in Scheme 2.1 was carried out. After the 'click' reaction, the product **7** was characterized by SEC (Table 2.3), ^{1}H NMR and MALDI-TOF mass spectra. Figure 2.3D showed the ^{1}H NMR spectrum of **7a**; compared with **6a** (Figure 2.3C), new peaks were observed at 7.25-7.50 ppm that were ascribed to the methine proton of triazole ring and aromatic protons from (1-azidoethyl)benzene. Other new peaks at 5.75 ppm and 4.45 ppm were ascribed to the methine proton (**s**) and methylene protons (**b**) adjacent to the triazole ring, respectively. For the other 'click' product **7b**, **7c** and **7d**, more resolved spectra showed the successful click reaction of (1-azidoethyl)benzene to the polymer **6b**, **6c** and **6d** without the interference of aromatic protons compared to PSTY **7a** (see appendix Figure A2.12, A2.16 and A2.20) . Moreover, MALDI-TOF mass spectrum in Figure 2.4D showed a single population of which was attributed to the **7a** and matched with theoretic isotopic resolution. By comparison of **7a** with **6a**, a 147 amu difference was observed and attributed to the molecular weight of (1-azidoethyl)benzene (147.08). The same characterizations were also applied to the other three cyclic polymer **7b**, **7c** and **7d** (see appendix Figure A2.44, Figure A2.52 and Figure A2.60). Both ^{1}H NMR and MALDI-TOF mass spectra characterization indicated the high functionality and click reactivity of the alkyne functional cyclic polymer **6**.

2.4 Conclusion

In summary, we have demonstrated the versatility of polymers made by RAFT to be cyclized in one-pot using the thiol-ene reaction. The optimum conditions for the thiol-ene cyclization reaction was found to be 1:125:3 (PSTY:hexylamine:TCEP), which allowed rapid rates and high percentages of cyclic (~80 %) using 5 mg mL^{-1} of polymer in a DMF solution with hexylamine. Under feed conditions the results showed that side reactions between the hexylamine and acrylate on either end of the polymer chain became a competing pathway with cyclization. The percent cyclic found from the feed experiments was less than 55 %. We were able to produce cyclic polymers with an alkyne functional group in a one-pot reaction, ranging from PSTY, P^{t}BA, PNIPAm and PDMA that were produced with over 80 % cyclic purity. These alkyne moieties on cyclic polymers were then coupled with a small molecule azide to confirm the high alkyne reactivity. Attempts to use the thio-bromo reaction to cyclize PSTY were not as successful as the thiol-ene cyclization reaction, producing less than 25 % cyclic. The thiol-ene procedure is a highly efficient strategy to produce a wide range of cyclic polymers, especially water soluble polymers.

This method also provides the synthesis of cyclic polymers with an alkyne functionality for the construction of more complex polymer topologies. Cyclic polymers are endless, therefore, no chain entanglement in the solution. The hydrophilic cyclic polymers will be coupled onto the periphery of hydrophobic dendritic core to prepare amphiphilic dendrimers, which are possible to form unimolecular micelle in aqueous solution. The endless and compact nature of hydrophilic cyclic polymers supresses the potential aggregation of micelles in aqueous solution.

2.5 References

1. Bielawski, C. W.; Benitez, D.; Grubbs, R. H. *Science* **2002,** 297, (5589), 2041-2044.
2. Chen, B.; Jerger, K.; Frechet, J. M. J.; Szoka, F. C. *Journal of Controlled Release* **2009,** 140, (3), 203-209.
3. Percec, V.; Kawasumi, M. *Macromolecules* **1993,** 26, (14), 3663-3675.
4. Percec, V.; Asandei, A. D.; Chu, P. *Macromolecules* **1996,** 29, (11), 3736-3750.
5. Percec, V.; Asandei, A. D. *Macromolecules* **1997,** 30, (25), 7701-7720.
6. Percec, V.; Turkaly, P. J.; Asandei, A. D. *Macromolecules* **1997,** 30, (4), 943-952.
7. Hadjichristidis, N.; Pitsikalis, M.; Pispas, S.; Iatrou, H. *Chemical Reviews* **2001,** 101, (12), 3747-3792.
8. Endo, K. *Advances in Polymer Science* **2008,** 217, (New Frontiers in Polymer Synthesis), 121-183.
9. Laurent, B. A.; Grayson, S. M. *Chemical Society Reviews* **2009,** 38, (8), 2202-2213.
10. Kricheldorf, H. R. *J Polym Sci Pol Chem* **2010,** 48, (2), 251-284.
11. Jia, Z. F.; Monteiro, M. J. *Journal of Polymer Science Part a-Polymer Chemistry* **2012,** 50, (11), 2085-2097.
12. Hawker, C. J.; Bosman, A. W.; Harth, E. *Chemical Reviews* **2001,** 101, (12), 3661-3688.
13. Moad, G.; Chong, Y. K.; Postma, A.; Rizzardo, E.; Thang, S. H. *Polymer* **2005,** 46, (19), 8458-8468.
14. Matyjaszewski, K.; Tsarevsky, N. V. *Nat Chem* **2009,** 1, (4), 276-288.
15. Konkolewicz, D.; Monteiro, M. J.; Perrier, S. *Macromolecules* **2011,** 44, (18), 7067-7087.
16. Iha, R. K.; Wooley, K. L.; Nystrom, A. M.; Burke, D. J.; Kade, M. J.; Hawker, C. J. *Chem Rev* **2009,** 109, (11), 5620-5686.
17. Laurent, B. A.; Grayson, S. M. *J. Am. Chem. Soc.* **2006,** 128, (13), 4238-4239.
18. Whittaker, M. R.; Goh, Y.-K.; Gemici, H.; Legge, T. M.; Perrier, S.; Monteiro, M. J. *Macromolecules* **2006,** 39, (26), 9028-9034.
19. Nicolay, R.; Matyjaszewski, K. *Macromolecules* **2011,** 44, (2), 240-247.
20. Qiu, X.-P.; Tanaka, F.; Winnik, F. M. *Macromolecules (Washington, DC, United States)* **2007,** 40, (20), 7069-7071.
21. Zhang, Y.; Wang, G.; Huang, J. *Macromolecules* **2010,** 43, (24), 10343-10347.

22. Glassner, M.; Blinco, J. P.; Barner-Kowollik, C. *Macromolecular Rapid Communications* **2011,** 32, (9-10), 724-728.

23. Hossain, M. D.; Valade, D.; Jia, Z. F.; Monteiro, M. J. *Polym Chem-Uk* **2012,** 3, (10), 2986-2995.

24. Goldmann, A. S.; Quemener, D.; Millard, P.-E.; Davis, T. P.; Stenzel, M. H.; Barner-Kowollik, C.; Mueller, A. H. E. *Polymer* **2008,** 49, (9), 2274-2281.

25. Jacobson, H.; Stockmayer, W. H. *Journal of Chemical Physics* **1950,** 18, (12), 1600-1606.

26. Stockmayer, H. J. W. H. *J. Chern. Phys.* **1950,** 18, 1600-1606.

27. Lonsdale, D. E.; Bell, C. A.; Monteiro, M. J. *Macromolecules* **2010,** 43, (7), 3331-3339.

28. Lonsdale, D. E.; Monteiro, M. J. *J Polym Sci Pol Chem* **2010,** 48, (20), 4496-4503.

29. Moses, J. E.; Moorhouse, A. D. *Chemical Society Reviews* **2007,** 36, (8), 1249-1262.

30. Roth, P. J.; Boyer, C.; Lowe, A. B.; Davis, T. P. *Macromol Rapid Comm* **2011,** 32, (15), 1123-1143.

31. Lowe, A. B. *Polymer Chemistry* **2010,** 1, (1), 17-36.

32. Killops, K. L.; Campos, L. M.; Hawker, C. J. *Journal of the American Chemical Society* **2008,** 130, (15), 5062-+.

33. Qiu, X. P.; Winnik, F. M. *Macromol Rapid Comm* **2006**, 1648–1653.

34. Jia, Z. F.; Liu, J. Q.; Davis, T. P.; Bulmus, V. *Polymer* **2009,** 50, (25), 5928-5932.

35. Stanford, M. J.; Pflughaupt, R. L.; Dove, A. P. *Macromolecules* **2010,** 43, (16), 6538-6541.

36. Lonsdale, D. E.; Monteiro, M. J. *Chem Commun* **2010,** 46, (42), 7945-7947.

37. Lonsdale, D. E.; Monteiro, M. J. *J Polym Sci Pol Chem* **2011,** 49, (21), 4603-4612.

38. Jia, Z. F.; Lonsdale, D. E.; Kulis, J.; Monteiro, M. J. *Acs Macro Letters* **2012,** 1, (6), 780-783.

39. Kulis, J.; Jia, Z. F.; Monteiro, M. J. *Macromolecules* **2012,** 45, (15), 5956-5966.

40. Ma, X. P.; Tang, J. B.; Shen, Y. Q.; Fan, M. H.; Tang, H. D.; Radosz, M. *Journal of the American Chemical Society* **2009,** 131, (41), 14795-14803.

41. Li, G. Z.; Randev, R. K.; Soeriyadi, A. H.; Rees, G.; Boyer, C.; Tong, Z.; Davis, T. P.; Becer, C. R.; Haddleton, D. M. *Polym Chem-Uk* **2010,** 1, (8), 1196-1204.

42. Cabaniss, S. E. Z., Q.H.; M aurice, P.A.; Chin Y.P.; Aiken, G. *Environ. Sci. Technol.* **2000,** 34, 1103-1109.

43. Roovers, J.; Toporowski, P. M. *Macromolecules* **1983,** 16, (6), 843-849.

44. Rosen, B. M.; Lligadas, G.; Hahn, C.; Percec, V. *Journal of Polymer Science Part a-Polymer Chemistry* **2009,** 47, (15), 3931-3939.

45. Rosen, B. M.; Lligadas, G.; Hahn, C.; Percec, V. *Journal of Polymer Science Part a-Polymer Chemistry* **2009,** 47, (15), 3940-3948.

46. Nicolay, R.; Kwak, Y.; Matyjaszewski, K. *Macromolecules* **2008,** 41, (13), 4585-4596.

47. Zhang, Y. Q.; Shen, Z.; Yang, D.; Feng, C.; Hu, J. H.; Lu, G. L.; Huang, X. Y. *Macromolecules* **2010,** 43, (1), 117-125.

48. Ladaviere, C.; Lacroix-Desmazes, P.; Delolme, F. *Macromolecules* **2009,** 42, (1), 70-84.

Chapter 3

Synthesis of ABCD mikto-arm star copolymers *via* sequential LRP and CuAAC 'click' chemistry

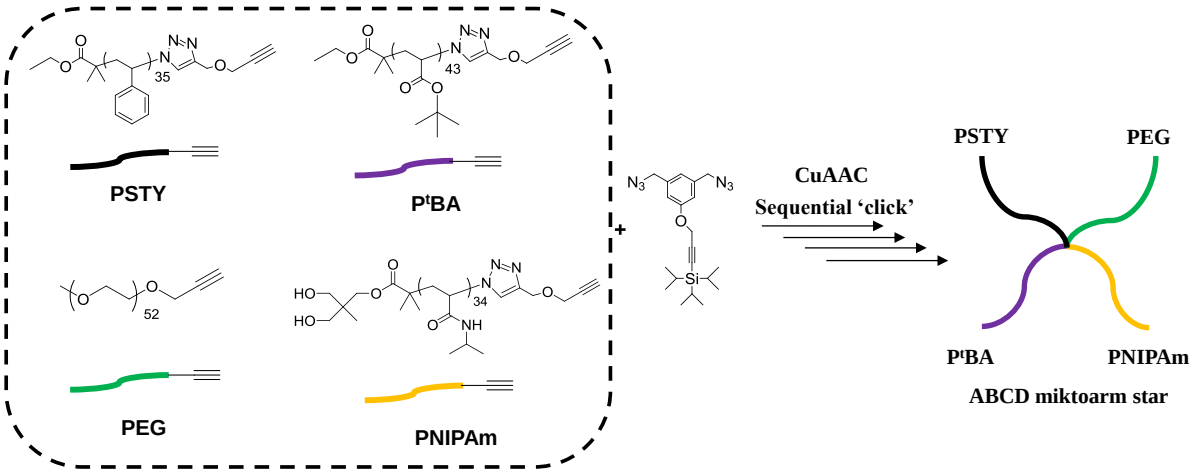

In this chapter, a novel synthetic strategy was used to prepare amphiphilic miktoarm star copolymers consisting of four different arm segments, including hydrophobic poly(styrene) PSTY and poly(*tert*-butyl acrylate)P^{t}BA which the latter can be hydrolysed to poly(acrylic acid) (i.e. PAA), hydrophiphilic poly(ethylene glycol) (PEG) and thermoresponsive poly(*N*-isopropylacrylamide) (PNIPAm). The polymeric building blocks were generated through either atom transfer radical polymerization (ATRP) or single electron transfer 'living' radical polymerization (SET-LRP) followed by post-functionalization to introduce alkyne functionality on the polymer chain-ends. These polymers were further coupled with a trifunctionallinker *via* stepwise iterative process using cascade CuAAC 'click' reaction/deprotection sequence. The strategy was first utilized for synthesis of 4-arm PSTY star that can be precisely characterized by SEC, NMR and MALDI-ToF MS to provide a proof of concept. The 4-arm PSTY star was constructed with high purity (98 %) low molecular weight distribution (1.04), and excellent 'click' efficiency (91 %). Afterwards, we extended this strategy to prepare PSTY-PEG-P^{t}BA-PNIPAm ABCD miktoarm star copolymers with well-controlled molecular weight, narrow polydispersity (1.03), and precise composition. Pre-synthesis of building blocks with a variety of different monomers, high reaction efficiency, and iterative method all together make this strategy very powerful for synthesis of amphiphilic miktoarm star copolymers with complex chemical composition (≥ 4 different polymers).

3.1 Introduction

Star-branched polymer which consists of polymer segments (arms) radiating from a central core have distinct properties compared to their liner analogues with similar molecular weight.[1-3] Among the star-branched polymers, asymmetric ones composed of chemically different arms, so-called miktoarm polymers (or μ-star polymers) have attached considerable attention due to their multi-arm segment structure. Miktoarm star polymers readily undergo phase-separation at molecular level resulting in nano-ordered superstructures through self-organizing and/or supermolecular assemblies in both bulk and selective solvent.[4-8] For example, amphiphilic miktoarm star polymers can form unimolecular containers or nanoreactors in water with special multivalent functionality on the shell surface and within the core, and could have applications in biological fields (e.g, gene delivery, drug release, and bio-catalysis).[9-13 14]

Living anionic polymerization (LAP) by far is the widely used methodology to synthesize well-defined miktoarm star polymers composed of three or more different arm segments.[15-20] Hirao and colleagues developed a superior strategy to make a variety of star-branched multicomponent polymers in a stepwise and iterative methodology using living anionic polymerization.[15] The combination of LAP and linking chemistries afforded the generation of miktoarm stars with many arms and multiple composition involving 4-arm ABCD, 5-arm ABCDE, and even up to 7-arm ABCDEFG with quite narrow polydispersity (< 1.05).[21, 22] The utilization of the LAP technique has a couple of synthetic drawbacks, such as the limited choice of monomers, low tolerance to functionalities on the monomer (i.e., any labile proton source in monomer or system terminates reaction), sensitivity to the moisture, and extreme reaction conditions (e.g., -70 ^{o}C).[15, 23] Therefore, the diversity of miktoarm macromolecular that can be constructed from LAP is limited, especially for the synthesis of amphiphilic and stimuli-responsive star copolymers.

Recent advances in 'living' radical polymerization (LRP), such as nitroxide-mediated polymerization(NMP),[24] reversible addition-fragmentation chain transfer (RAFT),[25-27] atom transfer radical polymerization (ATRP),[28-30] ring-opening polymerization (ROP),[31, 32] and single electron transfer living radical polymerization (SET-LRP), [33-35] provide a great opportunity to make well-defined functional polymer building blocks. When these polymerization techniques are combined with robust and highly efficient 'click' reaction, such as copper catalyzed azide alkyne cycloaddition (CuAAC), star-branched polymers with greater compositional variation are available, such as 3-arm ABC,[5, 36-40] 4-arm ABCD,[41-43]

and 5-arm ABCDE.[44] In addition, hydrophilic arm segments are able to be incorporated into the miktoarm structure due to the wide range choice of monomers utilized in LRP.[45-48]

Herein, we reported a new iterative coupling strategy for the synthesis of ABCD miktoarm star consisting of PSTY, PEG, P^{t}BA, and PNIPAm segments *via* combination of ATRP or SET-LRP and CuAAC 'click' chemistry. A trifunctional linker which contained two azide groups and one protected alkyne group was synthesized as key compound to covalently attach to the polymer chain-end and allow for an iteratively method to produce the ABCD miktoarms star. The methodology given in this chapter represents a proof-of-concept to not only generate miktoarm stars but provide a general methodology for the production of more complex architectures with control over the polymer composition.

3.1.1 Aim of Chapter

The aim of this work is to develop a new iterative coupling strategy to make miktoarm 4-arm star consisting of four very different polymeric blocks as shown in Scheme 3.1 (e.g., both hydrophobic and hydrophilic building blocks). The approach was first demonstrated in the synthesis of a 4-arm PSTY star for both ease of purification and more importantly characterization through SEC, NMR and MALDI-ToF MS (see Scheme 3.2). This method was then successfully applied for the construction of a miktoarm 4-arm star.

Scheme 3.1 Synthetic route of four-arm ABCD star copolymer

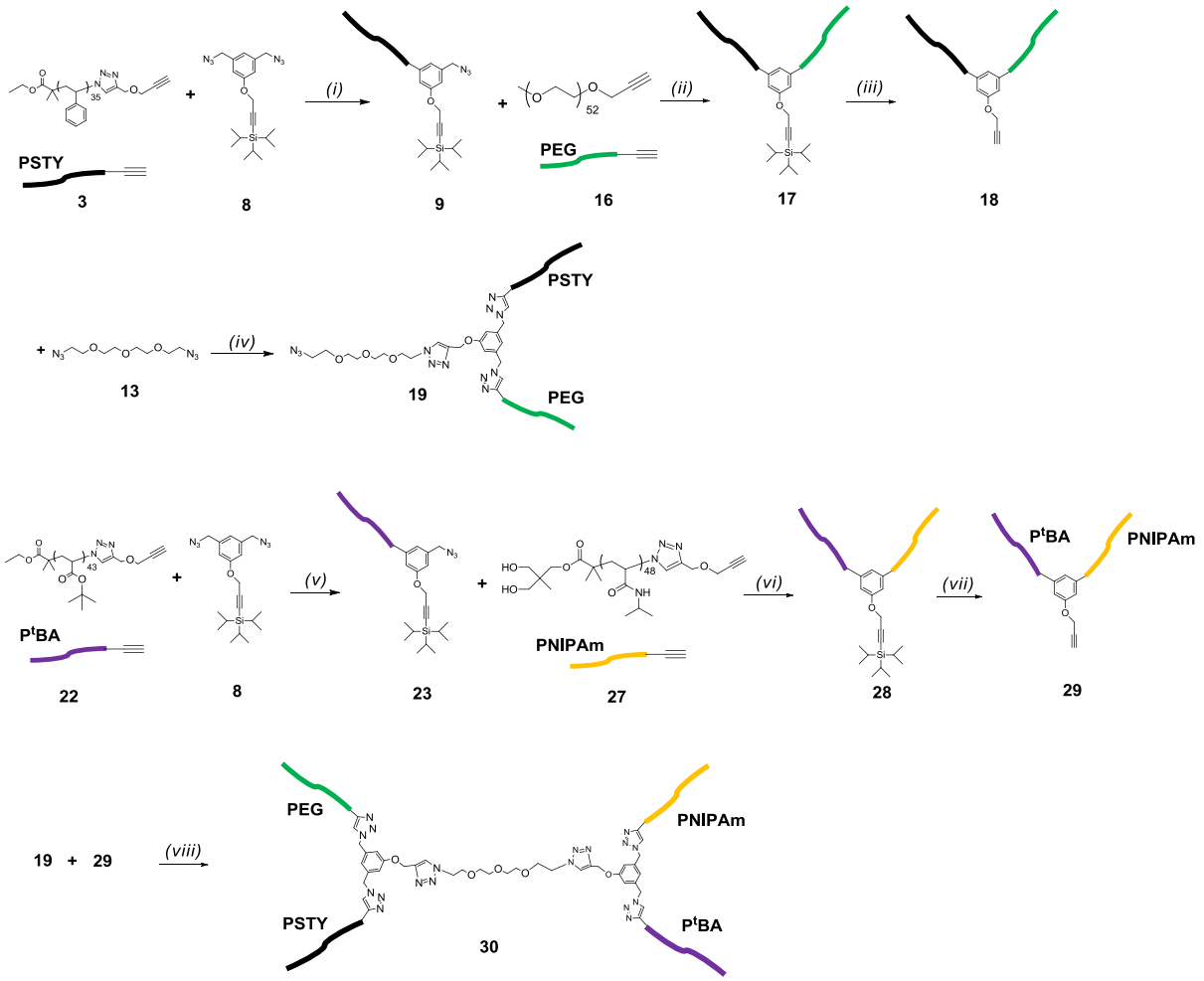

(i) CuBr, Cu wire, PMDETA, toluene, 25 ^{o}C, feeding; (ii) CuBr, Cu wire, PMDETA, toluene, 25 ^{o}C, 1h; (iii) TBAF, THF, argon, 25 ^{o}C, 24 h. (iv) CuBr, Cu wire, PMDETA, toluene, 25 ^{o}C, feeding; (v) CuBr, Cu wire, PMDETA, toluene, 25 ^{o}C, feeding; (iv) CuBr, Cu wire, PMDETA, DMF, 25 ^{o}C, 2h; (vii) TBAF, THF, argon, 25 ^{o}C, 24 h; (viii) CuBr, Cu wire, PMDETA, DMF, 50 ^{o}C, 2 h;

3.2 Experimental

3.2.1 Materials

The following chemicals were used as received: alumina, activated basic (Aldrich, Brockmann I, standard grade, ~150 mesh, 58 Å), magnesium sulfate ($MgSO_4$: anhydrous, Scharlau, extra pure), sodium chloride (NaCl: Univar, 99.9 %), sodium iodide (NaI: Aldrich, 99.5 %), sodium azide (NaN_3: Aldrich, 99.5 %), 1,1,1-triisopropylsilyl chloride (TIPS-Cl: Aldrich, 99 %), ethylmagnesium bromide solution (EtMgBr, Aldrich, 3.0 M in diethyl ether), triethylamine (TEA: Fluka, 98 %), TLC plates (silica gel 60 F254), silica gel 60 (230-400 mesh ATM (SDS)), potassium carbonate (K_2CO_3, analaR, 99.9 %), ethyl 2-bromo-2-methylpropionate (EBiB, Aldrich, 98%) 2-bromoisobutyryl bromide (BiB, Aldrich, 98%), lithium aluminium hydride ($LiAlH_4$, Aldrich, 98 %), diphenyl phosphoryl azide (DPPA, Aldrich, 97 %), 1,8-diazabicylco[5,4,0]undec-7-ene (DBU, Aldrich, 98 %), tetrabutylammonium fluoride hydrate (TBAF, Aldrich, 1.0 M in THF), 18-crown-6 ether (18-C-6, Aldrich, 99 %), imidazole (Aldrich, 99 %), propargyl bromide (Aldrich, 80wt % in toluene), propargyl amine (Aldrich, 98 %), tetraethlyene glycol (Aldrich, 98 %), Tetrabromomethane (Aldrich, 99 %), triphenylphosphine (Aldrich, 99 %), Propargyl ether (Aldrich, 98 %), Dowex® 50W X8-200 ion-exchange resin (Aldrich, 200-400 mesh) Sodium borohydride (Aldrich, 99 %), Poly(ethylene glycol) methyl ether. Styrene (Aldrich, 99 %) and *tert*-Butyl acrylate (^{t}BA, Aldrich, HPLC grade) were purified from inhibitor by passage through a column of activated basic alumina (Aldrich, Brockmann I, standard grade, ~150 mesh, 58Å). *N*-isopropylacrylamide (NIPAm, Aldrich, 99 %) was purified twice by recrystallization in *n*-hexane and toluene (9:1, v:v).

The following solvents were used as received: acetone (ChemSupply, AR), dimethyl sulfoxide (DMSO: Labscan, AR grade), dichloromethane (DCM: Labscan, AR grade), ethyl acetate (EtOAc: ChemSupply, AR grade), methanol (MeOH: anhydrous, Lichrosolv, 99.9 %, HPLC grade), *N*,*N*-Dimethylformamide (DMF, Aldrich, HPLC grade), *N*,*N*-dimethylacetamide (DMAc: Aldrich, HPLC grade), petroleum spirit (BR 40-60 ^{o}C, Univar, AR grade), tetrahydrofuran (THF: Lichrosolv, HPLC grade), and toluene (TOL, Univar, AR grade).

N,*N*,*N*',*N*'',*N*''-pentamethyldiethylenetriamine (PMDETA: Aldrich, 99 %) was used as received, tris-[2-(dimethylamino)ethyl]amine (Me_6TREN) and Copper(I)bromide were synthesized in our group. Cu wire (diamter 0.9 mm) was treated with acetate acid before use.

3.2.2 Synthetic procedure

Scheme 3.2 Synthesis of 4-arm PSTY star (**15)**

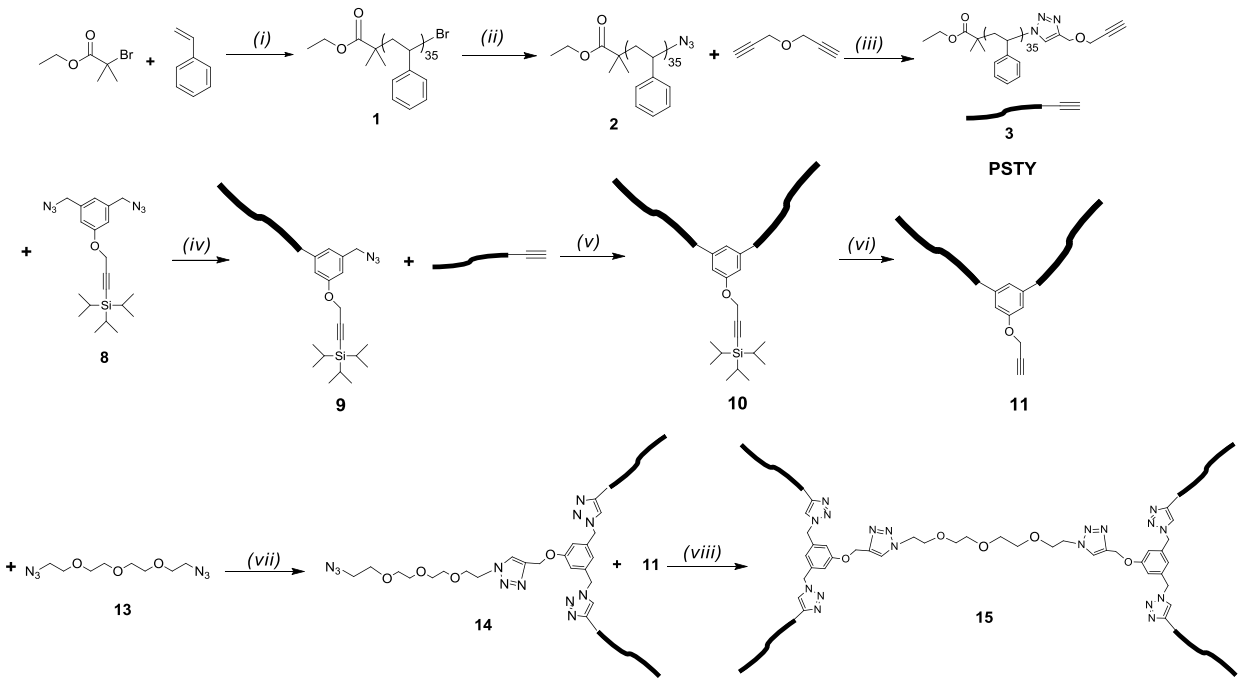

(i) CuBr, $CuBr_2$/PMDETA, PMDETA, 80^oC, 5 h; (ii) DMF, NaN_3, 24 h; (iii) CuBr, Cu wire, PMDETA, toluene, 25 ^oC, 30min; (iv) CuBr, Cu wire, PMDETA, toluene, 25 ^oC, feeding; (v) CuBr, Cu wire, PMDETA, toluene, 25 ^oC, 1 h; (iv) TBAF, THF, argon, 25 ^oC, 24 h. (vii) CuBr, Cu wire, PMDETA, toluene, 25 ^oC, feeding; (viii) CuBr, Cu wire, PMDETA, toluene, 25 ^oC, 2 h.

3.2.2.1 Synthesis of PSTY-alk (3)

Synthesis of (1)

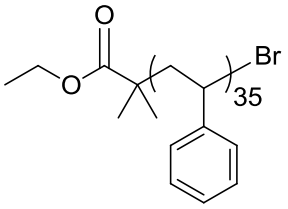

$PSTY_{35}$-Br (**1**) was synthesized according to the reference.[51] Styrene (16 g, 0.153 mol), PMDETA (0.240 mL, 1.154 x 10^{-3} mol), ethyl 2-bromo-2-methylpropionate (EBiB, 0.225 mL, 1.538 x 10^{-3} mol) and Cu(II)Br_2/ PMDETA complex (0.15 g, 3.787 x 10^{-4} mol) were

added to a Schlenk flask and purged with argon for 60 min with vigorous stirring. Cu(I)Br (0.165 g, 1.154 x 10^{-3} mol) was added under a positive argon flow and the contents bubbled with argon for 10 more min. The reaction vessel was then sealed, placed in an oil bath at 80 °C and the reaction mixture stirred for 6.5 h. The reaction was terminated by quenching in ice followed by exposure to air. The contents were diluted with dichloromethane and passed through activated basic alumina. The solvent was removed under reduced pressure and the residue dissolved in a minimal amount of dichloromethane. The polymer was precipitated in 10 x volume of MeOH. The resulting white precipitate was collected by vacuum filtration and dried under vacuum ($M_{n,RI}$=3860, $M_{p,RI}$=4050, PDI = 1.10, monomer conversion %=45.0 %, determined from gravimetric method).

Synthesis of (2)

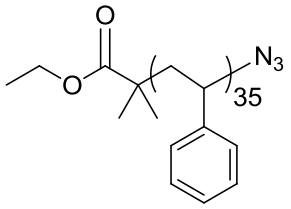

NaN_3 (0.93 g, 1.432 x 10^{-2} mol) was added to a stirring solution of PSTY-Br (**1**) (3.63 g, 9.552 x 10^{-4} mol) in DMF (8.0 mL). The reaction mixture was stirred for 20 h at 25 °C. The polymer was precipitated in 10 x volume of 10 % water/MeOH, recovered by vacuum filtration and washed exhaustively with water and MeOH. The polymer was redissolved in DCM, reprecipitated in 10 x volume MeOH and recovered by vacuum filtration. The polymer was dried under vacuum. ($M_{n,RI}$ = 3840, $M_{p,RI}$=4030, PDI = 1.08).

Synthesis of (3)

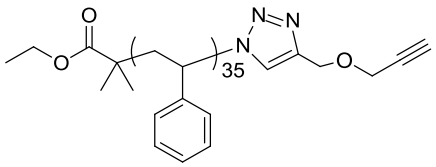

Propargyl ether (0.723 g, 7.69 x 10^{-3} mol), PMDETA (8.0 µL, 3.84 × 10^{-5} mol), PSTY-N_3 (**2**) (1.0 g, 2.604 x 10^{-4} mol) and toluene (5 mL) were added to a 20 mL vial and purged with argon for 30 min, degassed solution was transferred into a Schlenk tube containing Cu(I)Br (5.5 mg, 3.84 x 10^{-5} mol) under a positive argon flow. The reaction vessel was then sealed, placed in an oil bath at 25 °C and the reaction mixture stirred for 30 min. The reaction contents were diluted with dichloromethane and passed through activated basic alumina. The solvent was removed under reduced pressure and the residue dissolved in a minimal amount of dichloromethane. The polymer was precipitated in 10 x volume of MeOH. The resulting white precipitate was collected by vacuum filtration and dried under high vacuum. The resultant crude polymer was then further purified by preparative SEC to remove high molecular weight impurities. The resultant polymer was then re-precipitated from THF into 10 x volume of MeOH, filtered and dried under high vacuum obtained as white powder ($M_{n,RI}$ = 3900, $M_{p,RI}$=4060, PDI = 1.07, yield %= 86 %).

3.2.2.2 Synthesis of trifunctional (8)

Scheme 3.3 Synthetic route for trifunctional linker (**8)**

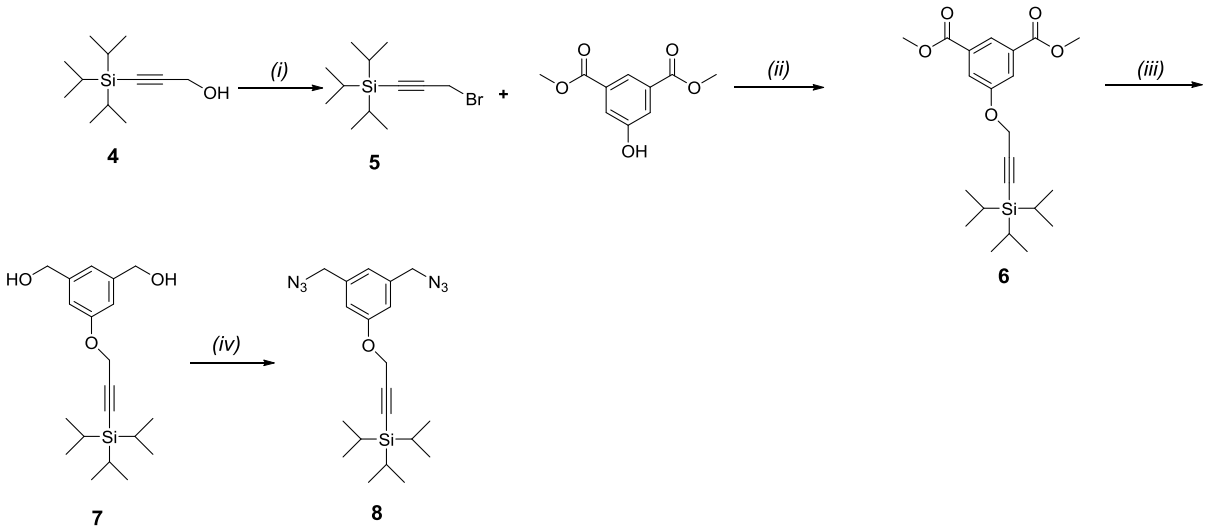

i) CBr_4, PPh_3. ii): 18-C-6, K_2CO_3, Acetone, reflux, 48 h. iii): $LiAlH_4$, THF, 0 ^oC-R.T., 16 h, iv): DPPA, DBU, toluene, 0 ^oC-R.T., dark.

Synthesis (6)

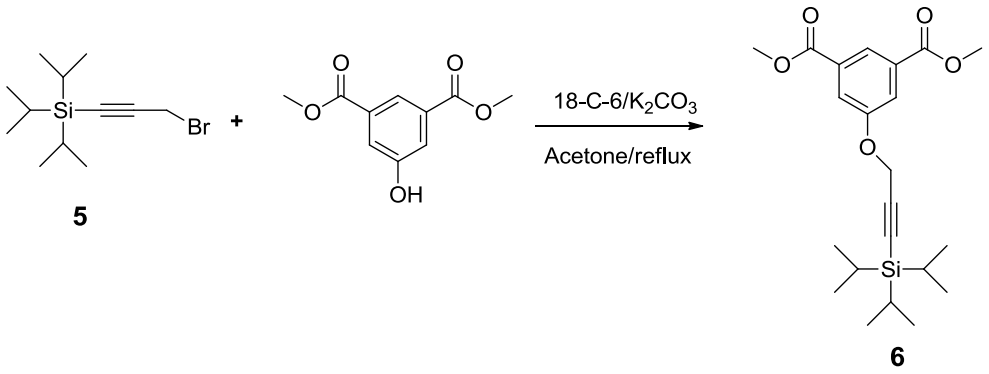

Compound **5** was synthesized according to reference.[52] Dimethyl 5-hydroxyisophthalate (3.2 g, 1.53 x 10^{-2} mol), **5** (2.8 g, 1.01 x 10^{-2} mol) and 18-crown-6 ether (0.40 g, 1.53 x 10^{-2} mol) were dissolved in 80 mL of acetone. Anhydrous potassium carbonate (2.1 g, 0.028 mol) was added and the reaction was refluxed at 70 ^oC for 48 h. The reaction was then cooled to room temperature, filtered, and the filtrate was concentrated by rotary evaporation. The crude product was purified by column chromatography using ethyl acetate/petroleum spirit (1/5,

v/v, R_f=0.43) as the eluent. Upon drying the product, **6** was obtained as white wax solid (3.0 g, 62.0 %).

^{1}H NMR ($CDCl_3$, 298K, 500 MHz): δ 8.30 (t, *J*=1.79 Hz, 1H; aromatic proton), 7.83 (d, *J*=1.80 Hz, 2H; aromatic proton), 4.79 (s, 2H; -SiCCC***H***$_2$O-), 3.91 (s, 6H; C***H***$_3$O-), 0.98 (s, 21H; -SiC***H***$(CH_3)_2$- and -SiCH(C***H***$_3)_2$-). ^{13}C NMR ($CDCl_3$, 298K, 500 MHz) δ, ppm: 11.10, 18.50, 52.46, 57.16, 90.53, 100.89, 120.77, 123.76, 131.78, 157.63, 166.07.

Synthesis (7)

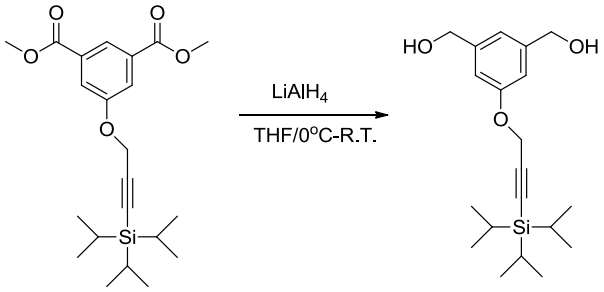

6 **7**

6 (3.0 g, 7.42 x 10^{-3} mol) was dissolved in 60 mL of dry THF at 0 ^{o}C under argon. Lithium aluminium hydride (0.65 g, 0.017 mol) was added to the solution portion-wise over 30 min. After stirring for 16 h, the reaction was quenched by slowly adding crushed $Na_2SO_4.10H_2O$. *Caution! Hydrogen is produced.* The mixture was filtered and the filtrate concentrated by rotary evaporation. The product was purified by column chromatography using MeOH/DCM (1/10, v/v, R_f=0.38) as the eluent, and the product, **7**, was obtained as white solid (1.8 g, 70 %).

^{1}H NMR ($CDCl_3$, 298K, 400 MHz): δ 6.92 (s, 1H; aromatic proton), 6.93 (s, 2H; aromatic proton), 4.72 (s, 2H; -SiCCC***H***$_2$O-), 4.64 (s, 4H; OHC***H***$_2$C-), 1.01 (s, 21H; -SiC***H***$(CH_3)_2$- and -SiCH(C***H***$_3)_2$-). ^{13}C NMR ($CDCl_3$, 298K, 400 MHz) δ, ppm: 11.05, 18.48, 56.76, 65.04, 89.30, 101.87, 112.86, 118.07, 142.67, 158.10.

Synthesis (8)

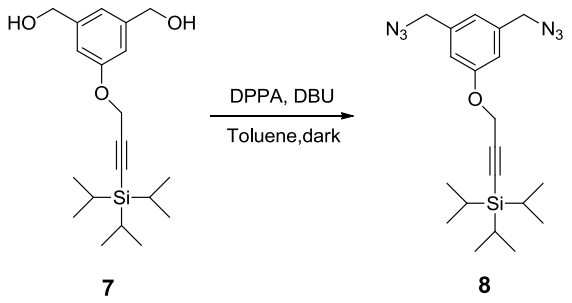

7 **8**

7 (1.8 g, 5.17 x 10^{-3} mol), DPPA (3.55 g, 1.29 x 10^{-2} mol) and DBU (1.96 g, 1.29 x 10^{-2} mol) were added to 35 mL of dry toluene at 0 ^{o}C. The flask was wrapped in aluminium foil to avoid light. The solution was stirred for 16 h, and then poured into a separation funnel. The colorless toluene phase was then collected and concentrated by rotary evaporation. The product was purified by column chromatography using ethyl acetate/petroleum spirit (1/6, v/v, R_f=0.48) as the eluent and the product, **8**, was obtained as a colorless oil (1.62 g, 79.0 %).

^{1}H NMR ($CDCl_3$, 298K, 500 MHz): δ 6.92 (s, 2H; aromatic proton), 6.86 (s, 1H; aromatic proton), 4.732 (s, 2H; -SiCCC***H***$_2$O-), 4.30 (s, 4H; N_3C***H***$_2$C-), 1.01 (s, 21H; -SiC***H***$(CH_3)_2$- and -SiCH(C***H***$_3)_2$-). ^{13}C NMR ($CDCl_3$, 298K, 500 MHz) δ, ppm: 11.15, 18.58, 54.59, 56.76, 89.94, 101.53, 114.85, 120.50, 137.55, 158.47.

3.2.2.3 Synthesis of Tips-alk-PS(N_3) (9)

Synthesis of (9)

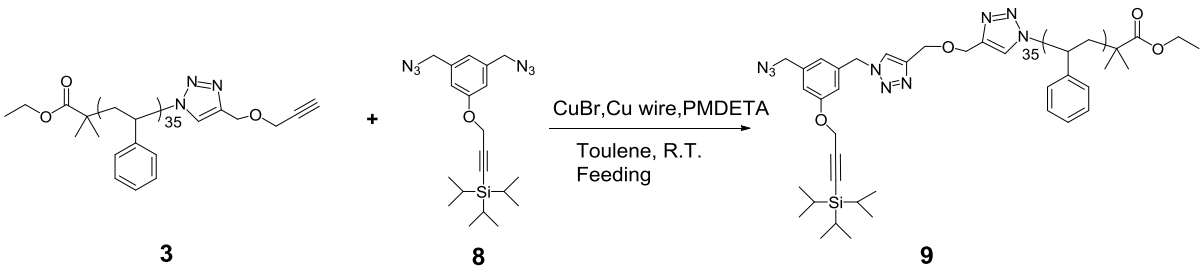

3 **8** **9**

A solution of **3** (0.40 g, 1.038 x 10^{-4} mol) in 6 mL toluene was purged with argon for 45 min to remove oxygen. Meanwhile, a mixture of **8** (0.398 g, 1.038 x 10^{-3} mol), PMDETA (20.8 µL, 1.038 x 10^{-4} mol), 4 mL toluene was degassed by argon for 45 min, the

deoxygenated mixture above was then added into a Schlenk tube containing Cu(I)Br and Cu wire (12.5 cm, surface area 3.54 cm^3) under positive argon flow. After that, the solution of **3** was added via syringe pump, at a flow rate of 0.04 mL min^{-1}, and after feeding the reaction was allowed to react for 1 h. The copper salts were removed by passage through activated basic alumina. The solvent was removed under reduced pressure. The resultant crude polymer was then further purified by preparative SEC to remove high molecular weight impurities. The resultant polymer was then precipitated from THF into 10 x volume of MeOH, filtered and dried under high vacuum obtained as white powder ($M_{n,RI}$ = 4350, $M_{p,RI}$=4530, PDI = 1.06, yield %= 67 %).

3.2.2.4 Synthesis of Tips-alk-$(PSTY)_2$ (10)

Synthesis of (10)

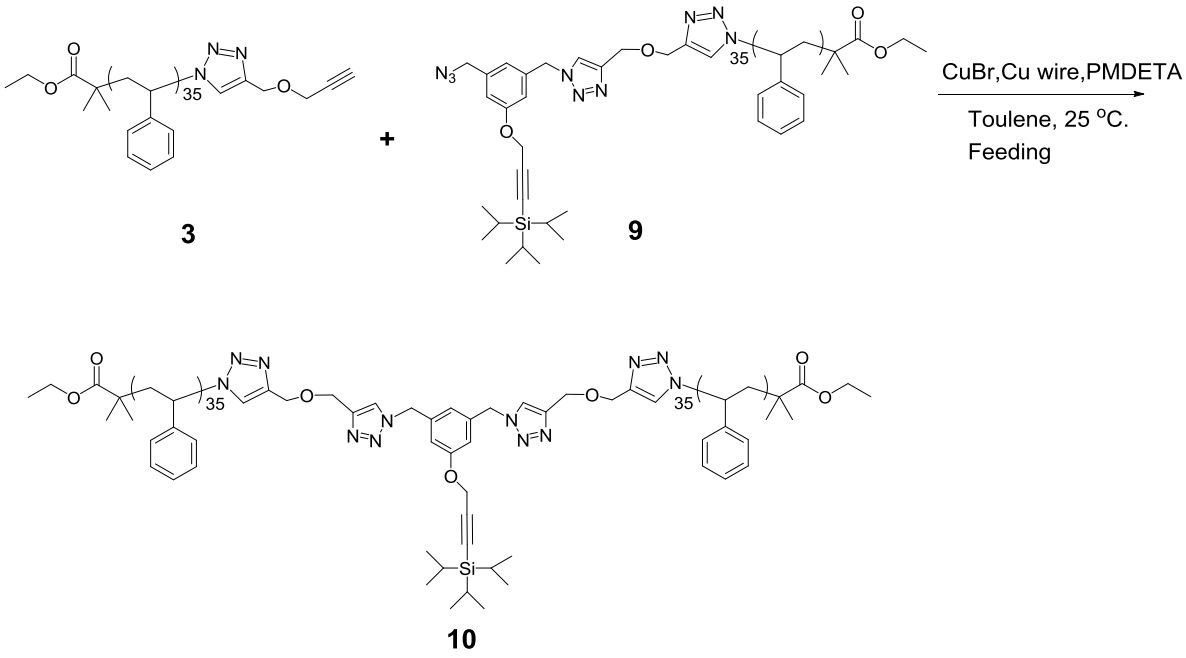

A mixture of **3** (0.2 g, 5.256 x 10^{-5} mol), **9** (0.24 g, 5.518 x 10^{-5} mol), PMDETA (54.7 µL, 2.628 x 10^{-5} mol) and 8 mL toluene was purged with argon for 45 min to remove oxygen. The deoxygenated mixture above was then added into a Schlenk tube containing Cu(I)Br (37 mg, 2.628 x 10^{-5} mol) and Cu wire (12.5 cm, surface area 3.54 cm^3) under positive argon flow. The reaction was allowed to react for 1 h. The copper salts were removed by passage through activated basic alumina. The solvent was removed under reduced pressure. The resultant crude polymer was then further purified by preparative SEC to remove low

molecular weight impurities. The resultant polymer was then re-precipitated from THF into 10 x volume of MeOH, filtered and dried under high vacuum obtained as white powder ($M_{n,RI}$ = 8880, $M_{p,RI}$=8970, PDI = 1.03, yield %= 80 %).

3.2.2.5 Synthesis of Alk-$(PSTY)_2$ (11)

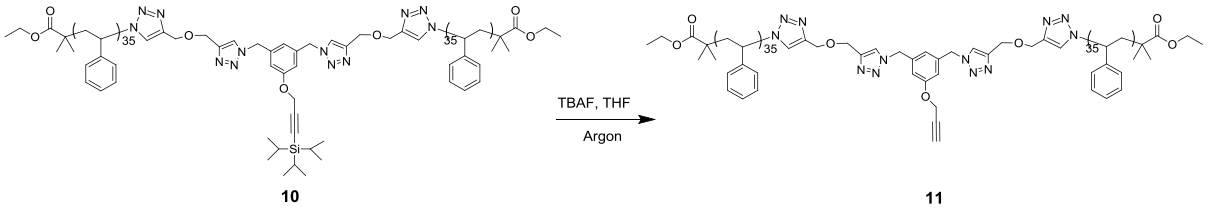

10 11

10 (0.2 g, 2.25 x 10^{-5} mol) was dissolved in 4 mL dry THF in a Schlenk tube equipped with magnetic stirrer. To this solution, 22 µL TBAF (1M in THF) was added and the mixture stirred for 24 h at 25 ^{o}C under argon protection. The polymer solution was directly precipitated into 10 x volume of MeOH, filtered and dried under high vacuum obtained as white powder ($M_{n,RI}$ = 8420, $M_{p,RI}$=8610, PDI = 1.04, yield %= 90 %).

3.2.2.6 Synthesis of difunctional linker (13)

Scheme 3.4 Synthesis of diazide linker

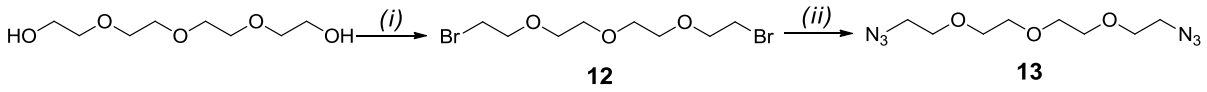

12 13

(i) CBr_4, PPh_3; (ii) NaN_3, DMF, 24 h.

Synthesis of (12)

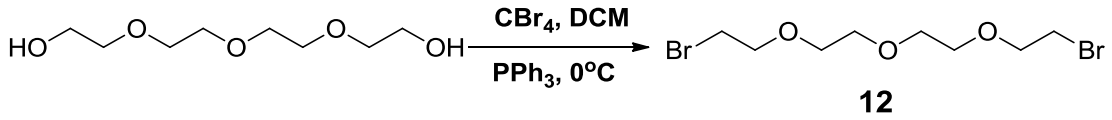

12

To a 250 mL round bottom flask, tetraethylene glycol (5g, 0.258 mol) and tetrabromomethane (21.3 g, 0.644 mol) were dissolved in 60 mL DCM with virgrous stirring. The triphenylphosphine (21.5 g, 0.824 mol) was added protion-wise into the solution above in 30 min. The reaction was kept stirring for 12 h. The solid content was filtered out, and filtrate was concentrated via reduced pressure. The brown crude product was further purified by column chromatography using ethyl acetate/petroleum spirit (1/2, v/v, R_f=0.40) as the eluent and the product, **12** was obtained as a colorless oil (6.7 g, 78.0 %).

^{1}H NMR ($CDCl_3$, 298K, 400 MHz): δ 3.81 (t, 2H; -$CH_2C\boldsymbol{H}_2O$-), 3.68 (s, 8H; -$C\boldsymbol{H}_2CH_2O$-,-$CH_2C\boldsymbol{H}_2O$-), 3.47 (t, 2H, Br$C\boldsymbol{H}_2CH_2$-). ^{13}C NMR ($CDCl_3$, 298K, 400 MHz) δ, ppm: 30.48, 70.62, 70.74, 71.29.

Synthesis of (13)

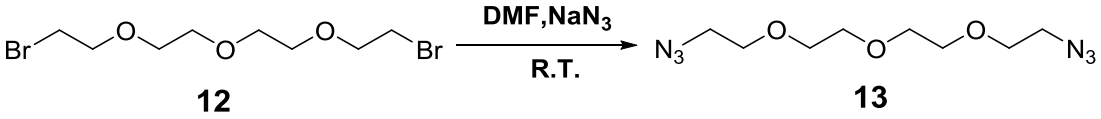

12 **13**

NaN_3 (9.3 g, 1.432 x 10^{-1} mol) was added to a stirring solution of **12** (5 g, 1.56 x 10^{-2} mol) in DMF (6.0 mL). The reaction mixture was stirred for 20 h at 25 °C. The solvent was remove by reduced pressure, and the residue was redissolved in DCM (150 mL) followed by washing with water (twice, 30 mL). The organic phase was dried over anhydrous $MgSO_4$, the solvent was removed by reduced pressure and resultant sample was dried in high vacuum for 24 h, obtained as colorless oil **13** (3.2 g, 84.2%)

^{1}H NMR ($CDCl_3$, 298K, 500 MHz): δ 3.69 (s, 12H; -$C\boldsymbol{H}_2CH_2O$-,-$CH_2C\boldsymbol{H}_2O$-), 3.37 (t, 4H, *J*=5.02 Hz, Br$C\boldsymbol{H}_2CH_2$-).^{13}C NMR ($CDCl_3$, 298K, 500 MHz) δ, ppm: 50.8, 70.15, 70.83.

3.2.2.7 Synthesis of N_3-$(PSTY)_2$ (14)

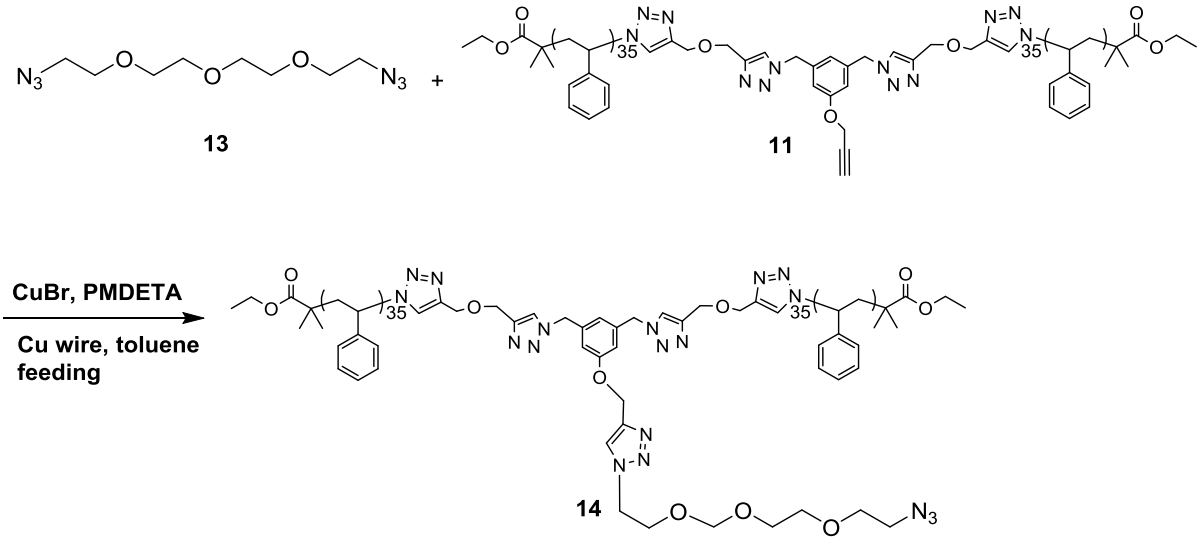

A solution of **11** (0.1 g, 1.18 x 10^{-5} mol) in 2.5 mL toluene was purged with argon for 45 min to remove oxygen. Meanwhile, a mixture of **13** (87 mg, 3.54 x 10^{-4} mol), PMDETA (2.0

µL, 1.18 x 10^{-5} mol), 1.5 mL toluene was degassed by argon for 45 min, the deoxygenated mixture above was then added into a Schlenk tube containing Cu(I)Br and Cu wire (12.5 cm, surface area 3.54 cm^3) under positive argon flow. After that, the solution of **11** was added via syringe pump, at a flow rate of 0.02 mL/min, and after feeding the reaction was allowed to react for 1 h. The copper salts were removed by passage through activated basic alumina. The solvent was removed under reduced pressure. The resultant crude polymer was then further purified by preparative SEC to remove high molecular weight impurities. The resultant polymer was then precipitated from THF into 10 x volume of MeOH, filtered and dried under high vacuum obtained as white powder ($M_{n,RI}$ = 8700, $M_{p,RI}$=8980, PDI = 1.03, yield %= 66 %).

3.2.2.8 Synthesis of 4-arm PSTY (15)

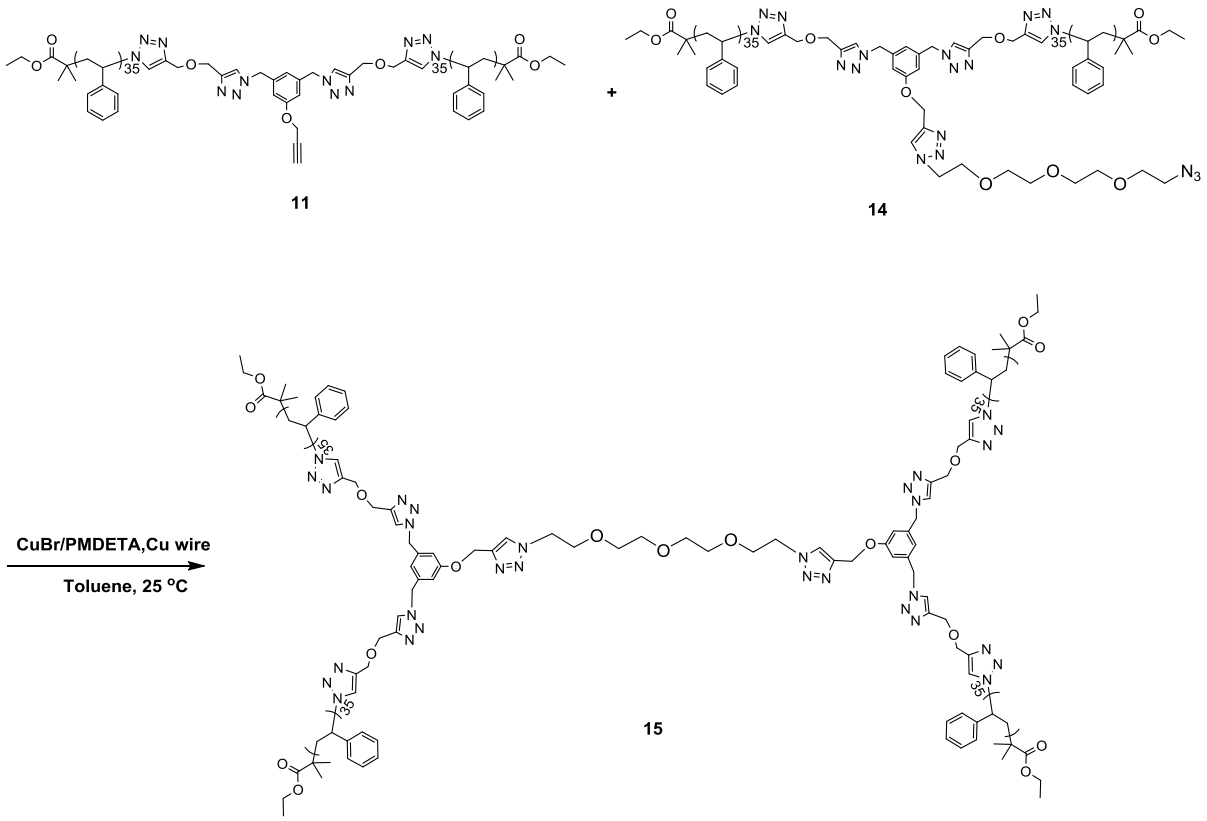

A mixture of **11** (0.0176 g, 2.089 x 10^{-6} mol), **14** (0.020 g, 2.298 x 10^{-6} mol) , PMDETA (1.44 µL, 8.359 x 10^{-6} mol) and 4 mL toluene was purged with argon for 30 min to remove oxygen. The deoxygenated mixture above was then added into a Schlenk tube containing Cu(I)Br (1.2 mg, 8.359 x 10^{-6} mol) and Cu wire (12.5 cm, surface area 3.54 cm^3) under positive argon flow. The reaction was allowed to react for 1 h at 25 °C. The copper salts were

removed by passage through activated basic alumina. The solvent was removed under reduced pressure. The resultant crude polymer was then further purified by preparative SEC to remove low molecular weight impurities. The resultant polymer was then re-precipitated from THF into 10× volume of MeOH, filtered and dried under high vacuum obtained as white powder ($M_{n,RI}$ = 15820, $M_{p,RI}$ =16320, PDI = 1.04, $M_{n,TD}$ = 17200, $M_{p,TD}$ =18030, PDI = 1.02, yield %= 70 %, overall yeild %=24 %).

3.2.2.9 Synthesis of PEG-alk (16)

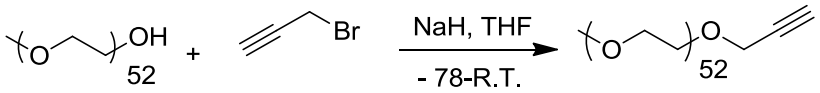

16

Briefly, Sodium hydride (0.15 g, 3.75 x 10^{-3} mol, 60 % in mineral oil) was added to 30 mL of dry THF under argon and cooled to 0 ^{o}C. To this suspension, PEG_{52}-OH (5.00 g, 2.50 x 10^{-3} mol) was added portionwise and stirred until dissolved before propargyl bromide (1.39 mL, 1.25 x 10^{-2} mol, 80 % in toluene) was added directly. The solution was stirred at 0 ^{o}C for 30 min then R.T. for 24 h after which saturated NH_4Cl solution (10 mL) was slowly added to quench the reaction. The solution was then extracted with DCM (50 mL) and the organic phase was then washed with brine (3 x 50 mL). The organic phase was collected, dried with anhydrous $MgSO_4$, filtered and taken to dryness. The light brown solid was redissolved in a minimum volume of DCM and precipitated (twice) into diethyl ether. The solid was then collected by vacuum filtration, washed with diethyl ether, collected and dried under high vacuum obtained as white powder ($M_{n,RI}$ = 2780, $M_{p,RI}$ =2870, PDI = 1.04, $M_{n,TD}$ = 2200, $M_{p,TD}$ =2390, PDI = 1.04).

3.2.2.10 Synthesis of Tips-alk-PSTY-PEG (17)

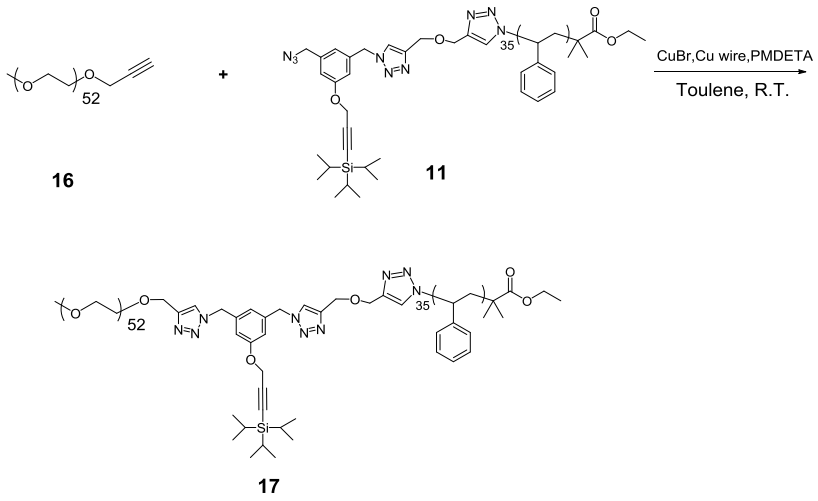

A mixture of **16** (0.059 g, 2.681 x 10^{-5} mol), **11** (0.093 g, 2.137 x 10^{-5} mol), PMDETA (1.84 µL, 1.068 x 10^{-5} mol) and 5 mL toluene was purged with argon for 30 min to remove oxygen. The deoxygenated mixture above was then added into a Schlenk tube containing Cu(I)Br (1.59 mg, 1.068 x 10^{-5} mol) and Cu wire (12.5 cm, surface area 3.54 cm^3) under positive argon flow. The reaction was allowed to react for 1 h. The copper salts were removed by passage through activated basic alumina. The solvent was removed under reduced pressure. The resultant crude polymer was then further purified by preparative SEC to remove low molecular weight impurities. The resultant polymer was recovered by freeze-drying and obtained as white powder ($M_{n,RI}$ = 7450, $M_{p,RI}$=7550, PDI = 1.03; $M_{n,TD}$ = 7040, $M_{p,TD}$=7160, PDI = 1.02, Yield %= 73 %).

3.2.2.11 Synthesis of Alk-PSTY-PEG (18)

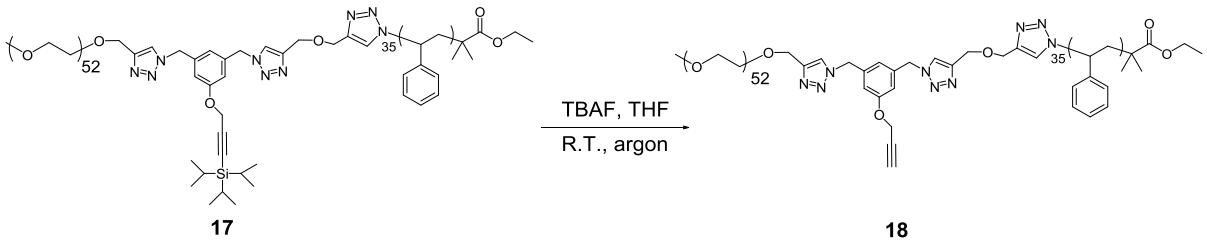

17 18

17 (0.076 g, 1.492 x 10^{-4} mol) was dissolved in 2 mL dry THF in a Schlenk tube equipped with magnetic stirrer. To this solution, 149 µL TBAF (1M in THF) was added and the mixture stirred for 24 h at 25 ^{o}C under argon protection. The TBAF salts were removed by passage through activated basic alumina. The product was recovered by freeze-drying obtained as white powder **18**. ($M_{n,RI}$ = 6600, $M_{p,RI}$=7100, PDI = 1.05; $M_{n,TD}$ = 6390, $M_{p,TD}$=6680, PDI = 1.02, , Yield %= 75 %).

3.2.2.12 Synthesis of N_3-PSTY-PEG (19)

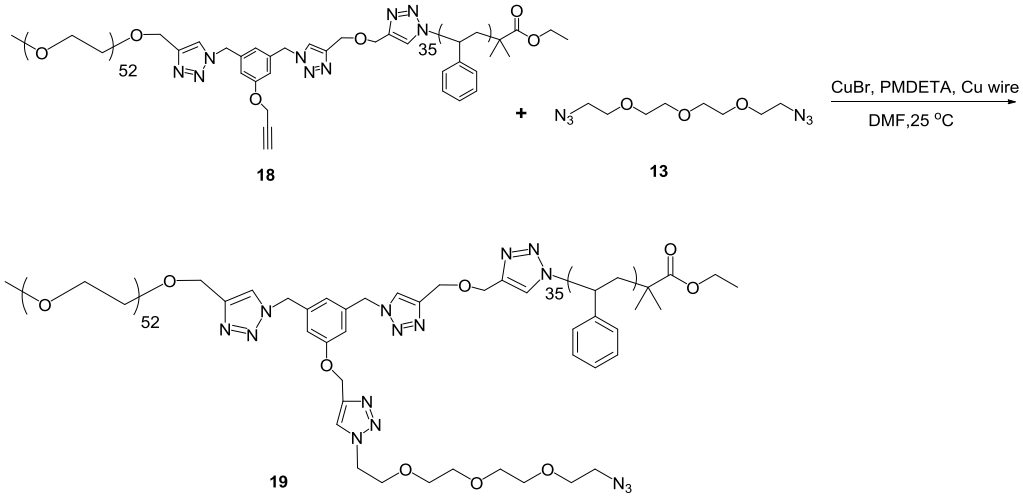

18 13 19

A solution of **18** (0.030 g, 4.40 x 10^{-6} mol) in 1.5 mL toluene was purged with argon for 30 min to remove oxygen. Meanwhile, a mixture of **13** (32 mg, 1.32 x 10^{-5} mol), PMDETA (1.8 µL, 8.80 x 10^{-6} mol), 1.5 mL toluene was degassed by argon for 30 min, the deoxygenated mixture above was then added into a Schlenk tube containing Cu(I)Br and Cu wire (12.5 cm, surface area 3.54 cm^3) under positive argon flow. After that, the solution of **18** was added via syringe pump, at a flow rate of 0.02 mL min^{-1}, and after feeding the reaction was allowed to react for 1 h at 25 ^{o}C. The copper salts were removed by passage through activated basic alumina. The solvent was removed under reduced pressure. The resultant

crude polymer was then further purified by preparative SEC to remove any low or high molecular weight impurities. The resultant polymer was then recovered by freeze-drying obtained as white powder ($M_{n,RI}$ = 6730, $M_{p,RI}$=7070, PDI = 1.05; $M_{n,TD}$ = 6640, $M_{p,TD}$=6860, PDI = 1.02, Yield %= 86 %).

3.2.2.13 Synthesis of P^{t}BA-alk (22)

Scheme 3.5 Synthesis of alk-P^{t}BA, 22

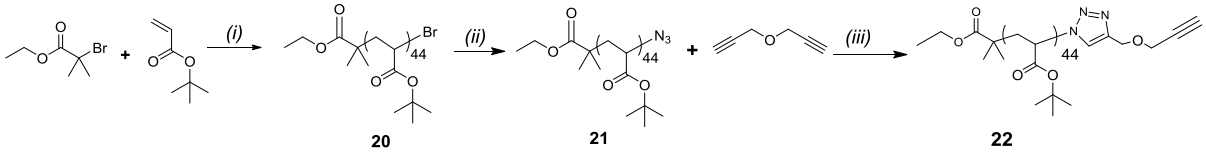

(i) Cu(0), <425µm, Me_6TREN, $CuBr_2$/Me_6TREN, DMSO, Acetone, 22 ^oC; (ii) DMF, NaN_3, 24 h; (iii) CuBr, Cu wire, PMDETA, toluene, 25 ^oC, 30min.

Synthesis of (20)

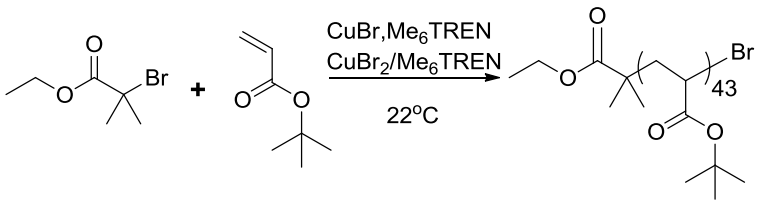

P^{t}BA was synthesized according the literature.[53] *tert*-Butyl Acrylate (^{t}BA) (9.84 g, 0.076 mol), Me_6TREN (0.308 mL, 1.15 x 10^{-3} mol), Cu(II)Br_2/Me_6TREN (0.105 g, 2.3 x 10^{-4} mol), ethyl 2-bromo-2-methylpropionate (0.226 mL, 1.54 x 10^{-3} mol), DMSO (0.7 mL) and acetone (8 mL) were added to a 25 mL Schlenk flask equipped with a magnetic stirrer. The reaction mixture was cooled down to 0 ^oC and purged with argon for 30 min to remove oxygen. Cu powder (0.074 g, 1.15 x 10^{-3} mol) was then carefully added to the solution under an argon blanket. The reaction mixture was further degassed for 5 min at 0 ^oC and then placed into a temperature controlled water bath at 22 ^oC for 50 min. The reaction was quenched by cooling in liquid nitrogen, exposure to air, and dilution with DCM (*ca.* 3 fold to the reaction mixture volume). The copper salts were removed by passage through an activated basic alumina column. The solution was concentrated by rotary evaporator and the

polymer was precipitated into cold MeOH/water mixture (40:60 v/v, 20 fold excess to polymer solution) twice. The polymer (viscous glassy solid) was dried *in vacuo* for 24 h at 25 ^{o}C obtained as white powder ($M_{n,RI}$ = 5950, $M_{p,RI}$= 6150, PDI = 1.05).

Synthesis of (21)

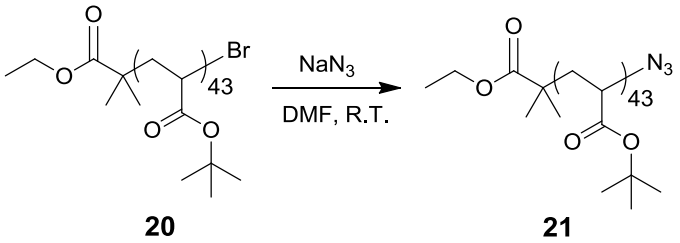

20 (3.8 g, 6.22 x 10^{-4} mol) was dissolved in 25 mL of DMF in a 50 mL reaction vessel equipped with magnetic stirrer. To this solution NaN_3 (0.61 g, 9.34 x 10^{-3} mol) was added and the mixture stirred overnight at 25 ^{o}C. The polymer solution was concentrated by airflow to approximately a third of the original volume and precipitated into cold MeOH/water mixture (20:80 v/v, ~10 fold excess to polymer solution) from DMF. All liquid was decanted and the polymer **21** (viscous solid) was then dried *in vacuo* for 24 h at 25 ^{o}C. ($M_{n,RI}$ = 6030, $M_{p,RI}$=6180, PDI = 1.06).

Synthesis of (22)

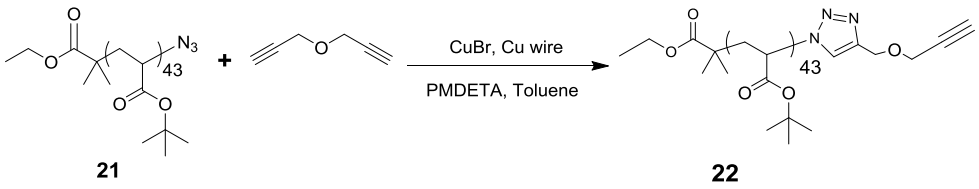

Propargyl ether (0.462 g, 4.91 x 10^{-3} mol), PMDETA (5.1 µL, 2.46 x 10^{-5} mol), P^{t}BA-N_3 (**20**) (1 g, 1.63 x 10^{-4} mol) and toluene (5 mL) were added to a 20 mL vial and purged with argon for 30 min, degassed solution was transferred into a Schlenk tube containing CuBr (3.5 mg, 2.46 x 10^{-5} mol) and Cu wire (12.5 cm, surface area 3.54 cm^3) under a positive argon flow. The reaction vessel was then sealed, placed in an oil bath at 25 °C and the reaction mixture stirred for 30 min. The reaction contents were diluted with dichloromethane and passed through activated basic alumina. The solvent was removed under reduced pressure

and the residue dissolved in a minimal amount of acetone. The polymer was precipitated in cold MeOH/water mixture (20:80 v/v, ~10 fold excess to polymer solution). The resulting white precipitate was collected by vacuum filtration and dried under high vacuum. The resultant crude polymer was then further purified by preparative SEC to remove high molecular weight impurities. The resultant polymer was then re-precipitated from THF into cold MeOH/water mixture (20:80 v/v, ~10 fold excess to polymer solution), filtered and dried under high vacuum obtained as white powder ($M_{n,RI}$ = 5930, $M_{p,RI}$=6110, PDI = 1.05, Yield %= 81 %).

3.2.2.14 Synthesis of Tips-alk-P^{t}BA(N_3) (23)

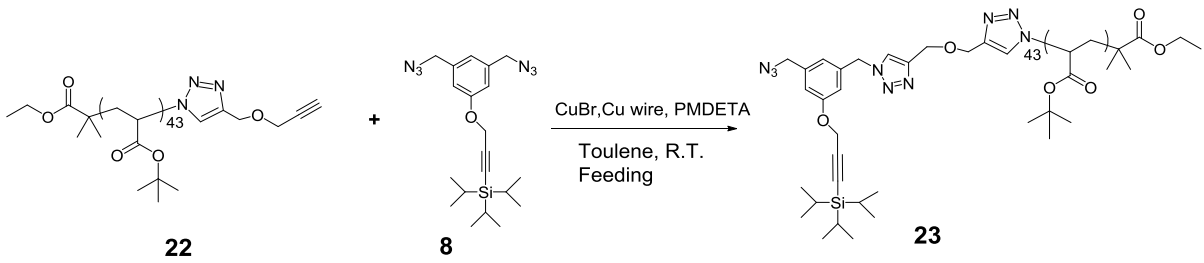

22 8 23

A solution of **22** (0.34 g, 5.11 x 10^{-5} mol) in 7 mL toluene was purged with argon for 45 min to remove oxygen. Meanwhile, a mixture of **8** (0.345 g, 7.65 x 10^{-4} mol), PMDETA (10.6 µL, 5.11 x 10^{-5} mol), 3 mL toluene was degassed by argon for 45 min, the deoxygenated mixture above was then added into a Schlenk tube containing CuBr (7.3 mg, 5.11 x 10^{-5} mol) and Cu wire (12.5 cm, surface area 3.54 cm^3) under positive argon flow. After that, the solution of **22** was added via syringe pump, at a flow rate of 0.04 mL min^{-1}, and after feeding the reaction was allowed to react for 1 h. The copper salts were removed by passage through activated basic alumina. The solvent was removed under reduced pressure. The resultant crude polymer was then further purified by preparative SEC to remove high molecular weight impurities. The resultant polymer was then precipitated from THF into 10 x volume of MeOH, filtered and dried under high vacuum obtained as white powder ($M_{n.RI}$ = 6240, $M_{p,RI}$ = 6360, PDI = 1.03, Yield %= 76 %).

3.2.2.15 Synthesis of PNIPAm-alk (27)

Scheme 3.6 Synthetic route of PNIPAm-alk, 27.

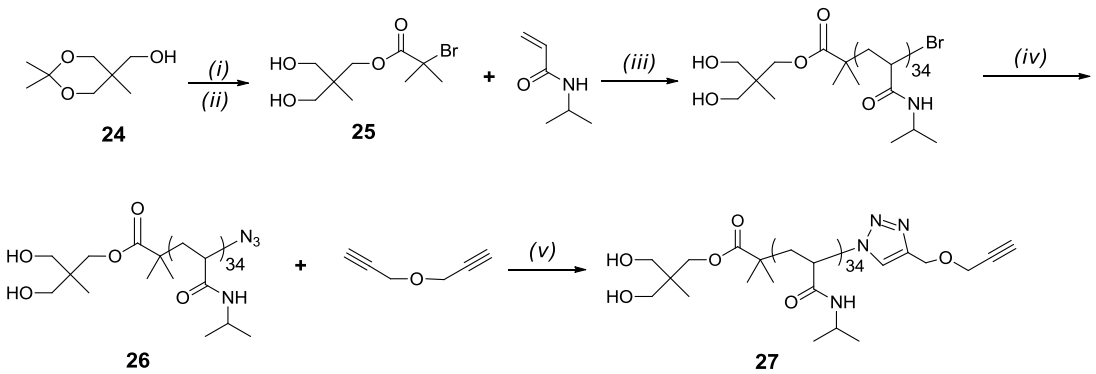

24 25 26 27

(i) TEA, 2-bromoisobutyryl bromide, THF, 0 ^oC-R.T.; (iii) $CuBr_2$, $NaBH_4$, Me_6TREN, H_2O, 0 ^oC; (iv) NaN_3, H_2O; (v) CuBr, Cu wire, PMDETA, DMF, 50 ^oC, 30min.

Synthesis of (25)

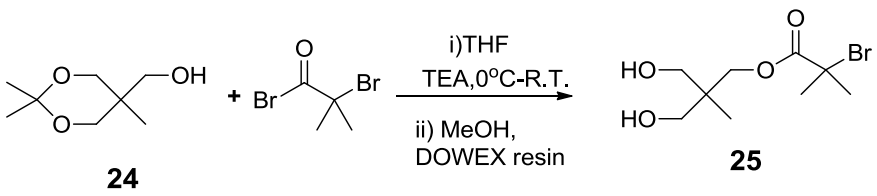

24 **25**

(2,2,5-trimethyl-1,3-dioxan-5-yl)methanol, **24** was synthesized according to the literature.[53] **24** (8.11 g, 0.051 mol) and TEA (7.81 g, 0.0765 mol) were dissolved in 140 mL of dry THF and cooled to 0 °C in an ice-bath. To the above solution, 2-bromoisobutyryl bromide (15.41 g, 0.0663 mol) was added drop-wise over 30 min. The reaction was allowed to slowly warm up to RT and then stirred overnight. The reaction mixture was filtered to remove salts, concentrated and dried under high vaccum at RT. The brown crude product was directly dissolved in 60 mL of dry methanol, and DOWEX (5.00 g) was added to the solution and stirred overnight. The DOWEX resin was filtered and the solution was concentrated and further purified by distillation under reduced pressure, followed by column chromatography with EtOAc/petroleum spirit (3/2, v/v) as eluent. The fraction with R_f as 0.40 was collected and concentrated to obtain a colorless viscous liquid (6.5 g, yield = 42 %).

^{1}H NMR ($CDCl_3$, 298K, 500 MHz); δ 4.25 (s, 2H, -CC***H***$_2$O-), 3.59 (dd, 4H, *J*=11.3 Hz *J*=4.35 Hz; OHC***H***$_2$C-), 2.61 (b, 2H; O***H***CH_2-), 1.92 (s, 6H; C***H***$_3$CBr), 0.87 (s, 3H; C***H***$_3$C-); ^{13}C NMR ($CDCl_3$, 298K, 500 MHz); 68.08, 67.77, 55.83, 41.24, 30.84, 16.86.

Synthesis of (26)

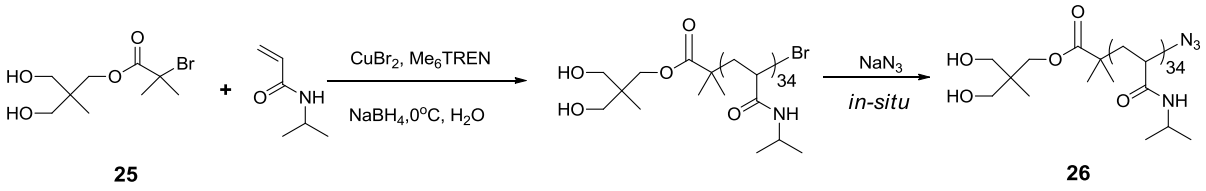

25 **26**

To a 100 mL Schlenk flask equipped with magnetic stirrer, $CuBr_2$ (0.132 g, 5.94 x 10^{-4} mol), Milli-Q water (28.4 mL), Me_6TREN (0.238 mL, 8.92 x 10^{-4} mol), NIPAm (3.36 g, 0.297 mol), and initiator **25** (0.2 g, 7.43 x 10^{-4} mol) were added. The tube was sealed with rubber septum and bubbled with argon for 30 min. After that, the tube was immersed in an ice-bath and bubbled with argon for another 30 min. Meanwhile, $NaBH_4$ and Milli-Q water

were sealed in 20 mL vial and purged with argon for 60 min. Degassed Milli-Q water (5.6 mL) was transferred into the vial containing $NaBH_4$ (5.6 mg, 1.486 x 10^{-4} mol) to form 1 mg mL^{-1} stock solution. The stock solution was added into the Schlenk tube to initiate the SET-LRP. A mixture of NaN_3 (1.93 g, 0.0297 mol) and Milli-Q water (19.2 mL) was purged by argon for 60 min. After 60 min, the SER-LRP was quenched by adding the degassed NaN_3 solution into the Schlenk flask above via syringe, and kept stirring for 24 h. The reaction mixture was then recovered by freeze-drying directly, redissolved in DCM followed by passing through activated basic alumina to remove copper salts. The solution was concentrated, and precipitated in 10× volume of Et_2O. The white precipitate was collected by vacuum filtration and dried under high vacuum obtained as white powder. ($M_{n,RI}$ = 2200, $M_{p,RI}$=2410, PDI = 1.10; $M_{n,TD}$ =4050 , $M_{p,TD}$=4180, PDI = 1.02).

Synthesis of (27)

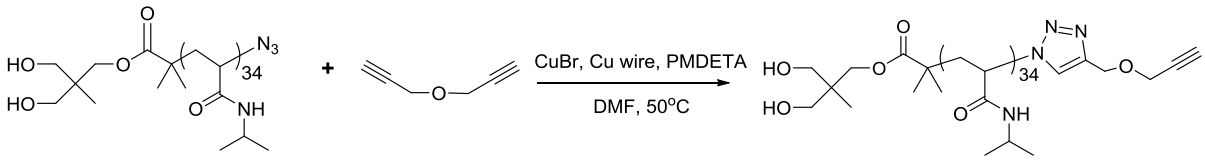

26 **27**

Propargyl ether (1.85 g, 1.98 x 10^{-2} mol), PMDETA (13 µL, 6.17 x 10^{-5} mol), PNIPAm-N_3 (**26**) (1 g, 2.46 x 10^{-4} mol) and DMF (8 mL) were added to a 20 mL vial and purged with argon for 60 min, degassed solution was transferred into a Schlenk tube containing Cu(I)Br (8.8 mg, 6.17 x 10^{-5} mol) and Cu wire (12.5 cm, surface area 3.54 cm^3) under a positive argon flow. The reaction vessel was then sealed, placed in an oil bath at 25 °C and the reaction mixture stirred for 30 min. The reaction contents were diluted with DCM and passed through activated basic alumina. The solvent was removed under reduced pressure and the residue dissolved in a minimal amount of DCM. The solution was dialysis against with MeOH for 2 days to remove unreacted propargyl ether. The polymer was precipitated in 10 x volume of Et_2O. The white precipitate was collected by vacuum filtration and dried under high vacuum obtained as white powder ($M_{n,RI}$ = 2650, $M_{p,RI}$=2820, PDI = 1.09; $M_{n,TD}$ =4230 , $M_{p,TD}$=4290, PDI = 1.02, Yield %= 84 %).

3.2.2.16 Synthesis of Tips-alk-P^{t}BA-PNIPAm (28)

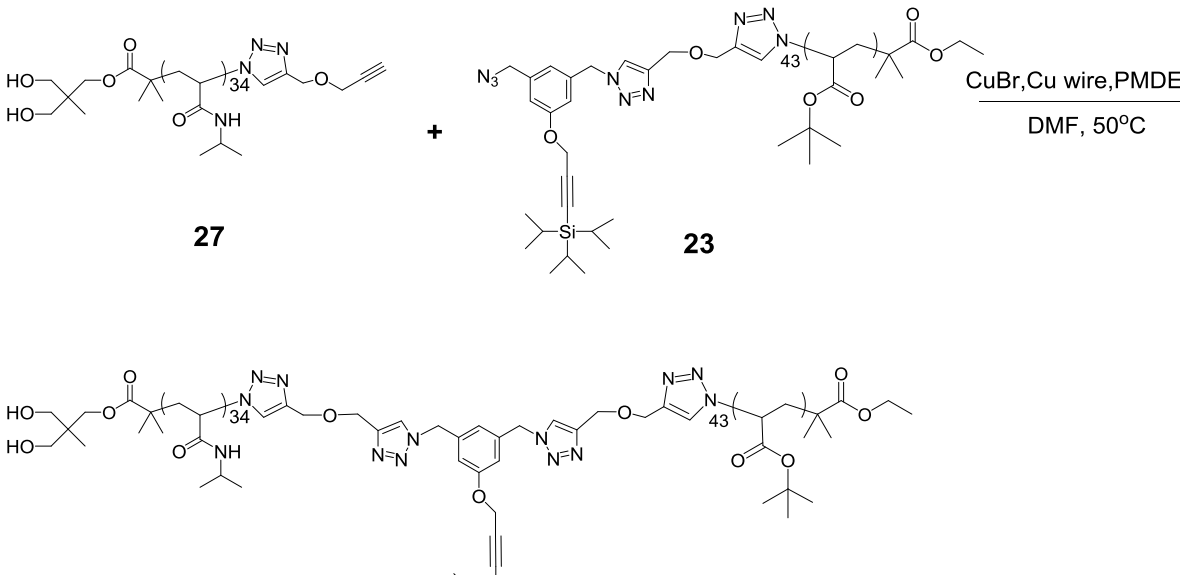

A mixture of **23** (0.075 g, 1.20 x 10^{-5} mol), **27** (0.056 g, 1.32 x 10^{-5} mol), PMDETA (2.5 µL, 1.20 x 10^{-5} mol) and 5 mL toluene was purged with argon for 30 min to remove oxygen. The deoxygenated mixture above was then added into a Schlenk tube containing CuBr (1.71 mg, 1.20 x 10^{-5} mol) and Cu wire (12.5 cm, surface area 3.54 cm^3) under positive argon flow. The reaction was allowed to react for 2 h at 50 ^oC. The copper salts were removed by passage through activated basic alumina. The solvent was removed under reduced pressure. The resultant crude polymer was then further purified by preparative SEC to remove low molecular weight impurities. The resultant polymer was then recovered from freeze dry obtained as white powder ($M_{n,RI}$ = 9450, $M_{p,RI}$=9471, PDI = 1.05; $M_{n,TD}$ = 10694, $M_{p,TD}$=10958, PDI = 1.03, Yield %= 75 %).

3.2.2.16 Synthesis of Alk-P^{t}BA-PNIPAm (29)

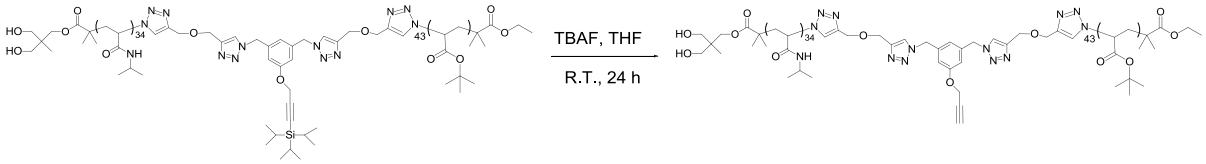

28 **29**

28 (0.092 g, 7.80 x 10^{-6} mol) was dissolved in 4 mL dry THF in a Schlenk tube equipped with magnetic stirrer. To this solution, 156 µL TBAF (1 M in THF) was added and the mixture stirred for 24 h at 25 ^{o}C under argon protection. The TBAF salts were removed by passage through activated basic alumina. The product was recovered by freeze-drying obtained as white powder **29**. ($M_{n,RI}$ = 9000, $M_{p,RI}$=9150, PDI = 1.05; $M_{n,TD}$ = 10220, $M_{p,TD}$=10580, PDI = 1.03, Yield %= 93 %).

Synthesis of (30)

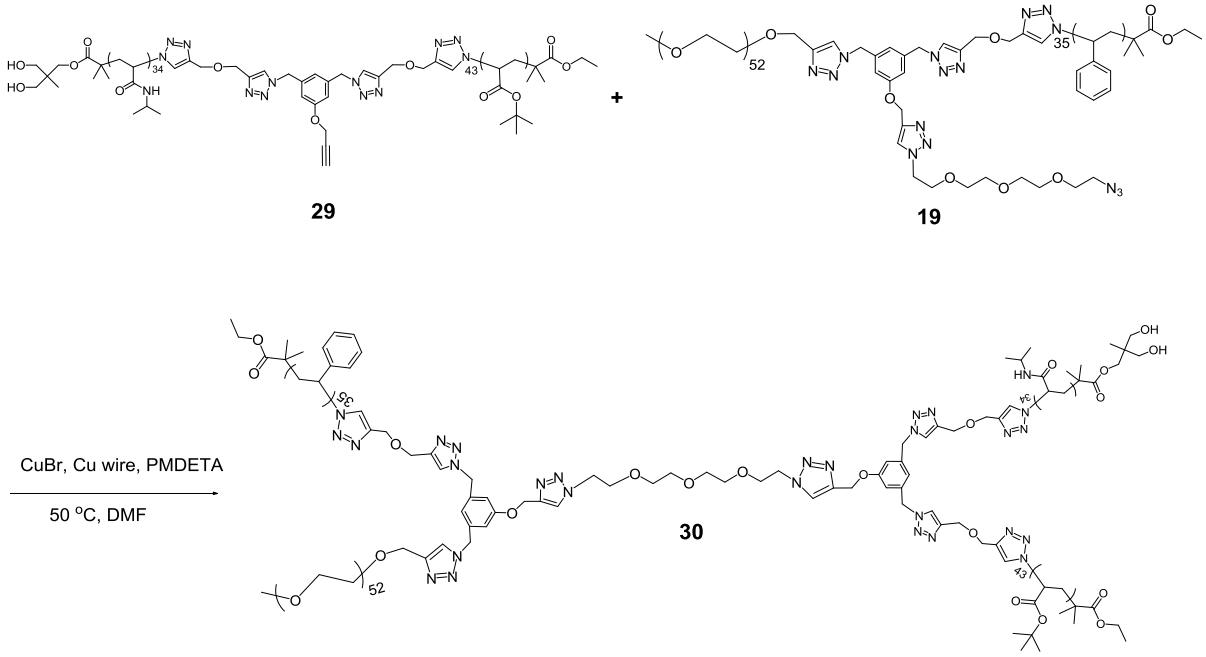

29 **19** **30**

A mixture of **19** (0.05 g, 7.5 x 10^{-6} mol), **29** (0.064 g, 6.2 x 10^{-6} mol), PMDETA (1.1 µL, 5.7 x 10^{-6} mol) and 2 mL DMF was purged with argon for 30 min to remove oxygen. The deoxygenated mixture above was then added into a Schlenk tube containing Cu(I)Br (0.8 mg, 5.7 x 10^{-6} mol) and Cu wire (12.5 cm, surface area 3.54 cm^{3}) under positive argon flow. The reaction was allowed to react for 2 h at 50 ^{o}C. The copper salts were removed by passage through activated basic alumina. The solvent was removed under reduced pressure. The

resultant crude polymer was then further purified by preparative SEC to remove low molecular weight impurities. The resultant polymer was then recovered from freeze dry obtained as white powder ($M_{n,RI}$ = 15860, $M_{p,RI}$ =15940, PDI = 1.03, $M_{n,TD}$ = 16760, $M_{p,TD}$ =17020, PDI=1.02, Yield %= 36 %)

3.2.3 Analytical Methodologies

Size Exclusion Chromatography (RI-SEC)

All polymer samples were dried prior to analysis in a vacuum oven for 2 days at 25 ^{o}C. The dried polymer was dissolved in tetrahydrofuran (THF) to a concentration of 1 mg mL^{-1} and then filtered through a 0.45 μm PTFE syringe filter. Analysis of the molecular weight distributions of the polymers was accomplished using a Waters 2695 separations module, fitted with a Waters 410 refractive index detector maintained at 35 ^{o}C, a Waters 996 photodiode array detector, and two Ultrastyragel linear columns (7.8 x 300 mm) arranged in series. These columns were maintained at 40 ^{o}C for all analyses and are capable of separating polymers in the molecular weight range of 500 to 4 million g mol^{-1} with high resolution. All samples were eluted at a flow rate of 1.0 mL min^{-1}. Calibration was performed using narrow molecular weight PSTY standards ($PDI_{RI} \leq 1.1$) ranging from 500 to 2 million g mol^{-1}. Data acquisition was performed using Empower software, and molecular weights were calculated relative to polystyrene standards.

Absolute Molecular Weight Determination by Triple Detection SEC (TD-SEC)

Absolute molecular weights of polymers were determined using a Polymer Laboratories GPC50 Plus equipped with dual angle laser light scattering detector, viscometer, and differential refractive index detector. HPLC grade *N*,*N*-dimethylacetamide (DMAc, containing 0.03 wt % LiCl) was used as the eluent at a flow rate of 1.0 mL min^{-1}. Separations were achieved using two PLGel Mixed B (7.8 x 300 mm) SEC columns connected in series and held at a constant temperature of 50 ^{o}C. The triple detection system was calibrated using a 2 mg mL^{-1} PSTY standard (Polymer Laboratories: Mw = 110 K, dn/dc = 0.16 mL g^{-1} and IV = 0.5809). Samples of known concentration were freshly prepared in DMAc + 0.03 wt % LiCl and passed through a 0.45 μm PTFE syringe filter prior to injection. The absolute

molecular weights and *d*n/*d*c values were determined using Polymer Laboratories Multi Cirrus software based on the quantitative mass recovery technique.

Preparative Size Exclusion Chromatography (Prep-SEC)

Crude polymers were fractionated (i.e. purified) using a Varian Pro-Star preparative SEC system equipped with a manual injector, differential refractive index detector, and single wave-length ultraviolet visible detector. The flow rate was maintained at 10 mL min^{-1} and HPLC grade tetrahydrofuran was used as the eluent. Separations were achieved using a PL Gel 10 μm 10 x 10^3 Å, 300 x 25 mm preparative SEC column at 25 °C. The dried crude polymer was dissolved in THF at 100 mg mL^{-1} and filtered through a 0.45 μm PTFE syringe filter prior to injection. Fractions were collected manually, and the composition of each was determined using the Polymer Laboratories GPC50 Plus equipped with triple detection as described above.

Nuclear Magnetic Resonance (NMR)

All NMR spectra were recorded on either a Bruker DRX 400 or 500 MHz spectrometer using an external lock ($CDCl_3$), and all spectra were referenced to the residual nondeuterated solvent ($CHCl_3$). 1D DOSY experiments were also run to acquire ^1H NMR spectra of all polymers by increasing the pulse gradient from 2 to 90 % of the maximum gradient strength and increasing d (p30) from 1 to 2 ms, using 256-512 scans.

Attenuated Total Reflectance-Fourier Transform Spectroscopy (ATR-FTIR)

ATR-FTIR spectra were obtained using a horizontal, single bounce, diamond ATR accessory on a Nicolet Nexus 870 FT-IR. Spectra were recorded between 4000 and 500 cm^{-1} for 32 scans at 4 cm^{-1} resolution with an OPD velocity of 0.6289 cm s^{-1}. Solids were pressed directly onto the diamond internal reflection element of the ATR without further sample preparation.

Matrix-Assisted Laser Desorption Ionization-Time-of-Flight (MALDI-ToF) Mass Spectrometry

MALDI-ToF MS spectra were obtained using a Bruker MALDI-ToF autoflex III smart beam equipped with a nitrogen laser (337 nm, 200 Hz maximum firing rate) with a mass range of 600-400 000 Da. Spectra were recorded in both reflectron mode (1500-4500 Da) and linear mode (4000-20000 Da). Trans- 2-[3-(4-tert- butylphenyl)-2-methyl-propenylidene] malononitrile (DCTB; 20 mg mL^{-1} in THF) was used as the matrix and $Ag(CF_3COO)$ (1 mg mL^{-1} in THF) as the cation source of all the polystyrene samples. 20 μL polymer solution (1 mg mL^{-1} in THF), 20 μL DCTB solution and 2 μL $Ag(CF_3COO)$ solution were mixed in an ependorf tube, vortexed and centrifuged. 1 μL of solution was placed on the target plate spot, evaporated the solvent at ambient condition and run the measurement.

LND simulations

We used a log-normal distribution (LND) model based on a Gaussian function to fit the experimental MWD. One can simulate the molecular weight distributions, and in particular the weight distribution[49], with a log-normal distribution (see ref[50] for more details) using the following equations:

$$w(M) = \frac{\exp(-(\ln M - \ln \overline{M})^2 / 2\sigma^2}{M(2\pi\sigma^2)^{0.5}} \quad (1)$$

where

$$\overline{M} = (M_n M_w)^{0.5} \quad (2)$$

and

$$\sigma^2 = \ln(PDI) \quad (3)$$

where equation **1** is the Gaussian distribution function of w(M) (the weight distribution of the SEC trace), M_n is the number-average molecular weight, M_w is the weight-average molecular weight, and the polydispersity PDI = M_w/M_n.

Determination of dn/dc value

$$\left(\frac{dn}{dc}\right)_{copolymer} = \frac{M_{n,p1}}{M_{n,p1}+M_{n,p2}}\left(\frac{dn}{dc}\right)_{p1} + \frac{M_{n,p2}}{M_{n,p1}+M_{n,p2}}\left(\frac{dn}{dc}\right)_{p2} \quad (4)$$

Where, $M_{n,p1}$ and $M_{n,p2}$ refer to the apparent molecular weight of polymer 1 and 2, respectively, determined by RI SEC. $(dn/dc)_{p1}$ and $(dn/dc)_{p2}$ refer to the dn/dc value of polymer 1 and 2, respectively, at 36 ^{o}C, in THF.

3.3 Results and discussion

Synthesis of mikoarm stars consisting of 4 or more arms with any desired chemical compositions is still a challenge. Compared to the methods utilizing 'living' anionic polymerizations (LAP), the LRP techniques enable the synthesis of polymers from a variety of monomers, with higher tolerance of functionalities. Moreover, the utilization of CuAAC 'click' reaction has been proved as a mild and highly efficient coupling reaction which can be carried out in wide range of conditions. The combination of LRP and CuAAC 'click' reaction enables the iterative synthesis of polymer structures with chemical diversity.

To test the feasibility of our new iterative strategy to make 4-arm star, we first made 4-arm PSTY star via sequentially coupling of alkyne-terminated PSTY to a small molecular linker which contained two azide groups and one protected alkyne group (Scheme 3.2). The resulting 4-arm polystyrene star can readily be characterized by SEC, NMR and MALDI-ToF mass spectrometers, and provides an assumption-free system to check the viability of our synthetic method.

3.3.1 Synthesis of 4-arm PSTY star (proof-of-concept)

Synthesis of building block PSTY-alk (3).

PSTY-Br **1** was synthesized from the ATRP of styrene using EBiB as initiator at 80 ^{o}C for 6.5 h (Scheme 3.2), and produced a polymer with a number-average molecular weight by SEC-RI ($M_{n,RI}$) of 3860 and polydispersity index (PDI) of 1.09 (see Table 3.1 and appendix Figure A3.1). The percentage of chains with bromine end-group functionality is important for subsequent coupling reactions and final formation of the 4-arm star. There was a 96 % Br chain-end functionality determined by integrating the areas of ^{1}H NMR at ~4.5 ppm (**d**) to 3.6 ppm (**b**) (see Figure A3.2). Analysis of the MALDI-ToF spectrum further confirmed the high chain-end functionality (see Figure A3.3). The bromine end-group on **1** was then converted to azide group using NaN_3 to produce PSTY-N_3 **2** in near quantitative yield through the shift of the proton (-CH(Ph)Br) at ~4.5 ppm to with the azide (-CH(Ph)N_3) at 3.9 ppm (see Figure A3.5). The percentage of -CH(Ph)N_3 calculated from the respective areas of peaks **d** and **b** in the ^{1}H NMR spectrum (Figure A3.5) was near quantitative at 96 %. The SEC trace of **2** did not change to that observed for **1**, with an $M_{n,RI}$ of 3840 and PDI of 1.08 (Table 3.1 and FigureA3.4). There were three main peaks observed in the MALDI-ToF

spectrum of **2** (Figure A3.6). The main peak corresponds to the expected product while the two small peaks originated from fragmentation of the azide on the polymer chain-end.[54] The PSTY-N_3 (**2**) was subsequently coupled with excess propargyl ether to yield PSTY-alk, **3**. To suppress the bimolecular coupling, a 30 fold excess of propargyl ether was used in the CuAAC 'click' reaction. The resulting crude product **3** ($M_{n,RI}$ = 3940, PDI=1.10) contained a small shoulder at the high molecular part of the MWD, indicating the formation of a bimolecular product. This product was removed by preparative-SEC to give **3** ($M_{n,RI}$ = 3850, PDI=1.07, SEC traces see Figure 3.1A) with high purity (> 99 %, Table 3.1). The small amount of Cu(I)Br (5.5 mg, 0.005 equiv. to propargyl ether) used in the reaction minimized the potential of the Glazer coupling reaction between alkyne groups. The concomitant addition of Cu(0) wire further allowed a low and relatively constant concentration of Cu(I) in the system over the course of the reaction. This is a result of the formation of Cu(II) species and its reduction to Cu(I) through comproportionation.[28] After the 'click' reaction, the ^{1}H NMR spectrum showed three new peaks at ~4.6, 4.1 and 2.4 ppm, ascribed to two methylene and alkyne protons respectively, suggesting the successful conjugation of the propargyl ether moiety onto the PSTY chain (Figure 3.1B). Integration of the peaks for the protons adjacent to the triazole ring (i.e., peaks **d**, **e**, and **f**,) suggested high alkyne chain-end functionality. In addition to the NMR analysis, the main peak with *m/z* as 3900.43 in MALDI-ToF spectrum that was close to the calculated value of 3900.16 supported the structure for $PSTY_{34}$-alk, **3** (Figure A3.7).

Table 3. 1 SEC data for all building blocks and star polymers

Entry	Polymer code	RI detection[a]			Triple detection[b]			Purity % [c]		Click efficiency[d]
		M_n	M_p	PDI	M_n	M_p	PDI	Crude	Prep	
1	PSTY-Br	3860	4050	1.10						
2	PSTY-N_3	3840	4030	1.08						
3[e]	PSTY-alk	3900	4060	1.07				95.8	>99	
9[e]	Tips-alk-PSTY(N_3)	4350	4530	1.06				95.0	>99	
10[e]	Tips-alk-$(PSTY)_2$	8880	8970	1.03				92	>99	94 %
11	Alk-$(PSTY)_2$	8420	8610	1.04						
14[e]	N_3-$(PSTY)_2$	8700	8980	1.04				93	97	
15[e]	$(PSTY)_4$	15820	16320	1.04	17200	18030	1.02	87	98	91 %
16	PEG-alk	2780	2870	1.04	2200	2390	1.04			
17[e]	Tips-alk-PSTY-PEG	7450	7550	1.03	7040	7160	1.02	77	>99	88%
18	Alk-PSTY-PEG	6600	7100	1.05	6390	6680	1.02			
19[e]	N_3-PSTY-PEG	6730	7065	1.05	6640	6860	1.02	68	88	
20	P^tBA-Br	5950	6150	1.05						
21	P^tBA-N_3	6030	6180	1.06						
22[e]	P^tBA-alk	5930	6110	1.05				94	99	
23[e]	Tips-alk-$P^tBA(N_3)$	6240	6360	1.03				91	>99	
26	N_3-PNIPAm-$(OH)_2$	2200	2412	1.10	4050	4180	1.02			
27	Alk-PNIPAm-$(OH)_2$	2650	2820	1.09	4230	4290	1.02			
28[e]	Tips-alk-PNIPAm-P^tBA	9450	9470	1.05	10690	10960	1.03	94	99	96 %
29	alk-PNIPAm-P^tBA	9000	9150	1.05	10220	10580	1.03			
30[e]	PSTY-PEG-P^tBA-PNIPAm	15860	15940	1.03	16760	17020	1.02	70	97	75 %

[a] The data was acquired using SEC (RI detector) and is based on PSTY calibration curve. [b] The data was acquired using THF Triple Detection SEC. [c] Determined from the LND simulation. [e] Sample purified by prep-SEC. [d] Click efficiency of copolymer calculated as following: Experimental Purity(LND)/max purity by theory x 100.

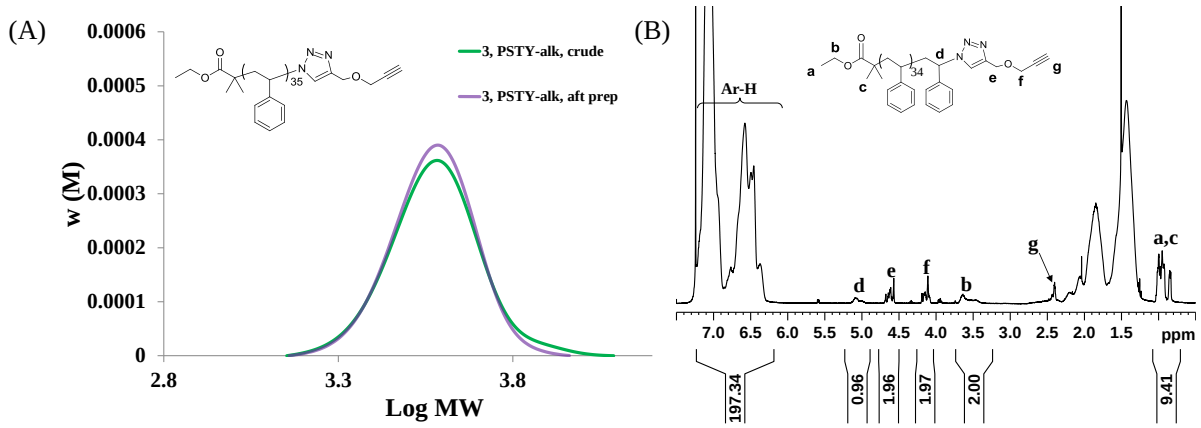

Figure 3.1 (A) SEC traces and LND simulations of PSTY-alk (**3**) before and after purification by prep-SEC. Determined from THF SEC, RI detector, PSTY standard. (B) ^{1}H NMR spectrum of PSTY-alk (**3**), recorded in $CDCl_3$ at 298K , 500MHz.

Synthesis of trifunctional linker 8.

Linker **8** was a key compound in the construction of the star polymer *via* our sequential CuAAC reaction strategy. The synthetic route to make **8** was illustrated in Scheme 3.3. The precursors **4** and **5** were synthesized according to the previous literature procedures.[52] Precursor **6** was made through an esterification of **5** with dimethyl 5-hydroxyisophthalate.[55] The methyl ester groups (-$PhCOOCH_3$) on compound **6** were then converted to benzyl alcohol (-$PhCH_2OH$) through a reduction process using $LiAlH_4$ to yield compound **7**. Subsequent azidation of resulting benzyl alcohol to the corresponding azide groups (-$PhCH_2N_3$) using DPPA and DBU produced **8**. The trifuntional linker **8** consisting of two free azide groups and a Tips-protected alkyne group is the key linker for the iterative coupling of the other polymer blocks to form the multiarm star (Scheme 3.1). The successful synthesis of molecule **8** was confirmed by both ^{1}H and ^{13}C NMR as shown in Figure 3.2; all precursors NMRs were given in appendix (Figure A3.14 to A3.15).

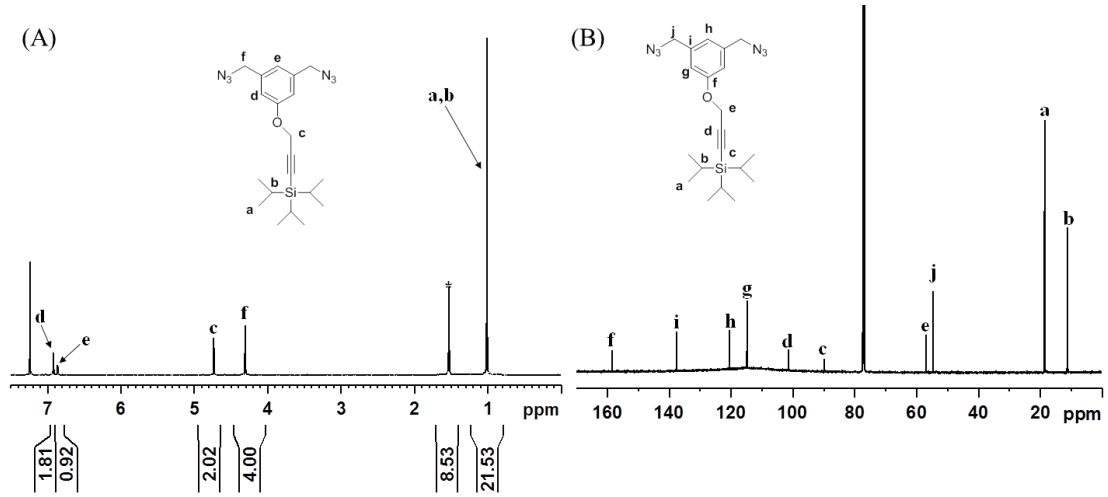

Figure 3.2 ^{1}H NMR (A) and ^{13}C NMR (B) spectra of **8**, recorded in $CDCl_3$ at 298 K, 500 M.

Synthesis of PSTY 4-arm star

The synthetic route to make 4-arm PSTY star was described at Scheme 3.2.The first arm PSTY-alk **3** was grafted onto **8** by the CuAAC 'click' reaction to generate product **9** containing a pendant azide group and a Tips-protected alkyne group. This allowed the introduce of additional arm segments to the core. To minimize the formation of 2-arm byproduct, a 10 fold excess of **8** was used in the coupling reaction. Moreover, a degassed solution of **3** was fed into the solution of **8** *via* syringe pump. This procedure favored the generation of **9** rather than the 2-arm byproduct. As a result, only a small shoulder (representing 5% of the 2-arm product determined by the LND simulation) at high MWD was generated, which was later removed by preprative SEC to give **9** ($M_{n,RI}$ = 4350, PDI=1.06) with ~100 % purity by the LND simulation (Figure 3.3A, Table 3.1).

After the CuAAC 'click' reaction, the ^{1}H NMR spectrum of **9** (Figure A3.3B) showed two characteristic peaks at 4.7 ppm (**j**) and 1.1 ppm (**k**, **l**) originating from **8**, which together with the complete disappearance of alkyne proton peak at 2.4 ppm and the appearance of a new peak ascribed to triazole ring proton (**g**) at 7.4 ppm confirmed the 'click' reaction was carried out in nearly quantitative. The high N_3 functionality (98 %) was determined by integrating the areas of the ^{1}H NMR at ~4.3 ppm (**i**) and to 5.4 ppm (**h**). This high functionality is crucial for the subsequent coupling of the second arm. The high purity of **9** was further supported by MALDI-ToF analysis given in the appendix (Figure A3.16).

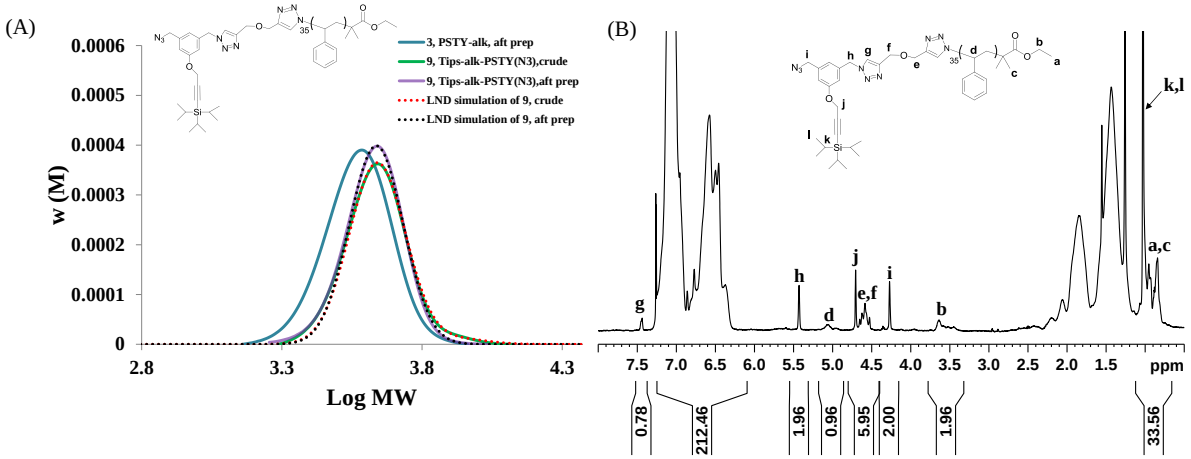

Fgiure 3.3 (A) SEC trace of PSTY-alk (**3**), Tips-alk-PSTY(N_3) (**9**) (before and after prep) and LND simulation of (**9**). Determined from THF SEC, RI detector, PSTY standard. (B) ^{1}H 1DOSY NMR spectrum of Tips-alk-PSTY(N_3) (**9**), recorded in $CDCl_3$ at 298K , 500MHz.

Coupling polymers **3** and **9** by CuAAC resulted in an increase in the molecular weight to nearly double, which corresponed to **10** as shown by the SEC chromatograms in Figure 3.4A. The introduction of a 10 % excess of **9** was used to drive the reaction of **10** to near full completion and also suppressed the potential of the bimolecular coupling between PSTY-alk, **3**.[56] The SEC trace of **10** (Figure 3.4A) showed a low MWD tail associated with unreacted **9**, and there was no observable bimodal distribution at high the MWD. As determined by the LND simulation, it showed greater than 92 % purity of crude product **10** (prior to fractionation),which increased to nearly 100 % after the removal of unreacted **9** by preparative SEC (Figure 3.4A, Table 3.1).The ^{1}H NMR of **10** (Figure 3.4B), in which the N_3 group was converted to the triazole ring, showed near complete loss of protons associated with azide and a nearly double integration of protons (**h**) adjacent to triazole ring after the CuAAC 'click' reaction. The MALDI-ToF spectrum given in Figure A3.17 showed a main peak with *m/z* of 9340.89, which was closed to theoretical value (e.g., 9340.41), and confirmed the high purity of product **10**.

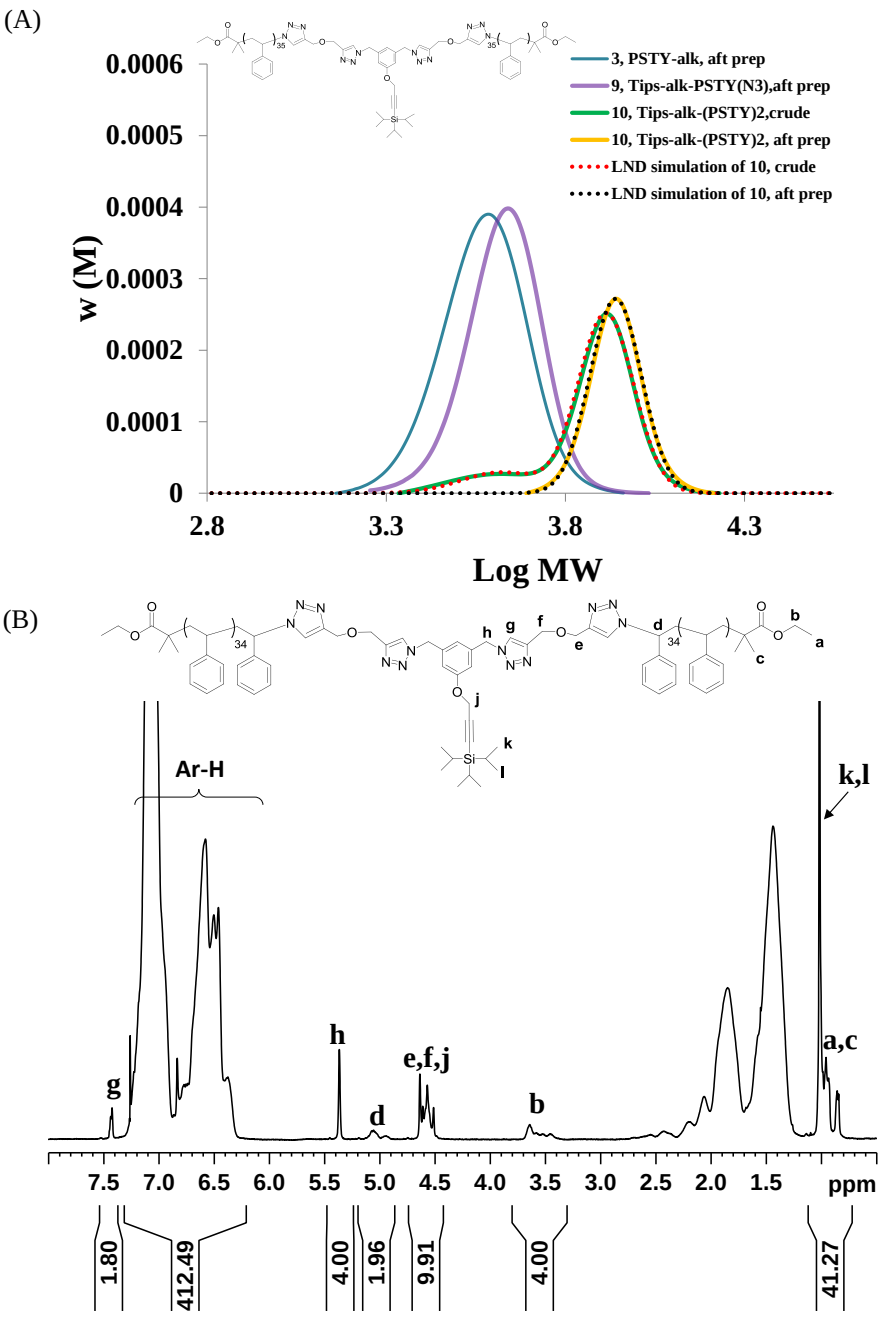

Figure 3.4 (A) SEC trace of PSTY-alk (**3**) , Tips-alk-PSTY(N_3) (**9**), Tips-alk-$(PSTY)_2$ (**10**) (before and after prep) and LND simulation of (**10**). Determined from THF SEC, RI detector, PSTY standard. (B) ^{1}H 1DOSY NMR spectrum of Tips-alk-ph-$(PSTY)_2$ (**10**), recorded in $CDCl_3$ at 298K , 500MHz.

The deprotection of the Tips of the alkyne group from **10** using TBAF gave **11** with near complete loss of Tips as shown from in ^{1}H NMR (i.e., loss of proton at 1.1 ppm in Figure 3.5B). In addition, after deprotection, the SEC chromatogram showed little change to the MWD and maintained a unimodal distribution, suggesting minimal Glaser coupling (Figure 3.5A).

The good agreement between the experimental (9340.89) and theoretical (9340.41) values of $PSTY_{78}$ from the MALDI-ToF spectrum of **11** further supported the successful deprotection Tips group from polymer **10** (Figure A3.18). Product **11** was an important intermediate as it can undergo a post-modification using diazide linker **13** to introduce N_3 functionality in the middle of the polymer chain of **11** to give N_3-$(PSTY)_2$, **14**. This allowed the subsequent CuAAC 'click' reaction between **11** and **14** to give 4-arm PSTY star (Scheme 3.2).

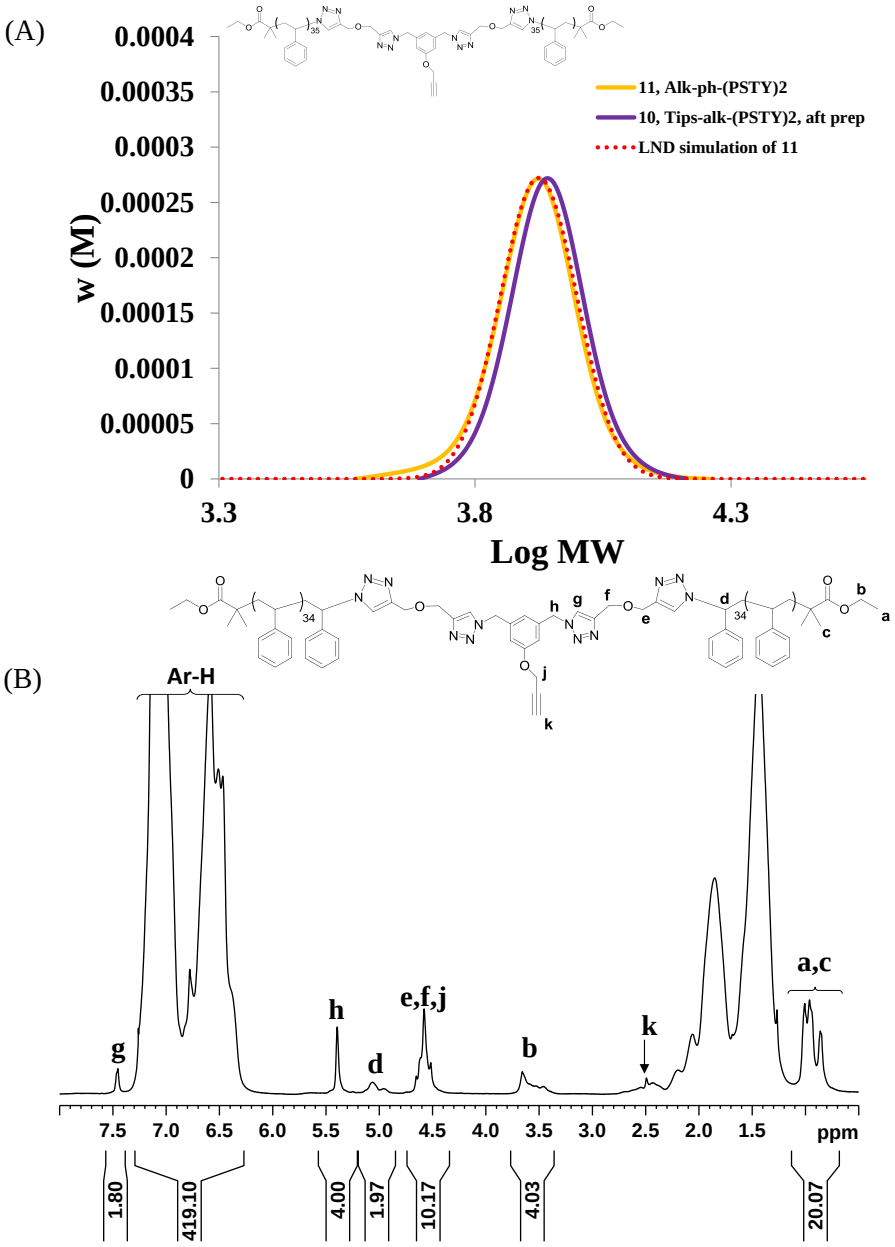

Figure 3.5 (A) SEC traces of alk-$(PSTY)_2$ (**11**), Tips-alk-$(PSTY)_2$ (**10**) and LND simulation of (**11**). Determined from THF SEC, RI detector, PSTY standard. (B) ^{1}H 1DOSY NMR spectrum of alk-$(PSTY)_2$ (**11**), recorded in $CDCl_3$ at 298K , 500MHz.

Diazide linker **13** was synthesized from tetra ethylene glycol through subsequent bromination and azidation (Scheme 3.3). The NMR and ATR-FTIR analyses of **13** were given in the appendix (Figure A3.19 to A3.22).

The alkyne functionality of polymer **11** was then converted to N_3 group through a CuAAC reaction with excess diazide linker **13** (see Scheme 3.2). Similar with the preparation of **9** using diazide compound, **14** was prepared by feeding a degassed solution of **11** into **13** (30 fold excess to 14) to suppress undesirable coupling reactions (e.g., alkyne-alkyne coupling of **11** and bimolecular coupling between **13** and two **11**). The product from the CuAAC reaction between polymer **11** and the linker **13** showed high coupling efficiency. There was only a small amount (i.e., 7 %) of high MWD impurities observed from SEC traces of **14** after CuAAC reaction(Figure 3.6A), which was removed by prep-SEC and led to an increase of purity of **14** ($M_{n,RI}$= 8700, PDI=1.04) from 93 % to 97 % determined by LND simulation. There was a 98 % N_3 functionality of **14** determined by integrating the areas of ^{1}H NMR spectrum at 3.3 ppm (**s**) to 5.4 ppm (**d**) (see Figure 3.6B). The MALDI of **14** showed a dominant specie with *m/z* as 8386.81, which was in agreement with the theoretical value (8386.78) including Ag^+ suggested high N_3 functionality of **14**(see Figure A3.24 in appendix).

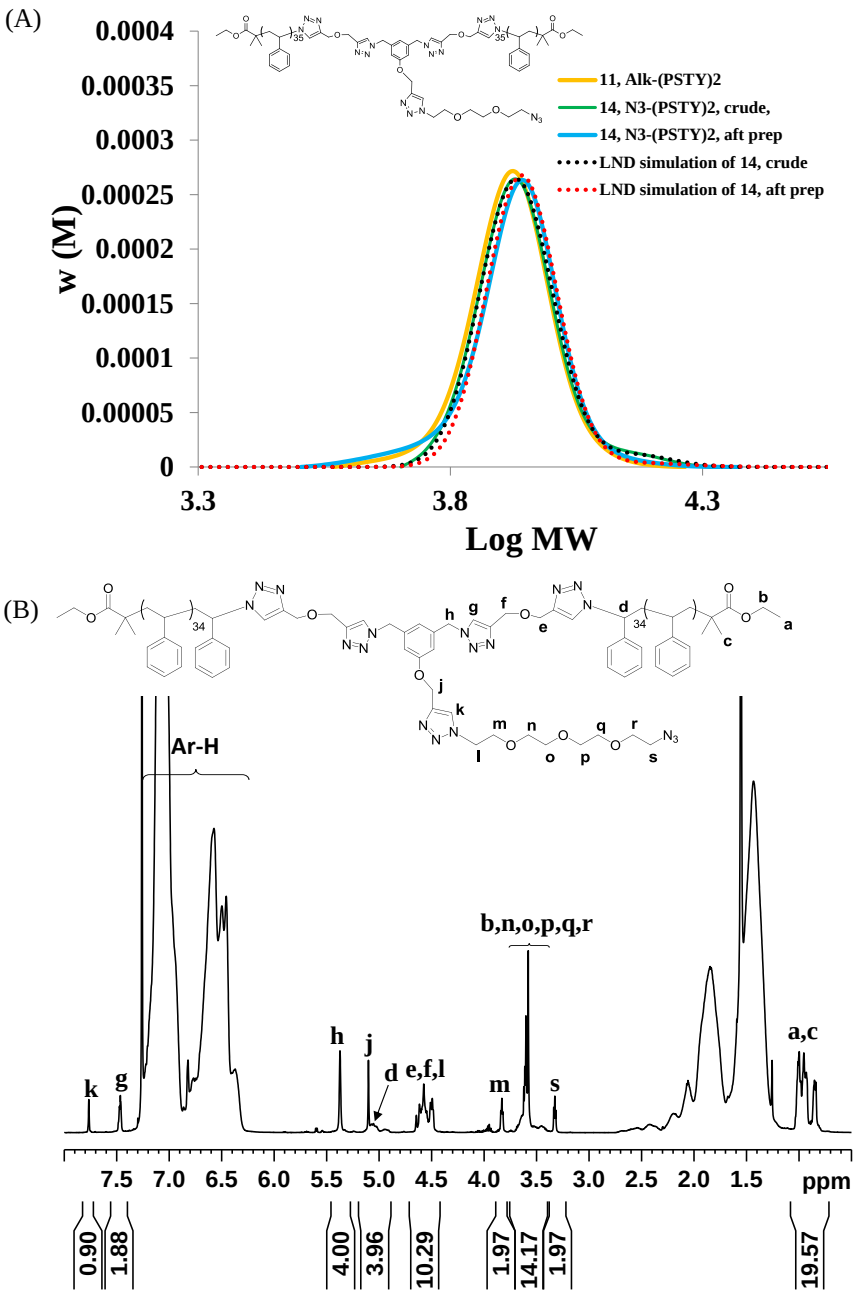

Figure 3.6 (A) SEC trace of alk-$(PSTY)_2$ (**11**), N_3-$(PSTY)_2$ (**14**) (before and after prep-SEC) and LND simulations of (**14**). Determined from THF SEC, RI detector, PSTY standard. (B) ^1H NMR spectrum of $(PSTY)_2$-N_3(**14**), recorded in $CDCl_3$ at 298K , 500MHz.

The 4-arm PSTY **15** star was formed by coupling of N_3-$(PSTY)_2$ **14** (1.1 equiv.) and alk-$(PSTY)_2$ **11** (1.0 equiv.) using CuAAC 'click' reaction in one-pot at 25 ^oC in 1h. The SEC trace (Figure 3.7A) showed MWD corresponding to the product of **15** (87 % purity, and 'click' efficiency 91 % determined by LND simulation), 12 % of the starting polymer **14**, little or no of the other starting polymer **11.** After fractionation of **15** (crude) by preparative SEC, the purity increased to 98 %. Obtaining the high purity satr-like polymer is currently a

chanllenge for polymer chemist, and the minor strcutral-defect may dramatically change the properties of star polymer. The overall yeild of PS-star is 24 % after 8-step synthesis. The relatively low yield is due to the multi-step purifications to remove impurities by prep-SEC. However, the purification by prep-SEC gave the highly pure final star. The $M_{n,RI}$ of **15** (prep) was 15820 with a PDI of 1.04 through refractive index (RI) detector, and the $M_{n,TD}$ was 17200 with a PDI of 1.02 through triple detection (i.e., absolute molecular weight determination) as given in Table 3.1. The value of $M_{n,TD}$ (17200) was close to the theoretical value (17120) of **15** calculated from the addition of the absolute molecular weights of the starting polymers **11** and **14**.

Because of the more compact conformation of 4-arm star, the apparent molecular weight ($M_{n,RI}$=15820) determined by RI SEC was lower than that of absolute molecular weight obtained from triple detection SEC ($M_{n,TD}$=17200,), resulting in a change in hyrodynamic volume (ΔHDV) of 0.92 (calculated from $M_{P,RI}/M_{P,TD}$, Table 3.1), which is accorded well with previous report.[57] The low PDI (≤ 1.04) revealed the minimal amount of structural defect in final polymer star. In ^{1}H NMR spectrum of PSTY star (Figure 3.7B), characteristic resonance signal at 7.6 ppm (**k**) could be ascribed to proton in new generated 1,2,3-triazole ring, and the methylene protons (**s**) beside the new triazole ring showed a distinct shift from 3.4 ppm to ~4.5 ppm.

The MALDI-ToF (Figure 3.8) spectrum acquired in linear mode showed that the distributions (i.e., the full spectrum, Figure 3.8A) were similar to that found by SEC, with the main peak corresponding to the expected molecular weight of the **15**. For example, the experimental peak at *m/z* = 18099.57 (adduct with Ag^+) matched closely with the theoretical *m/z* 18102.74 for polymer chain with 140 STY units, suggesting high purity of resulting product. The high 'click' efficiency (91 %, determined by LND simulation) of coupling reaction and the high purity of purified product **15** (98 %) demonstrated that our model synthesis strategy can successfully afford the synthesis of miktoarm star with predetermined molecular weight, narrow polydispersity, and precise composition.

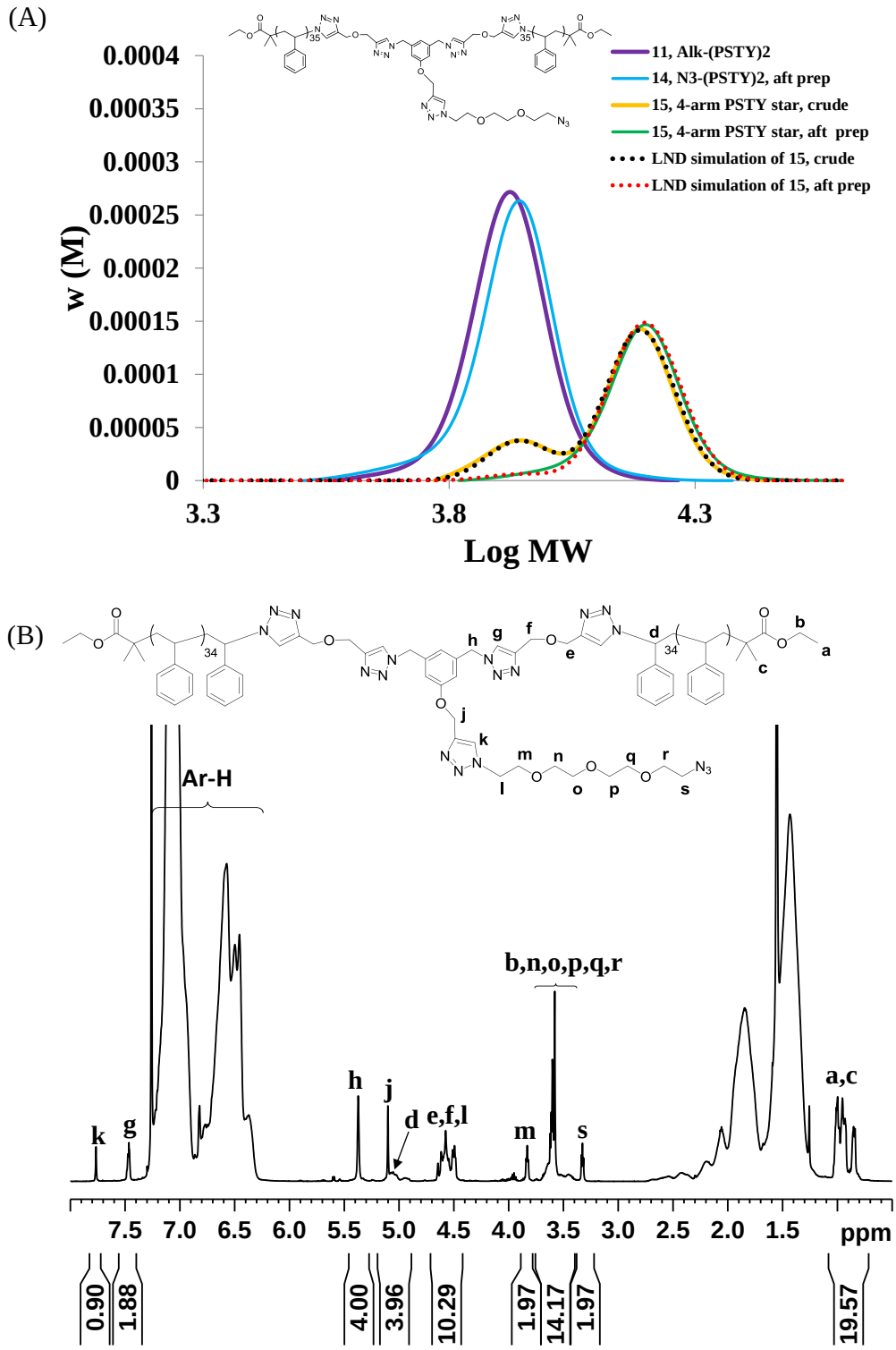

Fgiure 3.7 (A) SEC trace of alk-$(PSTY)_2$ (**11**), N_3-$(PSTY)_2$ (**14**), and 4-arm PSTY star (**15**). Determined from THF SEC, RI detector, PSTY standard. (B) ^{1}H 1D DOSY NMR spectrum of 4-arm PSTY(**15**), recorded in $CDCl_3$ at 298K , 500MHz.

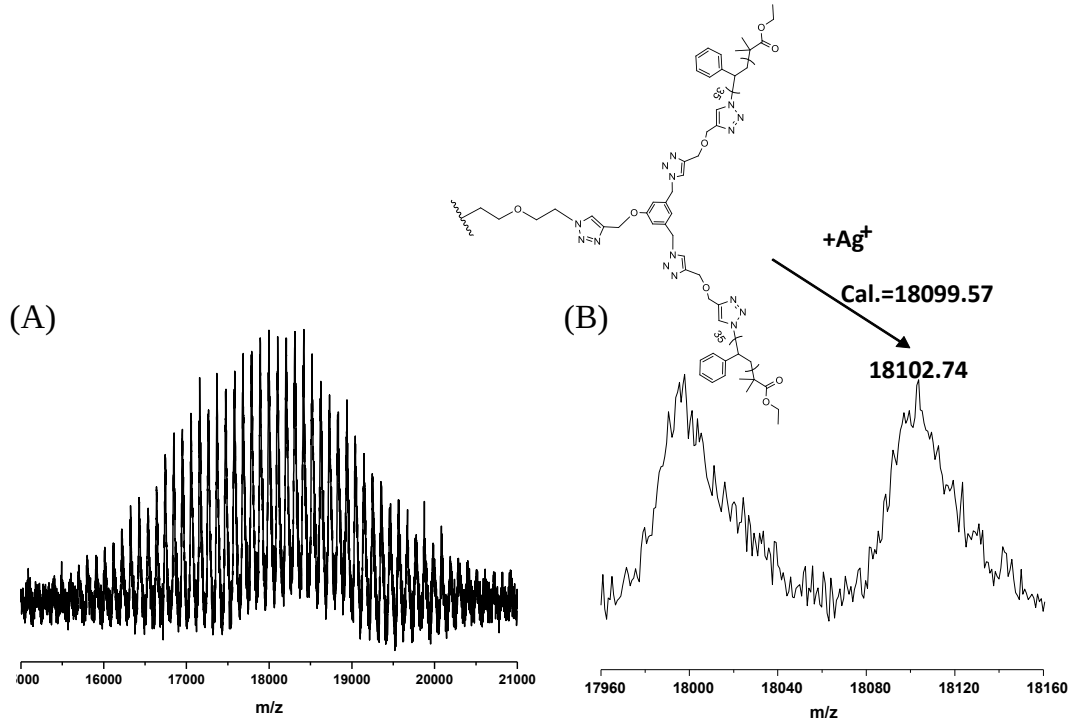

Figure 3.8 The full (A) and expanded (B) MALDI-TOF mass spectra of 4-arm PSTY star (**15**), the spectra were recorded in linear mode using DCTB as the matrix and $AgCF_3COO$ as the cation source.

3.3.2 Synthesis of 4-arm ABCD miktoarm star

After the successful synthesis of four arm PSTY star through the iterative coupling reaction method, we further applied this strategy to synthesize an ABCD miktoarm star polymer (Scheme 3.1). We chose four different polymer building blocks including PSTY, P^{t}BA, PEG and PNIPAm which represented a hydrophobic, pH sensitive (i.e. hydrolysis of P^{t}BA to PAA), neutral and water soluble, and thermos-responsive properties, respectively. More importantly, the synthesis of these polymer precursors involved ATRP (i.e. for PSTY), SET-LRP in organic solvent (i.e. for P^{t}BA), and SET-LRP in the water phase (i.e. PNIPAm).

Synthesis of building block 16.

The alkyne-functionalized PEG_{52}-alk, **16**, was prepared by an etherification reaction of MeO-PEG_{52}-OH and propargyl bromide.[58] The SEC trace of **16** showed a slight shift to a higher molecular weight after etherification (Figure 3.9A). The ^{1}H NMR analysis revealed two new peaks ascribed to the methylene (**b**) and alkyne protons (**c**) respectively, suggesting the successful conjugation of the propargyl ether moiety onto the PEG chain-end (Figure 3.9B). The MALDI-ToF spectrum (Figure 3.10B) exhibited two isotope peaks; for example,

adduct with Na^+ (*m/z* =2205.96) and K^+ (*m/z* =2222.26) were close to their theoretical values (*m/z* 2206.28 for Na^+, and 2221.95 for K^+).

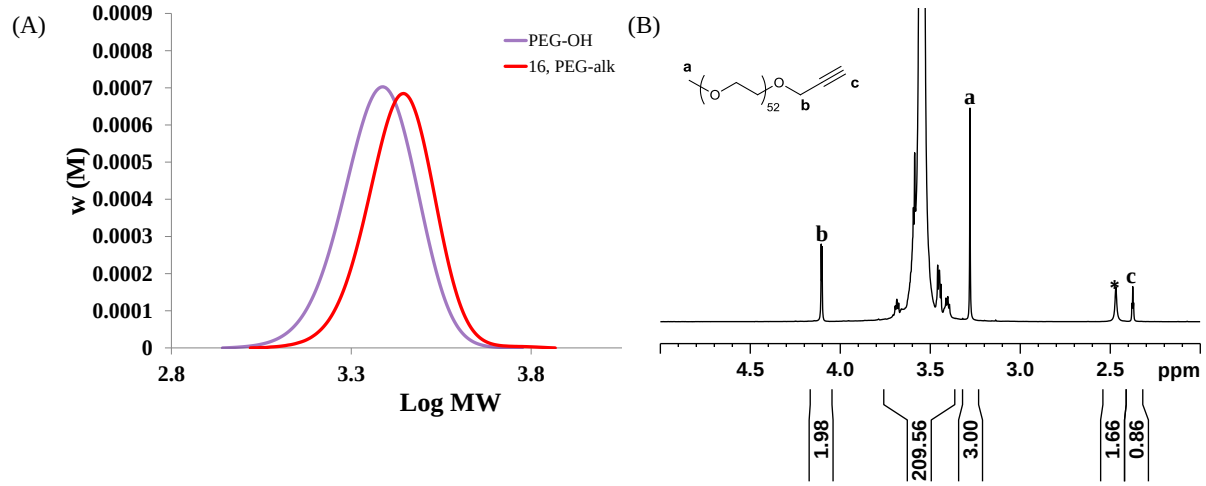

Figure 3.9 (A) SEC traces of PEG-OH, PEG-alk (**16**) and LND simulation of (**16**). Determined from THF SEC, RI detector, PSTY standard. (B) ^{1}H NMR spectrum of alk-PEG (**16**), recorded in $CDCl_3$ at 298K , 500MHz,*=H_2O.

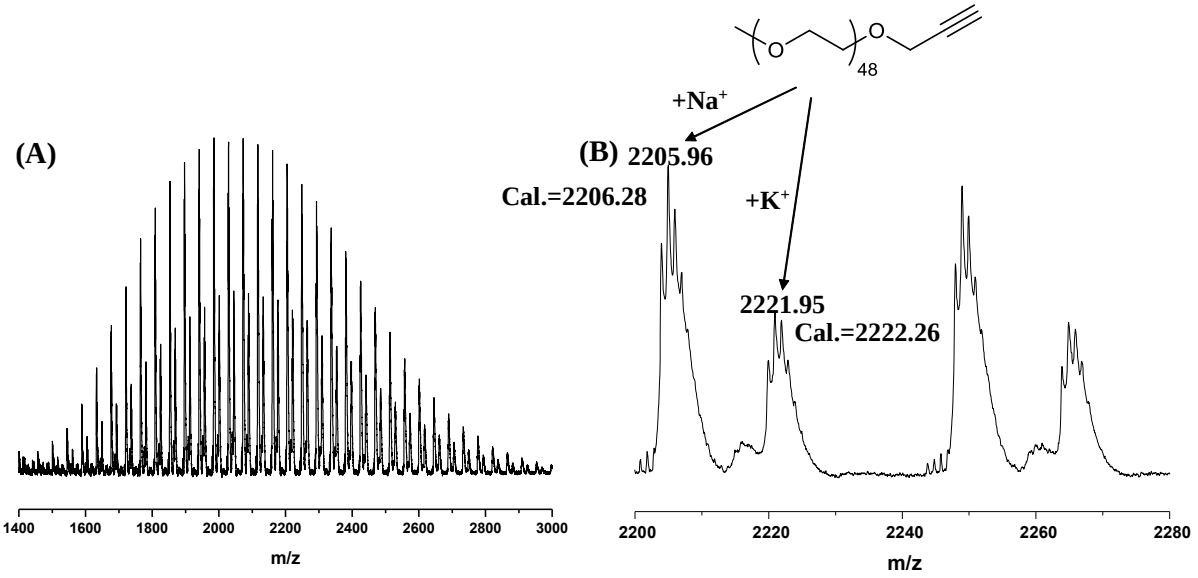

Fgiure 3.10 The full (A) and expanded (B) MALDI-TOF mass spectra of PEG-alk (**16**), the spectra were recorded in reflect mode using DCTB as the matrix and $NaCF_3COO$ as the cation source.

Synthesis of alk-PEG-PSTY (18) and N_3-PEG-PSTY (19) copolymers

PEG-alk **16** was then used to couple with azide group on polymer **9** to give PSTY-PEG copolymer **17** with a protected alkyne group in the middle of the chain. A slight excess (0.1 equiv.) of PEG-alk (**16**) was used to drive the coupling reaction to completion. The SEC trace after the 'click' reaction gave a MWDs that corresponded to the product of 17 (88 %, Figure 3.13A), 4.1 % unreacted **16,** and 8 % Glazer coupling product of **16** (i.e., PEG-≡-≡-PEG), respectively. These two byproducts (low MWD tail on SEC trace) were removed by preparative SEC to give **17** ($M_{n,RI}$ = 7450, PDI=1.03, SEC traces see Figure 3.11A) with high purity (> 99 %, Table 3.1). In ^{1}H NMR spectrum of **17** (Figure 3.11B), the typical signals of PEG was observed at ~3.6 ppm and a new sharp peak ascribed to triazole ring proton **n** at 7.45 ppm demonstrated the incorporation of the second block PEG. The dn/dc value of PSTY-b-PEG copolymer was determined by equation 4 based on the dn/dc of PSTY and PEG, and given in Table 3.2.

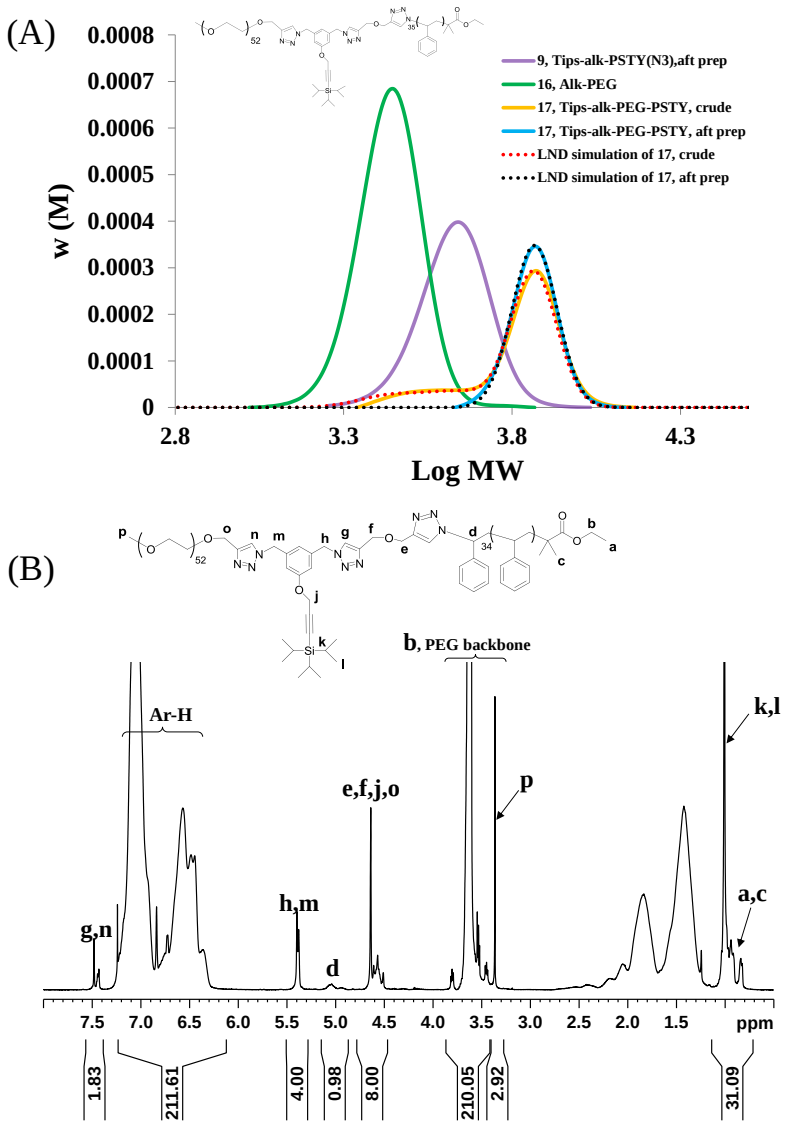

Figure 3.11 (A) SEC traces of alk-PEG (16), Tips-alk-PSTY(N_3) (**9**), Tips-alk-PEG-PSTY (**17**) (before and after prep-SEC) and LND simulation of (**17**), Determined from THF SEC, RI detector, PSTY standard. (B) ^{1}H 1D DOSY NMR spectrum of Tips-alk-PEG-PSTY (**17**), recorded in $CDCl_3$ at 298K, 500MHz.

Table 3.2 dn/dc value of building blocks and copolymers

Entry	Polymer code	$M_{n,RI}$	dn/dc (mL g^{-1})[a]
3	PSTY-alk	3900	0.183
16	PEG-alk	2780	0.06
17	Tips-alk-PEG-PSTY	7450	0.135
22	P^{t}BA-alk	5930	0.042
27	Alk-PNIPAm-(OH)2	2650	0.095
28	Tips-alk-PNIPAm-P^{t}BA	9450	0.058
30	PSTY-PEG-P^{t}BA-PNIPAm	15860	0.091

[a] dn/dc of PSTY was known as 0.1828 mL g^{-1}, at 36 ^oC, THF. The dn/dc values of PEG, PtBA and PNIPAm were determined by comparison of intensity of RI signal with PSTY sample with same mass concentration, at 36 ^oC, THF. The dn/dc values of copolymers were calculated using equation 4.

TBAF was then used to remove the Tips group from copolymer **17** to give **18** (alk-PEG-PSTY) with purity of 88 % by LND simulation (Figure 3.12A). After deprotection, the SEC trace showed a slight shift to low molecular weight distribution due to the removal of Tips group (Figure 3.12A). There is no high MWD byproduct was observed in SEC trace, but a small MWD tail (12 % by LND fit) was detected which probably due to the Glazer coupling of PEG-alk. The removal of Tips group was also verified by the completed loss of the signals at 1.0 ppm from ^{1}H NMR spectrum of **18** (Figure 3.12B)

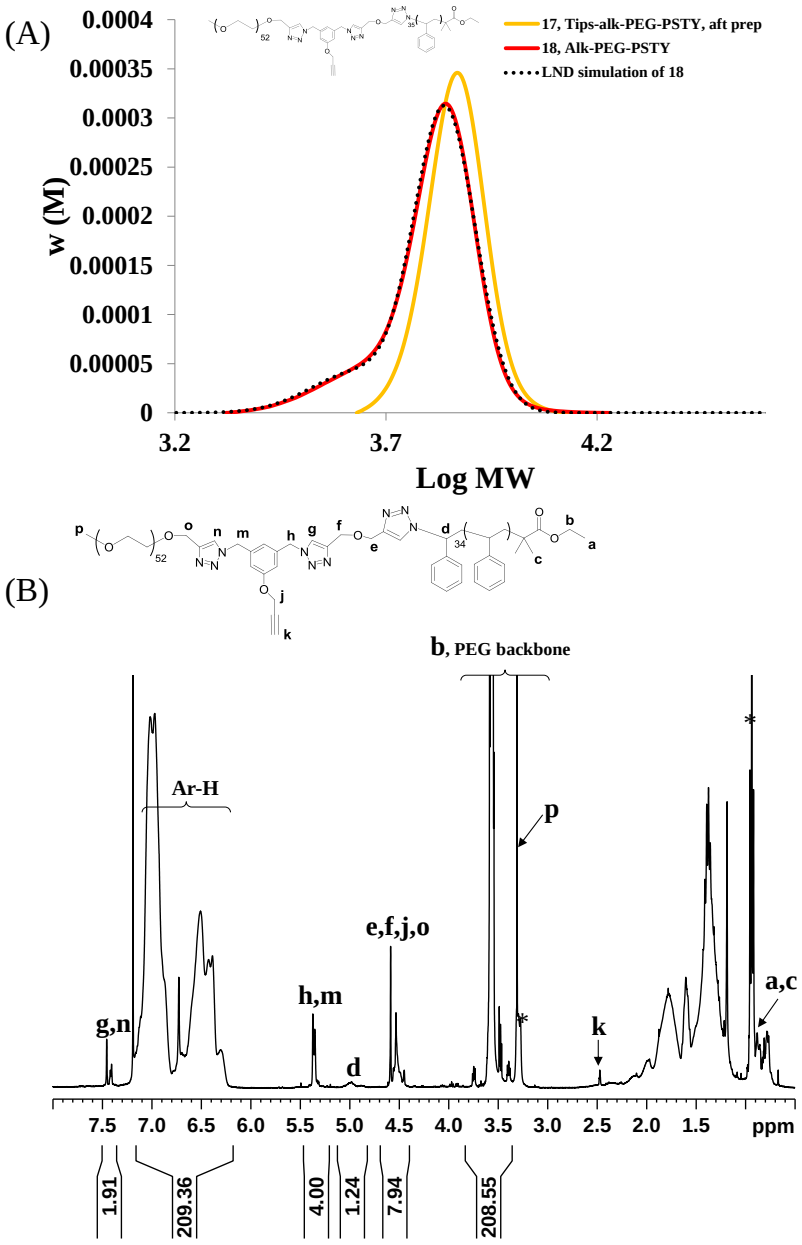

Fgiure 3.12 (A) SEC traces of Tips-alk-PEG-PSTY (**17**), alk- PEG-PSTY (**18**) and LND simulation of (**18**), Determined from THF SEC, RI detector, PSTY standard. (B) ^{1}H NMR spectrum of Tips-alk-PSTY-PEG (**18**), recorded in $CDCl_3$ at 298K, 500MHz, *=TBAF salt.

Followed the successful strategy in preparation of 4-arm star PSTY, we then coupled alkyne-terminated copolymer **18** with diazide linker **13** to give N_3-PEG-PSTY copolymer, **19**. A 30 fold excess of **13** was fed into the solution of **18** to suppress bimolecular coupling. After the reaction, a small peak was detected at MWD in SEC trace indicated the small proportion of bimolecular coupling which was ~22% obtained by LND simulation (Figure

3.13A). The high molecular weight impurities were removed by preparative SEC resulting in an increase of purity from 68 % (crude product) to 88 % (after prep) (Figure 3.13A).

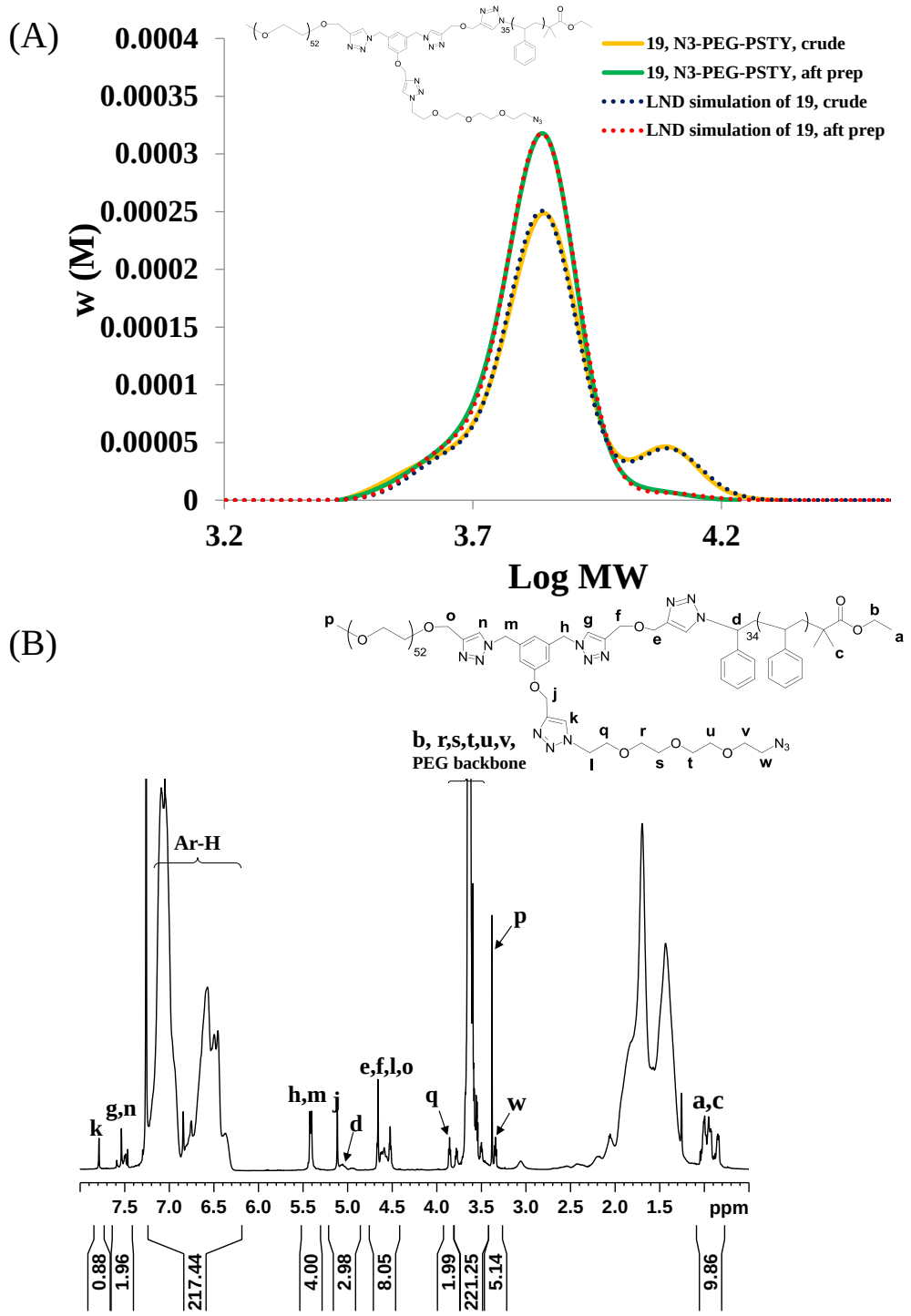

Figure 3.13 (A) SEC traces and LND simulation of N_3-PEG-PSTY (**19**, before and after prep). Determined from THF SEC, RI detector, PSTY standard. (B) ^{1}H NMR spectrum of N_3-PEG-PSTY (**19**), recorded in $CDCl_3$ at 298K, 500MHz.

Synthesis of building blocks P^{t}BA-alk, 22

The synthetic route of P^{t}BA-alk building block was similar to PSTY-alk but using SET-LRP technique (Scheme 3.5) to prepare precursor P^{t}BA-Br ,**20**. SET-LRP technique allows to make acrylate polymer with high chain end functionality and narrow polydispersity in a very short time.[53]

P^{t}BA-Br was synthesized from the SET-LRP of *tert*-butyl acrylate using EBiB as initiator at 22 ^{o}C for 50 min with M_n=5950 and PDI=1.05 (Scheme 3.5, Tables 3.1, Figure A3.26). The ^{1}H NMR (Figure A3.27) and MALID-ToF spectra (Figure A3.28) confirmed the high Br functionality (96 % from ^{1}H NMR). The Br group was further converted to N_3 group using NaN_3 with nearly quantitative conversion (96 % N_3 functionality from ^{1}H NMR, Figure A3.30) to produce P^{t}BA-N_3,**21**. A distinct shift of peak **d** from 4.1 ppm to ~3.6 ppm in ^{1}H NMR spectrum (Figure A3.30) together with single peak ascribed to adduct Na^+ in MALDI-ToF spectrum (Figure A3.31) proved the successful azidation. Apart, the typical azide stretching signal at 2100 cm^{-1} in ATR-FTIR (Figure A3.32B) also suggested the azide functionality.

P^{t}BA-N_3 **21** was subsequently converted to P^{t}BA-alk **22** by 'click' reaction with a 30 fold excess of propargyl ether. After the reaction, the SEC trace of the crude product showed almost unimodal distribution with small high MWD shoulder which was then removed by preparative SEC to give **22** (Figure 3.14A, Table 3.1) with M_n=5930 and PDI= 1.05. ^{1}H NMR spectra (Figure 3.14B) of **22** showed three new peaks at 7.7 ppm, 4.7 ppm, and 4.2 ppm ascribed protons in and beside the new genretaed triazole ring (i.e., peaks **e**, **f**, **g**), suggesting the incorporation of prapargyl ether moiety. Integration of the peaks for the protons adjacent to the triazole ringe (i.e., peaks **d**, **f** ,**g**) suggested high alkyne chain-end functionality. . The main peak was observed with *m/z* 5913.49 in MALDI-ToF spectrum of **22** (Figure 3.15B) was close to the theoretical value (5913.81) proved the structure of P^{t}BA-alk. SET-LRP together with CuAAC 'click' reaction provided the polymers with very high alkyne chain-end functionality which is a prerequisite for further successful iterative coupling reactions.

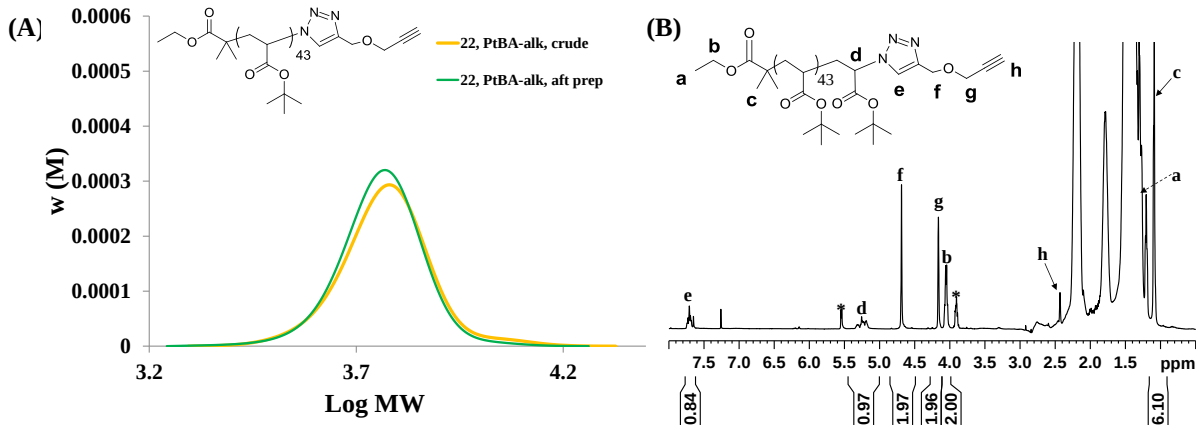

Figure 3. 14 (A) ^{1}H 1D DOSY NMR spectrum of P^{t}BA-alk (**22**), recorded in $CDCl_3$ at 298K , 500MHz. (B) ^{1}H 1D DOSY NMR spectrum of P^{t}BA-alk (**22**), recorded in $CDCl_3$ at 298K , 500MHz.

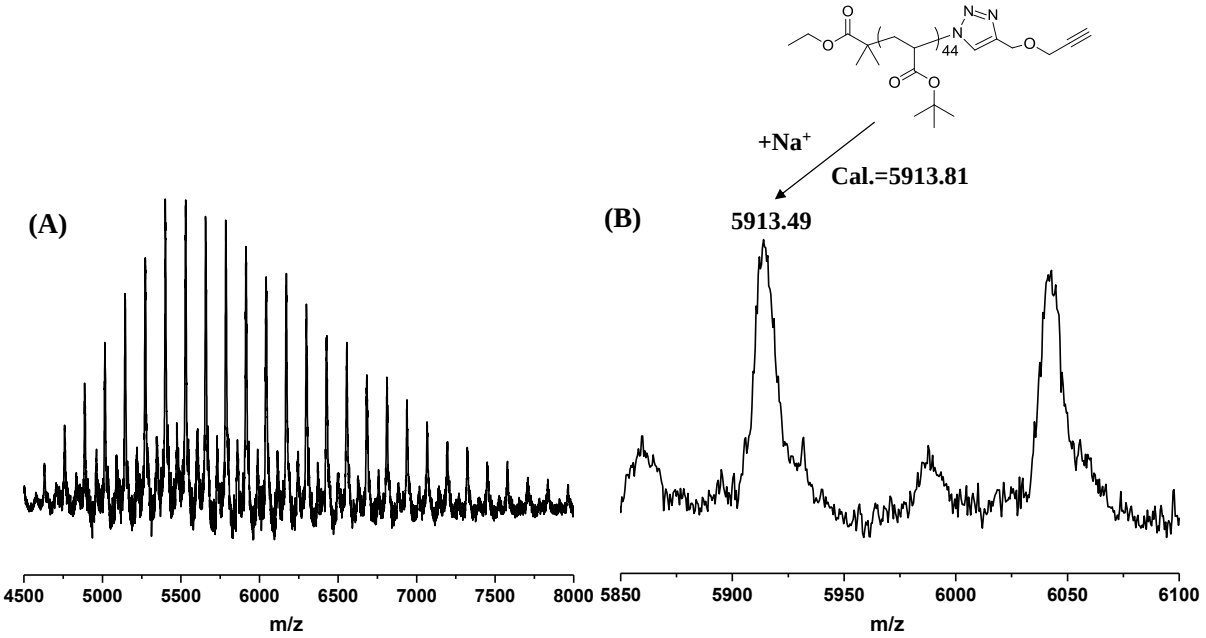

Fgiure 3.15 The full (A) and expanded (B) MALDI-ToF mass spectra of P^{t}BA-alk (**22**), the spectra were recorded in linear mode using DCTB as the matrix and $NaCF_3COO$ as the cation source.

Synthesis of Tips-alk-ph-P^{t}BA(N_3), 23

The P^{t}BA-alk (**22**) was then coupled onto the one of azide groups of trifunctional linker (**8**) to give **23** with another free azide group allowing the further attachment of the second arm (Scheme 3.1). The degassed solution of **22** was fed into the solution containing a 10 fold excess of **8** to create a reaction system that instant molar ratio of **8** to **22** was high enough to favour the formation of one-arm product **23** and minimized two-arm side product. Coupling **22** and **8** using CuAAC reaction resulted in a slight shift of SEC trace to higher MWD to produce **23** (91 % purity, prior to fractionation, by LND method) as shown in Figure 3.16A. The SEC trace of 23 (Figure 3.16A, crude) showed a very small shoulder at high MWD

indicated the formation of 2-arm byproduct, which was removed by preparative SEC to give **23** (,Figure 3.16A, aft prep, > 99 % purity by LND fit) with $M_{n,RI}$=6240, PDI=1.03.

After click reaction, the typical resonance signals of protons ascribed to the compound **8,** such as aromatic protons **k**, **j** at 6.8~7.0 ppm, Tips group protons **m**, **n** at 1.0 ppm, and methylene protons **o**, **i** at 4.3 ppm and 5.5 ppm, respectively, were detected in ^{1}H NMR spectrum (Figure 3.16B). In addition,, a new triazole ring proton (**h**) emerged at 7.5 ppm suggested P^{t}BA was coupled onto the trifuctional core 8 via CuAAC 'click' reaction (Figure 3.16B). Integration of the peaks for the protons adjacent to the triazole ring (**i**) and N_3 group (**o**), respectively, suggesting high N_3 chain-end functionality,which is crucial for further coupling of another arm. A single peak at MALDI-ToF spectrum which the *m/z* found (6055.76) was close to the theoretical value (6055.87) suggested the formation and the high purity of targeted product **23** (Figure 3.17).

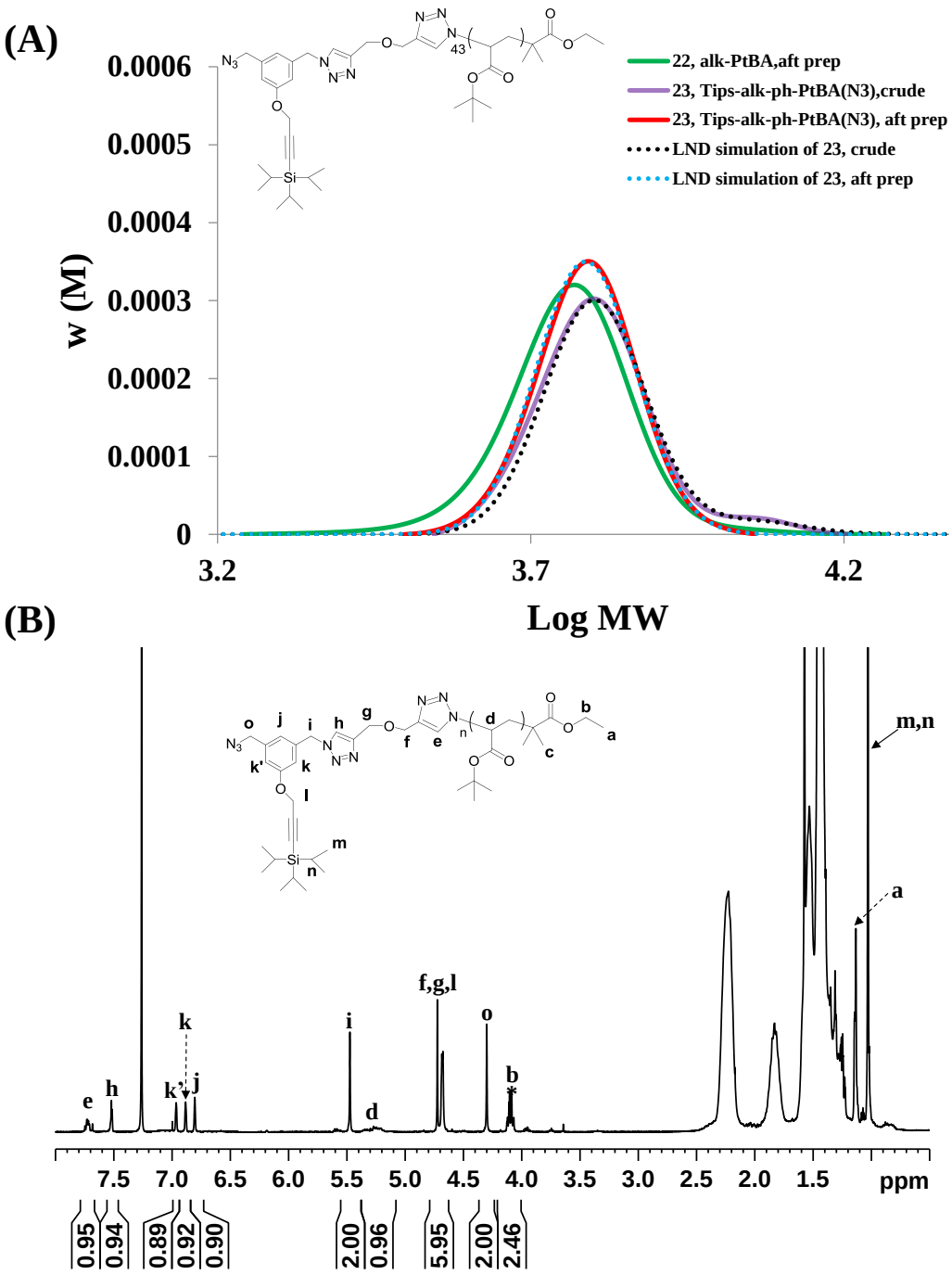

Figure 3.16 (A) SEC trace of P^{t}BA-alk (**22**), Tips-alk-P^{t}BA(N_3) (**23**) (before and after prep) and LND simulation of (**23**).Determined from THF SEC, RI detector, PSTY standard. (B) ^{1}H NMR spectrum of Tips-alk-P^{t}BA(N_3) (**23**), recorded in $CDCl_3$ at 298K , 500MHz, *=peroxide.

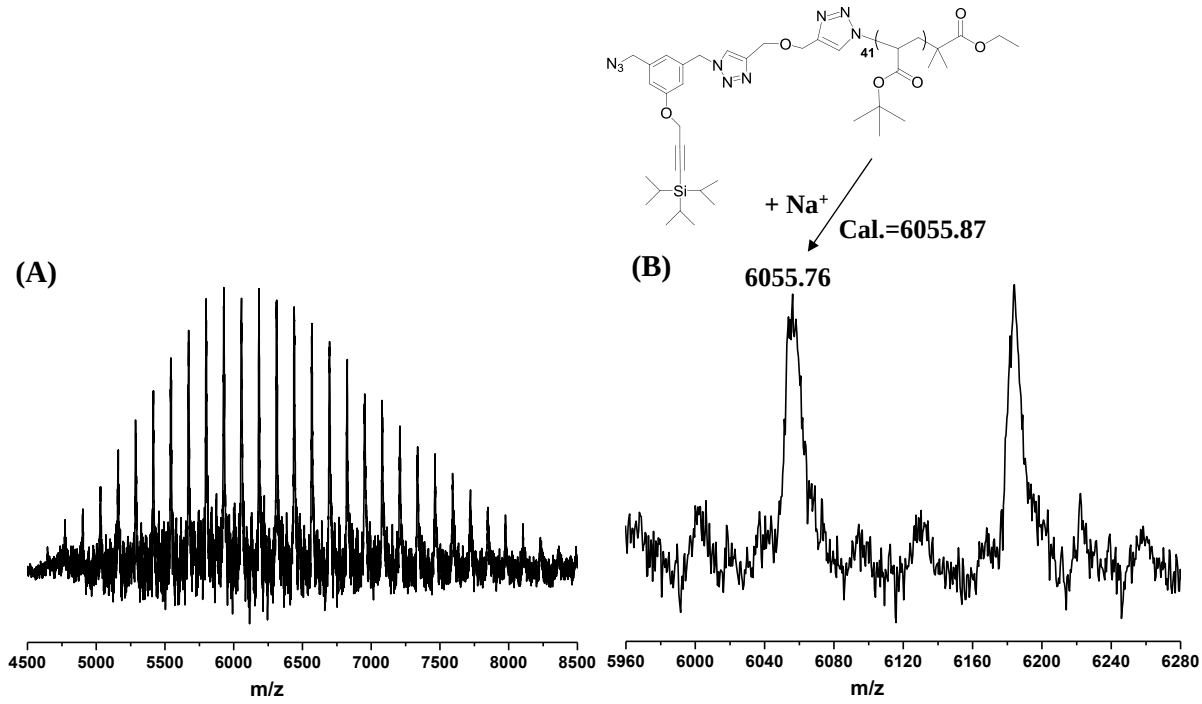

Figure 3. 17 The full (A) and expanded (B) MALDI-ToF mass spectra of Tips-alk-P^{t}BA(N_3)(**23**), The spectra were recorded in linear mode using DCTB as the matrix and $NaCF_3COO$ as the cation source.

Synthesis of $(OH)_2$-PNIPAm-alk, 27

The alk-terminal PNIPAm building block was generated from SET-LRP of NIPAm in water followed by two steps of post-modification (Scheme 3.6). The SET-LRP is capable for the polymerization of acrylamide monomer in aqueous condition resulting in corresponding polymer (e.g, PNIPAm). However, the Br chain-end functionality was suspected to hydrolyze during the work up.[35] In this work, we polymerized NIPAm monomer in water and at the end of polymerization the Br chain end was directly converted to azide. To polymerize the NIPAm in water, water-soluble initiator **25** was designed, synthesized and characterized by NMR to confirm the structure (Figure A3.33 and 3.34). In the presence of reducing agent $NaBH_4$, the Cu(II)Br_2 was readily converted to Cu(I)Br followed by a fast disproportionation of itself to form nascent Cu(0) to initiate the SET-LRP of PNIPAm.[35, 59, 60] The polar solvent H_2O and *N*-containing ligand Me_6TREN favor instantaneous disproportionation of Cu(I)Br into Cu(II)Br_2 and Cu(0).[61] The polymerization was carried out in 0 ^oC with very fast propagation rate and finished within 60 min followed by *in-situ* adization by adding degassed NaN_3 solution into reaction system to convert Br group to N_3 group of PNIPAm chain end. The addition of NaN_3 allowed the *in-situ* azidation which reduced the possibility of potential hydrolysis of Br group to hydroxyl group in water.[35, 62] The narrow polydisperity (1.10, Table

3.1) of resulting PNIPAm-N_3 ($M_{n,RI}$=2200) **26** demonstrated that aqueous phase SET-LRP had an excellent control of polymerization of NIPAm (Table 3.1, Figure A3.35).

The further analysis by ^{1}H NMR (Figure A3.36) and MALDI-ToF (Figure A3.37) confirmed the high N_3 functionality of resulting PNIPAm-N_3 also suggesting that the *in-situ* conversion of Br group to N_3 group is an effective strategy to achieve high chain-end fidelity. Again, the propargyl ether was used to modify the azide-functional polymer **26** to prepare alkyne-terminated polymer **27** which will be coupled onto the pendant azide group of **23** (Scheme 3.6). A 50 fold excess. of propargyl ether was used in the 'click' reaction with **26**. After 'click' reaction, there was no obvious high molecular shoulder observed (Figure 3.18A) suggesting little or no biomolecular coupling product. The dialysis was used to remove excess of propargyl ether resulted in PNIPAm-alk **27** with ($M_{n,RI}$=2650, PDI=1.09, $M_{n,TD}$=4230, PDI=1.02, Table 3.1). ^{1}H NMR spectrum (Figure 3.18B) of **27** showed the appearance of triazole ring proton (**i**) at 7.9 ppm and protons (peak **j**, **k**, and alkyne proton **l**) ascribed to propargyl ether moiety provided the direct proof of incorporation of propargyl ether moiety by CuAAC reaction. The dominant peak with *m/z* as 4533.90 in MALDI-ToF spectrum was close with the calculated value 4534.26 for PNIPAm$_{37}$-alk also suggested the high purity of resulting polymer **27** (Figure 3.19).

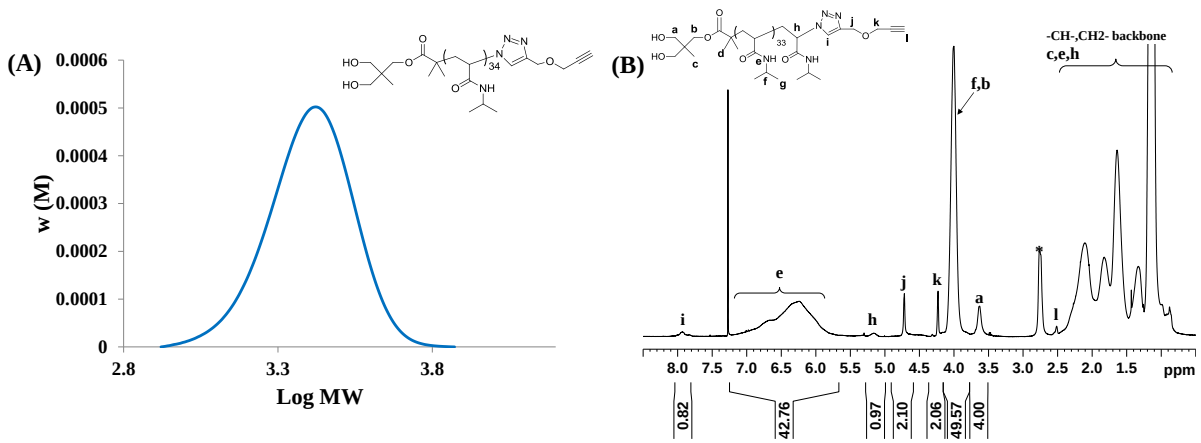

Figure 3.18 (A) SEC trace of alk-PNIPAm-$(OH)_2$ (**27**). Determined from THF SEC, RI detector, PSTY standard. (B) ^{1}H 1D DOSY NMR spectrum of alk-PNIPAm-$(OH)_2$ (**27**), recorded in $CDCl_3$ at 298K , 400MHz, *=H_2O.

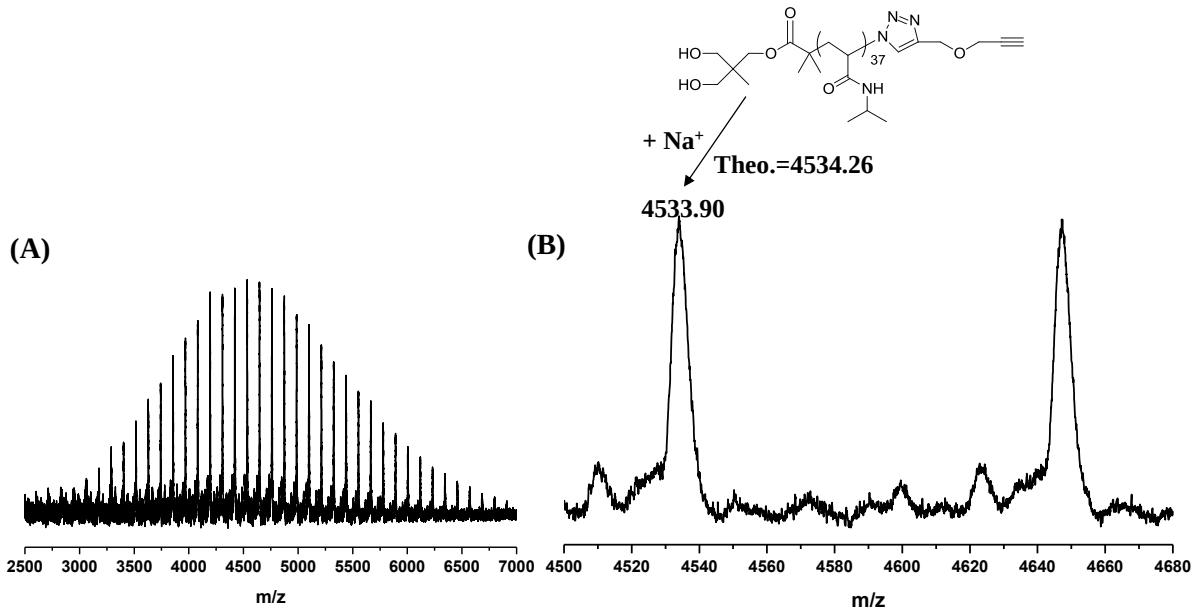

Figure 3.19 The full (A) and expanded (B) MALDI-TOF mass spectra of alk-PNIPAm-$(OH)_2$ (**27**), The spectra were recorded in linear mode using DCTB as the matrix and $NaCF_3COO$ as the cation source.

Synthesis of alkyne-terminal P^{t}BA-b-PNIPAm copolymer, 29

The P^{t}BA-b-PNIPAm copolymer with protected alkyne group was prepared *via* coupling building blocks **23** and **27** in DMF. A higher temperature (50 ^oC) was used to accelerate the 'click' reaction. A slightly excess (0.1 equiv. excess) of **27** was used to drive the reaction to higher conversion. The small tail at low MWD represents 5 % impurity of the double MW of **27** by LND simulation, which probably originated from the Glazer coupling of excess reactant PNIPAm-alk (Figure 3.20A). The Glazer coupling byproduct was subsequently removed by preparative SEC and led to an increase of purity of **28** from 94 % to 99 % by LND simulation. The purified copolymers **28** exhibited a narrow PDI_{RI} (1.03) with $M_{n,RI}$ of 9450 and $M_{n,TD}$ of 10690 that is close to theoretical molecular weight (10470, calculated from the addition of absolute molecular weight of **23** and **27**) of **28** (Table 3.1). After 'click' reaction, the ^1H NMR spectrum showed a new peak at 7.6 ppm ascribed to new triazole ring proton (**h**), suggesting the successful 'click' reaction. And two new broad peaks at ~4.0 ppm (**t**) and 6.0 to 7.2 ppm (**u**) ascribed to the protons of NIPAm units also demonstrated the incorporation of PNIPAm block (Figure 3.20B). The dn/dc value of P^{t}BA-b- PNIPAm copolymer was determined by equation 4 based on the dn/dc of P^{t}BA and PNIPAm, and given in Table 2.

TBAF was used for deprotecting **28** to produce **29** ($M_{n,RI}$=9000, PDI=1.05, $M_{n,TD}$=10690, PDI=1.03, Table 3.1) bearing free alkyne group. The SEC trace of **29** also showed a slightly

lower MWD than that of Tips-protected precursor **28**, and no high or low MWD byproducts observed after deprotection (Figure 3.21A). The disappearance of signal assigned for Tips group (~ 1.1 ppm) in ^{1}H NMR spectrum is another direct proof of quantitative derpotection (Figure 3.21B).

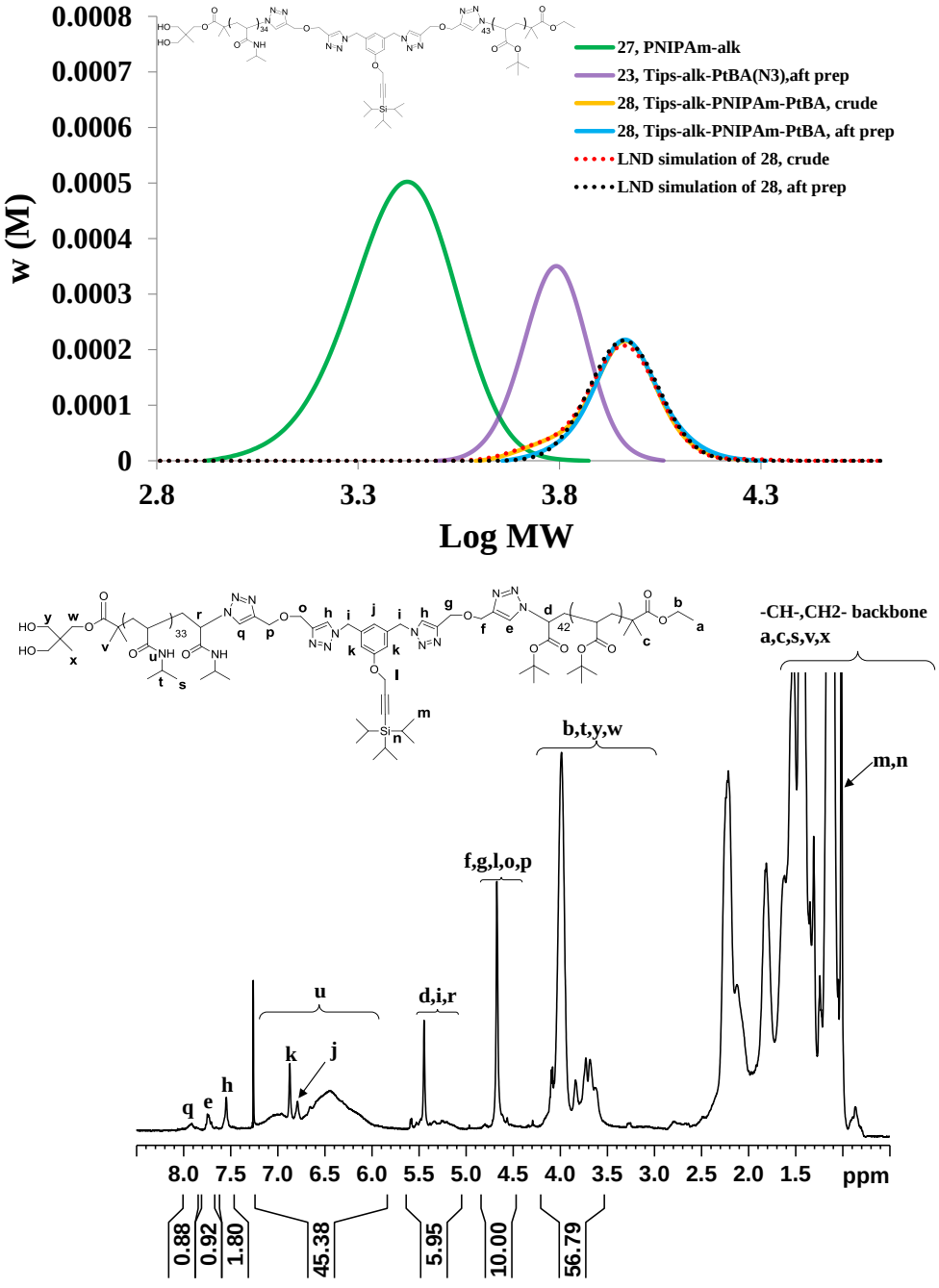

Figure 3.20 (A) SEC traces of alk-PNIPAm (**27**), Tips-alk-P^{t}BA-(N_3) (**23**), Tips-alk-ph-PNIPAm-P^{t}BA (28) (before and after prep-SEC) and LND simulation of (**28**), Determined from THF SEC, RI detector, PSTY standard. (B) ^{1}H 1D DOSY NMR spectrum of Tips-alk-ph-PNIPAm-P^{t}BA (**28**), recorded in $CDCl_3$ at 298K, 400MHz.

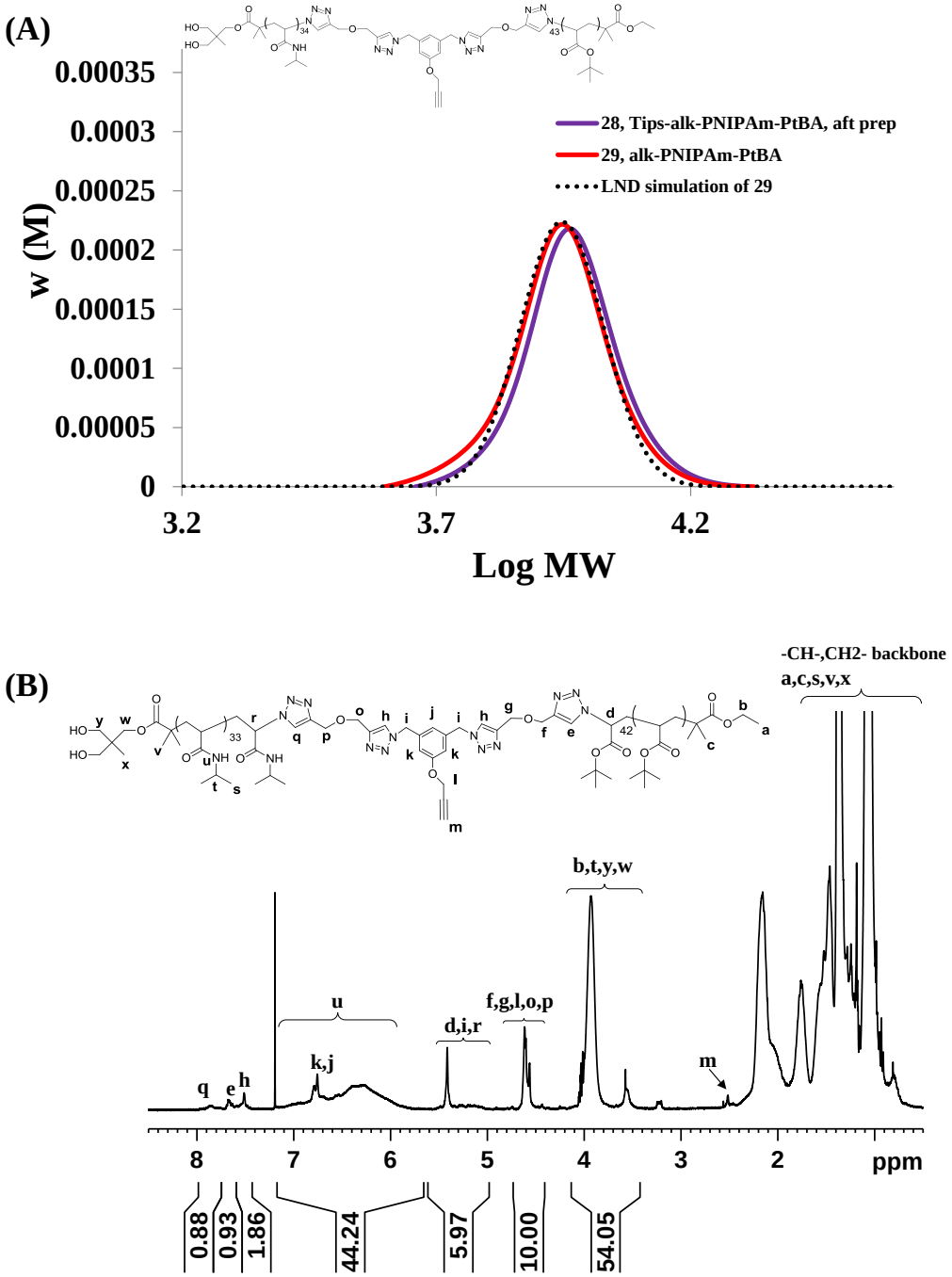

Figure 3.21 (A) SEC trace of Tips-alk-ph-PtBA-PNIPAm (**28**), alk-ph-PtBA-PNIPAm (**29**) and LND simulation of (**11**). Determined from THF SEC, RI detector, PSTY standard. (B) ^{1}H 1D DOSY NMR spectrum of alk-PNIPAm(P^{t}BA) (**29**), recorded in $CDCl_3$ at 298K , 400MHz.

Synthesis of 4-arm ABCD miktoarm star, 30

The ABCD miktoarm **30** star was formed by coupling of N_3-PEG-PSTY**19** (1.1 equiv.) and alk-PNIPAm-P^{t}BA**29** (1.0 equiv.) using the CuAAC 'click' reaction in one-pot at 50 ^{o}C in 2h. The SEC trace (Figure 3.31A) showed a MWD corresponding to the product of **30** (70 % purity, and click efficiency 75 % determined by LND simulation and dn/dc value of 4-arm ABCE star, Table 1 and Table 2), 13.2 % of the starting polymer **19**, 11.8 % starting polymer **29**, and 3.3 % low MWD impurities, respectively. After fractionation of **30** (crude) by preparative SEC, the purity increased to 97 %. The moderate 'click' efficiency (75 %) of CuAAC reaction utilized in synthesis of ABCD star may due to the impurity of starting materials, which therefore led to a difficulty in determining the stoichiometry of reactants. The $M_{n,RI}$ of **30** (prep) was 15860 with a PDI of 1.03 using refractive index (RI) detector, and the $M_{n,TD}$ was 16760 with a PDI of 1.02 using triple detection (i.e., absolute molecular weight determination) as given in Table 3.1. The value of $M_{n,TD}$ (16760) was close to the theoretical value (16860) of **30** calculated from the addition of the absolute molecular weights of the starting polymers **19** and **29**.

In the ^{1}H NMR spectrum of ABCD star (Figure 3.22B), characteristic resonance signals were detected at 6.2 to 7.2 ppm (PhH of PSTY and -NH- of PNIPAm), 3.8 to 4.2 ppm (-CH- of PNIPAm), 3.3 to 3.7 ppm (-CH_2-,CH_3O- of PEG). On the basis of integration areas ascribed to 3 different polymers, the chemical composition of **30** was determined to be $PSTY_{37}$-PEG_{51}-$PNIPAm_{36}$, which was close to the theoretical composition calculated from the ^{1}H NMR spectra of each polymer building blocks (i.e., $PSTY_{35}$-PEG_{52}-$PNIPAm_{34}$). For the PtBA block, the main characteric peaks were overlapped and the DP can not be calculated. The good agreement between experimental and theoretical molecular weight data (DP), and narrow PDI (1.03) suggested the precise and controlled compositions of resulting miktoarm star.

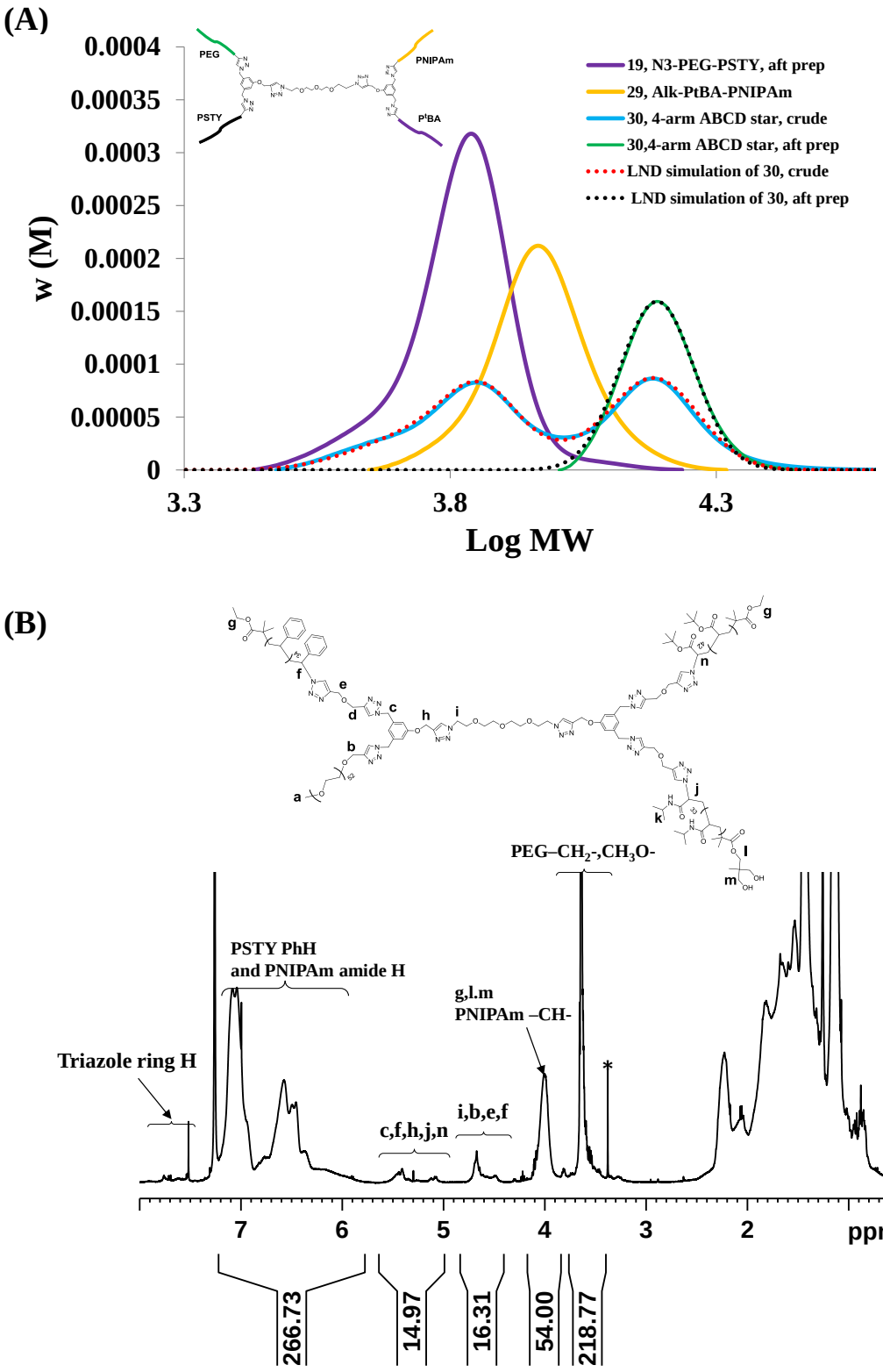

Figure 3.22 (A) SEC trace of N_3-PSTY-PEG (**19**), alk-PNIPAm-P^{t}BA (**29**), and 4-arm PSTY-PEG-PNIPAm-P^{t}BA star (**30**). Determined from THF SEC, RI detector, PSTY standard. (B) ^{1}H NMR spectrum of PSTY-PEG-P^{t}BA-PNIPAm (**30**), recorded in $CDCl_3$ at 298K , 400MHz, *=MeOH.

3.4 Conclusion

In conclusion, we developed a facile strategy to synthesize multi-compositional ABCD miktoarm star copolymers. The versatile LRP techniques (ATRP and SET-LRP) together with the quantitative post-functionalization provided access to alkyne-terminated and well-defined building blocks, including PSTY, P^{t}BA, PNIPAm and PEG. The clickable trifunctional and difunctional azide linkers were employed to couple the pre-synthesized arm segments via an iterative and sequential strategy. A 4-arm PSTY star was first synthesized *via* sequential CuAAC 'click' reaction with high click efficiency (91 %), the resulting PSTY star possessed a low polydispersity (1.04) and high purity (98 %) evident from NMR, SEC and MALDI-ToF MS analyses. This strategy was further employed to prepare 4-arm PSTY-PEG-PNIPAm-P^{t}BA miktoarm star with low PDI (1.03) and high purity after purification (97 %) Because of its mild reaction condition and good 'click' efficiencies for a wide range of polymers, our versatile method based on CuAAC 'click' reaction and LRP can be utilized to construct many types of miktoarm star copolymers with various chemical composition up to 4 or more arm segments. Our method is an efficient and versatile method for the construction of multiarm star branched polymers.

3.5 References

1. Bauer, B. J.; Fetters, L. J. *Rubber Chem Technol* **1978,** 51, (3), 406-436.
2. Grest, G. S.; Fetters, L. J.; Huang, J. S.; Richter, D. *Adv Chem Phys* **1996,** 94, 67-163.
3. Kricheldorf, H. R. *Macromol Symp* **1997,** 122, 15-23.
4. Moughton, A. O.; Hillmyer, M. A.; Lodge, T. P. *Macromolecules* **2012,** 45, (1), 2-19.
5. Li, Z. B.; Kesselman, E.; Talmon, Y.; Hillmyer, M. A.; Lodge, T. P. *Science* **2004,** 306, (5693), 98-101.
6. Lodge, T. P.; Rasdal, A.; Li, Z. B.; Hillmyer, M. A. *J Am Chem Soc* **2005,** 127, (50), 17608-17609.
7. Li, Z. B.; Hillmyer, M. A.; Lodge, T. P. *Langmuir* **2006,** 22, (22), 9409-9417.
8. Li, Z. B.; Hillmyer, M. A.; Lodge, T. P. *Macromolecules* **2006,** 39, (2), 765-771.
9. Gao, H. F. *Macromol Rapid Comm* **2012,** 33, (9), 722-734.
10. Wu, W.; Wang, W. G.; Li, J. S. *Prog Polym Sci* **2015,** 46, 55-85.
11. Lapienis, G. *Prog Polym Sci* **2009,** 34, (9), 852-892.
12. Kuckling, D.; Wycisk, A. *J Polym Sci Pol Chem* **2013,** 51, (14), 2980-2994.
13. Iatridi, Z.; Tsitsilianis, C. *Polymers-Basel* **2011,** 3, (4), 1911-1933.
14. Mei, L.; Jiang, Y. Y.; Feng, S. S. *Nanomedicine-Uk* **2014,** 9, (1), 9-12.
15. Higashihara, T.; Hayashi, M.; Hirao, A. *Prog Polym Sci* **2011,** 36, (3), 323-375.
16. Hadjichristidis, N.; Pitsikalis, M.; Pispas, S.; Iatrou, H. *Chem Rev* **2001,** 101, (12), 3747-3792.
17. Higashihara, T.; Nagura, M.; Inoue, K.; Haraguchi, N.; Hirao, A. *Macromolecules* **2005,** 38, (11), 4577-4587.
18. Zhao, Y. L.; Higashihara, T.; Sugiyama, K.; Hirao, A. *J Am Chem Soc* **2005,** 127, (41), 14158-14159.
19. Hirao, A.; Hayashi, M.; Higashihara, T. *Macromol Chem Phys* **2001,** 202, (16), 3165-3173.
20. Higashihara, T.; Sugiyama, K.; Yoo, H. S.; Hayashi, M.; Hirao, A. *Macromol Rapid Comm* **2010,** 31, (12), 1031-1059.
21. Ito, S.; Goseki, R.; Ishizone, T.; Senda, S.; Hirao, A. *Macromolecules* **2013,** 46, (3), 819-827.
22. Ito, S.; Goseki, R.; Ishizone, T.; Hirao, A. *Eur Polym J* **2013,** 49, (9), 2545-2566.
23. Hong, K. L.; Uhrig, D.; Mays, J. W. *Curr Opin Solid St M* **1999,** 4, (6), 531-538.
24. Hawker, C. J.; Bosman, A. W.; Harth, E. *Chem Rev* **2001,** 101, (12), 3661-3688.

25. Barner, L.; Barner-Kowollik, C.; Davis, T. P.; Stenzel, M. H. *Aust J Chem* **2004,** 57, (1), 19-24.

26. Chiefari, J.; Chong, Y. K.; Ercole, F.; Krstina, J.; Jeffery, J.; Le, T. P. T.; Mayadunne, R. T. A.; Meijs, G. F.; Moad, C. L.; Moad, G.; Rizzardo, E.; Thang, S. H. *Macromolecules* **1998,** 31, (16), 5559-5562.

27. Moad, G.; Rizzardo, E.; Thang, S. H. *Polymer* **2008,** 49, (5), 1079-1131.

28. Gao, H. F.; Matyjaszewski, K. *Macromolecules* **2006,** 39, (15), 4960-4965.

29. Matyjaszewski, K. *Abstr Pap Am Chem S* **2014,** 248.

30. Matyjaszewski, K.; Gaynor, S. G. *Abstr Pap Am Chem S* **1999,** 217, U428-U428.

31. Cameron, D. J. A.; Shaver, M. P. *Chem Soc Rev* **2011,** 40, (3), 1761-1776.

32. Khanna, K.; Varshney, S.; Kakkar, A. *Macromolecules* **2010,** 43, (13), 5688-5698.

33. Rosen, B. M.; Percec, V. *Chem Rev* **2009,** 109, (11), 5069-5119.

34. Nguyen, N. H.; Rosen, B. M.; Percec, V. *J Polym Sci Pol Chem* **2010,** 48, (8), 1752-1763.

35. Zhang, Q.; Wilson, P.; Li, Z. D.; McHale, R.; Godfrey, J.; Anastasaki, A.; Waldron, C.; Haddleton, D. M. *J Am Chem Soc* **2013,** 135, (19), 7355-7363.

36. Shi, P. H.; Li, Y. G.; Pan, C. Y. *Eur Polym J* **2004,** 40, (7), 1283-1290.

37. Zhang, Y. F.; Li, C. H.; Liu, S. Y. *J Polym Sci Pol Chem* **2009,** 47, (12), 3066-3077.

38. Yuan, Y. Y.; Wang, Y. C.; Du, J. Z.; Wang, J. *Macromolecules* **2008,** 41, (22), 8620-8625.

39. Iskin, B.; Yilmaz, G.; Yagci, Y. *J Polym Sci Pol Chem* **2011,** 49, (11), 2417-2422.

40. Nunns, A.; Ross, C. A.; Manners, I. *Macromolecules* **2013,** 46, (7), 2628-2635.

41. Wang, G. W.; Luo, X. L.; Liu, C.; Huang, J. L. *J Polym Sci Pol Chem* **2008,** 46, (6), 2154-2166.

42. Altintas, O.; Hizal, G.; Tunca, U. *J Polym Sci Pol Chem* **2008,** 46, (4), 1218-1228.

43. Yang, L. P.; Zhou, H. X.; Shi, G. Y.; Wang, Y.; Pan, C. Y. *J Polym Sci Pol Chem* **2008,** 46, (19), 6641-6653.

44. Ye, C. N.; Zhao, G. D.; Zhang, M. J.; Du, J. Z.; Zhao, Y. L. *Macromolecules* **2012,** 45, (18), 7429-7439.

45. Mu, C. G.; Fan, X. D.; Tian, W.; Bai, Y.; Zhou, X. *Polym Chem-Uk* **2012,** 3, (5), 1137-1149.

46. Sun, W. Q.; He, X. H.; Gao, C. Y.; Liao, X. J.; Xie, M. R.; Lin, S. L.; Yan, D. Y. *Polym Chem-Uk* **2013,** 4, (6), 1939-1949.

47. Almeida, C. C.; Monteiro, M. L. G.; da Costa-Lima, B. R. C.; Alvares, T. S.; Conte, C. A. *Lwt-Food Science and Technology* **2015,** 61, (1), 7-11.

48. Li, C. H.; Ge, Z. S.; Liu, H. W.; Liu, S. Y. *J Polym Sci Pol Chem* **2009,** 47, (16), 4001-4013.

49. Gavrilov, M.; Monteiro, M. J. *Eur Polym J* **2015,** 65, 191-196.

50. Monteiro, M. J. *Eur Polym J* **2015,** 65, 197-201.

51. Kulis, J.; Jia, Z. F.; Monteiro, M. J. *Macromolecules* **2012,** 45, (15), 5956-5966.

52. Hossain, M. D.; Jia, Z. F.; Monteiro, M. J. *Macromolecules* **2014,** 47, (15), 4955-4970.

53. Jia, Z. F.; Lonsdale, D. E.; Kulis, J.; Monteiro, M. J. *Acs Macro Lett* **2012,** 1, (6), 780-783.

54. Li, Y. J.; Hoskins, J. N.; Sreerama, S. G.; Grayson, S. M. *Macromolecules* **2010,** 43, (14), 6225-6228.

55. Jia, Z. F.; Bell, C. A.; Monteiro, M. J. *Chem Commun* **2011,** 47, (14), 4165-4167.

56. Duxbury, C. J.; Cummins, D.; Heise, A. *J Polym Sci Pol Chem* **2009,** 47, (15), 3795-3802.

57. Lu, D. R.; Hossain, M. D.; Jia, Z. F.; Monteiro, M. J. *Macromolecules* **2015,** 48, (6), 1688-1702.

58. Bell, C. A.; Jia, Z. F.; Perrier, S.; Monteiro, M. J. *J Polym Sci Pol Chem* **2011,** 49, (21), 4539-4548.

59. Percec, V.; Popov, A. V.; Ramirez-Castillo, E.; Monteiro, M.; Barboiu, B.; Weichold, O.; Asandei, A. D.; Mitchell, C. M. *J Am Chem Soc* **2002,** 124, (18), 4940-4941.

60. Percec, V.; Guliashvili, T.; Ladislaw, J. S.; Wistrand, A.; Stjerndahl, A.; Sienkowska, M. J.; Monteiro, M. J.; Sahoo, S. *J Am Chem Soc* **2006,** 128, (43), 14156-14165.

61. Levere, M. E.; Nguyen, N. H.; Leng, X. F.; Percec, V. *Polym Chem-Uk* **2013,** 4, (5), 1635-1647.

62. Rademacher, J. T.; Baum, R.; Pallack, M. E.; Brittain, W. J.; Simonsick, W. J. *Macromolecules* **2000,** 33, (2), 284-288.

Chapter 4

One-Pot Orthogonal Copper-Catalyzed Synthesis and Self-Assembly of L-Lysine Decorated Polymeric Dendrimers

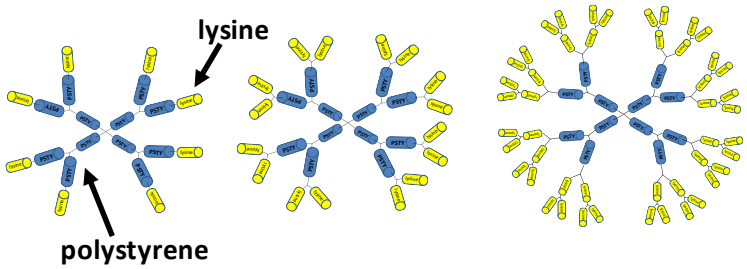

In this chapter, we developed a synthetic methodology to rapidly prepare polymeric synthetic peptides (peptidomimetics) with high yields. Synthetic peptides, including cyclic peptides and peptidomimetics, provide stability, protection and long circulation times compared to free-circulating peptides. Dendritic structures with amino acids or peptides attached to the peripheral layer represent one form of peptidomimetics (i.e. a hybrid peptide/dendrimer construct) that has found use in biological applications. Constructing such dendritic structures from linear polymeric building blocks provides a further advantage of generating a highly ordered and defined structure in the nanoparticle size range. However, the rapid synthesis of such well-defined structures is still a challenge. In this work, we demonstrate that through modulating the copper-activity concomitantly of the nitroxide radical coupling (NRC) and the azide-alkyne cycloaddition (CuAAC) reactions, polymeric dendrimers decorated with L-lysine on the periphery could be made rapidly in one-pot at 25 ^{o}C. Three polymeric dendrimers were constructed with high purity (>94 %) and with varying L-lysine density coated on the peripheral generation layer. The self-assembly of these dendrimers in water gave similar sizes to that found in organic solvents, suggesting that the aggregation number of dendritic structures in water was very low and possibly consisting of unimolecular micelles. The findings support the conclusion that the self-assembly of a dendritic architecture in water produces nanoparticles with predictable and well-controlled sizes. This synthetic methodology and the self-assembly properties represents an important step towards synthesizing peptide-decorated dendrimers targeted towards therapeutic applications.

4.1 Introduction

Recently, there has been a rapid increase in the number of synthetic peptides with therapeutic efficacy covering a diverse range of bioapplications.[1] The synthesis of cyclic peptides and peptidomimetics helped to overcome many of the drawbacks limiting the use of peptides as therapeutics in the past. These drawbacks included low stability in plasma, rapid degradation by proteases and rapid clearance from circulation.[2] Synthetic peptides in the form of dendrimers (i.e. peptidomimetics) were found to be much more stable when incubated with human plasma and serum.[3] Dendrimers consisting of a 4th generation poly(L-lysine) with multivalent ligands on the peripheral layer are in clinical trials as an antiviral topical ointment.[4, 5] Although dendrimers built from small molecules in each generation (with sizes < 15 nm) have been widely researched for many biological applications,[6, 7] dendrimers synthesized from polymeric building blocks[8-15] (denoted here as polymeric dendrimers) have extended the applications to where larger sizes (> 15 nm) were required, including a self-adjuvanting vaccine[16] and a cancer vaccine.[17] Polymeric dendrimers combine the attributes of the highly branched and symmetrical dendrimer structure, consisting of well-defined functionality within the generational layers and periphery, with the advantages of size and shape associated with nanoparticles.[13, 18]

Considerable work has been carried out to produce a wide range of polymeric dendrimers either through divergent or convergent methods.[8, 9, 11, 14, 19-21] One of the first strategies to combine 'living' radical polymerization (LRP) and a chain-end coupling process was denoted as TERMINI (Terminator Multifunctional INItiator), in which polymers were divergently grown via LRP, terminated with a difunctional molecule that after deprotection acted as an initiator for further polymer growth; a process repeated until the desired generation was achieved.[8] Other strategies included the divergent coupling of already synthesized linear polymers.[11] More recently, with the combination of LRP and 'click' reactions, polymers were synthesized with precise control over their architecture, including stars,[12, 22] dendrimers,[12, 14, 23-25] hyperbranched polymers,[26-28] multiblock polymers,[29] and bioconjugates.[30, 31] There are now many examples of using 'click' reactions to couple linear polymers together; these include the copper(I)-catalyzed azide-alkyne cycloaddition (CuAAC) reaction, strain-promoted azide-alkyne coupling (SPAAC),[32] Diels-Alder[33] and thiol-ene reactions.[34-37]

Most dendrimers made from linear polymer building blocks are synthesized divergently in a sequential and iterative manner. This synthetic process requires multiple reaction steps, including protection and deprotection of terminal end-groups, and time-consuming purification before growth of the next generational layer. The use of orthogonal 'click' coupling reactions avoids many of these

issues and increases the coupling efficiency with fewer reaction steps,[37-39] but in many cases a change in experimental conditions are required for the next 'click' reaction.

Here, a new process[40] of using two orthogonal 'click'-type reactions (i.e. nitroxide radical coupling (NRC) and CuAAC) modulated by a copper catalyst was utilized to produce 3 or 4 generation layered polymer dendrimers that are densely coated with L-lysine groups in one-pot at 25 ^{o}C (Scheme 4.1). This represents an advance on the previous techniques which relied on changing experimental conditions and purification at each generation step. By controlling the experimental conditions through selection of solvent and ligand, the synthesis of polymeric dendrimers in one-pot could proceed via a divergent, convergent, or a parallel process. The relative rates of the CuAAC and NRC reactions could be controlled to be comparable or with one significantly faster than the other. Utilizing the tool kit of building blocks shown in Scheme 1, the lysine peripheral density could be well controlled. The purity of the foundational building block, **5**, is critical to the success of the polymer dendrimer synthesis. In general, the synthesis of 4-arm stars produces higher order star architectures through star-star radical coupling.[41] Limiting the amount of star-star coupling allowed high purity 4-arm star polymer to be produced, enabling the high peripheral density of L-lysine on the dendrimer. This method of producing well-defined polymeric dendrimers with densely decorated amino acids (or amino acid dendrons) on the periphery represents an important step towards synthetic peptides designed as therapeutics. To further validate the potential use for these dendrimers as peptidomimetic nanoparticles, the self-assembly of these structures in water was compared to that in organic solvent.

4.1.1 Aim of Chapter

The aim of this work is to demonstrate the feasibility of using two orthogonal 'click'-type reactions (i.e. nitroxide radical coupling (NRC) and CuAAC) to couple well-defined polymer and amino acid or peptide building blocks in a one-pot reaction to produce high generation dendrimers (e.g., third or fourth generation), containing a polymer core and amino acid or peptide periphery.

Scheme 4.1 Synthetic route for lysine decorated polymeric 3rd and 4th generational layered dendrimers.

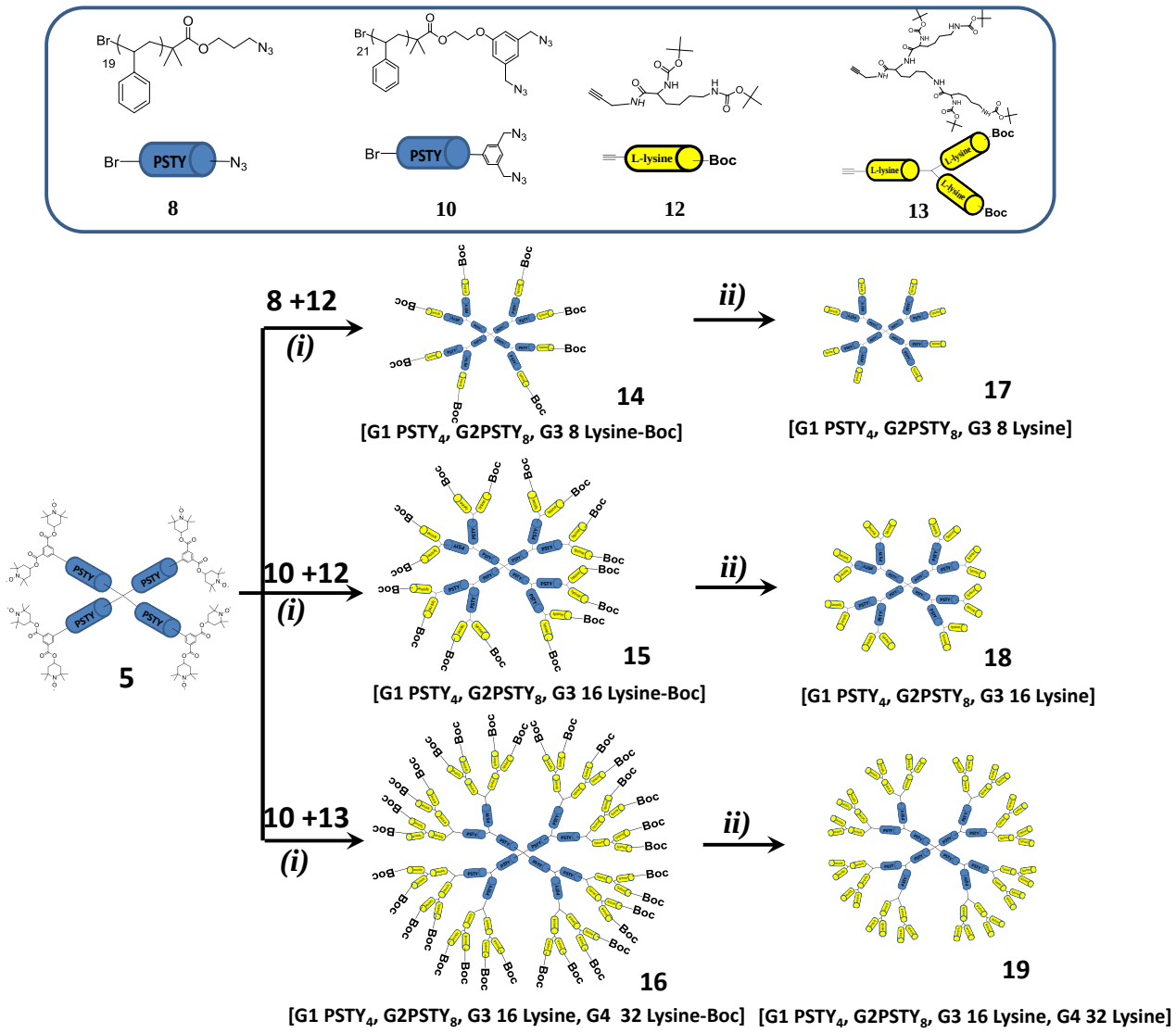

(*i*) One-pot, parallel CuAAC and NRC reaction. Polymer reactants with CuBr/PMDETA in a mixture of toluene/DMSO (50:50) for 30 min at 25 ^{o}C. (*ii*) Deprotection of Boc groups with TFA.

4.2 Experimental

4.2.1 Materials

Inhibitor was removed from styrene (STY: Aldrich, >99 %) before use by passing through a basic alumina column. The following chemicals were used as received: alumina, activated basic (Aldrich, Brockmann I, standard grade, ~150 mesh, 58 Å), magnesium sulfate ($MgSO_4$: anhydrous, Scharlau, extra pure), sodium chloride (NaCl: Univar, 99.9 %), sodium iodide (NaI: Aldrich, 99.5 %), sodium azide (NaN_3: Aldrich, 99.5 %), 1,1,1-triisopropylsilyl chloride (TIPS-Cl: Aldrich, 99 %), tetrabutylammonium fluoride (TBAF: Aldrich, 1.0 M in THF), ethylmagnesium bromide solution (Aldrich, 3.0 M in diethyl ether), triethylamine (TEA: Fluka, 98 %), TLC plates (silica gel 60 F254), silica gel 60 (230-400 mesh ATM (SDS)), potassium carbonate (K_2CO_3, analaR, 99.9 %), 2-bromoisobutyryl bromide (BIB, Aldrich, 98 %), lithium aluminium hydride ($LiAlH_4$, Aldrich, 98 %), diphenyl phosphoryl azide (DPPA, Aldrich, 97 %), 1,8-diazabicylco[5,4,0]undec-7-ene (DBU, Aldrich, 98 %), tetrabutylammonium fluoride hydrate (TBAF, Aldrich, 1.0 M in THF), 18-crown-6 ether (18-C-6, Aldrich,99 %), 2-Bromoethanol (Aldrich,98 %), imidazole (Aldrich,99 %) *N*,*N*′-dicyclohexylcarbodiimide (DCC, Aldrich, 99 %), *N*-hydroxysuccinimide (NHS, Aldrich, 98 %).

The following solvents were used as received: acetone (ChemSupply, AR), chloroform ($CHCl_3$: Labscan, AR grade), dimethyl sulfoxide (DMSO: Labscan, AR grade), dichloromethane (DCM: Labscan, AR grade), diethyl ether (Merck, GR grade), ethyl acetate (EtOAc: ChemSupply, AR grade), methanol (MeOH: anhydrous, Lichrosolv, 99.9 %, HPLC grade), *N*,*N*-dimethylformamide (DMF: Labscan, AR grade), *N*,*N*-dimethylacetamide (DMAc: Aldrich, HPLC grade), petroleum spirit (BR 40-60 ^{o}C, Univar, AR grade), tetrahydrofuran (THF: Lichrosolv, HPLC grade), and toluene (TOL, Univar, AR grade).

The following initiators, ligands, and metals for the various polymerizations are given below and used as received unless otherwise stated: *N*,*N*,*N*’,*N*’’,*N*’’-pentamethyldiethylenetriamine (PMDETA: Aldrich, 99 %), copper(II) bromide (Cu(II)Br_2: Aldrich, 99 %), Copper(I)bromide and Cu(II)Br_2/PMDETA complex were synthesized in our group.

4.2.2 Synthetic procedure

Scheme 4.2 Synthetic route for building block 5 (4-arm PSTY-$(NO^{\cdot})_2$)

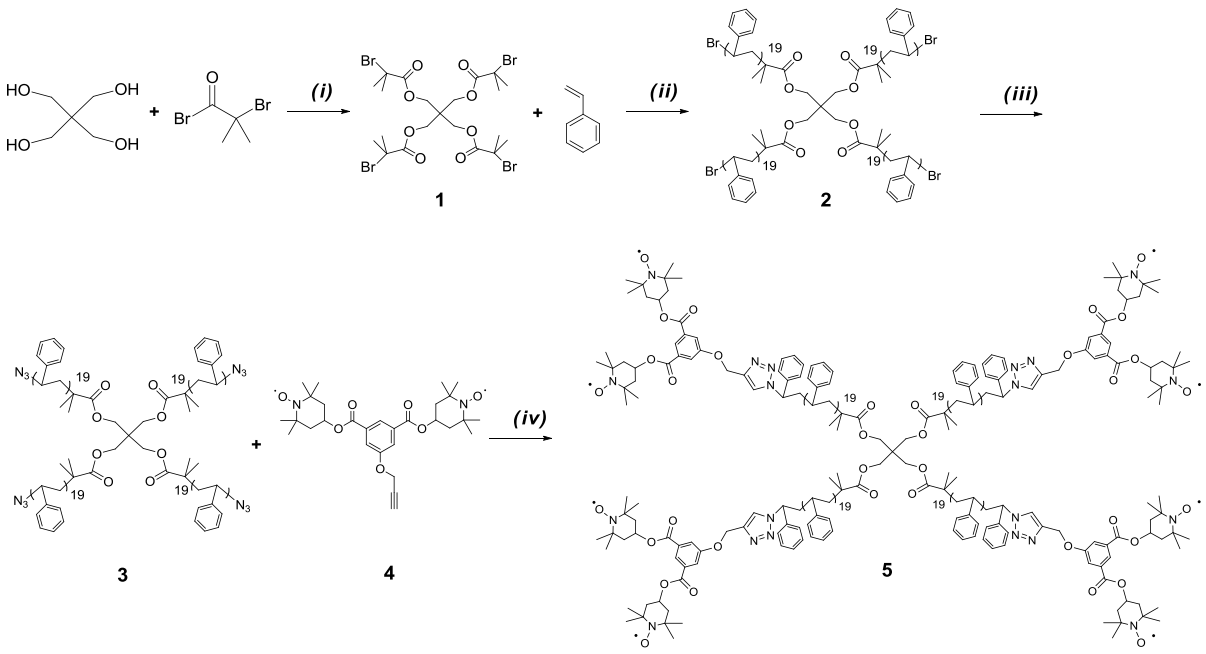

(*i*): THF, TEA, 0 ^{o}C-R.T., 6 h. (*ii*): CuBr, PMDETA, Cu(II)Br_2/PMDETA, anisole, 80 ^{o}C, 9 h; (*iii*): DMF, NaN_3, 25 ^{o}C, 24 h; (*iv*): CuBr, PMDETA, Toluene, 25 ^{o}C, 1 h.

4.2.2.1 Synthesis of 4-arm ATRP initiator, 1.

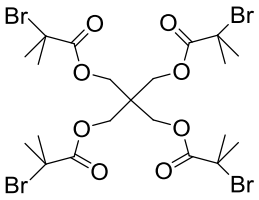

A solution containing 2-bromoisobutyryl bromide (25.1 g, 0.109 mol) dissolved in 80 mL of dry THF was added dropwise to another solution containing pentaerythritol (3.0 g, 2.2 x 10^{-2} mol) and triethylamine (11.1 g, 0.109 mol) dissolved in 220 mL of dry THF at 0 ^{o}C. The reaction was allowed to stir for 6 h, filtered to remove the salts, and then the filtrate concentrated by rotary evaporation. The resulted product was dissolved in 300 mL ether and sequentially washed with 10 wt% HCl, saturated $NaHCO_3$ solution, and brine. The organic layer was collected, dried over anhydrous $MgSO_4$ and filtered. The filtrate was concentrated by rotary evaporation. The concentrate was purified by silica gel column chromatography

using ethyl acetate/petroleum spirit (1/6, v/v) as the eluent. Product **1** was obtained as white crystals (10.65 g, 66.0 %). R_f (1/6 EtOAc/petroleum spirit) 0.61.

^{1}H NMR ($CDCl_3$, 298K, 400 MHz): δ 1.92 (s, 24H, C***H***$_3$-), 4.30 (s, 8H, -OC***H***$_2$C-). ^{13}C NMR ($CDCl_3$, 298K, 400 MHz): 30.62, 43.64, 55.18, 62.88, 170.89.

4.2.2.2 Synthesis of building block (4-arm PSTY-Br), 2

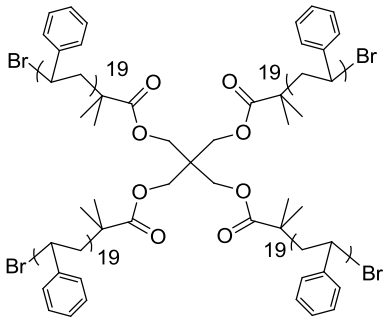

Freshly purified styrene (9.02 g, 8.66 x 10^{-2} mol), PMDETA (0.078 mL, 3.76 x 10^{-4} mol), **1** (0.254 g, 3.76 x 10^{-4} mol), anisole (10 mL) and Cu(II)Br_2/PMDETA (0.037 g, 9.41 x 10^{-5} mol) were added to a 20 mL Schlenk tube equipped with a magnetic stirrer and purged with argon for 20 min. Cu(I)Br (0.054 g, 3.77 x 10^{-4} mol) was carefully added under positive argon flow and the reaction mixture purged with argon for a further 5 min. The flask was placed in a temperature controlled oil bath at 80 ^{o}C for 9 h. The reaction was stopped by quenching in ice and exposed to air. The polymerization mixture was diluted with DCM and the copper salts removed by passage through an activated basic alumina column. The solution was concentrated by rotary evaporation and the polymer recovered by precipitation into methanol, filtered and dried for 48 h under high vacuum at 25 ^{o}C. The resultant polymer was precipitated from DCM into MeOH, filtered and dried under high vacuum for 48 h at 25 ^{o}C to give a white polymer, which was further purified by preparative SEC. The resultant polymer was re-precipitated from THF into MeOH, filtered, dried under high vacuum for 48 h at 25 ^{o}C and obtained as peach powder ($M_{n,RI}$ = 8670, $M_{p,RI}$ = 8710, PDI,$_{RI}$ = 1.05, $M_{n,TD}$ = 9700, $M_{p,TD}$ = 9840, PDI,$_{TD}$ = 1.02, $M_{n,NMR}$ =10820, monomer conversion 39.0 % as determined by gravimetric method).

4.2.2.2 Synthesis of building block (4-arm PSTY-N_3), 3

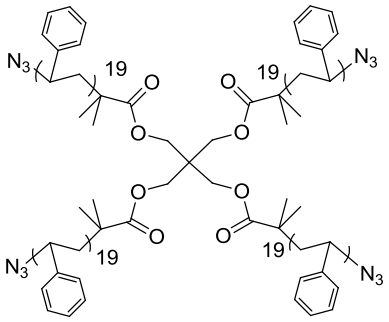

NaN_3 (0.34 g, 5.25 x 10^{-3} mol) was added to a stirred solution of **2** (1.16 g, 1.31 x 10^{-4} mol) in 6 mL of DMF. The reaction mixture was stirred for 24 h at room temperature. The polymer was twice precipitated into methanol (once from DMF, once from DCM), recovered by vacuum filtration and washed extensively with water and methanol. The polymer was dried under high vacuum for 48 h at 25 ^{o}C obtained as white powder. ($M_{n,RI}$ = 8730, $M_{p,RI}$ = 8810, $PDI_{,RI}$ = 1.05, $M_{n,TD}$ = 9630, $M_{p,TD}$ = 9790, $PDI_{,TD}$ = 1.02, $M_{n,NMR}$ =10670).

4.2.2.3 Synthesis of (4-arm PSTY-$(NO^{\cdot})_2$), 5

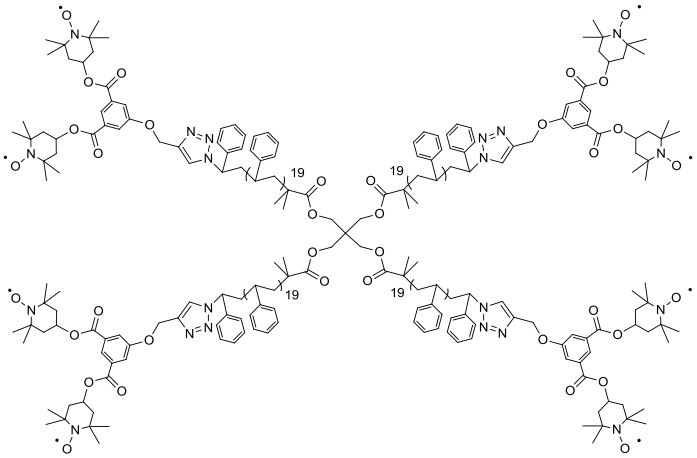

The trifunctional linker, **4**, was synthesized according to the literature procedure.[40] In a 20 mL Schlenk tube, **4** (0.096 g, 1.82 x 10^{-4} mol) was added to a stirred solution of **3** (0.35 g, 4.04 x 10^{-5} mol) and PMDETA (7.0 x 10^{-3} g, 4.04 x 10^{-5} mol) in 6 mL of toluene. The reaction mixture was purged with argon for 15 min. Cu(I)Br (5.7 x 10^{-3} g, 4.04 x 10^{-5} mol) was added to the solution under a positive flow of argon, sealed and stirred for 1 h at 25 ^{o}C. The polymer was diluted with DCM and the copper salts removed by passage through an

activated basic alumina column. The solution was concentrated by rotary evaporation and the polymer recovered by two precipitations (once from toluene and once from DCM) into methanol, collected by vacuum filtration and washed extensively with methanol. The polymer was dried under high vacuum for 48 h at 25 ^{o}C to give a peach colored polymer. The resultant polymer was re-precipitated from THF into MeOH, filtered and dried under high vacuum for 48 h at 25 ^{o}C and obtained as peach powder ($M_{n,RI}$ = 10200, $M_{p,RI}$ = 10320, PDI,$_{RI}$ = 1.04, $M_{n,TD}$ = 11600, $M_{p,TD}$ = 11760, PDI,$_{TD}$ = 1.01, $M_{n,NMR}$ =12640).

Scheme 4.3 Synthetic route for building block **8**.

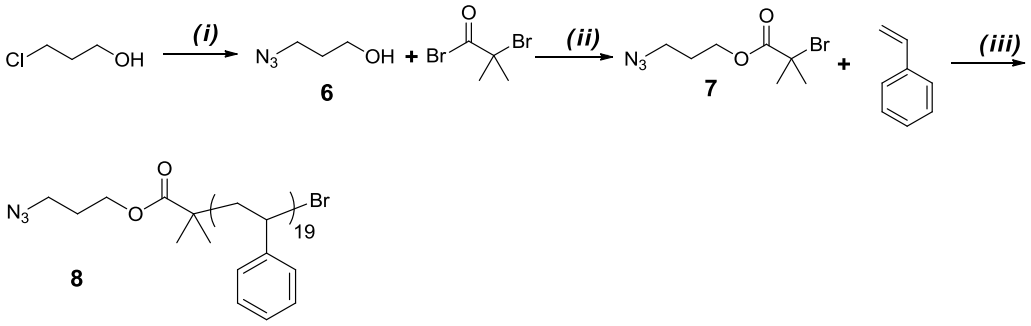

(*i*): NaI, NaN_3, DMSO/H_2O, 80 ^{o}C, 2 days. *(ii)*: TEA, THF, 0 ^{o}C-R.T., 6 h. (*iii*): CuBr, PMDETA, Cu(II)Br_2/PMDETA, bulk, 80 ^{o}C, 7.5 h;

4.2.2.4 Synthesis of 3-azidopropan-1-ol,6

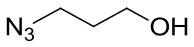

To a 100 mL flask, 3-chloropropan-1-ol (10 g, 0.106 mol), NaN_3 (17.2 g, 0.269 mol) and NaI (0.158 g, 1.06 x 10^{-3} mol) were dissolved in 25 mL DMSO and 25 mL water, kept stirring at 80 ^{o}C for 2 days. The solution was cooled and extracted with ether (3 x 100 mL), the organic phase was dried over anhydrous $MgSO_4$, filtered and concentrated. The product was **6** was obtained as a colourless oil (9.33 g, 88.0 %). The product was used in the next step without further purification. *Warning: The prodcut is not safe in high vaccum.*

^{1}H NMR ($CDCl_3$, 298K, 500 MHz): δ 3.69 (t, 2H, *J*=6.05 Hz, -C***H***$_2$OH), 3.39 (t, 2H, *J*=6.50 Hz -C***H***$_2$$N_3$), 2.25 (b, 1H, -O***H***), 1.78 (dt, 2H, *J*=6.15 Hz and 6.50 Hz, -CH_2C***H***$_2$$CH_2$-). ^{13}C NMR ($CDCl_3$, 298K, 500 MHz): 31.50, 48.47, 59.68.

4.2.2.5 Synthesis of mono-azide functional, 7

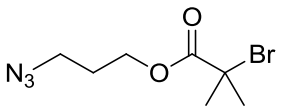

The ATRP initiator **7** (Scheme 4.3) was synthesized according to the literature procedure.[42] To a 250 mL flask, **6** (2.4 g, 2.37 x 10^{-2} mol) and triethylamine (3.0 g, 2.97 x 10^{-2} mol) were dissolved in 70 mL of dry THF at 0 ^{o}C. A mixture of bromine isobutyl bromide (6.53 g, 2.85 x 10^{-2} mol) and 30 mL dry THF was added dropwise into the solution above in 30 min. The reaction was allowed to stir for 6 h, filtered to remove the salts and the filtrate concentrated by rotary evaporation. The brown crude product was dissolved in 200 mL ether and sequentially washed with 10 % (m/m) HCl, saturated $NaHCO_3$ solution, and saturated brine. The organic layer was collected, and dried over anhydrous $MgSO_4$. The solvent was removed *in vacuo*, and followed by column chromatography using ethyl acetate/petroleum spirit (1/8, v/v) as the eluent. The product **7** was obtained as a colourless oil (6.1 g, 73.0 %). R_f (1/8 EtOAc/petroleum spirit) 0.43.

^{1}H NMR ($CDCl_3$, 298K, 500 MHz): δ 4.25 (t, 2H, *J*=6.1 Hz, -C***H***$_2$OCO-), 3.42 (t, 2H, *J*=6.7 Hz -C***H***$_2$N$_3$), 1.95 (dt, 2H, *J*=6.3 Hz and 6.5 Hz, -CH$_2$C***H***$_2$CH$_2$-), 1.92 (s, 6H, -C***H***$_3$). ^{13}C NMR ($CDCl_3$, 298K, 500 MHz): 28.04, 30.77, 48.09, 55.77, 62.82, 171.58.

4.2.2.6 Synthesis of building block N_3-PSTY-Br 8.

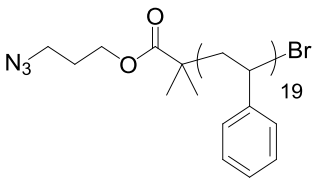

Building block **8** was synthesized *via* a typical ATRP polymerization. Freshly purified styrene (22.4 g, 0.215 mol), PMDETA (0.798 mL, 3.82 x 10^{-3} mol), **7** (1.19 g, 4.78 x 10^{-3} mol), and Cu(II)Br_2/PMDETA (0.284 g, 7.17 x 10^{-4} mol) were added to a 100 mL Schlenk flask equipped with a magnetic stirrer then purged with argon for 60 min. Cu(I)Br (0.548 g, 3.82 x 10^{-3} mol) was added under positive argon flow and the reaction mixture purged with argon for a further 5 min. The flask was placed in a temperature controlled oil bath at 80 ^{o}C for 7.5 h. The reaction was stopped by quenching in ice and then exposed to air. The

polymerization mixture was diluted with DCM and the copper salts removed by passage through an activated basic alumina column. The solution was concentrated by rotary evaporation and the polymer recovered by precipitation into methanol, filtered and dried for 48 h under high vacuum at 25 ^{o}C, and then further purified by preparative SEC. The resultant polymer was then re-precipitated from THF into MeOH, filtered and dried under high vacuum for 48 h at 25 ^{o}C obtained as white powder ($M_{n,RI}$ = 2370, $M_{p,RI}$ = 2490, PDI = 1.08, $M_{n,NMR}$=2870, monomer conversion %=47.6 %, determined from gravimetric method, yield %= 87 % after prep-SEC).

Scheme 4.4 Synthetic route for building block **10**.

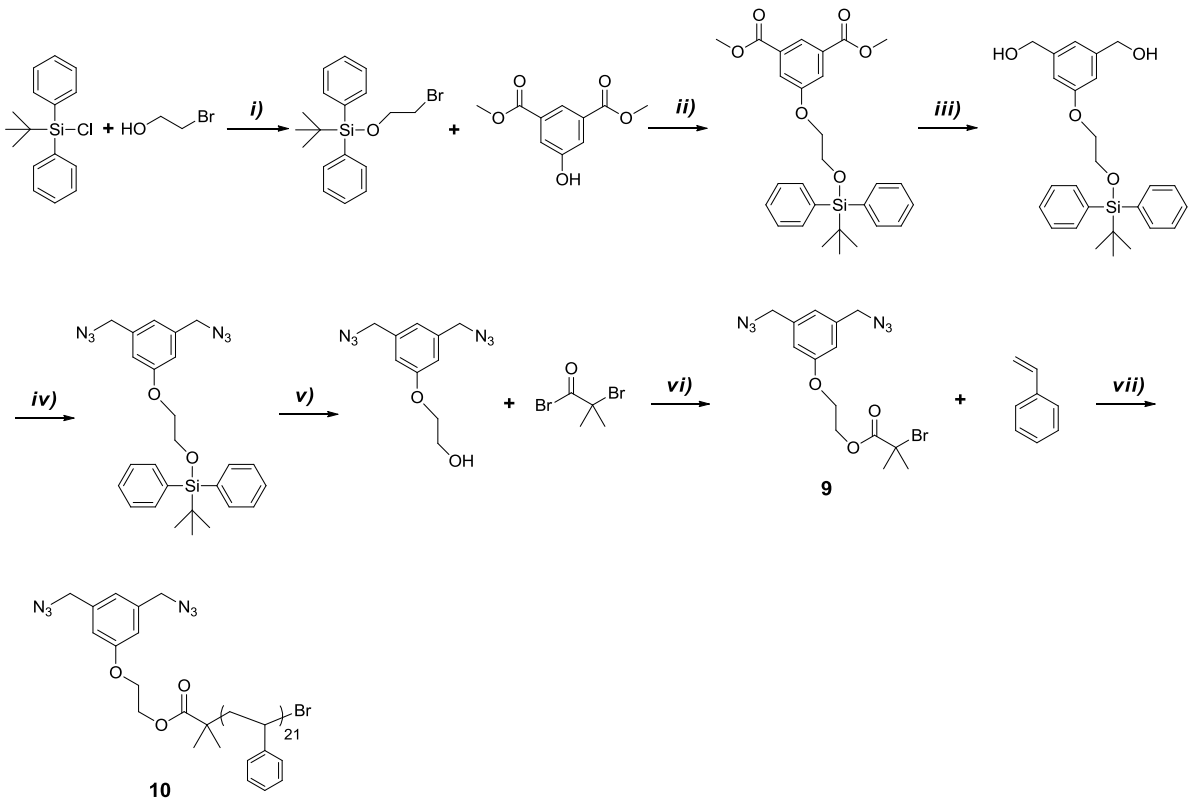

(*i*): Imidazole, THF, 0 ^{o}C-R.T., 12 h. (*ii*): 18-C-6, K_2CO_3, Acetone, reflux, 48 h. (*iii*): $LiAlH_4$, THF, 0 ^{o}C-R.T., 16 h, (*iv*): DPPA, DBU, toluene, 0 ^{o}C-R.T., dark, 16 h. (*v*): TBAF, THF, argon, R.T., 12 h. (*vi*): TEA, THF, 0 ^{o}C-R.T., 12 h. (*vii*): CuBr, PMDETA, Cu(II)Br_2/PMDETA, bulk, 80 ^{o}C, 220 min.

4.2.2.7 Synthesis of di-azide functional, 9

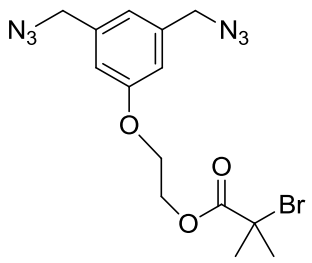

To a 250 mL flask, 2-(3,5-bis(azidomethyl)phenoxy)ethanol (3.0g, 0.014 mol) and triethylamine (2.14 g, 0.021 mol) were dissolved in 60 mL dry THF and cooled to 0 ^{o}C in an ice-bath. A mixture of bromine isobutyl bromide (4.81 g, 0.021 mol) and 30 mL dry THF was added dropwise into the solution above in 30 min. The reaction was stirring overnight and warmed to RT. The reaction mixture was filtered to remove the solid, concentrated and dried under vaccum at RT. The brown crude product was redissolved in 300 mL ether, and washed sequentially with 10 % (m/m) HCl, saturated $NaHCO_3$ solution, and then brine. The organic layer was collected, dried with anhydrous $MgSO_4$, the solvent was removed *in vacuo*, followed by column chromatography using ethyl acetate/petroleum spirit (1/3, v/v) as the eluent. The product **9** was obtained as a colourless oil (2.96 g, 58.2 %). R_f (1/3 EtOAc/petroleum spirit) 0.34.

^{1}H NMR ($CDCl_3$, 298K, 500 MHz): δ 6.85 (bd, 1H, aromatic proton), 6.83 (bd, 1H, aromatic proton), 4.51 (t, 2H, *J*=4.8 Hz, -$CH_2C\boldsymbol{H}_2$OCO-), 4.31 (s, 4H, -$C\boldsymbol{H}_2N_3$), 4.23 (t, 2H, *J*=4.8 Hz, -$OC\boldsymbol{H}_2CH_2$-), 1.94 (s, 6H, -$C\boldsymbol{H}_3$). ^{13}C NMR ($CDCl_3$, 298K, 500 MHz): 30.68, 54.41, 55.47, 64.04, 65.80, 114.16, 120.42, 137.72, 159.20, 171.63.

4.2.2.8 Synthesis of building block $(N_3)_2$-PSTY-Br, 10

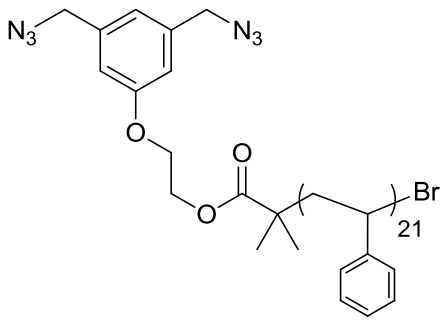

Freshly purified styrene (7.15 g, 0.068 mol), PMDETA (0.798 mL, 1.03 x 10^{-3} mol), **9** (0.546 g, 1.37 x 10^{-3} mol), and Cu(II)Br_2/PMDETA (0.082 g, 2.06 x 10^{-4} mol) were added to

a 20 mL Schlenk tube equipped with a magnetic stirrer then purged with argon for 20 min. Cu(I)Br (0.147 g, 1.03 x 10^{-3} mol) was added under positive argon flow and the reaction mixture purged with argon for a further 5 min. The flask was placed in a temperature controlled oil bath at 80 ^{o}C for 220 min. The reaction was stopped by quenching in ice and exposure to air. The polymerization mixture was diluted with DCM and the copper salts removed by passage through an activated basic alumina column. The solution was concentrated by rotary evaporation and the polymer recovered by precipitation into methanol, filtered and dried for 48 h under high vacuum at 25 ^{o}C, and then further purified by preparative SEC. The resultant polymer was then re-precipitated from DCM into MeOH, filtered and dried under high vacuum for 48 h at 25 ^{o}C, and characterized by SEC ($M_{n,RI}$ = 2600, $M_{p,RI}$ = 2690, PDI = 1.07, M_{NMR}=2830, monomer conversion %=46.9 %, determined from gravimetric method, yield %= 84 % after prep-SEC).

Scheme 4.5 Synthesis of alk-lysine-Boc 12 and alk-lysine-Boc dendron **13**

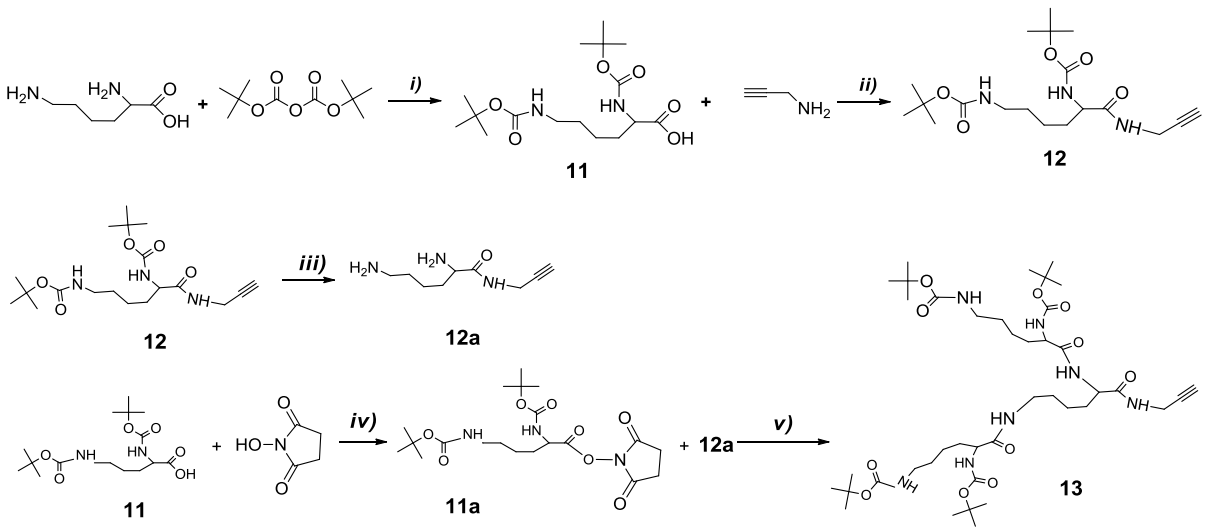

i): NaOH, H_2O, 1,4-Dioxane, 0 ^{o}C-R.T., 7 h, ii): DCC, DMAP, DCM, 0 ^{o}C-R.T., 24 h, iii): TFA, DCM, R.T., 2 h, iv): DCM, DCC, NHS, 0 ^{o}C-R.T., 2 h, v): DMF, TEA, R.T., 12 h.

4.2.2.9 Synthesis of building block alkyne-Lysine-Boc, 12

The Boc-Lysine-OH, **11**, was synthesized according to the reference(Scheme 5).[43] To a 500 mL flask, **11** (6.0 g, 0.172 mol), propargyl amine (1.90 g, 0.0345 mol), and DMAP (0.316 g, 2.59 x 10^{-3} mol) were dissolved in 120 mL dry DCM and cooled to 0 ^{o}C in an ice-bath. A mixture of DCC and 50 mL DCM was added dropwise into the solution over 30 min. The mixture was allowed to react for 36 h at room temperature. The solid content was

removed by filtration and the filtrate was washed by saturated brine (2 x 50 mL). The organic layer was collected, dried over anhydrous $MgSO_4$, the solvent removed *in vacuo* followed by column chromatography using ethyl acetate/petroleum spirit (3/1, v/v) as the eluent. Product **12** was obtained as a white solid (2.86 g, yield%=41.7 %). R_f (3/1 EtOAc/petroleum spirit) 0.65.

^{1}H NMR ($CDCl_3$, 298K, 500 MHz): δ 6.91 (s, 1H, $CHCCH_2N\boldsymbol{H}CO$-), 5.32 (s, 1H, -$CHN\boldsymbol{H}CO$-), 4.69 (s, 1H, -$CH_2N\boldsymbol{H}CO$), 3.97-4.07 (b, 3H, $CH_2CC\boldsymbol{H}_2NH$- and –$CH_2C\boldsymbol{H}CO$-), 3.08 (t, 2H, *J*=6.6 Hz, -$CH_2C\boldsymbol{H}_2NH$-), 2.20 (t, 1H, *J*=2.5 Hz, $\boldsymbol{H}CCCH_2$-), 1.2-2.0 (m, 24H, $C\boldsymbol{H}_2$-Lys and $C\boldsymbol{H}_3$-Boc). ^{13}C NMR ($CDCl_3$, 298K, 500 MHz): 22.69, 28.44, 28.53, 29.09, 29.70, 32.23, 40.07, 54.24, 71.60, 79.16, 79.53, 80.10, 155.97, 156.26, 172.22.

4.2.2.10 Synthesis of building block alkyne-Lysine-Boc Dendron, 13

11 (2.25 g, 6.51 x 10^{-3} mol), NHS (1.5 g, 0.013 mol) and DCC (2.63 g, 0.013 mol) were dissolved in 50 mL DCM, which was cooled to 0 ^oC in an ice bath. The reaction mixture was heated to room temperature and stirred for 2 h; the solid was filtered, the filtrate was evaporated and the concentrate, **11a**, was dissolved in 20 mL DMF and used without further purification. **12** (1.12 g, 2.93 x 10^{-3} mol) was dissolved in 6 mL TFA/DCM mixture (1:1, v/v), stirred for 2 h, and the solvent evaporated. The concentrate, **12a,** was dissolved in 20 mL DMF, and then added dropwise into the 20 mL DMF/**11a** mixture above over 20 min. The mixture was stirred for another 12 h. The reaction mixture was then concentrated. The concentrate was dissolved in 200 mL DCM, washed sequentially with 10 wt% HCl solution, saturated $NaHCO_3$ solution, and brine. The organic layer was collected, dried over anhydrous $MgSO_4$ and filtered. The filtrate was concentrated by rotary evaporation. The concentrate was purified by silica gel column chromatography using 100% EtOAc as the eluent. Product **13** was obtained as white solid (1.4 g, yield%=56.9 %). R_f (100% EtOAc) 0.51.

MALDI-ToF MS: [M+Na^+] Calc.=862.52, Found=862.89; [M+K^+] Calc.=878.50, Found=878.72.

4.2.2.11 Synthesis of dendrimer 14 in a one-pot reaction

In a 10 mL Schlenk tube, **5** (90.0 mg, 7.76 x 10^{-6} mol), **8** (156 mg, 6.51 x 10^{-5} mol), **12** (48.0 mg, 1.24 x 10^{-4} mol), and PMDETA (20 µL, 9.31 x 10^{-5} mol) were dissolved in 2 mL of toluene and 2 mL DMSO. The reaction mixture was then purged with argon for 30 min.

Cu(I)Br (13.5 mg, 9.31 x 10^{-5} mol) was added to the solution under a positive flow of argon, sealed and stirred for 30 min at 25 ^{o}C in a temperature controlled oil bath. The polymer was diluted with DCM and the copper salts removed by passage through an activated basic alumina column. The solution was concentrated by rotary evaporation and the polymer recovered by precipitation into methanol, collected by vacuum filtration and washed extensively with methanol. The polymer was dried under high vacuum for 48 h at 25 ^{o}C to give a white polymer, and further purified by preparative SEC. The resultant polymer was re-precipitated from DCM into MeOH, filtered and dried under high vacuum for 48 h at 25 ^{o}C and obtained as white powder ($M_{n,RI}$ = 26590, $M_{p,\ RI}$=27650, PDI= 1.08; $M_{n,TD}$ = 35120, $M_{p\ TD}$=35990, PDI = 1.05, $M_{n,NMR}$ =39340, yield %= 69 % after prep-SEC).

4.2.2.12 Synthesis of dendrimer 15 in a one-pot reaction

In a 10 mL Schlenk tube, **5** (90.0 mg, 7.76 x 10^{-6} mol), **10** (171 mg, 6.51 x 10^{-5} mol), **12** (71.9 mg, 1.86 x 10^{-4} mol), and PMDETA (26 µL, 1.24 x 10^{-4} mol) were dissolved in 1 mL of toluene. The reaction mixture was then purged with argon for 15 min. Cu(I)Br (18 mg, 1.24 x 10^{-4} mol) was then added to the solution under a positive flow of argon, sealed and stirred for 30 min at 25 ^{o}C in a temperature controlled oil bath. The polymer was diluted with DCM and the copper salts were removed by passage through an activated basic alumina column. The solution was concentrated by rotary evaporation and the polymer recovered by precipitation into methanol, collected by vacuum filtration and washed extensively with methanol. The polymer was dried under high vacuum for 48 h at 25 ^{o}C to give a white polymer, and further purified by preparative SEC. The resultant polymer was then re-precipitated from DCM into MeOH, filtered, dried under high vacuum for 48 h at 25 ^{o}C and obtained as white powder ($M_{n,RI}$ = 29140, $M_{p,\ RI}$=30520, PDI= 1.08; $M_{n,TD}$ = 37540, $M_{p\ TD}$=38590, PDI = 1.05, $M_{n,NMR}$ =43990, yield %= 67 % after prep-SEC).

4.2.2.13 Synthesis of dendrimer 16 in a one-pot reaction

In a 10 mL Schlenk tube, **5** (90.0 mg, 7.76 x 10^{-6} mol), **10** (171 mg, 6.51 x 10^{-5} mol), **13** (160 mg, 1.86 x 10^{-4} mol), and PMDETA (26 µL, 1.24 x 10^{-4} mol) were dissolved in 1 mL of toluene. The reaction mixture was then purged with argon for 15 min. Cu(I)Br (18 mg, 1.24 x 10^{-4} mol) was then added to the solution under a positive flow of argon, sealed and stirred for 30 min at 25 ^{o}C in a temperature controlled oil bath. The polymer was diluted with DCM and

the copper salts were removed by passage through an activated basic alumina column. The solution was concentrated by rotary evaporation and the polymer recovered by precipitation into methanol, collected by vacuum filtration and washed extensively with methanol. The polymer was dried under high vacuum for 48 h at 25 ^{o}C to give a white solid, and further purified by preparative SEC. The resultant polymer was then re-precipitated from DCM into MeOH, filtered and dried under high vacuum for 48 h at 25 ^{o}C obtained as white powder ($M_{n,RI}$ = 31200, $M_{p,\ RI}$=33360, PDI= 1.08; $M_{n,TD}$ = 45640, $M_{p,TD}$=46330, PDI = 1.03, $M_{n,NMR}$ =53540, yield %= 59 % after prep-SEC).

4.2.2.14 Deprotection of Boc groups from Boc-Lysine units of dendrimer

Typically, dendrimer (30 mg) was dissolved in a mixture of DCM (1 mL) and TFA (1 mL). The solution was kept stirring for 12 h at room temperature, the solvent was removed by evaporation and the residual content was dried in high vacuum for 24 h. The resulting product was used for further micellization in water directly.

4.2.2.15 Micellization of dendrimers

Typically, dendrimer (5 mg, after removal of Boc groups from Boc-Lysine units) was dissolved in DMF (3 mL), a common solvent for both PSTY and Lysine units followed by gradual addition (0.013 mL min^{-1}) of a nonsolvent (water, 3 mL) for the hydrophobic PSTY blocks. The resulting mixture of DMF and water was transferred to pre-soaked and rinsed dialysis bag (Pierce Snakeskin, MWCO 3.5 K) and dialyzed against a large volume of Milli-Q water for 2 days to remove the organic solvent. After dialysis, the volume of all three samples increased but was less than 10 mL. To make the similar concentration for all three samples, the volume was made up to 10 mL by adding water. The final micelle concentration for sample **18** and **19** were 0.5 mg mL^{-1}. However, a small amount of precipitant was observed after the self-assembly of sample **17**, therefore the concentration for sample 17 was slightly lower than 0.5 mg mL^{-1}.

4.2.3 Analytical Methodologies

Size Exclusion Chromatography (RI-SEC)

All polymer samples were dried prior to analysis in a vacuum oven for 2 days at 25 ^{o}C. The dried polymer was dissolved in tetrahydrofuran (THF) to a concentration of 1 mg mL^{-1} and then filtered through a 0.45 μm PTFE syringe filter. The molecular weight distributions of the polymers was determined through separation on a Waters 2695 separations module, fitted with a Waters 410 refractive index (RI) detector maintained at 35 ^{o}C, a Waters 996 photodiode array detector, and two Ultrastyragel linear columns (7.8 x 300 mm) arranged in series. These columns were maintained at 40 ^{o}C for all analyses and are capable of separating polymers in the molecular weight range of 500 to 4 million g mol^{-1} with high resolution. All samples were eluted at a flow rate of 1.0 mL min^{-1}. Calibration was performed using narrow molecular weight PSTY standards ($PDI_{RI} \leq 1.1$) ranging from 500 to 2 million g mol^{-1}. Data acquisition was performed using Empower software, and molecular weights were calculated relative to polystyrene standards.

Absolute Molecular Weight Determination by Triple Detection SEC (TD-SEC)

Absolute molecular weights of polymers were determined using a Polymer Laboratories GPC50 Plus equipped with dual angle laser light scattering detector, viscometer, and differential refractive index detector. HPLC grade *N*,*N*-dimethylacetamide (DMAc, containing 0.03 wt % LiCl) was used as the eluent at a flow rate of 1.0 mL min^{-1}. Separations were achieved using two PLGel Mixed B (7.8 x 300 mm) SEC columns connected in series and held at a constant temperature of 50 ^{o}C. The triple detection system was calibrated using a 2 mg mL^{-1} PSTY standard (Polymer Laboratories: Mw = 110 K, dn/dc = 0.165 mL g^{-1} and IV = 0.5809). Samples of known concentration were freshly prepared in DMAc + 0.03 wt % LiCl and passed through a 0.45 μm PTFE syringe filter prior to injection. The absolute molecular weights and dn/dc values were determined using Polymer Laboratories Multi Cirrus software based on the quantitative mass recovery technique.

Preparative Size Exclusion Chromatography (Prep-SEC)

Crude polymers were fractionated (i.e. purified) using a Varian Pro-Star preparative SEC system equipped with a manual injector, differential refractive index detector, and single wave-length ultraviolet visible detector. The flow rate was maintained at 10 mL min^{-1} and HPLC grade THF was used as the eluent. Separations were achieved using a PL Gel 10 μm 10×10^3 Å, 300 x 25 mm preparative SEC column at 25 °C. The dried crude polymer was dissolved in THF at 100 mg/mL and filtered through a 0.45 μm PTFE syringe filter prior to injection. Fractions were collected manually, and the composition of each was determined using the Polymer Laboratories GPC50 Plus equipped with triple detection as described above.

Nuclear Magnetic Resonance (NMR)

All NMR spectra were recorded on either a Bruker DRX 400 or 500 MHz spectrometer using an external lock ($CDCl_3$), and all spectra were referenced to the residual nondeuterated solvent ($CHCl_3$). Spectra of functional molecules and polymers containing nitroxide radicals were measured in the presence of phenylhydrazine under an inert atmosphere to reduce the nitroxides to their incipient hydroxylamines.

Diffusion-Ordered Spectroscopy (DOSY) NMR

1D DOSY experiments were run to suppress solvent and organic peroxide impurity (from THF) which appeared in ^1H NMR spectra for all polymers (including starting building blocks and dendrimers) by using the gradient strength (gpz6) 85 % (for starting building blocks) and 90 % (for dendrimers) ,gradient pulse length (p30, little delta, δ=p30 x 2) 2 ms (for starting building blocks) and 2.5 ms (for dendrimers), and relaxation delay (d1) 5s (≥ 5T1) with 256-512 scans.

2D DOSY experiments were carried out to determine the diffusion coefficients (*D*) for dendrimers (14, 15 and 16) in $CDCl_3$. The dendrimer sample concentration was 10 mg mL^{-1} in $CDCl_3$. All 2D DOSY experiments were conducted at 298 K using a Bruker Avance DRX 500 spectrometer operating at 500.13 MHz for protons and equipped with a 5 mm triple-resonance (1H, 13C, 15N) *z*-gradient probe equipped with actively shielded gradients. The *z*-gradient was calibrated at 298 K with a HDO sample containing 0.1 mg mL^{-1} $GdCl_3$. The

maximum *z*-gradient amplitude was 50 G cm^{-1}. A 90° pulse calibration was performed for each new sample for DOSY experiments. A bipolar pulse longitudinal eddy current delay (BPPLED) pulse sequence was used. The pulse sequences included a 5 ms delay to allow residual eddy currents to decay. Sine-shaped gradient pulses were utilized to further minimize eddy currents. The gradient pulse length (p30, little delta, δ=p30 x 2) 2.5 ms was chosen for diffusion time in order to obtain the minimum residual signal for each component at maximum gradient strength. The diffusion delay (Δ) was set to 200 ms. The pulse gradients were incremented from 2 to 95 % of the maximum gradient strength in a linear ramp (16 steps). A spectral window of 6000 Hz was accumulated in an acquisition time of 1.38 s. The relaxation time *T*1 was determined by inversion recovery method. A relaxation delay of 5*T*1 of the slowest relaxing signal was used (5s). The FIDs were collected into 16K data points; 128 scans and 4 dummy scans were acquired on each sample. Following acquisition the FIDs were Fourier transformed applying zero-filling to 16K data points and an exponential window function with line broadening factor 1-5 Hz. Data were processed using Bruker XWIN NMR software. The signal decay due to gradients was fitted using:

$$I=I_0\exp(-D\gamma^2g^2\delta^2(\Delta-\delta/3) \qquad (1)$$

where *I* is the resonance intensity measured for a given gradient strength, *g*, I_0 is the signal intensity with no gradient applied, γ is the gyromagnetic ratio, δ is the gradient duration (p30 x 2), and Δ is the diffusion delay. The resulting diffusion coefficients (*D*) of the polymer signals and the solvent are the result of the fitting procedure (see appendix Figure A3.28, A3.30 and A3.32).

The hydrodynamic diameter ($D_{h,NMR}$) was determined using the Stokes-Einstein equation:

$$D_h = 2R_h = \frac{kT}{3\pi\eta D} \qquad (2)$$

where *k* is the Boltzmann constant (1.380 x 10^{-23} J K^{-1}), T is the temperature in Kelvin (298 K), η is the viscosity of the solvent in Pascal seconds (5.3 x 10^{-4} Pa S for $CDCl_3$) and *D* is the diffusion coefficient obtained from 2D DOSY experiment.[44]

Attenuated Total Reflectance-Fourier Transform Spectroscopy(ATR-FTIR)

ATR-FTIR spectra were obtained using a horizontal, single bounce, diamond ATR accessory on a Nicolet Nexus 870 FT-IR. Spectra were recorded between 4000 and 500 cm^{-1} for 32 scans at 4 cm^{-1} resolution with an OPD velocity of 0.6289 cm s^{-1}. Solids were pressed directly onto the diamond internal reflection element of the ATR without further sample preparation.

Matrix-Assisted Laser Desorption Ionization-Time-of-Flight (MALDI-ToF) Mass Spectrometry

MALDI-ToF MS spectra were obtained using a Bruker MALDI-ToF autoflex III smart beam equipped with a nitrogen laser (337 nm, 200 Hz maximum firing rate) with a mass range of 600-400 000 Da. Spectra were recorded in either reflectron mode (1500-4500 Da) or linear mode (4000-20000 Da). Trans- 2-[3-(4-tert- butylphenyl)-2-methyl-propenylidene] malononitrile (DCTB; 20 mg mL^{-1}in THF) was used as the matrix and $Ag(CF_3COO)$ (1 mg mL^{-1} in THF) as the cation source for all the polystyrene samples. 20 μL polymer solution (1 mg mL^{-1} in THF), 20 μL DCTB solutions and 2 μL $Ag(CF_3COO)$ solution were mixed in an eppendorf tube, vortexed and centrifuged. 1 μL of solution was placed on the target plate spot, evaporated the solvent at ambient condition and run the measurement. For lysine Dendron **13**, $Na(CF_3COO)$ (1 mg mL^{-1} in THF) was used as cation source.

Dynamic Light Scattering (DLS)

Dynamic Light Scattering measurements were performed using a Malvern Zetasizer Nano Series running DTS software and operating a 4 mW He-Ne laser at 633 nm. Analysis was performed at an angle of 173° and a constant temperature of 25 °C. The hydrodynamic diameter of dendrimer before the removal of Boc groups from Boc-Lysine units was measured in $CDCl_3$ (5 mg mL^{-1}). The hydrodynamic diameter and zeta potential of dendrimer after the removal of Boc groups was measured in water (0.5 mg mL^{-1}, micelle solution). All the samples were filtered by 0.45 μm filter before measurements. The number-average hydrodynamic particle size, polydispersity index and zeta potential are reported. The polydispersity index (PDI) was used to describe the width of the particle size distribution. It was calculated from a Cumulants analysis of the DLS measured intensity autocorrelation

function and is related to the standard deviation of the hypothetical Gaussian distribution (i.e. $PDI_{PSD} = \sigma^2/Z_D^2$, where σ is the standard deviation and Z_D is the Z average mean size).

Transmission Electron Microscopy (TEM)

The samples for TEM analysis were prepared by placing a drop of the micelle solution (0.5 mg mL^{-1}) of dendrimer onto a formavar precoated copper TEM support grid and allowed to air-dry before measurement. The micelles were characterized on a Jeol-1010 instrument utilizing an accelerating voltage of 80 kV at ambient temperature.

LND simulations

We used a log-normal distribution (LND) model based on a Gaussian function to fit the experimental MWD. One can simulate the molecular weight distributions, and in particular the weight distribution,[45] with a log-normal distribution (see ref[46] for more details) using the following equations:

$$w(M) = \frac{\exp(-(\ln M - \ln \overline{M})^2 / 2\sigma^2}{M(2\pi\sigma^2)^{0.5}} \qquad (3)$$

where

$$\overline{M} = (M_n M_w)^{0.5} \qquad (4)$$

and

$$\sigma^2 = \ln(PDI) \qquad (5)$$

where equation **3** is the Gaussian distribution function of w(M) (the weight distribution of the SEC trace), M_n is the number-average molecular weight, M_w is the weight-average molecular weight, and the polydispersity $PDI = M_w/M_n$.

4.3 Results and discussion

4.3.1Synthesis of Building Blocks

The synthesis of a 4-arm polystyrene star (**2**) by ATRP using a tetrafunctional bromine initiator, **1** (NMR spectra of **1** see Figure A4.1), was given in Scheme 4.2. The produced 4-arm star exhibited a narrow molecular weight distribution (MWD) with an $M_{n,RI}$ of 9140 and polydispersity index (PDI) of 1.09. The SEC trace (i.e. weight distribution) of **2** (crude, curve a) given in Figure 4.1 showed a high molecular weight tail most likely the result of star-star coupling, which was removed by preparative SEC (i.e. **2** after prep, curve b). The purity of the 4-arm star (**2** crude) relative to the higher molecular weight species formed through star-star radical coupling was determined by simulating the weight distributions from SEC based on a log-normal distribution (model) using a Gaussian function (Figure A4.2 and Table A4.1 in appendix). The purity of the crude 4-arm star was 87.3 %, which increased to 96.1 % after purification by preparative SEC (Table 4.1). In addition, the chain-end functionality of **2** after preparative SEC was 98 % determined by ^{1}H NMR (Figure 4.2A), and from the MALDI-ToF (Figure 4.3A) the only species detected was the chain-end fragmentation with added Ag^+ (e.g. m/z found was 9266.20 which was close to that calculated 9266.37). These results suggested that this 4-arm star would provide a suitable core building block to produce the final dendrimers in high yields.

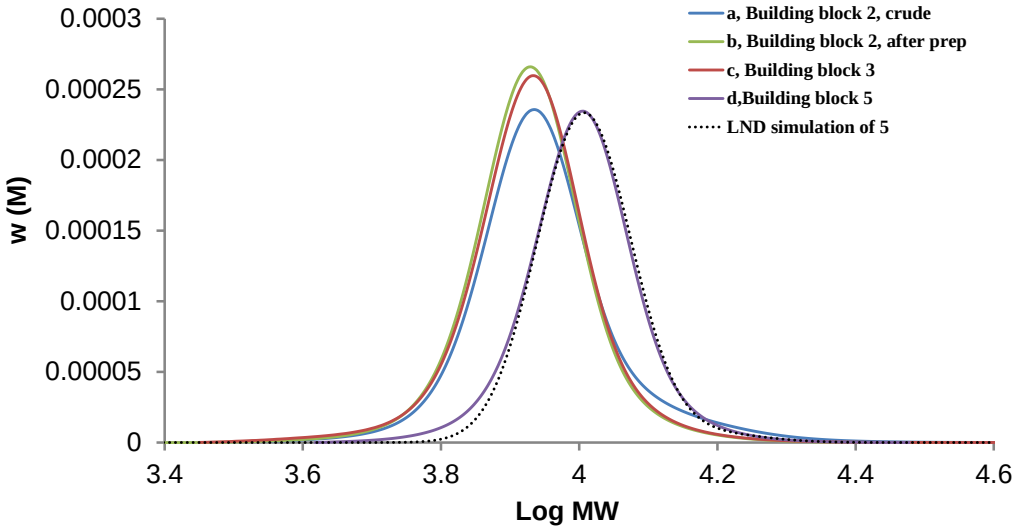

Figure 4.1 Molecular weight distributions (MWDs) for starting polymer (**2** and **3**) and product (**5**) obtained from SEC-RI based on a polystyrene calibration curve: (a) 4-arm PSTY-Br (**2** crude), (b) 4-arm PSTY-Br (**2** after prep), (c) 4-arm PSTY-N_3 (**3**), (d) 4-arm PSTY-$(NO^-)_2$ (**5**). Dotted line represents the LND fit to 5. All SEC traces were normalized to weight.

Table 4.1 SEC and NMR data for all building blocks

Polymer	$M_{n,RI}$ [a]	$M_{p,RI}$ [a]	PDI	$M_{n,TD}$ [b]	$M_{p,TD}$ [b]	PDI[f]	$M_{n,theo}$	ΔHDV[c]	$M_{n,NMR}$	Chain-end Functionality% [d]	Purity[i]
2	9140	8730	1.09								87.3
2[e]	8670	8710	1.05	9700	9840	1.02		0.89	10820	98.0	96.1
3	8730	8810	1.05	9630	9790	1.02	9550[g]	0.90	10670	98.0	94.9
5	10200	10310	1.04	11600	11760	1.01	11660[g]	0.88	12640	96.0	96.0
8	2500	2570	1.11								95.4
8[e]	2370	2490	1.08				2480[h]		2870	99.0	99.0
10	2600	2690	1.07				2820[h]		2830	96.0	97.9

[a] SEC (RI detector) was based on a PSTY calibration curve; [b] MWD determined from DMAc triple detection SEC; [c] Hydrodynamic volume change (ΔHDV = $M_{p,RI}/M_{p,TD}$). [d] Chain-end functionality calculated from ^{1}H NMR. [e] Polymers fractionated (purified) by preparative SEC; [f] Underestimation of true PDI value as light scattering has less sensitivity to low molecular weights. [g] $M_{n,theo.}$ determined from $M_{n,TD}$ of **2** (after prep) plus the Mw of functional groups. [h] $M_{n,theo.}$ determined by: $M_{n,theo.}$ =([M]/[I])*M_m*con%+M_i, where [M], [I], M_m, con%, and M_i are the monomer concentration, initiator concentration, molecular weight of monomer, monomer conversion, and molecular weight of initiator respectively. [i] Determined from log-normal distributions(LND) simulation.

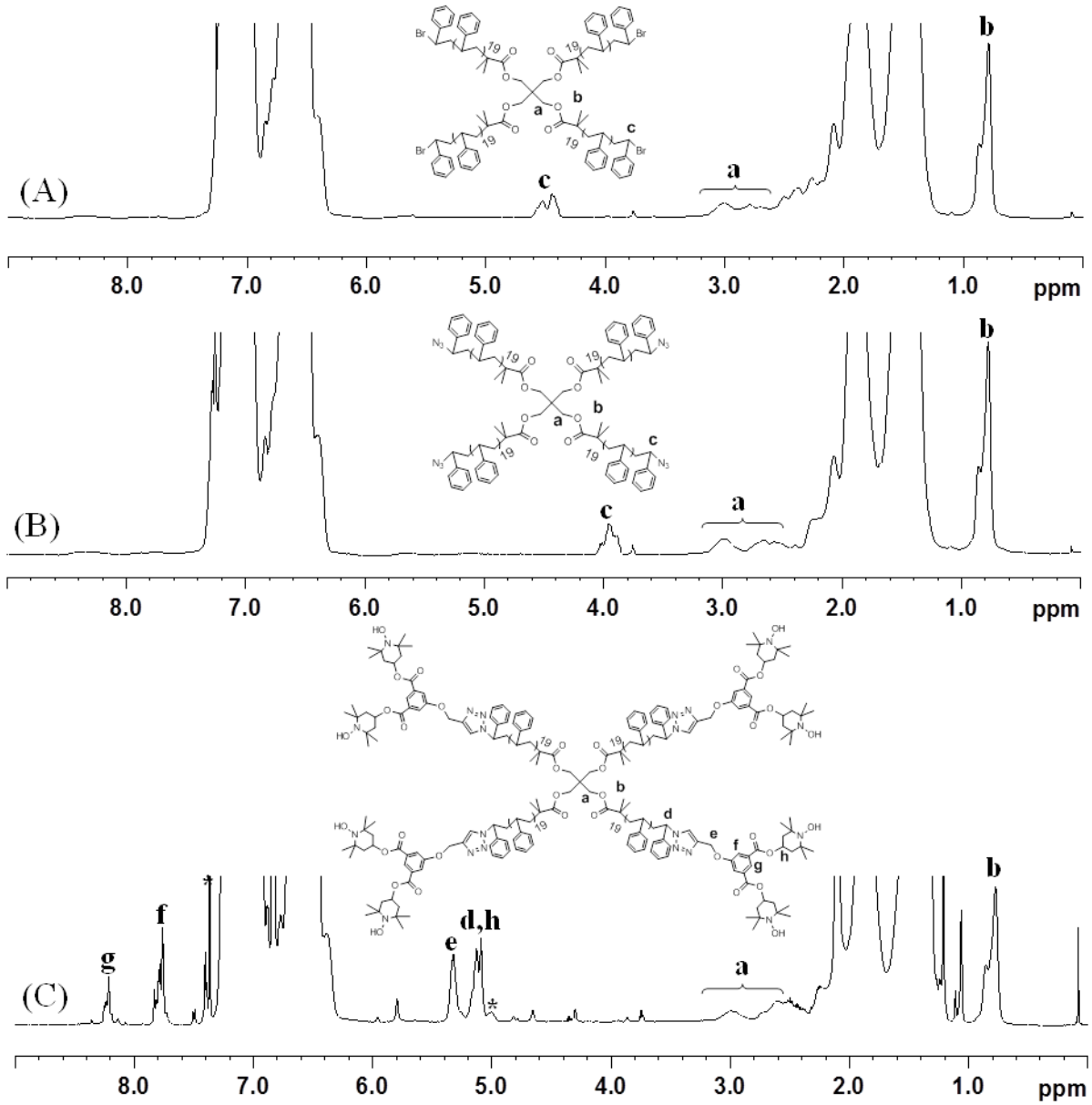

Figure 4.2 Comparison of ^{1}H 1D DOSY NMR spectra of (A) 4-arm PSTY-Br (**2**); (B) 4-arm PSTY-N_3 (**3**); (C) 4-arm PSTY-$(NO^{\cdot})_2$ (**5**). Recorded in $CDCL_3$, 298K, 500MHz, gradient strength (gpz6) 85%, gradient pulse length (p30) 2.0 ms, *- residual phenylhydrazine.

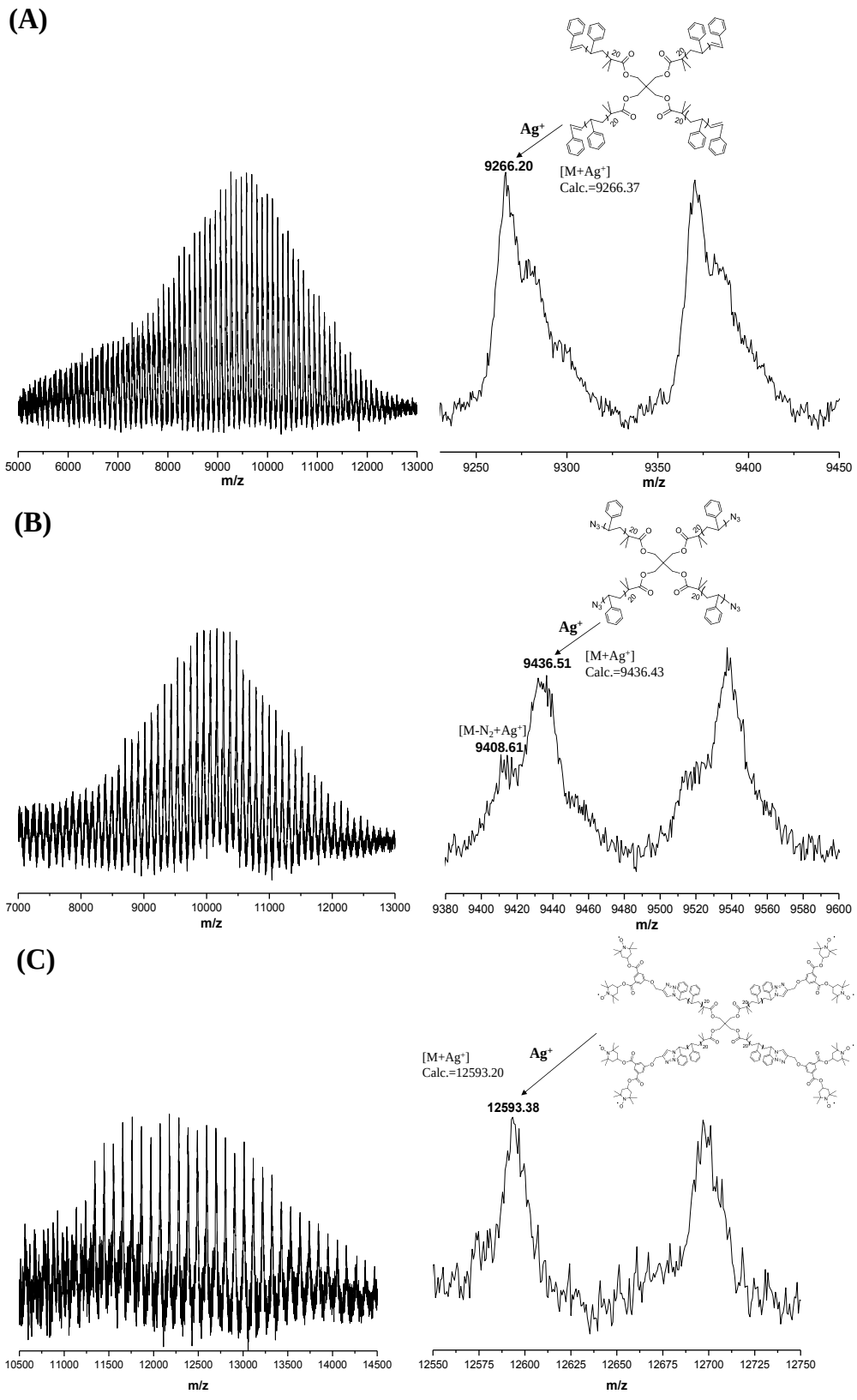

Figure 4.3 MALDI-TOF mass spectra of (A) 4-arm PSTY-Br (**2**), (B) 4-arm PSTY-N_3 (**3**), and (C) 4-arm PSTY-$(NO^{\cdot})_2$ (**5**). The spectra were recorded in linear mode using DCTB as the matrix and $Ag(CF_3COO)$ as the cation source, (i) full spectra and (ii) expanded spectra.

Azidation of the bromine groups on **2** (i.e. after purification) to produce **3** showed a distinct shift of the proton adjacent to the azide from ~4.5 to 4 ppm (Figure 4.2), a slight increase in the $M_{n,\ RI}$ value (Table 4.1), and the near quantitative conversion further confirmed by analysis of the MALDI (Figure 4.3B) spectrum. The SEC trace of **3** (i.e. **2** after azidation) was near identical to that of **2** (after prep) as shown in Figure 3.1. The trifunctional linker, **4**, consisted of an alkyne and two nitroxide moiteies (see Scheme 4.2), with its characterization given in appendix (Figure A4.4-4.6). Coupling **3** and **4** using the CuAAC reaction resulted in a slight shift of the MWD to the expected molecular weight to produce **5** (Scheme 4.1). The 4-arm star **5** consisted of 8 free-nitroxides on its periphery. The MALDI-ToF given in Figure 4.3C showed that the peaks corresponded to the expected nitroxide end-functionalized **5** (e.g. m/z found was 12593.38 which was close to 12593.20 calculated with Ag^+) in agreement with the MALDI analysis of the previously synthesized polymers with nitroxide chain-end functionality[19]. The ^{1}H NMR of the free nitroxides on **5** led to line broadening and poor resolution, whereas converting these nitroxides to hydroxylamines allowed us to obtain accurate NMR spectra. The ^{1}H NMR of **5**, in which the nitroxides have been converted to hydroxylamines, showed near complete loss of the proton associated with the azide and presence of peaks at 5.1, 5.3, 7.8 and 8.2 ppm associated with peaks d, e, f and g from the coupling reaction to produce **5** (Figure 4.2C). It was also found that the absolute $M_{n,TD}$ (11600) was close to that calculated (11660) from the addition of all the end-groups to the 4-arm star (Table 4.1).

The ATRP of initiator **7** with styrene (Scheme 4.3) gave telechelic polymer **8** (crude) with approximately 4.6 wt% of double molecular weight polymer formed through radical-radical coupling (see Figure A4.11 and Table A4.2 in appendix). After purification by preparative SEC, its purity increased to 99.0 % (Figure A4.11 and Table A4.2) and chain-end functionality was close to 99 % as determined by ^{1}H NMR (Figure 4.4A) from the near 4:1 ratio of proton e to that of a and c. Telechelic polymer **10** (Scheme 4.4), with a diazide functionality on one chain-end and a bromine on the other, was formed again using ATRP. As determined by the LND simulations, it showed greater than 97.9 % purity (Figure A4.14 and Table A4.3) and approximately 96 % chain-end functionality by ^{1}H NMR (Figure 4.4B) as given in Table 1, and thus **10** was used without further purification by preparative SEC. The high purity of both **8** and **10** was further supported by the MALDI analysis in Figure A4.12 and A4.15 in appendix. The other two building blocks **12** and **13** (see Scheme 3.1) consisted of Boc protected L-lysine groups. The synthetic strategy to make **12** and **13** is shown in Scheme 4.5. The amidation of **11** and propagyl amine afforded **12** in a good yield of

41.7 %. The Boc protected L-lysine dendron **13** formed through the reaction of **11a** and **12a** to give a yield of 56.9 %. Characterization of **12** and **13** is given in appendix (Figure A4.17-A4.23).

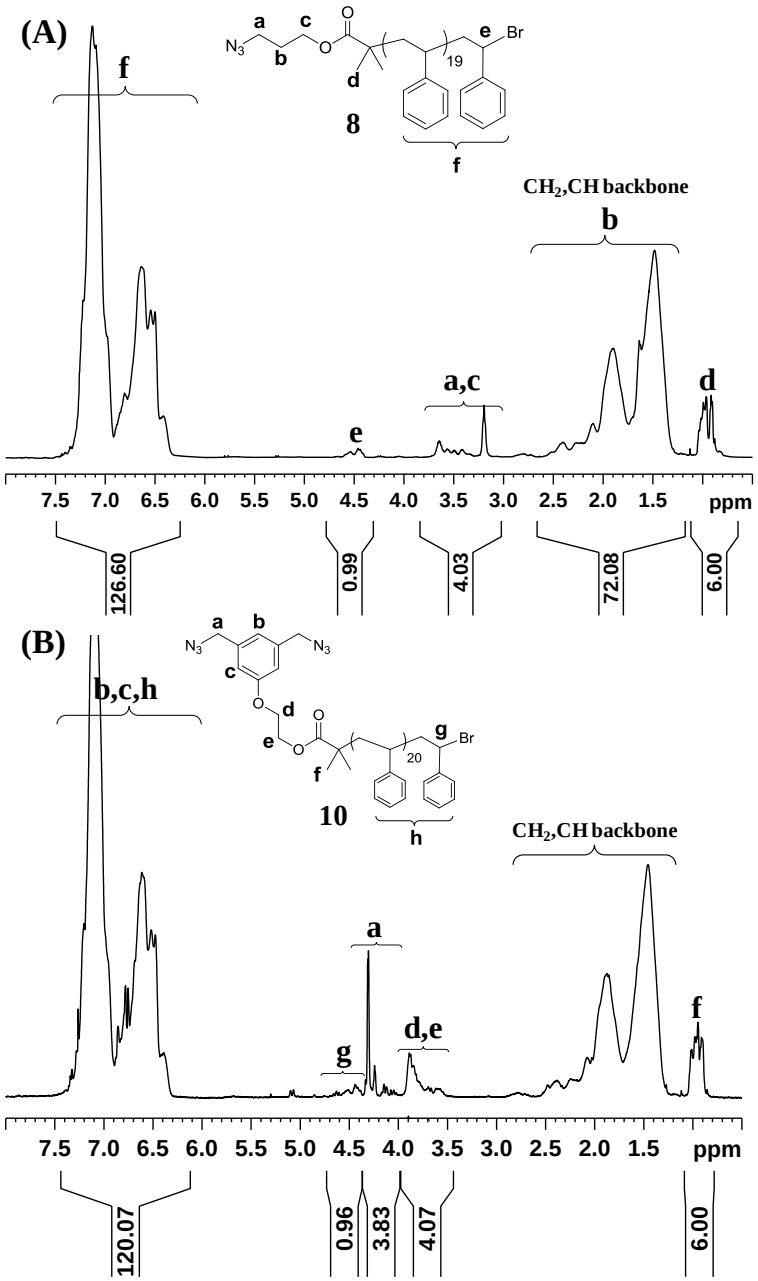

Figure 4.4 ^{1}H 1D DOSY NMR spectra of (A) N_3-PSTY-Br, (**8**) and (B) $(N_3)_2$-PSTY-Br (**10**), recorded in $CDCl_3$ at 298 K, 500MHz, gradient strength (gpz6) 85%, gradient pulse length (p30) 2.0 ms, the sample (**8**) was purified by preparative-SEC.

.

4.3.2 One-Pot Synthesis of Boc protected L-lysine Decorated Polymeric Dendrimers

Modulating the catalytic activity of copper for the orthogonal 'click'-type reactions of NRC and CuAAC produced 3rd or 4th generational layer dendrimers coated on the periphery with L-lysine in one-pot at 25 °C (Scheme 4.1). The NRC process occurs through the reaction of a nitroxide and a free-radical to form an alkoxyamine.[47, 48] A method to produce radicals rapidly *in situ* employed the abstraction of the halide from the polymer end-group with either Cu(I) or Cu(0).[47] It was found that in DMSO, Cu(I)Br/Me_6TREN was highly reactive, rapidly producing radicals that were subsequently trapped by nitroxides to form the resultant alkoxyamines with little or no radical-radical coupling product[48]. As a solvent, DMSO has also been demonstrated to induce disproportionation of Cu(I)Br/Me_6TREN to the highly active Cu(0) and Cu(II) species.[49] Recent results showed that in DMSO, the NRC reaction was rapid and complete within less than 2 min.[19, 40] By changing the ligand to PMDETA and the solvent to toluene, the NRC reaction slowed down significantly with coupling times greater than 2 h. Copper also catalyzes the CuAAC reaction. The coupling reaction using Cu(I)Br/PMDETA in toluene, in contrast to the NRC reaction, was rapid with complete coupling in less than 2 min. Conversely, using Cu(I)Br/Me_6TREN in DMSO slowed the CuAAC reaction with complete coupling in more than 30 min. However, using Cu(I)Br/PMDETA in a mixture of toluene and DMSO (50:50 v/v%) allowed the NRC and CuAAC reactions to proceed with similar rates of coupling. This latter method should produce the dendrimer much faster than in the other two solvent/ligand conditions.[50]

Polymeric dendrimer **14** formed through the orthogonal NRC and CuAAC 'click' reactions of **5**, **8** and **12** in a molar ratio of 1:8.4:16 (Scheme 4.1), respectively, utilizing an excess of reactants **8** and **12** to the core **5**. The parallel process using CuBr/PMDETA in a solvent mixture of toluene and DMSO (50:50 v/v%) produced **14** (crude) in 30 min at 25 °C. The SEC trace in Figure 4.5A showed that all core **5** (blue dotted line) was consumed and that the MWD contained the remaining excess of **8** (green dotted line) and **12** (orange dotted line). We determined a purity of 79 wt% from a fit of the theoretical MWD of **14**, denoted as 'LND (**14**, pure)' in Figure 4.5A by the black dotted line calculated from the addition of molecular weight of all arms to the core using a change in hydrodynamic volume (ΔHDV) of 0.77 in the LND method. Polymeric dendrimer **14** was then purified by preparative SEC to remove all starting reagents and other low molecular weight coupled products. After preparative SEC (see Figure 4.5A), the purity of **14** (after prep) determined by the LND method was 94 % based on the fit of the theoretical MWD of **14**. The 6 % of by-products most probably results

from the non-fully coupled L-lysine-alkyne to the polymeric dendrimer. The $M_{n,RI}$ of **14** (prep) was 26590 with a PDI of 1.08 using the refractive index (RI) detector, and the $M_{n,TD}$ was 35120 with a PDI of 1.05 using triple detection (i.e. absolute molecular weight determination) as given in Table 3.2. The value of $M_{n,TD}$ determined by triple detection was slightly higher than the theoretical value (33640) of the dendrimer calculated from the addition of the absolute molecular weights of the building blocks (**5**, **8** and **12**) due to the removal of low molecular weight fraction by preparative SEC. It should be noted that the PDI from triple detection SEC was always lower due to a lower sensitivity of the light scattering at lower molecular weights. The change in ΔHDV from $M_{p,RI}$ to $M_{p,TD}$ of 0.77 was the same as that used in the LND method above, supporting the calculated high purity of 94 %. The lower apparent molecular weight (i.e. ΔHDV of 0.77) suggested that the polymeric dendrimer was much more compact than its corresponding linear analogue as a result of the many tethering links in each generational layer. Each link will reduce the amount of solvent required to swell the polymer arms.[51] Further support for the high purity comes from analysis of the ^{1}H NMR (see Figure 4.6A and Figure A4.24) from integration of peaks corresponding to the three building blocks. Table 3.2 showed that the ratio of the number of arms in each generational layer was 4:8.2: 8 and close to theory (4:8:8).

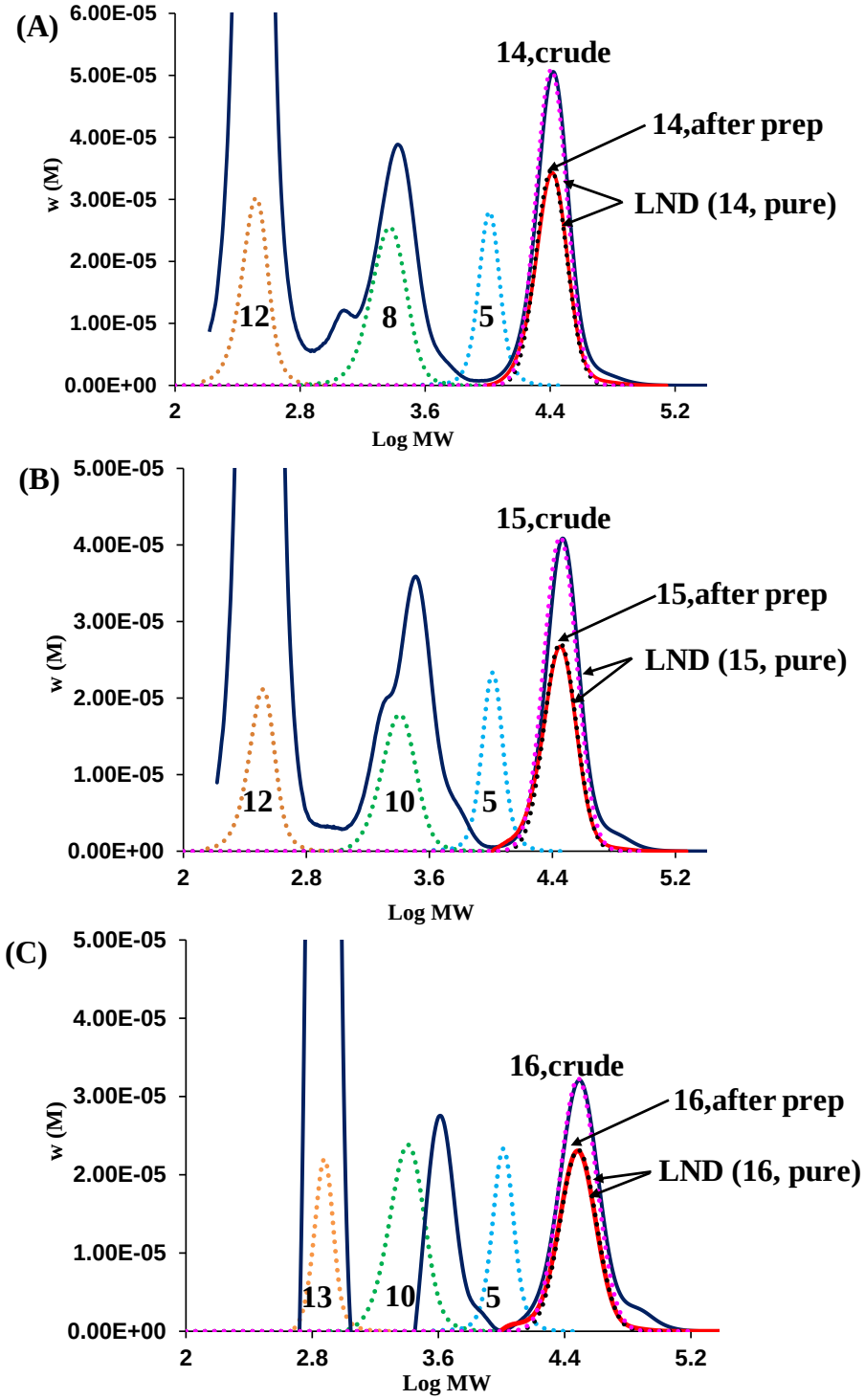

Figure 4.5 SEC traces of starting building blocks (**5**, **8**, **10**, **12**, **13**; dotted lines) to produce the respective dendrimers. Dendrimers before (crude, dark blue solid line) and after purification by preparative SEC (after prep, red solid line). All SEC traces were determined by THF SEC (RI). (A) dendrimer **14** and LND simulation of pure (theoretical, dotted lines) **14**. (B) dendrimer **15** and LND simulation of pure (theoretical, dotted lines)**15**. (C) dendrimer **16** and LND simulation of pure (theoretical, dotted lines)**16**.

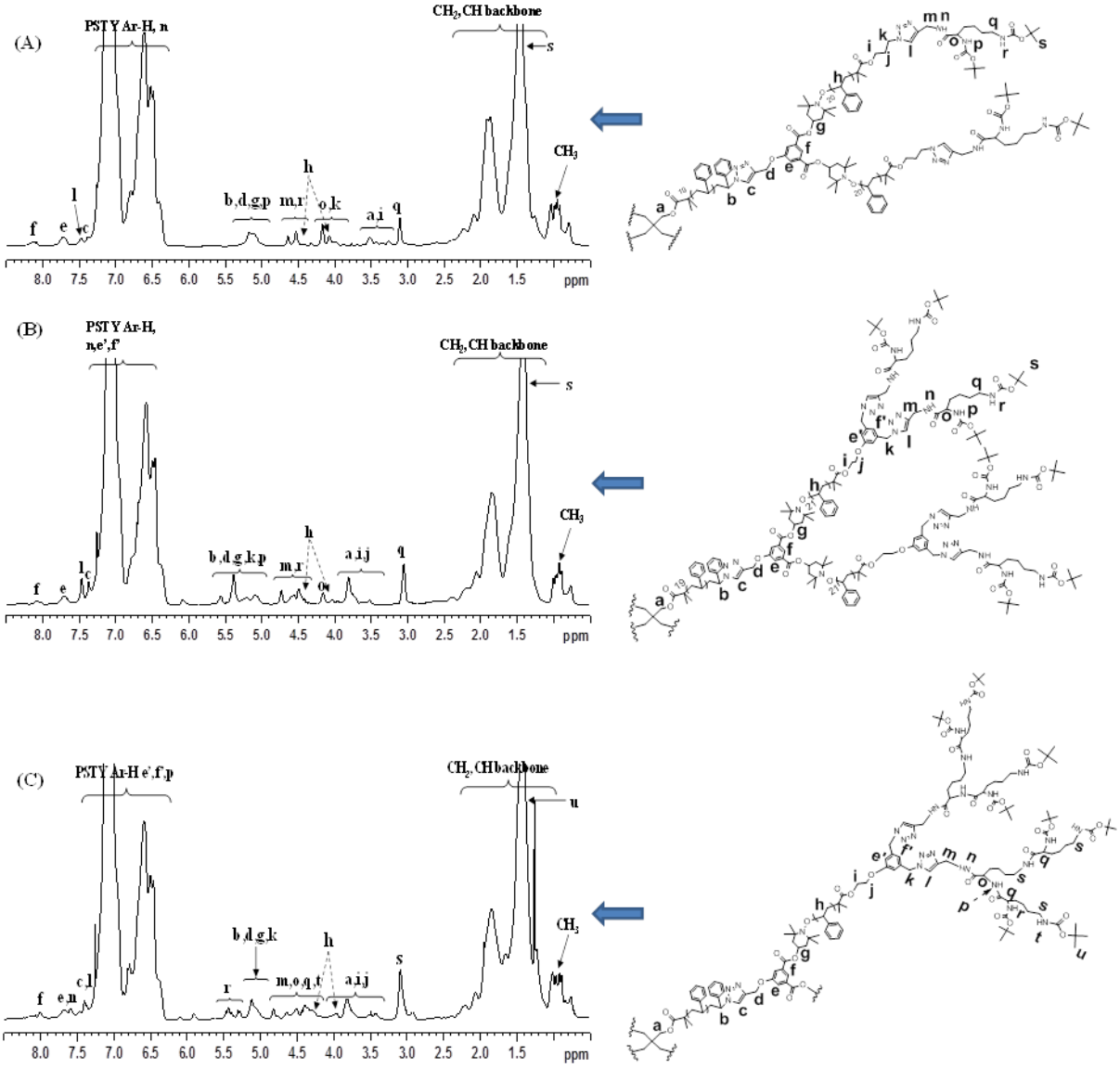

Figure 4.6 ^{1}H 1D DOSY NMR spectra of dendrimers (A)**14**, (B)**15**, and (C)**16**, recorded in $CDCl_3$ at 298K, 500MHz, gradient strength (gpz6) 90%, gradient pulse length (p30) 2.5 ms.

.

Table 4. 2 SEC, LND and NMR data for dendrimers

Dendrimer	Reactants	$M_{n,RI}$ [a]	$M_{p,RI}$ [a]	PDI	$M_{n,TD}$ [b]	$M_{p,TD}$ [b]	PDI [c]	$M_{n,theo.}$ [d]	ΔHDV		$M_{n,NMR}$	Number of arms [g]			Purity% [h]
									SEC [e]	LND [f]		G1	G2	G3	
14	**5,8,12**	26590	27650	1.08	35120	35990	1.05	33640	0.77	0.77	39340	4	8.20	8	94
15	**5,10,12**	29140	30520	1.07	37540	38590	1.05	38530	0.79	0.76	43990	4	8.12	16	96
16	**5,10,13**	31200	33360	1.08	45640	46330	1.03	46420	0.72	0.70	53540	4	8.14	16[i]	97

All the dendrimer products fractionated (purified) using preparative SEC. [a] MWD from SEC (RI). [b] MWD determined by DMAc triple detection SEC; [c] Underestimation of true PDI value as light scattering has less sensitivity to low molecular weights. [d] $M_{n,theo.}$ calculated from M_n of starting materials (Table 1) . [e] Hydrodynamic volume change (ΔHDV) determined from peak molecular weight (ΔHDV = $M_{p,RI}/M_{p,TD}$). [f] ΔHDV used in log-normal distributions(LND) simulation. [g] Determined from integration of each generation by ^{1}H NMR. [h] Determined from log-normal distributions(LND) simulation. [i] Represents 16 units of dendron **13**, which includes 16 and 32 L-lysine groups in the 3rd and 4th generation layers, respectively.

The next polymeric dendrimer synthesized was **15** with double the number of L-lysine on the periphery (Scheme 4.1). The molar ratio of starting reagents **5**, **10** and **12** was 1:8.4:24, and using the same reaction conditions as those to produce **14**. The SEC trace showed that 15 was produced (Figure 4.5B) with near complete loss of starting polymer 5 and remaining excess of reactants **10** and **12**. The SEC trace showed products corresponding to the coupling of **10** and **12** through the CuAAC reaction. The purity of **15** (crude) was 74 % determined by the LND method using the theoretical molecular weight of **15** and a ΔHDV of 0.76 (Figure 4.5B). After fractionation of **15** (crude) by preparative SEC, the purity increased to 96 %. The $M_{n,RI}$ and PDI were 29140 and 1.07, and the $M_{n,TD}$ and PDI by triple detection was 37540 and 1.05, respectively (Table 4.2). The value of $M_{n,TD}$ (38590) was close to the theoretical value (38530) of the dendrimer calculated from the absolute molecular weight of the building blocks (**5**, **10** and **12**). In addition, the ΔHDV determined from the ratio of $M_{p,RI}$ to $M_{p,TD}$ was 0.79, which was close to that used in the LND method above for **15** (crude). Analysis by ^{1}H NMR (Figure 4.6B and Figure A4.25) gave the number of arms in each generational layer as equal to 4:8.1:16, which was very close to expected for a polymeric dendrimer to form **15**.

One of the main goals of this work was to create a dendrimer with a densely coated L-lysine periphery (i.e. with 32 lysine groups on the periphery and 16 lysine groups as the penultimate generational layer) as shown in Scheme 1. To do this, we produced a small molecule L-lysine dendron **13** with an alkyne end-functionality that was then coupled to **10**

and **5** to produce a 4th generation layered (G4) polymeric dendrimer **16**. The molar ratio of starting reagents **5**, **10** and **13** was 1:8.4:24, and using the same reaction conditions as for the previously made **14** and **15**. The MWD after the reaction showed a loss of reactants **5** and **10**, with new MWD peaks appearing that corresponded to the coupling of **10** and **13** and the final polymeric dendrimer **16**. There was still a large peak corresponding to the starting dendron **13**, which was used in large excess. The purity of the crude product **16** was lower (69 %) compared to both **14** and **15** using a ΔHDV of 0.70 in the LND simulation (Figure 4.5C). Purification using preparative SEC gave an $M_{n,RI}$ of 31200 (PDI=1.08) and $M_{n,TD}$ of 45640 (PDI=1.03), in which the value of $M_{n,TD}$ (45640) was close to the theoretical one (46420) of the dendrimer calculated from the absolute molecular weight of the building blocks (**5**, **10** and **13**). The purity after preparative SEC increased to 97 %. In addition, the ΔHDV calculated from the ratio of $M_{p,RI}$ to $M_{p,TD}$ was 0.72, which was close to the value used in the LND simulation (Table 4.2). This lower ΔHDV value suggested that **16** was more compact due to the higher peripheral lysine branching compared to either **14** or **15**. Analysis by ^{1}H NMR further showed that the ratio of the number of arms in each generational layer (i.e. 4:8.1:16:32) was close to theory (Figure 4.6C and Figure A4.26). The results taken together strongly support that all three polymeric dendrimers were produced in excellent purity. We could not obtain MALDI-ToF of the dendrimers, presumably due to the high molecular weights of the dendrimers.

4.3.3 Self-assembly of dendrimers in organic and aqueous media

We used three different methods to determine the hydrodynamic diameter (D_h) in organic solvents. The first method used SEC to determine D_h in THF based on polystyrene standards.[46, 52] Using the Mark-Houwink relationship between molecular weight and intrinsic viscosity, one can determine the hydrodynamic radius (R_h) from the following relationship[52]

$$R_h^3 = \frac{3KM^{a+1}}{10\pi N_A} \qquad (6)$$

where K = 0.0141 cm^3 g^{-1}, a = 0.7 (in a good solvent), and N_A is Avogadro's number. It can be seen from Table 3.3 that the $D_{h,SEC}$ increased from 8.41 to 9.21 nm for dendrimers **14** to **16** with an increase in the number of L-lysines on the periphery. It should be noted that the value of K is based on linear PSTY chains, and would be expected to change for dendritic

structures. The second and more precise method allowed determination of the diffusion coefficient (D) from a concentration dependent diffusion-ordered NMR spectroscopy (DOSY).[44] The value of $D_{h,NMR}$ can be calculated from the Stokes-Einstein equation (see Eq. 2 above). The diameter (i.e. $D_{h,\ NMR}$) in $CDCl_3$ increased from 5.97 to 9.06 nm respectively for **14** to **16**, which was supported from the very close values found by DLS (the third method). These sizes are expected, since the solvent is good for both PSTY and Boc-protected L-lysine, to represent the unimolecular diameter (i.e. without aggregation or self-assembly of the dendrimers). In addition, the excellent agreement between the $D_{h,DLS}$ and $D_{h,NMR}$ suggests that the size determined by DLS is accurate and should provide some insight into the self-assembly of these dendrimers in water.

Table 4.3 Self-assembly of dendrimers in water and organic solvents. The diameters were measured from three methods: (i) SEC, (ii) DOSY NMR, and (iii) DLS.

Dendrimer	$D_{h,SEC}$[a] (nm)	Diffusion coefficient ($m^2.s^{-1}$)[b]	$D_{h,NMR}$ (nm)[c]	$D_{h,DLS}$ (nm)	PDI_{DLS}	$D_{h,TEM}$ (nm)[d]	$D_{h,DLS}$ (nm)	PDI_{DLS}	Zeta potential (mV)
	THF	**$CDCl_3$**				**water**			
14	8.41	1.38×10^{-10}	5.97	5.80	0.168				
15	8.86	1.03×10^{-10}	8.00	8.44	0.164				
16	9.21	9.06×10^{-11}	9.06	10.44	0.228				
17						10.8	8.38	0.374	27.5
18						13.0	9.83	0.447	34.1
19						13.5	11.07	0.673	40.4

[a] Determined from Eq 6 using the Mark−Houwink parameters (K = 0.0141 $cm^3\ g^{-1}$, a = 0.7 in a good solvent); [b]diffusion coefficient (D) determined by 2D DOSY NMR in $CDCl_3$ at 298K; [c]determined from Eq 2.; [d]determined by averaging the size of over 50 single particles in the TEM micrograph.

The self-assembly of L-lysine decorated dendrimers into peptidomimetic nanoparticles represents the next step towards biological efficacy. The three Boc protected L-lysine dendrimers were deprotected to the free L-lysine periphery by addition of TFA (Scheme 4.1). Micelles of three L-lysine dendrimers (**17-19**) were formed through the slow addition of water to a solution of dendrimer dissolved in DMF over a 6.5 h period, and then further dialyzed with Milli-Q water for 2 days to remove organic solvent. It should be noted that there was a small amount of precipitant found after the self-assembly of **17**. All samples were

filtered before analysis. The $D_{h,DLS}$ found in water increased from 8.38 to 11.07 nm for the three dendrimers **17** to **19** (Table 4.3). A similar trend was found from TEM (see Figure A4.33 in appendix), although the TEM diameters ($D_{h,TEM}$) were slightly larger by ~2.5 nm. The zeta potential increased from +27.5 to +40.4 mV, as expected, with the increased number of cationic L-lysine groups on the periphery. The small size of the dendrimer micelles in water could be assumed to represent crew-cut unimolecular micelles or multimolecular micelles with quite a low aggregation number. This postulate is in agreement with the low aggregation number found from the self-assembly of amphiphilic 4-arm block stars (consisting of an anionic outer block and a hydrophobic core block),[53, 54] and more particularly, with the low aggregation number (Z) of 9 found for polymeric dendrimers decorated with anionic blocks.[18] Due to the presence of both unimolecular and multimolecular micelles, the PDIs of micelles measured by DLS in water is relatively high.From the TEM (Figure A4.33) we can also observe both multimolecular micelles (long rod-like particles) and unimolecular micelles (single particles). The reason for such low aggregation numbers compared to linear diblock copolymers (where Z ranges from 150 to 300)[53] is ascribed to junction points[55] and loops[54]. It was found the number of junction points between polymer chains and their location within the structure. [54,55] For linear amphiphilic copolymer, it has only one junction point. The dendrimer, generally, containing multiple junction points. The PSTY core of our dendrimers consists of a 4-arm star tethered to a second generational layer of linear PSTY with a cationic peripheral layer (i.e. L-lysine groups). The many junction points between PSTY building blocks results in stretching of the PSTY chains[51] in the core, which further stretches due to the cationic peripheral groups. This stretching together with the formation of loops leads to an increase in the free energy, which can only be reduced by significantly lowering the aggregation number. Therefore, the data for our dendrimers suggests that the aggregation number is very low and consisting of unimolecular micelles (i.e. where Z =1), and that the L-lysine groups on one side of the dendrimer must be as far from the L-lysine groups on the other side of the dendrimer to reduce loop formation and thus entropy, thus limiting the diameter to the length of a single dendrimer in the core. The amphiphilic dendrimer architecture also directed self-assembly towards spherical micelles compared to the lamella structure normally found from crew-cut diblock copolymer self-assembly. This is due to the hydrophobic PSTY blocks are well shileded by hydrophilic lysine units after deprotection. The $D_{h,DLS}$ (Table 4.3) in water represents the average size of formed nanoparticles after self-assembly. During self-assembly, it is possible to form multimolecular micelles and unimolecular micelles, leading

to a slight increase of average size compared the size in organic slovent (before self-assembly).

4.4 Conclusion

In summary, we have demonstrated that by using copper to catalyze two orthogonal reactions (i.e. NRC and CuAAC) polymeric dendrimers with 3 and 4 generational layers could be constructed rapidly and with high purity. The purity of the 4-arm star core, **5**, was essential to the success of creating polymeric dendrimers coated with L-lysine on the periphery. The ATRP of the 4-arm star produced **2,** the precursor to **5,** with a purity of 87.3 % with the other 16.7% corresponding to higher molecular weight star-star coupling products. After purification by preparative SEC, the purity increased to 96.1 %. Coupling various building blocks to **5,** in a process where the rates of reaction for the NRC and the CuAAC were similar (i.e. the parallel process), allowed us to produce three polymeric dendrimers with an increase in L-lysine peripheral density. The purity for **14**, **15** and **16** was found to be 94, 96 and 97 %, respectively, as determined using the LND method. Our work showed that the copper-catalyzed CuAAC and NRC reactions represent a powerful synthetic method to produce dendrimers in one-pot at 25 ^{o}C. The versatility of this synthetic approach will have utility in the synthesis of polymeric dendrimers coated with a wide range of biomolecules. The self-assembly of these dendrimers in water demonstrates that due to the junction points within the dendrimer, the particle sizes were slightly larger than that found in organic solvents. We show here that utilizing amphiphilic dendrimers leads to control over the particles size due to its very low aggregation numbers. This represents an important step to implementing these peptidomimetic nanoparticles to increase the biological efficacy. We will carry out in vitro and *in vivo* studies in the future to confirm our hypothesis.

4.5 References

1. Kaspar, A. A.; Reichert, J. M. *Drug Discovery Today* **2013,** 18, (17-18), 807-817.
2. Vlieghe, P.; Lisowski, V.; Martinez, J.; Khrestchatisky, M. *Drug Discovery Today* **2010,** 15, (1-2), 40-56.
3. Bracci, L.; Falciani, C.; Lelli, B.; Lozzi, L.; Runci, Y.; Pini, A.; De Montis, M. G.; Tagliamonte, A.; Neri, P. *J. Biol. Chem.* **2003,** 278, (47), 46590-46595.
4. Jiang, Y. H.; Emau, P.; Cairns, J. S.; Flanary, L.; Morton, W. R.; McCarthy, T. D.; Tsai, C. C. *Aids Research and Human Retroviruses* **2005,** 21, (3), 207-213.
5. Bourne, N.; Stanberry, L. R.; Kern, E. R.; Holan, G.; Matthews, B.; Bernstein, D. I. *Antimicrob. Agents Chemother.* **2000,** 44, (9), 2471-2474.
6. Lee, C. C.; MacKay, J. A.; Frechet, J. M. J.; Szoka, F. C. *Nat. Biotechnol.* **2005,** 23, (12), 1517-1526.
7. Gajbhiye, V.; Palanirajan, V. K.; Tekade, R. K.; Jain, N. K. *J. Pharm. Pharmacol.* **2009,** 61, (8), 989-1003.
8. Percec, V.; Barboiu, B.; Grigoras, C.; Bera, T. K. *J. Am. Chem. Soc.* **2003,** 125, (21), 6503-6516.
9. Trollsas, M.; Hedrick, J. L. *J. Am. Chem. Soc.* **1998,** 120, (19), 4644-4651.
10. Hedrick, J. L.; Trollsas, M.; Hawker, C. J.; Atthoff, B.; Claesson, H.; Heise, A.; Miller, R. D.; Mecerreyes, D.; Jerome, R.; Dubois, P. *Macromolecules* **1998,** 31, (25), 8691-8705.
11. Matsuo, A.; Watanabe, T.; Hirao, A. *Macromolecules* **2004,** 37, (17), 6283-6290.
12. Whittaker, M. R.; Urbani, C. N.; Monteiro, M. J. *J. Am. Chem. Soc.* **2006,** 128, (35), 11360-11361.
13. Urbani, C. N.; Bell, C. A.; Lonsdale, D.; Whittaker, M. R.; Monteiro, M. J. *Macromolecules* **2008,** 41, (1), 76-86.
14. Urbani, C. N.; Bell, C. A.; Whittaker, M. R.; Monteiro, M. J. *Macromolecules* **2008,** 41, (4), 1057-1060.
15. Hossain, M. D.; Jia, Z. F.; Monteiro, M. J. *Macromolecules* **2014,** 47, (15), 4955-4970.
16. Skwarczynski, M.; Zaman, M.; Urbani, C. N.; Lin, I. C.; Jia, Z. F.; Batzloff, M. R.; Good, M. F.; Monteiro, M. F.; Toth, I. *Angewandte Chemie-International Edition* **2010,** 49, (33), 5742-5745.

17. Liu, T. Y.; Hussein, W. M.; Jia, Z. F.; Ziora, Z. M.; McMillan, N. A. J.; Monteiro, M. J.; Toth, I.; Skwarczynski, M. *Biomacromolecules* **2013,** 14, (8), 2798-2806.

18. Lonsdale, D. E.; Whittaker, M. R.; Monteiro, M. J. *Journal of Polymer Science Part a-Polymer Chemistry* **2009,** 47, (22), 6292-6303.

19. Bell, C. A.; Jia, Z. F.; Kulis, J.; Monteiro, M. J. *Macromolecules* **2011,** 44, (12), 4814-4827.

20. Trollsas, M.; Claesson, H.; Atthoff, B.; Hedrick, J. L. *Angewandte Chemie-International Edition* **1998,** 37, (22), 3132-3136.

21. Trollsas, M.; Atthof, B.; Wursch, A.; Hedrick, J. L.; Pople, J. A.; Gast, A. P. *Macromolecules* **2000,** 33, (17), 6423-6438.

22. Lammens, M.; Fournier, D.; Fijten, M. W. M.; Hoogenboom, R.; Du Prez, F. *Macromol. Rapid Commun.* **2009,** 30, (23), 2049-2055.

23. Urbani, C. N.; Lonsdale, D. E.; Bell, C. A.; Whittaker, M. R.; Monteiro, M. J. *Journal of Polymer Science Part a-Polymer Chemistry* **2008,** 46, (5), 1533-1547.

24. Urbani, C. N.; Bell, C. A.; Lonsdale, D. E.; Whittaker, M. R.; Monteiro, M. J. *Macromolecules* **2007,** 40, (19), 7056-7059.

25. Hutchings, L. R.; Roberts-Bleming, S. J. *Macromolecules* **2006,** 39, (6), 2144-2152.

26. Konkolewicz, D.; Monteiro, M. J.; Petrie, S. *Macromolecules* **2011,** 44, (18), 7067-7087.

27. Kimani, S. M.; Hutchings, L. R. *Macromol. Rapid Commun.* **2008,** 29, (8), 633-637.

28. Hutchings, L. R. *Soft Matter* **2008,** 4, (11), 2150-2159.

29. Hu, D.; Zheng, S. X. *Eur. Polym. J.* **2009,** 45, (12), 3326-3338.

30. Pan, P. J.; Fujita, M.; Ooi, W. Y.; Sudesh, K.; Takarada, T.; Goto, A.; Maeda, M. *Polymer* **2011,** 52, (4), 895-900.

31. Lutz, J. F.; Borner, H. G.; Weichenhan, K. *Macromolecules* **2006,** 39, (19), 6376-6383.

32. Sumerlin, B. S.; Vogt, A. P. *Macromolecules* **2010,** 43, (1), 1-13.

33. Inglis, A. J.; Sinnwell, S.; Stenzel, M. H.; Barner-Kowollik, C. *Angewandte Chemie-International Edition* **2009,** 48, (13), 2411-2414.

34. Kade, M. J.; Burke, D. J.; Hawker, C. J. *Journal of Polymer Science Part a-Polymer Chemistry* **2010,** 48, (4), 743-750.

35. Campos, L. M.; Killops, K. L.; Sakai, R.; Paulusse, J. M. J.; Damiron, D.; Drockenmuller, E.; Messmore, B. W.; Hawker, C. J. *Macromolecules* **2008,** 41, (19), 7063-7070.

36. Campos, L. M.; Meinel, I.; Guino, R. G.; Schierhorn, M.; Gupta, N.; Stucky, G. D.; Hawker, C. J. *Advanced Materials* **2008,** 20, (19), 3728-+.

37. Killops, K. L.; Campos, L. M.; Hawker, C. J. *J. Am. Chem. Soc.* **2008,** 130, (15), 5062-+.

38. Antoni, P.; Robb, M. J.; Campos, L.; Montanez, M.; Hult, A.; Malmstrom, E.; Malkoch, M.; Hawker, C. J. *Macromolecules* **2010,** 43, (16), 6625-6631.

39. Ma, X. P.; Tang, J. B.; Shen, Y. Q.; Fan, M. H.; Tang, H. D.; Radosz, M. *J. Am. Chem. Soc.* **2009,** 131, (41), 14795-14803.

40. Jia, Z. F.; Bell, C. A.; Monteiro, M. J. *Chemical Communications* **2011,** 47, (14), 4165-4167.

41. Matyjaszewski, K.; Davis, T. P., *Handbook of Radical Polymerization*. John Wiley and Sons: USA, 2002.

42. Mantovani, G.; Ladmiral, V.; Tao, L.; Haddleton, D. M. *Chemical Communications* **2005**, (16), 2089-2091.

43. Agrawal, P.; Gupta, U.; Jain, N. K. *Biomaterials* **2007,** 28, (22), 3349-3359.

44. Altintas, O.; Krolla-Sidenstein, P.; Gliemann, H.; Barner-Kowollik, C. *Macromolecules* **2014,** 47, (17), 5877-5888.

45. Gavrilov, M.; Monteiro, M. J. *Eur. Polym. J.* **2015**. doi:10.1016/j.eurpolymj. 2014.11.018

46. Monteiro, M. J. *Eur. Polym. J.* **2015**. doi:10.1016/j.eurpolymj.2015.01.009

47. Kulis, J.; Bell, C. A.; Micallef, A. S.; Jia, Z. F.; Monteiro, M. J. *Macromolecules* **2009,** 42, (21), 8218-8227.

48. Kulis, J.; Bell, C. A.; Micallef, A. S.; Monteiro, M. J. *Journal of Polymer Science Part a-Polymer Chemistry* **2010,** 48, (10), 2214-2223.

49. Percec, V.; Guliashvili, T.; Ladislaw, J. S.; Wistrand, A.; Stjerndahl, A.; Sienkowska, M. J.; Monteiro, M. J.; Sahoo, S. *J. Am. Chem. Soc.* **2006,** 128, (43), 14156-14165.

50. Kulis, J.; Jia, Z. F.; Monteiro, M. J. *Macromolecules* **2012,** 45, (15), 5956-5966.

51. Daoud, M.; Cotton, J. P. *Journal De Physique* **1982,** 43, (3), 531-538.

52. Hossain, M. D.; Lu, D. R.; Jia, Z. F.; Monteiro, M. J. *Acs Macro Letters* **2014,** 3, (12), 1254-1257.

53. Whittaker, M. R.; Monteiro, M. J. *Langmuir* **2006,** 22, (23), 9746-9752.

54. Iatrou, H.; Willner, L.; Hadjichristidis, N.; Halperin, A.; Richter, D. *Macromolecules* **1996,** 29, (2), 581-591.

55. Kim, K. H.; Kim, S. H.; Huh, J.; Jo, W. H. *J. Chem. Phys.* **2003,** 119, (11), 5705-5710.

Chapter 5

Star molecules as drug scaffolds targeting biological ion channels

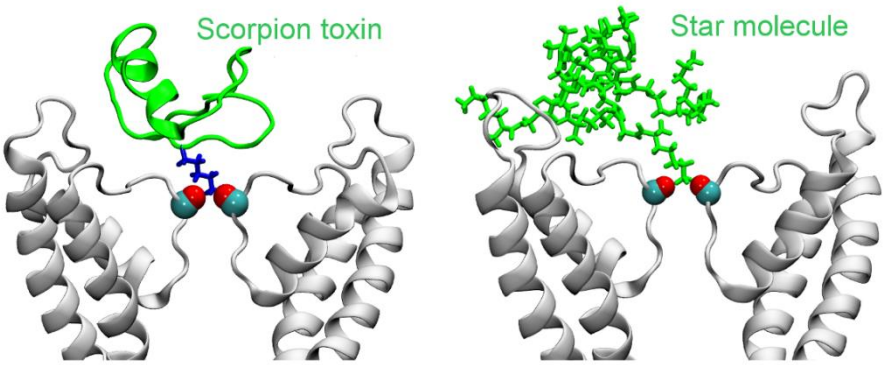

In this chapter, four peripherally functionalized star dendrimers were successfully synthesized to mimic the action of scorpion toxins on voltage-activated K^+ channels. Pre-synthesized alkyne or azide functional ethylene glycol (EG) backbones were attached to either lysine-Boc or MFK-Boc peptides, resulting in alkyne-terminal EG-Lysine-Boc and EG-MKF-Boc conjugates, which were further tethered with a tetraazide core *via* CuAAC 'click' reaction to form the corresponding dendrimers. The size, types and density of surface functional groups of dendrimers were adjusted by changing the repeating unit of the EG backbone, attaching different molecules (amino acid or peptide), and utilizing the trifuntional linker to create alternative branch points. The resulting dendrimers were characterized by MALDI-ToF MS and NMR to confirm the formation of the desired structures. Generating these diverse architectures enabled the study of the effect of different structures on ion channel inhibition. Future work will consist of computer modeling of these dendrimers within the ion channel and then biological testing.

5.1 Introduction

Ion channels are integral membrane proteins that selectively allow the passage of certain ionic species across the cell membrane. Malfunction of ion channels is implicated in the development of a host of human diseases such as neurological, muscular and immunological disorders. Various ion channels have been identified as pharmaceutical targets,[1, 2] and a range of currently available drugs such as local anesthetics and anticonvulsants modulate ion channel function.[3] Many natural peptides isolated from the venom of arachnids, reptiles and marine invertebrates modulate the function of ion channels, either by physically occluding the ion conduction pathway or by interfering with their gating mechanisms. As some of these venom peptides are highly specific inhibitors for certain channel isoforms, extensive research has been undertaken to develop novel drugs using venom peptides as scaffolds.[4, 5]

The peptidic nature of these toxins, however, generates several undesired properties. Peptides are relatively expensive to manufacture, and thus the cost for drug development can be high,[6] the immune system may generate antibodies against the peptides and compromise the efficacy of the peptide toxins, further peptides are also susceptible to proteolysis, which could result in low oral activity and limited lifetime in plasma.[7, 8] It is therefore desirable to replace peptides with equally effective synthetic compounds (e.g, Peptidomimetics) that overcome these drawbacks.[9]

Peptidomimetics, are compounds derived from native peptides and obtained by structural modification using unnatural amino acids which may help to overcome many of the drawbacks limiting the application of peptides as therapeutics in the past.[10-14] Very recently, polymer-peptide (or polymer peptidomimetic) conjugates has been adopted to modify the properties and conformation of short peptides, the resulting conjugates possessing both advantages of peptidomimetic and synthetic polymer.[15-17] For example, the conjugation of polyethylene glycol (PEG) to peptides, so-called PEGylation, has been demonstrated to be a promising method to overcome some delivery issues of peptide drugs by increasing their water solubility and circulating lifetime, and thus reducing toxicity and improving stability.[18-22] Recent experimental studies and computational simulation showed that the topologies of PEG backbones (e.g, size and grafting density of PEG) would exert great influence on the biological activity of PEGylated complex.[21-23] Interestingly, 4-arm PEG-peptide conjugates showed significantly improved DNA binding and gene transfection capabilities compared to their linear derivative.[22] The limitations of linear peptide-polymer conjugates was further verified by simulation, which suggested that linear PEG chains warp peptides into polymeric

coils and therefore decrease their binding interactions.[23] These results supported the previous theory that the mobility of linear peptides (or linear peptide-polymer conjugates) weakens chemical interactions, while conformationally restricted peptides (e.g, cyclic peptide, dendritic peptide) show enhanced biological activities.[15, 24, 25] In contrast to linear PEG, dendritic PEG cores possess controllable sizes, topologies, and multivalent terminal groups. Moreover, the steric hindrance on the outer shell restricts the flexibility of attached peptides, resulting in improved biological performance.[26-29] Thus, the synthetically accessible dendritic PEG-peptidomimetic conjugates offer superior properties in comparison to their linear counterparts.

In order to prepare PEG-peptidomimetic conjugates that retain the biological activity of amino acids or peptide precursors, the chemical synthesis applied for both modification of peptidomimetics and conjugation of PEG-peptidomimetics should fulfill the following criterions. First, experimental conditions should be sufficiently mild to avoid reduction of the biological activity of the peptide; second the chemistry should be compatible with the side chains of the amino acids, at least in protected form; and finally it should afford efficient coupling to form peptidomimectics with few or negligible side products. The copper(I)-catalyzed alkyne-azide cycloaddition(CuAAC), a robust coupling reaction meets the requirements above and has been extensively used in the biological fields.[20, 30-32] The versatility of organic chemistry enables the generation of functional peptidomimectics and polymer backbones bearing either alkyne or azide functionality, which can be readily coupled by further CuAAC reactions. The CuAAC reaction therefore offers structural diversity in complex polymer- peptidomimectics conjugates.

Herein, a series of 4-arm star-like ethylene glycol lysine (EG-lysine) and ethylene glycol peptide (EG-MKF) dendrimers were prepared to mimic the structure of scorpion toxins (e.g, charybdotoxin) with the potential to inhibit several K^+ channels including Kv1.3.[33] The resultant conjugates could be used as potential inhibitors of the voltage-gated K^+ channel Kv1.3, which is involved in autoimmune diseases.[34, 35] The molecules were all constructed convergently using the copper-catalyzed azide-alkyne cycloaddition (CuAAC) reaction and were designed to consist of a common core, a second generational layer of EG that was either longer or twice as dense, and an outer generational layer with the lysine or MKF tripeptide.

5.1.1 Aim of Chapter

The aim of this chapter is to synthesize 4-arm PEG-lysine or EG-peptide structure which will be used in a later biological experiment to block the Kv1.3 ion channel, as well as in computational simulation experiments (these will be carried out by other groups). By comparing simulation and biological testing, it may be possible to develop an approach for exploring the structure-property relationship of peptidimetics architectures for therapeutic use.

Scheme 5.1 Synthetic route of EG-Lysine and EG-MKF dendrimers

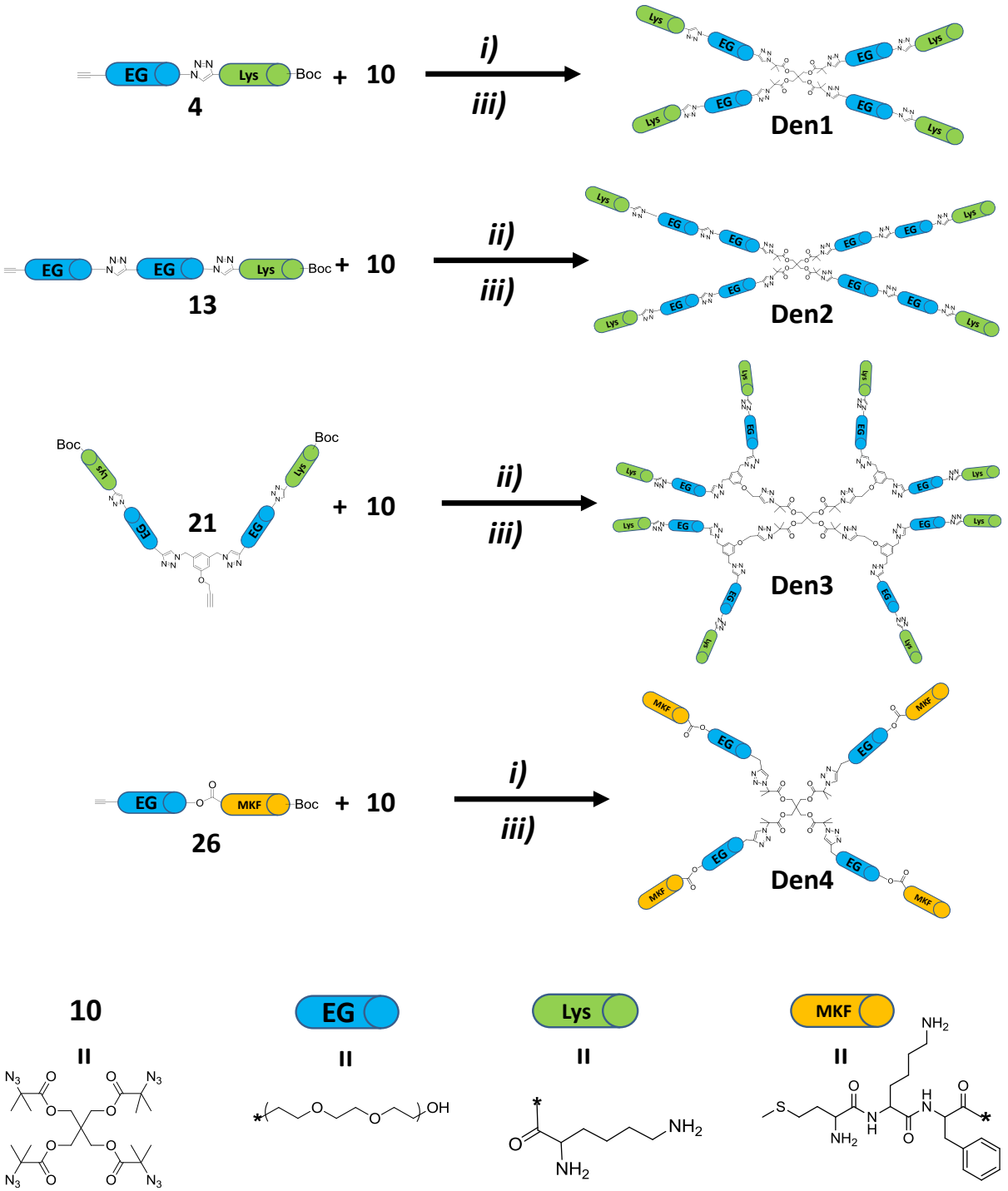

i) CuBr, PMDETA, Toluene, 25 ^{o}C, 120 min; ii) CuBr, PMDETA, Toluene, DMSO, 25 ^{o}C, 120 min; iii) TFA, DCM, 6h.

5.2 Experimental

5.2.1 Materials

The following chemicals were used as received: alumina, activated basic (Aldrich, Brockmann I, standard grade, ~150 mesh, 58 Å), magnesium sulfate ($MgSO_4$: anhydrous, Scharlau, extra pure), sodium chloride (NaCl: Univar, 99.9%), sodium iodide (NaI: Aldrich, 99.5%), sodium azide (NaN_3: Aldrich, 99.5%), 1,1,1-triisopropylsilyl chloride (TIPS-Cl: Aldrich, 99%), ethylmagnesium bromide solution (EtMgBr, Aldrich, 3.0 M in diethyl ether), triethylamine (TEA: Fluka, 98%), TLC plates (silica gel 60 F254), silica gel 60 (230-400 mesh ATM (SDS)), potassium carbonate (K_2CO_3, analaR, 99.9%), 2-bromoisobutyryl bromide (BIB, Aldrich, 98%), lithium aluminium hydride ($LiAlH_4$, Aldrich, 98%), diphenyl phosphoryl azide (DPPA, Aldrich, 97%), 1,8-diazabicylco[5,4,0]undec-7-ene (DBU, Aldrich, 98%), tetrabutylammonium fluoride hydrate (TBAF, Aldrich, 1.0 M in THF), 18-crown-6 ether (18-C-6, Aldrich, 99%), imidazole (Aldrich, 99%) *N*,*N*′-dicyclohexylcarbodiimide (DCC, Aldrich, 99%), pentaerythritol (Aldrich, 99%), 2-(2-(2-chloroethoxy)ethoxy)ethanol (Aldrich, 96%), 4-(Dimethylamino)pyridine (DMAP, Aldrich, >99%), propargyl bromide (Aldrich, 80wt% in toluene), propargyl amine (Aldrich, 98%), triethlyene glycol (Aldrich, 98%), lithium aluminium hydride (LAH, Aldrich, 98%), di-*tert*-butyl dicarbonate (Boc, Aldrich, >99%), L-lysine (Lys, Aldrich, >98%), trifluoroacetic acid (TFA, Aldrich, 99%). The custom peptide Boc-Met-Lys(Boc)-Phe-OH (Boc-MKF-OH) was purchased from Auspep Pty Ltd, the peptide was purified by HPLC chromatogram, and used as received.

The following solvents were used as received: acetone (ChemSupply, AR), dimethyl sulfoxide (DMSO: Labscan, AR grade), dichloromethane (DCM: Labscan, AR grade), ethyl acetate (EtOAc: ChemSupply, AR grade), methanol (MeOH: anhydrous, Lichrosolv, 99.9%, HPLC grade), *N*,*N*-dimethylacetamide (DMAc: Aldrich, HPLC grade), petroleum spirit (BR 40-60 ^oC, Univar, AR grade), tetrahydrofuran (THF: Lichrosolv, HPLC grade), and toluene (TOL, Univar, AR grade).

The following initiators, ligands, and metals for the various polymerizations are given below and used as received unless otherwise stated: *N*,*N*,*N*’,*N*’’,*N*’’-pentamethyldiethylenetriamine (PMDETA: Aldrich, 99%), Copper(I)bromide were synthesized in the Monteiro group.

5.2.2 Synthetic procedures

5.2.2.1 Synthesis of dendrimer (1)

Scheme 5.2 Synthesis of EG-Lysine dendrimer 1 (**Den 1**)

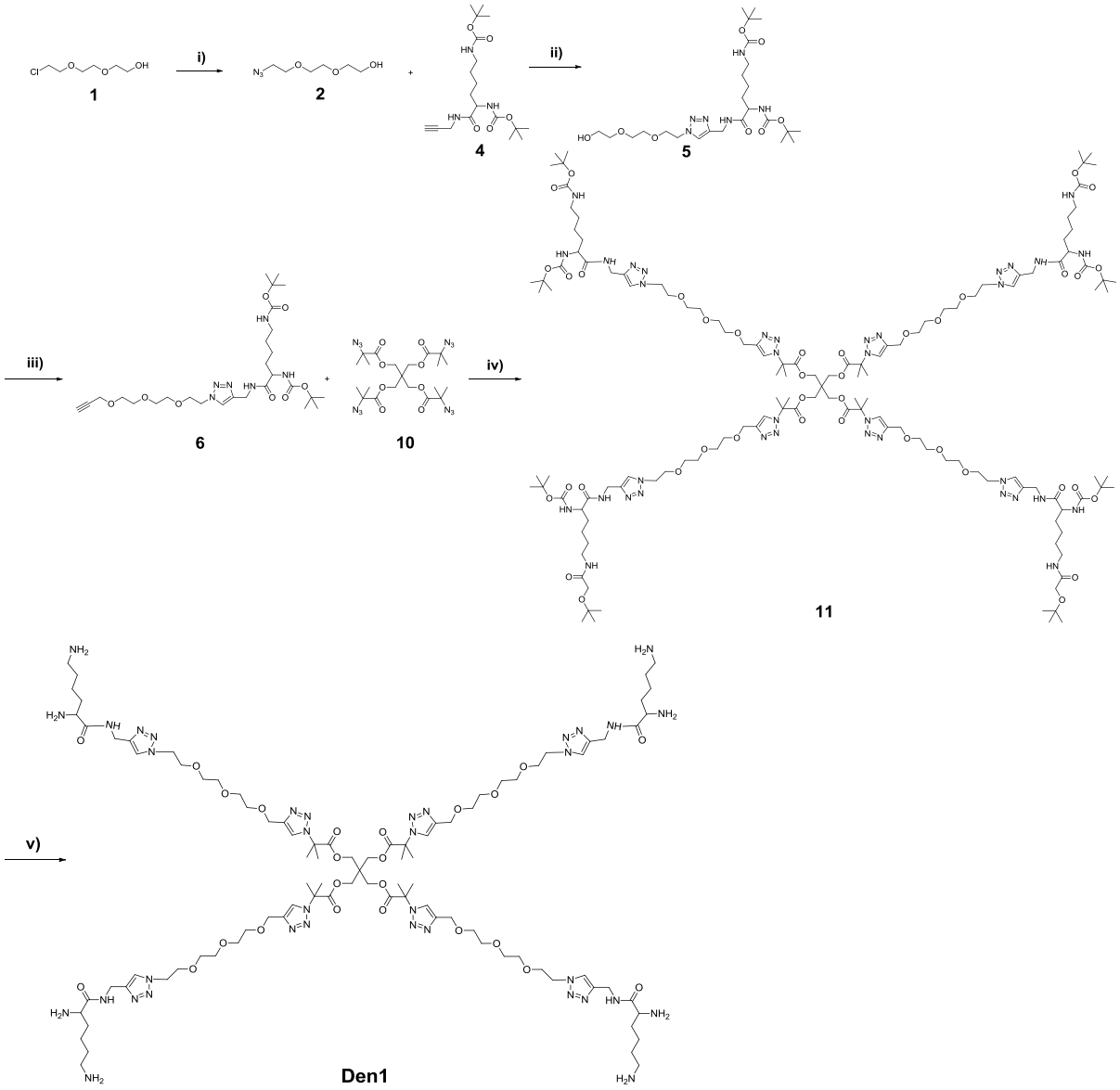

(i) NaN_3, NaI, H_2O, 60 ^oC, 16h; (ii) CuBr, PMDETA, Toluene, DMSO, 25 ^oC, 30 min; (iii) THF, NaH, propargyl bromide, -78 ^oC, 16 h; (iv) CuBr, PMDETA, Toluene, 25 ^oC, 120 min; (v) TFA, DCM, R.T., 6h.

Synthesis of 2-(2-(2-azidoethoxy)ethoxy)ethanol, 2.

A mixture of 2-(2-(2-chloroethoxy)ethoxy)ethanol (**1**, 3 mer, 5 g, 2.976 x 10^{-2} mol), NaN_3 (19.3 g, 2.976 x 10^{-1} mol), NaI (0.9 g, 6.0 x 10^{-3} mol) and H_2O (30 mL) was added into a 100 mL flask and was then placed into a 60 ^oC oil bath. The reaction was allowed to react for 16 h with stirring. After removal of the solvent under reduced pressure, the product was diluted in 50 mL DCM, washed with saturated brine (2 x 20 mL) and the organic phase was dried over anhydrous $MgSO_4$. The solvent was concentrated under reduced pressure. 4.47 g viscous oil **2** was obtained with the yield of 86% and used for next step directly without further purification.

^{1}H NMR ($CDCl_3$, 298K, 500 MHz): δ 3.65 (t, 2H, *J*=4.52 Hz, -C***H***$_2$OH), 3.59 (s, 6H, -C***H***$_2$-), 3.58 (t, 2H, *J*=4.52 Hz, -C***H***$_2$CH$_2$OH), 3.37 (t, 2H, *J*=5.00 Hz, -C***H***$_2$N$_3$), 1.96 (bd, 1H, -O***H***), ^{13}C NMR ($CDCl_3$, 298K, 500 MHz): 50.67, 61.68, 70.03, 70.39, 70.65, 72.62.

Synthesis of alk-Lysine-Boc, 4.

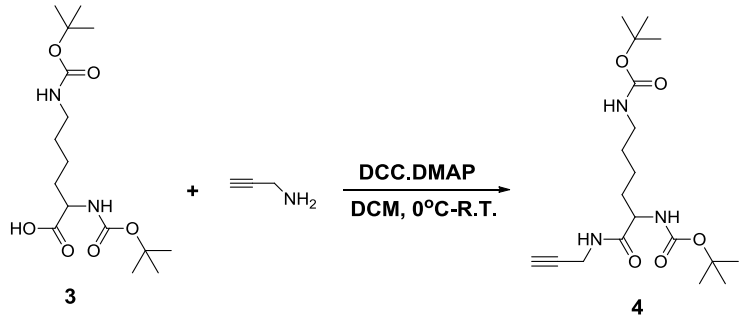

OH-Lysine-OH (**3**) and alk-Lysine-Boc (**4**) were synthesized according to reference.[36] In a 500 mL flask, **3** (6.0 g, 0.172 mol), propargyl amine (1.90 g, 0.0345 mol), and DMAP (0.316 g, 2.59 x 10^{-3} mol) were dissolved in 120 mL dry DCM and cooled to 0 ^oC in an ice-bath. A mixture of DCC and 50 mL DCM was added dropwise into the solution over 30 min. The mixture was allowed to react for 36 h at room temperature. The solid content was removed by filtration and the filtrate was washed by saturated brine (2 x 50 mL). The organic layer was collected, dried over anhydrous $MgSO_4$, the solvent removed *in vacuo* followed by

column chromatography using ethyl acetate/petroleum spirit (3/1, v/v, R_f=0.65) as the eluent. Product **4** was obtained as a white solid (2.86 g, yield%=41.7 %). ^{1}H NMR ($CDCl_3$, 298K, 500 MHz): δ 6.91 (s, 1H, $CHCCH_2N\boldsymbol{H}CO$-), 5.32 (s, 1H, -$CHN\boldsymbol{H}CO$-), 4.69 (s, 1H, -$CH_2N\boldsymbol{H}CO$), 3.97-4.07 (b, 3H, $CH_2CC\boldsymbol{H}_2NH$- and –$CH_2C\boldsymbol{H}CO$-), 3.08 (t, 2H, *J*=6.6 Hz, -$CH_2C\boldsymbol{H}_2NH$-), 2.20 (t, 1H, *J*=2.5 Hz, $\boldsymbol{H}CCCH_2$-), 1.2-2.0 (m, 24H, $C\boldsymbol{H}_2$-Lys and $C\boldsymbol{H}_3$-Boc). ^{13}C NMR ($CDCl_3$, 298K, 500 MHz): 22.69, 28.44, 28.53, 29.09, 29.70, 32.23, 40.07, 54.24, 71.60, 79.16, 79.53, 80.10, 155.97, 156.26, 172.22.

Synthesis of OH-EG-Lysine-Boc, 5.

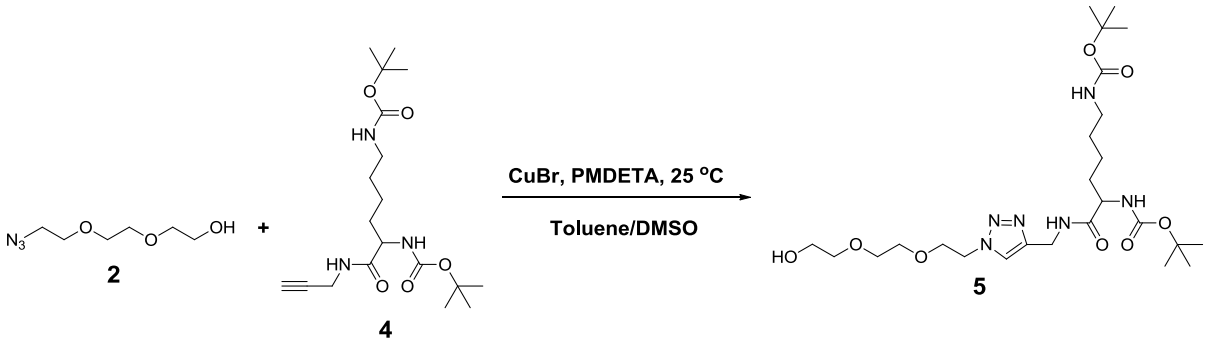

2 **4** **5**

2 (0.684 g, 3.909 x 10^{-3} mol) and **4** (0.650 g, 1.699 x 10^{-3} mol) were placed in a Schlenk tube and dissolved in a mixture of PMDETA (0.0293 g, 1.70 x 10^{-4} mol), toluene (4 mL), DMSO (2 mL). Oxygen was removed from the solution by purging with argon for 30 min. Cu(I)Br (0.024 g, 1.70 x 10^{-4} mol) was added under a positive argon flow and the solution was purged with argon for another 5 minutes. The reaction vessel was then sealed and placed in an oil bath at 25 ^{o}C and kept stirring for 30 min. The mixture was diluted in DCM and passed through activated basic alumina. The solvent was removed under reduced pressure, and the residue was purified by column chromatography with DCM-MeOH (6:1, v/v, R_f=0.55) as eluent. 2.26 g viscous oil **5** was obtained with the yield as 79%.

^{1}H NMR ($CDCl_3$, 298K, 500 MHz): δ 7.85 (s, 1H, -NC***H***C-, triazole ring proton), 7.48 (bd, 1H, -CCH_2N***H***CO-), 5.40 (bd, 1H, -CHN***H***C(O)O-), 4.77 (bd, 1H, -CH_2N***H***C(O)O-), 4.47-4.48 (m, 4H, -CH_2C***H***$_2$N-, -CC***H***$_2$NH-), 4.05 (s, 1H, -C(O)C***H***(CH_2)NH-), 3.81 (t, 2H, *J*=4.90 Hz, -COC***H***$_2$$CH_2$N-), 3.69 (t, 2H, *J*=4.58 Hz, OHC***H***$_2$$CH_2$O-), 3.57 (bd, 4H, -OC***H***$_2$$CH_2$O-, -$OCH_2$C***H***$_2$O-), 3.51 (t, 2H, *J*=4.55 Hz, $OHCH_2$C***H***$_2$O-), 3.44 (bd, 1H, -O***H***), 3.02 (t, 2H, *J*=6.6 Hz, -CH_2C***H***$_2$NH-), 1.2-2.0 (m, 24H, C***H***$_2$-Lys and C***H***$_3$-Boc). ^{13}C NMR ($CDCl_3$, 298K, 500 MHz): 22.68, 28.40, 28.52, 29.64, 32.32, 34.85, 40.08, 50.38, 54.48, 61.64, 69.21, 70.21, 70.51, 72.60, 79.17, 79.99, 124.03, 144.54, 155.86, 156.30, 172.66.

Synthesis of alk-EG-Lysine-Boc conjugate, 6.

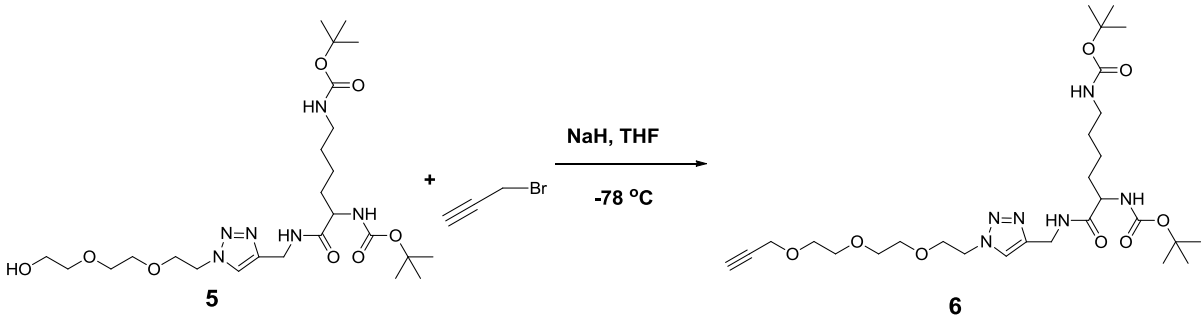

5 (0.6 g, 1.075 x 10^{-3} mol) was dissolved in 10 mL dry THF in a 25 mL two-neck round bottom flask, the flask was connected to the argon line and the solution was cooled to 0^{o}C in an ice-bath. NaH (0.043 g, 1.075 x 10^{-3} mol) (60 % in mineral oil) was added proportionally in the above solution over 5 min. The reaction was stirred for 1 h and there was no bubbling if the argon was stopped. The reaction vessel was then cooled down to -78 ^{o}C in dry ice/acetone mixture. Propargyl bromide (0.237 g, 1.6 x 10^{-3} mol) (80 wt % in toluene) was added to the solution dropwise over 10 min. The reaction was then kept stirring overnight and warmed to RT. The reaction mixture was filtered to remove the salt and concentrated to remove all the solvent and low b.p impurities at RT. The crude brown liquid product was purified by column chromatography with DCM-MeOH (10:1, v/v, R_f=0.45) as eluent. 0.21 g viscous oil **6** was obtained with the yield as 27.8 %.

^{1}H NMR ($CDCl_3$, 298K, 500 MHz): δ 7.72 (s, 1H, -NC***H***C-, triazole ring proton), 6.95 (bd, 1H, -CCH_2N***H***CO-), 5.18 (bd, 1H, -CHN***H***C(O)O-), 4.63 (bd, 1H, -CH_2N***H***C(O)O-), 4.51-4.49 (m, 4H, -CH_2C***H***$_2$N-, -CC***H***$_2$NH-), 4.17 (d, 2H, *J*=2.5 Hz, CHC***H***$_2$O-), 4.05 (s, 1H, -C(O)C***H***(CH_2)NH-), 3.83 (t, 2H, *J*=4.90 Hz, -COC***H***$_2CH_2$N-), 3.67 (m, 2H, OHC***H***$_2CH_2$O-), 3.62 (m, 2H, $OHCH_2$C***H***$_2$O-), 3.59 (bd, 4H, -OC***H***$_2CH_2$O-, -OCH_2C***H***$_2$O-), 3.05 (t, 2H, *J*=6.6 Hz, -CH_2C***H***$_2$NH-), 2.43 (t, 1H, *J*=2.3 Hz, C***H***CCH_2-), 2.0-1.2 (m, 24H, C***H***$_2$-Lys and C***H***$_3$-Boc). ^{13}C NMR ($CDCl_3$, 298K, 500 MHz): 22.68, 29.76, 32.31, 34.98, 40.05, 50.37, 54.52, 58.48, 69.18, 69.47, 70.45, 70.56, 70.63, 74.86, 79.19, 79.66, 80.05, 123.48, 144.45, 155.82, 156.30, 172.36.

Scheme 5.3 Synthetic route for tetrafunctional core **10**

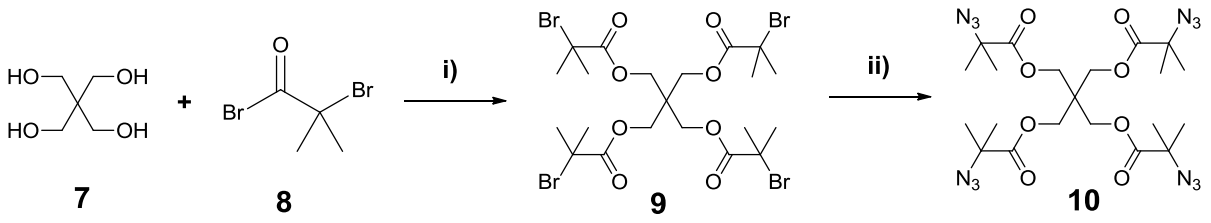

i) THF, TEA, 0°C-R.T., 6 h. ii) NaN_3, DMF, 24 h.

Synthesis of tetrabromo core, 9.

A solution containing 2-bromoisobutyryl bromide (**8**, 25.1 g, 0.109 mol) and 80 mL of dry THF was added dropwise to another solution containing pentaerythritol (**7**, 3.0 g, 2.2 x 10^{-2} mol), triethylamine (11.1 g, 0.109 mol) and 220 mL of dry THF at 0 °C. The reaction was allowed to stir for 6 h, filtered to remove the salts, and then the filtrate concentrated by rotary evaporation. The resulted product was dissolved in 300 mL ether and sequentially washed with 10 wt% HCl, saturated $NaHCO_3$ solution, and brine. The organic layer was collected, dried over anhydrous $MgSO_4$ and filtered. The filtrate was concentrated by rotary evaporation. The concentrate was purified by silica gel column chromatography using ethyl acetate/petroleum spirit (1/6, v/v) as the eluent. Product **9** was obtained as white crystals (10.65 g, 66.0 %). R_f (1/6 EtOAc/petroleum spirit) 0.61.

^{1}H NMR ($CDCl_3$, 298K, 400 MHz): δ 1.92 (s, 24H, C***H***$_3$-), 4.30 (s, 8H, -OC***H***$_2$C-). ^{13}C NMR ($CDCl_3$, 298K, 400 MHz): 30.62, 43.64, 55.18, 62.88, 170.89.

Synthesis of tetraazide core,10.

NaN_3 (1.77 g, 2.73 x 10^{-2} mol) was added to a stirred solution of **9** (1.00 g, 1.37 x 10^{-3} mol) in 6 mL of DMF. The reaction mixture was stirred for 24 h at room temperature. The resulted mixture was diluted by 30 mL DCM and passed through short basic alumina column to remove NaN_3. The filtrate was concentrated by rotary evaporation, and dried under high vacuum for 48 h at 25 °C obtained as light yellow powder **10**. The resulted product was used for next step without further purification.

^{1}H NMR ($CDCl_3$, 298K, 500 MHz): δ 1.48 (s, 24H, C***H***$_3$-), 4.27 (s, 8H, -OC***H***$_2$C-). ^{13}C NMR ($CDCl_3$, 298K, 500 MHz): 24.47, 43.09, 62.60, 63.33, 172.18.

Synthesis of 4-arm star-like EG-Lysine-Boc conjugate, 11.

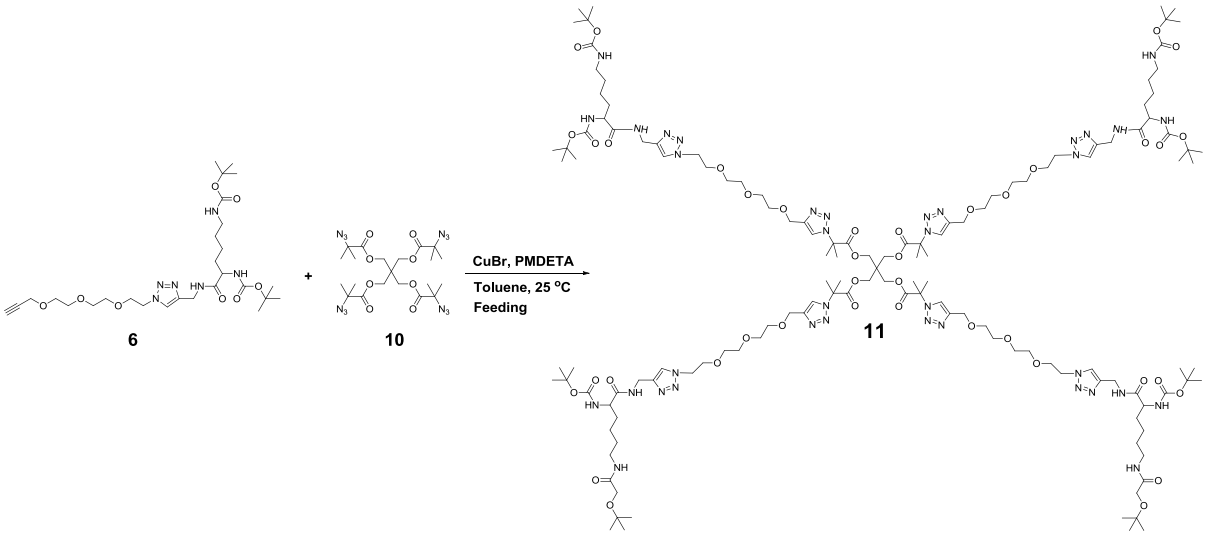

A solution of **6** (0.096 g, 1.613 x 10^{-4} mol) in toluene (5 mL) was purged argon for 30 min to remove oxygen. Meanwhile, a mixture of **10** (21.9 mg, 3.786 x 10^{-5} mol), PMDETA (6.56 mg, 3.786 x 10^{-5} mol) and toluene (5 mL) was degassed by argon for 30 min, to the deoxygenated mixture above, CuBr (5.24 mg, 3.786 x 10^{-5} mol) was added under positive argon flow. Then, the solution of **6** was added via syringe pump, at a flow rate of 0.025 mL/min, and after feeding the reaction was allowed to react for 2 h. The copper salts were removed by passage through activated basic alumina. The solvent was removed under reduced pressure. The crude product was purified using a Varian Pro-Star preparative SEC system equipped with a manual injector, differential refractive index detector, and single wave-length ultra-violet visible detector. Flow rate was maintained 10 mL min^{-1} and HPLC grade THF was used as the eluent. Separations were achieved using a PL gel 10 mm 1x103 Å, 300 mm x 25 mm preparative SEC column held at 25 ^{o}C. After injection, the expected fraction was collected manually with the yield as 18.7 mg. (yielding %=15.9 %).

SEC: (M_n=2220, M_p=2370, PDI=1.025)

MALDI-ToF MS: [**11**+Na^+]=2986.84 (Cal.=2986.67)

Synthesis of 4-arm star-like EG-Lysine conjugate, Den 1.

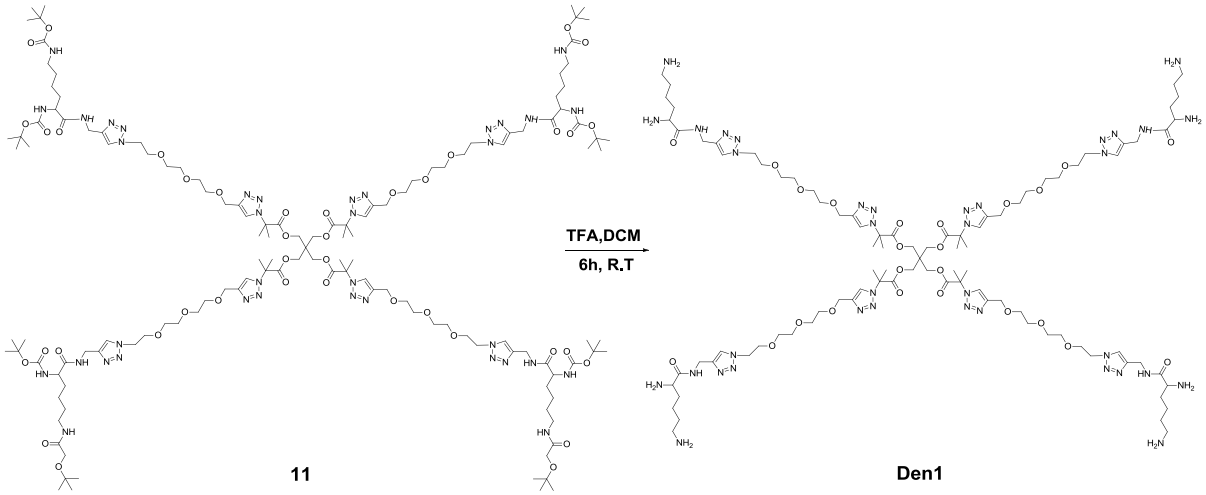

11 (0.015 g) was dissolved in 3 mL mixture of TFA and DCM (1:1, v:v). And the solution was kept stirring for 6 h at room temperature The solvent was remove by reduced pressure, and dried in high vacuum for 24 h, grey yellow oil **Den 1** was produced with near quantitative conversion.

5.2.2.2 Synthesis of dendrimer (2)

Scheme 5.4 Synthesis of EG-Lysine dendrimer 2 (**Den 2**)

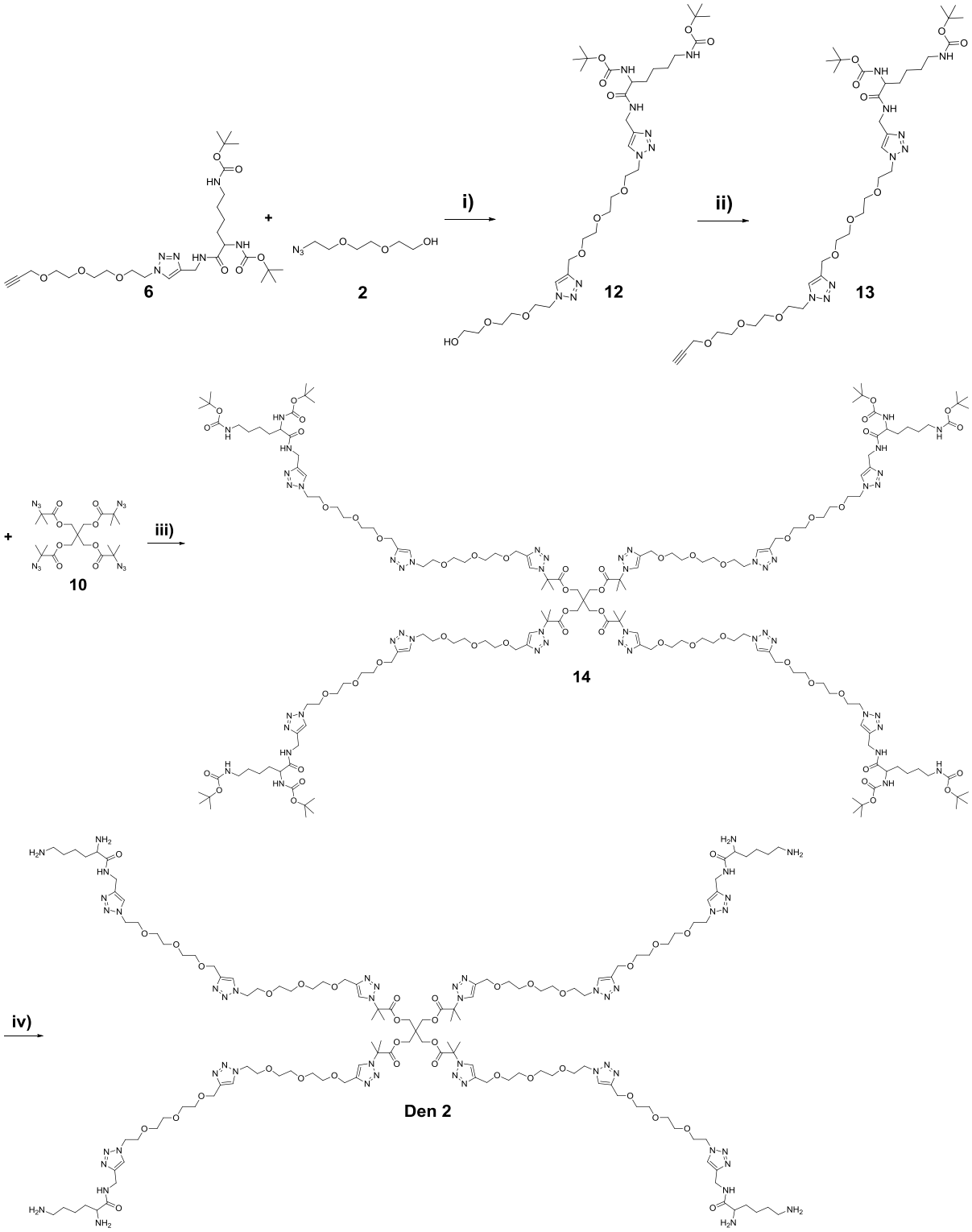

(i) CuBr, PMDETA, Toluene, DMSO, 25 ^{o}C, 30 min; (ii) THF, NaH, propargyl bromide, -78^{o}C, 16 h; (iii) CuBr, PMDETA, Toluene,DMSO 25 ^{o}C, 120 min; (iv) TFA, DCM, R.T., 6h.

Synthesis of OH-EG-Lysine-Boc conjugate,12.

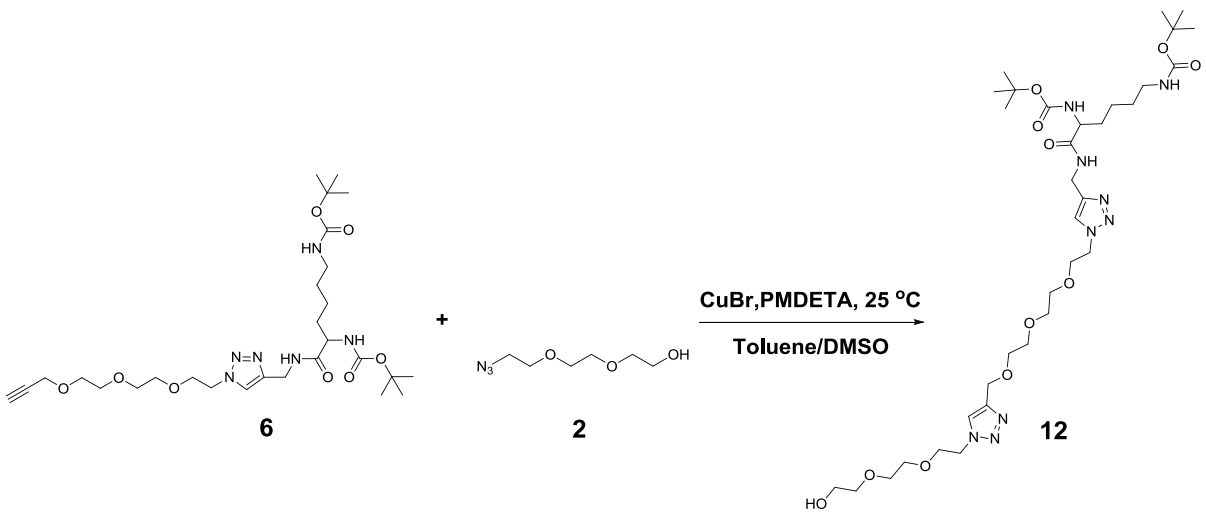

2 (0.095 g, 5.43 x 10^{-4} mol) and **6** (0.21 g, 3.62 x 10^{-4} mol) were placed in a Schlenk tube and dissolved in a mixture of PMDETA (0.0156 g, 9.05 x 10^{-5} mol), toluene (6 mL). Oxygen was removed from the solution by purging with argon for 30 min. Cu(I)Br (0.013 g, 9.05 x 10^{-5} mol) was added under a positive argon flow. The reaction vessel was then sealed and placed in an oil bath at 25 ^{o}C and kept stirring for 60 min. The mixture was diluted in DCM and passed through activated basic alumina. The solvent was removed under reduced pressure, and the residue was purified by column chromatography with EtOAc-MeOH (4:1, v/v, R_f=0.23) as eluent. 0.16 g viscous oil **12** was obtained with the yield as 59%.

^{1}H NMR ($CDCl_3$, 298K, 500 MHz): δ 7.79 (s, 1H, -NC***H***CCH_2O-, triazole ring proton), 7.68 (s, 1H, -NC***H***C-, triazole ring proton), 7.32 (bd, 1H, -CCH_2N***H***CH-), 5.38 (bd, 1H, -CHN***H***C(O)O-), 4.78 (bd, 1H, -CH_2N***H***C(O)O-), 4.61 (s, 2H, -CC***H***$_2CH_2O$-), 4.49-4.44 (m, 6H, -OCH_2C***H***$_2N$-, -CC***H***$_2$NH-), 4.05 (s, 1H, -C(O)C***H***(CH_2)NH-), 3.81 (m, 4H, -CH_2OC***H***$_2CH_2N$-), 3.82-3.54 (m, 16H, -C*H*$_2$- units on EG backbone), 3.02 (s, 2H, -CH_2C***H***$_2$NH-), 2.0-1.2 (m, 24H, C***H***$_2$-Lys and C***H***$_3$-Boc). ^{13}C NMR ($CDCl_3$, 298K, 500 MHz): 22.70, 28.54, 29.65, 32.43, 34.99, 40.09, 50.24, 50.33, 54.50, 61.59, 64.55, 69.39, 69.45, 69.69, 70.24, 70.47, 70.49, 70.53, 70.61,79.13, 79.92, 85.07, 123.48, 124.26, 144.61, 144.79, 155.83, 156.29, 171.48, 172.26.

Synthesis of alk-EG-Lysine-Boc conjugate, 13.

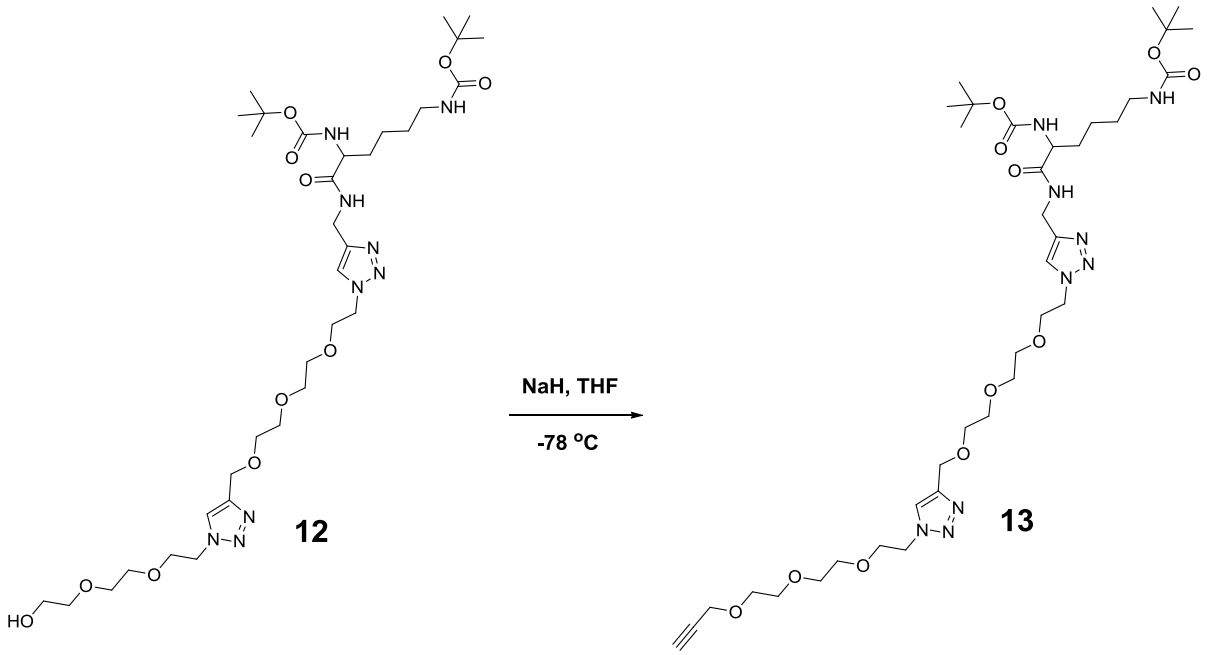

12 (0.11 g, 1.456 x 10^{-4} mol) was dissolved in 4 mL dry THF in a Schlenk tube, the tube was connected to the argon line and the solution was cooled to 0^{o}C in an ice-bath. NaH (0.0059 g, 1.456 x 10^{-4} mol) (60 % in mineral oil) was added in the above solution. The reaction was stirred for 30 min and there was no bubbling if stop the argonthe argon was stopped. The reaction vessel was then cooled down to -78 ^{o}C in dry ice/acetone mixture. Propargyl bromide (0.026 g, 2.18 x 10^{-4} mol) (80 wt % in toluene) was added to the solution dropwise in 5 min. The reaction was then kept stirring overnight and warmed to RT. The reaction mixture was filtered to remove the salt and concentrated to remove all the solvent and low b.p impurities at RT. The crude brown liquid product was purified by column chromatography with EtOAc-MeOH (6:1, v/v, R_f=0.50) as eluent. 0.02 g viscous oil **13** was obtained with the yield as 17 %.

^{1}H NMR ($CDCl_3$, 298K, 500 MHz): δ 7.78 (s, 2H, -NC***H***CCH_2O-, triazole ring protons), 7.29 (bd, 1H, -CCH_2N***H***CH-), 5.30 (bd, 1H, -CHN***H***C(O)O-), 4.68 (bd, 1H, -CH_2N***H***C(O)O-), 4.64 (s, 2H, -CC***H***$_2$$CH_2$O-), 4.49-4.44 (m, 6H, -OCH_2C***H***$_2$N-, -CC***H***$_2$NH-), 4.16 (d, 2H, *J*=2.35 Hz, CHC***H***$_2$O-), 4.09 (s, 1H, -C(O)C***H***(CH_2)NH-), 3.83 (m, 4H, -CH_2OC***H***$_2$$CH_2$N-), 3.67-3.55 (m, 16H, -C*H*$_2$- units on EG backbone), 3.02 (s, 2H, -CH_2C***H***$_2$NH-), 2.43 (t, 1H, *J*=2.3 Hz, C***H***CCH_2-), 2.0-1.2 (m, 24H, C***H***$_2$-Lys and C***H***$_3$-Boc).

Synthesis of 4-arm star-like EG-Lysine-Boc conjugate, 14.

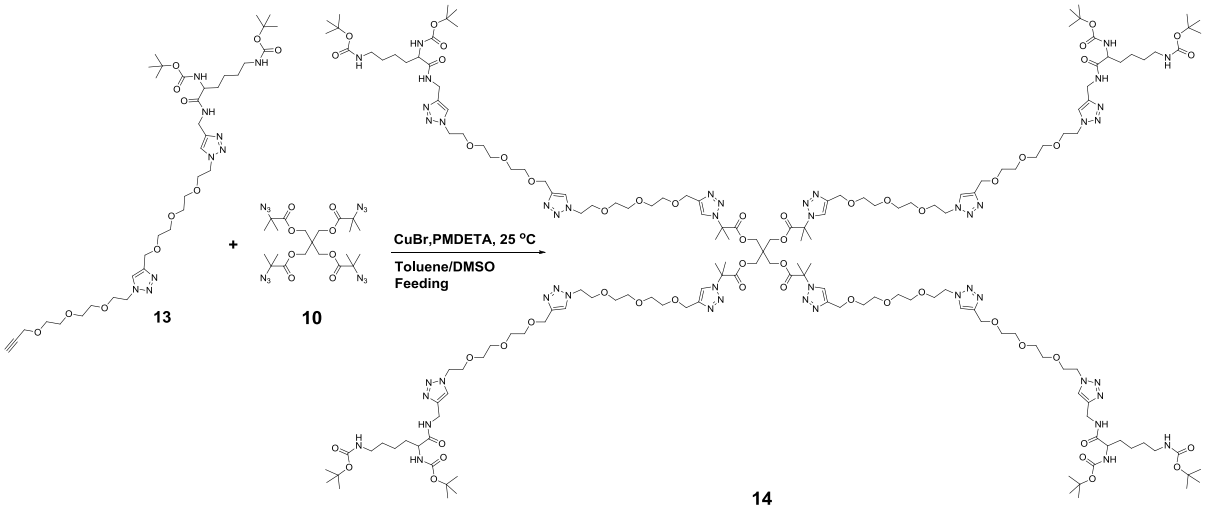

A solution of **13** (19.2 mg, 2.379 x 10^{-5} mol) in toluene (1.6 mL) and DMSO (0.4 mL) was purged with argon for 15 min to remove oxygen. Meanwhile, a mixture of **10** (0.0023 g, 3.966 x 10^{-6} mol), PMDETA (2.74 mg, 1.586 x 10^{-5} mol), toluene (1.6 mL) was degassed by argon for 15 min, to the deoxygenated mixture above, CuBr (2.3 mg, 1.586 x 10^{-5} mol) was added under positive argon flow. Then, the solution of **13** was added *via* syringe pump, at a flow rate of 0.003 mL/min, and after feeding the reaction was allowed to react for 2 h. The copper salts were removed by passage through activated basic alumina. The solvent was removed under reduced pressure. The crude product was purified using a Varian Pro-Star preparative SEC system equipped with a manual injector, differential refractive index detector, and single wave-length ultra-violet visible detector. Flow rate was maintained 10 mL min^{-1} and HPLC grade THF was used as the eluent. Separations were achieved using a PL gel 10 mm 1x103 Å, 300 mm x 25 mm preparative SEC column held at 25 ^{o}C. After injection, the expected fraction was collected manually with the yield as 4.26 mg (yielding%=23.2%).

SEC: (M_n=2610, M_p=2660, PDI=1.028)

MALDI-ToF MS: [**14**+Na^+]=3840.95 (Cal.=3841.09)

Synthesis of 4-arm star-like EG-Lysine conjugate, Den 2.

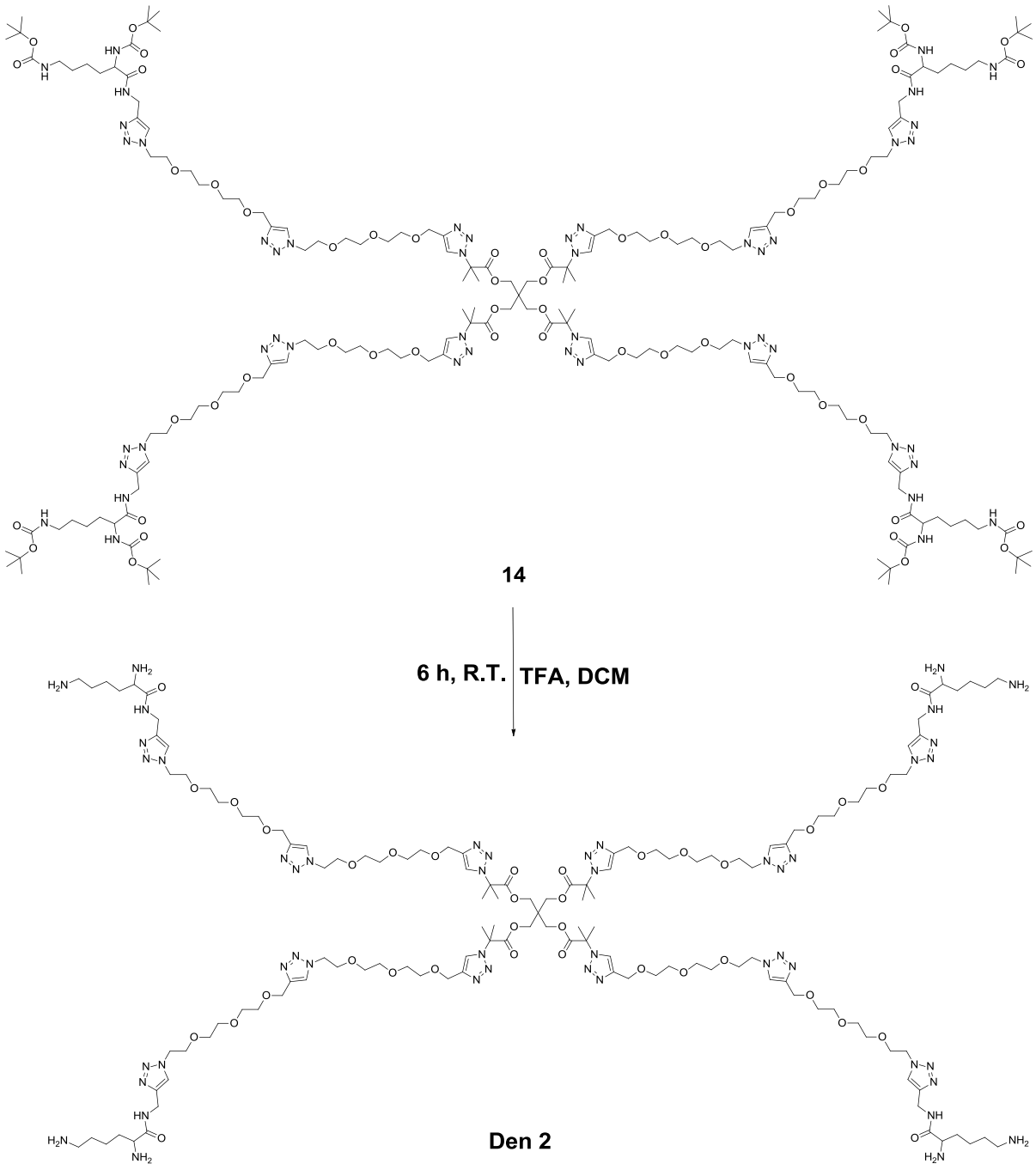

14 (0.015 g) was dissolved in 3 mL mixture of TFA and DCM (1:1, v:v). And the solution was kept stirring for 6 h at room temperature The solvent was remove by reduced pressure, and dried in high vacuum for 24 h, grey yellow oil **Den 2** was produced with near quantitative conversion.

5.2.2.3 Synthesis of dendrimer (3)

Scheme 5.5 Synthesis of EG-Lysine dendrimer 3 (**Den 3**)

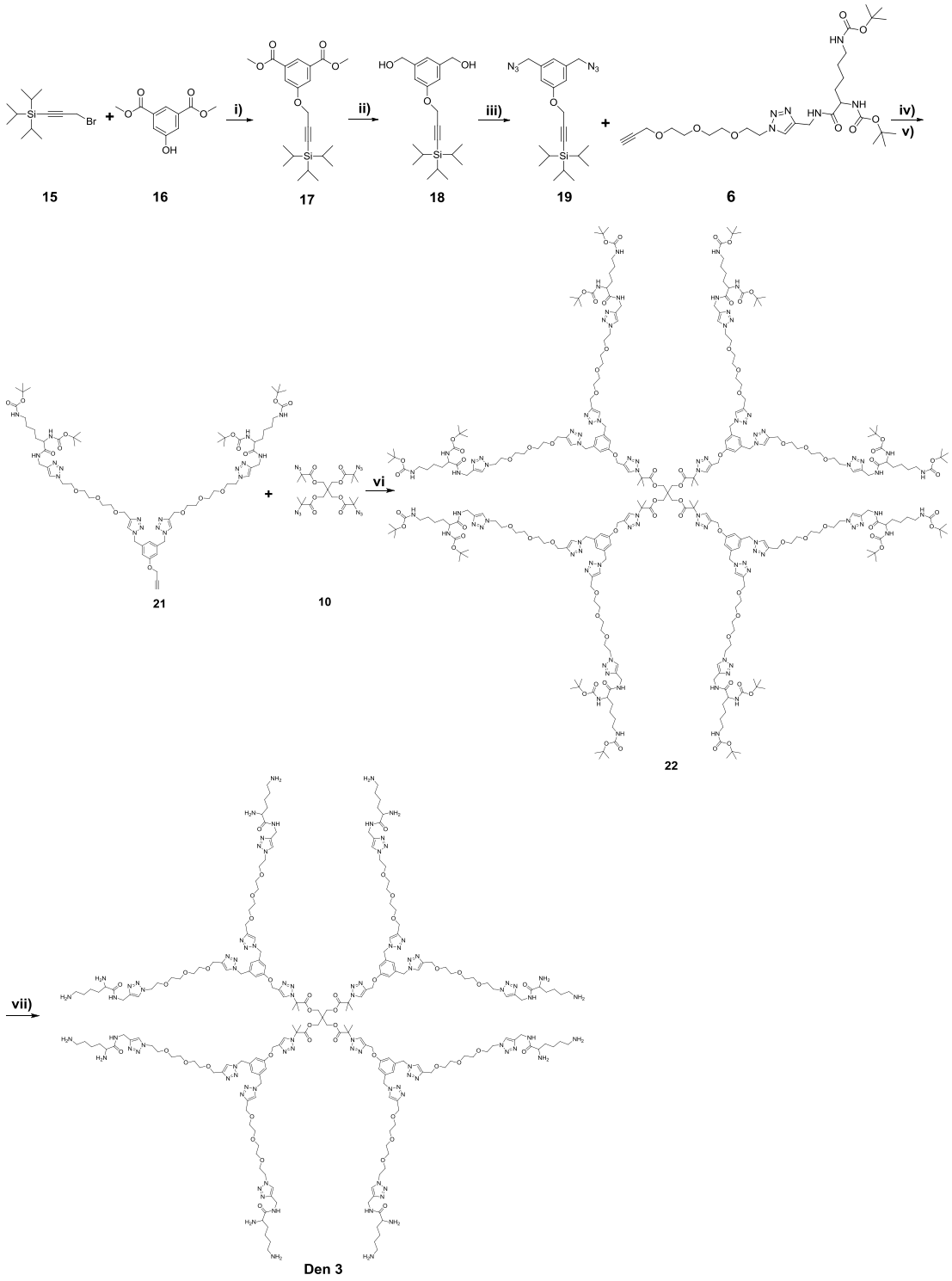

i): 18-C-6, K_2CO_3, Acetone, reflux, 48 h. ii): $LiAlH_4$, THF, 0 ^oC-R.T., 16 h, iii): DPPA, DBU, toluene, 0 ^oC-R.T., dark.(iv) CuBr, PMDETA, Toluene, DMSO, 25 ^oC, 30 min; (v) TBAF, THF, argon, 25 ^oC; (vi) CuBr, PMDETA, Toluene, DMSO 25 ^oC, 120 min; (vii) TFA, DCM, R.T., 6h.

Synthesis of alk-EG-(Lysine-Boc)$_2$ conjugate, 21.

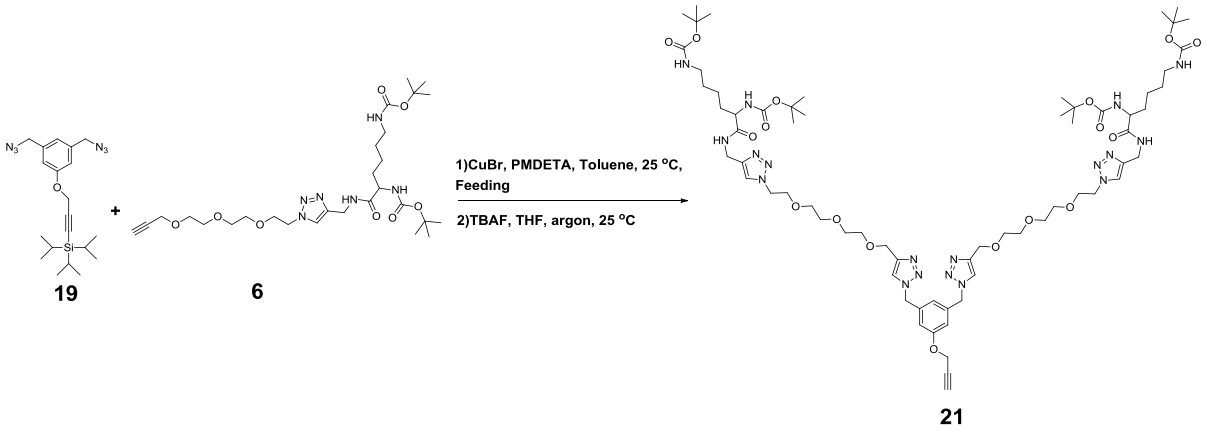

The synthetic details of **19** and its precursors **15** to **18** see **Chapter 3**

A mixture of **19** (12.2 mg, 3.065 x 10^{-5} mol), PMDETA (5.30 mg, 3.065 x 10^{-5} mol), and toluene (1 mL) was purged with argon for 15 min to remove oxygen. To the deoxygenated mixture above, CuBr (4.51 mg, 3.065 x 10^{-5} mol) was added under positive argon flow. Meanwhile, a solution of **6** (0.046 g, 7.718 x 10^{-5} mol), toluene (2 mL) was degassed by argon for 15 min. The degassed solution of **6** was added via syringe pump, at a flow rate of 0.004 mL/min, and after feeding the reaction was allowed to react for 2 h. The copper salts were removed by passage through activated basic alumina. The residue was concentrated by rotary evaporation and dried in high vacuum for 24 h, followed by adding TBAF (0.125 mL, 1M in THF) and 0.2 mL THF. The reaction was kept stirring for 24 h under protection of argon. The product was concentrated by rotary evaporation and purified by column chromatography using DCM/MeOH/petroleum spirit (10/6/2, v/v/v, R_f=0.24) as the eluent and the product, **21**, was obtained as a colorless oil (17.6 mg, 49.0 %).

^{1}H NMR ($CDCl_3$, 298K, 500 MHz): δ 7.72 (s, 1H, -CH_2NC***H***C-, triazole ring proton), 7.59 (s, 1H, -NC***H***C-, triazole ring proton) 7.30 (bd, 1H, -CCH_2N***H***CO-), 6.85 (s, 1H; aromatic proton), 6.80 (s, 2H; aromatic proton), 5.46 (s, 2H, -CC***H***$_2$N-), 5.33 (bd, 1H, -CHN***H***C(O)O-), 4.73 (bd, 1H, -CH_2N***H***C(O)O-), 4.59-4.57 (m, 4H, CHC***H***$_2$NO-, -CC***H***$_2$O-) 4.60-4.45 (m, 4H, -CH_2C***H***$_2$N-, -CC***H***$_2$NH-), 4.08 (s, 1H, -C(O)C***H***(CH_2)NH-), 3.81 (t, 2H, *J*=4.90 Hz, -COC***H***$_2$$CH_2$N-), 3.81-3.44 (m, 8H, -C*H*$_2$- units on EG backbone), 3.04 (t, 2H, *J*=6.6 Hz, -CH_2C***H***$_2$NH-), 2.57 (t, 1H, *J*=2.3 Hz, C***H***CCH_2-), 1.80-1.37 (m, 24H, C***H***$_2$-Lys and C***H***$_3$-Boc). ^{13}C NMR ($CDCl_3$, 298K, 500 MHz): 22.69, 28.41, 29.65, 29.76, 32.38, 34.96, 40.07, 50.32, 53.65, 54.52, 56.03, 64.53, 69.42, 69.84, 70.47, 70.58, 76.80, 77.98, 79.16, 79.95, 114.87, 120.63, 123.14, 123.50, 137.33, .144.53, 145.46, 155.86, 156.32, 158.45, 172.54.

Synthesis of 4-arm star-like EG-(Lysine-Boc)$_2$ conjugate, 22.

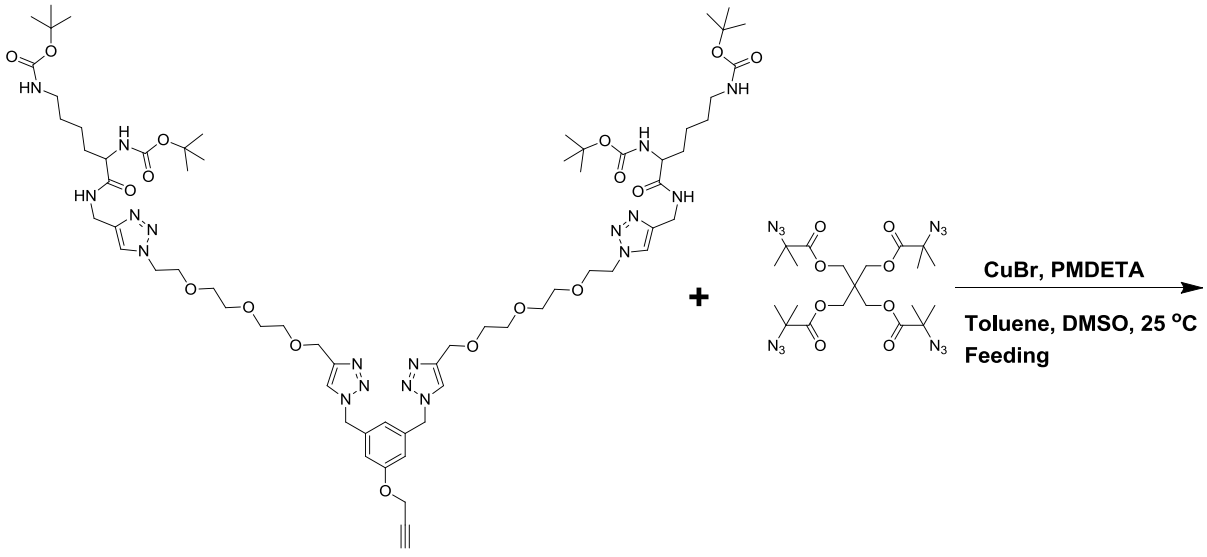

21 **10**

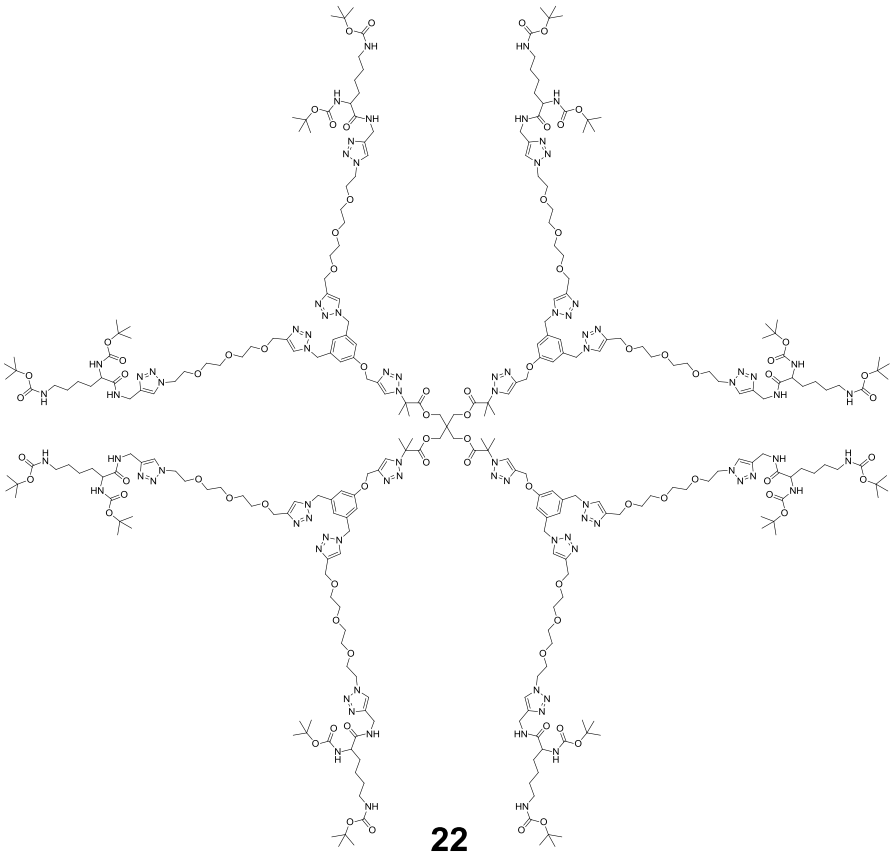

22

A solution of **21** (13.6 mg, 9.482 x 10^{-6} mol) in toluene (2 mL) and DMSO (0.5 mL) was purged with argon for 15 min to remove oxygen. Meanwhile, a mixture of **10** (1.1 mg, 1.896 x 10^{-6} mol), PMDETA (1.64 mg, 9.482 x 10^{-6} mol), toluene (1.0 mL) was degassed by argon for 15 min, to the deoxygenated mixture above, CuBr (1.36 mg, 9.482 x 10^{-6} mol) was added

under positive argon flow. The degassed solution of **21** was added via syringe pump, at a flow rate of 0.008 mL/min, and after feeding the reaction was allowed to react for 2 h. The copper salts were removed by passage through activated basic alumina. The solvent was removed under reduced pressure. The crude product was purified using a Varian Pro-Star preparative SEC system equipped with a manual injector, differential refractive index detector, and single wave-length ultra-violet visible detector. Flow rate was maintained 10 mL min^{-1} and HPLC grade THF was used as the eluent. Separations were achieved using a PL gel 10 mm 1x103 Å, 300 mm x 25 mm preparative SEC column held at 25 ^{o}C. After injection, the expected fraction was collected manually with the yield as 4.32 mg, (yielding%=29.9 %).

SEC: (M_n=3870, M_p=3930, PDI=1.025)

MALDI-ToF MS: [**22**+Na^+]=6344.96 (Cal.=6345.76)

Synthesis of 4-arm star-like EG-(Lysine)$_2$ conjugate, Den 3.

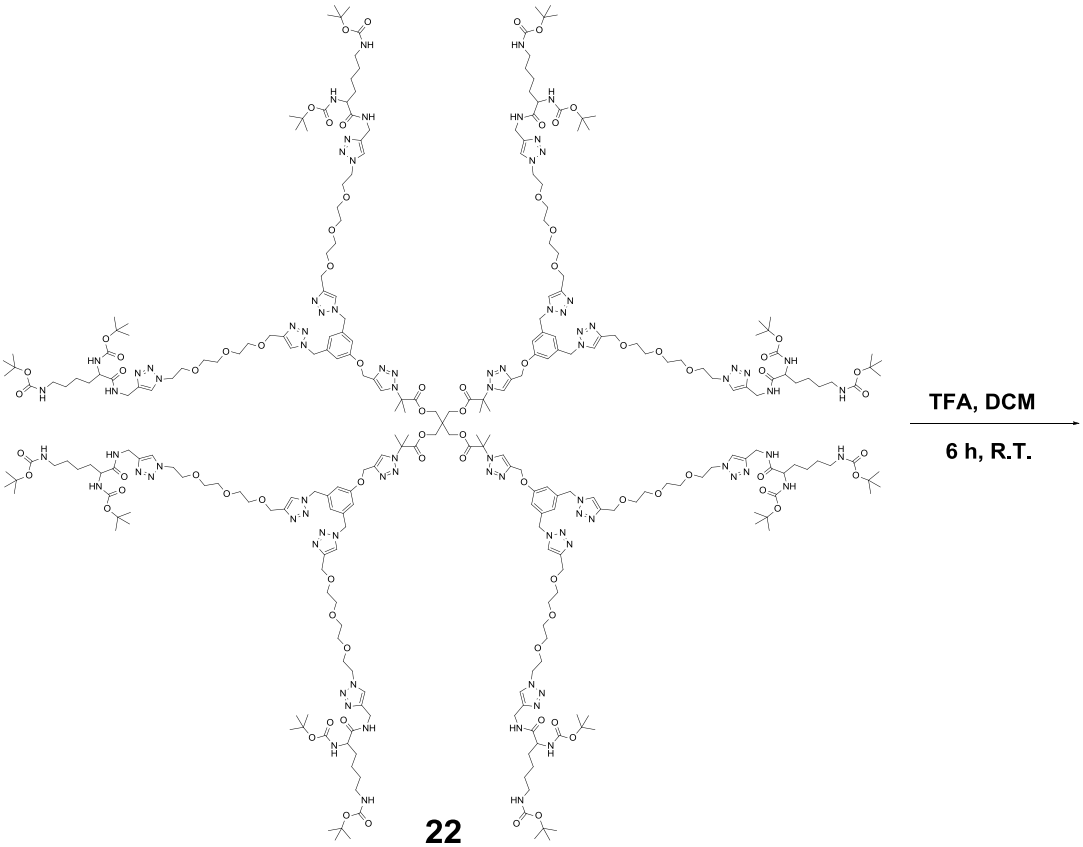

22

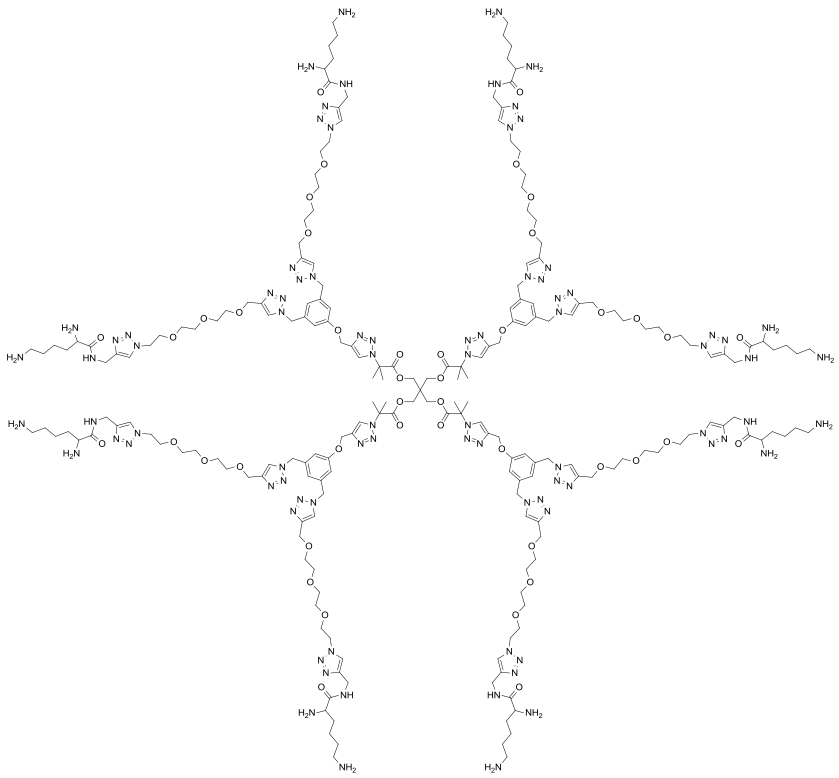

Den 3

22 (0.0056 g) was dissolved in 2 mL mixture of TFA and DCM (1:1, v:v). And the solution was kept stirring for 6 h at room temperature The solvent was remove by reduced pressure, and dried in high vacuum for 24 h, grey yellow oil **Den 3** was produced with near quantitative conversion.

5.2.2.4 Synthesis of dendrimer (4)

Scheme 5.6 Synthesis of EG-MKF dendrimer 4 (**Den 4**)

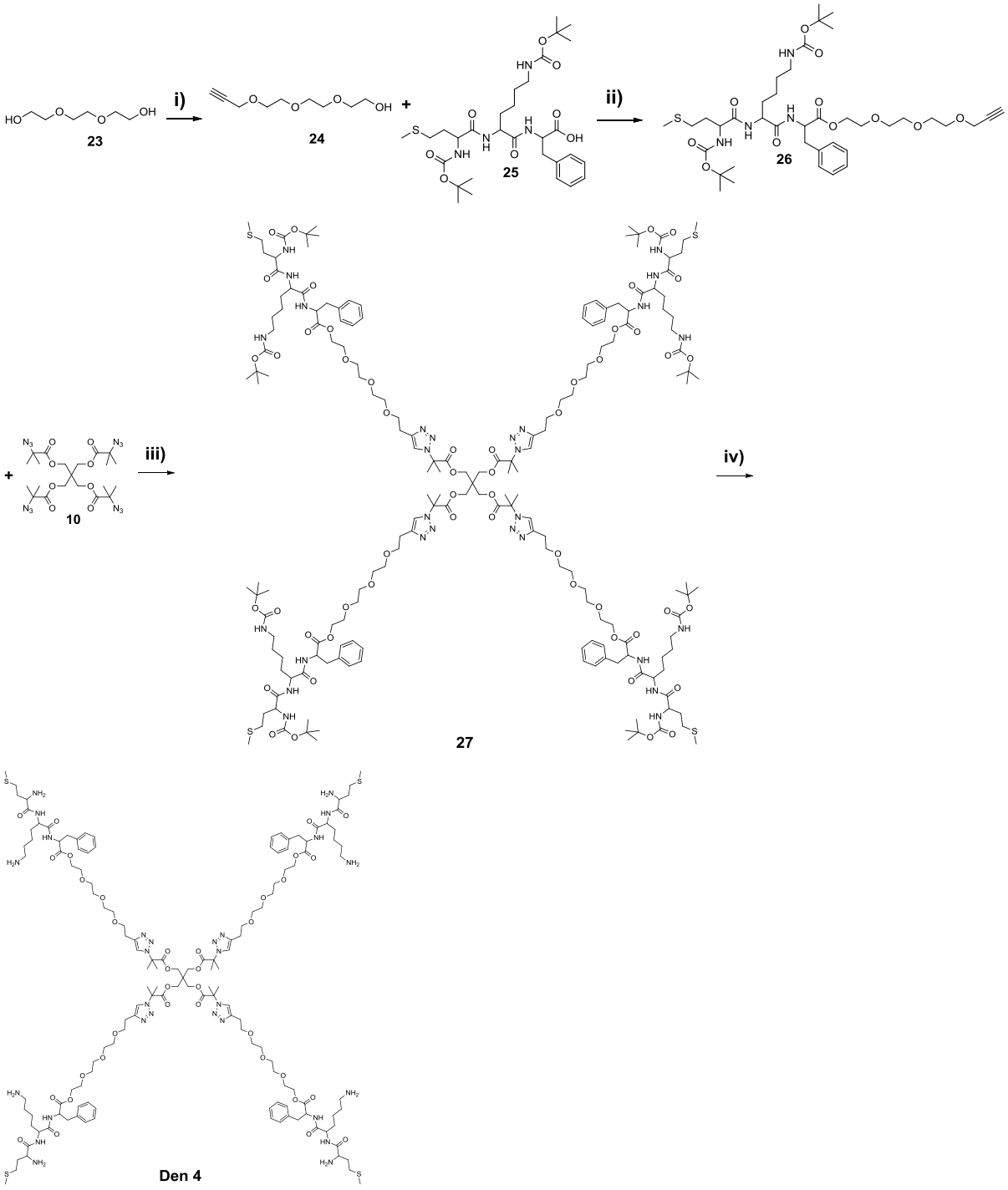

i) THF, NaH, propargyl bromide, -78 ^{o}C, 16 h; ii) DCC, DMAP, DCM, 0^{o}C-R.T.; iii) CuBr, PMDETA, Toluene, 25 ^{o}C, 120 min; iv) TFA, DCM, R.T., 6h.

Synthesis of 2-(2-(2-(prop-2-yn-1-yloxy)ethoxy)ethoxy)ethanol, 24.

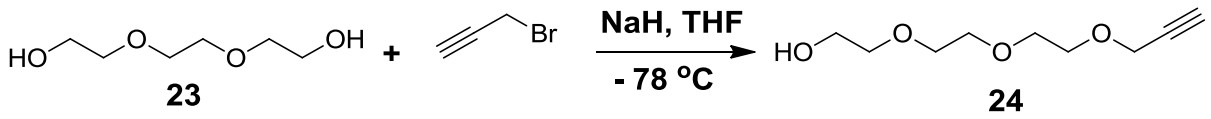

Triethylene glycol (**23**, 15.0 g, 0.1 mol) was dissolved in 10 mL dry THF in a 25 mL two-neck round bottom flask, the flask was connected to the argon line and the solution was cooled to 0^{o}C in an ice-bath. NaH (3 g, 7.50 x 10^{-2} mol) (60 % in mineral oil) was added proportionally in the above solution in 30 min. The reaction was stirred for 1 h and there was no bubbling if the argon was stopped. The reaction vessel was then cooled down to -78 ^{o}C in dry ice/acetone mixture. Propargyl bromide (9.83 g, 6.67 x 10^{-2} mol) (80 wt % in toluene) was added to the solution dropwise in 1 h. The reaction was then kept stirring overnight and warmed to RT. The reaction mixture was filtered to remove the salt and concentrated to remove all the solvent and low b.p impurities at RT. The crude brown liquid product was purified by column chromatography with DCM-MeOH (4:1, v/v, R_f=0.49) as eluent. 6.7 g viscous oil **24** was obtained with the yield as 43 %.

^{1}H NMR ($CDCl_3$, 298K, 500 MHz): δ 4.17 (d, 2H, *J*=2.35 Hz, CHCC***H***$_2$O-), 3.71-3.63 (m, 12H, -C***H***$_2$-), 3.58 (t, 2H, *J*=4.55 Hz, -C***H***$_2$CH$_2$OH), 2.44 (bd, 1H, O***H***CH$_2$-), 2.40 (bd, 1H, *J*=4.55 Hz, -OCH$_2$CC***H***); ^{13}C NMR ($CDCl_3$, 298K, 500 MHz): 58.51, 61.85, 69.17, 70.45, 70.48, 72.73, 72.56, 74.70, 79.67.

NMR analysis of OH-Met-Lys-Phe-Boc, 25.

Peptide **25** was purchased from Auspep Pty Ltd and fully characterized by NMR. The data shown as following:

^{1}H NMR ($CDCl_3$, 298K, 500 MHz): 7.30 (bd, 1H, -CH(NH)C(O)N***H***CH(CH$_2$)-), δ 7.28-7.20 (m, 5H, aromatic proton), 6.90-7.03 (dd, 1H, *J*=7.65 Hz, *J*=7.35 Hz -C(O)N***H***CH(CH$_2$)-), 5.52 (bd, 1H, -CHN***H***C(O)O-), 4.91 (bd, 1H, -CH$_2$N***H***C(O)O-), 4.75 (m, 1H, -NHC***H***C(O)CH$_2$-), 4.41 (m, 1H, -NHC***H***C(O)CH$_2$-), 4.24 (m, SCH$_2$CH$_2$C***H***C(O)NH-), 3.19-2.98 (m, 4H, -OC(O)NHC***H***$_2$CH$_2$-, -CHC***H***$_2$C-), 2.45 (m, -SC***H***$_2$CH$_2$-), 2.02 (d, *J*=2.35 Hz, C***H***$_3$S-) 1.98-1.82 (mm, -SCH$_2$C***H***$_2$CH-), 1.70-1.20 (m, 24H, C***H***$_2$-Lys and C***H***$_3$-Boc); ^{13}C NMR ($CDCl_3$, 298K, 500 MHz): 15.44, 22.38, 28.44, 28.55, 30.23, 31.95, 32.18, 33.43,37.36, 40.13, 52.79, 53.09, 53.37, 79.53, 80.38, 127.14, 128.67, 129.50, 136.24, 155.83, 157.74, 171.70, 172.05, 173.76.

Synthesis of alk-EG-Met-Lys-Phe-Boc, 26.

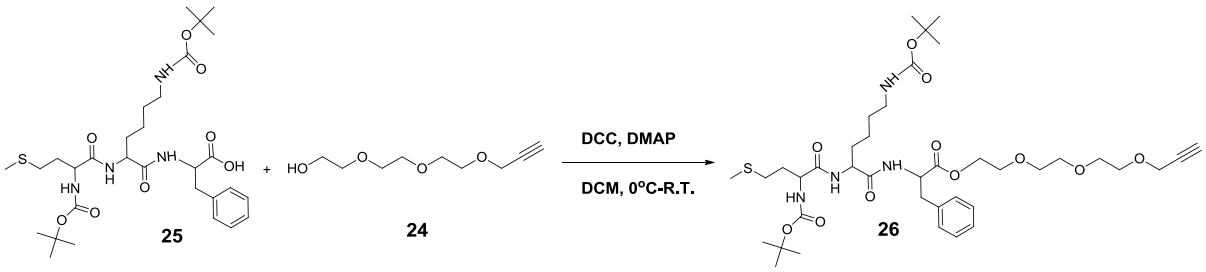

To a 100 mL flask, Boc-Met-Lys(Boc)-Phe-OH (Boc-MKF-OH) **25** (0.5 g, 8.01 x 10^{-4} mol), **24** (0.55 g, 2.80 x 10^{-3} mol), and DMAP (0.015 g, 2.59 x 10^{-3} mol) were dissolved in 20 mL dry DCM and cooled to 0 ^{o}C in an ice-bath. A mixture of DCC (0.32 g, 1.58 x 10^{-3} mol) and 10 mL DCM was added dropwise into the solution over 30 min. The mixture was allowed to react for 48 h at room temperature. The solid content was removed by filtration and the filtrate was washed by saturated brine (2 x 50 mL). The organic layer was collected, dried over anhydrous $MgSO_4$, the solvent removed *in vacuo* followed by column chromatography using ethyl acetate/petroleum spirit (5/1, v/v, R_f=0.48) as the eluent. Product **26** was obtained as a white powder (0.31 g, yield%=46.0 %).

^{1}H NMR ($CDCl_3$, 298K, 500 MHz): δ 7.28-7.20 (m, 5H, aromatic proton), 6.74 (bd, 1H, -CH(NH)C(O)N***H***CH(CH_2)-), 6.67-6.53 (dd, 1H, *J*=7.65 Hz, *J*=7.35 Hz -C(O)N***H***CH(CH_2)-), 5.25 (bd, 1H, -CHN***H***C(O)O-), 4.82 (m, 1H, -NHC***H***C(O)CH_2-), 4.71 (bd, 1H, -CH_2N***H***C(O)O-), 4.34 (m, 1H, -NHC***H***C(O)CH_2-), 4.30-4.16 (m, 5H, -SCH_2CH_2C***H***C(O)NH-, -OC***H***$_2$CCH, -C(O)OC***H***$_2$$CH_2$-), 3.66-3.62 (m, 10H, -C*H*$_2$- units on EG backbone), 3.19-3.01 (m, 4H, -OC(O)NHC***H***$_2$$CH_2$-, -CHC***H***$_2$C-), 2.50 (m, -SC***H***$_2$$CH_2$-), 2.42 (t, -$CH_2$C***H***), 2.06 (d, *J*=2.35 Hz, C***H***$_3$S-) 2.03-1.88 (mm, -SCH_2C***H***$_2$CH-), 2.0-1.2 (m, 24H, C***H***$_2$-Lys and C***H***$_3$-Boc); ^{13}C NMR ($CDCl_3$, 298K, 500 MHz): 15.40, 22.41, 28.42, 28.56, 31.75, 31.93, 34.30, 37.80, 40.13, 52.79, 52.98, 53.37, 58.47, 64.59, 68.87, 69.17, 70.50, 70.65, 70.68, 74.78, 79.21, 79.67, 80.40, 127.25, 128.72, 129.46, 135.24, 155.75, 156.14, 170.94, 171.27, 171.32.

Synthesis of 4-arm star-like EG-MKF-Boc conjugate, 27.

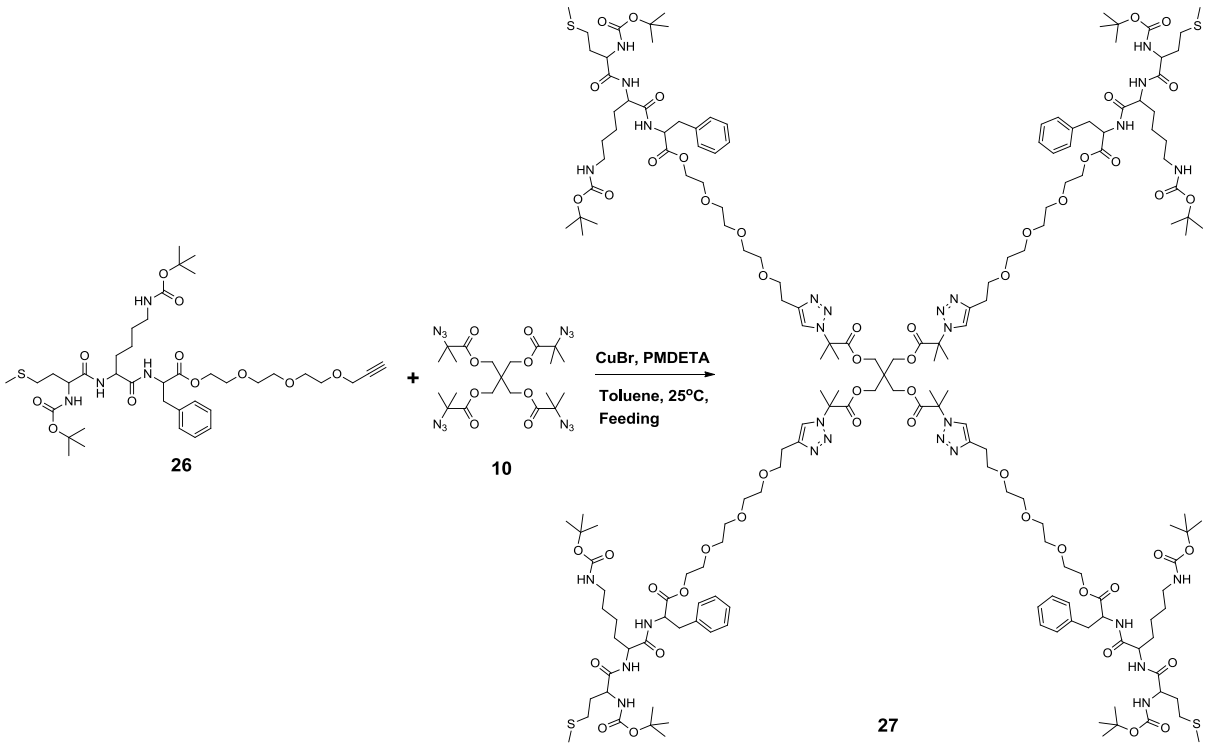

A solution of **26** (0.184 g, 2.327 x 10^{-4} mol) in toluene (20 mL) was purged with argon for 60 min to remove oxygen. Meanwhile, a mixture of **10** (0.027 g, 4.655 x 10^{-5} mol), PMDETA (5.3 mg, 3.007 x 10^{-5} mol), toluene (20 mL) was degassed by argon for 60 min, to the deoxygenated mixture above, CuBr (4.3 mg, 3.007 x 10^{-5} mol) was added under positive argon flow. Then, the solution of **26** was added via syringe pump, at a flow rate of 0.06 mL/min, and after feeding the reaction was allowed to react for 2 h. The copper salts were removed by passage through activated basic alumina. The solvent was removed under reduced pressure. The crude product was purified using a Varian Pro-Star preparative SEC system equipped with a manual injector, differential refractive index detector, and single wave-length ultra-violet visible detector. Flow rate was maintained 10 mL min^{-1} and HPLC grade THF was used as the eluent. Separations were achieved using a PL gel 10 mm 1x103 Å, 300 mm x 25 mm preparative SEC column held at 25 ^{o}C. After injection, the expected fraction was collected manually with the yield as 39 mg. (yielding%=13.8 %).

SEC: (M_n=3380, M_p=3475, PDI=1.023)

MALDI-ToF MS: [**27**+Na^+]=3782.59 (Cal.=3782.89); [**27**+Na^++4O]=3846.06 (Cal.= 3846.87); [**27**+K^++4O]=3862.71 (Cal.= 3862.06)

Synthesis of 4-arm star-like EG-MKF conjugate ,Den 4.

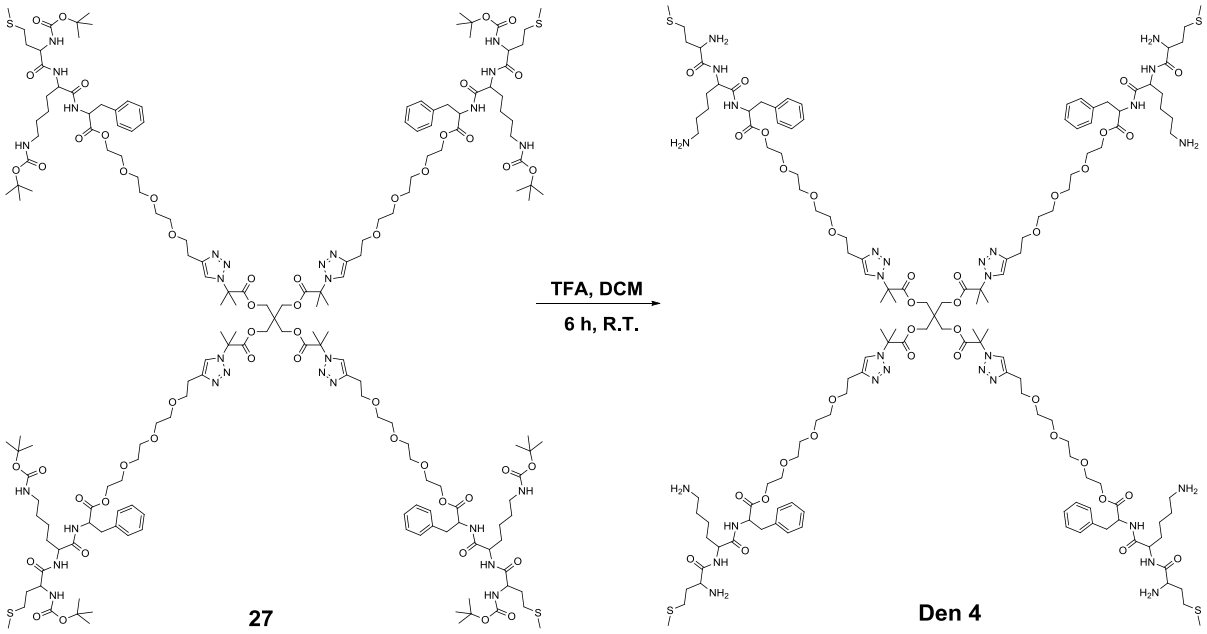

27 (0.015 g) was dissolved in 3 mL mixture of TFA and DCM (1:1, v:v). And the solution was kept stirring for 6 h at room temperature The solvent was remove by reduced pressure, and dried in high vacuum for 24 h, grey yellow oil **Den 4** was produced with near quantitative conversion.

5.2.3 Analytical Methodologies

Size Exclusion Chromatography (RI-SEC)

All polymer samples were dried prior to analysis in a vacuum oven for 2 days at 25 ^{o}C. The dried polymer was dissolved in tetrahydrofuran (THF) to a concentration of 1 mg mL^{-1} and then filtered through a 0.45 μm PTFE syringe filter. The molecular weight distributions of the polymers was determined through separation on a Waters 2695 separations module, fitted with a Waters 410 refractive index (RI) detector maintained at 35 ^{o}C, a Waters 996 photodiode array detector, and two Ultrastyragel linear columns (7.8 x 300 mm) arranged in series. These columns were maintained at 40 ^{o}C for all analyses and are capable of separating polymers in the molecular weight range of 500 to 4 million g mol^{-1}with high resolution. All samples were eluted at a flow rate of 1.0 mL min^{-1}. Calibration was performed using narrow molecular weight PSTY standards ($PDI_{RI} \leq 1.1$) ranging from 500 to 2 million g mol^{-1}. Data acquisition was performed using Empower software, and molecular weights were calculated relative to polystyrene standards.

Nuclear Magnetic Resonance (NMR)

All NMR spectra were recorded on either a Bruker DRX 400 or 500 MHz spectrometer using an external lock ($CDCl_3$), and all spectra were referenced to the residual nondeuterated solvent ($CHCl_3$).

Matrix-Assisted Laser Desorption Ionization-Time-of-Flight (MALDI-ToF) Mass Spectrometry

MALDI-ToF MS spectra were obtained using a Bruker MALDI-ToF autoflex III smart beam equipped with a nitrogen laser (337 nm, 200 Hz maximum firing rate) with a mass range of 600-400 000 Da. Spectra were recorded in either reflectron mode (1500-4500 Da) or linear mode (4000-20000 Da). Trans- 2-[3-(4-tert- butylphenyl)-2-methyl-propenylidene] malononitrile (DCTB; 20 mg mL^{-1}in THF) was used as the matrix and Na(CF_3COO) (1 mg mL^{-1} in THF) as the cation source for all the polystyrene samples. The 20 μL sample solution (0.5 mg mL^{-1} in THF), 20 μL DCTB solution and 2 μL Na(CF_3COO) solution were mixed in

an eppendorf tube, vortexed and centrifuged. A 1 μL of solution was placed on the target plate spot, evaporated the solvent at ambient condition and the measurement taken.

5.3 Results and discussion

5.3.1 Synthesis of dendrimer 1 (Den 1)

The synthesis of azide terminal ethylene glycol (**2**, EG-N_3) was accomplished by the azidation of commercial available 2-(2-(2-chloroethoxy)ethoxy)ethanol (**1**) using NaN_3 (Scheme 5.2). The detailed NMR analyses of **1** was given in the appendix (Figure A5.1 to A5.4). The resulting EG-N_3 was then coupled with alkyne-Lysine-Boc *via* a CuAAC click reaction gave hydroxyl functional EG-Lysine-Boc conjugate **5** (Scheme 5.2) with a 79% yield. In the ^{1}H NMR spectrum of 5, the complete disappearance of the alkyne proton (-C≡C*H*) at 2.20 ppm (Figure A5.5) and the emergence of a proton in new triazole ring at 7.85 ppm (Figure A5.8) suggested the quantitative conversion of the reactants and a high efficiency CuAAC reaction. The -OH group on **5** was converted *via* an etherification reaction to the alkyne group to give **6** with a 27.8% yield. After etherification, the typical resonance of signals at 2.4 ppm and 4.1 ppm ascribed to alkyne proton (**s**) and methylene protons (**r**) verified the successful incorporation of propargyl ether moiety (Figure 5.1). The more detail NMR analyses of compound **6** is given in the appendix (Figure A5.11 to A5.12).

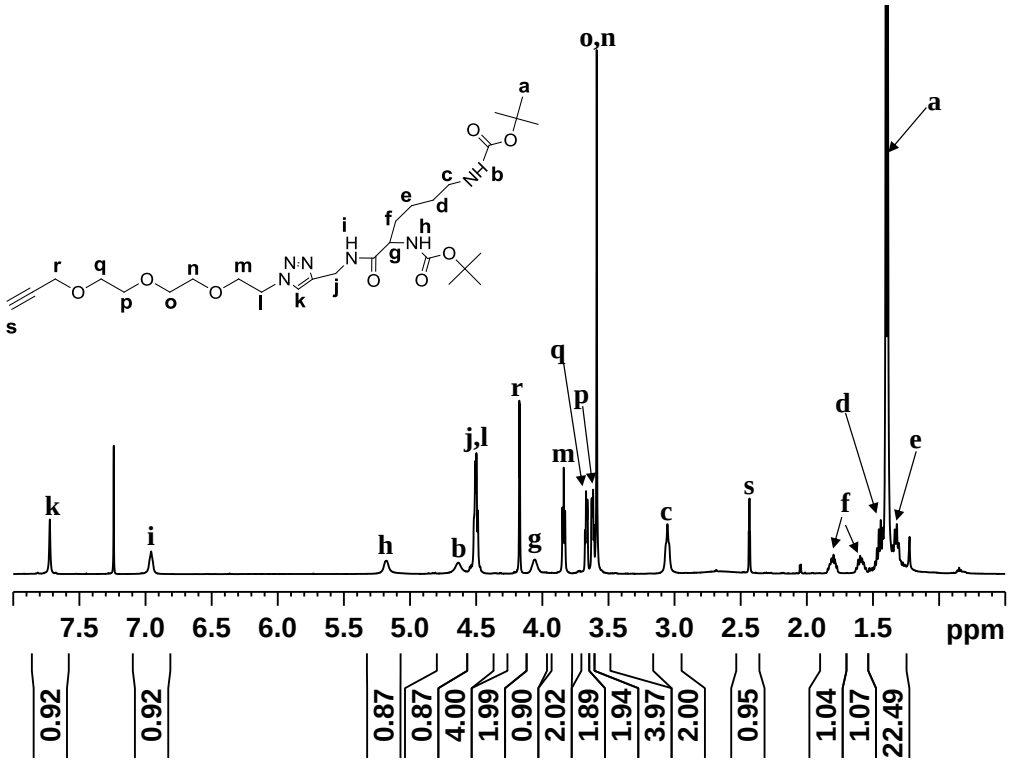

Figure 5.1 ^{1}H NMR spectrum (500 MHz) of **6**, recorded in $CDCl_3$ at 298K.

The synthesis of the tetraazide core **10** was generated from the bromination of pentaerythritol followed by the azidation using NaN_3 (Scheme 5.3). The structure of **10** was confirmed by ^{1}H NMR and ^{13}C NMR given in Figure A5.13 to Figure A5.15. The CuAAC reaction of **6** and **10** (tetraazide core) produced **11** with a purity of 60.9% as determined from the log-normal distribution (LND) simulations[38, 39] of the size exclusion chromatography (SEC) trace (Figure 5.2A). There was a considerable amount of 3-arm (25.4%), 2-arm (9.1%) and a small amount of 1-arm and unreacted core **10**. Upon purification of crude **11** by preparative SEC (Figure 5.1A), 95% of the product consisted of **11** and the other 5% consisted of 3-arm. This was further supported from the MALDI-ToF data, in which the products before purification were in agreement with the LND fit (Figure 5.2B) and after purification (Figure 5.2C) the product consisted of predominantly **11** (i.e. **11** + Na^{+}) showed one mass peak at 2986.84 and a small peak at 2389.08 (corresponding to the 3-arm product). The structure of **11** was further confirmed by the ^{1}H NMR spectrum in Figure 5.3. The distinct shift of proton (**r**, Figure 5.2) adjacent to alkyne from ~4.1 to 4.6 ppm and the new board peak (**s,** Figure 5.2) at 7.9 ppm suggested conjugation of **6** onto the core **11** *via* the triazole ring. The high purity of resulting dendrimer **11** could be further confirmed from integration of peaks corresponding to the protons of core, EG backbone and lysine moiety. The ratio of integration for protons **u**, **r** and **c** in each generational layer was 8:7.95:8 which was close to theoretical (8:8:8). The Boc-protecting groups on **11** were then removed using TFA for 6 h at room temperature to give **Den 1**.

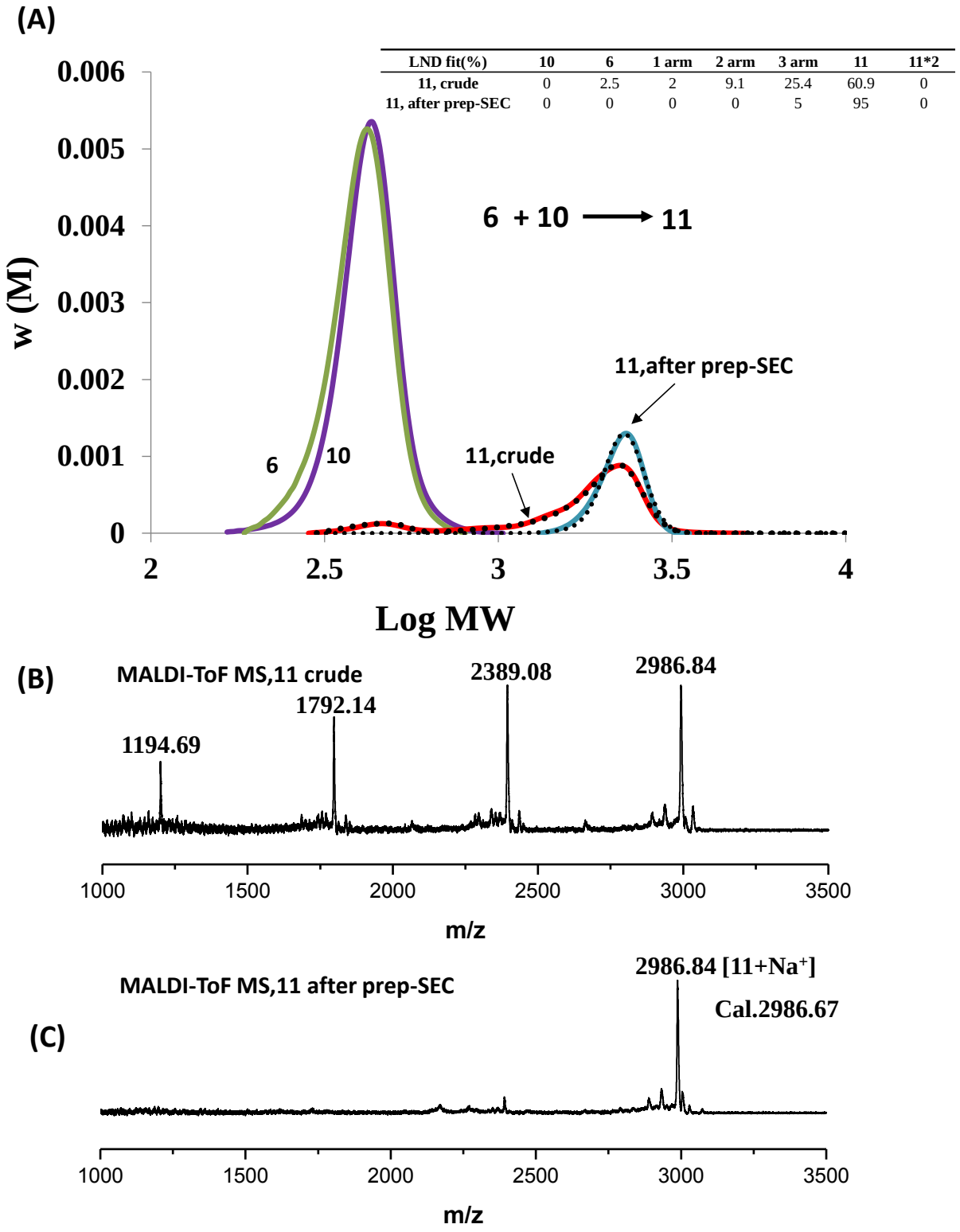

Figure 5.2 (A) SEC traces of **6**, **10**, **11** (crude and after prep) in THF and LND simulation of **11** (black dots) . (B) MALDI-ToF MS of **11** crude, and (C) MALDI-ToF MS of **11** after prep. The spectrum was recorded in reflection mode using DCTB as the matrix and $NaCF_3COO$ as the cation source.

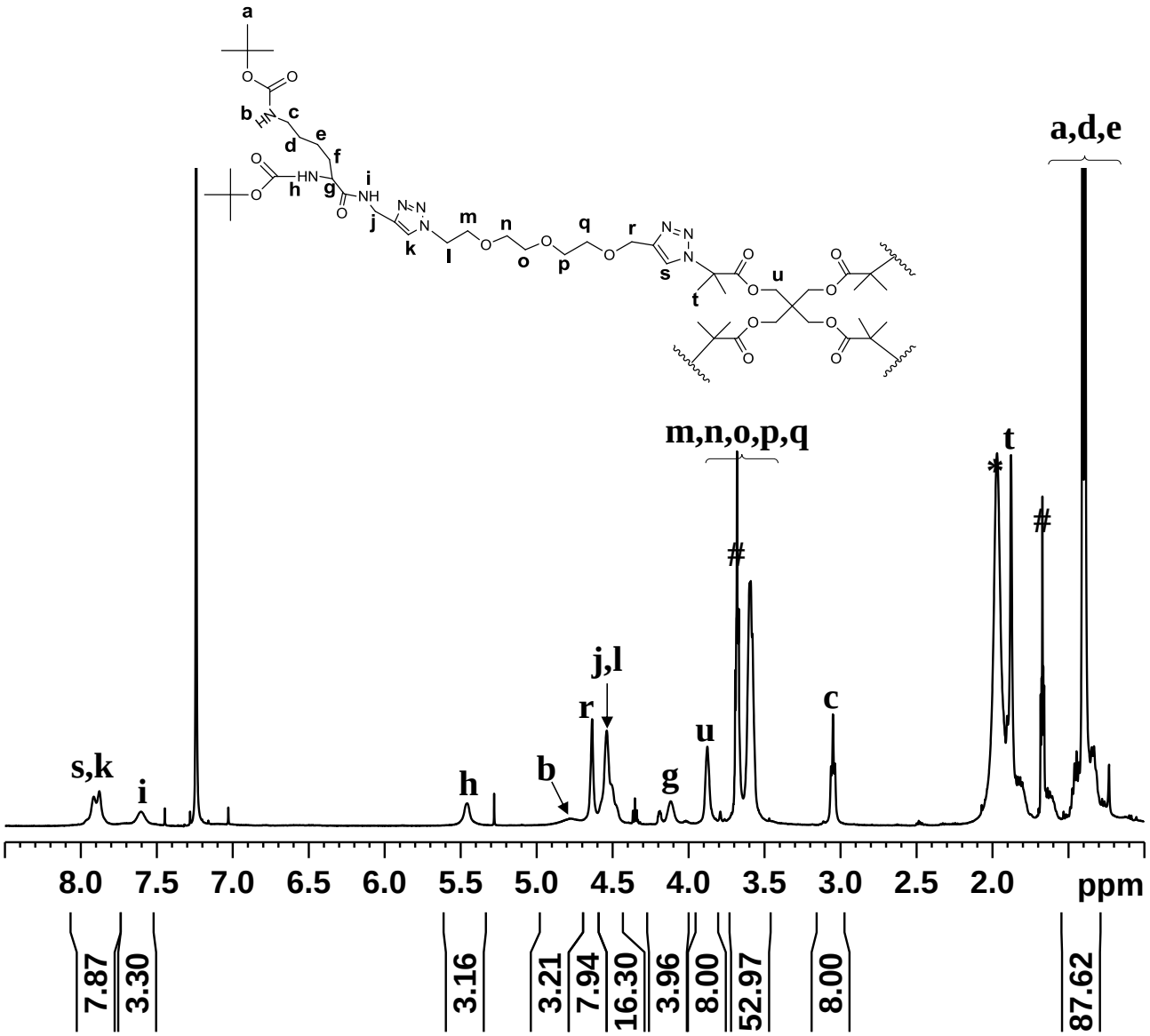

Figure 5.3 ^{1}H NMR spectrum of **11**, recorded in $CDCl_3$ at 298 K, 500 MHz. *=H_2O,#=THF.

5.3.2 Synthesis of dendrimer 2 (Den 2)

Dendrimer **2** (**Den 2**) was designed with a longer spacer (i.e. two EG units per arm) within the second generational layer (Scheme 5.4). Compound **12** was synthesized through the CuAAC coupling of **6** and **2** to produce **12** (two EG units). The integration increased by two times around 3.1ppm (methylene protons onto ethylene glycol units) compared to **5** indicating the attachment of another EG unit (Figure A5.16). The complete disappearance of alkyne proton signal at 2.4 ppm and the appearance of new triazole ring proton peak at 7.9 ppm revealed the full conversion of click reaction (Figure A5.16). ^{13}C NMR and 2D NMR analyses of **12** was given in the appendix (Figure A5.17 and A5.18). The following

etherfication was carried out to introduce the alkyne group onto the chain end of **12** to produce **13,** which was evidenced by the appearance of alkyne proton (**a1**) and methylene (**r**) at ~2.4 and 4.6 ppm, respectively (Figure 5.4).

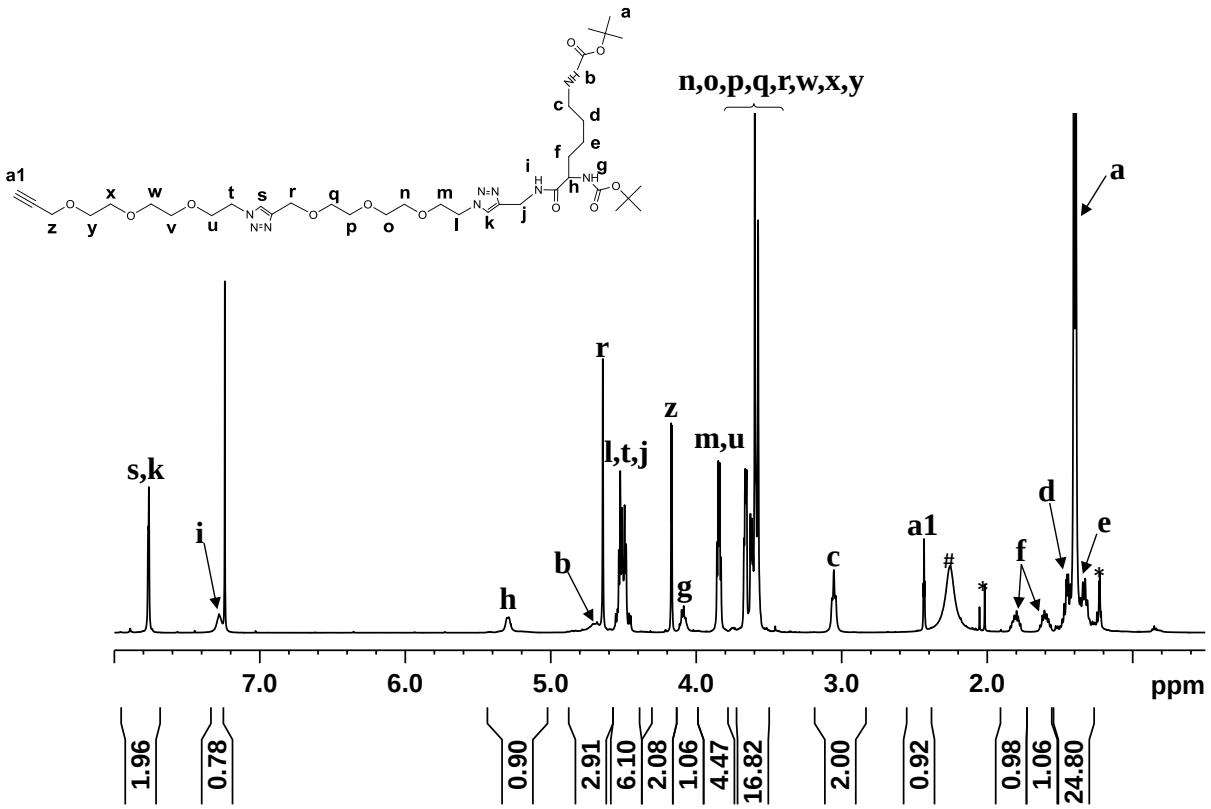

Figure 5.4 ^{1}H NMR spectrum (500 MHz) of **13**, recorded in $CDCl_3$ at 298K, #=H_2O, *=EtOAc.

The CuAAC reaction between **13** and **10** afforded **14** (crude) with a low purity of 35.6 % as determined by the LND fit (Figure 5.5A). The majority of the impurity was due to **13** (45%), which was used in excess to the azide core **10** (6.3% remaining). There was only a small amount of 1, 2 and 3-arm products, suggesting the excess of **13** drove the reaction to the 4-arm product **14**. After preparative SEC, the purity of **14** increased to 97 % with only 3 % of the 3-arm product remaining. The MALDI-ToF data confirmed the LND simulations, demonstrating that after preparative SEC the main product consisted of **14** (where M=**14**+Na^+=3841.16) as shown in Figure 5.5. Again, the integration of the ^{1}H NMR also showed that **14** was of a high purity (Figure 5.6). The ratio of integration for protons **c1**, **m, u** and **c** which were ascribed to the core, EG backbone and lysine moiety, respectively, were found as 16.61:16.58:8 (theoretical: 16:16:8, double the value of **11**). The high efficiency deprotection of Boc-groups on **14** using TFA gave **Den 2** with near quantitative conversion.

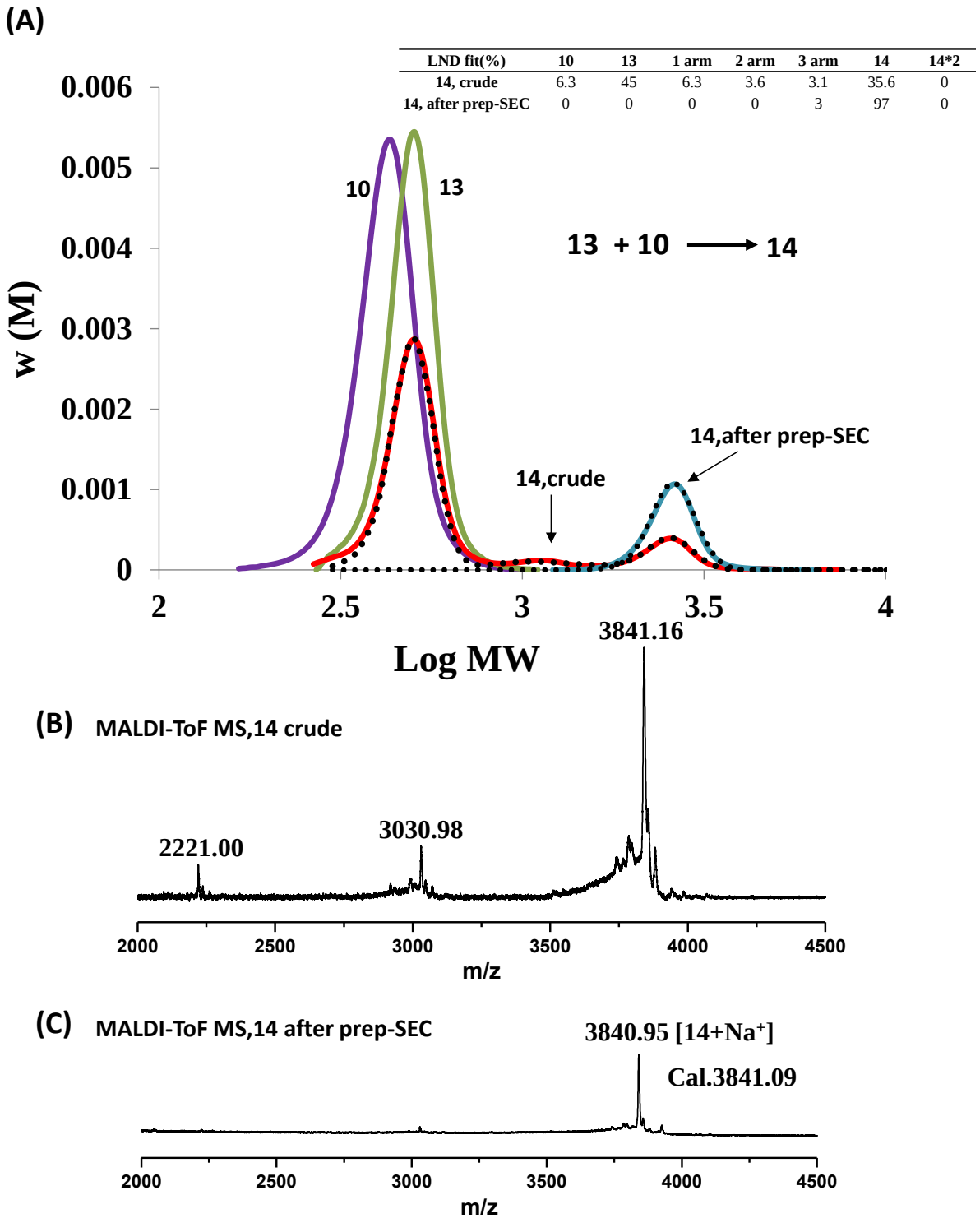

Figure 5.5 (A) SEC traces of **10**, **13**, **14** (crude and after prep) in THF and LND simulation of **14** (black dots), (B) MALDI-ToF MS of **14** crude, (C) MALDI-ToF MS of **14** after prep-SEC. The spectrum was recorded in reflection mode using DCTB as the matrix and $NaCF_3COO$ as the cation source.

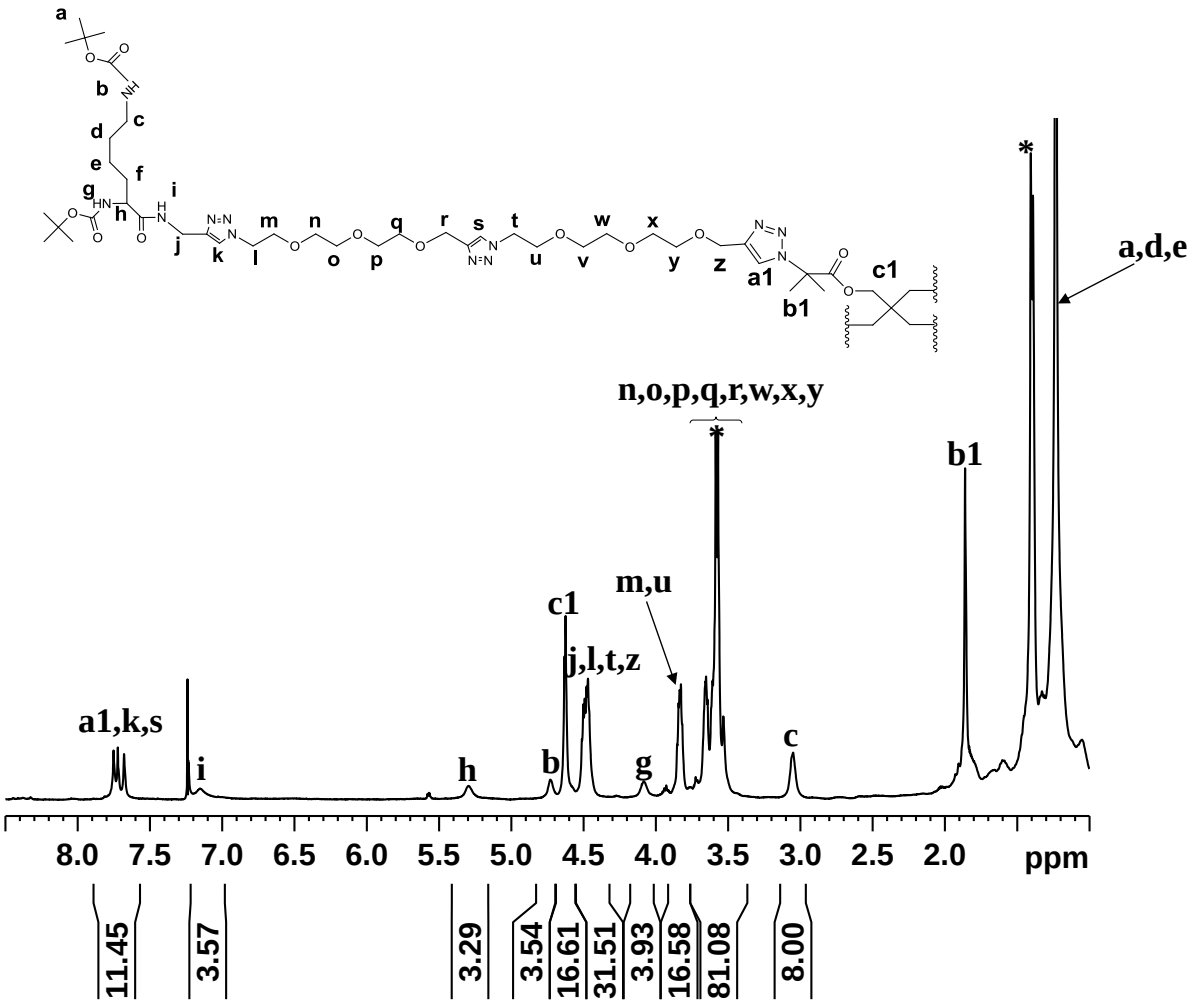

Figure 5.6 ^{1}H NMR spectrum of **14**, recorded in $CDCl_3$ at 298 K, 500 MHz. *THF.

5.2.3Synthesis of dendrimer 3 (Den 3)

Dendrimer **3** (**Den 3**) was designed with twice the number of lysine groups in the outer generational layer (Scheme 5.5). To accomplish this, we elaborated on synthesis an alkyne-protected trifunctional linker **19** (Scheme 5.5, detailed NMR analyses of **19** were given in Chapter 3, Figure 3.2 and appendix Figure A3.9 to A3.15) which afforded the conjugation of double lysine moieties for each arm. The coupling of **6** and **19** followed by the deprotection of the Tips group in TBAF resulted in alk-EG-(Lysine-Boc)$_2$ conjugate **21,** with a purity of 49 %. The conjugation of lysine moieties onto pending azide group onto linker **19** was evidenced by ^{1}H NMR analysis (Figure 5.7). After the click reaction, the resonance signal of protons on the new triazole ring was detected at 7.6 ppm, there was an obvious shift of proton **r** from 4.2 to 4.6 ppm, and a shift of proton **t** from 4.3 to 5.5 ppm collectively verified the attachment of **6** onto **19**. The signal for Tips group at 1.0 ppm and the detection of the alkyne

proton at 2.6 ppm suggested the complete removal of Tips group after hydrolysis by TBAF. ^{13}C NMR and 2D NMR analyses of **21** see appendix Figure A5.21 to A5.22.

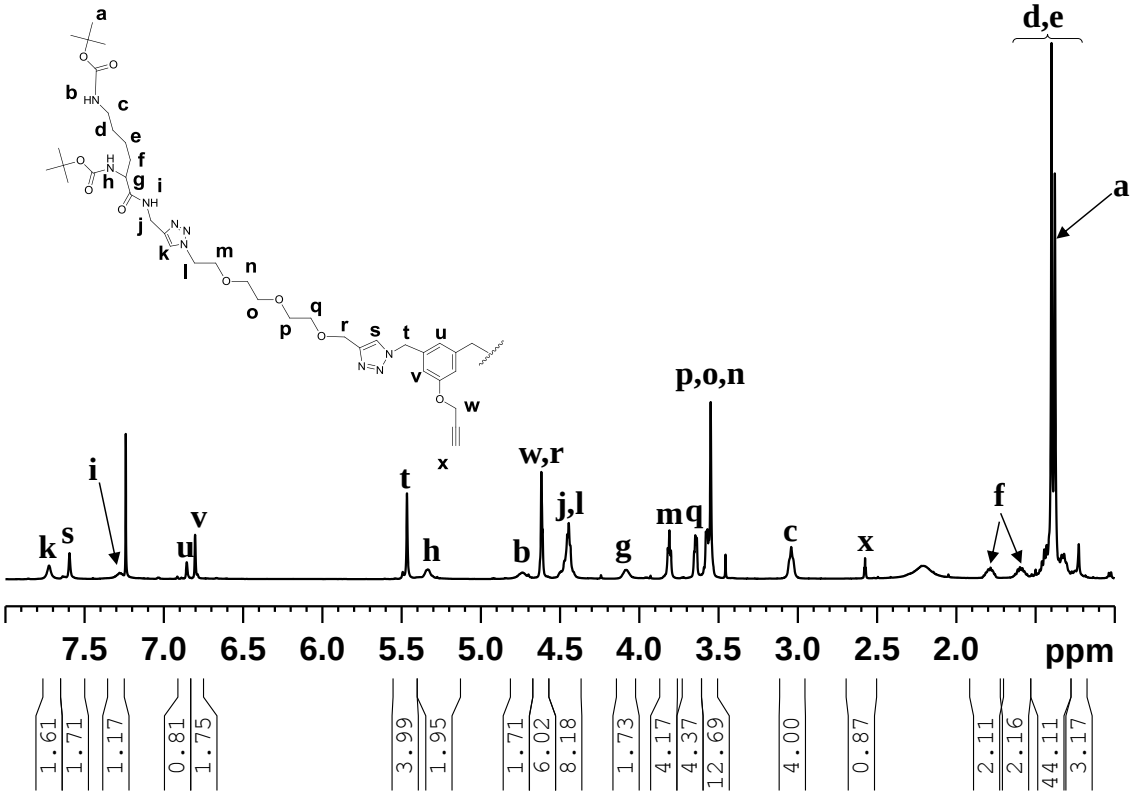

Figure 5.7 ^{1}H NMR spectrum of **21**, recorded in $CDCl_3$ at 298 K, 500 MHz.

Dendrimer **3** was formed through the CuAAC reaction of **10** with excess **21** with a yield of 29.9%. The LND simulation of the SEC traces in Figure 5.5A showed that **22** was formed with a purity of 43%, with impurities arising from the starting compounds **10** and **21**, and the formation of 1, 2 and 3-arm star products. After preparative SEC, the purity increased to 94% with 3% of both 2- and 3-arm star products. This was consistent with the MALDI-ToF data, in which one main mass peak was observed at 6344.96 corresponding to **22** with the Na ion (Figure 5.8C). Once again the ^{1}H NMR also showed that **22** was produced with a high purity (Figure 5.9). The observation of proton **x** of the triazole rings linked to the core demonstrates the CuAAC reaction was conducted successfully. In addition, the ratio of the interaction in each layer verify the purity of resultant dendrimer (e.g., protons **c**:**m**:**w**,**r**:**z**=15.9:16.4:23.84:8 which close to theoretical value, 16:16:24:8, Figure 5.9). The following deprotection of Boc-groups on **22** using TFA gave **Den3** with near quantitative conversion.

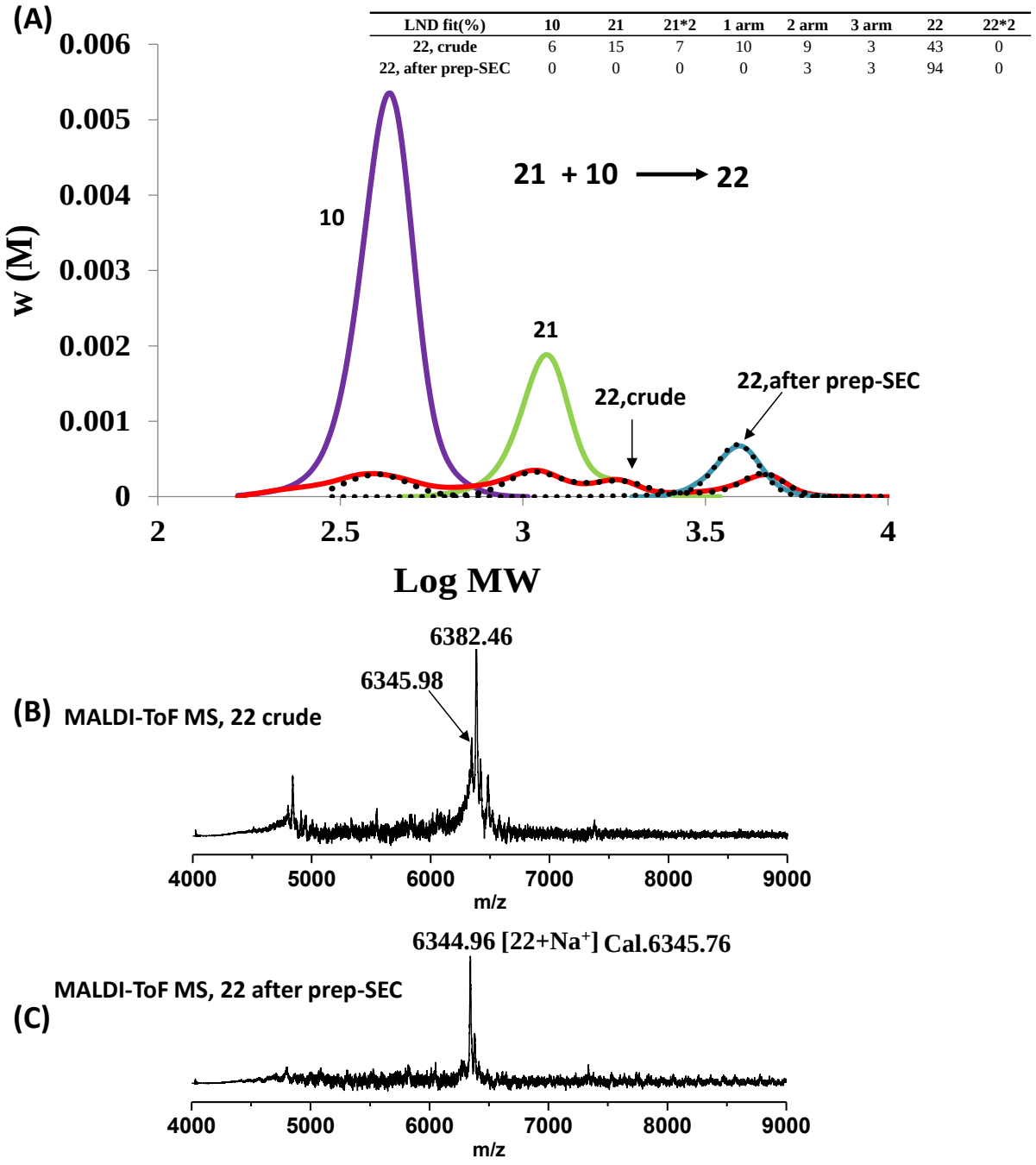

Figure 5.8 (A) SEC traces of **10**, **21**, **22** (crude and after prep) in THF and LND simulation of **22** , PSTY as standard, (B) MALDI-ToF MS of **22** crude, (C) MALDI-ToF MS of **22** after prep-SEC. the spectrum was recorded in linear mode using DCTB as the matrix and $NaCF_3COO$ as the cation source.

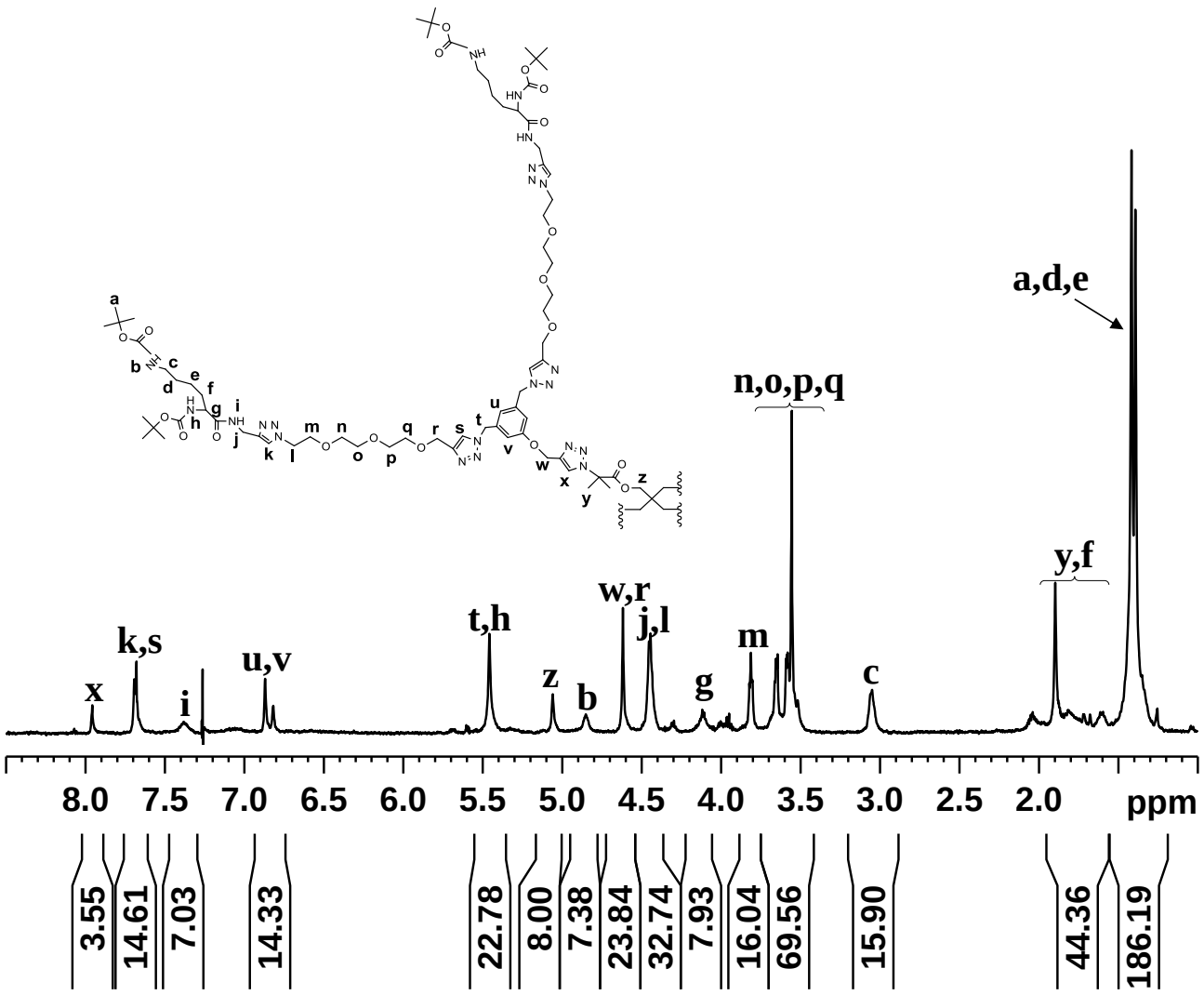

Figure 5.9 ^{1}H 1D DOSY NMR spectrum of **21**, recorded in $CDCl_3$ at 298 K, 500 MHz.

5.3.4 Synthesis of dendrimer 4 (Den 4)

Dendrimer **4** (**Den 4**) was designed so that the peripheral layer consisted of a three amino acid sequence of Met-Lys-Phe (MKF) (Scheme 5.6). The alk-EG-OH **24** was synthesized *via* etherfication between triethylene glycol and propargyl bromide (Scheme 5.6). The appearance of alkyne proton at 2.4 ppm and the methylene protons **b** at 4.2 ppm, suggesting the successful attachment of the alkyne group and the formation of **24** (Figure A5.23 to A5.25). The resulting alk-EG-OH was conjugated with MKF peptide bearing a carboxyl group by esterification (DCC coupling) to form alk-EG-MKF-Boc conjugate **26** with a yield of 46% (Scheme 5.6). The methylene protons previously adjacent to hydroxyl group shift from 3.5 ppm to 4.2 ppm due to the formation of ester bond after the coupling (Figure 5.10

and A5.26). A new peak appeared at 2.4 ppm assigned for the alkyne proton indicated the presence of alkyne functionality which afforded the further CuAAC reaction.

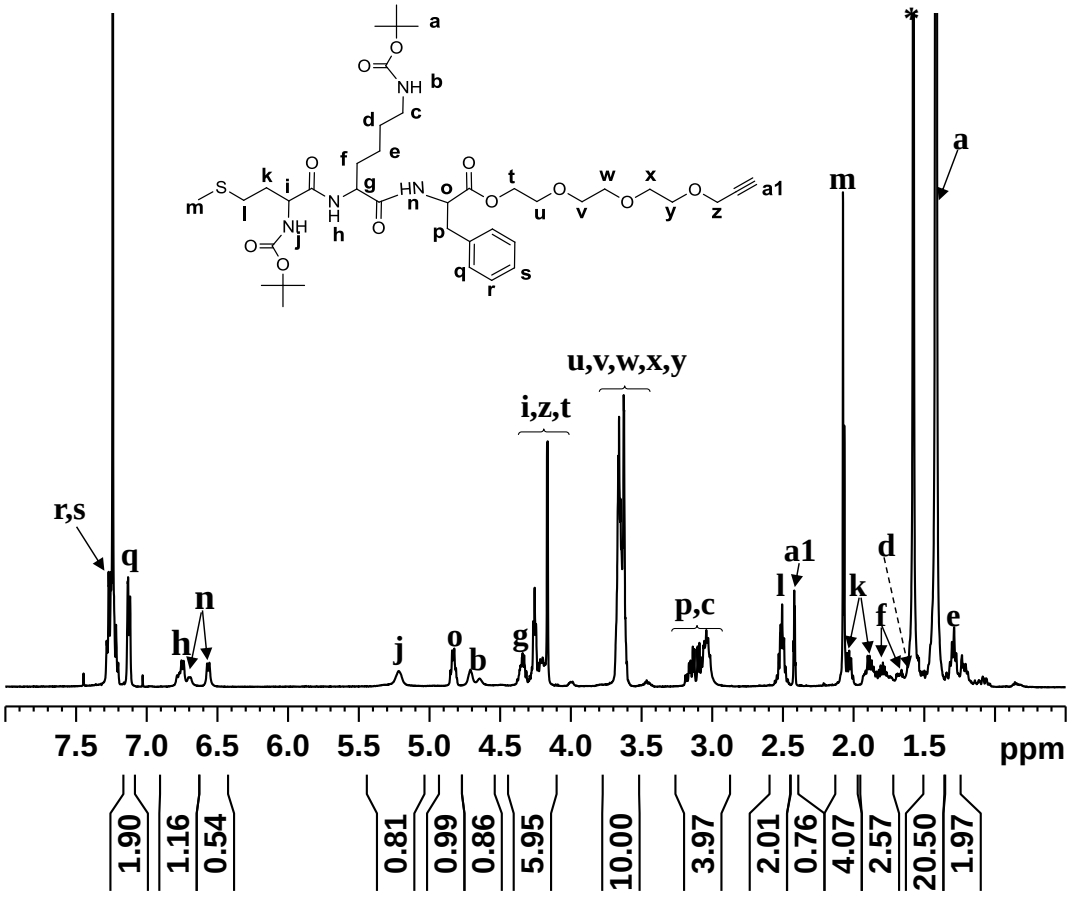

Figure 5.10 ^{1}H NMR spectrum (500 MHz) of **26**, recorded in $CDCl_3$ at 298K, *=H_2O.

The CuAAC reaction between **26** and excess **10** gave dendrimer **27** with a purity of 73% (Figure 5.11A). The impurities consisted of the starting compounds and formation of 1, 2 and 3-arm star products. After preparative SEC, the purity increased to 97 % with 3 % of 3-arm star remaining. The MALDI-ToF MS further confirmed the high purity with only one major peak after preparative SEC (Figure 5.11C) indicating that a number of species were formed after ionization through the MALDI. These species were consistent with the various oxidized species from the sulfur on the methionine group (Figure 5.11D). The emergence of the peak at 7.8 ppm is due to the formation of a triazole ring, the observation of peak 1.8 ppm is ascribed to methyl groups in the core, the characteristic resonance signal at 3.7 ppm is ascribed to EG units, the peaks at 7.3 ppm is the phenyl proton of Phe residue, and the multi-peaks from 4.0 to 5.0 ppm are assigned for Met and Lys residues. Collectively this verifies the formation of Dendrimer 4. Again, the ratio of integration (found: 24:16.87:41.97,

theoretical: 24:16:42) for methylene protons onto core (**b1**), EG backbone (**u** to **y**), and MKF structure (**p**,**c**) confirm the high purity of resulted dendrimer (Figure 5.12). The further deprotection of Boc-groups on **27** using TFA gave **Den 4** with near quantitative conversion.

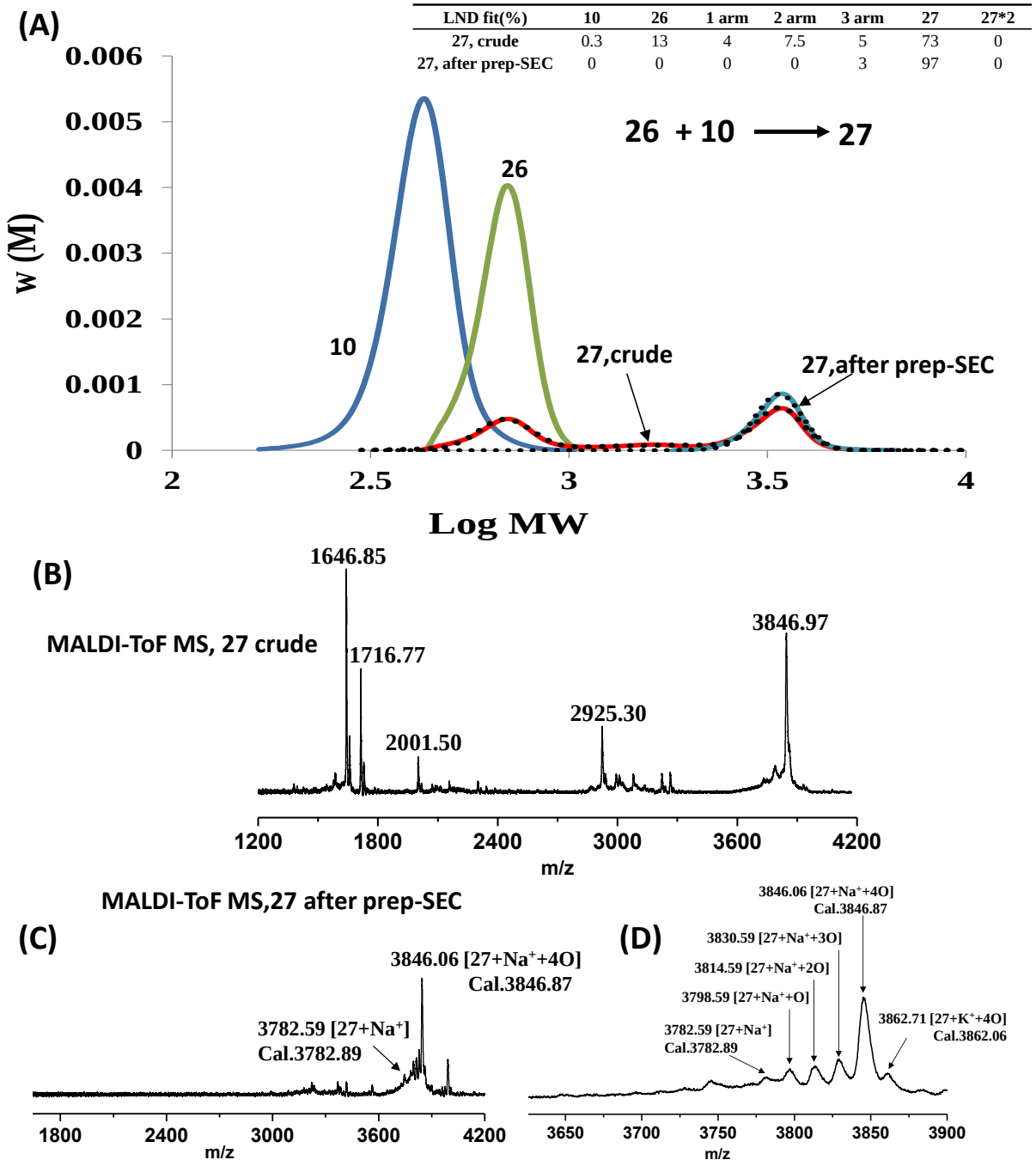

Figure 5.11 (A) SEC traces of **10**, **26**, **27** (crude and after prep) in THF and LND simulation of **27** (black dots), (B) MALDI-ToF MS of **27** crude, (C) MALDI-ToF MS of 27 after prep-SEC, and (D) expanded region of (C). The spectrum was recorded in reflection mode using DCTB as the matrix and $NaCF_3COO$ as the cation source.

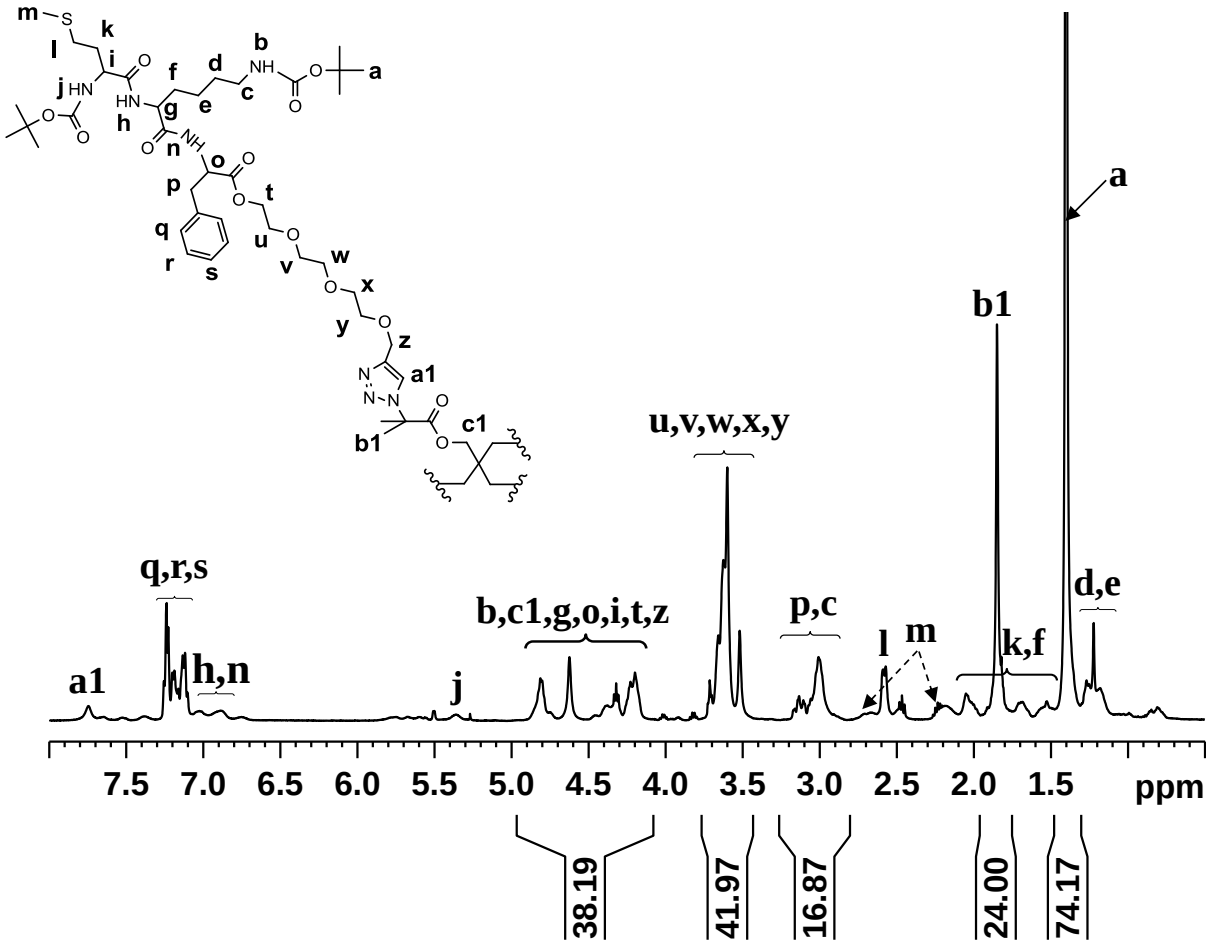

Figure 5. 12 ^{1}H NMR spectrum of **27**, recorded in $CDCl_3$ at 298 K, 500 MHz.

The SEC and MALDI-ToF MS data for all building blocks and dendrimers are given in following table.

Table 5.1 SEC and MALDI-ToF MS data for all starting materials and dendrimers

Compound	$M_{n,RI}$ [a]	$M_{p,RI}$ [a]	PDI	$M_{w,theo}$ [b]	ΔHDV [c]	$M_{n,MALDI}(+Na^+)$ [d]	Purity % [e]
6	410	430	1.03	597	0.693		
13	510	515	1.02	809	0.627		
26	670	710	1.03	795	0.843		
10	430	440	1.03	581	0.737		
11 [f]	2220	2370	1.03	2964	0.763	2986.84	95 %
14 [f]	2610	2660	1.03	3820	0.683	3841.97	97%
21	1220	1180	1.05	1436	0.848		
22 [f]	3870	3930	1.03	6323	0.512	6344.96	94%
27 [f]	3380	3480	1.02	3759	0.899	3782.89	97%

[a] SEC (RI detector) was based on a polystyrene calibration curve; [b] Theoretical molecular weight; [c] Hydrodynamic volume change (ΔHDV = $M_{n,RI}/M_{w,theo}$); [d] Molecular weight determined by MALDI-ToF MS; [e] Determined from log-normal distributions(LND) simulation. [f] Purified by prep-SEC.

5.4 Conclusion

In conclusion, we successfully synthesized four 4-arm ethylene glycol-lysine or ethylene glycol-MKF dendrimers. By utilizing a variety of coupling reactions (esterification, etherfication and CuAAC), we are able to construct dendritic polymer-peptidomimetics from small molecular organic compounds (poly ethylene) and biological entities (amino acids and peptides). The robust CuAAC click reaction together with purification by prep-SEC afforded the high purity of dendrimers. This synthetic strategy offers a route to make complex synthetic peptidomimetics for use in biological applications such as inhibition of selective ion channels.

5.5 References

1. Kaczorowski, G. J.; McManus, O. B.; Priest, B. T.; Garcia, M. L. *J. Gen. Physiol.* **2008,** 131, (5), 399-405.
2. Shieh, C. C.; Coghlan, M.; Sullivan, J. P.; Gopalakrishnan, M. *Pharmacol. Rev.* **2000,** 52, (4), 557-594.
3. England, S.; de Groot, M. J. *Br. J. Pharmacol.* **2009,** 158, (6), 1413-1425.
4. McGivern, J. G. *Neuropsychiatr. Dis. Treat.* **2007,** 3, 69-85.
5. Chi, V.; Pennington, M. W.; Norton, R. S.; Tarcha, E. J.; Londono, L. M.; Sims-Fahey, B.; Upadhyay, S. K.; Lakey, J. T.; Iadonato, S.; Wulff, H.; Beeton, C.; Chandy, K. G. *Toxicon* **2012,** 59, (4), 529-546.
6. Marr, A. K.; Gooderham, W. J.; Hancock, R. E. W. *Curr. Opin. Pharmacol.* **2006,** 6, (5), 468-472.
7. Dekan, Z.; Vetter, I.; Daly, N. L.; Craik, D. J.; Lewis, R. J.; Alewood, P. F. *J. Am. Chem. Soc.* **2011,** 133, (40), 15866-15869.
8. Clark, R. J.; Akcan, M.; Kaas, Q.; Daly, N. L.; Craik, D. J. *Toxicon* **2012,** 59, 446-455.
9. Reid, R. C.; Yau, M. K.; Singh, R.; Hamidon, J. K.; Reed, A. N.; Chu, P.; Suen, J. Y.; Stoermer, M. J.; Blakeney, J. S.; Lim, J.; Faber, J. M.; Fairlie, D. P. *Nat. Commun.* **2013,** 4, 2802.
10. Bracci, L.; Falciani, C.; Lelli, B.; Lozzi, L.; Runci, Y.; Pini, A.; De Montis, M. G.; Tagliamonte, A.; Neri, P. *J Biol Chem* **2003,** 278, (47), 46590-46595.
11. Vagner, J.; Qu, H. C.; Hruby, V. J. *Curr Opin Chem Biol* **2008,** 12, (3), 292-296.
12. Vlieghe, P.; Lisowski, V.; Martinez, J.; Khrestchatisky, M. *Drug Discov Today* **2010,** 15, (1-2), 40-56.
13. Avan, I.; Hall, C. D.; Katritzky, A. R. *Chem Soc Rev* **2014,** 43, (10), 3575-3594.
14. Duncan, R. *Nat Rev Cancer* **2006,** 6, (9), 688-701.
15. Skwarczynski, M.; Zaman, M.; Urbani, C. N.; Lin, I. C.; Jia, Z. F.; Batzloff, M. R.; Good, M. F.; Monteiro, M. F.; Toth, I. *Angew Chem Int Edit* **2010,** 49, (33), 5742-5745.
16. Kuhnle, H.; Borner, H. G. *Angew Chem Int Edit* **2009,** 48, (35), 6431-6434.
17. Shu, J. Y.; Panganiban, B.; Xu, T. *Annu Rev Phys Chem* **2013,** 64, 631-657.
18. Harris, J. M.; Chess, R. B. *Nat Rev Drug Discov* **2003,** 2, (3), 214-221.
19. Bonache, M. A.; Alaimo, A.; Malo, C.; Millet, O.; Villarroel, A.; Gonzalez-Muniz, R. *Org Biomol Chem* **2014,** 12, (44), 8877-8887.

20. Hamley, I. W. *Biomacromolecules* **2014,** 15, (5), 1543-1559.

21. Isimjan, T. T.; de Bruyn, J. R.; Gillies, E. R. *Macromolecules* **2010,** 43, (10), 4453-4459.

22. Albertazzi, L.; Mickler, F. M.; Pavan, G. M.; Salomone, F.; Bardi, G.; Panniello, M.; Amir, E.; Kang, T.; Killops, K. L.; Brauchle, C.; Amir, R. J.; Hawker, C. J. *Biomacromolecules* **2012,** 13, (12), 4089-4097.

23. Lee, H. *Polymers-Basel* **2014,** 6, (3), 776-798.

24. Hruby, V. J. *Life Sci* **1982,** 31, (3), 189-199.

25. Kojima, C.; Fukada, H.; Inui, T. *Polym J* **2013,** 45, (3), 339-345.

26. Roy, R.; Baek, M. G.; Rittenhouse-Olson, K. *J Am Chem Soc* **2001,** 123, (9), 1809-1816.

27. Darbre, T.; Reymond, J. L. *Curr Top Med Chem* **2008,** 8, (14), 1286-1293.

28. Kinberger, G. A.; Cai, W. B.; Goodman, M. *J Am Chem Soc* **2002,** 124, (51), 15162-15163.

29. Majoros, I. J.; Myc, A.; Thomas, T.; Mehta, C. B.; Baker, J. R. *Biomacromolecules* **2006,** 7, (2), 572-579.

30. Besanceney-Webler, C.; Jiang, H.; Zheng, T. Q.; Feng, L.; del Amo, D. S.; Wang, W.; Klivansky, L. M.; Marlow, F. L.; Liu, Y.; Wu, P. *Angew Chem Int Edit* **2011,** 50, (35), 8051-8056.

31. Fuaad, A. A. H. A.; Azmi, F.; Skwarczynski, M.; Toth, I. *Molecules* **2013,** 18, (11), 13148-13174.

32. Angell, Y. L.; Burgess, K. *Chem Soc Rev* **2007,** 36, (10), 1674-1689.

33. Grissmer, S.; Nguyen, A. N.; Aiyar, J.; Hanson, D. C.; Mather, R. J.; Gutman, G. A.; Karmilowicz, M. J.; Auperin, D. D.; Chandy, K. G. *Mol Pharmacol* **1994,** 45, (6), 1227-1234.

34. Wulff, H.; Calabresi, P. A.; Allie, R.; Yun, S.; Pennington, M.; Beeton, C.; Chandy, K. G. *J Clin Invest* **2003,** 111, (11), 1703-1713.

35. Beeton, C.; Wulff, H.; Standifer, N. E.; Azam, P.; Mullen, K. M.; Pennington, M. W.; Kolski-Andreaco, A.; Wei, E.; Grino, A.; Counts, D. R.; Wang, P. H.; LeeHealey, C. J.; Andrews, B. S.; Sankaranarayanan, A.; Homerick, D.; Roeck, W. W.; Tehranzadeh, J.; Stanhope, K. L.; Zimin, P.; Havel, P. J.; Griffey, S.; Knaus, H. G.; Nepom, G. T.; Gutman, G. A.; Calabresi, P. A.; Chandy, K. G. *P Natl Acad Sci USA* **2006,** 103, (46), 17414-17419.

36. Lu, D. R.; Hossain, M. D.; Jia, Z. F.; Monteiro, M. J. *Macromolecules* **2015,** 48, (6), 1688-1702.

37. Hossain, M. D.; Jia, Z. F.; Monteiro, M. J. *Macromolecules* **2014,** 47, (15), 4955-4970.

38. Gavrilov, M.; Monteiro, M. J. *Eur. Polym. J.* **2015,** 65, 191-196.

39. Monteiro, M. J. *Eur. Polym. J.* **2015,** 65, 197-201.

Chapter 6

Summary

The objective of this thesis was to develop new synthetic strategies using LRP and 'click' chemistry to produce complex architectures in with high purity. The advance of the combination of 'living' radical polymerizations and 'click' techniques has allowed macromolecular architectures with structural and compositional precsion to be built. With this chemistry, we now have the tools to design polymer structures with desired properties that can be made for specific applications.

In this thesis, small molecule chain transfer agents and initiators were used to mediate a variety of LRPs (such as RAFT polymerization, ATRP, and SET-LRP) to make well-defined polymeric building blocks with high chain-end functionalities. Alternatively, expected functionalities could be incorporated into the polymer backbone *via* post-modification. These site-specific functionalities (e.g., trithiocarbonate, activated double bond, bromine, alkyne, azide) on the polymer chains require robust and efficient 'click' reactions for further coupling reactions to form complex macromolecular structures. In addition, the mild reaction condition of 'click' chemistries (e.g. CuAAC) make it an excellent tool for building biomacromolecules structures (i.e., dendritic peptidomimetics) by coupling functional biomolecules (e.g., structurally-modified amino acids or peptides)

In this thesis, a library of complex polymer architectures such as cyclic polymers, ABCD 4-arm mkitoarm stars, dendrimers decorated with biological molecules (amino acid or peptides) were successfully synthesized.

6.1 RAFT polymerization and thiol-ene 'click' reaction to prepare cyclic polymers

RAFT polymerization is a powerful tool to make a wide range of well-defined polymers. The mild conditions of RAFT polymerization allows high tolerance for functionalities. A diverse range of functional groups can be introduced onto polymers for further chain-end modification or 'click' reactions. The RAFT end group can be readily converted to another functional group, or made into a complex polymer structure through the *in-situ* aminolysis and subsequent thiol-ene coupling reaction.

In this thesis, the trithiocarbonate RAFT agent bearing hydroxyl and alkyne functionalities was designed and synthesized to mediate the RAFT polymerization of STY, *t*-BA, NIPAm, and DMA. The resultant polymers were produced with a narrow PDI, high chain-end

functionality of RAFT group, and predetermined molecular weight. The alkyne functionality allowed the further CuAAC reaction with another moiety, while the hydroxyl group could be converted to an activated ene-group for the thiol-ene coupling reaction.

RAFT-made polymers bearing trithiolcarbonate at the chain-end readily form the corresponding thiol group through aminolysis of primary amine (e.g., hexylamine). In a typical Michael addition, hexylamine acts as an aminolysis reagent for the formation of the thiol-group, then as a base to form the thiolate anion, and finally as a nucleophilic catalyst for attack of the thiolate to the activated double bond. Therefore, hexylamine is a simplified catalytic reagent that allows the one-pot cyclization of RAFT-based polymers containing an ene functionality.

One-pot cyclization was achieved by *in-situ* aminolysis of trithiocarbonate moiety and intramolecular thiol-ene Michael Addition under non-dilute conditions (> 5 mg/mL) in less than 2 h at room temperature, yielding alkyne functional monocyclic polymers with high cyclic purity(> 80 %). The key to achieve one-pot cyclization was the concentration-dependent slow aminolysis of trithiocarbonate group which ensured the instant concentration of thiol termini was low enough to make sure the intramolecular thiol-ene reaction was the dominant reaction. As hexylamine can also react with acrylates, an optimized condition (PSTY :hexylamine : TCEP=1:125:3) was therefore required to maximize the purity of resulting mono-cyclic product. This was the reason why it was difficult to achieve higher pure cyclic polymers. In further work, the alkyne functionality on cyclic polymer chain allowed the further construction of more complex macrocyclic architechtures.

6.2 Synthesis of miktoarm star polymers *via* combination of LRP and CuAAC

The properties of polymeric materials is not only dictated by their architectures but also highly depended on their composition. Miktoarm stars, in which arm consists of a different polymer chain, can be constructed from LRP or living anionic polymerization. LRP is more advantageous over living anionic polymerization as LRP allows a wide range of monomers to be polymerized

The ATRP and SET-LRP techniques utilized in this work provide access to wide range of well-defined polymers with high chain-end functionality, which is crucial for further CuAAC 'click' reaction. One goal of this work was to incorporate any polymeric arm segments into the star. Herein, we selected hydrophobic PSTY and P^{t}BA, the latter which can be hydrolysed to poly(acrylic acid) (i.e. PAA), hydrophiphilic poly(ethylene glycol) (PEG) and

thermoresponsive poly(*N*-isopropylacrylamide) (PNIPAm). The amphiphilic nature of the miktoarm star allow self-assembly into micelles that have potential application in biological area. The chain ends of LRP generated polymers are easily modified to introduce desired functionality (i.e., alkyne) and subsequently 'click' with azide moiety *via* CuAAC.

The trifunctional linker containing two azide groups and one protected alkyne group is key for the introduction of different polymers to the core. By removal of the TIPS protecting group and further modification by a difunctional azide compound, diblock copolymers bearing either azide or alkyne functionality can be obtained. ABCD miktoarm star was made by coupling N_3 and alkyne diblock copolymers *via* the CuAAC click reaction. The characterization of the miktoarm star is a challenge due to their complex chemical composition. To confirm the synthetic feasibility of using such sequential/iterative CuAAC reaction to make miktoarmstar, a 4-arm PSTY homo star was made to obtain full information of structure through characterization by SEC, NMR and MALDI-ToF MS. The excellent click efficiency (> 92 %), high purity (> 98 %), and narrow molecular weight distribution demonstrated that it is a superior strategy to make star-like polymers. To synthesize ABCD miktoarm star consisting of PSTY, P^{t}BA, PNIPAm, and PEG arm segments, we followed this sequential CuAAC reaction strategy. The lower click efficiency (66 %) at final coupling step was probably due to the difficulty in determining the stoichiometry of reactants. After purification by prep-SEC, the purity increased from 67 % (before purification) to 97 % (after prep-SEC).

This synthetic protocol combined the recent advance of polymer chemistry, which represented a synthetic advance of preparing miktoarm star polymers. By using the LRP and CuAAC as well as the specially-designed trifunctional linker, star polymer with multi-arm segments up to 4 or more can be achieved. Moreover, a growing understanding of the behaviour of miktorarm copolymers in aqueous solution and relation between polymer arm (length or/and composition) and overall morphology is becoming increasingly important. Different immiscible and chemically-distinct polymeric blocks at one junction point suppresses the formation of concentric structures and results in a range of new morphologies with compartmentalized micellar cores. By far, the study of the response of morphology to external stimuli has just begun. In this work, the hydrophobic PSTY arm and hydrophilic PEG arm provide the amphiphilic nature of miktoarm star, while the PAA and PNIPAm blocks offer the possibility of PH-induced and thermoresponsive changes in the morphology during the self-assembly. More detailed study of self-assembly behaviour of our miktoarm star will be carried out in the future.

6.3 Synthesis of dendritic peptidomimetics

Numerous studies have demonstrated that the chemical and physical properties of dendritic macromolecules are dedicated by the nature of their functional peripheral groups. Thus, the function-bearing units on the periphery allows dendrimers to be designed for a variety of applications. When the periphery of dendrimers were decorated by amino acids or/and peptides, dendrimers can be serviced as peptidomimetics to mimic functions of natural peptides. Moreover, these structures overcome some of the inherent shortcomings of natural peptides.

In the past few years, our group developed a new and simple synthetic methodology to produce 3rd generation dendrimers in one step and in one pot in under 30 min. By selecting ligand and solvent conditions, two chemoselective click reactions, NRC (nitroxide radical coupling) and CuAAc (copper(I)-catalyzed azide-alkyne cycloaddition), can be carried out in one-pot system to rapidly coupled three polymer building blocks with nitroxide, azide, and alkyne functional groups on the chain ends. This is a significant advance on any methodology currently used to prepare dendrimers (both from small molecules and polymeric building blocks). This will provide the chemistry to couple special biomolecules and other macromolecules onto the periphery of the dendrimer.

We aim to extend this unique strategy to build a library of polymeric dendritic peptidomimitics with lysine or dendritic lysine peptide at the periphery. By combing ATRP, NRC and CuAAc techniques, we can produce 3rd and 4th generational lysine-decorated and peptide-decorated polymeric dendrimer in one-pot reaction within 1h, which is a great improvement over previous methods to make similar dendrimers originated from small molecular dendrimer (e.g. lysine-decorated PAMAM dendrimer). By choosing the core and controlling the chain length of building blocks, we can also change the structure and size of dendritic peptidomimetics. Later, we syntheiszed small molecular dendritic peptidomimitics targeting the mimicking the function of scorpion toxins on voltage-activated K^+ ion channel. Through the guidance of computational methods, it was feasible to design promising lead compounds, which can then be verified by biological experiments. In the synthesis, we first made a variety of alkyne-functional building blocks consist of ethylene glycol and spacer, lysine or MKF peptide as chain-ends. By using the CuAAC 'click' reaction, we successfully made 4 different small molecular dendritic peptidomimitics with variable size, types and density peripheral molecules (either amino acid or peptide). The detailed NMR and MALDI-

ToF MS analyses were carried out to confirm the formation of desired structures. In the future, the biological test will be performed to verify the potential of resultant small molecular dendritic peptidomimitics as a potent and selective ion channel inhibitors, which mimic the inhibition action of natural peptide (scorpion toxins) on biological targets (ion channels).

In general, this thesis presents a journal from small molecules to complex polymer archetectures using LRPs and Click chemistries. Not only have LRPs found increasingly widespread use in polymer synthesis in recent years, but also have 'Click' chemistries due to its efficiency, orthogonality to other functional moieties present, and compatibility with LRPs techniques. Consequently, numerous elegant synthetic strategies have been created by different combinations of LRPs and Click chemistries to construct complicated polymer structure with controllable properties toward the applications.

The functional cyclic polymers will be further coupled to other polymer building blocks (either cyclic or linear) to produce more complex macrocycles (e.g, dendritic cyclic structure).By far, many study have been carried out to examine the effect of molecular weight of homocyclic polymers on the glass transition temperature, diffusion behaviour and relaxation properties. Very few attention have been paid on the influence of topologies on these properties. The study on complex cyclic structure provide the new insight into the relationship of topologies and polymer physical properties. Similarly, the construction of complex miktoarm stars offer the feasibility to study phase-separation at molecular level due to the immiscible arm segments. Moreover, the amphiphilic nature of miktoarm star lead to a landmark studies in the self-assmebly behaviour, which renders miktoarm polymers as attractive candidates as a drug delivery vehicle.

Dendritic peptidomimetics circumvent some of the inherent problems associated with a natural peptide and therefore, expand the application of peptide library. The utilization of dendritic polymer structure is facilitated to modify and cluster bioactive molecules (e.g, amino acids, peptides) at the periphery of their structures. The clustering effect of dendritic polymers is useful multiple binding interactions due to the multivalent bonding. In the future, a library of polymeric dendritic peptidomimetics with biocompatible polymer core and biomolecules outer layer would be prepared by click chemistry, which to be used as antiviral and antibacterial agent. The series of EG-peptide conjugated peptidomimetics will be used as a potent inhibitor of the voltage-gated K^+ channel Kv1.3, a target for autoimmune diseases. These study highlight the potential of EG-peptide conjugates as drug scaffolds targeting biological potassium channels. The LRPs and Click techniques allow to expediently adjust

the structural parameters (i.e., size, density of surface molecules, composition of polymers, N/P ratio) of peptidomimetics to fulfil the certain biological application.

Appendix A

Synthesis of (1-azidoethyl)benzene

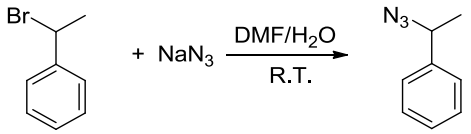

(1-bromomethyl)-benzene (3.0 g, 16.2 mmol) and sodium azide (2.1 g, 32.4 mmol) were dissolved in a mixtureof DMF (9 mL) and water (1 mL) and the resulting solution was stirred overnight. The mixture was added 30 mL brine and extracted withdiethyl ether (3 x 60 mL). The organic layer collected were dried over anydrous $MgSO_4$, after removal ofthe solvent under reduced pressure, colourless oil(1-azidoethyl)benzene was obtainedwith yield as 84 %.

^{1}H NMR ($CDCl_3$, 298 K, 400 MHz): δ 7.45 (d, 2H, *J*=7.48, benzene protons), 7.35 (dd, 2H, *J*=8.28 Hz, 7.40 Hz; benzene protons), 7.29 (d, 1H, *J*=7.12 Hz; benzene proton),4.60 (q, 1H, *J*=6.92 Hz; CH_3-***CH***-N_3), 1.53 (d, 3H; *J*=6.92 Hz; methyl protons);^{13}C NMR ($CDCl_3$, 298 K, 400 MHz); 140.9, 128.7, 128.1, 126.3, 61.1, 21.6.

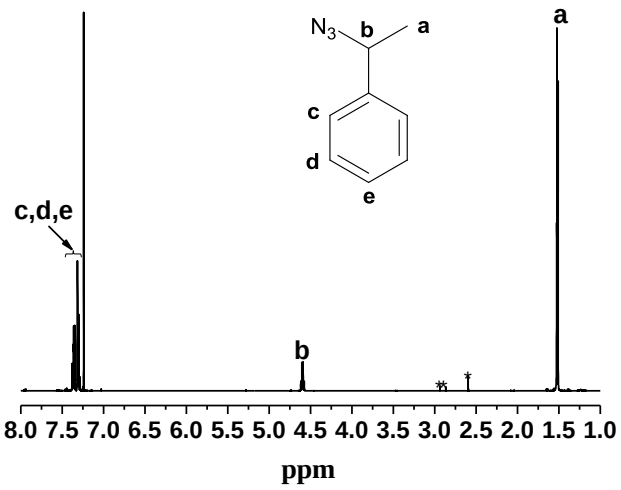

Figure A2.1: ^{1}H NMR spectrum (400 MHz) of (1-azidoethyl) benzene in $CDCl_3$ at 298 K, **=DMF. *=DMSO

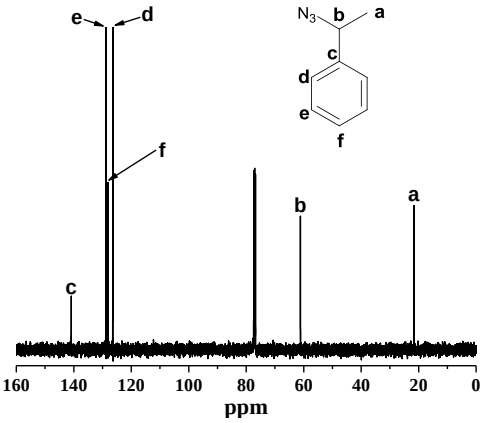

Figure A2.2: ^{13}C NMR spectrum (400 MHz) of (1-azidoethyl) benzene in $CDCl_3$ at 298 K.

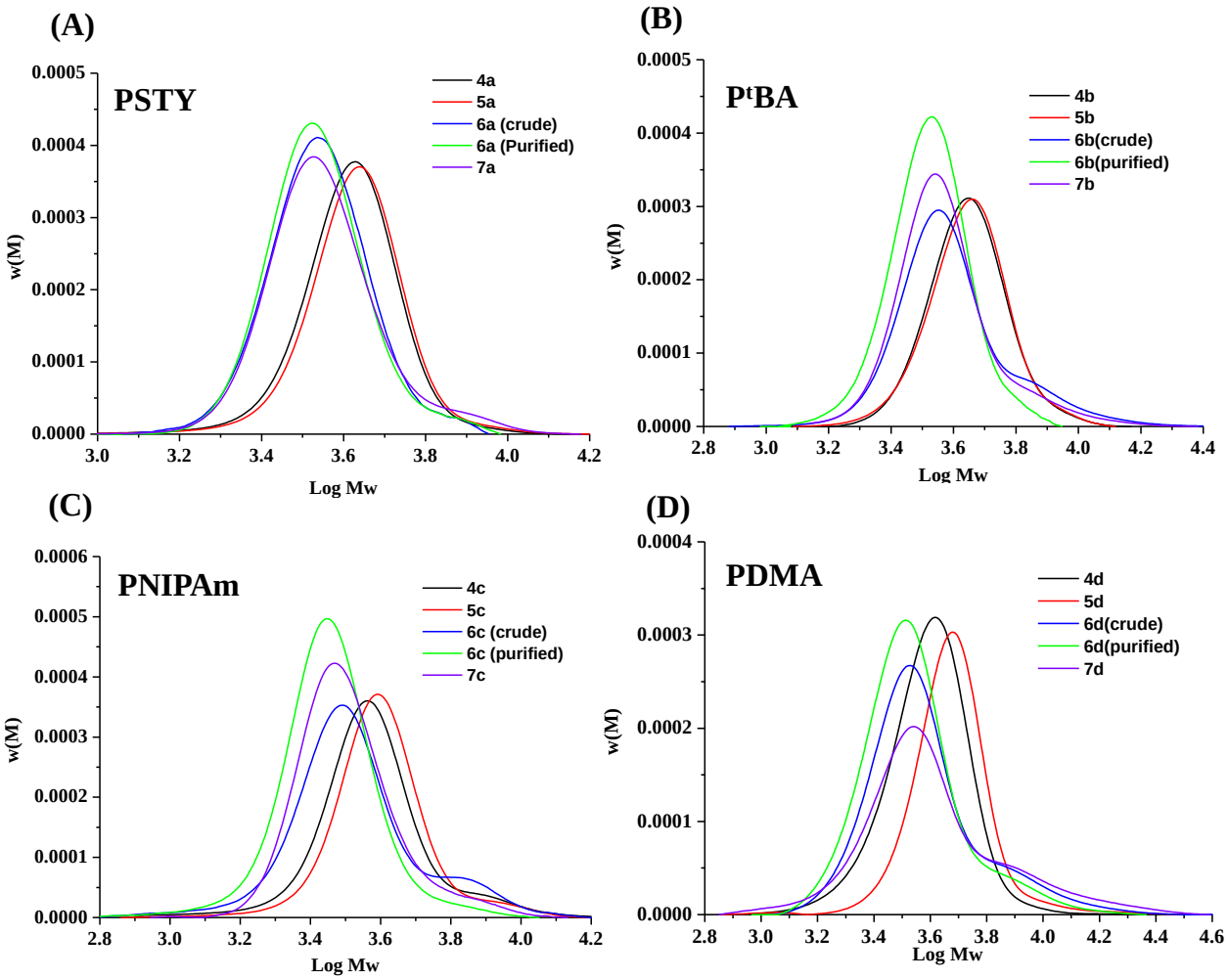

Figure A2.3: Overall SEC traces of polymers **4**, **5**, **6**, and **7**. (A) for **a**, (B) for **b**, and (C) for **c** were determined from THF SEC, RI detector, PSTY standard; (D) for **d** was determined from DMAc SEC, RI detector, PSTY standard.

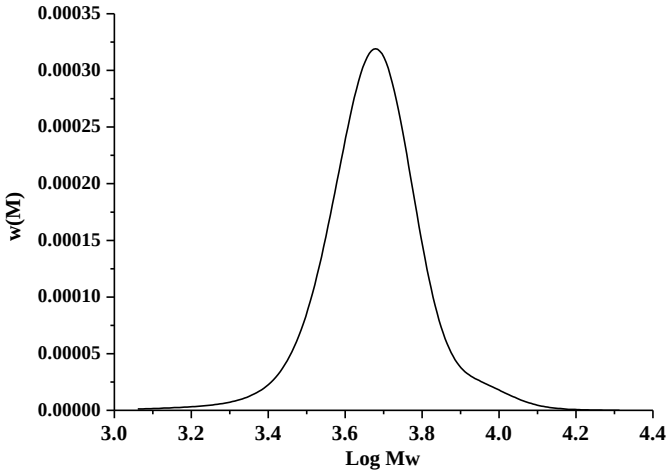

Figure A2.4:SEC trace of polymer **11**, determined from THF SEC, RI detector, PSTY standard, M_n=4480, PDI=1.10.

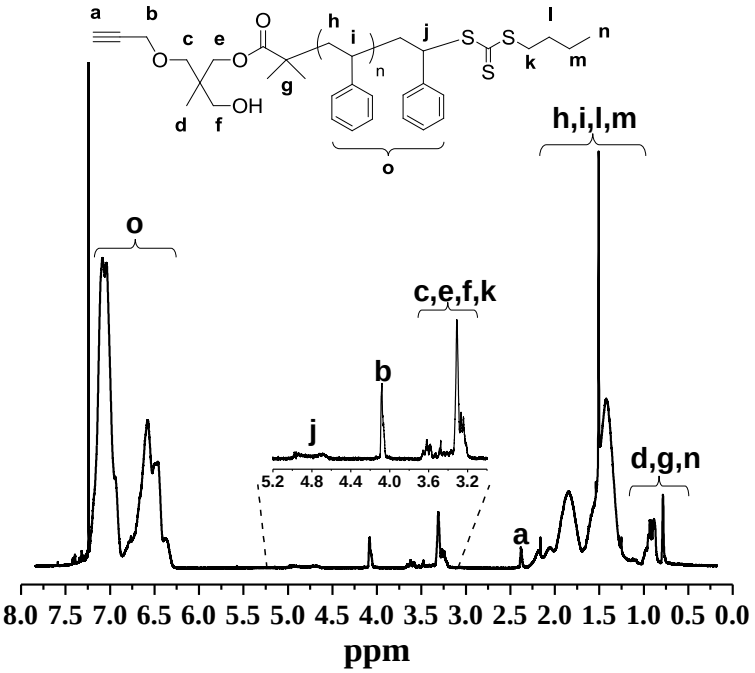

Figure A2.5:^{1}H NMR spectrum (400 MHz) of **4a**, recorded in $CDCl_3$ at 298 K.

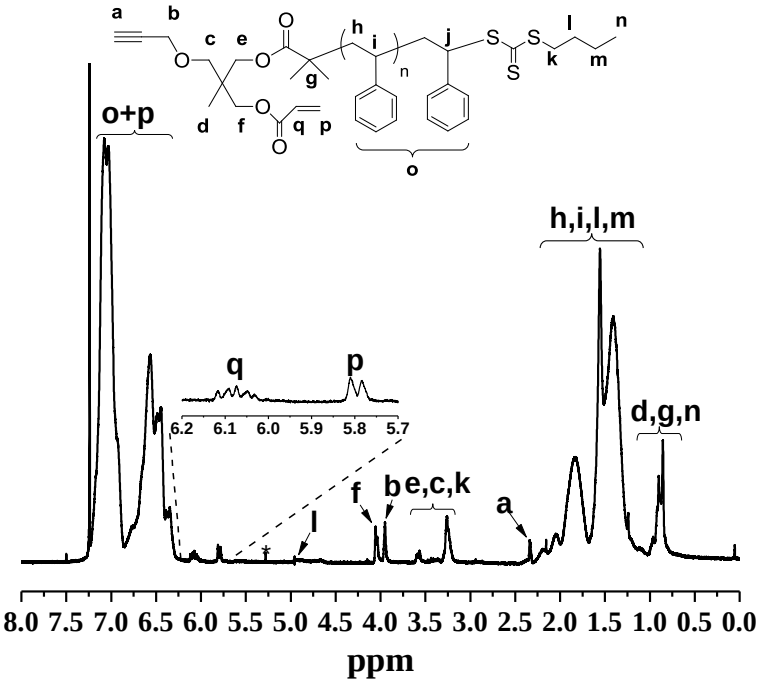

Figure A2.6: ^{1}H NMR spectrum (400 MHz) of **5a**, recorded in $CDCL_3$ at 298 K.

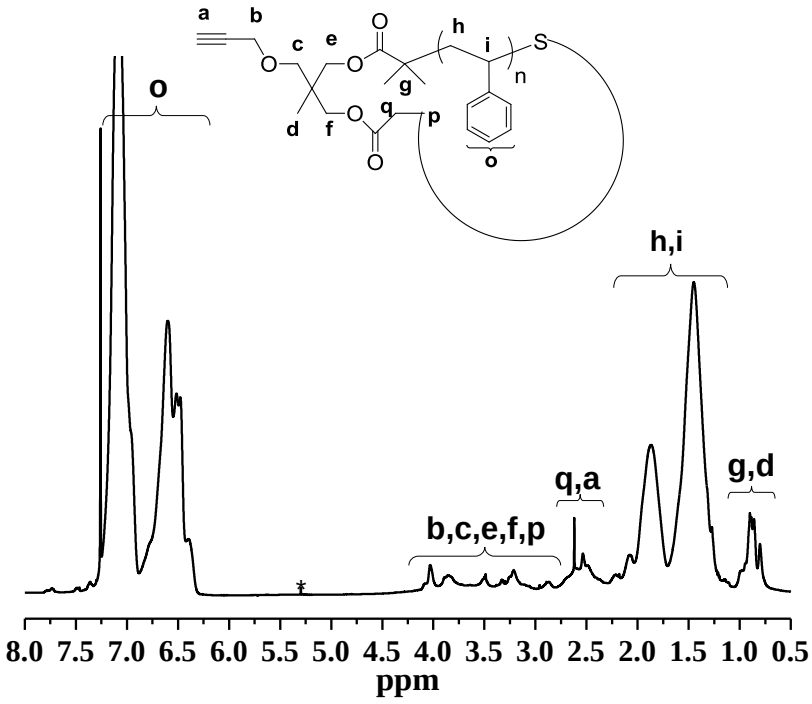

Figure A2.7: ^{1}H NMR spectrum (400 MHz) of **6a**, recorded in $CDCl_3$ at 298 K. *=DCM

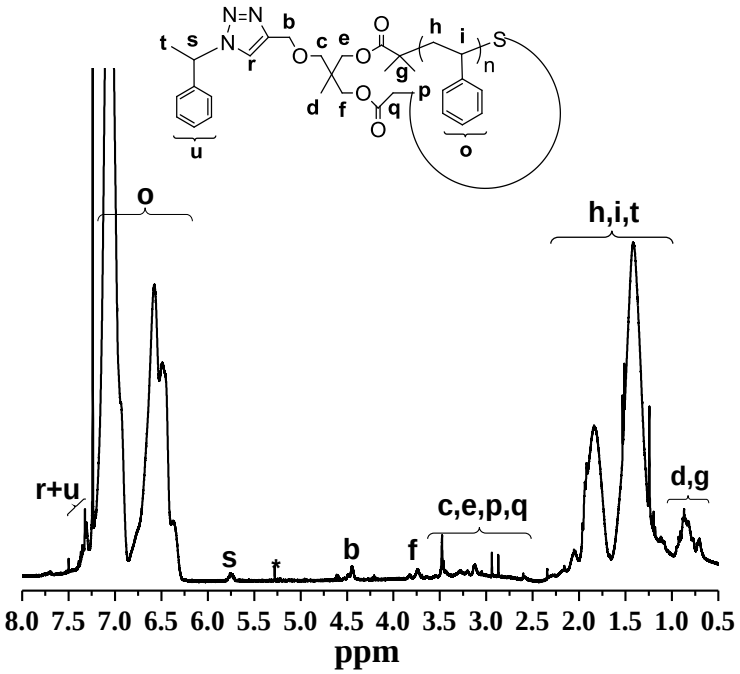

Figure A2.8: ^{1}H NMR spectrum (400 MHz) of **7a**, recorded in $CDCl_3$ at 298 K. *=DCM

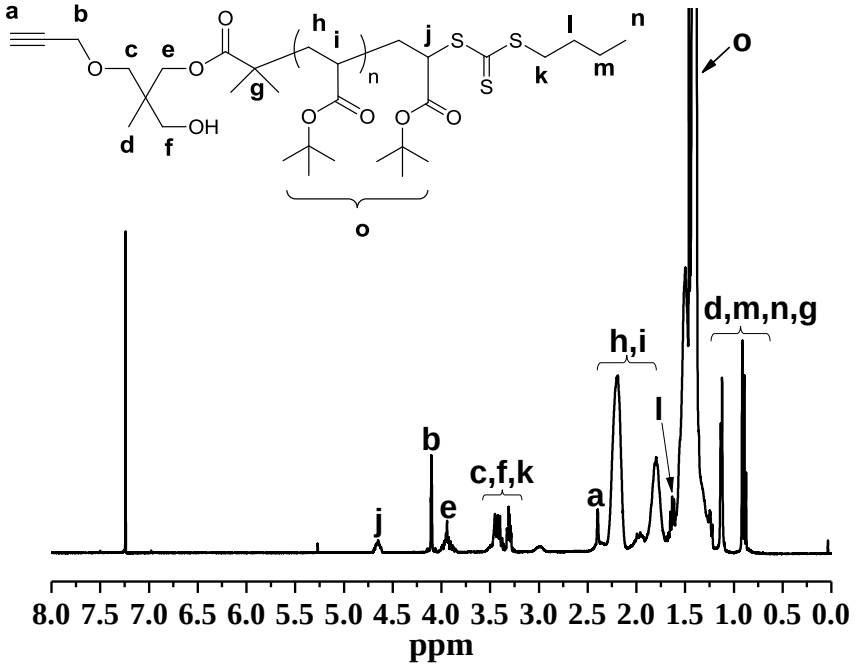

Figure A2.9: ^{1}H NMR spectrum (400 MHz) of **4b**, recorded in $CDCl_3$ at 298 K.

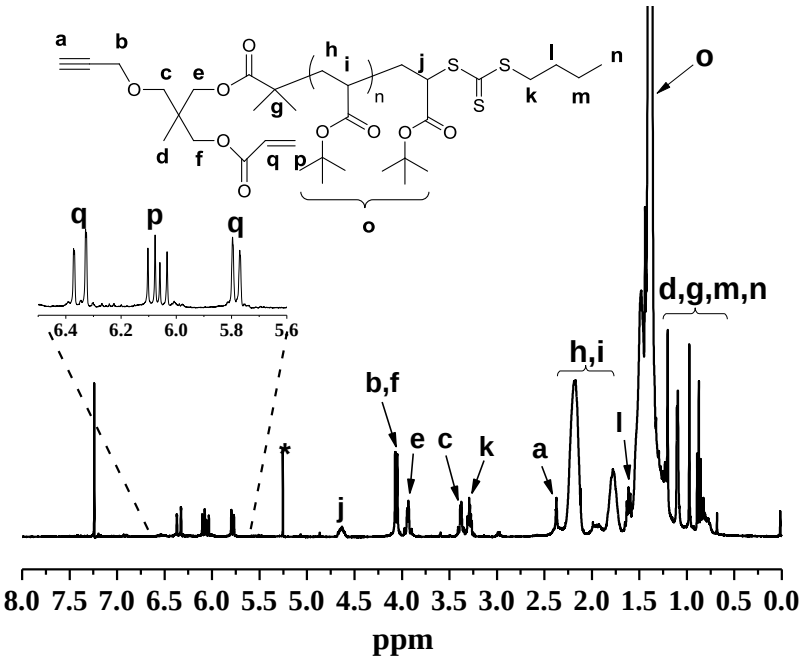

Figure A2.10: ^{1}H NMR spectrum (400 MHz) of **5b**, recorded in $CDCl_3$ at 298 K.*=DCM

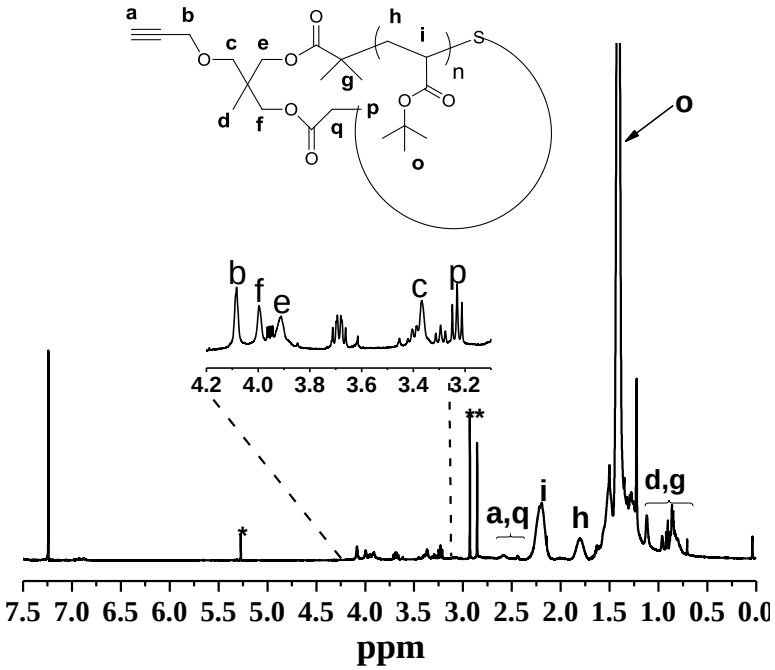

Figure A2.11: ^{1}H NMR spectrum (400 MHz) of **6b**, recorded in $CDCl_3$ at 298 K.*=DCM.

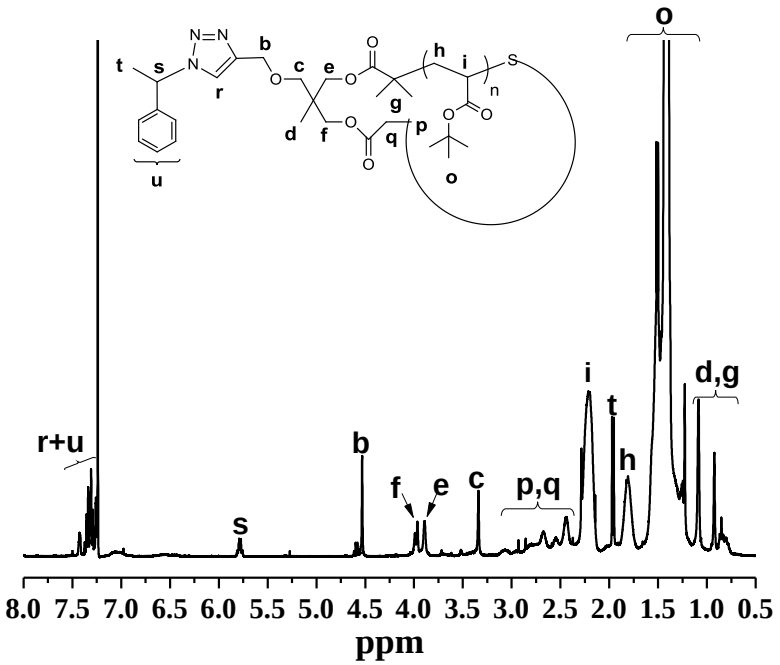

Figure A2.12: ^{1}H NMR spectrum (400 MHz) of **7b**, recorded in $CDCl_3$ at 298 K.

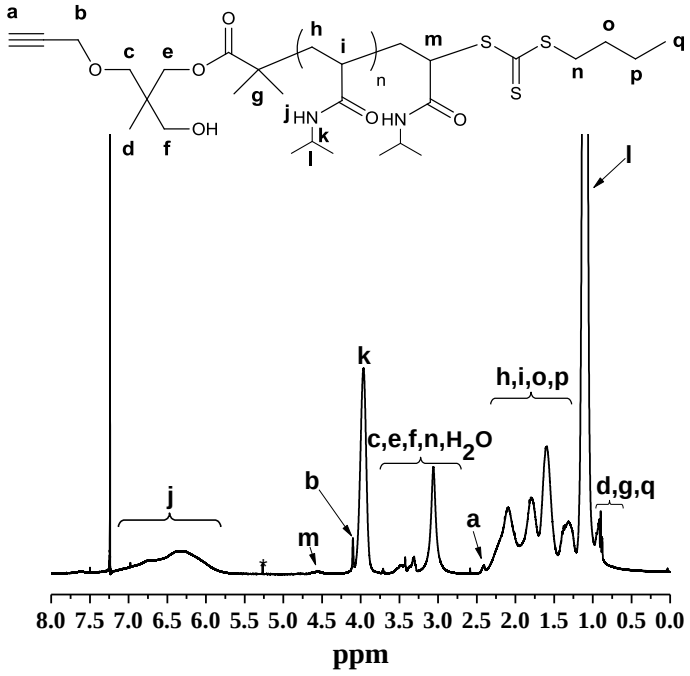

Figure A2.13: ^{1}H NMR spectrum (400 MHz) of **4c**, recorded in $CDCl_3$ at 298 K.

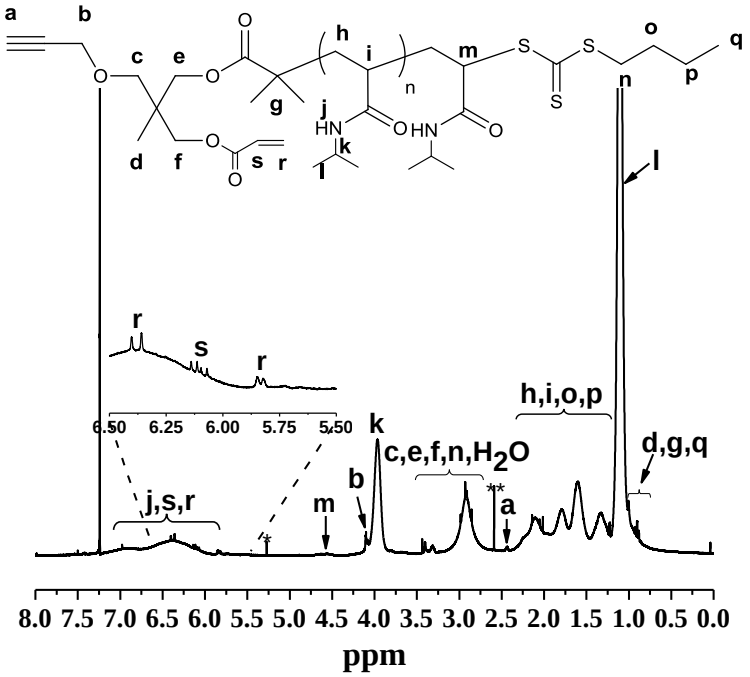

Figure A2.14: ^{1}H NMR spectrum (400 MHz) of **5c**, recorded in $CDCl_3$ at 298 K.*=DCM, **=DMSO.

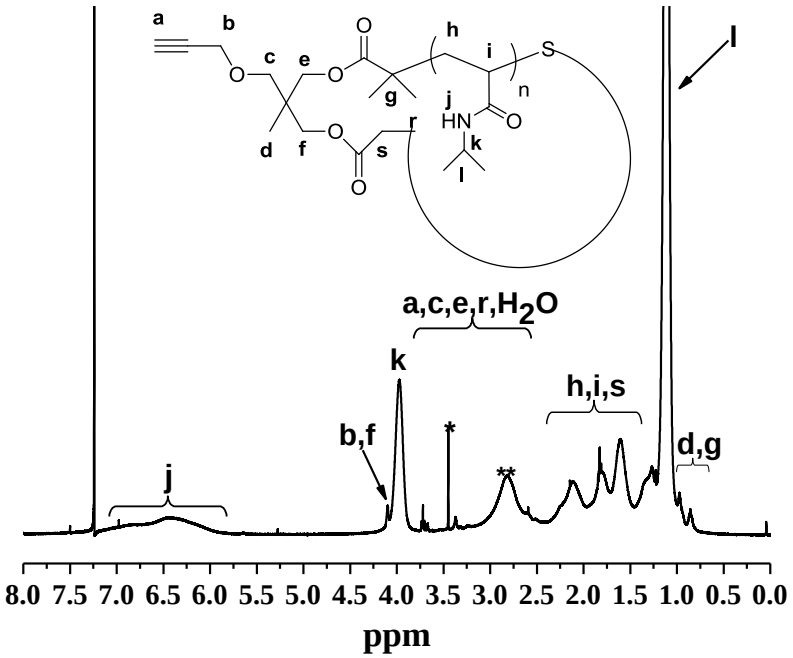

Figure A2.15: ^{1}H NMR spectrum (400 MHz) of **6c**, recorded in $CDCl_3$ at 298 K. *=Et_2O.

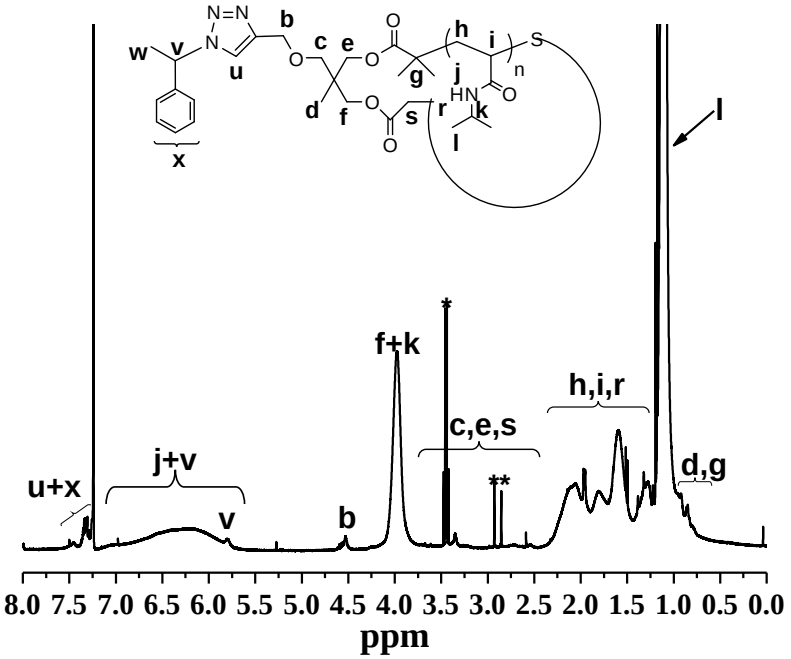

Figure A2.16: ^{1}H NMR spectrum (400 MHz) of **7c**, recorded in $CDCl_3$ at 298 K.*=Et_2O, **=DMF.

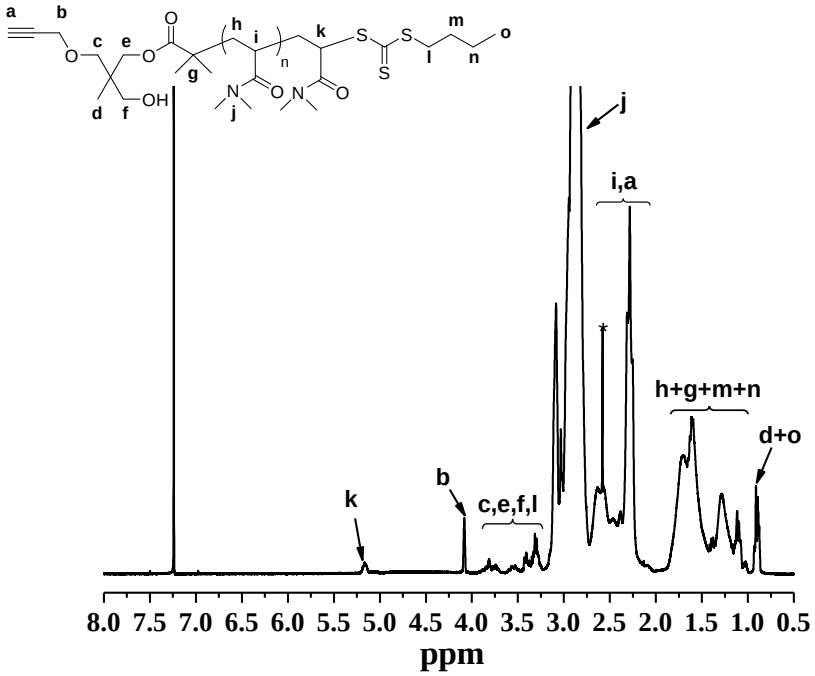

Figure A2.17: ^{1}H NMR spectrum (400 MHz) of **4d**, recorded in $CDCl_3$ at 298 K.

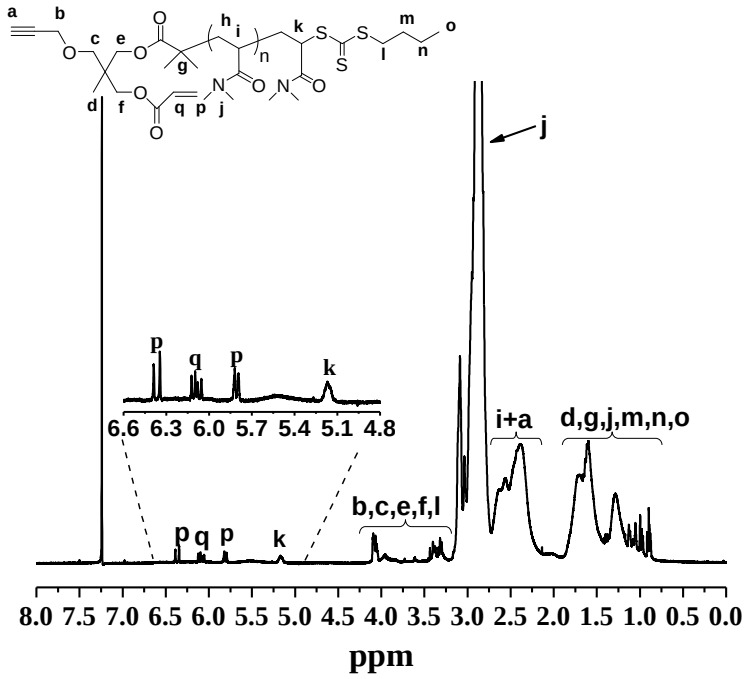

Figure A2.18: ^{1}H NMR spectrum (400 MHz) of **5d**, recorded in $CDCl_3$ at 298 K.

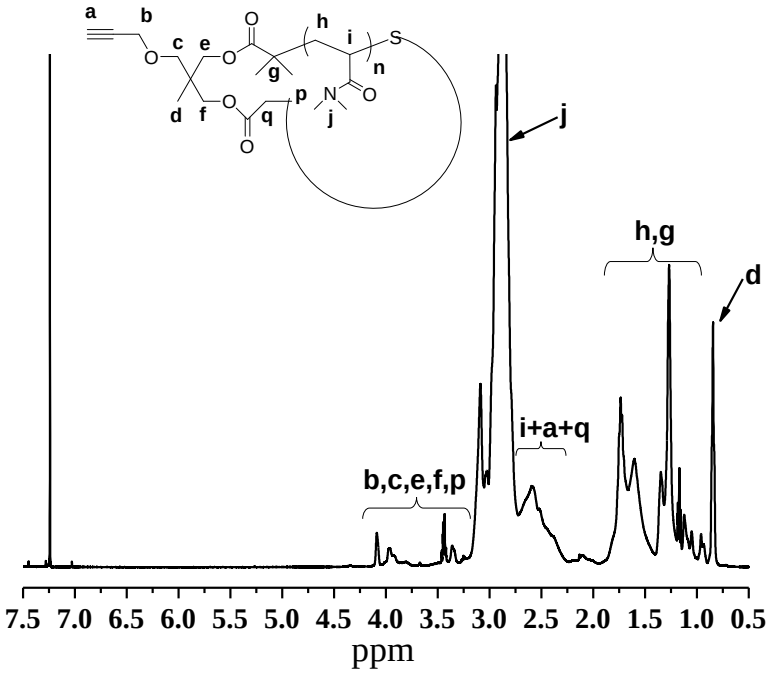

Figure A2.19: ^{1}H NMR spectrum (400 MHz) of **6d**, recorded in $CDCl_3$ at 298 K.

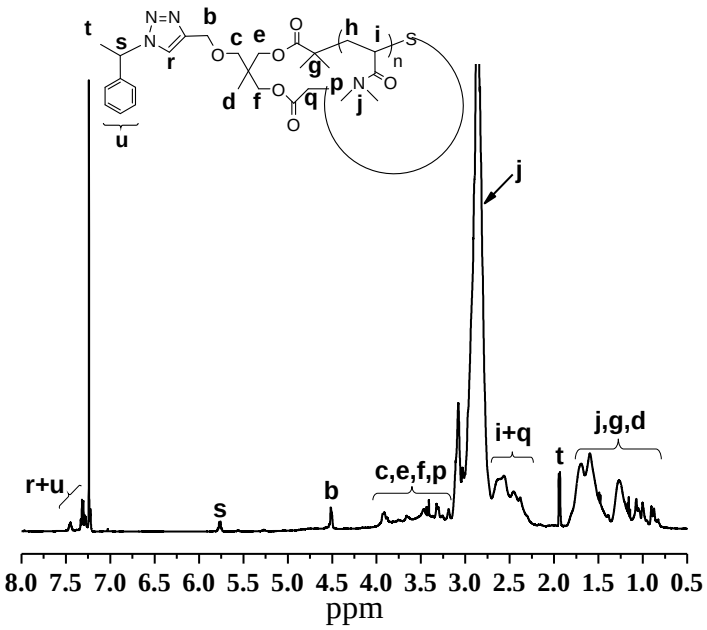

Figure A2.20: ^{1}HNMR spectrum (400 MHz) of **7d**, recorded in $CDCl_3$ at 298 K.

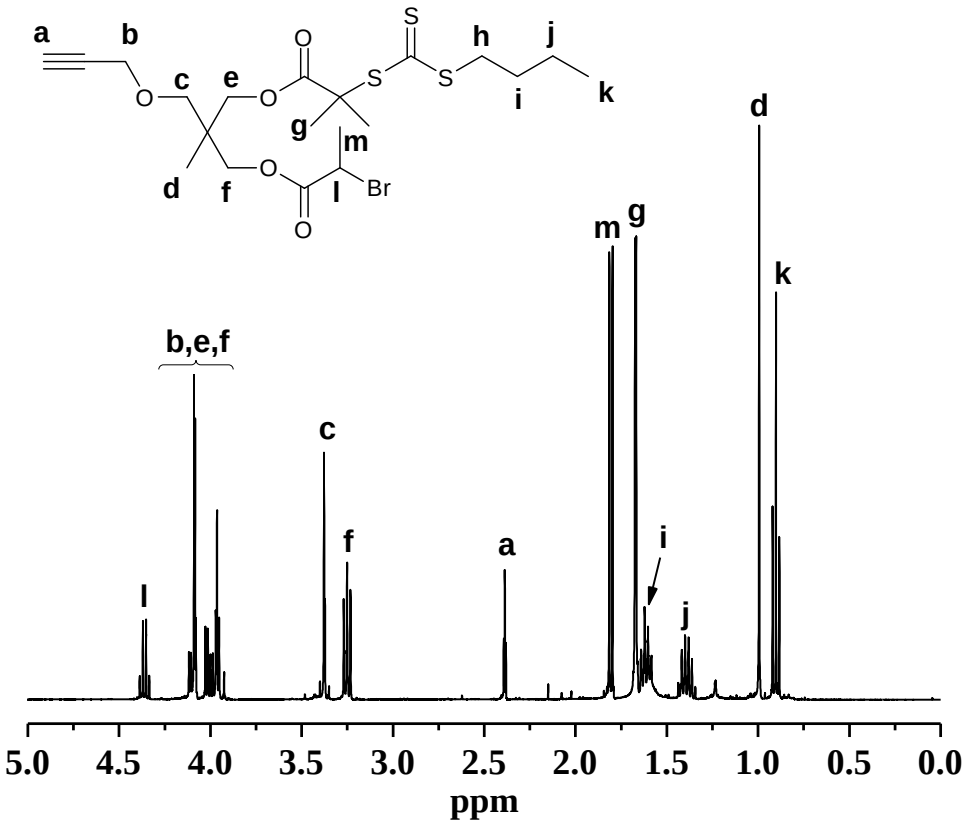

Figure A2.21: ^{1}H NMR spectrum (400 MHz) of **10**, recorded in $CDCl_3$ at 298 K.

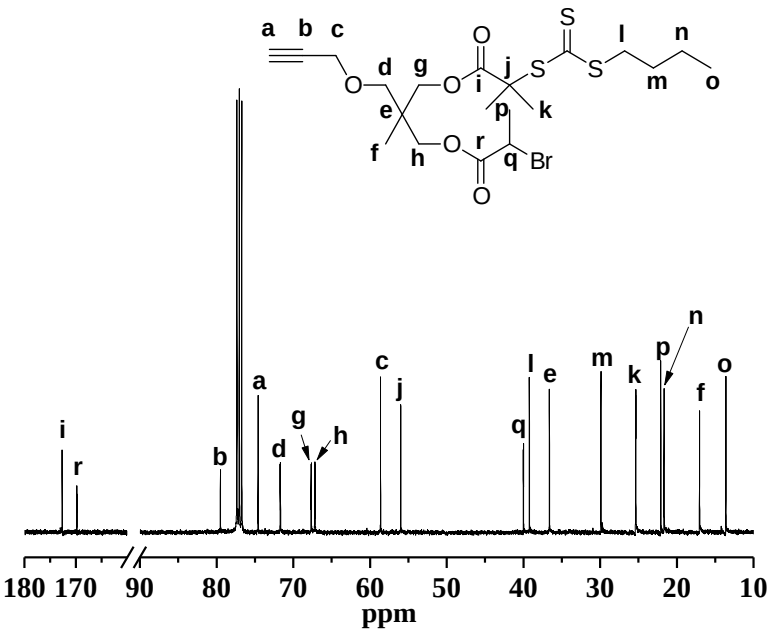

Figure A2.22: ^{13}C NMR spectrum (400 MHz) of **10**, recorded in $CDCl_3$ at 298 K.

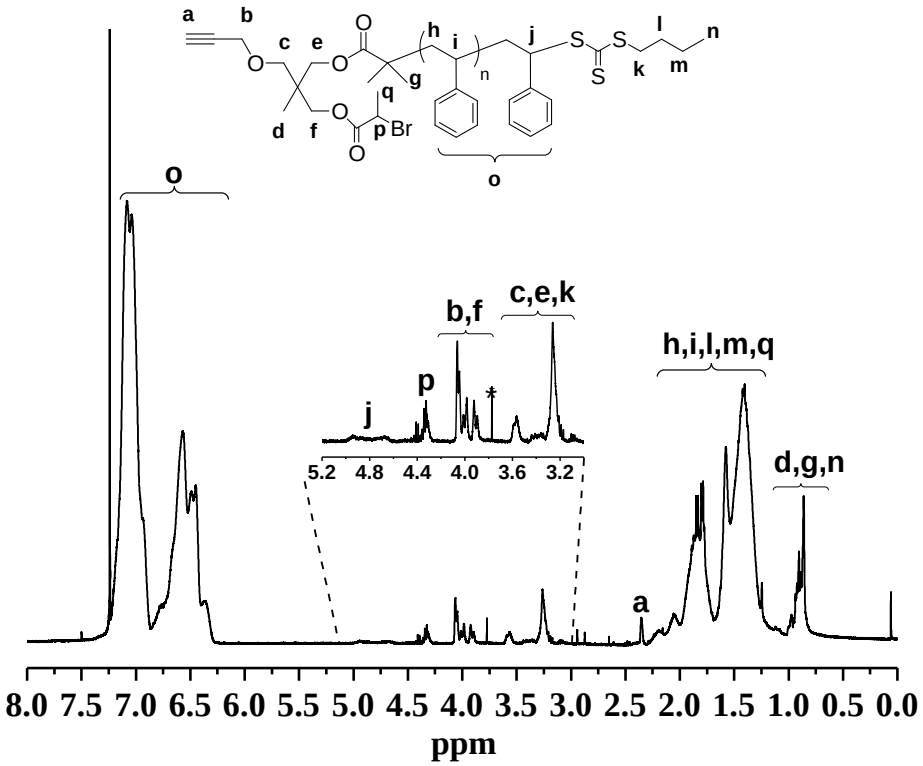

Figure A2.23: ^{1}H NMR spectrum (400 MHz) of **8**, recorded in $CDCl_3$ at 298 K.

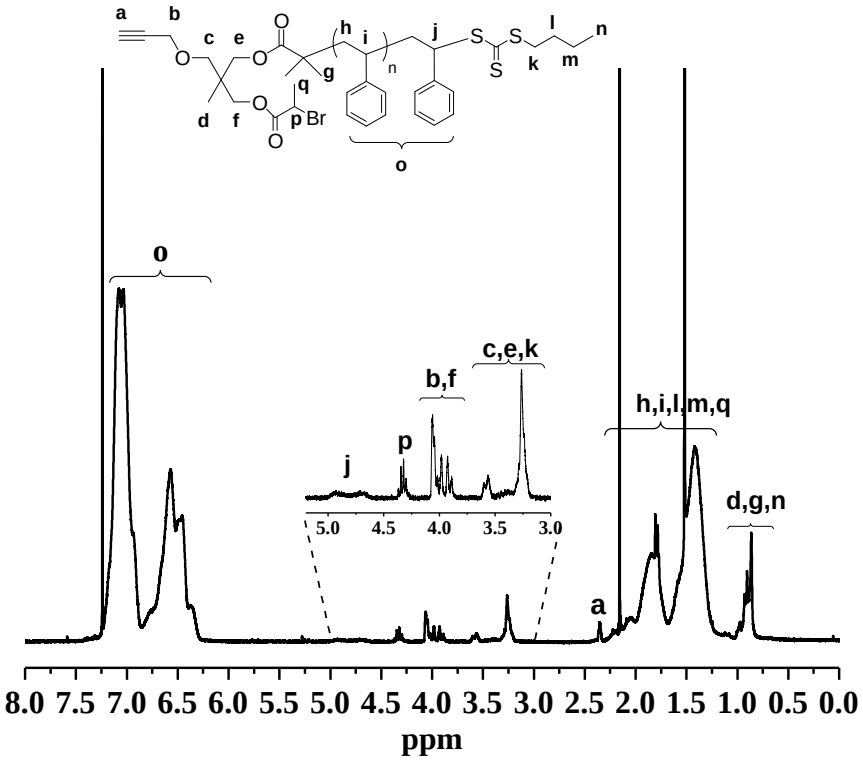

Figure A2.24: ^{1}H NMR spectrum (400 MHz) of **11**, recorded in $CDCl_3$ at 298 K.

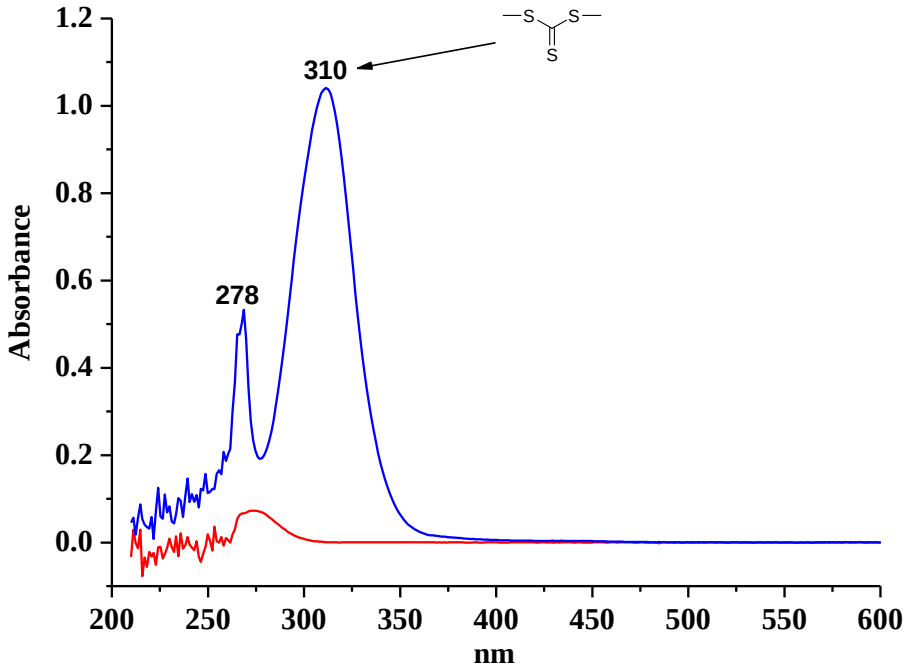

Figure A2.25: UV-vis absorbance of **5a** (blue) and **6a** (red). UV-vis spectrum was recorded by UV-detector of THF GPC with the same concentration of polymers. The peak at 310 nm is attributed to RAFT moiety.

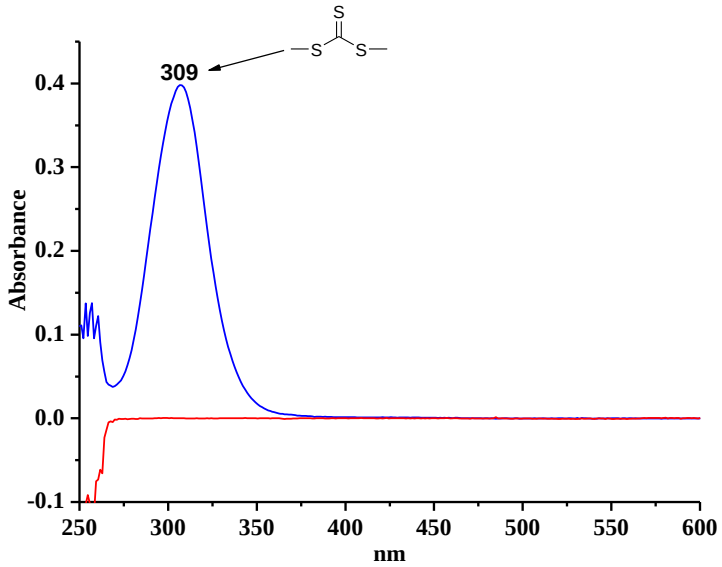

Figure A2.26: UV-vis absorbance of **5b** (blue) and **6b** (red). UV-vis spectrum was recorded by UV-detector of THF GPC with the same concentration of polymers. The peak at 309 nm is attributed to RAFT moiety.

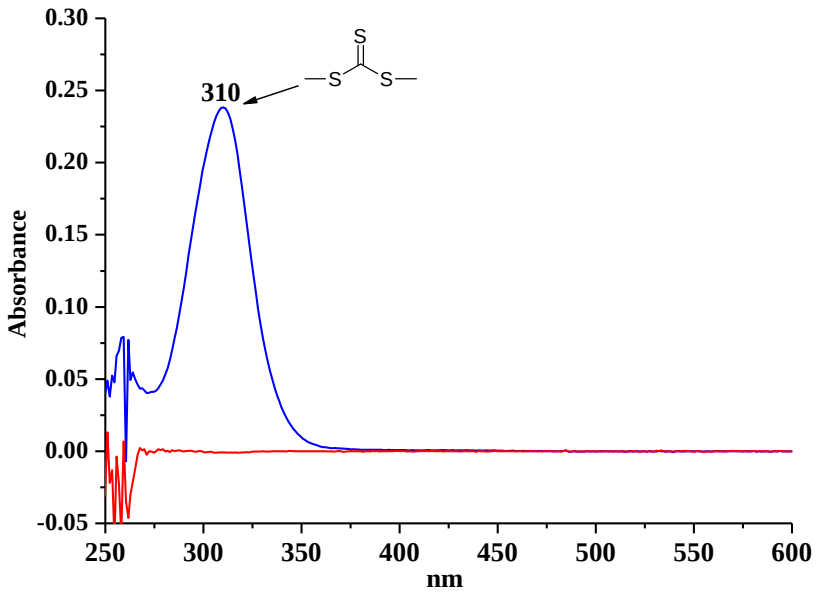

Figure A2.27: UV-Vis absorbance of **5c** (blue) and **6c** (red). UV-vis spectrum was recorded by UV-detector of THF GPC with the same concentration of polymers. The peak at 310 nm is attributed to RAFT moiety.

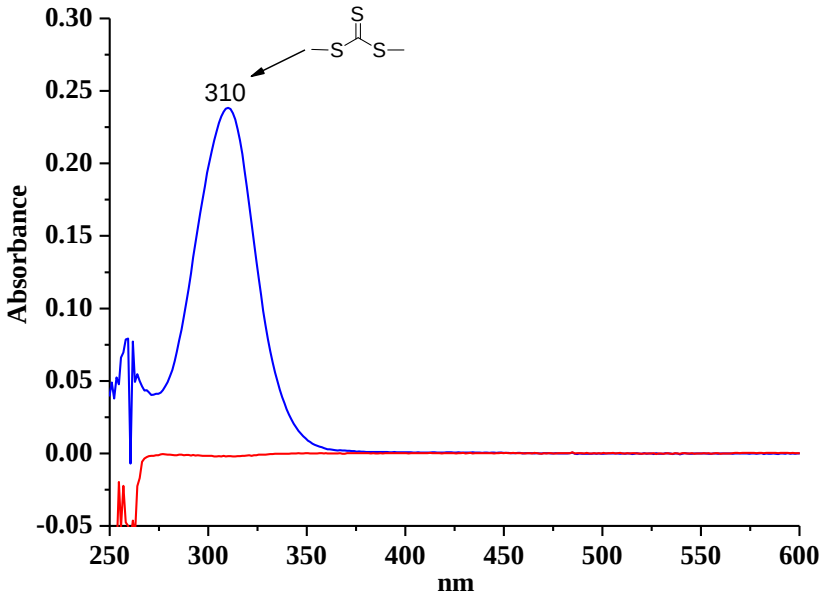

Figure A2.28: UV-vis absorbance of **5d** (blue) and **6d** (red). UV-vis spectrum was recorded by UV-detector of THF GPC with the same concentration of polymers. The peak at 310 nm is attributed to RAFT moiety.

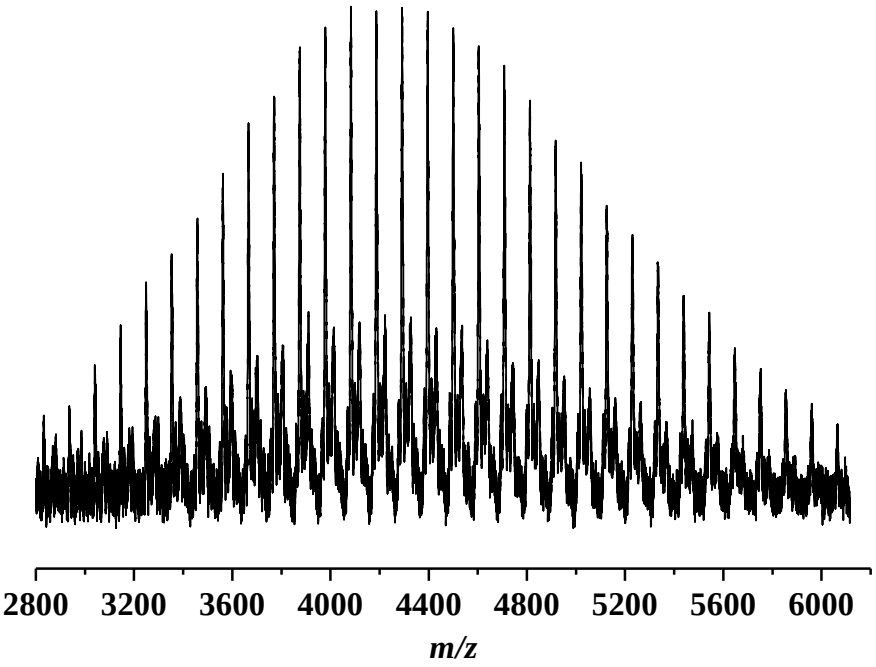

Figure A2.29: Full MALDI-ToF mass spectrum of **4a** with Ag(CF_3COO) as cationization agent from a DCTB matrix in reflectron mode.

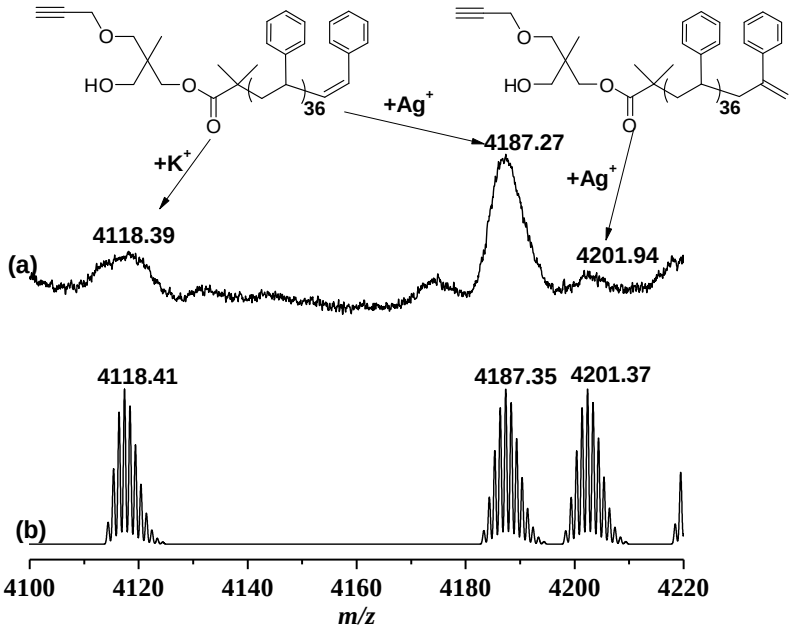

Figure A2.30: Expanded MALDI-ToF mass spectrum of **4a** with Ag(CF_3COO) as cationization agent from a DCTB matrix in reflectron mode. (a) experimental isotopic resolution of peaks (b) theoretical isotopic pattern of products.

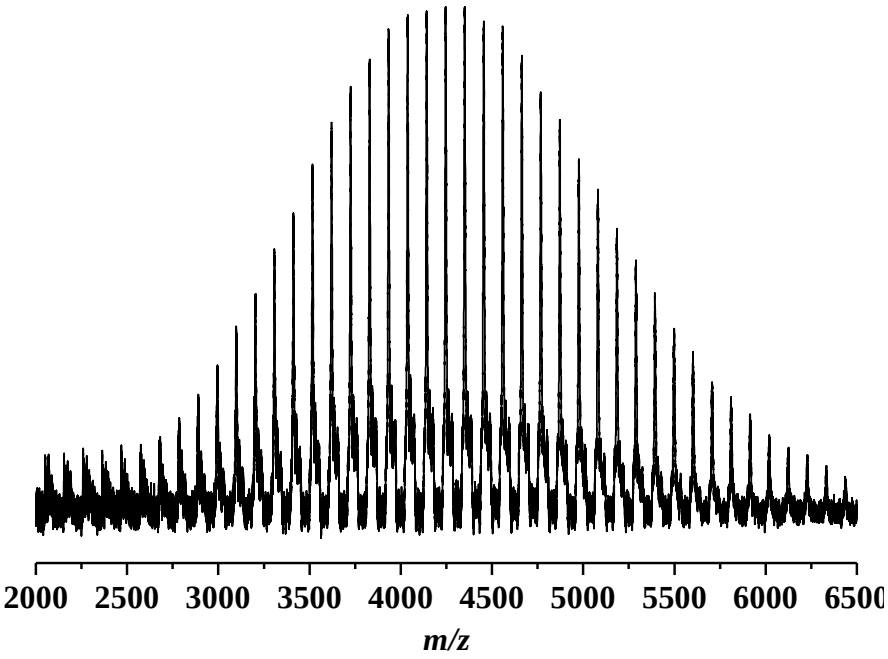

Figure A2.31: Full MALDI-ToF mass spectrum of **5a** with Ag(CF_3COO) as cationization agent from a DCTB matrix in reflectron mode.

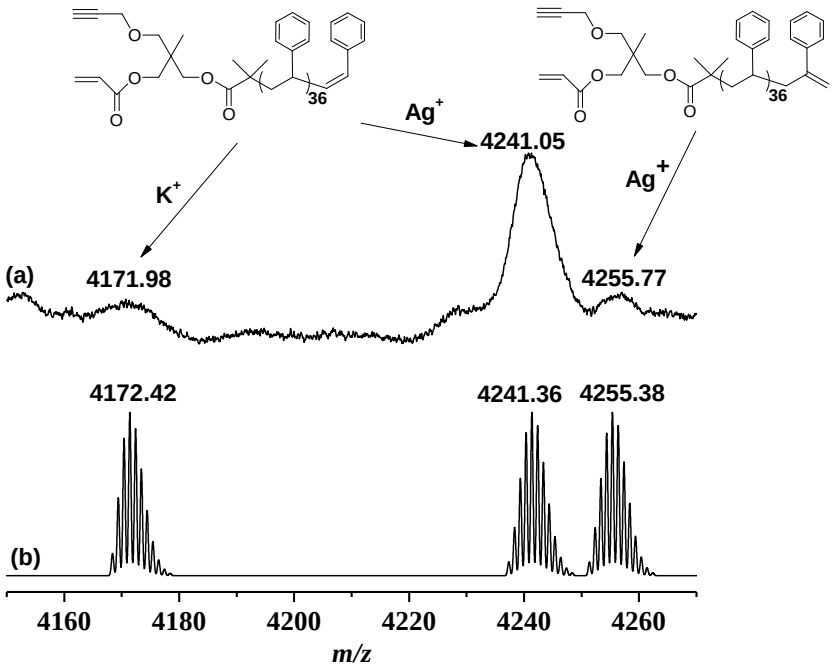

Figure A2.32: Expanded MALDI-ToF mass spectrum of **5a** with Ag(CF_3COO) as cationization agent from a DCTB matrix in reflectron mode. (a) experimental isotopic resolution of peaks (b) theoretical isotopic pattern of products.

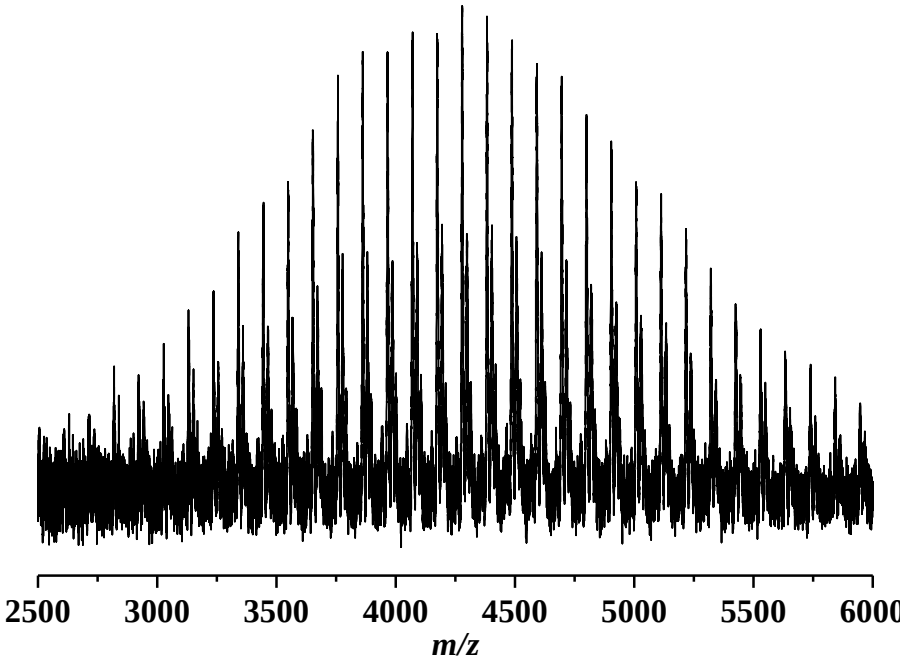

Figure A2.33: Full MALDI-ToF mass spectrum of **6a** with Ag(CF_3COO) as cationization agent from a DCTB matrix in reflectron mode.

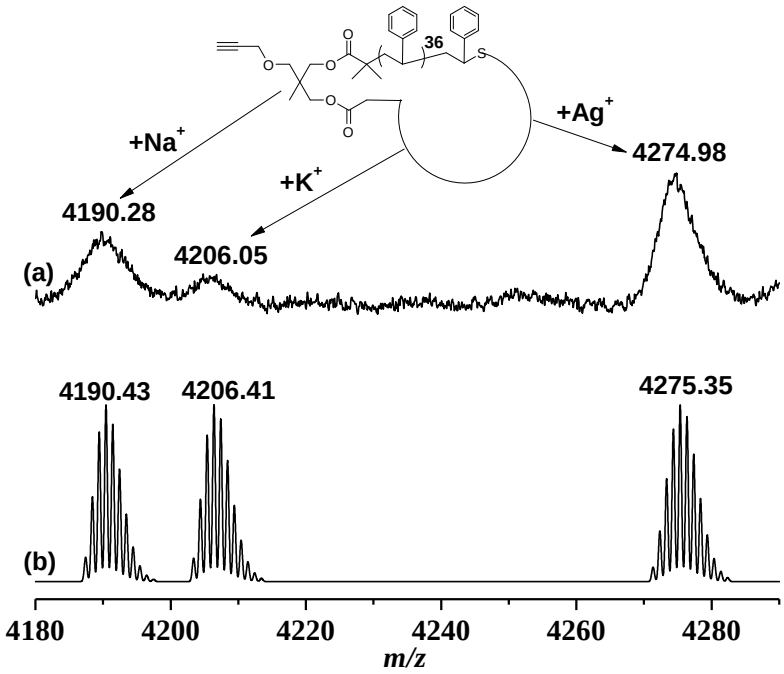

Figure A2.34: Expanded MALDI-ToF mass spectrum of **6a** with Ag(CF_3COO) as cationization agent from a DCTB matrix in reflectron mode. (a) experimental isotopic resolution of peaks (b) theoretical isotopic pattern of products.

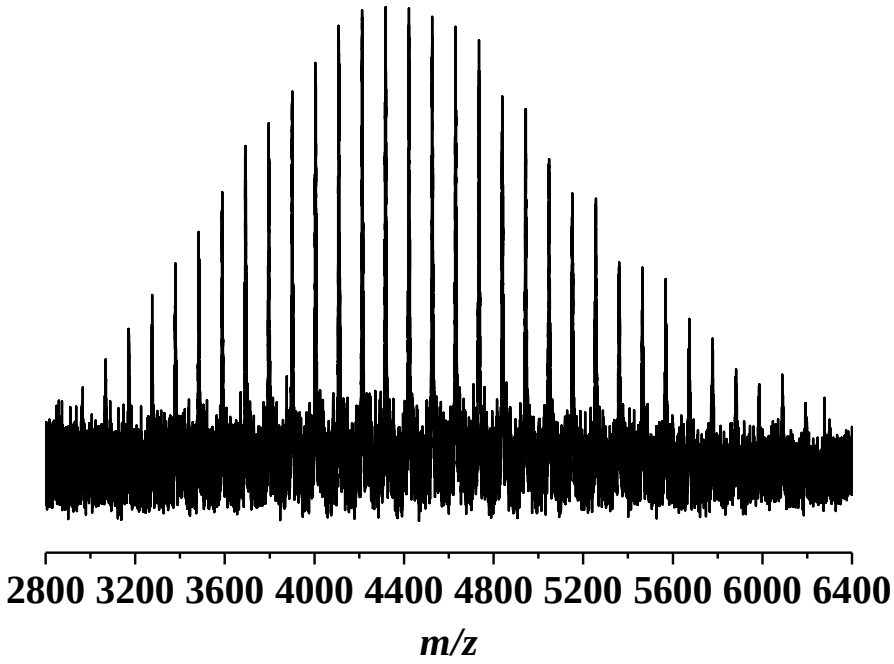

Figure A2.35: Full MALDI-ToF mass spectrum of **7a** with Ag(CF_3COO) as cationization agent from a DCTB matrix in reflectron mode.

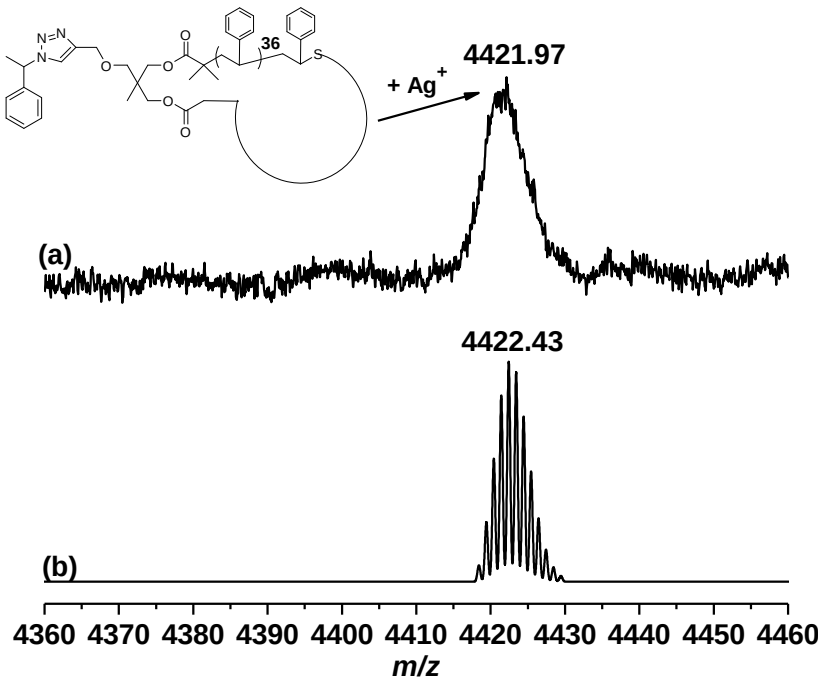

Figure A2.36: Expanded MALDI-ToF mass spectrum of **7a** with Ag(CF_3COO) as cationization agent from a DCTB matrix in reflectron mode. (a) experimental isotopic resolution of peaks (b) theoretical isotopic pattern of products.

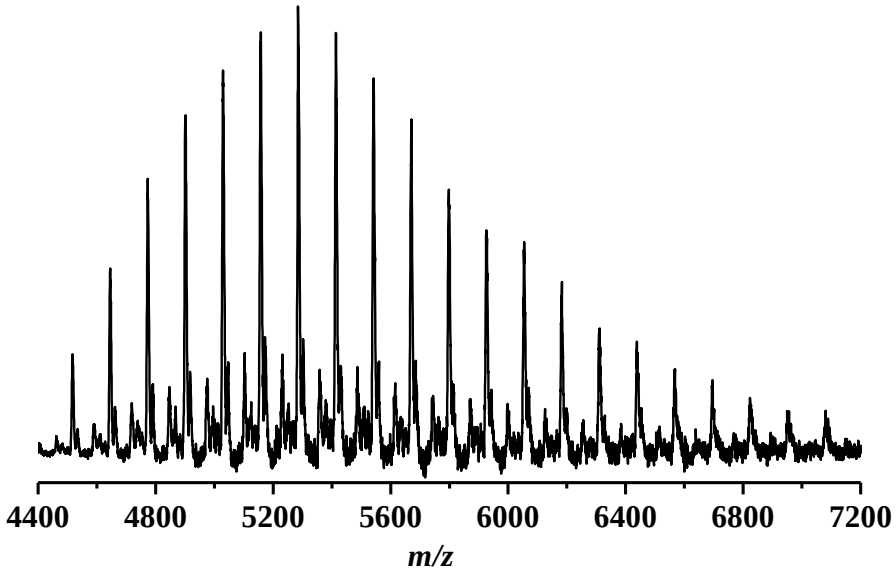

Figure A2.37: Full MALDI-ToF mass spectrum of **4b** with Na(CF_3COO) as cationization agent from a DCTB matrix in linear mode.

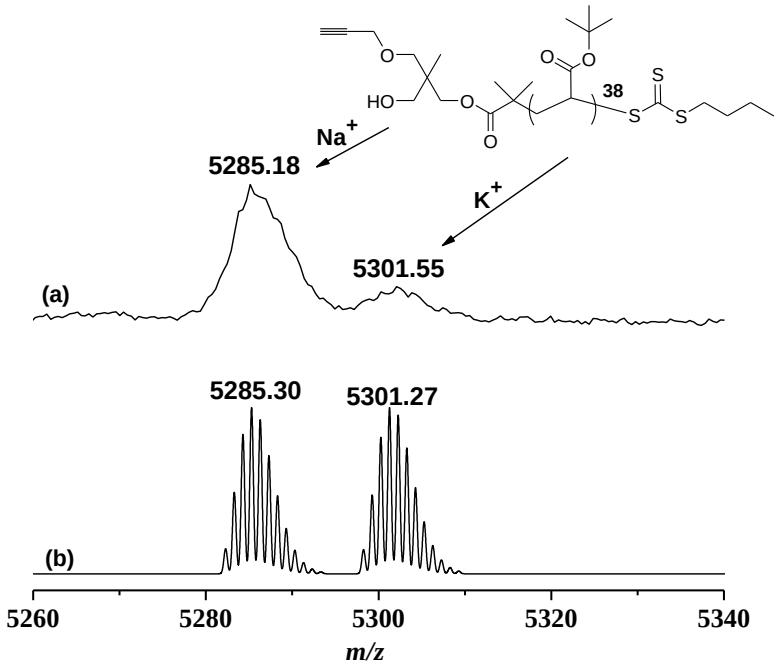

Figure A2.38: Expanded MALDI-ToF mass spectrum of **4b** with Na(CF_3COO) as cationization agent from a DCTB matrix in linear mode. (a) experimental isotopic resolution of peaks (b) theoretical isotopic pattern of products.

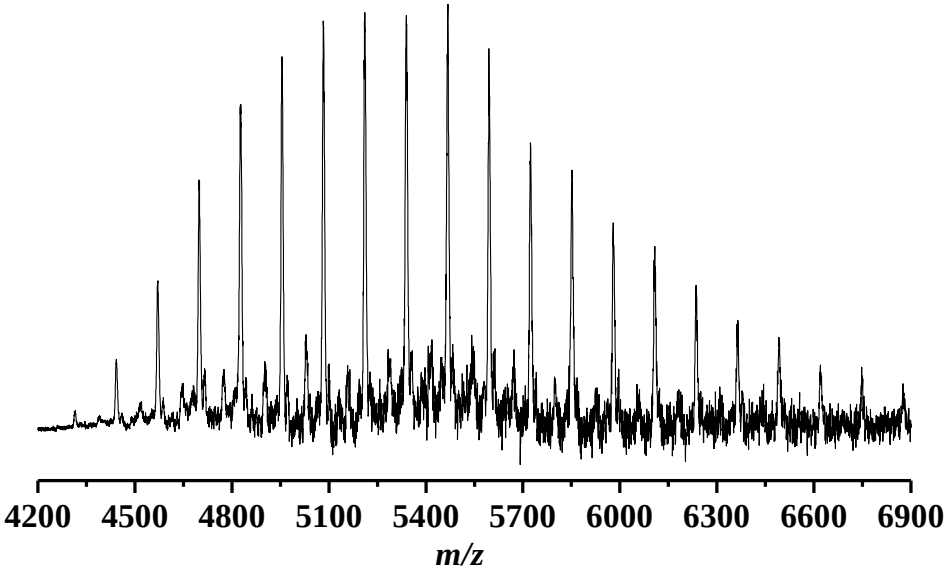

Figure A2.39: Full MALDI-ToF mass spectrum of **5b** with Na(CF_3COO) as cationization agent from a DCTB matrix in linear mode.

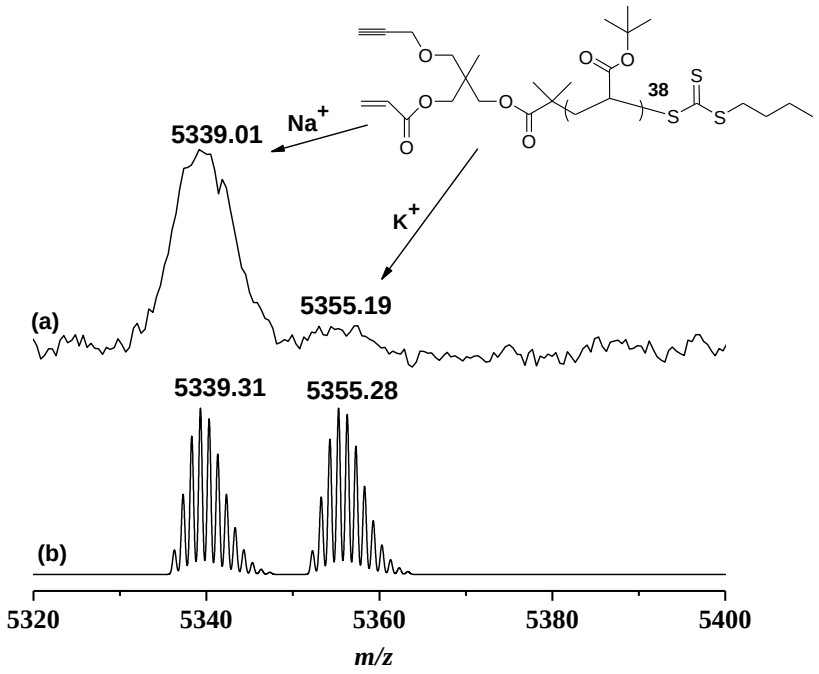

Figure A2.40: Expanded MALDI-ToF mass spectrum of **5b** with Na(CF_3COO) as cationization agent from a DCTB matrix in linear mode. (a) experimental isotopic resolution of peaks (b) theoretical isotopic pattern of products.

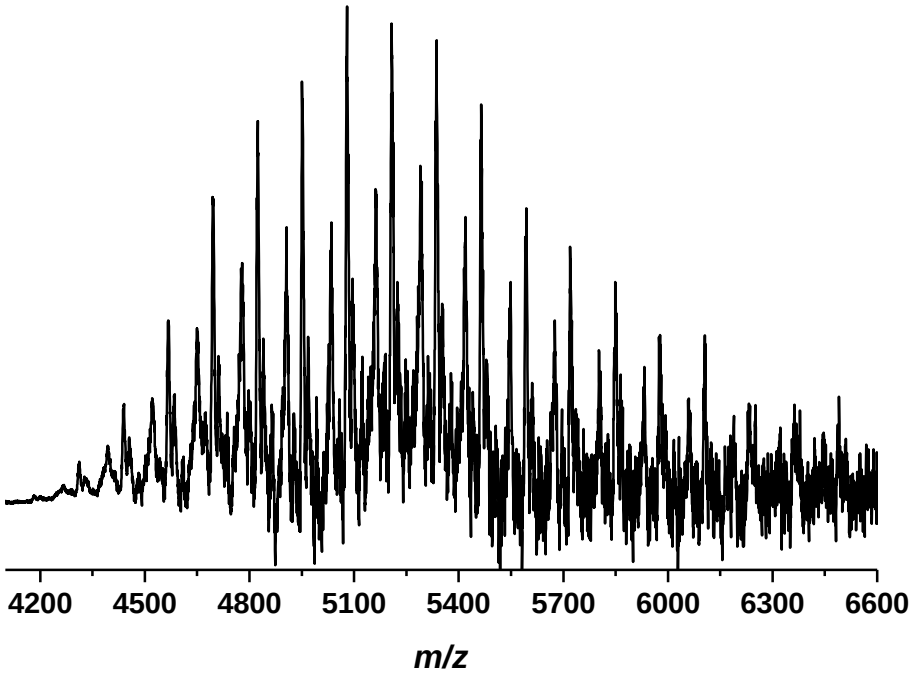

Figure A2.41: Full MALDI-ToF mass spectrum of **6b** with Na(CF_3COO) as cationization agent from a DCTB matrix in linear mode.

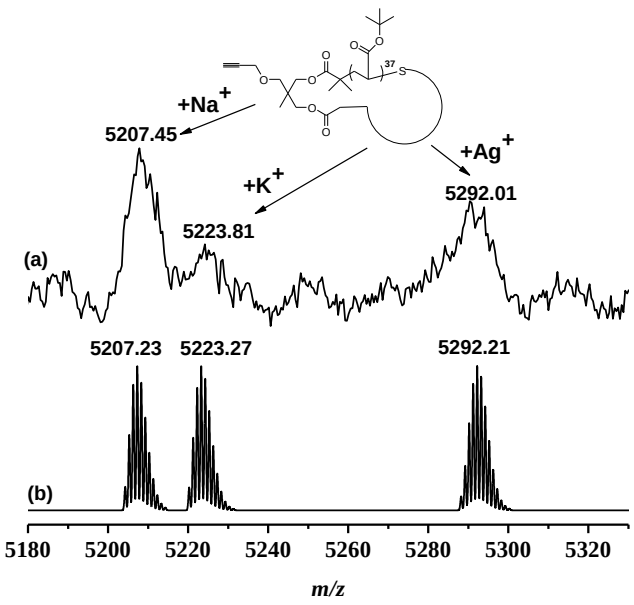

Figure A2.42: Expanded MALDI-ToF mass spectrum of **6b** with Na(CF_3COO) as cationization agent from a DCTB matrix in reflectron mode. (a) experimental isotopic resolution of peaks (b) theoretical isotopic pattern of products.

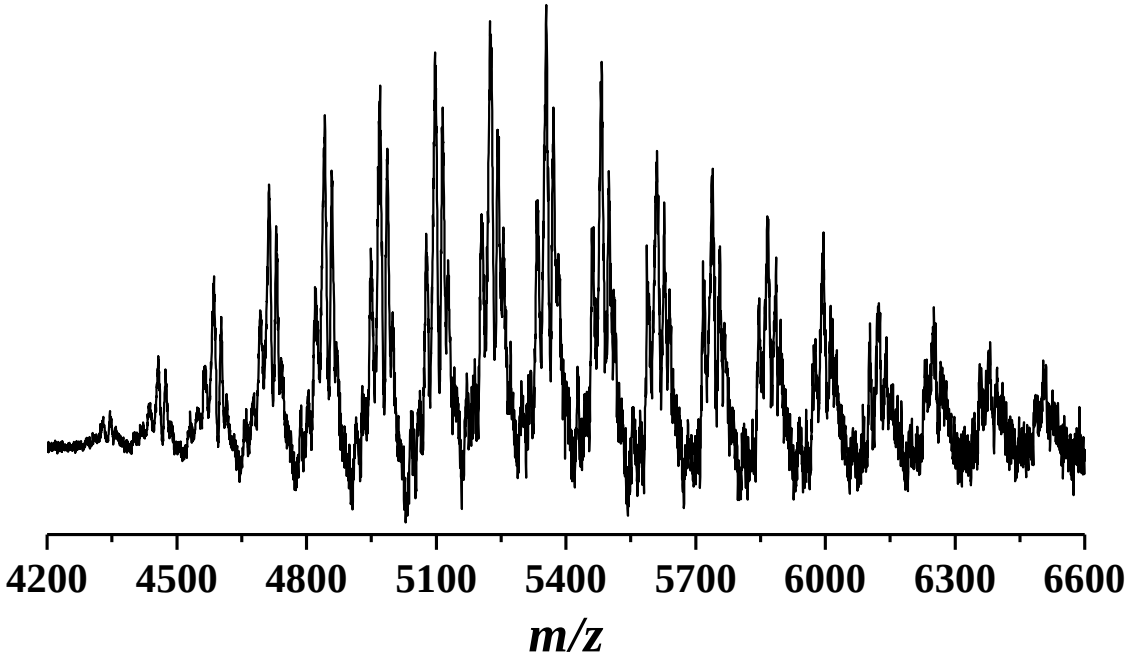

Figure A2.43: Full MALDI-ToF mass spectrum of **7b** with Na(CF_3COO) as cationization agent from a DCTB matrix in linear mode.

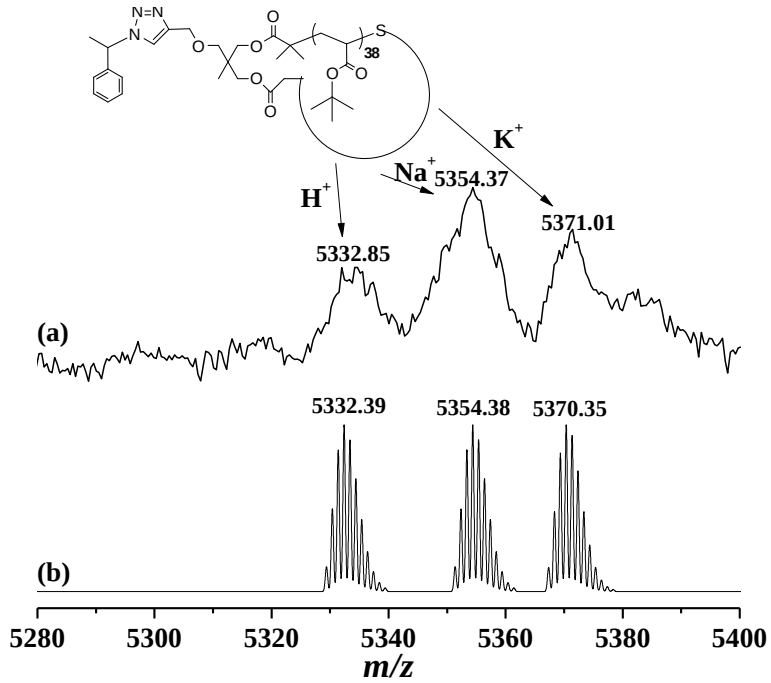

Figure A2.44: Expanded MALDI-ToF mass spectrum of **7b** with Na(CF_3COO) as cationization agent from a DCTB matrix in linear mode. (a) experimental isotopic resolution of peaks (b) theoretical isotopic pattern of products.

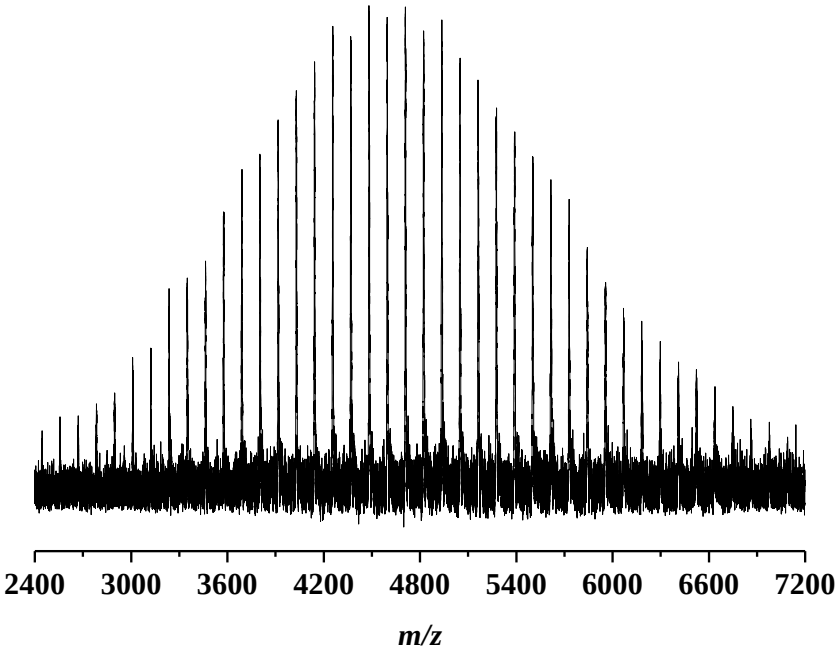

Figure A2.45: Full MALDI-ToF mass spectrum of **4c** with Na(CF_3COO) as cationization agent from a DCTB matrix in reflectron mode.

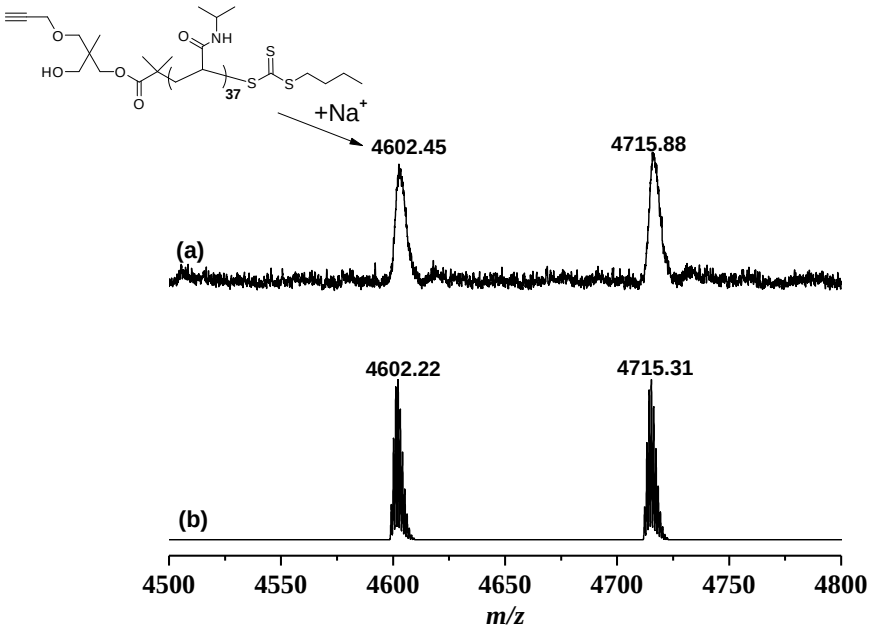

Figure A2.46: Expanded MALDI-ToF mass spectrum of **4c** with Na(CF_3COO) as cationization agent from a DCTB matrix in reflectron mode. (a) experimental isotopic resolution of peaks (b) theoretical isotopic pattern of products.

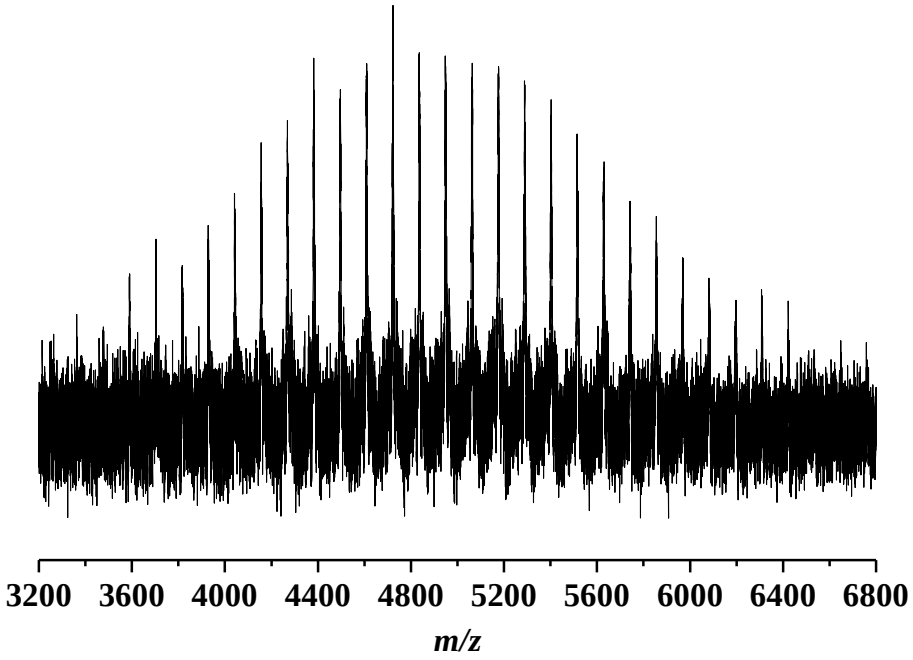

Figure A2.47: Full MALDI-ToF mass spectrum of **5c** with Na(CF_3COO) as cationization agent from a DCTB matrix in reflectron mode.

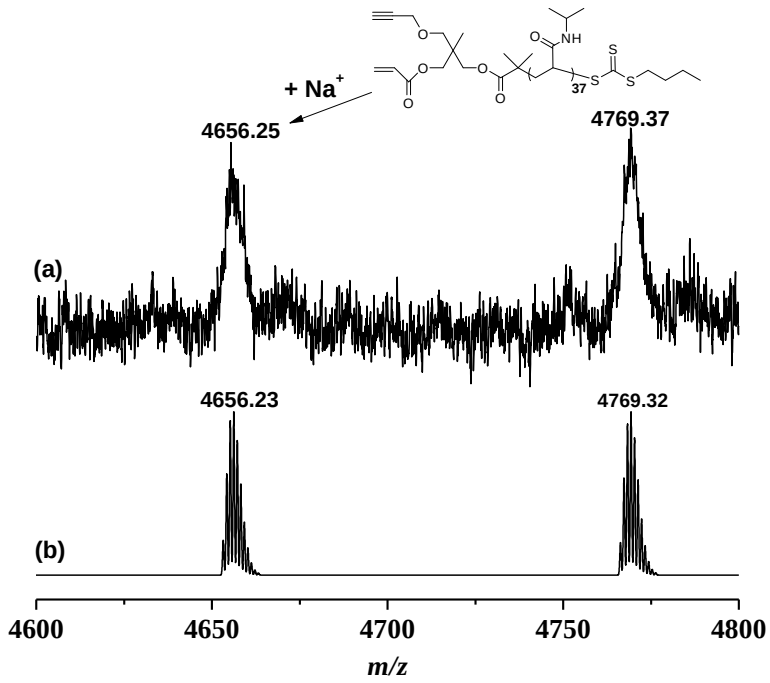

Figure A2.48: Expanded MALDI-ToF mass spectrum of **5c** with Na(CF_3COO) as cationization agent from a DCTB matrix in reflectron mode. (a) experimental isotopic resolution of peaks (b) theoretical isotopic pattern of products.

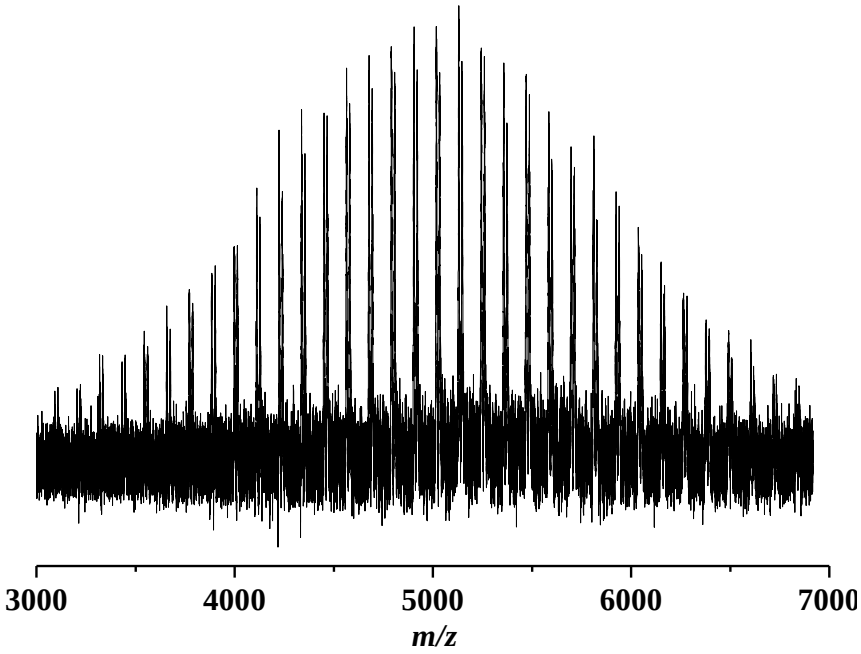

Figure A2.49: Full MALDI-ToF mass spectrum of **6c** with Na(CF_3COO) as cationization agent from a DCTB matrix in reflectron mode.

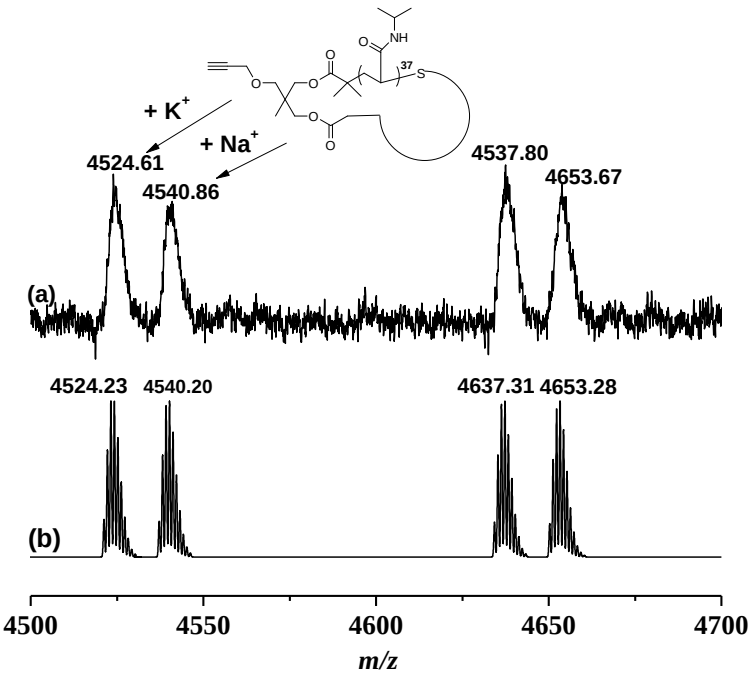

Figure A2.50: Expanded MALDI-ToF mass spectrum of **6c** with Na(CF_3COO) as cationization agent from a DCTB matrix in reflectron mode. (a) experimental isotopic resolution of peaks (b) theoretical isotopic pattern of products.

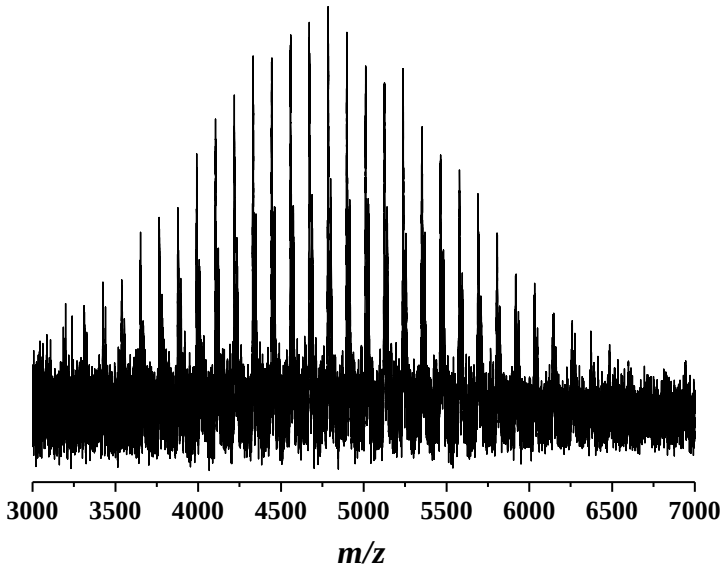

Figure A2.51: Full MALDI-ToF mass spectrum of **7c** with Na(CF_3COO) as cationization agent from a DCTB matrix in reflectron mode.

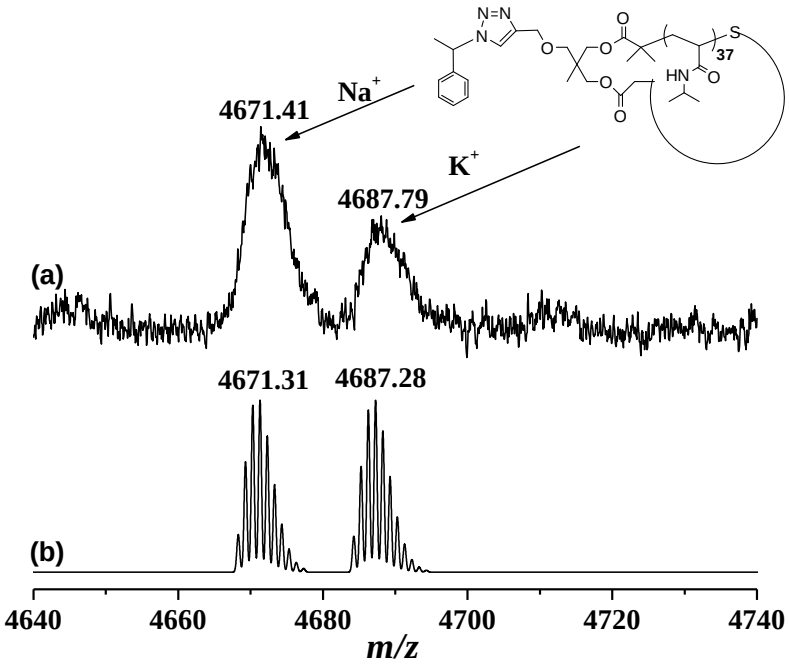

Figure A2.52: Expanded MALDI-ToF mass spectrum of **7c** with Na(CF_3COO) as cationization agent from a DCTB matrix in reflectron mode. (a) experimental isotopic resolution of peaks (b) theoretical isotopic pattern of products.

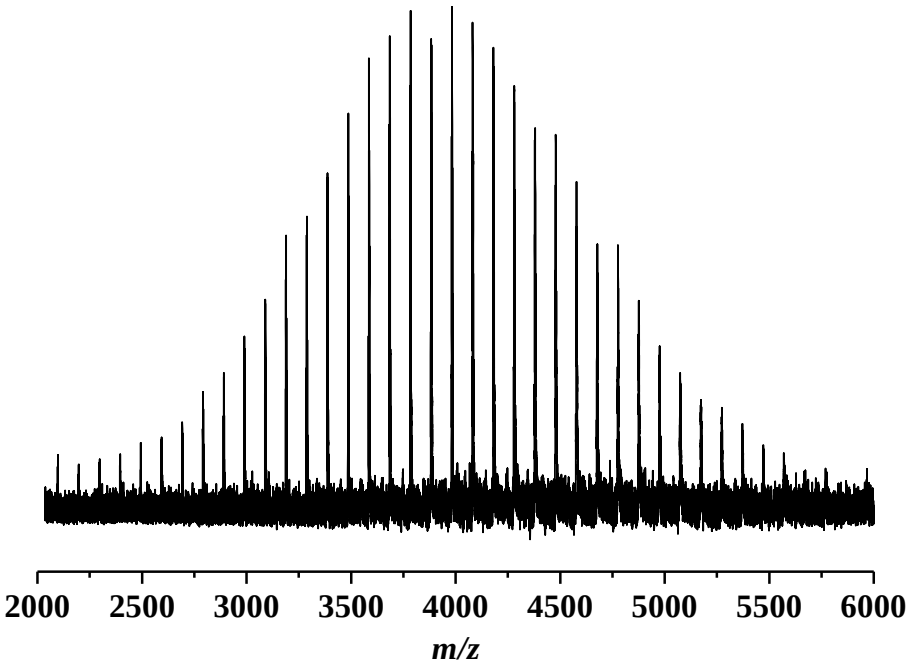

Figure A2.53: Full MALDI-ToF mass spectrum of **4d** with Na(CF_3COO) as cationization agent from a DCTB matrix in reflectron mode.

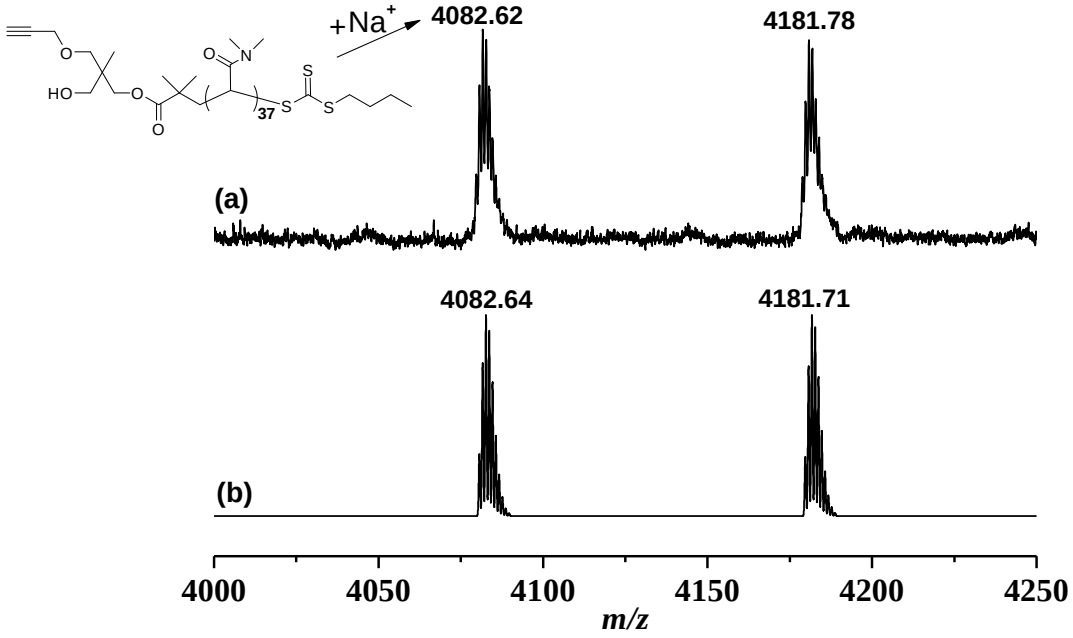

Figure A2.54: Expanded MALDI-ToF mass spectrum of **4d** with Na(CF_3COO) as cationization agent from a DCTB matrix in reflectron mode. (a) experimental isotopic resolution of peaks (b) theoretical isotopic pattern of products.

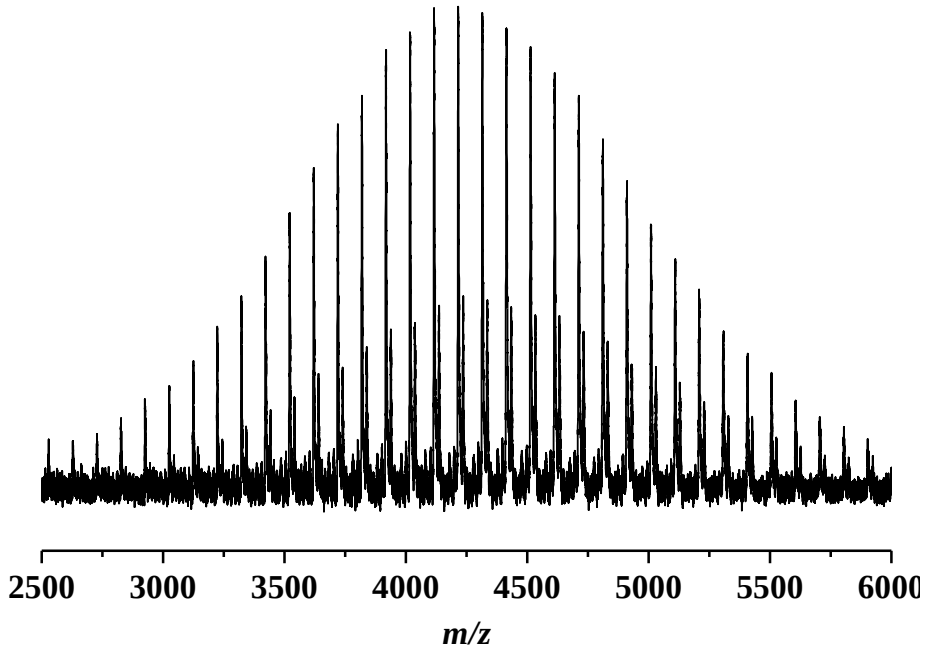

Figure A2.55: Full MALDI-ToF mass spectrum of **5d** with Na(CF_3COO) as cationization agent from a DCTB matrix in reflectron mode.

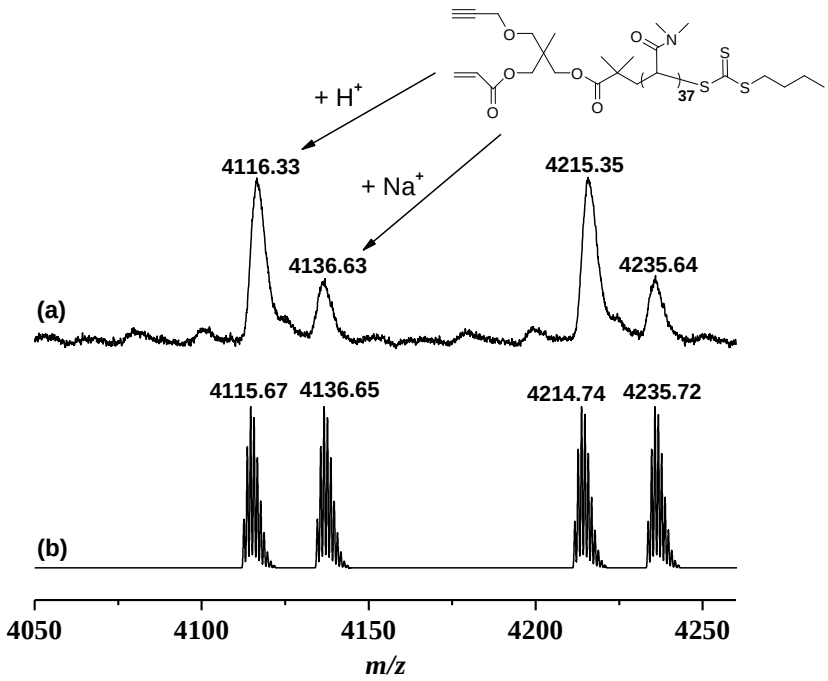

Figure A2.56: Expanded MALDI-ToF mass spectrum of **5d** with Na(CF_3COO) as cationization agent from a DCTB matrix in reflectron mode. (a) experimental isotopic resolution of peaks (b) theoretical isotopic pattern of products.

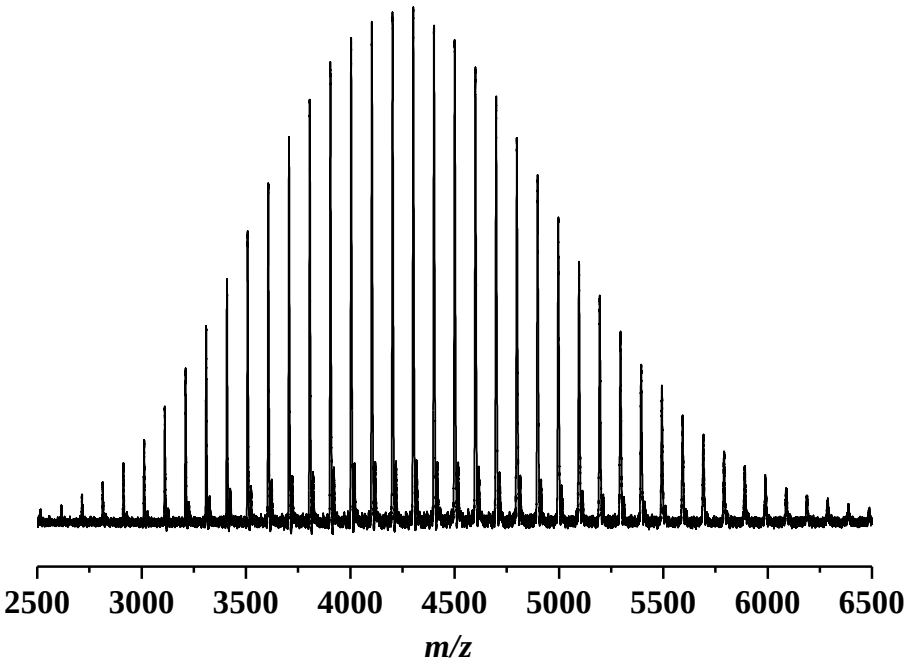

Figure A2.57: Full MALDI-ToF mass spectrum of **6d** with Na(CF_3COO) as cationization agent from a DCTB matrix in reflectron mode.

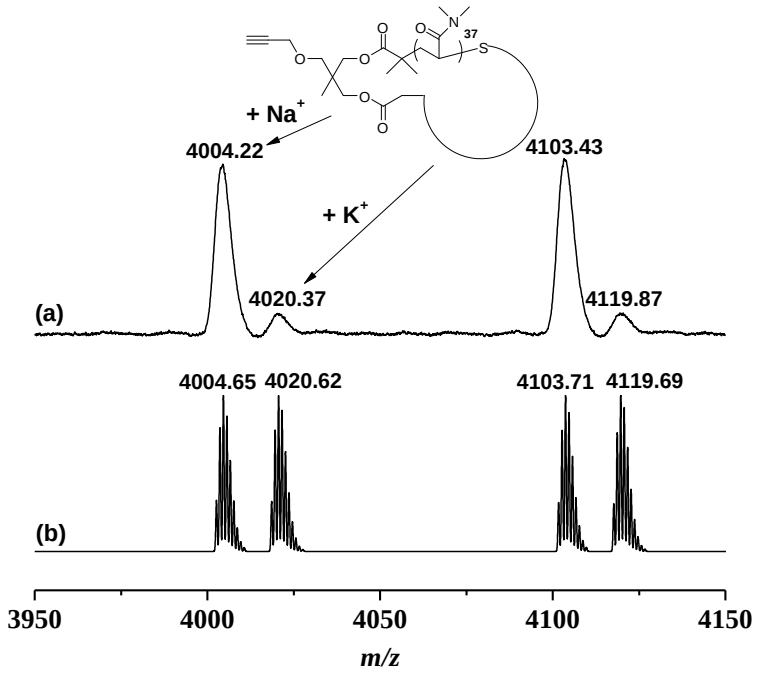

Figure A2.58: Expanded MALDI-ToF mass spectrum of **6d** with Na(CF_3COO) as cationization agent from a DCTB matrix in reflectron mode. (a) experimental isotopic resolution of peaks (b) theoretical isotopic pattern of products.

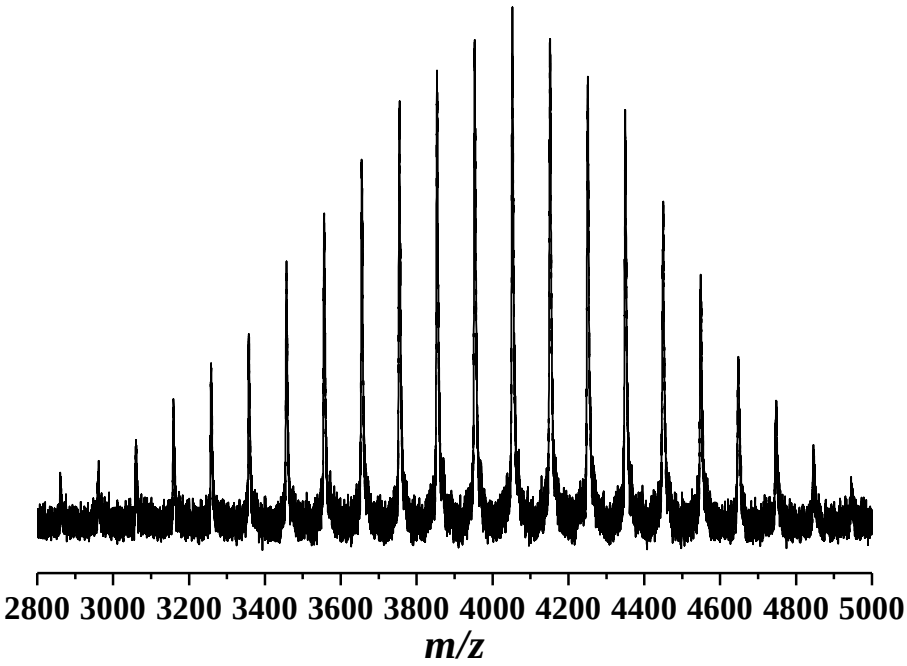

Figure A2.59: Full MALDI-ToF mass spectrum of **7d** with Na(CF_3COO) as cationization agent from a DCTB matrix in reflectron mode.

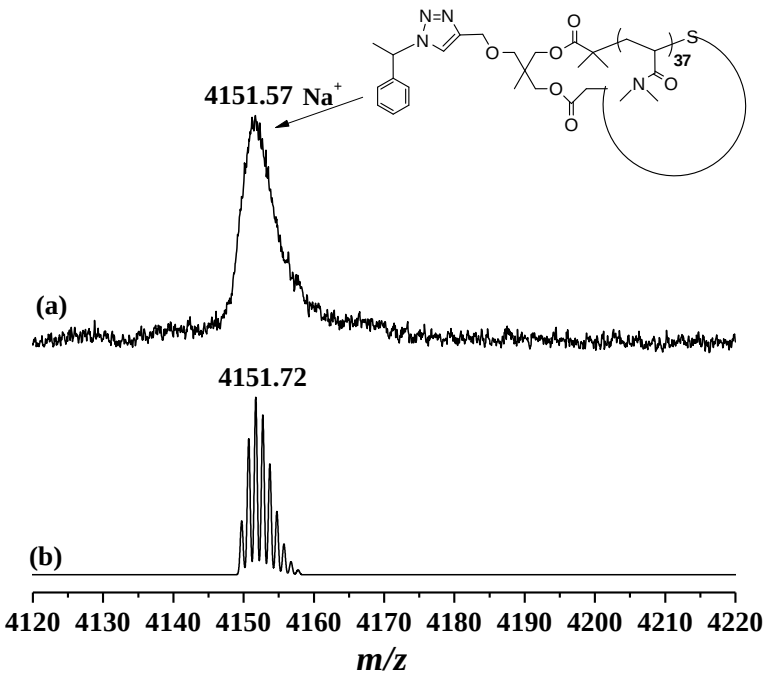

Figure A2.60: Expanded MALDI-ToF mass spectrum of **7d** with Na(CF_3COO) as cationization agent from a DCTB matrix in reflectron mode. (a) experimental isotopic resolution of peaks (b) theoretical isotopic pattern of products.

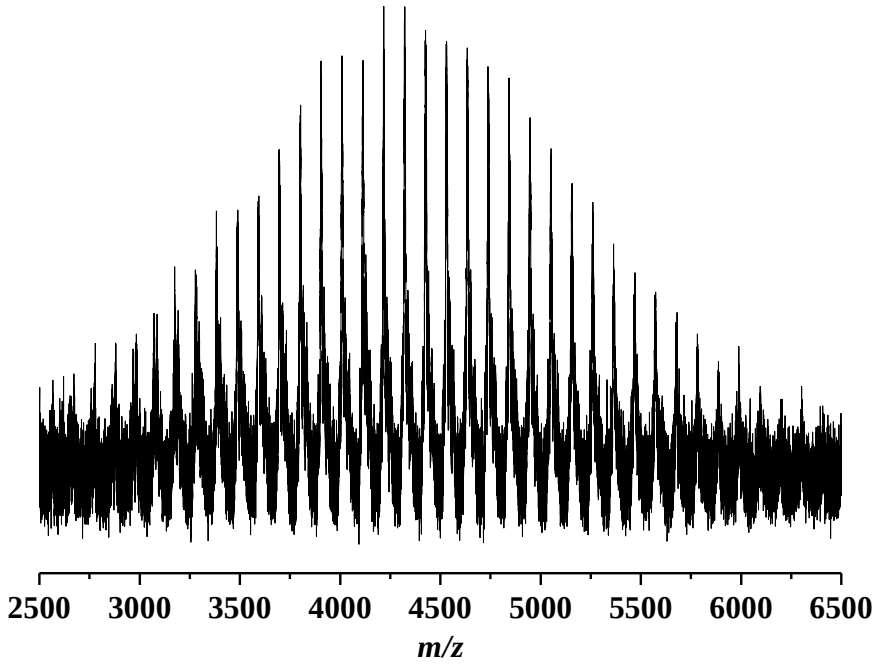

Figure A2.61: Full MALDI-ToF mass spectrum of **8** with Ag(CF_3COO) as cationization agent from a DCTB matrix in reflectron mode.

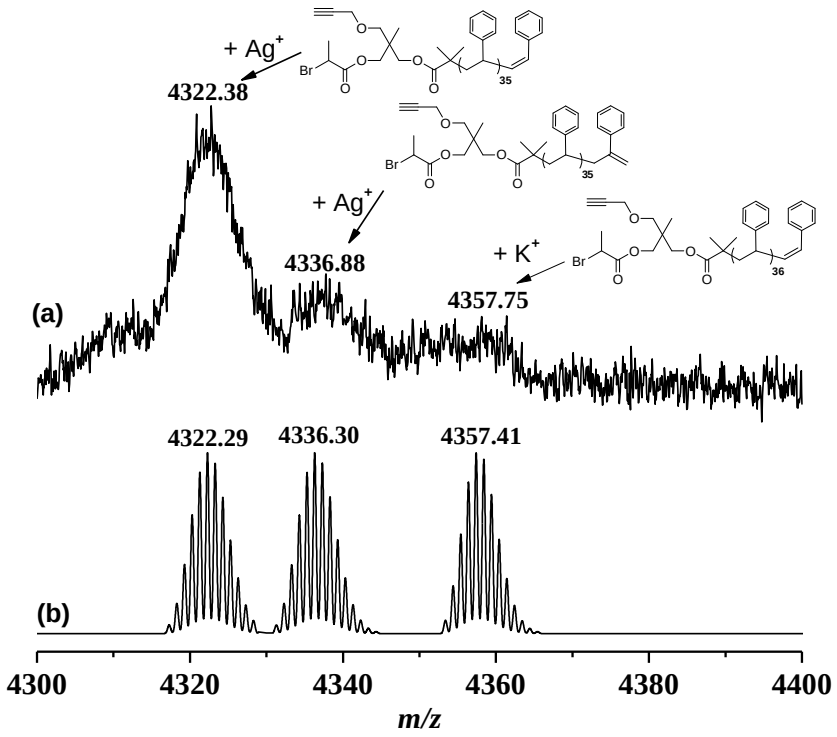

Figure A2.62: Expanded MALDI-ToF mass spectrum of **8** with Ag(CF_3COO) as cationization agent from a DCTB matrix in reflectron mode. (a) experimental isotopic resolution of peaks (b) theoretical isotopic pattern of products.

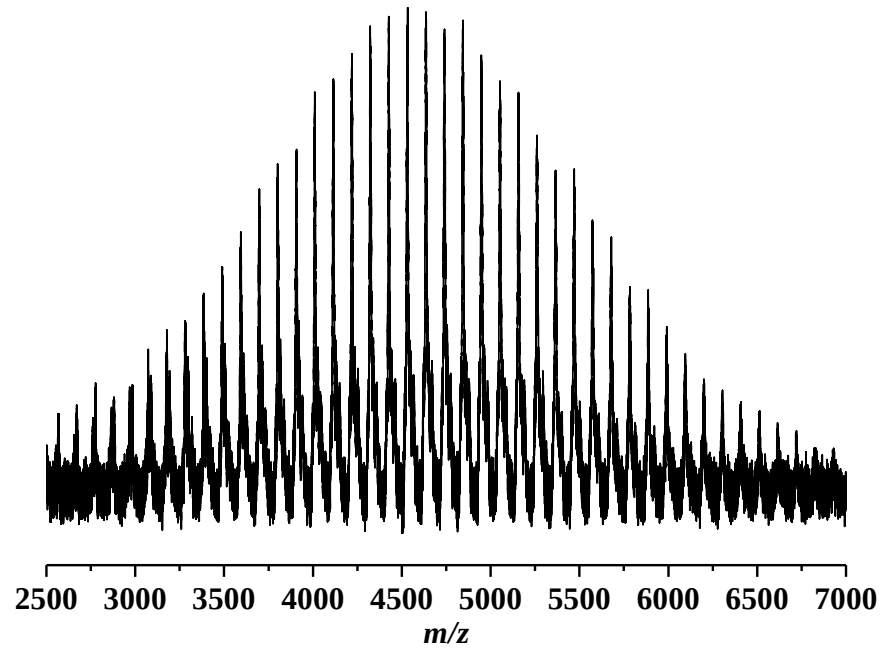

Figure A2.63: Full MALDI-ToF mass spectrum of **11** with Ag(CF_3COO) as cationization agent from a DCTB matrix in reflectron mode.

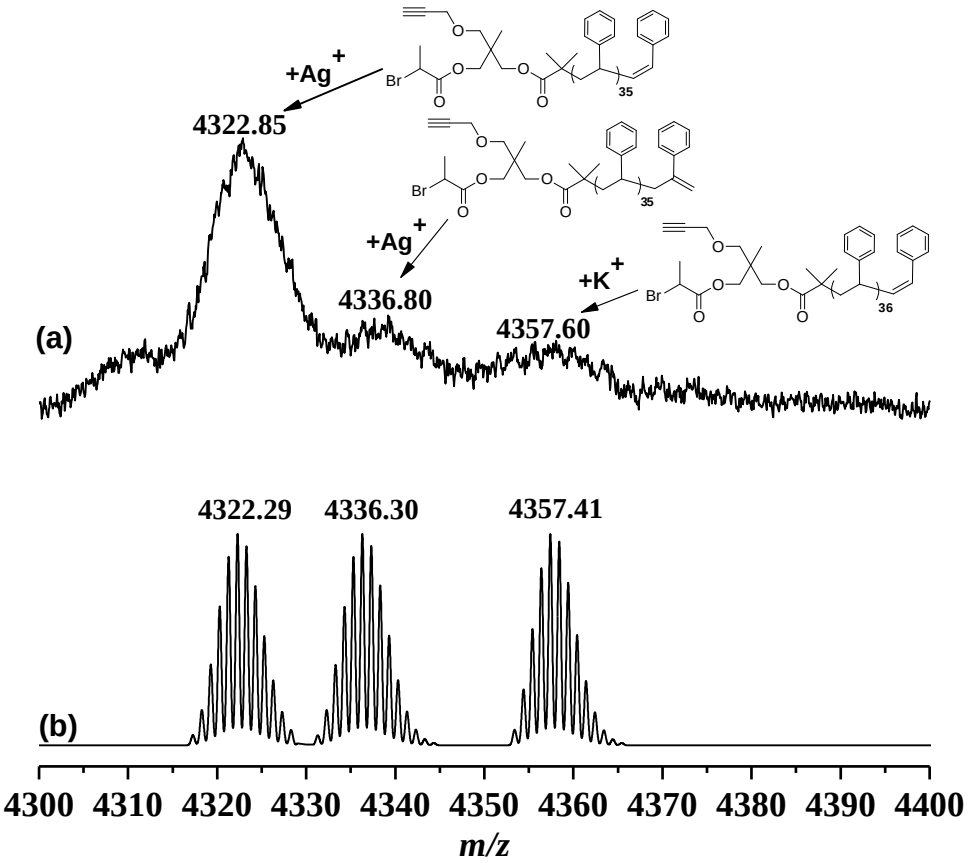

Figure A2.64: Expanded MALDI-ToF mass spectrum of **11** with Ag(CF_3COO) as cationization agent from a DCTB matrix in reflectron mode. (a) experimental isotopic resolution of peaks (b) theoretical isotopic pattern of products.

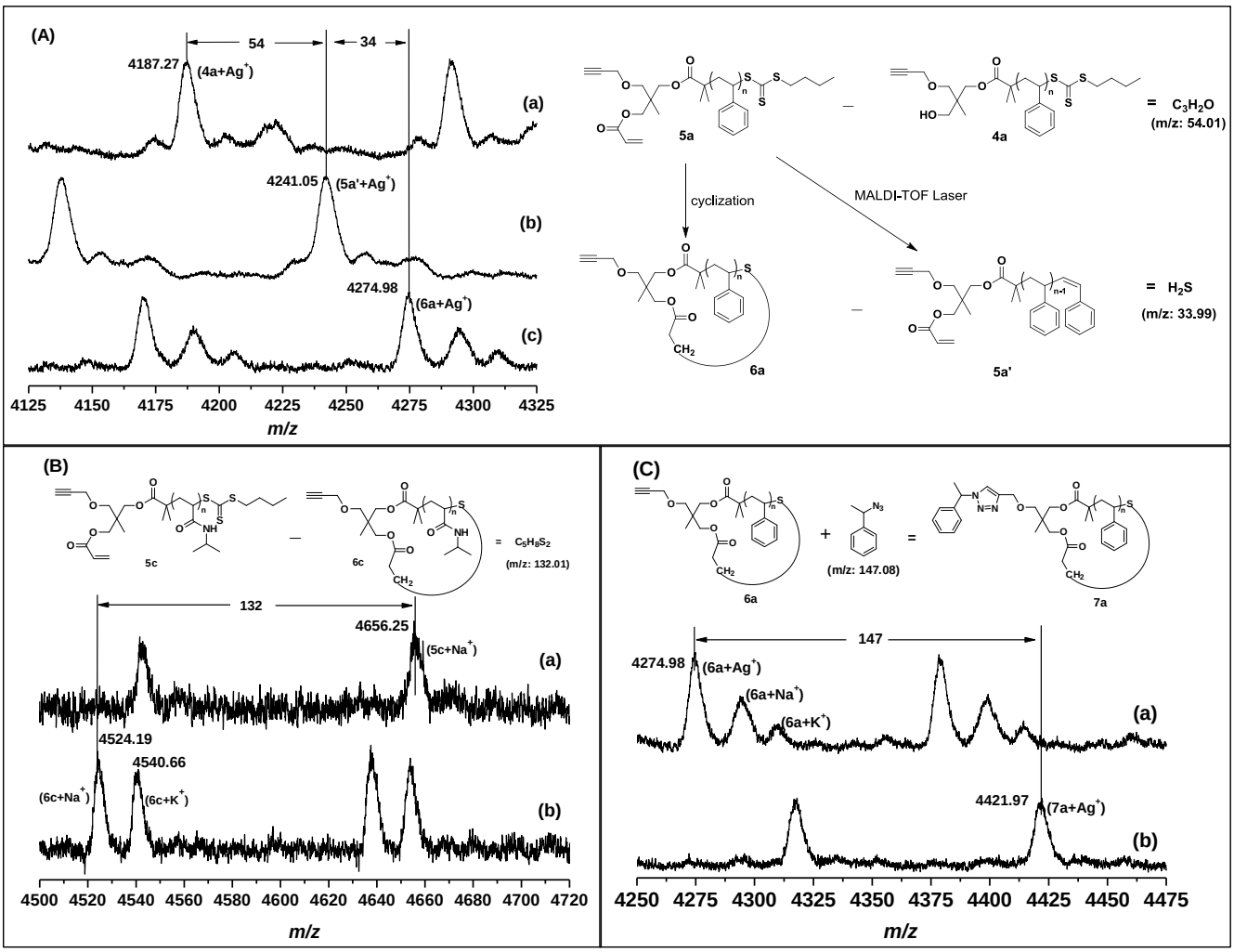

Figure A2.65: Expanded MALDI-TOF mass spectra comparison, for **4a**, **5a**, **6a** and **7a**, the spectra were acquired with Ag(CF_3COO) as cationization agent, for **5c** and **6c** with Na(CF_3COO) as cationization agent, and DCTB matrix in reflectron mode. (A) PSTY **4a** (a), PSTY **5a'** (b), and PSTY **6a** (c); (B) PNIPAm **5c** (a) and PNIPAm **6c** (b); and (C) PSTY **6a** (a) and PSTY **7a** (b). The schemes in the figure illustrated the formula change after the end-group modification and cyclization.

Appendix B

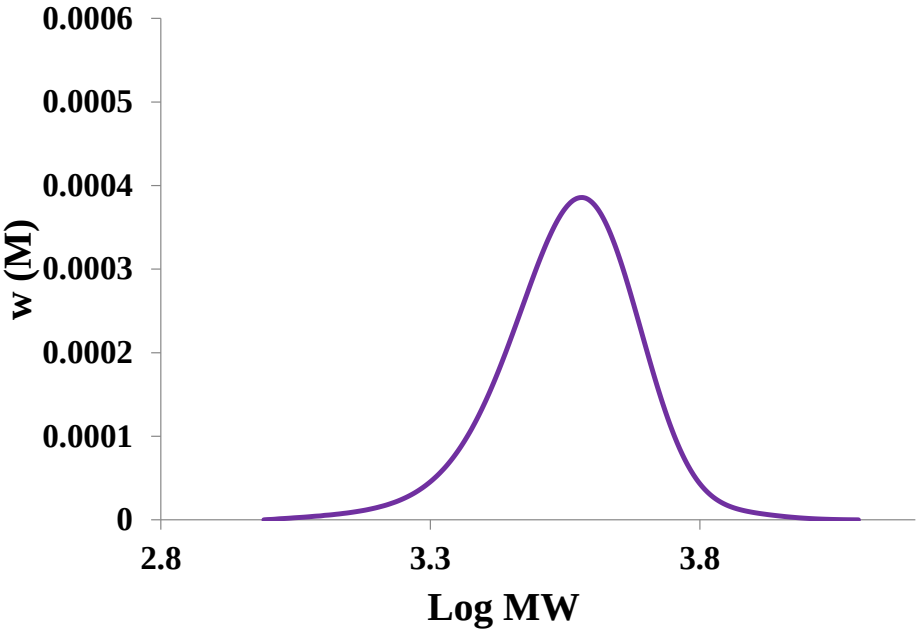

Figure A3.1:SEC trace of PSTY-Br (**1**). Determined from THF SEC, RI detector, PSTY standard.

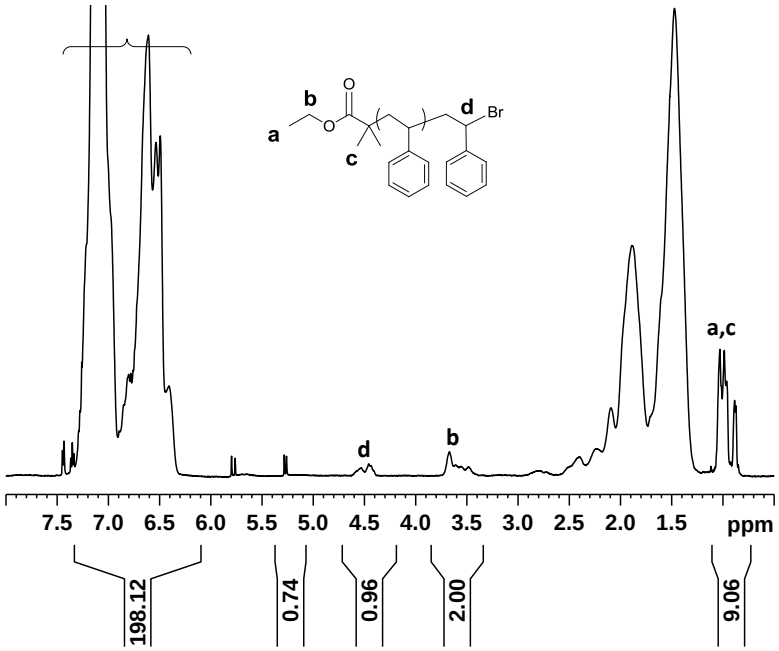

Figure A3.2: ^{1}H NMR spectrum of PSTY-Br (**1**),recorded in $CDCl_3$ at 298K , 500MHz, *=residual styrene monomer.

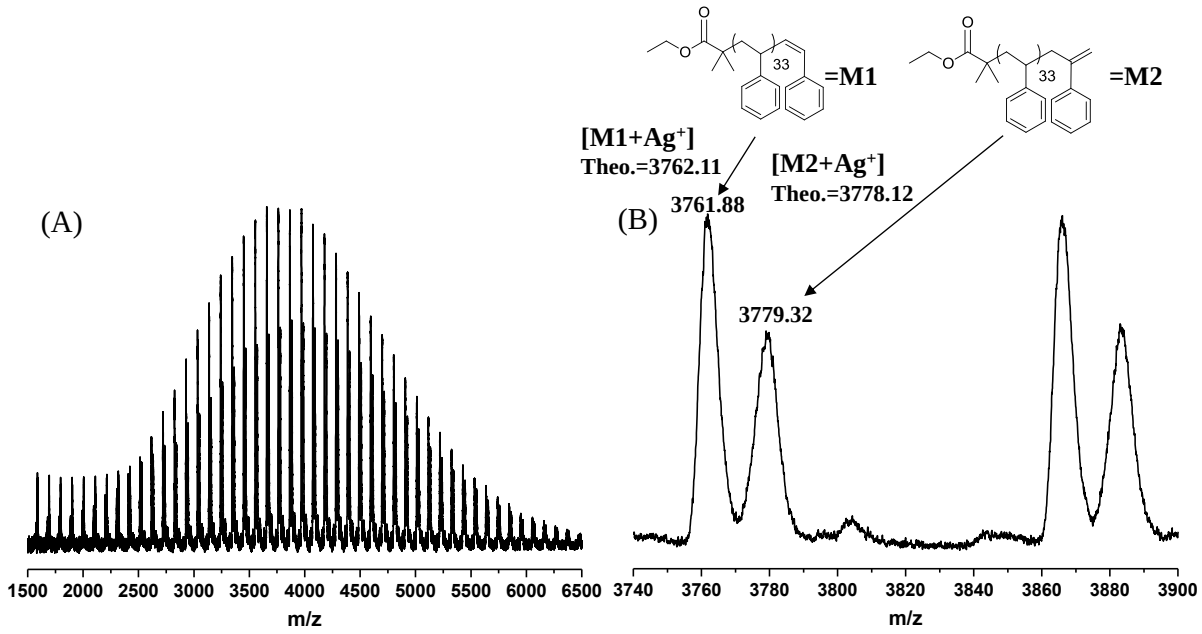

Figure A3.3:The full (A) and expanded (B) MALDI-TOF mass spectra of PSTY-Br (**1**). The spectra were recorded in reflect mode using DCTB as the matrix and $AgCF_3COO$ as the cation source.

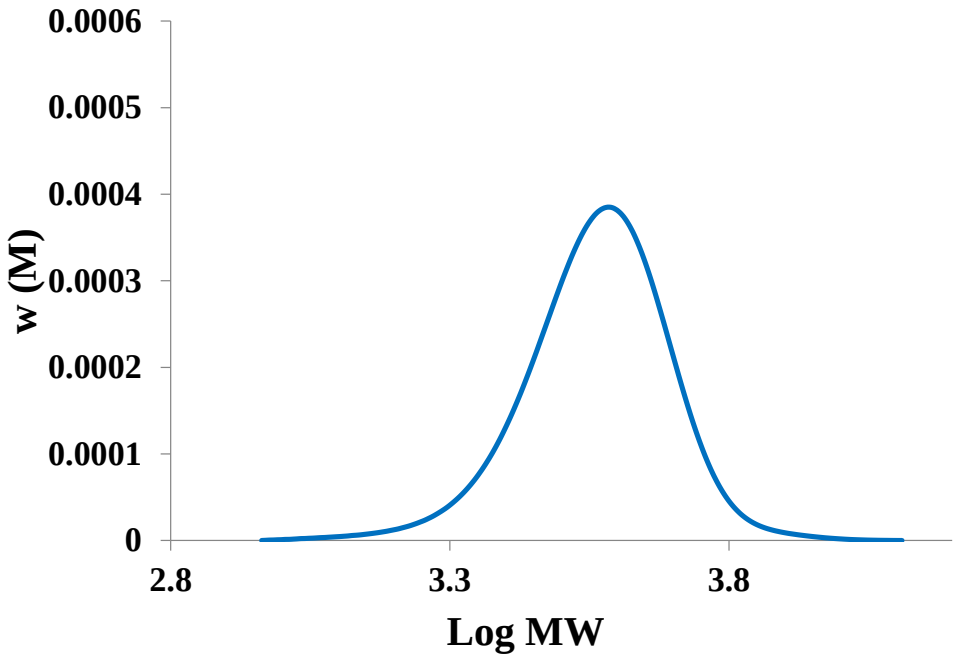

Figure A3.4: SEC trace and LND simulation of PSTY-N_3 (**2**). Determined from THF SEC, RI detector, PSTY standard.

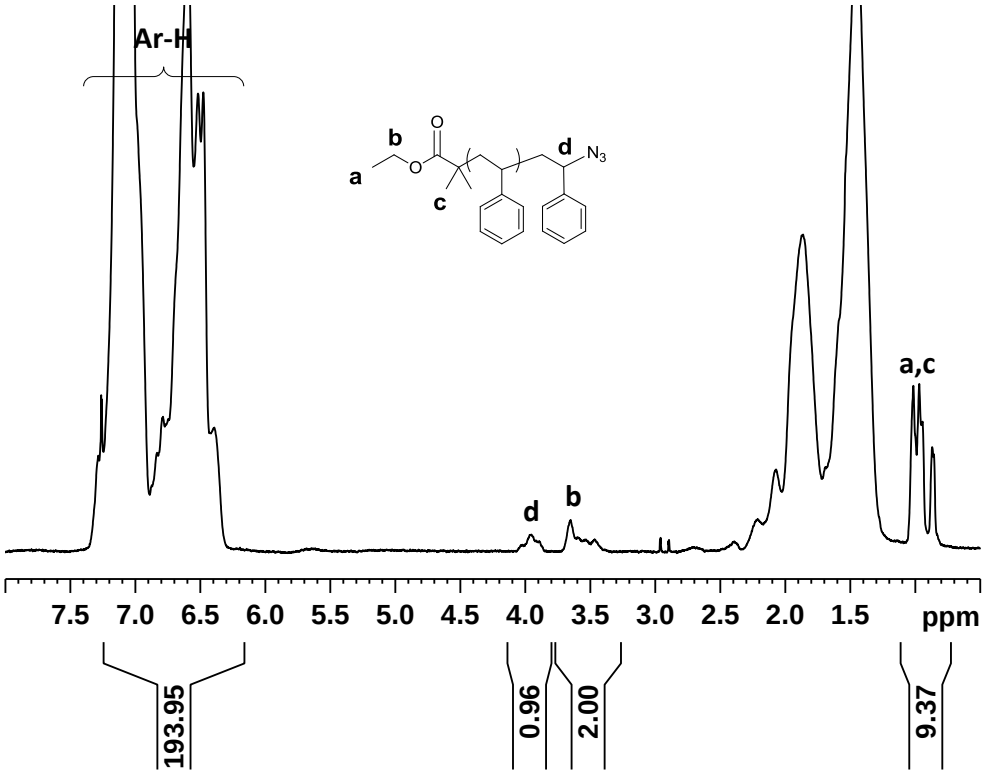

Figure A3.5: ^{1}H NMR spectrum of PSTY-N_3 (**2**),recorded in $CDCl_3$ at 298K , 500MHz.

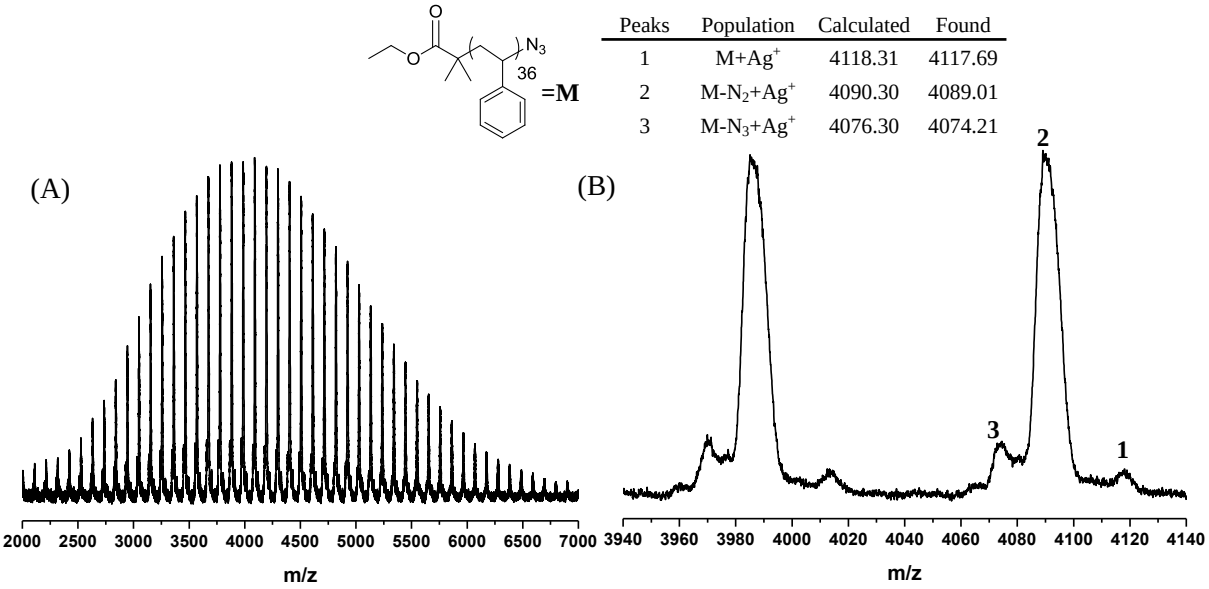

Peaks	Population	Calculated	Found
1	$M+Ag^+$	4118.31	4117.69
2	$M-N_2+Ag^+$	4090.30	4089.01
3	$M-N_3+Ag^+$	4076.30	4074.21

Figure A3.6:The full (A) and expanded (B) MALDI-TOF mass spectra of PSTY-N_3 (**2**). The spectra were recorded in reflect mode using DCTB as the matrix and $AgCF_3COO$ as the cation source.

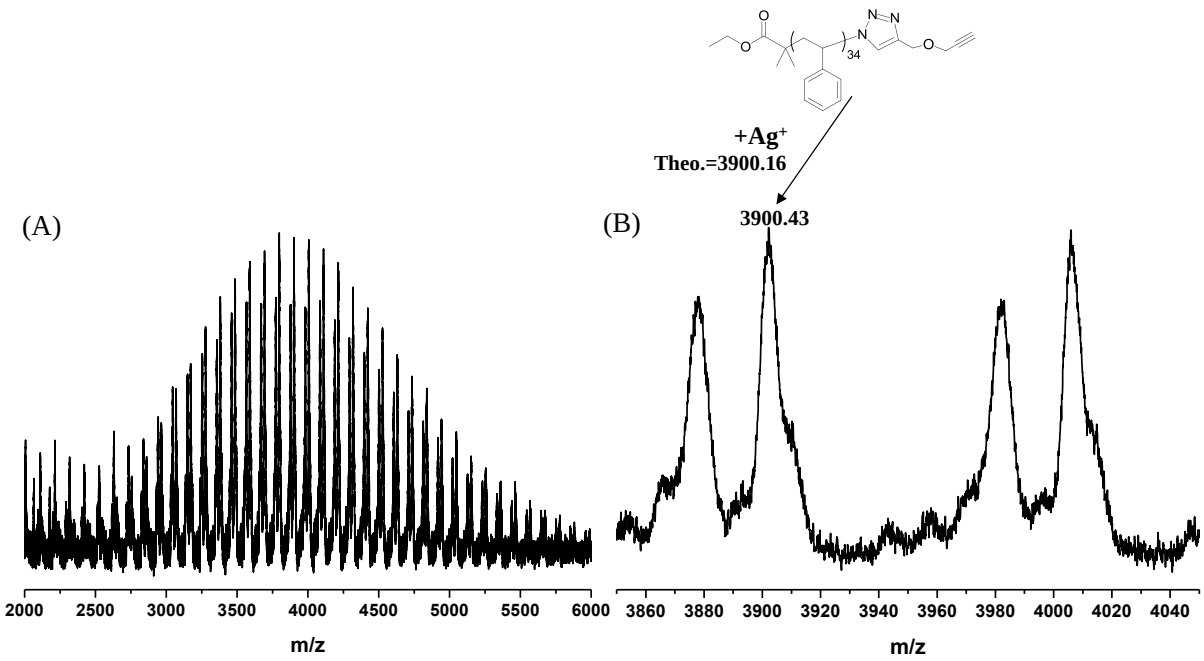

Figure A3.7: The full (A) and expanded (B) MALDI-TOF mass spectra of PSTY-alk (**3**). The spectra were recorded in reflect mode using DCTB as the matrix and $AgCF_3COO$ as the cation source.

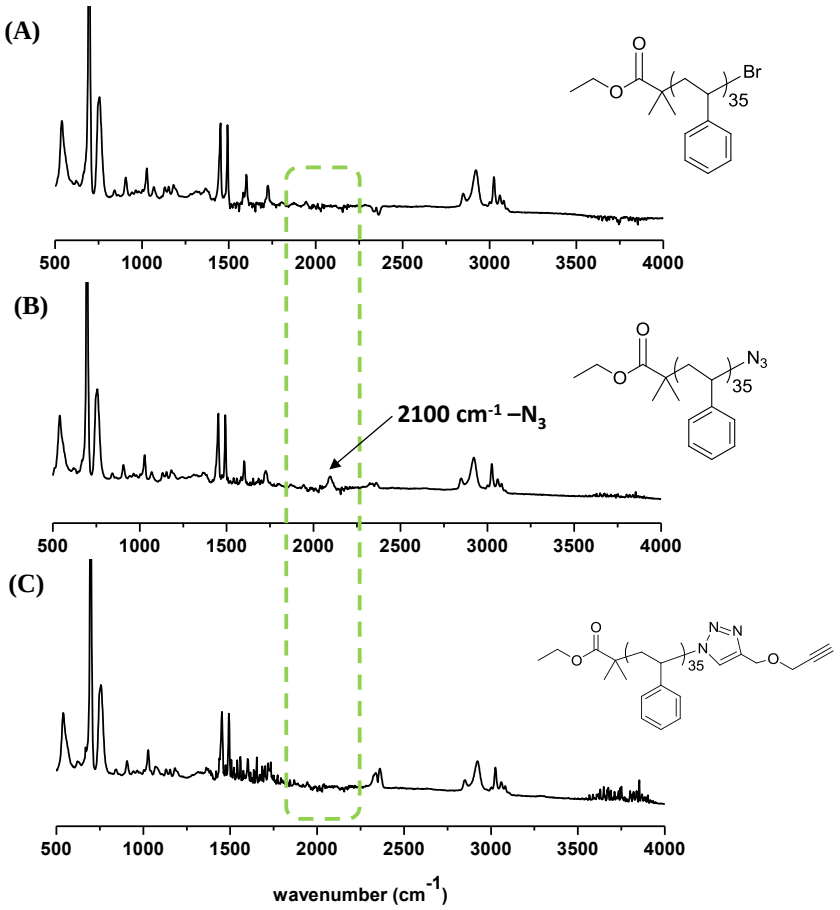

Figure A3.8: ATR-FTIR of spectra of (A) PSTY-Br (**1**); (B) PSTY-N_3**(2)**; and (C)PSTY-alk**(3)**.

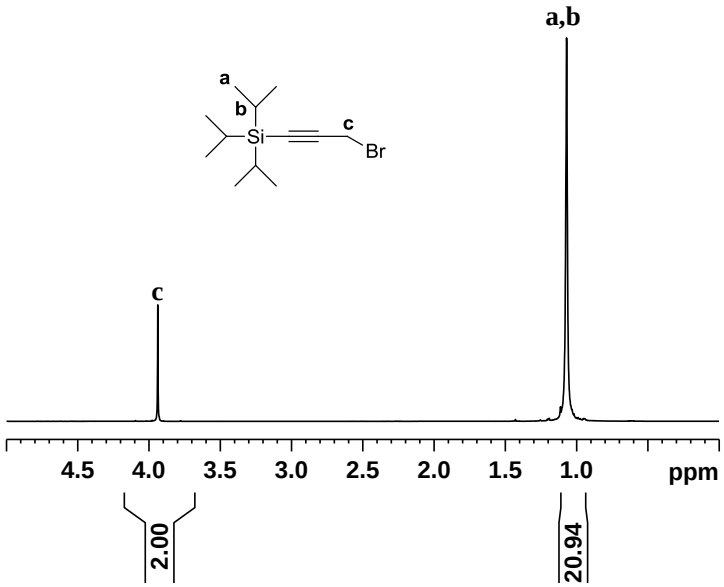

Figure A3.9: ^{1}H NMR spectrum of **5**,recorded in $CDCl_3$ at 298 K, 500 M.

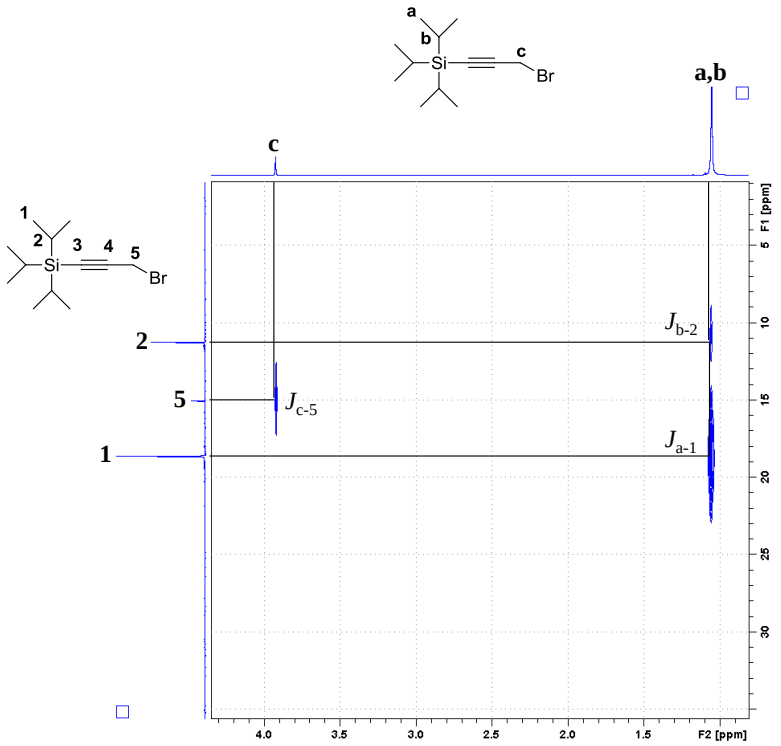

Figure A3.10: 2D-COSY spectrum of **5**,recorded in $CDCl_3$ at 298 K, 500 M.

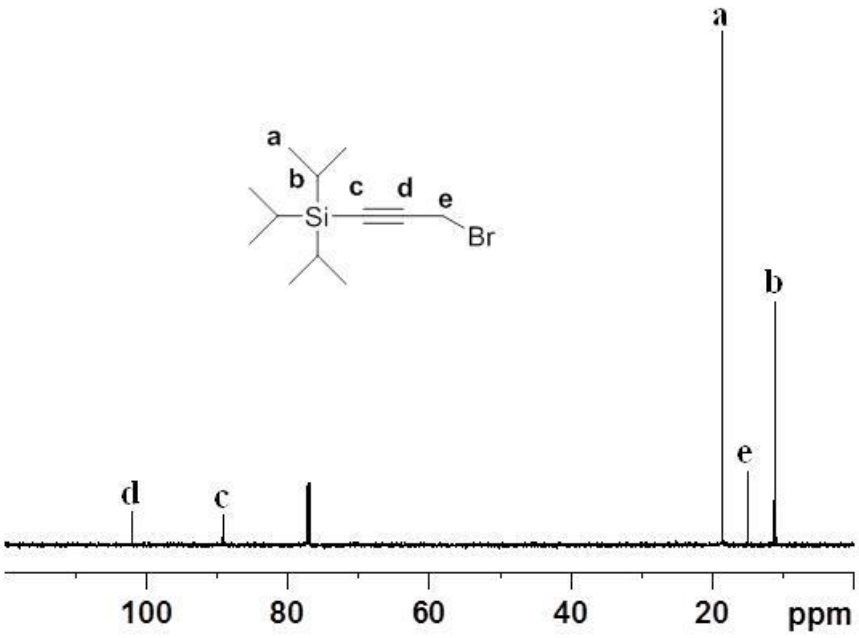

Figure A3.11: ^{13}C NMR spectrum of **5**,recorded in $CDCl_3$ at 298 K, 500 M.

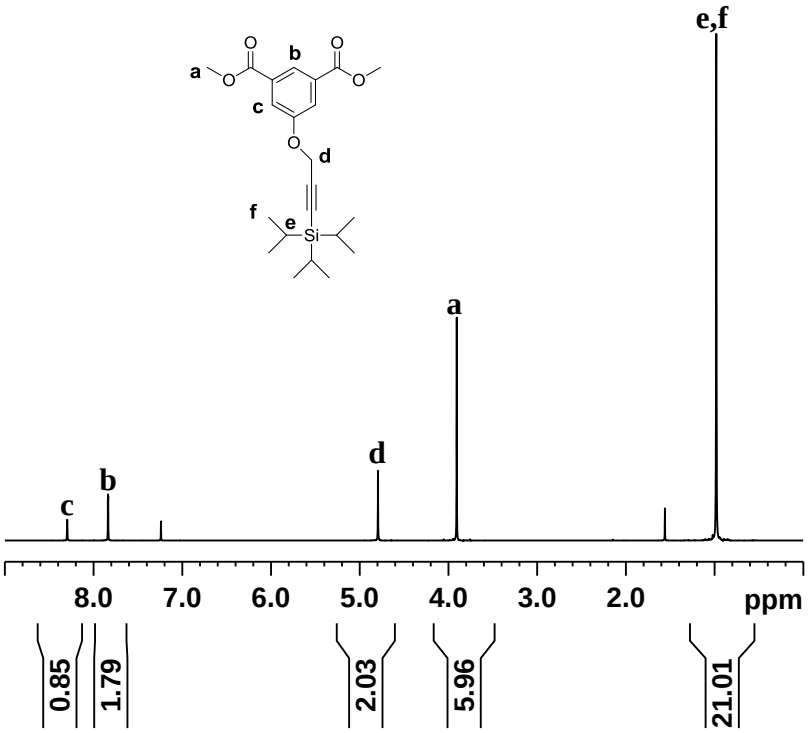

Figure A3.12: ^{1}H NMR spectrum of **6**, recorded in $CDCl_3$ at 298 K, 500 M.

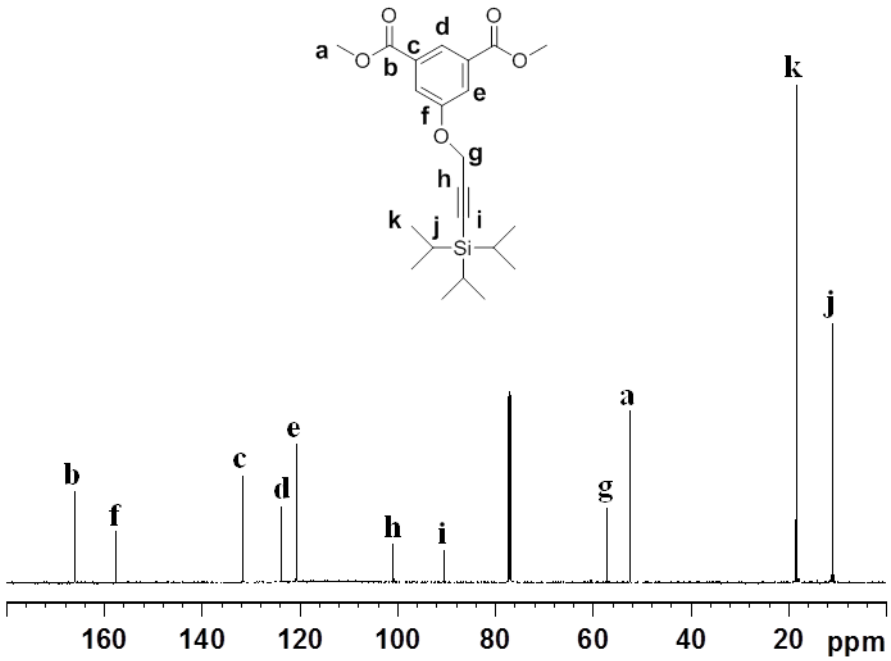

Figure A3.13:^{13}C NMR spectrum of **6**,recorded in $CDCl_3$ at 298 K, 500 M.

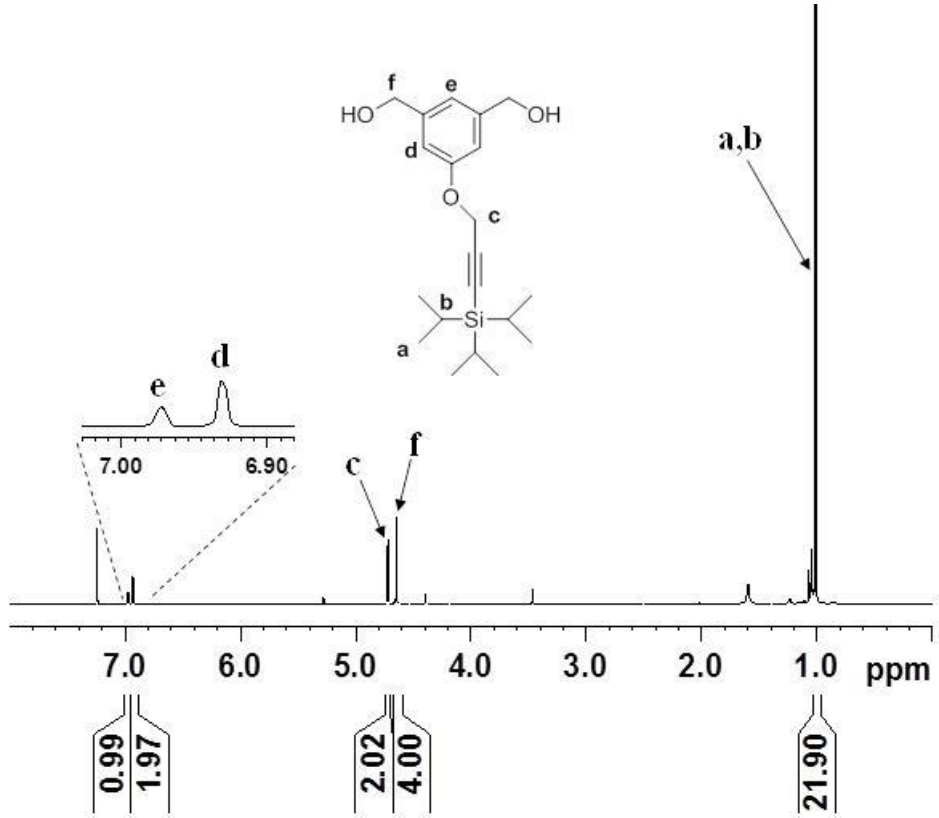

Figure A3.14: ^{1}H NMR spectrum of **6**, recorded in $CDCl_3$ at 298 K, 500 M.

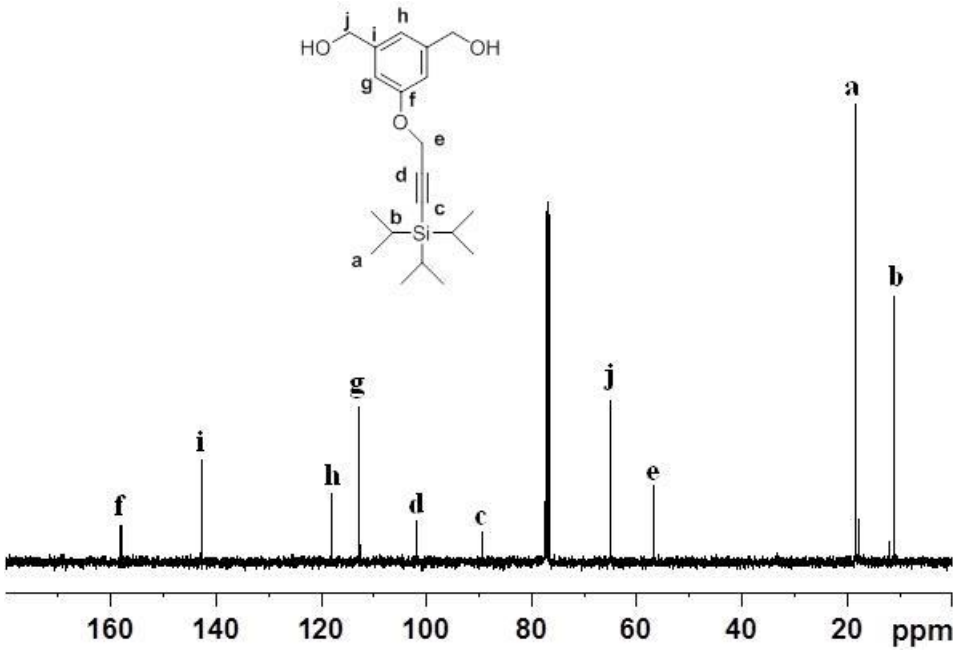

Figure A3.15: ^{13}C NMR spectrum of **7**, recorded in $CDCl_3$ at 298 K, 500 M.

Peaks	Population	Calculated	Found
1	$M+Ag^+$	4819.45	4819.71
2	$M-N_2+Ag^+$	4796.61	4791.71
3	$M-N_3+Ag^+$	4772.43	4777.71
4	$M+K^+$	4750.64	4750.77

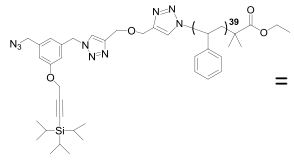

= **M**

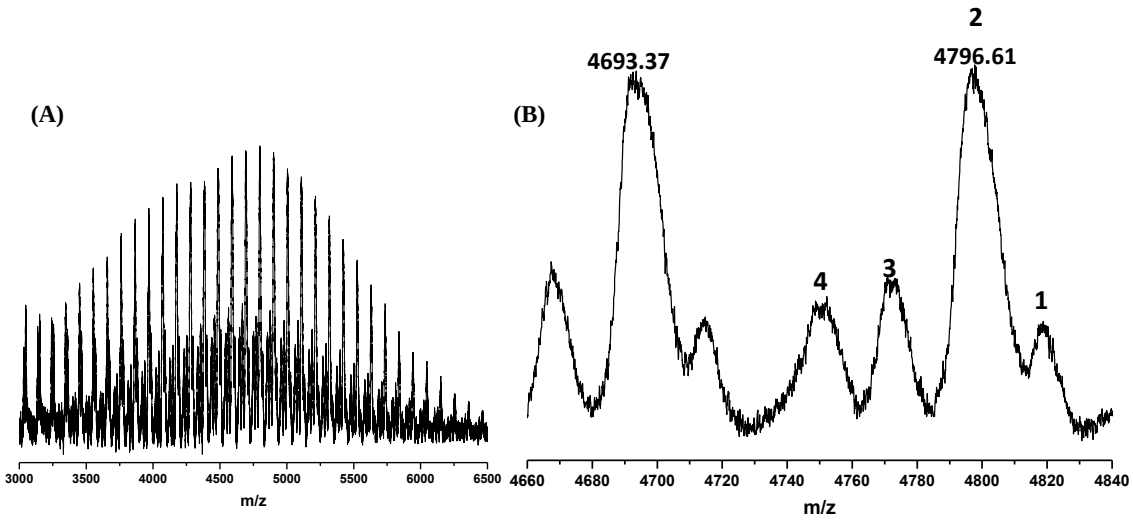

Figure A3.16: The full (A) and expanded (B) MALDI-TOF mass spectra of Tips-alk-PSTY(N_3) (**9**), The spectra were recorded in reflect mode using DCTB as the matrix and $AgCF_3COO$ as the cation source.

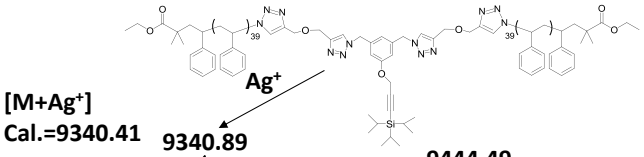

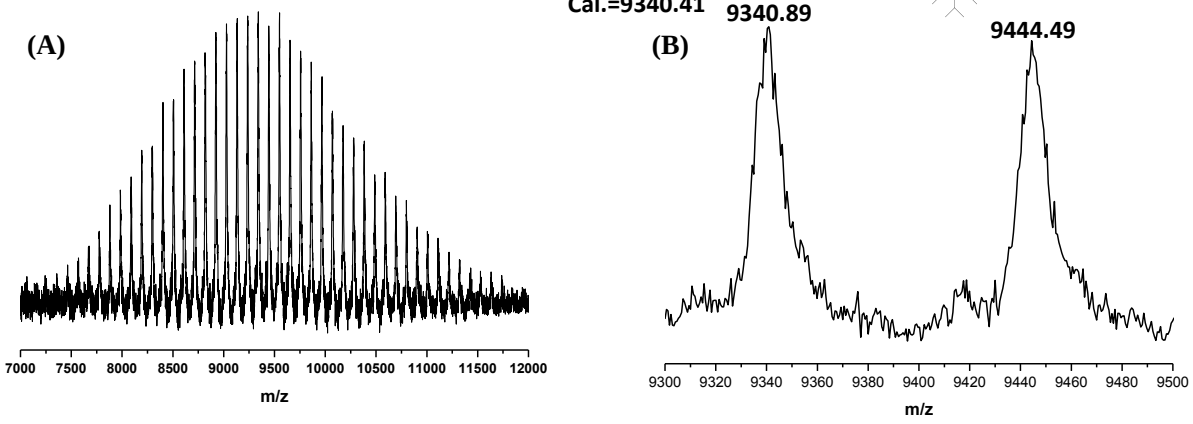

Figure A3.17: The full and expanded MALDI-TOF mass spectra of Tips-alk-$(PSTY)_2$ (**10**), The spectra were recorded in reflect mode using DCTB as the matrix and $AgCF_3COO$ as the cation source.

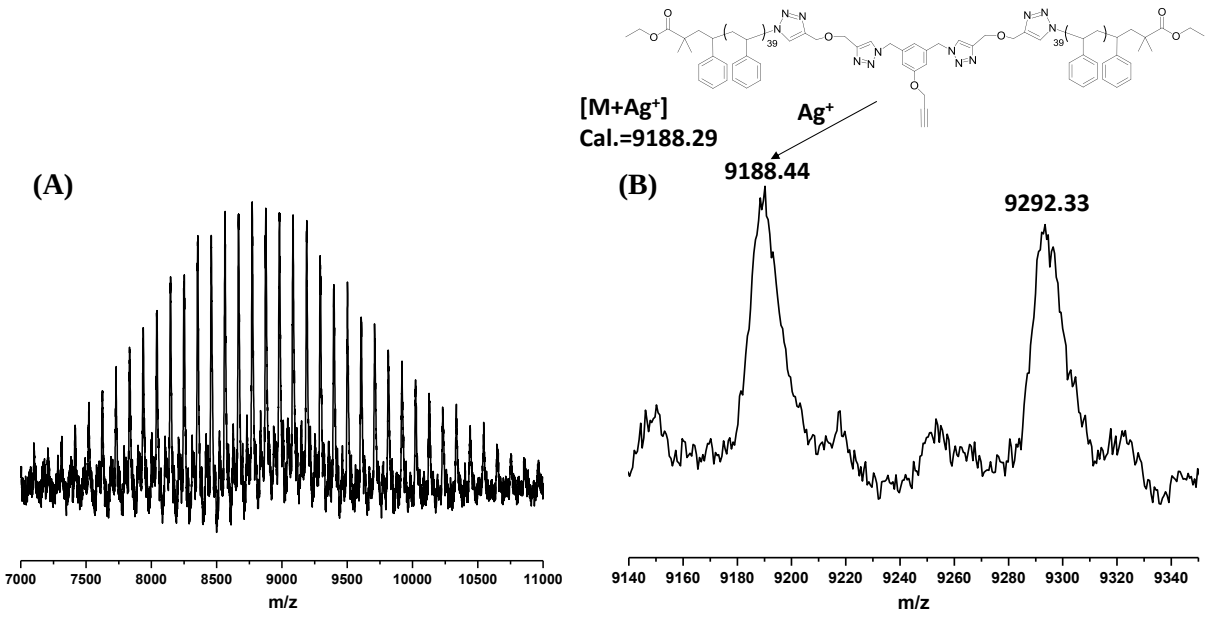

Figure A3.18:The full (A) and expanded (B) MALDI-TOF mass spectra of alk-$(PSTY)_2$ (**11**), The spectra were recorded in reflect mode using DCTB as the matrix and $AgCF_3COO$ as the cation source.

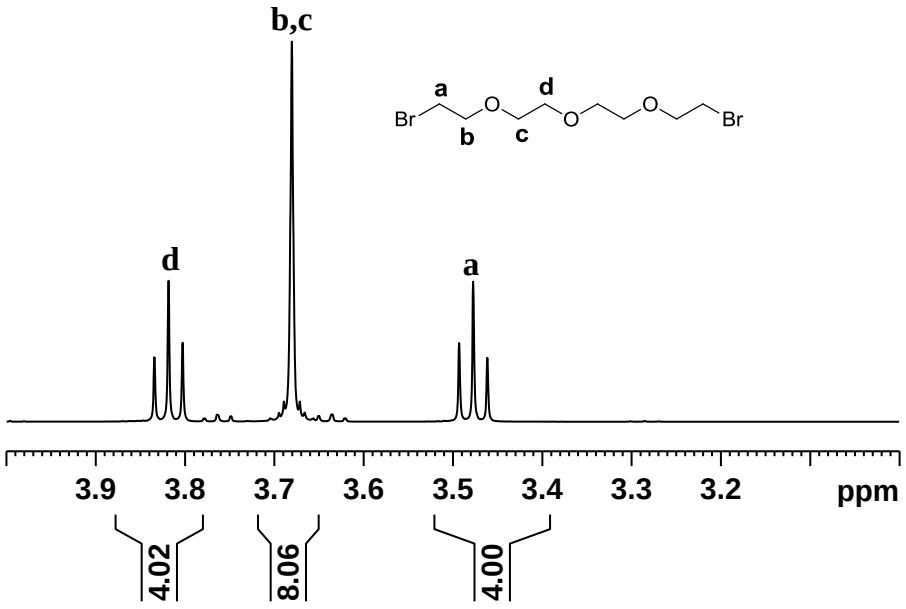

Figure A3.19:^{1}H NMR spectrum of **12**,recorded in $CDCl_3$ at 298 K, 500 M.

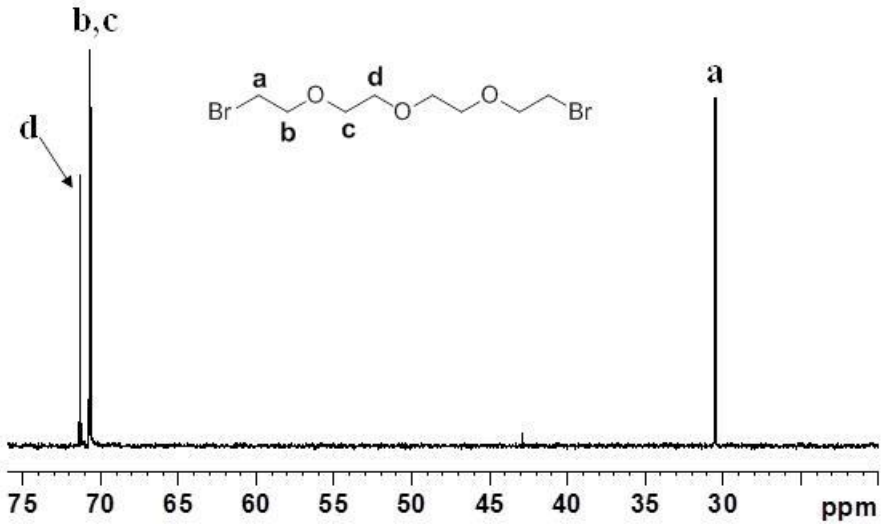

Figure A3.20: ^{13}C NMR spectrum of **12**,recorded in $CDCl_3$ at 298 K, 500 M.

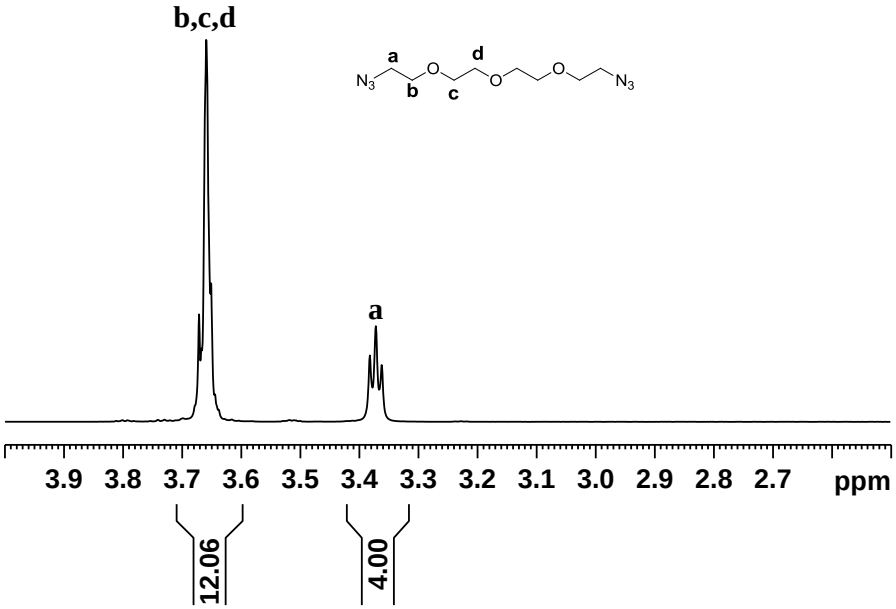

Figure A3.21: ^{1}H NMR spectrum of **13**,recorded in $CDCl_3$ at 298 K, 500 M.

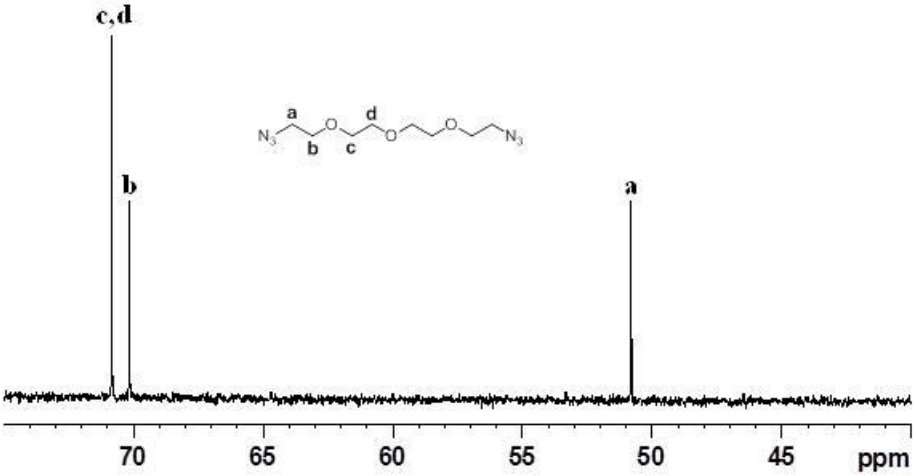

Figure A3.22: ^{13}C NMR spectrum of **13**,recorded in $CDCl_3$ at 298 K, 500 M.

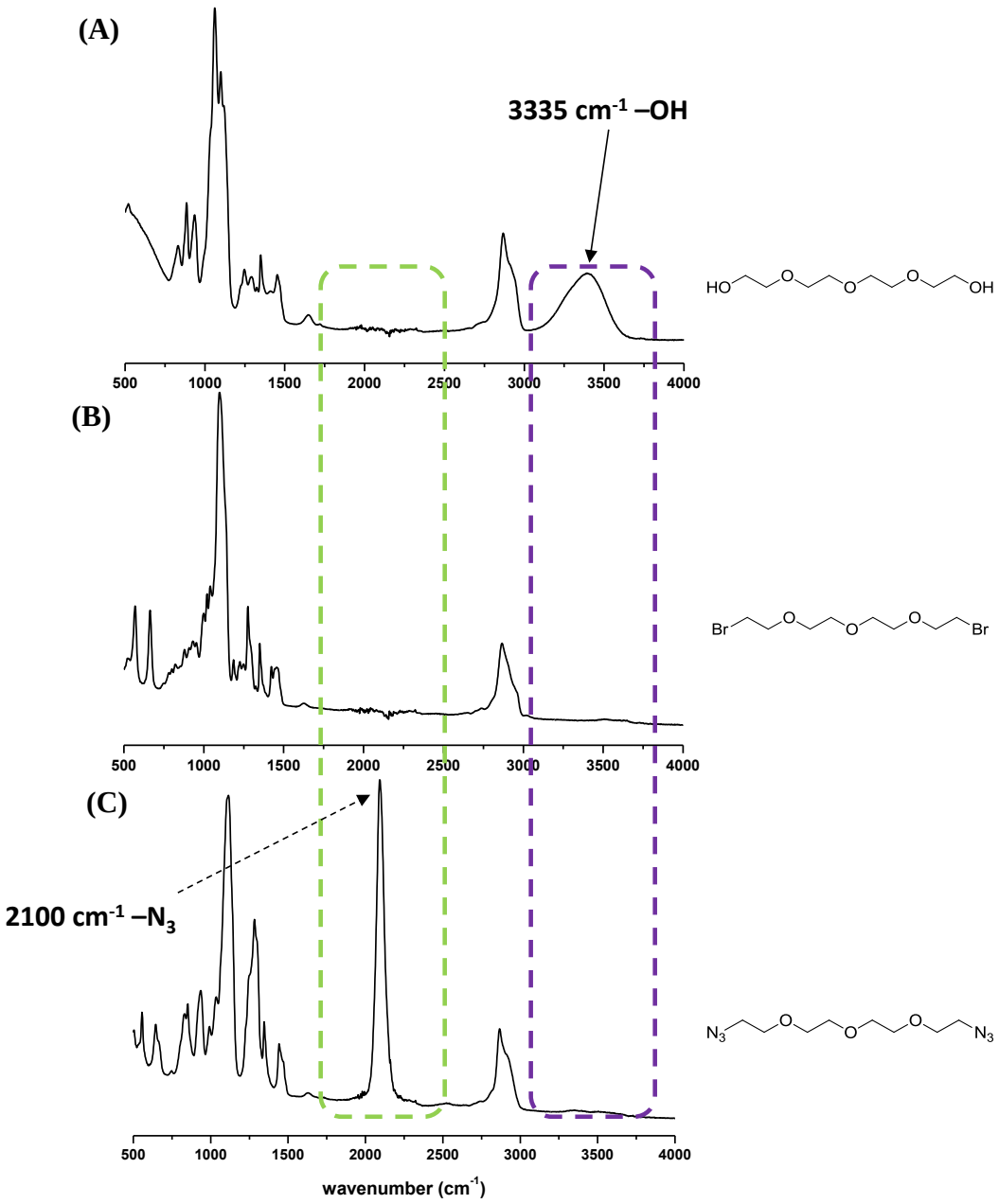

Figure A3.23:ATR-FTIR of spectra of (A) OH-EG-OH; (B) Br-EG-Br **(12)**; and (C)N_3-EG-N_3**(13)**.

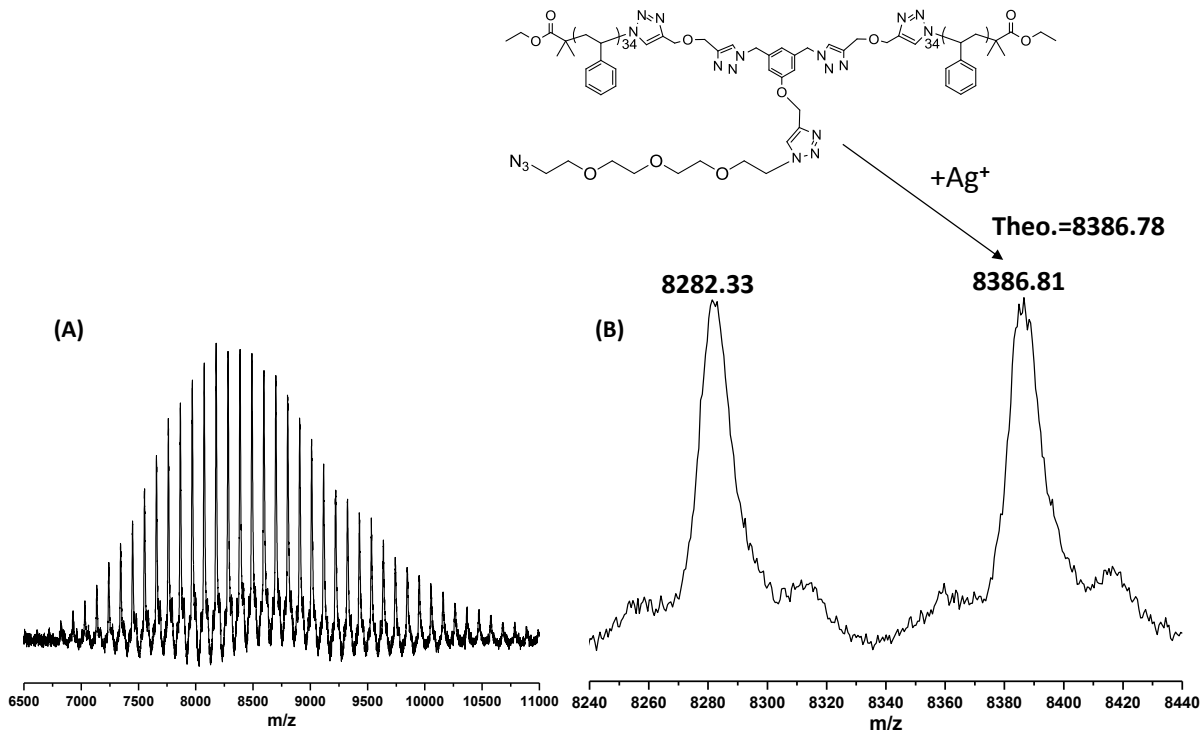

Figure A3.24:The full and expanded MALDI-TOF mass spectra of N_3-$(PSTY)_2$ (**14**), The spectra were recorded in linear mode using DCTB as the matrix and $AgCF_3COO$ as the cation source.

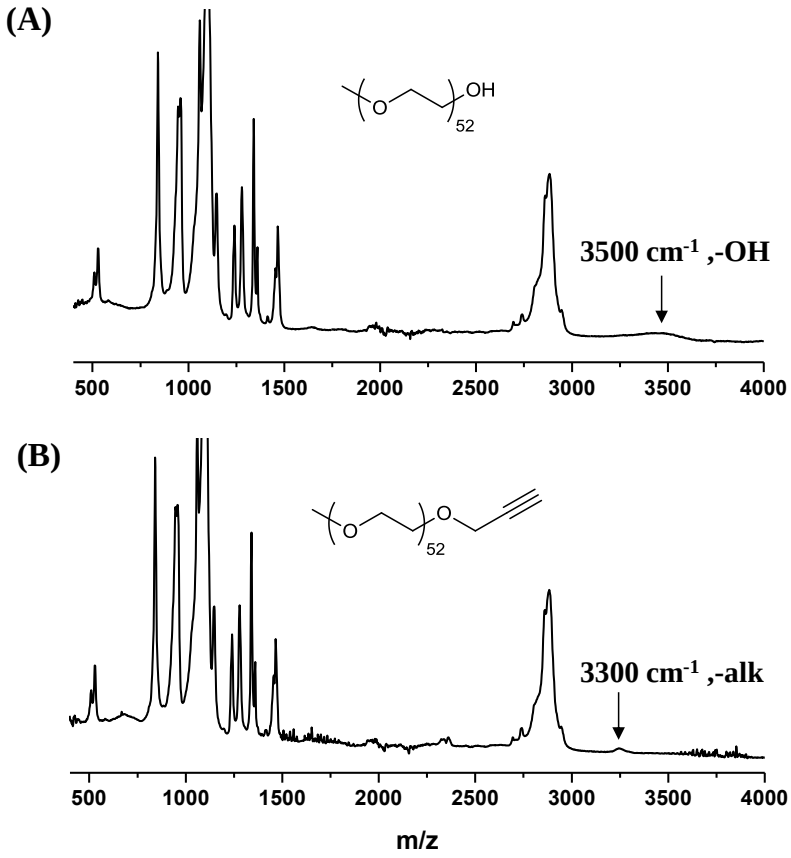

Figure A3.25: ATR-FTIR of spectra of (A) PEG-OH, (B) PEG-alk (**16**).

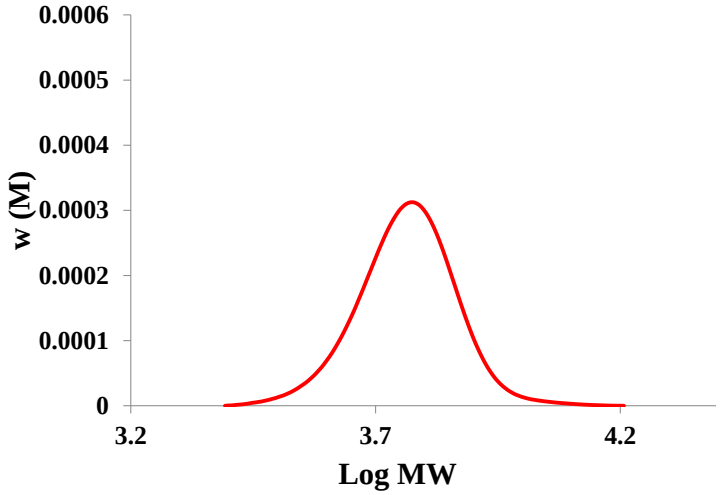

Figure A3.26: SEC trace of P^{t}BA-Br (**20**). Determined from THF SEC, RI detector, PSTY standard.

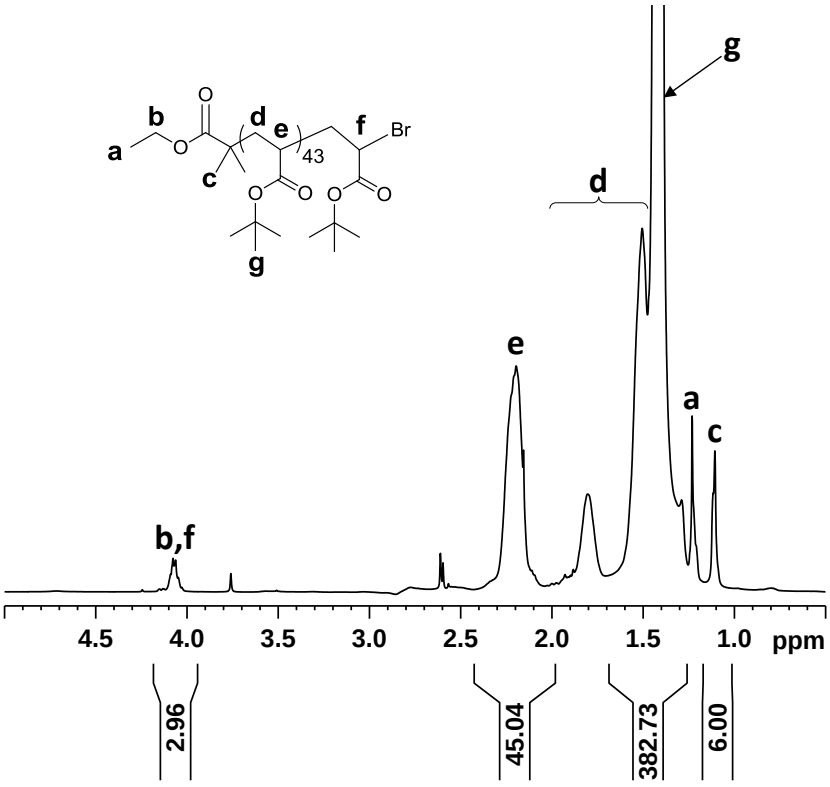

Figure A3.27: ^{1}H 1D DOSY NMR spectrum of P^{t}BA-Br (**20**), recorded in $CDCl_3$ at 298K , 500MHz.

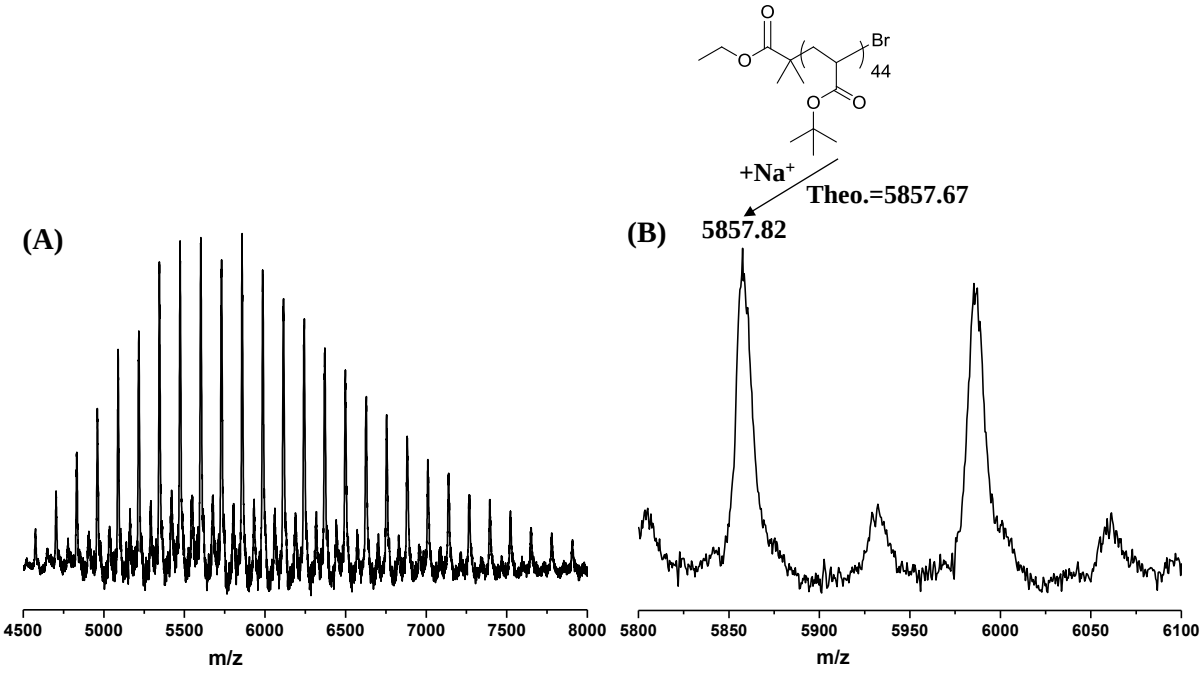

Figure A3.28:The full (A) and expanded (B) MALDI-TOF mass spectra of P^{t}BA-Br (**20**), The spectra were recorded in linear mode using DCTB as the matrix and $NaCF_3COO$ as the cation source.

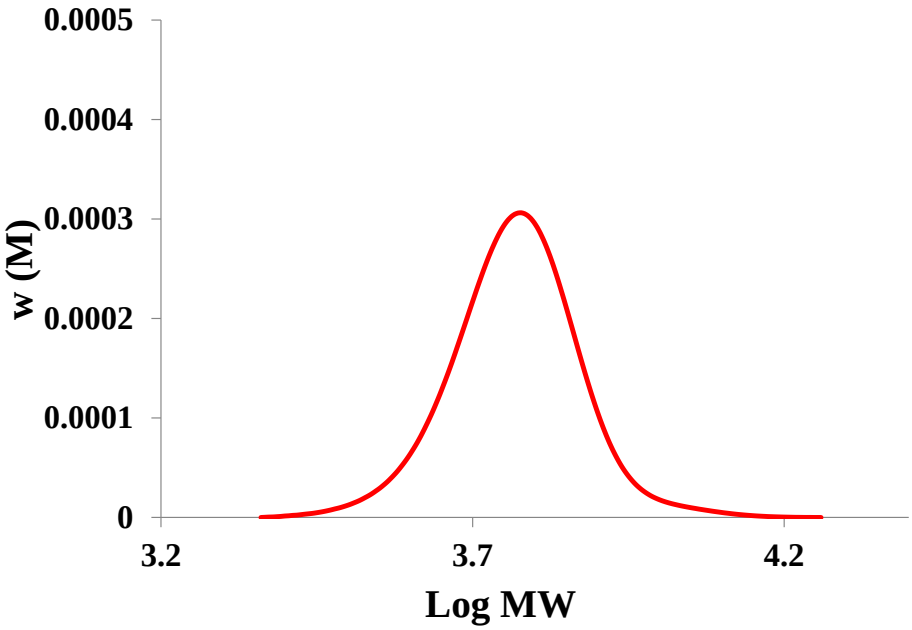

Figure A3.29: SEC trace of P^{t}BA-N_3 (**21**). Determined from THF SEC, RI detector, PSTY standard.

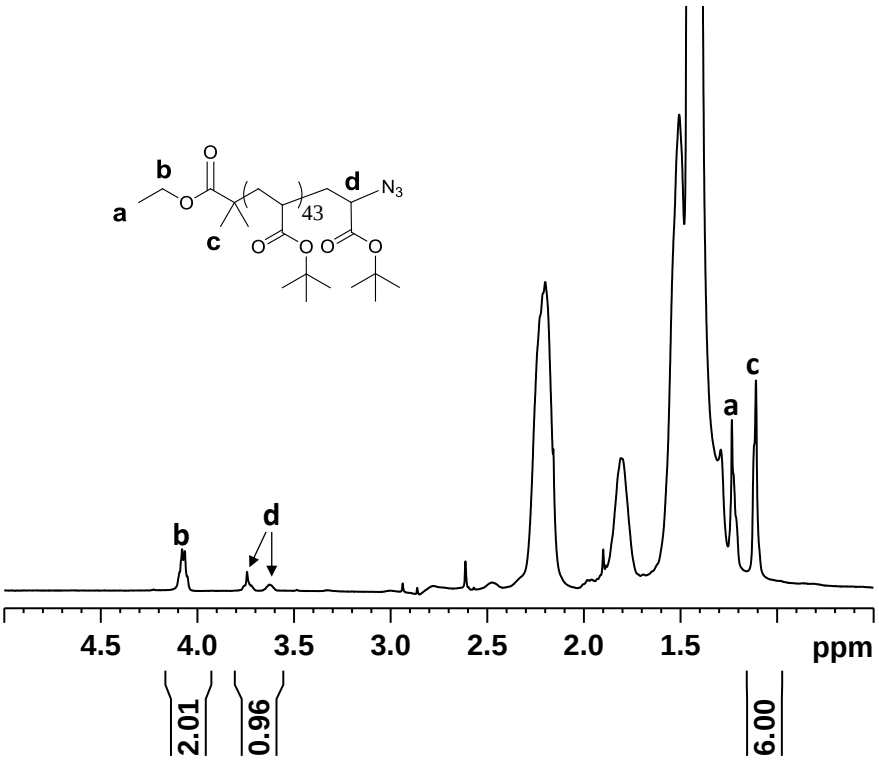

Figure A3.30:[1]H 1D DOSY NMR spectrum of $P^tBA\text{-}N_3$ (**20**), recorded in $CDCl_3$ at 298K , 500MHz.

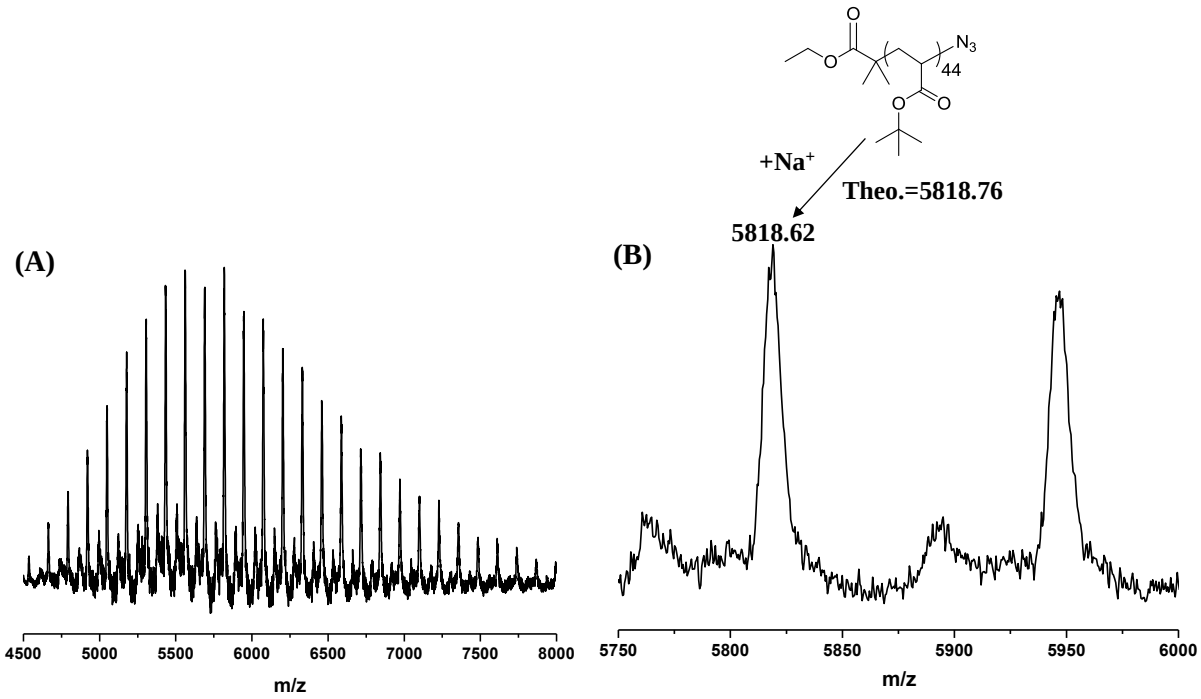

Figure A3.31: The full (A) and expanded (B) MALDI-TOF mass spectra of $P^tBA\text{-}N_3$ (**21**), The spectra were recorded in linear mode using DCTB as the matrix and $NaCF_3COO$ as the cation source.

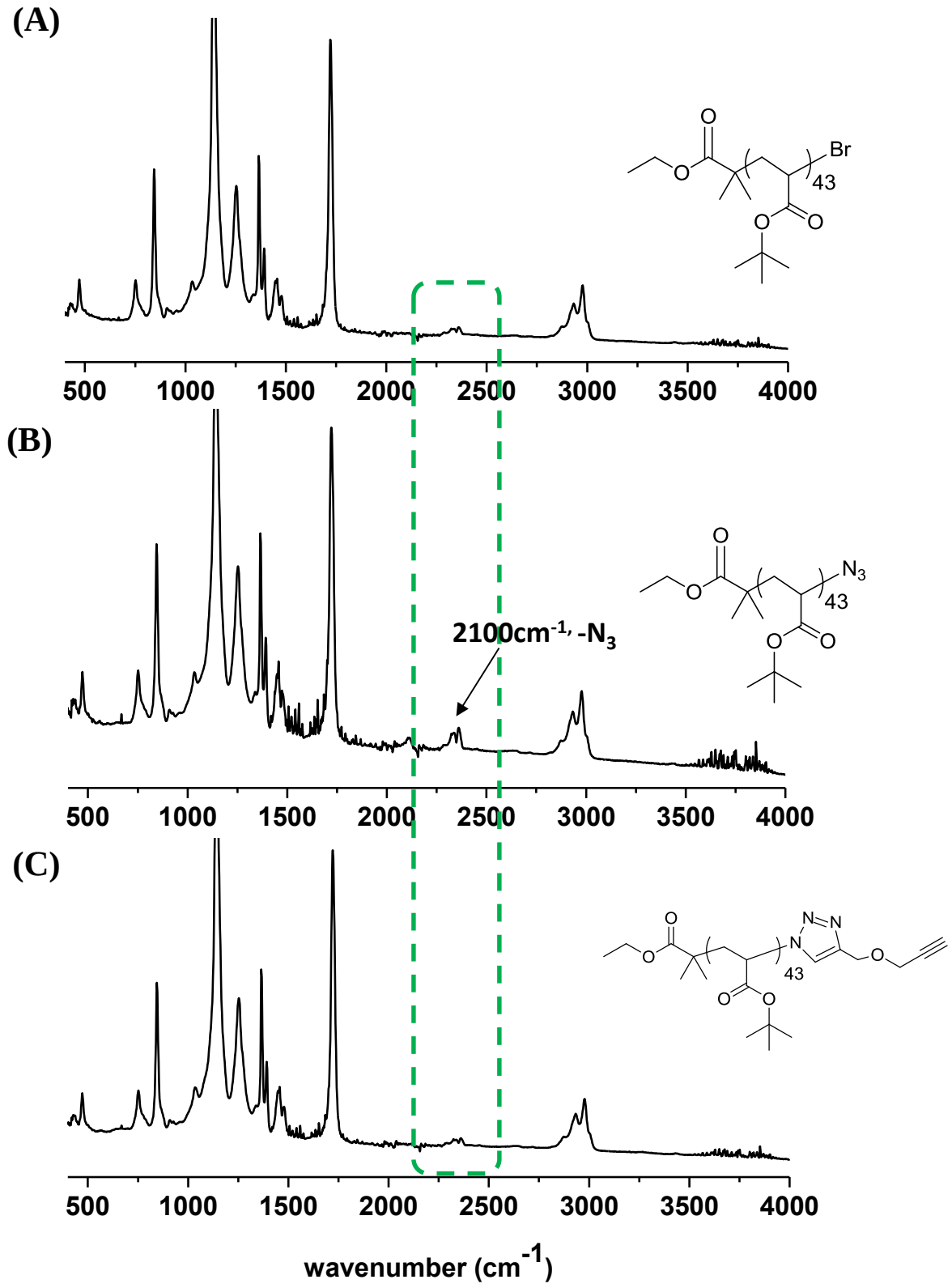

Figure A3.32: ATR-FTIR of spectra of (A) P^{t}BA-Br, (B) P^{t}BA-N_3 and (C) P^{t}BA-alk.

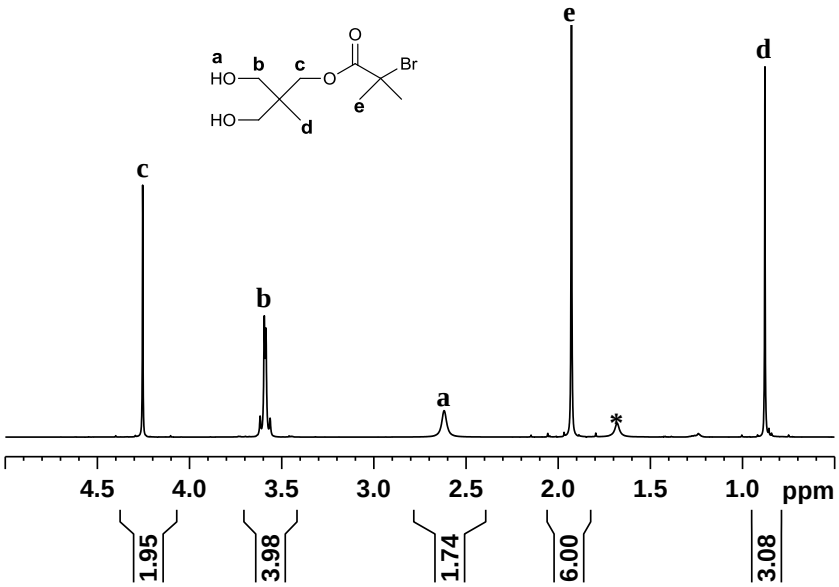

Figure A3.33: ^{1}H NMR spectrum of initiator (**25**), recorded in $CDCl_3$ at 298K , 500MHz, *=H_2O.

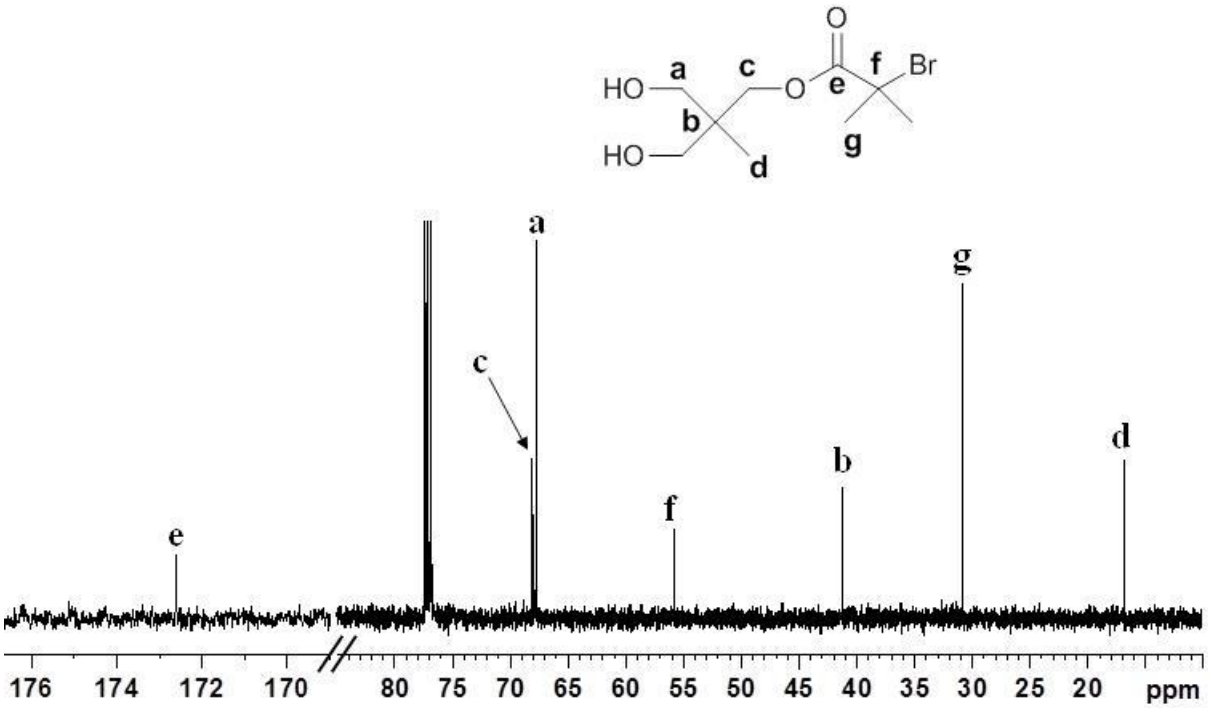

Figure A3.34: ^{13}C NMR spectrum of initiator (**25**), recorded in $CDCl_3$ at 298K , 500MHz.

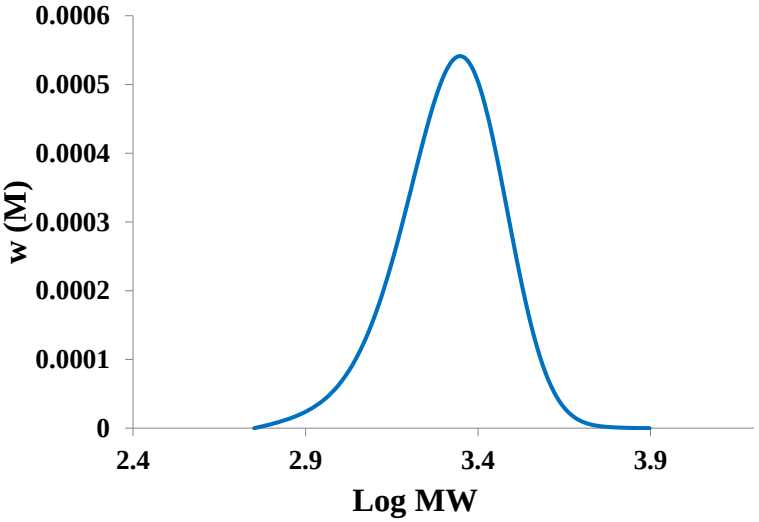

Figure A3.35: SEC trace of PNIPAm-N_3 (**26**). Determined from THF SEC, RI detector, PSTY standard.

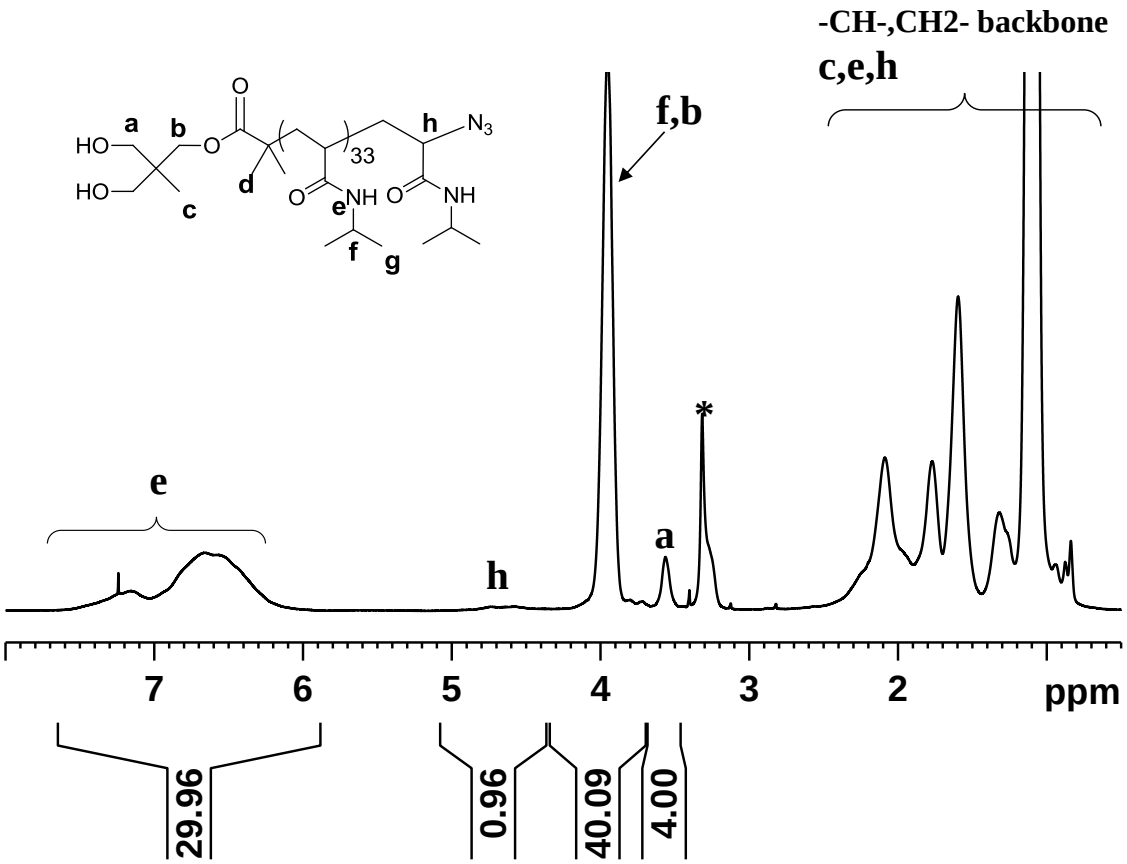

Figure A3.36: ^{1}H 1D DOSY NMR spectrum of $(OH)_2$-PNIPAm-N_3 (**26**), recorded in $CDCl_3$ at 298K , 400MHz, *=H_2O.

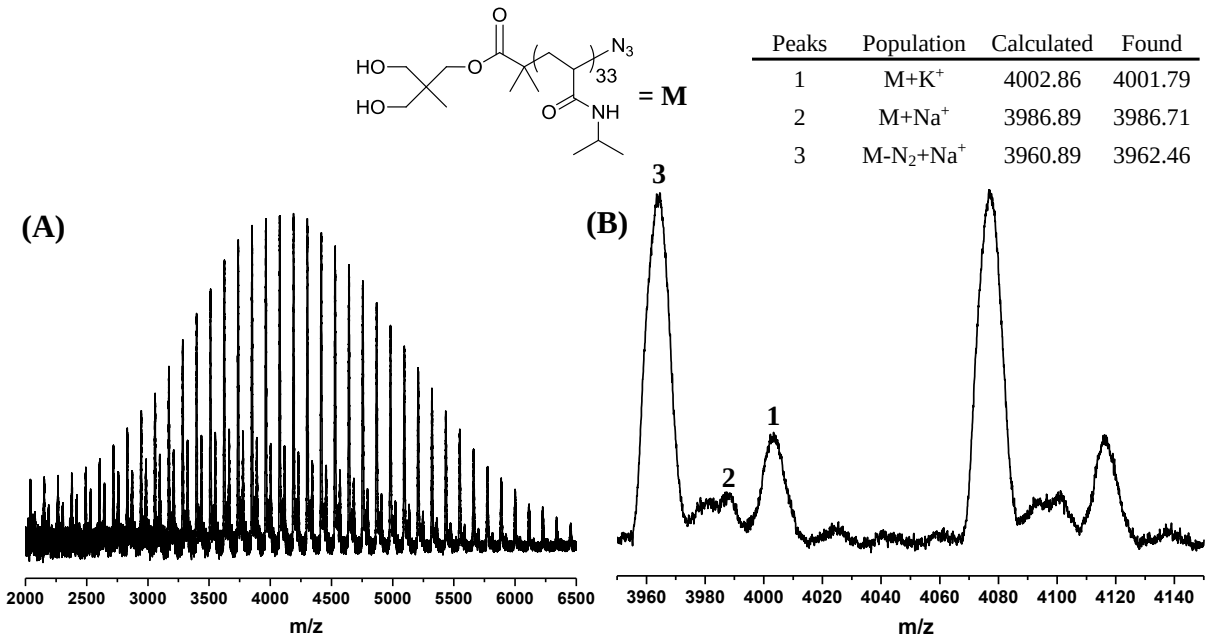

Peaks	Population	Calculated	Found
1	$M+K^+$	4002.86	4001.79
2	$M+Na^+$	3986.89	3986.71
3	$M-N_2+Na^+$	3960.89	3962.46

Figure A3.37: The full and expanded MALDI-TOF mass spectra of $(OH)_2$-PNIPAm-N_3 (**26**), The spectra were recorded in linear mode using DCTB as the matrix and $NaCF_3COO$ as the cation source.

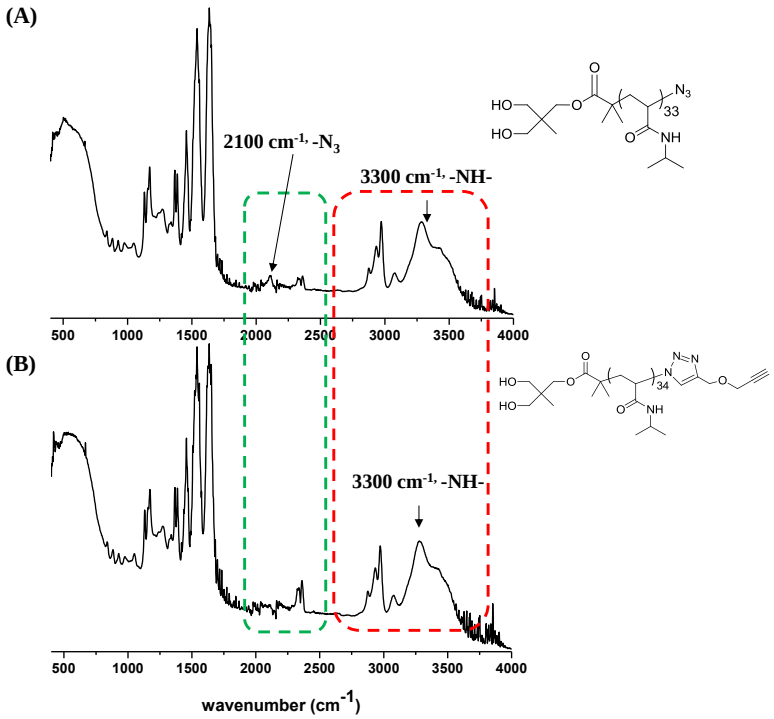

Figure A3.38: ATR-FTIR of spectra of (A) PNIPAm-N_3,**26** (B) PNIPAm-alk, **28.**

Appendix C

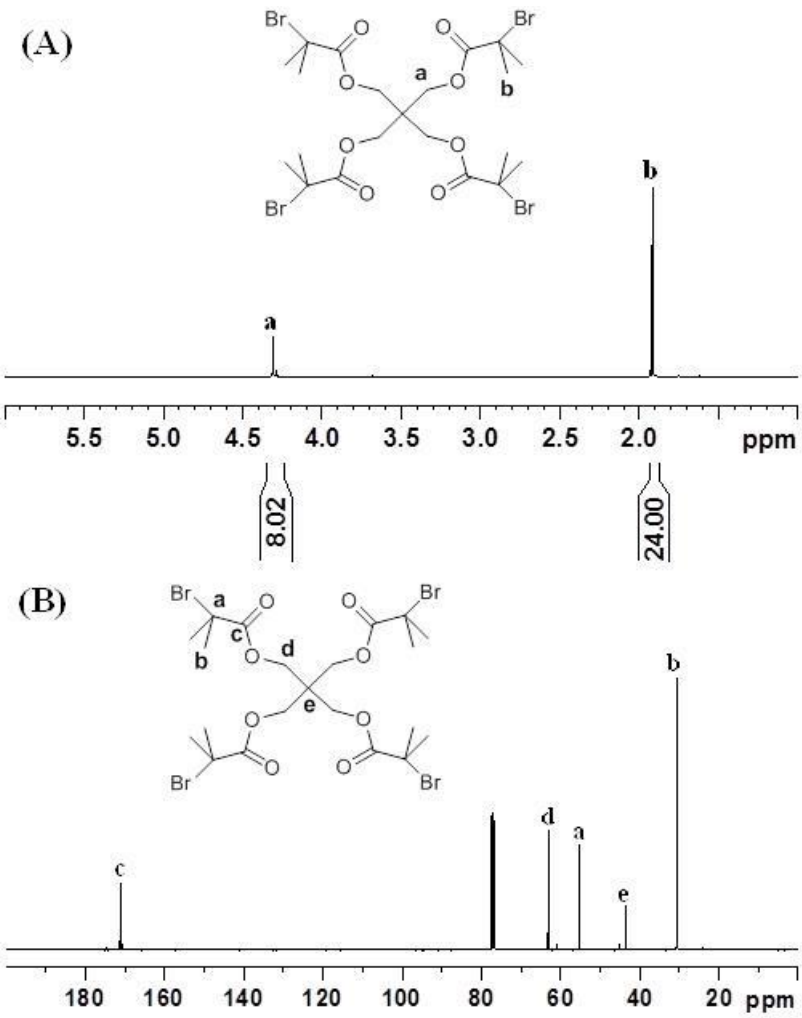

Figure A4.1: ^{1}H (A) and ^{13}C (B) NMR spectra of 4-arm ATRP initiator **(1)**. recorded in $CDCl_3$ at 298K 500MHz.

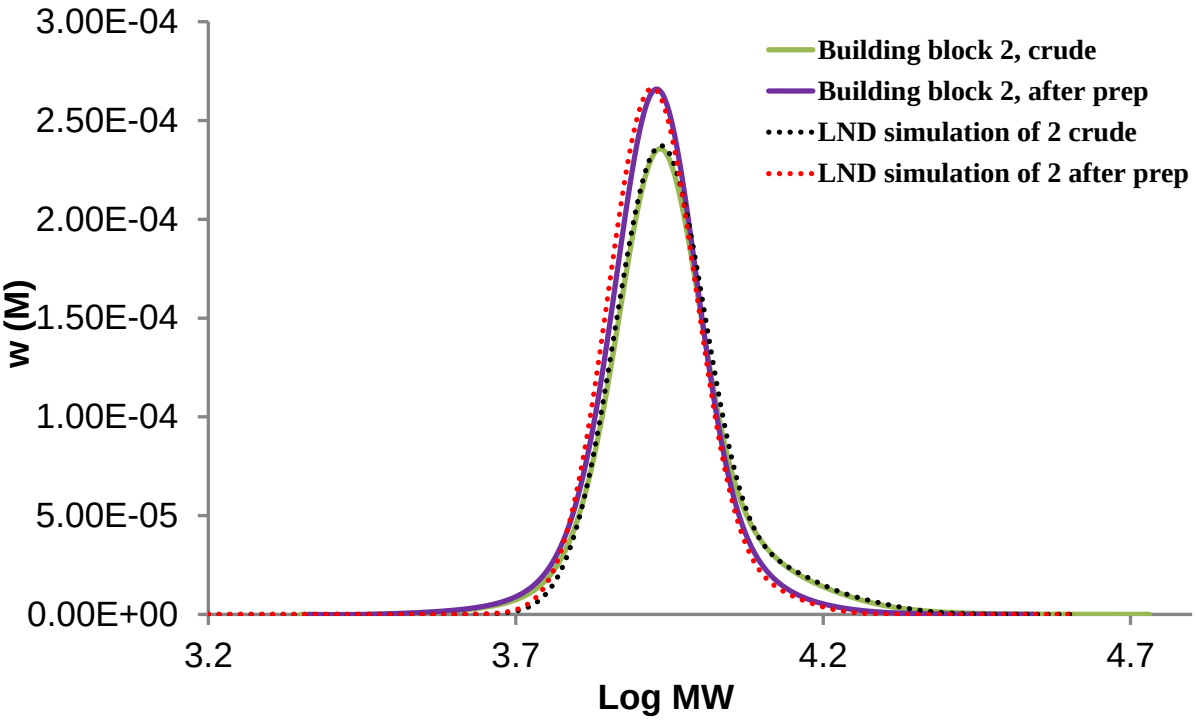

Figure A4.2: SEC traces of 4-arm PSTY-Br **(2)** before and after purification by preparative-SEC, and LND simulation for product before (A) and after prep (B). Determined from THF SEC, RI detector, PSTY standard.

Table A4.1: The molecular weight, change in hydrodynamic volume and weight percentages of the product (**2**) and higher molecular wieght species used in the LND method to simulate the experimental SEC traces in Figure A4.2.

Polymer	M_n[a]	PDI[a]	ΔHDV[a]	weight percentage%	
				Crude	After prep
2	9580	1.03	0.89	87.3	96.1
2+2	19160	1.02	0.7	7.84	3.8
2+2+2	28740	1.02	0.6	4.9	-

[a]Absolute molecular weight , PDI ,and hydrodynamic volume change used for LND simulation.

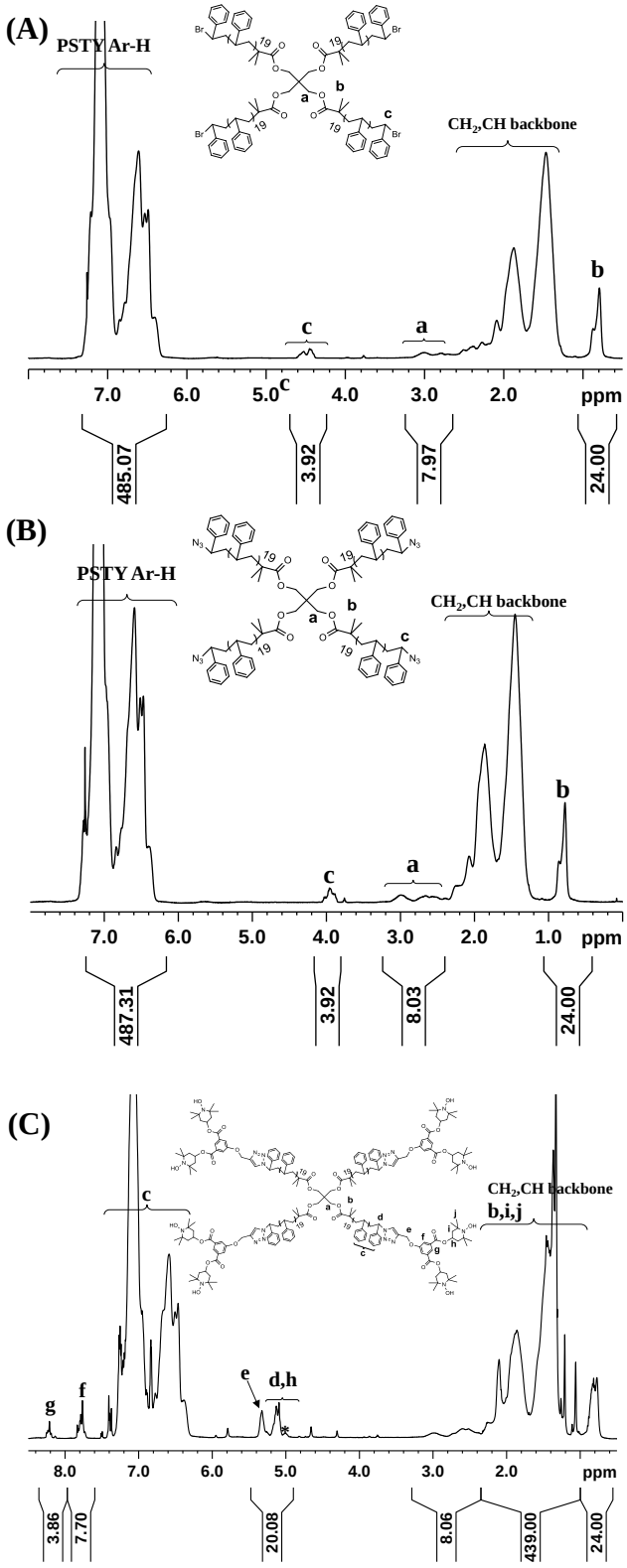

Figure A4.3: ^{1}H 1D DOSY NMR spectra of (A) 4-arm PSTY-Br **(2)**; (B) 4-arm PSTY-N_3**(3)**; and (C) 4-arm PSTY-$(NO^{\cdot})_2$**(5)**, *-residual phenylhydrazine, the gradient strength (gpz6) was used as 85% and gradient pulse length (p30) was used as 2.0 ms.

.

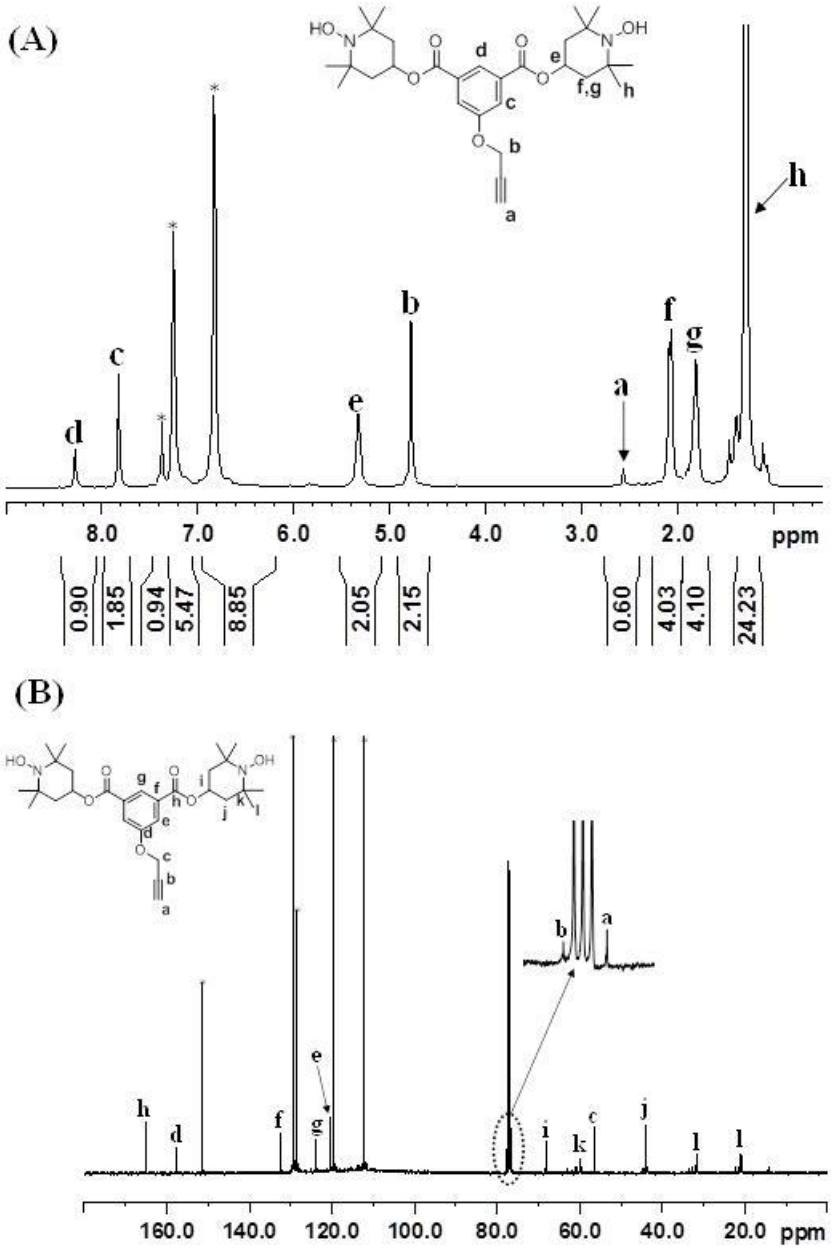

Figure A4.4: ^{1}H (A) and ^{13}C (B) NMR spectra of propargyl-$(NO^{\cdot})_2$ (**4**),recorded in $CDCl_3$ at 298K 500MHz, in the presence of phenylhydrazine.

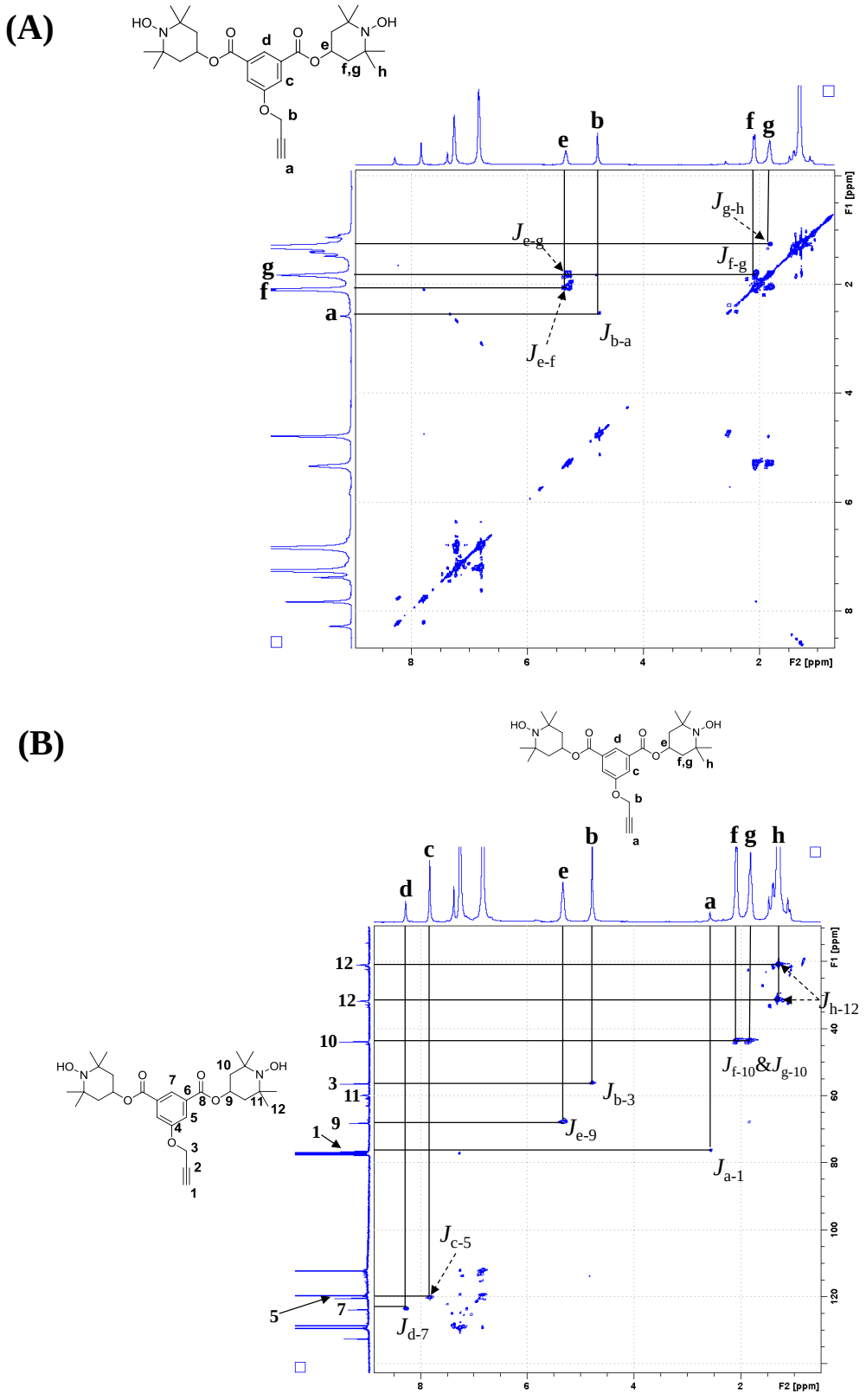

Figure A4.5:2D COSY (A) and HSQC (B) NMR spectra of propargyl-$(NO^{\cdot})_2$ (**4**),recorded in $CDCl_3$ at 298K, 500MHz,in the presence of phenylhydrazine.

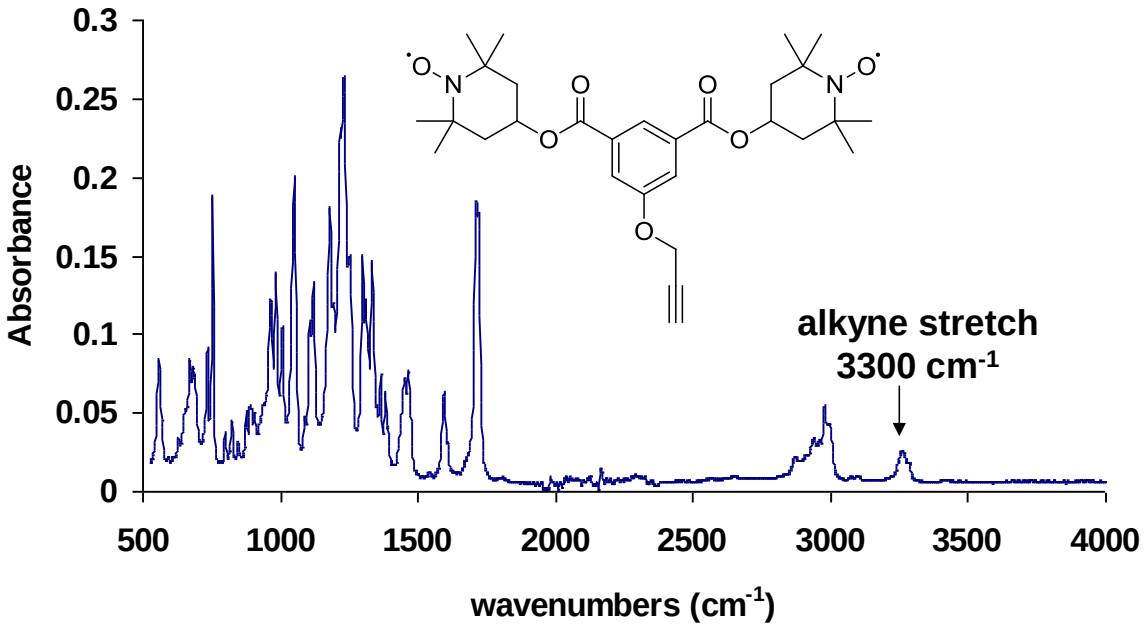

Figure A4.6: ATR-FTIR spectrum of propargyl-$(NO^{\cdot})_2$ (**4**).

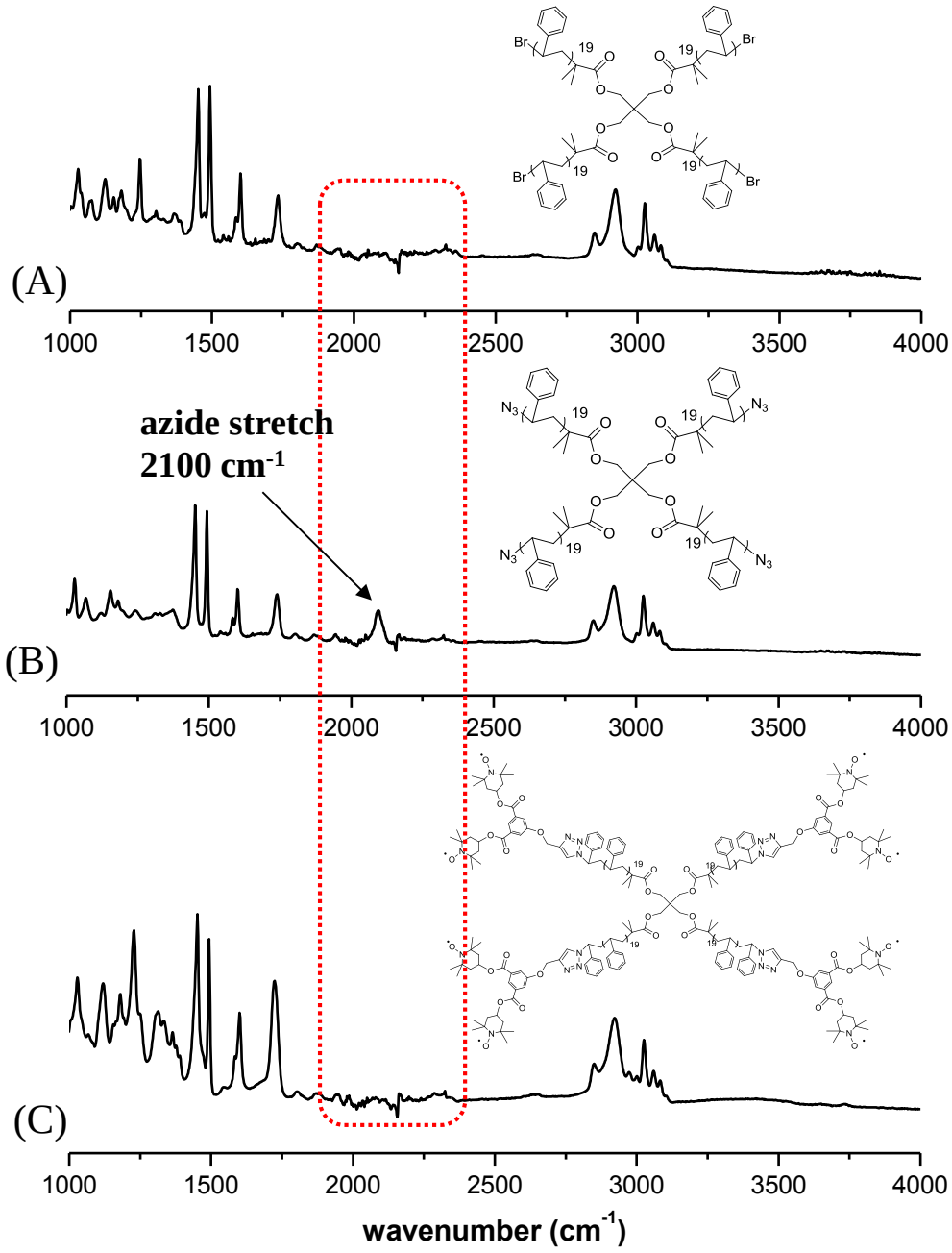

Figure A4.7: ATR-FTIR of spectra of (A) 4-arm PSTY-Br **(2)**; (B) 4-arm PSTY-N_3**(3)**; and (C) 4-arm PSTY-$(NO^{\cdot})_2$**(5)**.

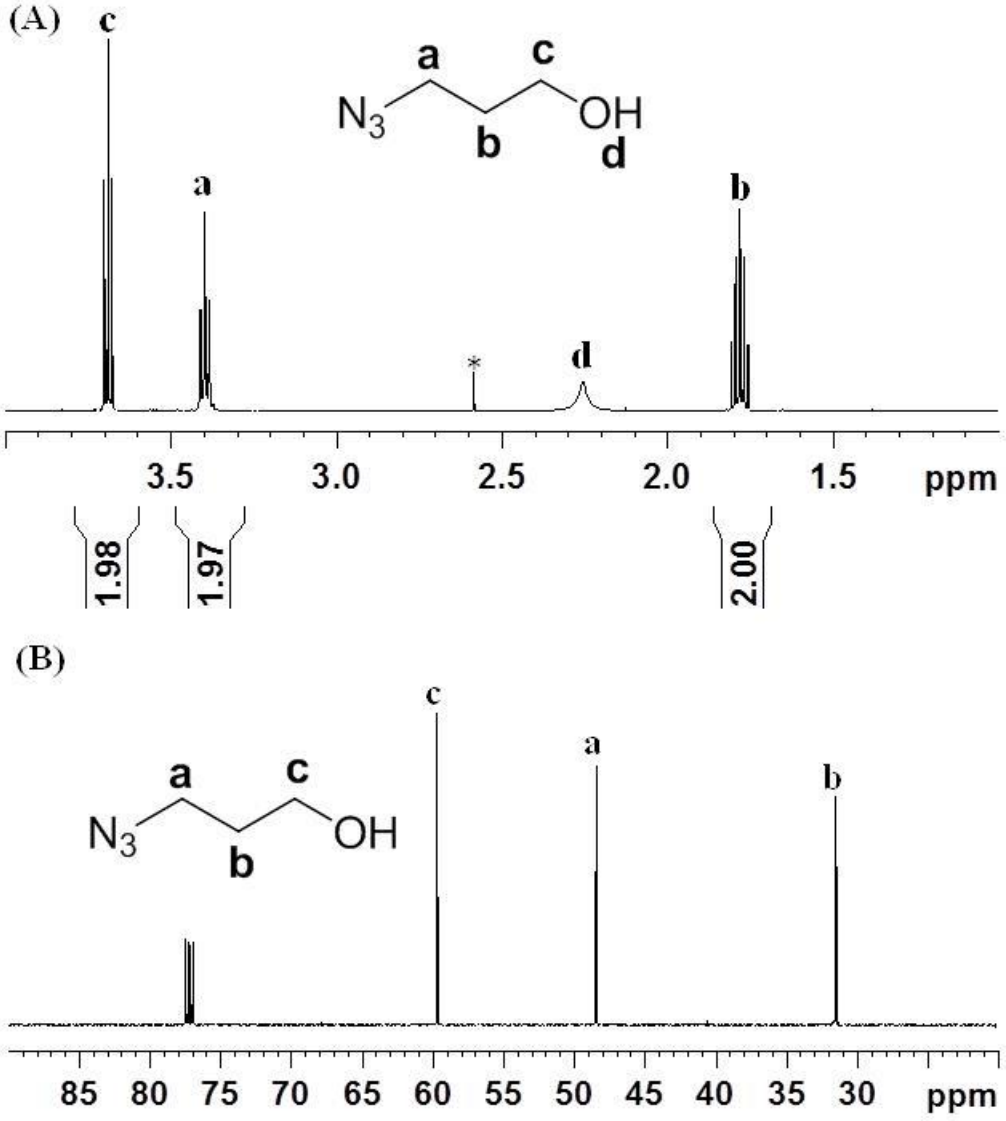

Figure A4.8: ^{1}H (A) and ^{13}C (B) NMR spectrum of (**6**),recorded in $CDCl_3$ at 298K 500MHz, *-DMSO.

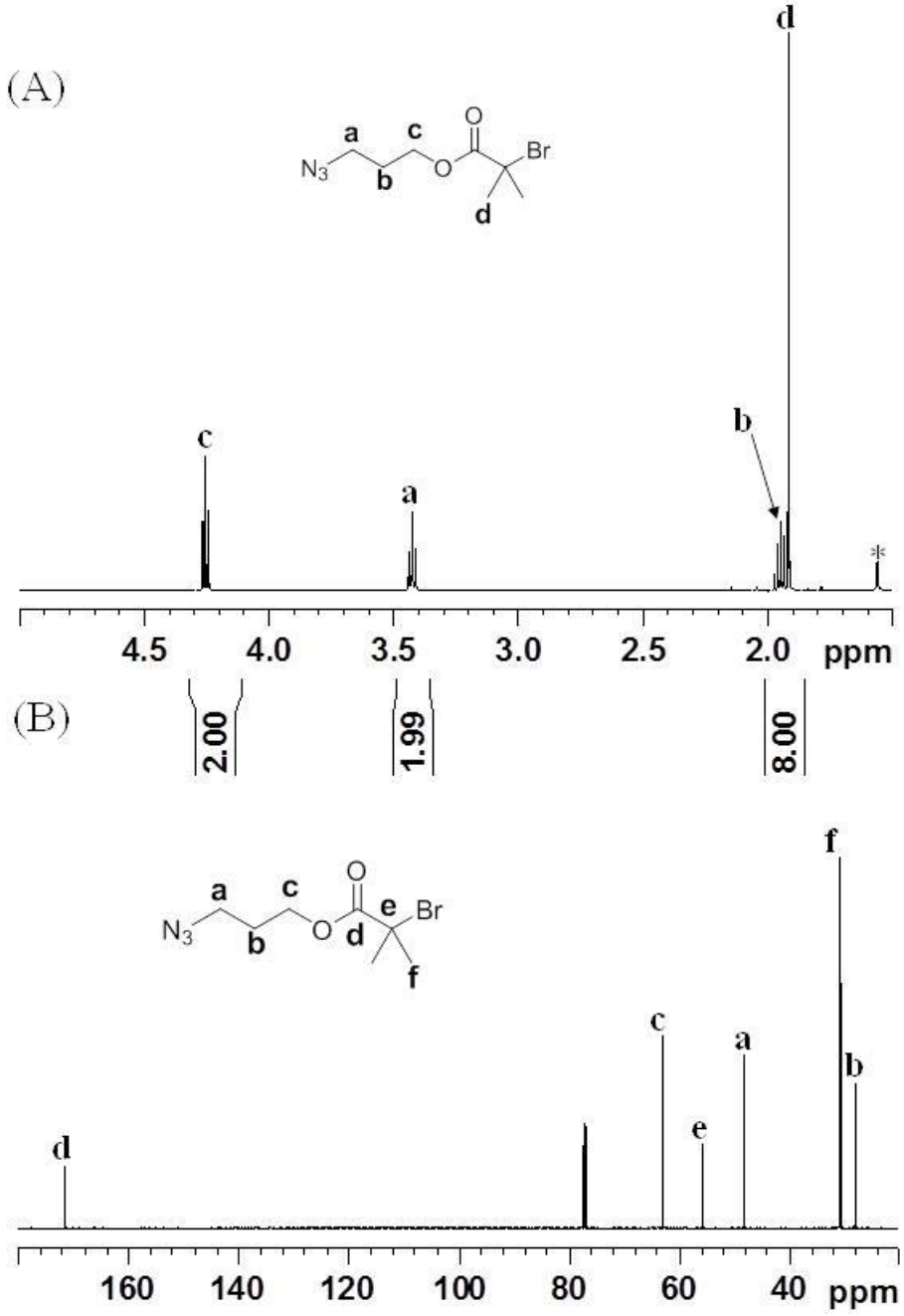

Figure A4.9: ^{1}H (A) and ^{13}C (B) NMR spectra of (**7**),recorded in $CDCl_3$ at 298K 500MHz.

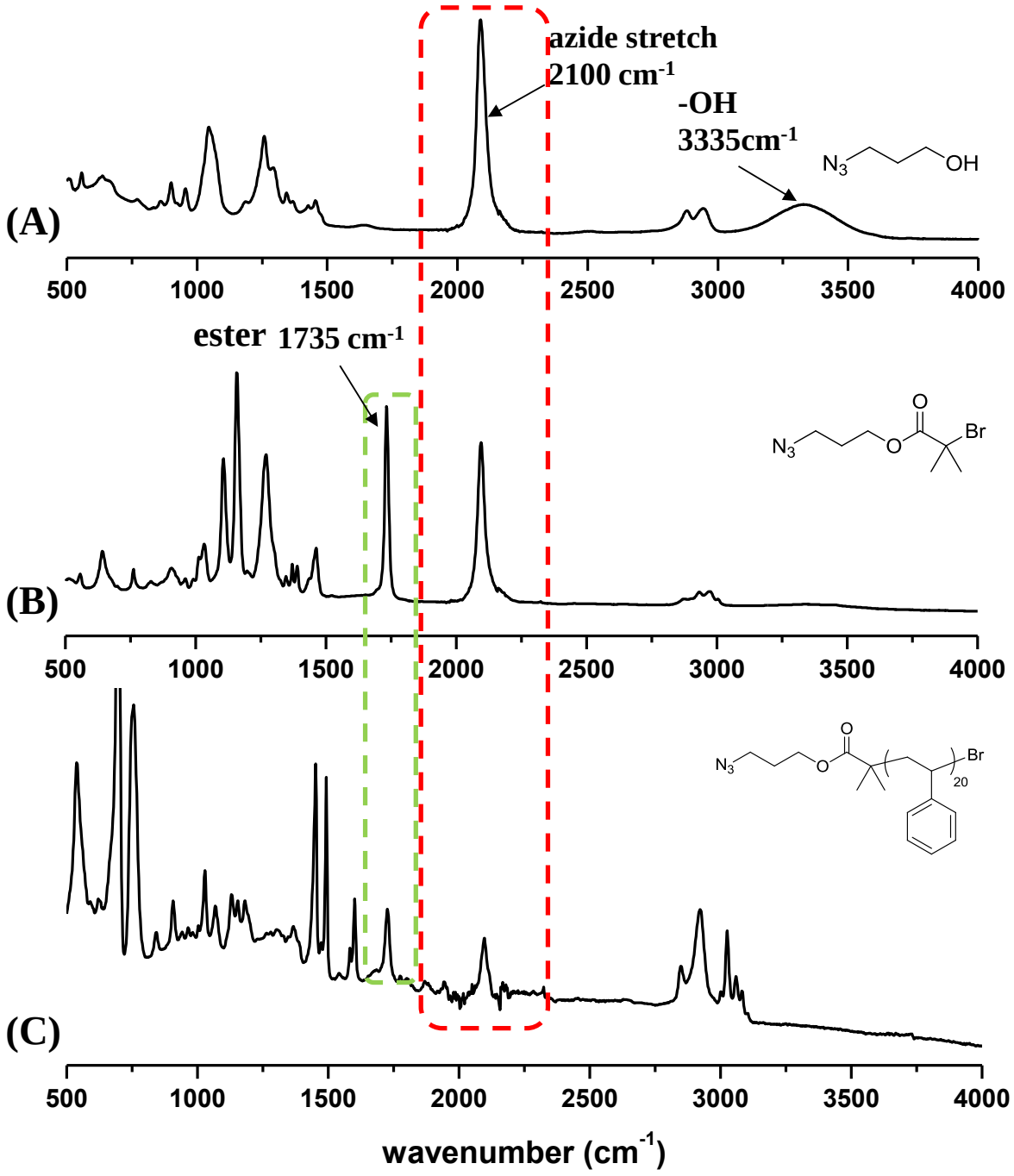

Figure A4.10:ATR-FTIR spectra of (A)**6**, (B) **7**, and (C) **8**.

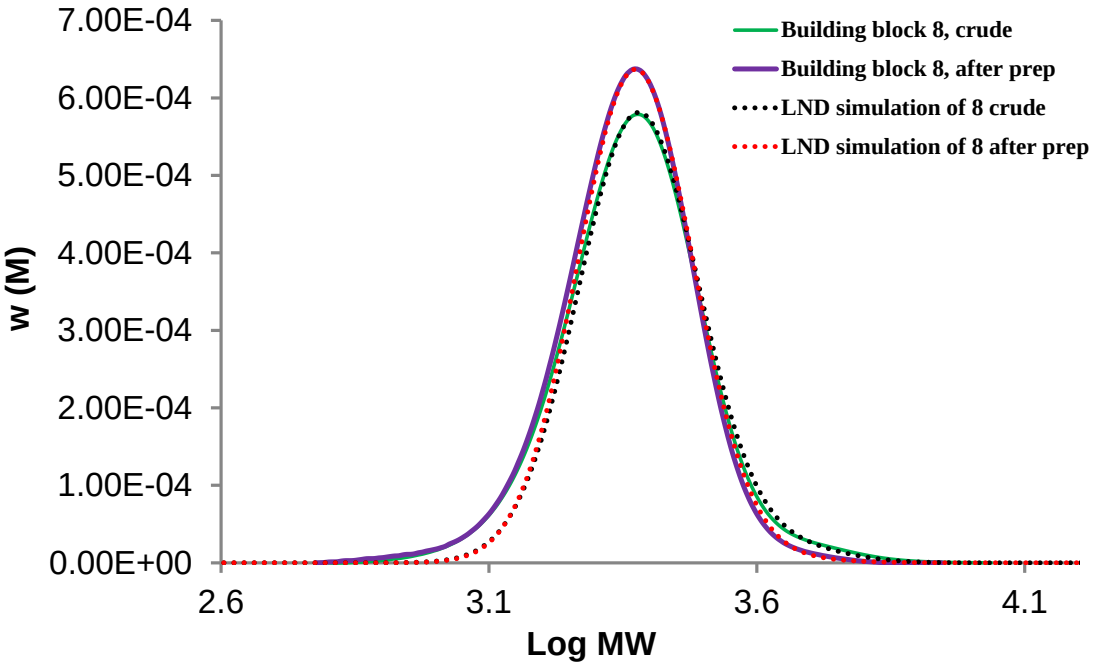

Figure A4.11: SEC traces of N_3-PSTY-Br **(8)** before and after purification by preparative-SEC, and LND simulation forproduct before and after prep. Determined from THF SEC, RI detector, PSTY standard.

Table A4.2: The molecular weight, change in hydrodynamic volume and weight percentages of the product (**8**) and higher molecular wieght species used in the LND method to simulate the experimental SEC traces in Figure A4.11.

Polymer	M_n[a]	PDI[a]	ΔHDV[a]	weight percentage%	
				Crude	After prep
8	2320	1.07	1	95.4	99.0
8+8	4640	1.05	1	4.6	1.0

[a]Absolute molecular weight , PDI ,and hydrodynamic volume change used for LND simulation.

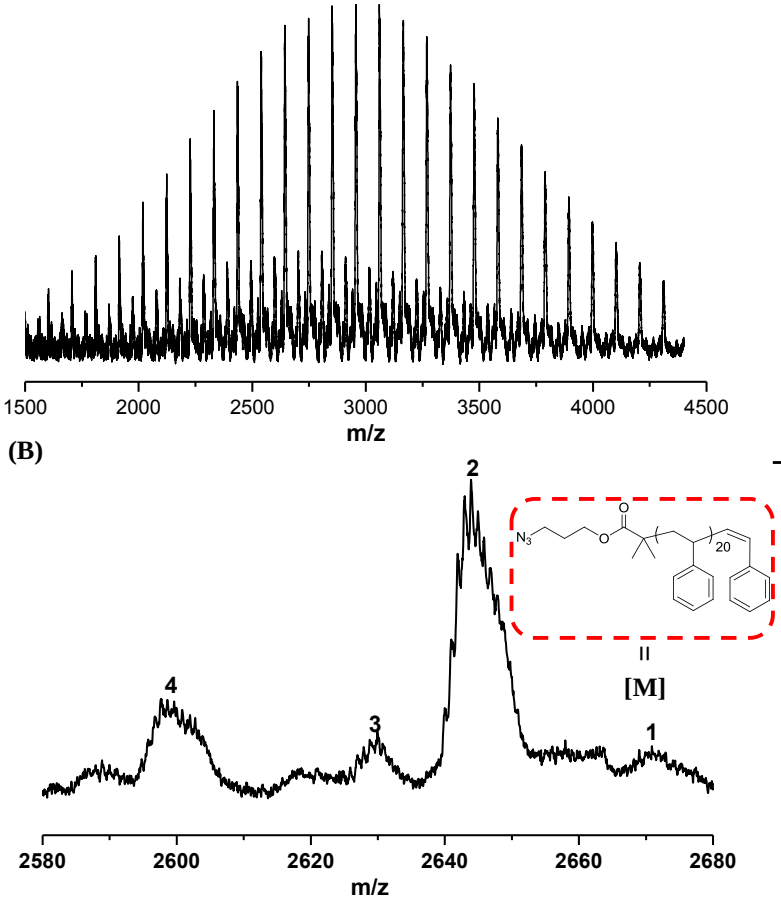

Peaks	Population	Calculated	Found
1	$M+Ag^+$	2672.43	2672.06
2	$M-N_2+Ag^+$	2644.43	2643.94
3	$M-N_3+Ag^+$	2630.42	2630.08
4	$M+K^+$	2602.43	2601.78

Figure A4.12: The full (A) and expanded (B) MALDI-ToF mass spectra of N_3-PSTY-Br (**8**). The spectra were recorded in reflect mode using DCTB as the matrix and $Ag(CF_3COO)$ as the cation source.

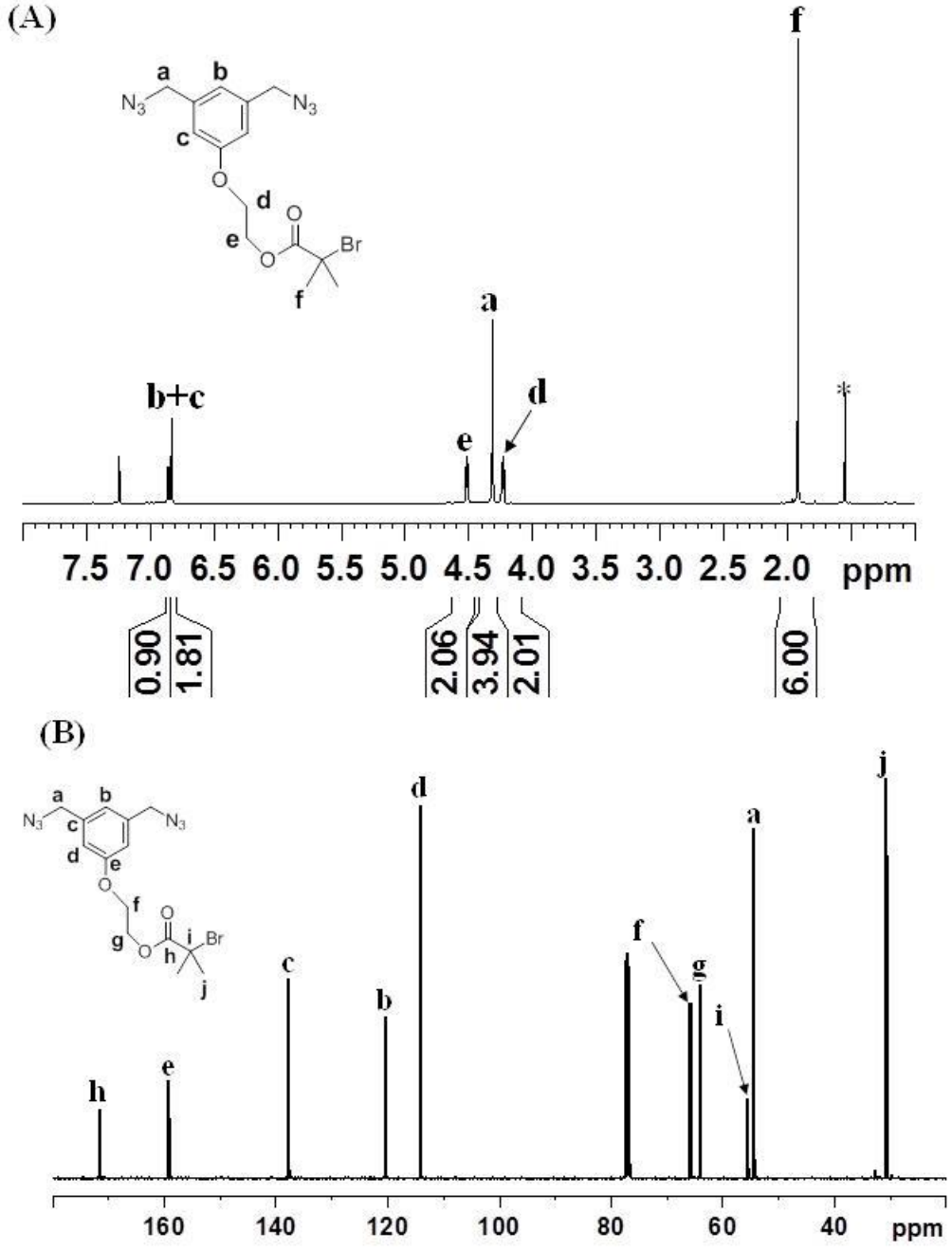

Figure A4.13: ^{1}H (A) and ^{13}C (B) NMR spectra of (**9**),recorded in $CDCl_3$ at 298K 500MHz.

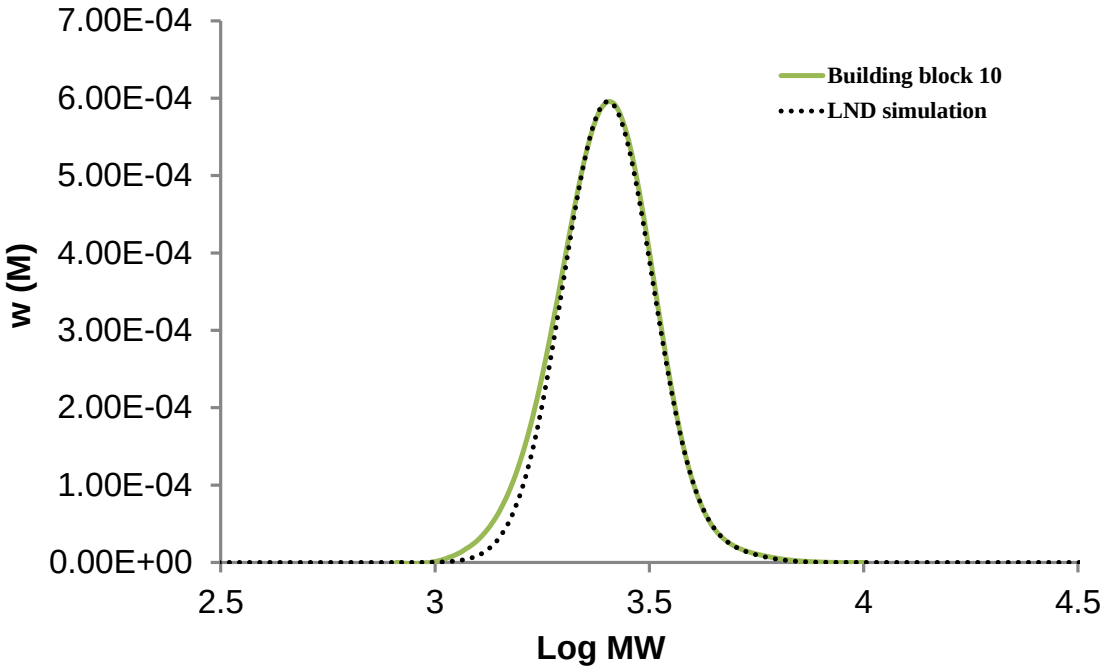

Figure A4.14: SEC trace of $(N_3)_2$-PSTY-Br (**10**).Determined from THF SEC, RI detector, PSTY standard.

Table A4.3: The molecular weight, change in hydrodynamic volume and weight percentages of the product (**10**) and higher molecular wieght species used in the LND method to simulate the experimental SEC traces in Figure A4.14.

Polymer	M_n[a]	PDI[a]	ΔHDV[a]	weight percentage%	
				Crude	After prep
10	2460	1.06	1	97.9	-
10+10	4920	1.03	1	2.08	-

[a]Absolute molecular weight , PDI ,and hydrodynamic volume change used for LND simulation.

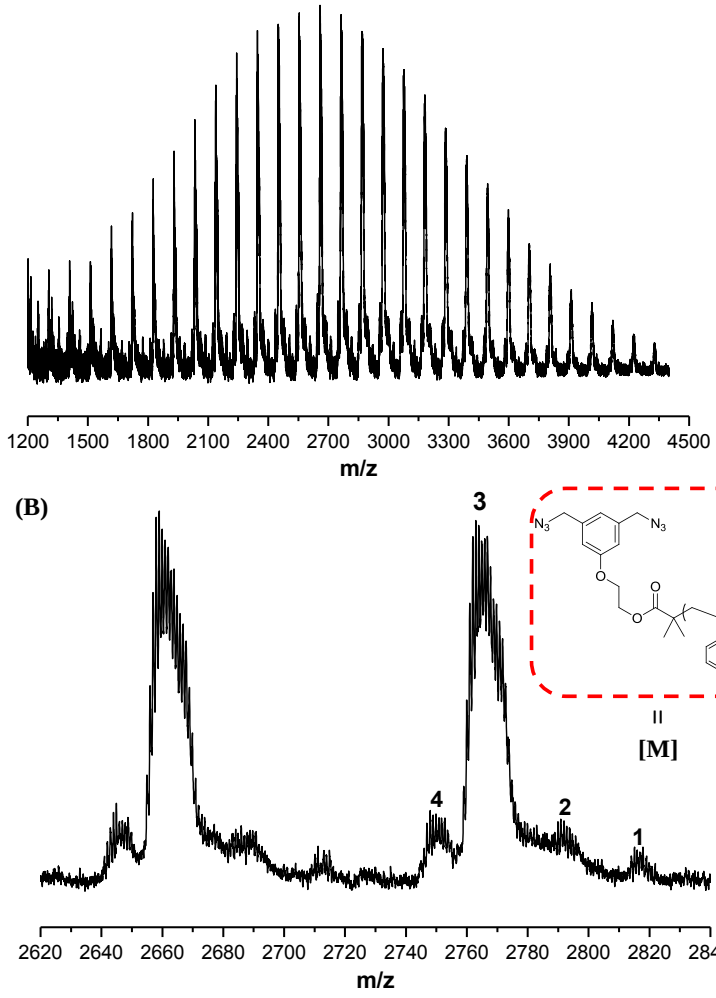

Peaks	Population	Calculated	Found
1	$M+Ag^+$	2816.47	2816.98
2	$M-N_2+Ag+$	2788.48	2789.76
3	$M-N_4+Ag+$	2760.49	2761.78
4	$M-N_5+Ag+$	2746.49	2748.27

Figure A4.15: The full (A) and expanded (B) MALDI-ToF mass spectra of $(N_3)_2$-PSTY-Br (**10**). The spectra were recorded in reflect mode using DCTB as the matrix and $Ag(CF_3COO)$ as the cation source.

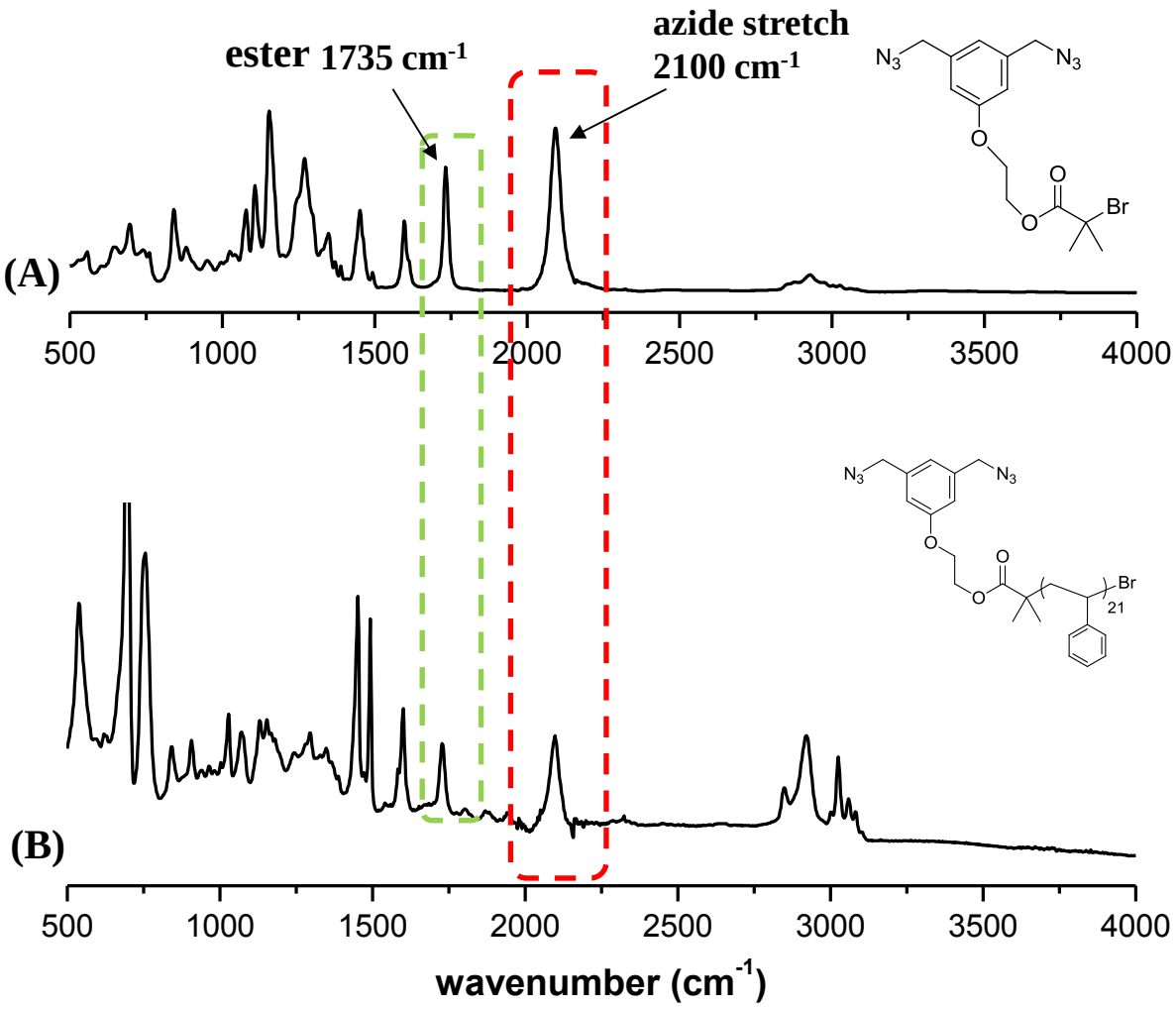

Figure A4.16:ATR-FTIR spectra of (A)**9** and (B) **10**.

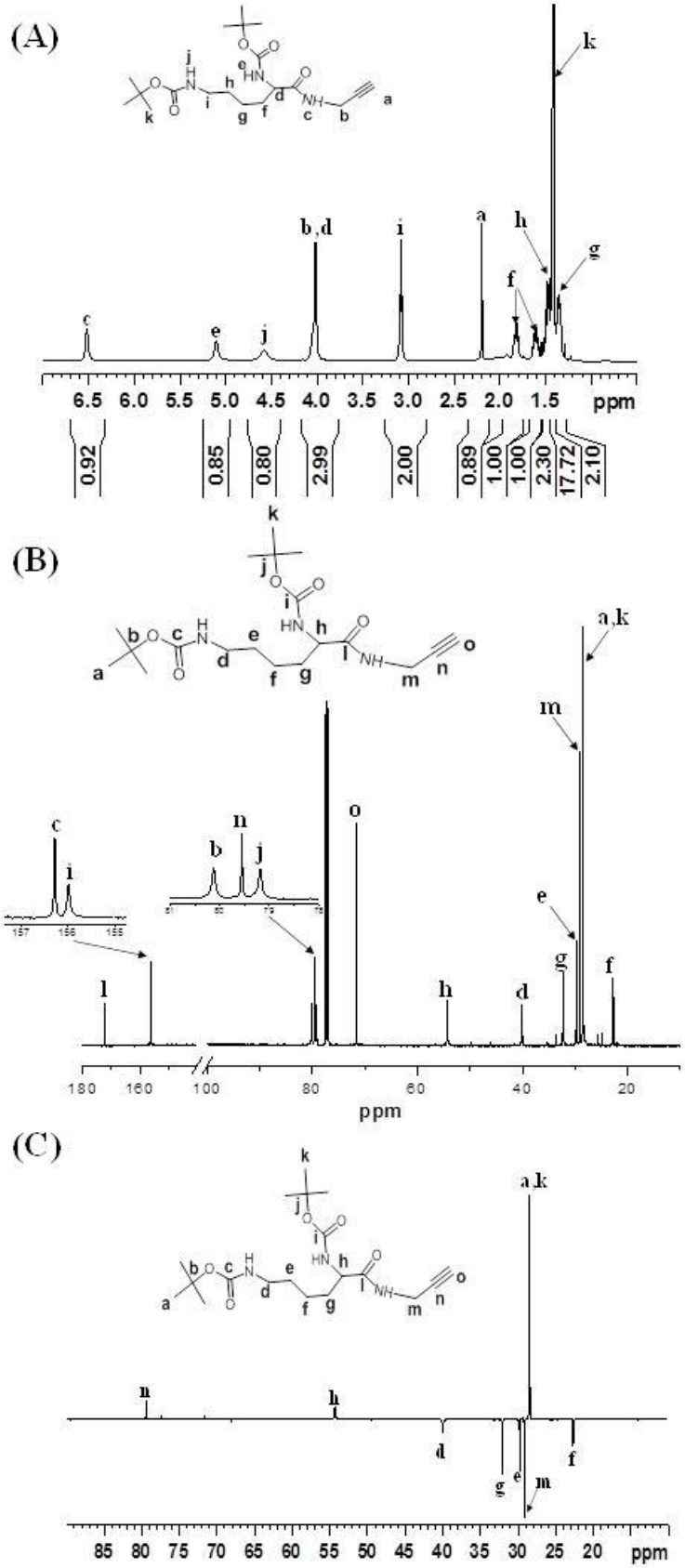

Figure A4.17: ^{1}H (A), ^{13}C (B) and ^{13}C DEPT-135^{o}(C) NMR spectra of alk-Lysine-Boc (**12**),recorded in $CDCl_3$ at 298 K, 500 MHz

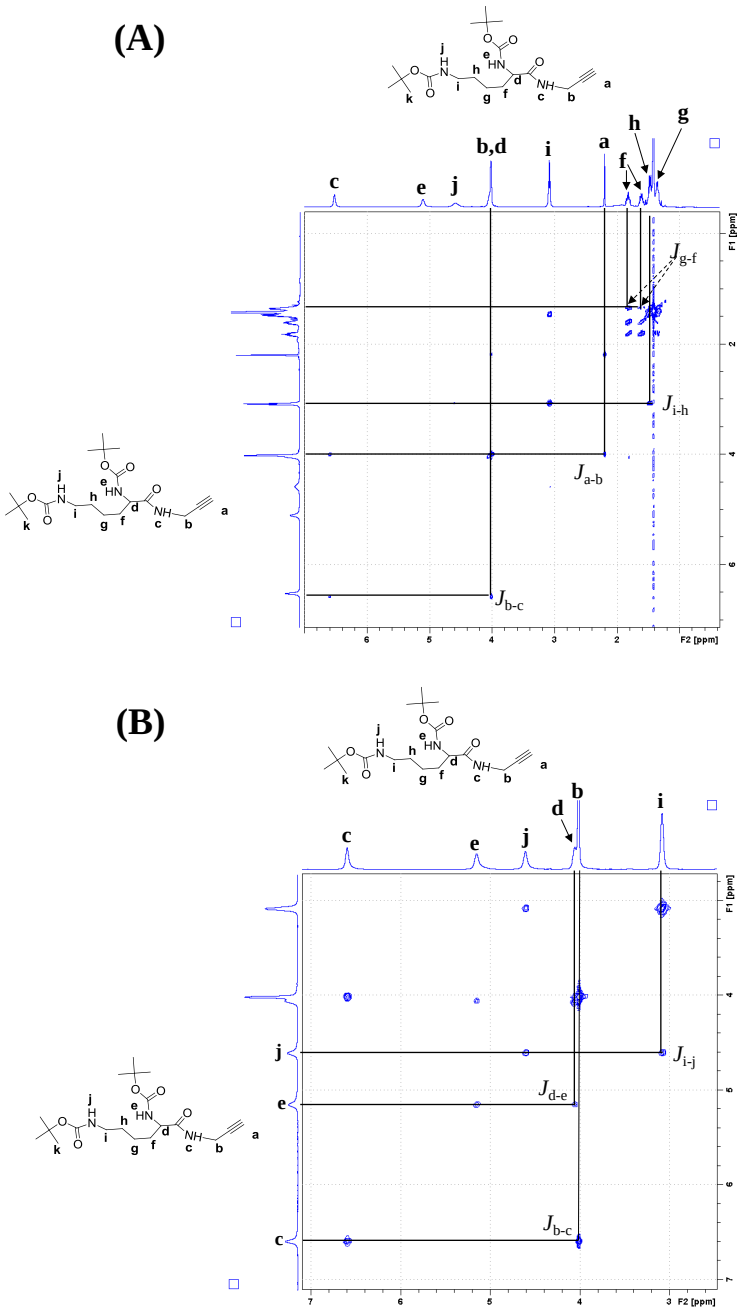

Figure A4.18: Full (A) and expanded (B) 2D-COSY NMR spectra of alk-Lysine-Boc (**12**), recorded in $CDCl_3$ at 298K, 500 MHz.

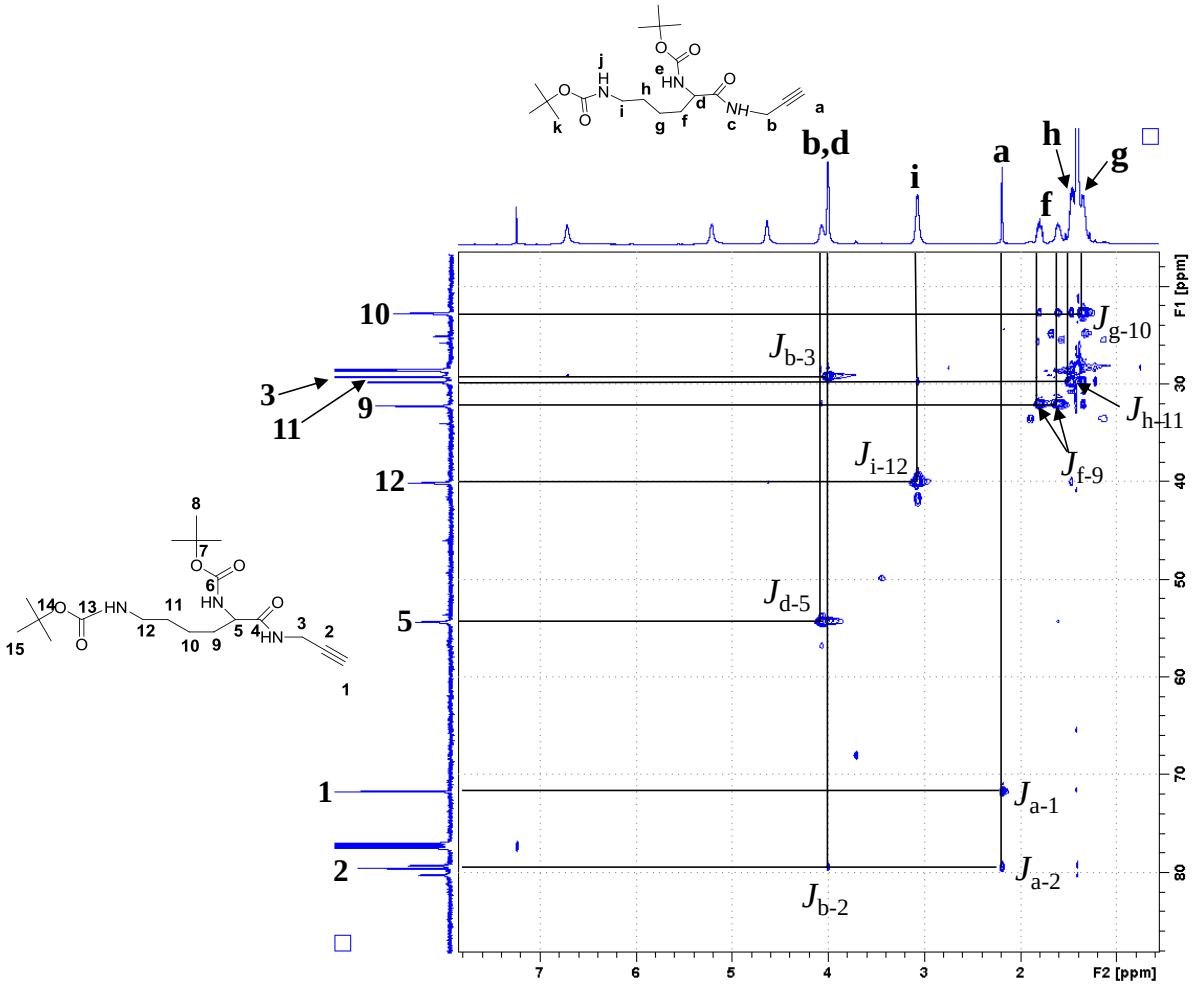

Figure A4.19: 2D HSQC NMR spectrum of alk-Lysine-Boc (**12**), recorded in $CDCl_3$ at 298 K, 500 MHz.

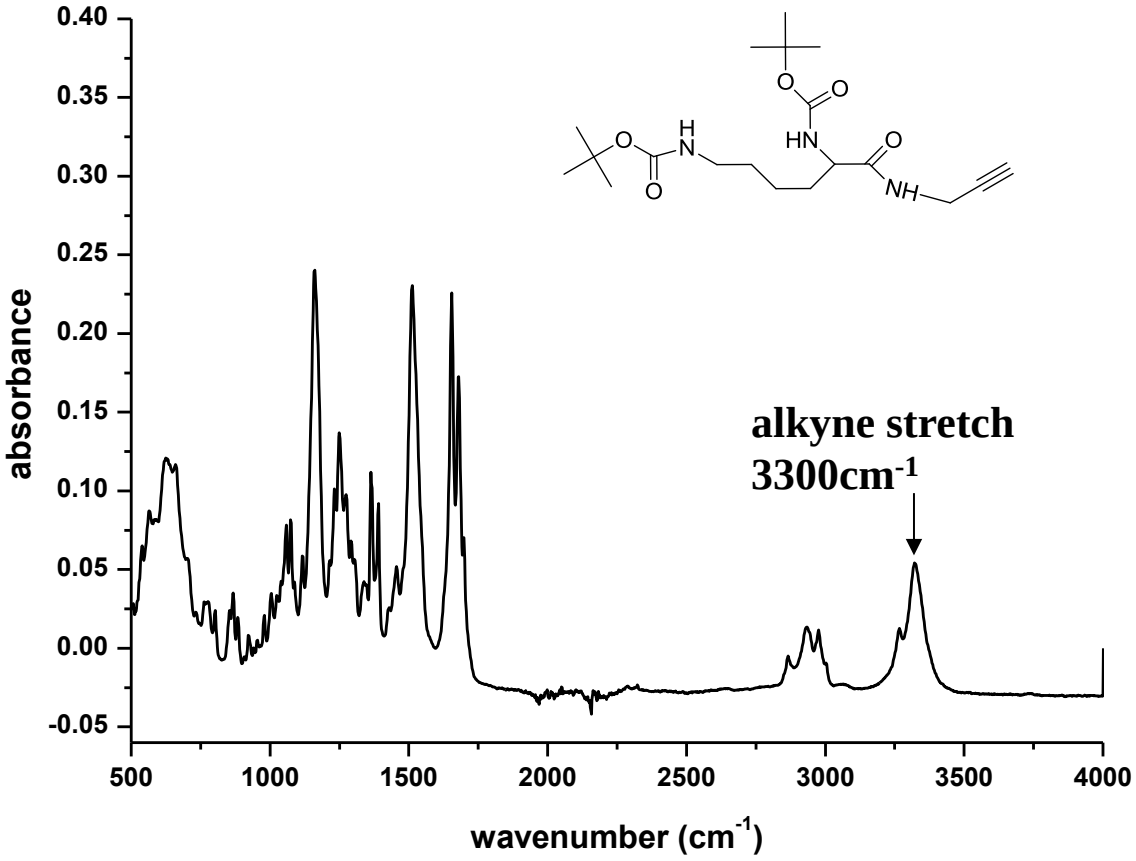

Figure A4.20: ATR-FTIR spectrum of alk-Lysine-Boc (**12**).

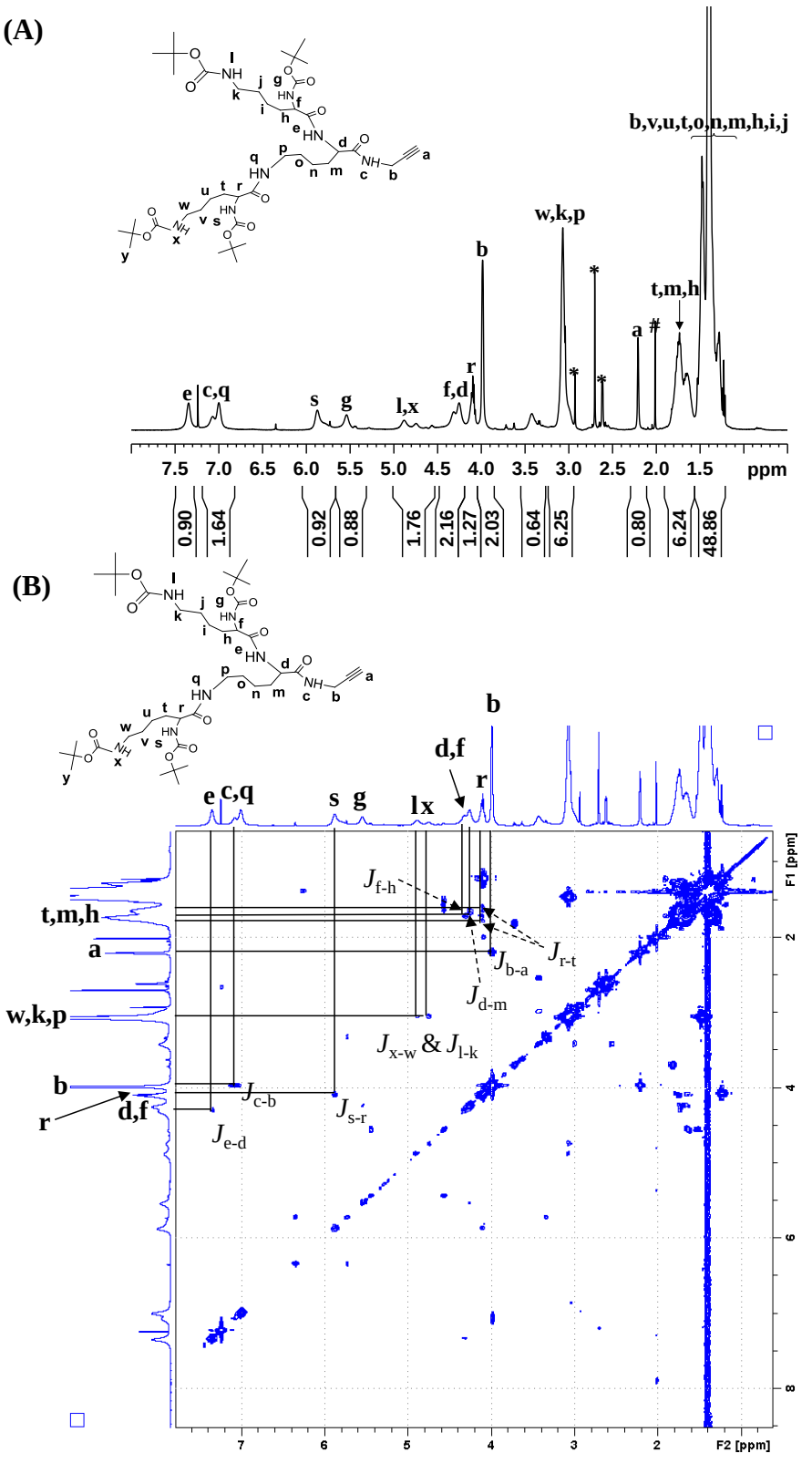

Figure A4.21: ^{1}H (A) and 2D COSY (B) NMR spectra of alk-Lysine-Boc dendron (**13**),recorded in $CDCl_3$ at 298K ,500MHz, #-EtOAc *-unknown impurities.

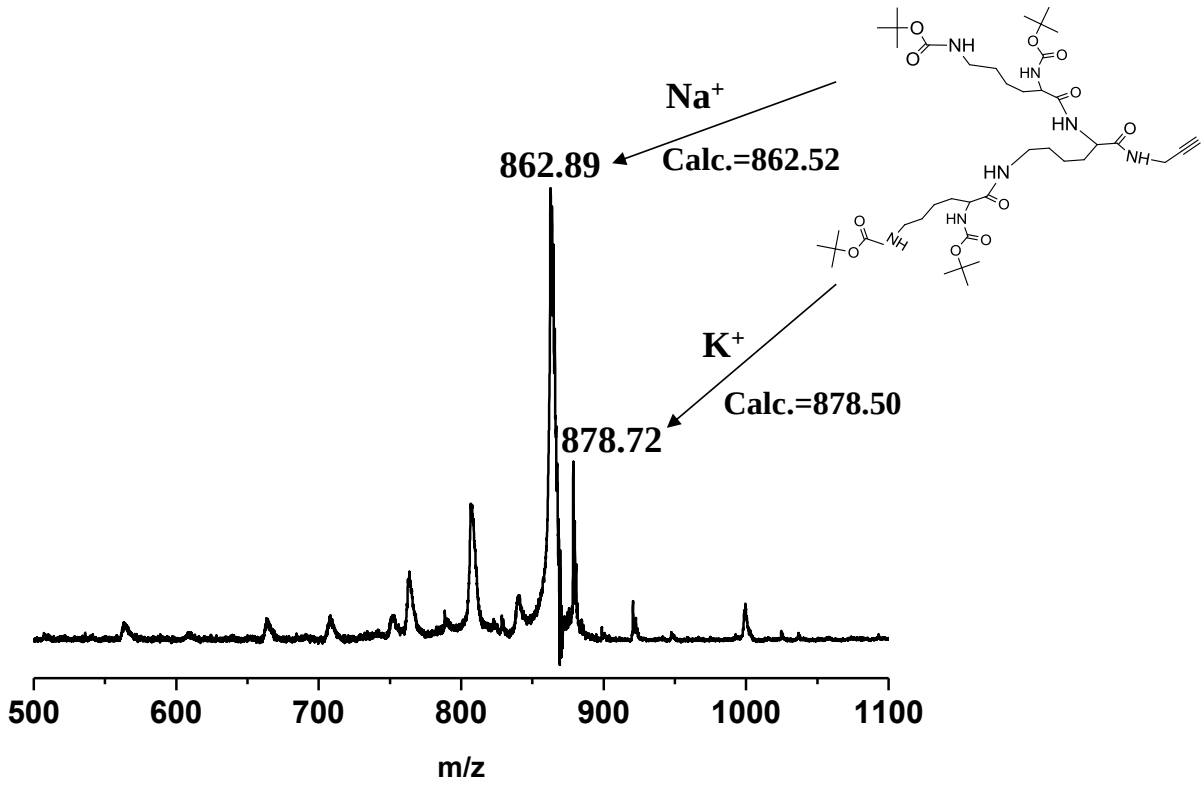

Figure A4.22: The MALDI-ToF mass spectrum of alk-Lysine-dendron (**13)**. The spectrum was recorded in reflect mode using DCTB as the matrix and Na(CF_3COO) as the cation source.

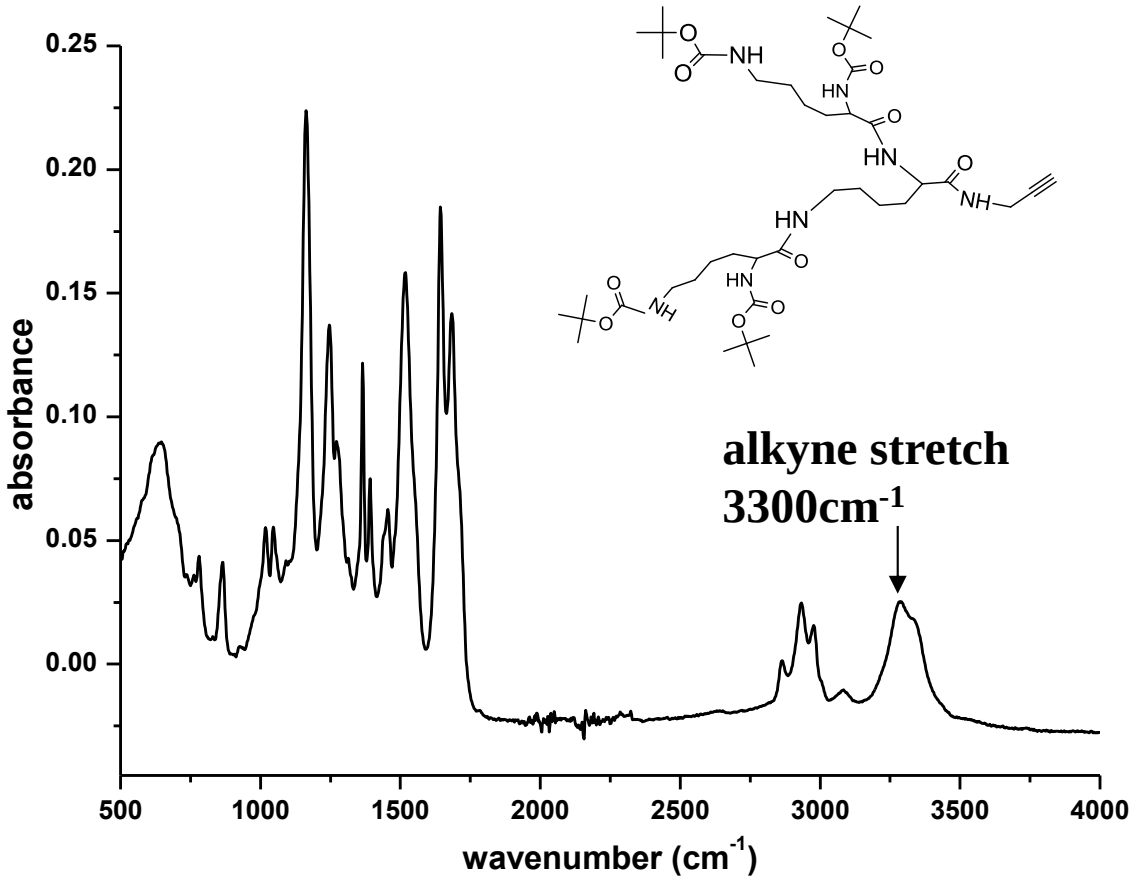

Figure A4.23: ATR-FTIRspectrumof alk-Lysine-Boc (**13**).

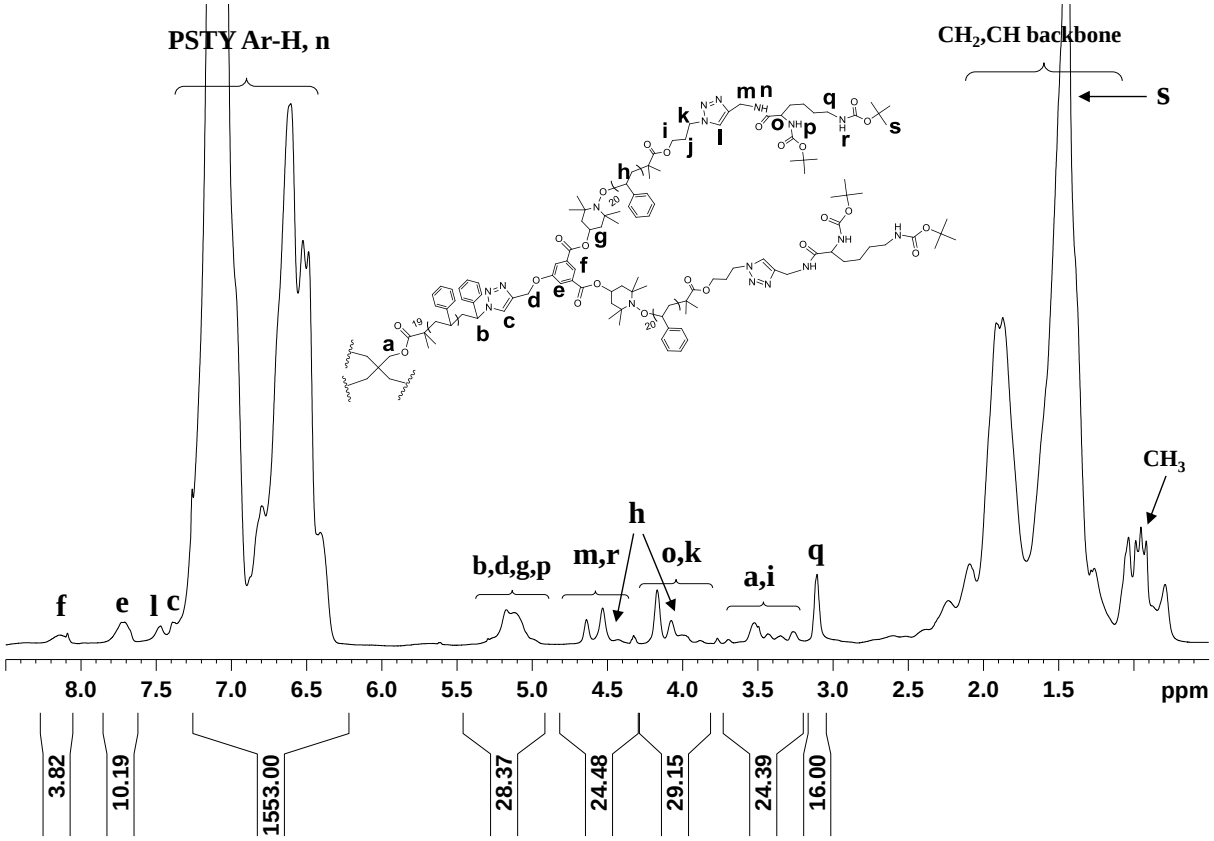

Figure A4.24: ^{1}H 1D DOSY NMR spectrum of **14**,recorded in $CDCl_3$ at 298K, 500MHz, the gradient strength (gpz6) was used as 90 % and gradient pulse length (p30) was used as 2.5 ms.

.

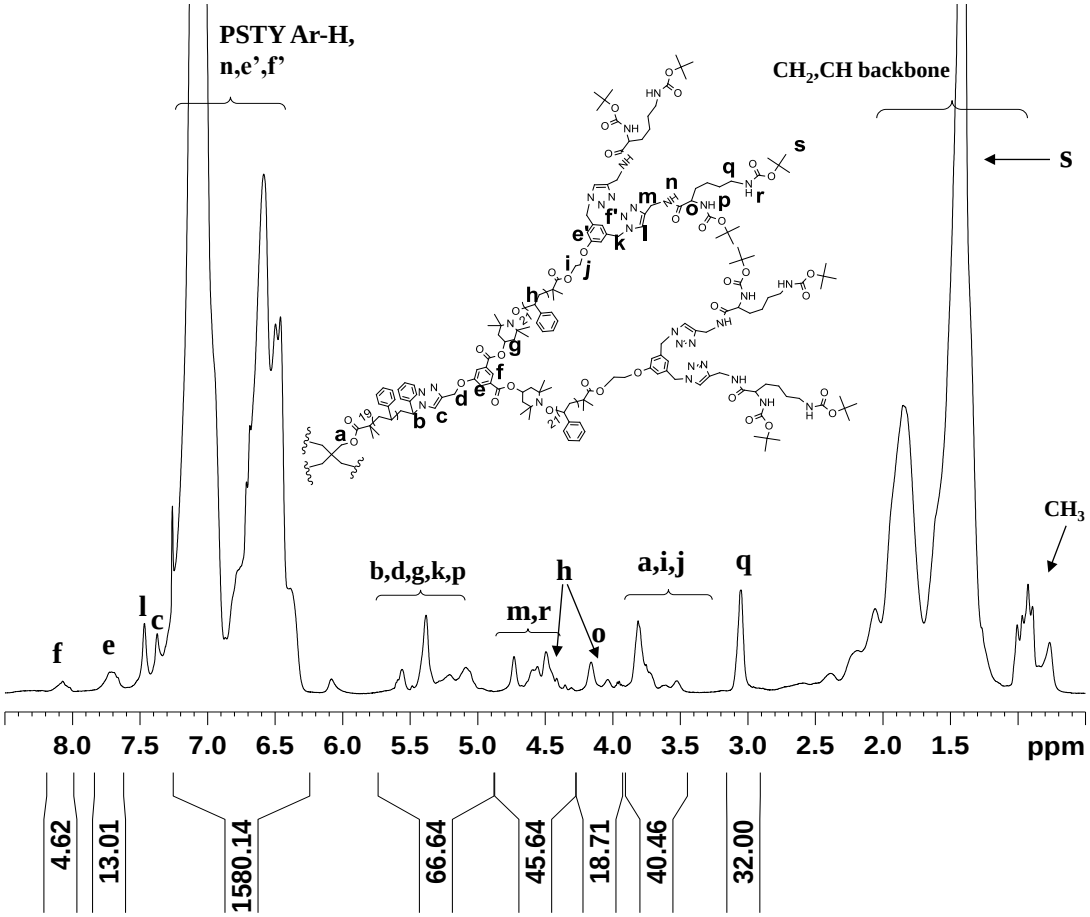

Figure A4.25: ^{1}H 1D DOSY NMR spectrum of **15**,recorded in $CDCl_3$ at 298K, 500MHz, the gradient strength (gpz6) was used as 90 % and gradient pulse length (p30) was used as 2.5 ms.

.

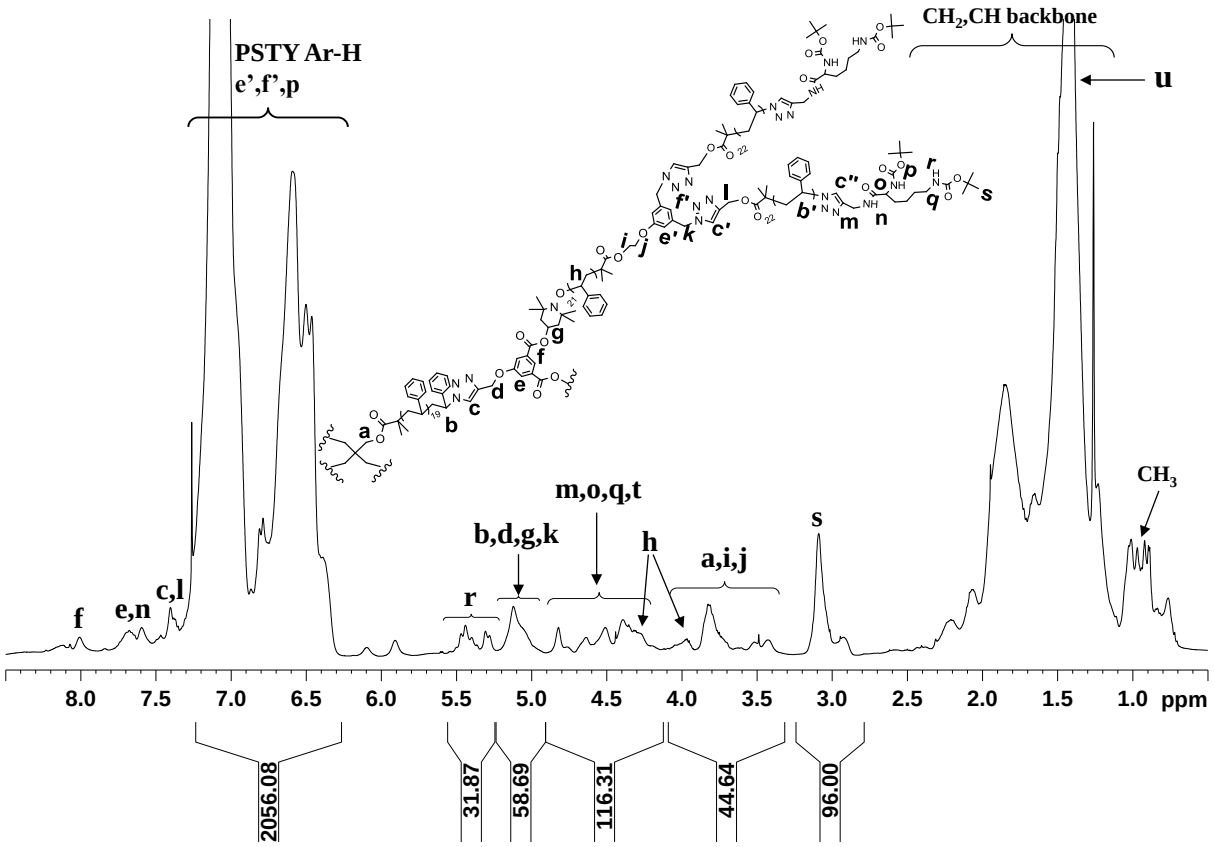

Figure A4.26: ^{1}H 1D DOSY NMR spectrum of (**16**),recorded in $CDCl_3$ at 298K, 500MHz, the gradient strength (gpz6) was used as 90 % and gradient pulse length (p30) was used as 2.5 ms.

.

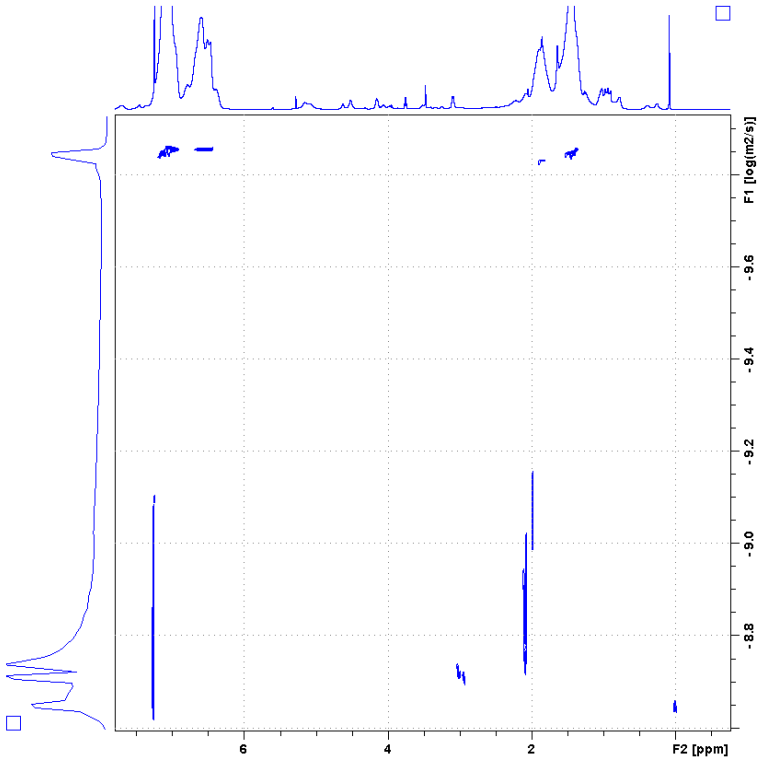

Figure A4.27:2D DOSY NMR spectrum of dendrimer **14**, recorded in $CDCl_3$, 298K, the parameter were used as following: diffusion delay (Δ , 200 ms) gradient pulse length (p30, 2.5 ms).

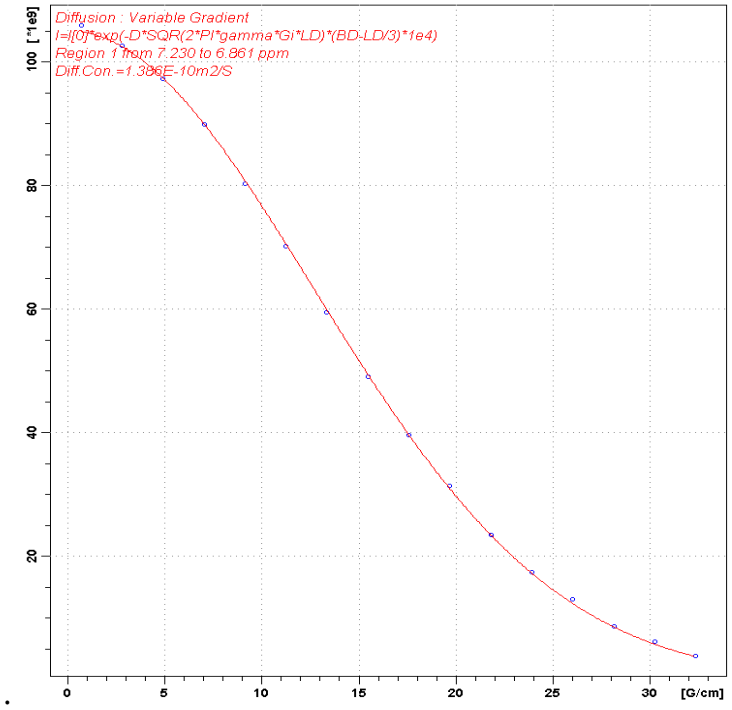

Figure A4.28: Exponential fit for NMR signal decay due to the gradients using equation (1) for dendrimer **14**. Processed with the Bruker XWIN NMR software using vargard fitting function giving diffusion coefficient $D=1.38 \times 10^{-10}\ m^2\ S^{-1}$.

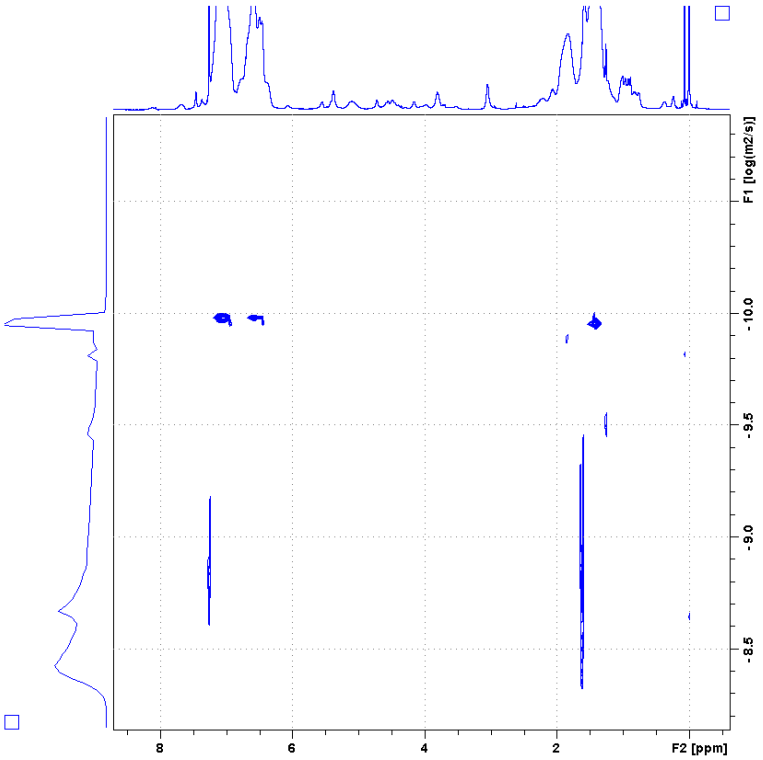

Figure A4.29: 2D DOSY NMR spectrum of dendrimer **15**, recorded in $CDCl_3$, 298K, the parameters were used as following: diffusion delay (Δ , 200 ms)gradient pulse length (p30, 2.5 ms).

.

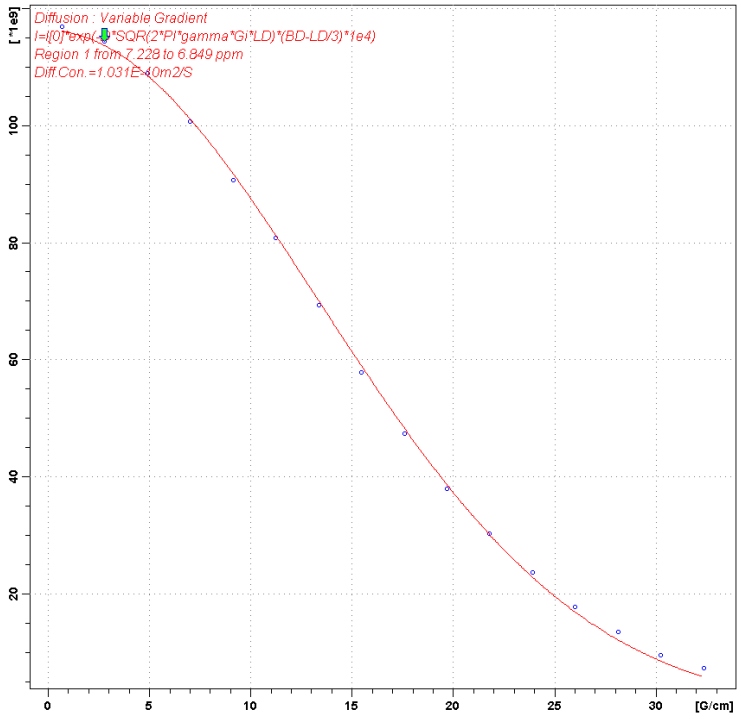

Figure A4.30: Exponential fit for NMR signal decay due to the gradients using equation (1) for dendrimer **15**. Processed with the Bruker XWIN NMR software using vargard fitting function giving diffusion coefficient D=1.03 x 10^{-10} m^2 S^{-1}.

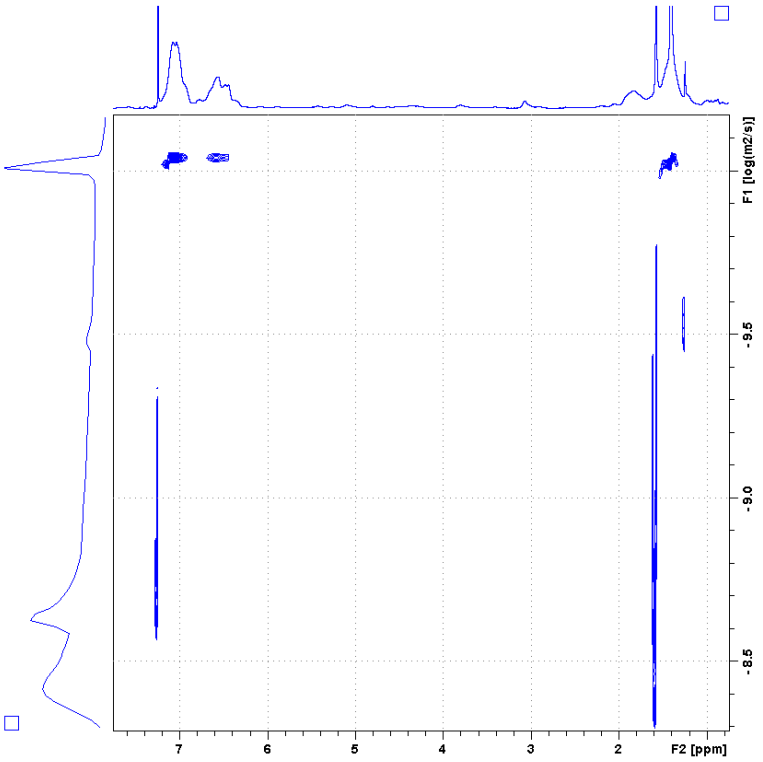

Figure A4.31: 2D DOSY NMR spectrum of dendrimer **16**, recorded in $CDCl_3$, 298K, the parameters were used as following: diffusion delay (Δ , 200 ms)gradient pulse length (p30, 2.5 ms).

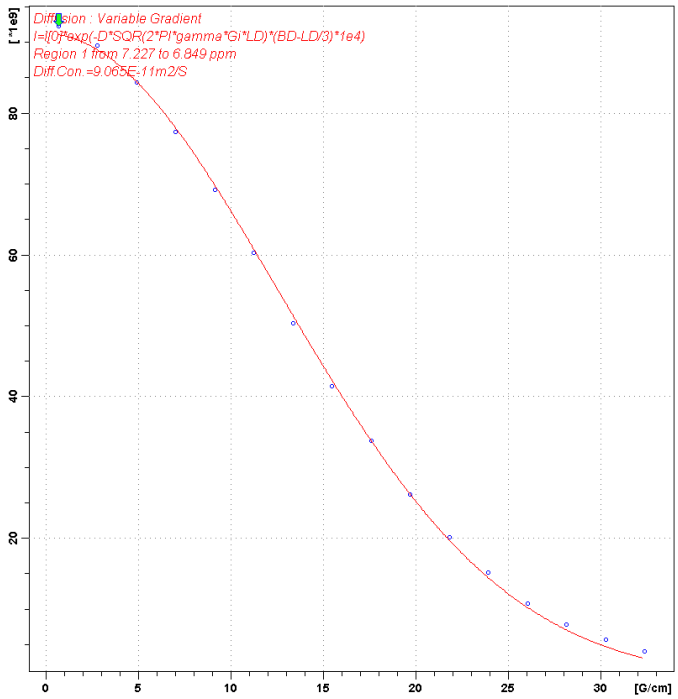

Figure A4.32: Exponential fit for NMR signal decay due to the gradients using equation (1) for dendrimer **16**. Processed with the Bruker XWIN NMR software using vargard fitting function giving diffusion coefficient D=9.06 x 10^{-11} m^2 S^{-1}.

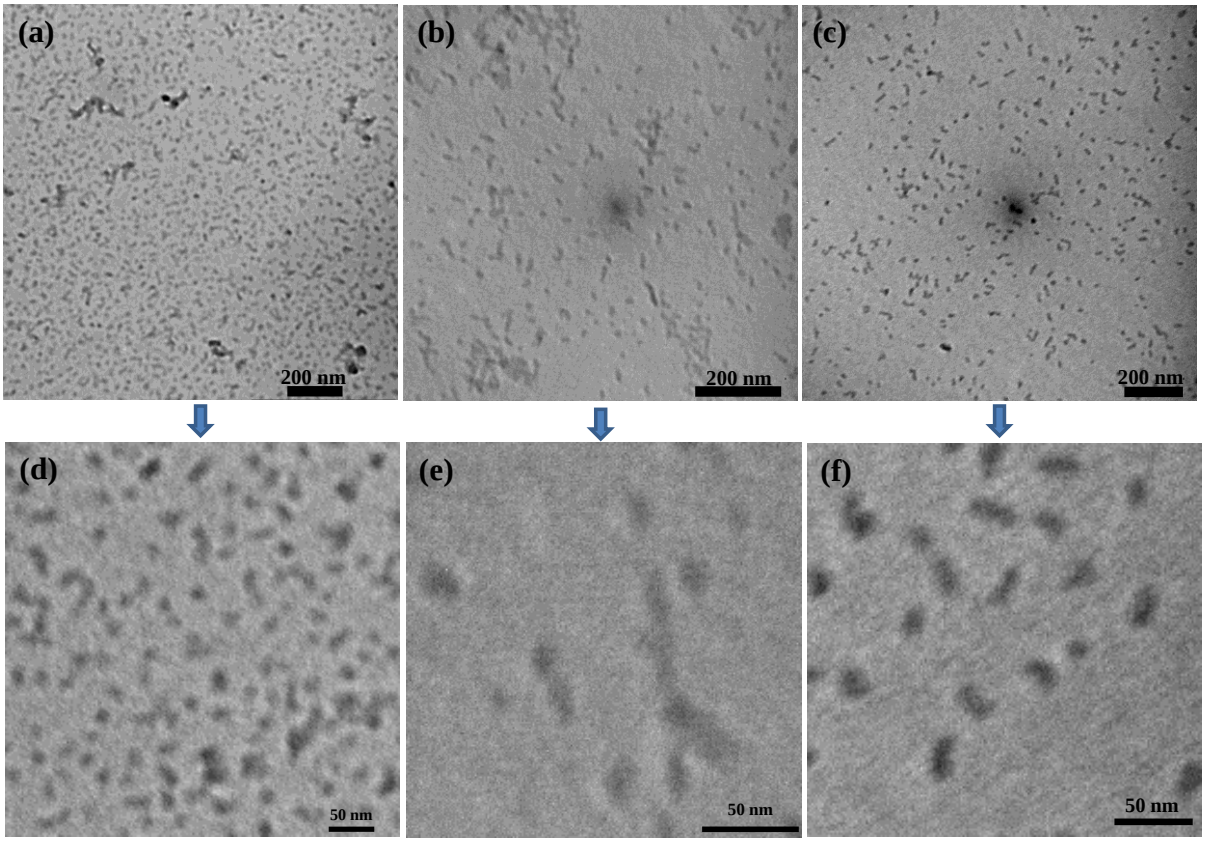

Figure A4.33: TEM images of dendrimers (a) and (d) **17**, (b) and (e) **18**, (b) and (f) **19** in water.

Appendix D

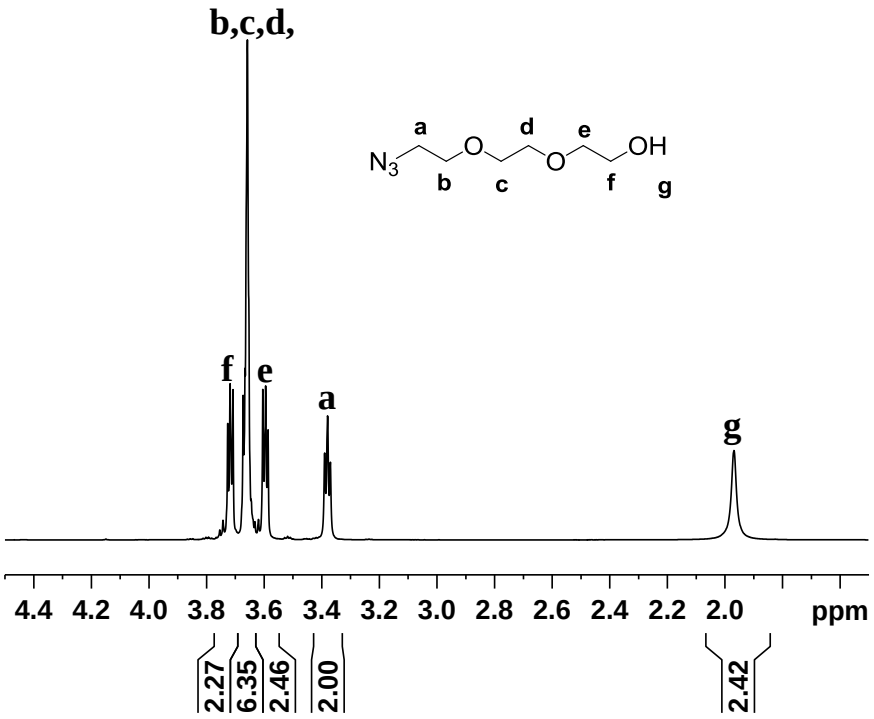

Figure A5.1: ^{1}H NMR spectrum (500 MHz) of **2**, recorded in $CDCl_3$ at 298K.

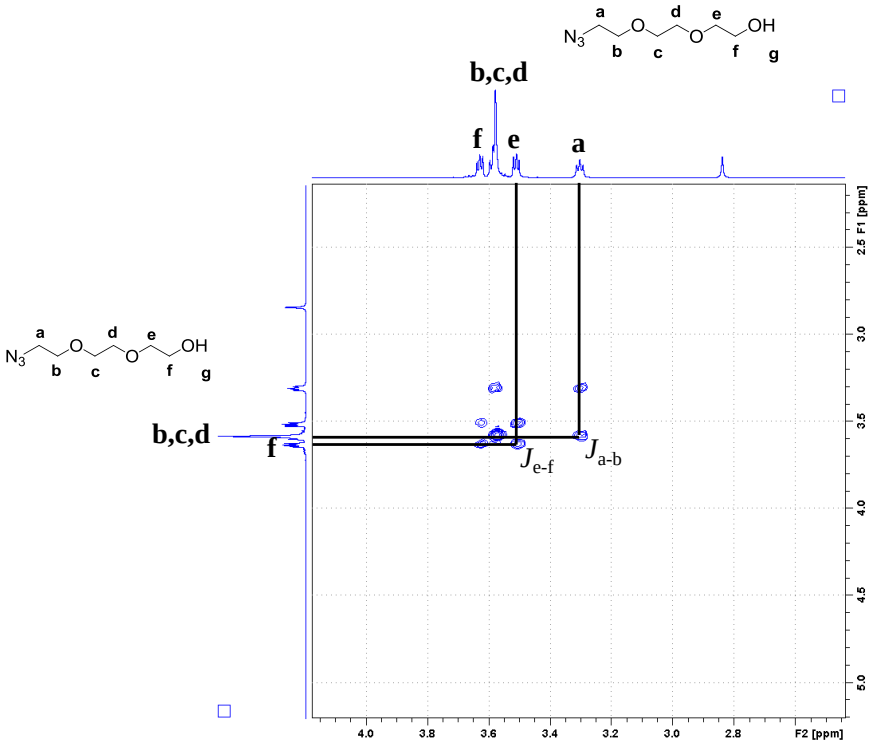

Figure A5.2: 2D-COSY spectrum (500 MHz) of **2**, recorded in $CDCl_3$ at 298K.

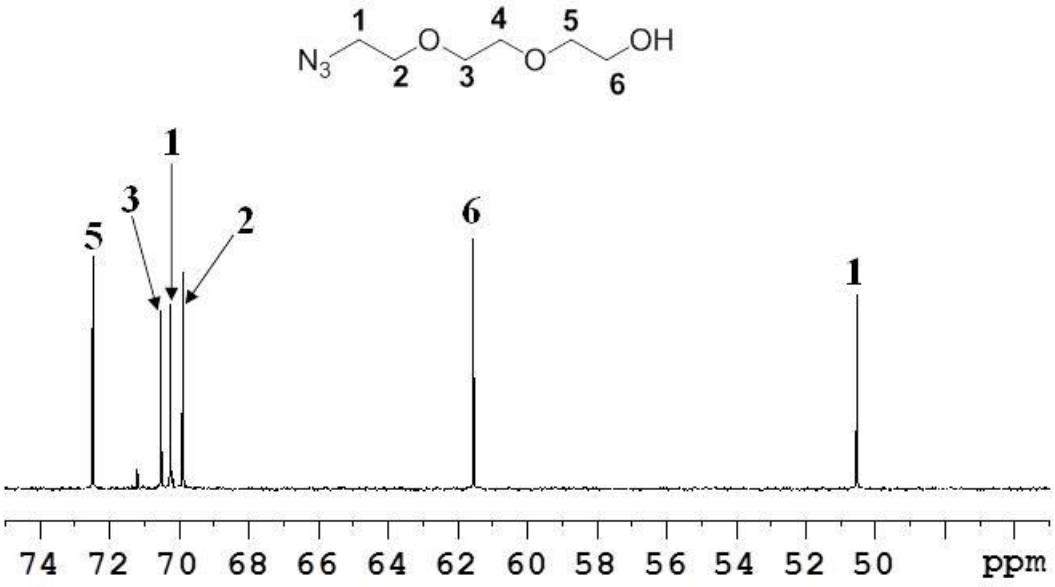

Figure A5.3: ^{13}C NMR spectrum (500 MHz) of **2**.

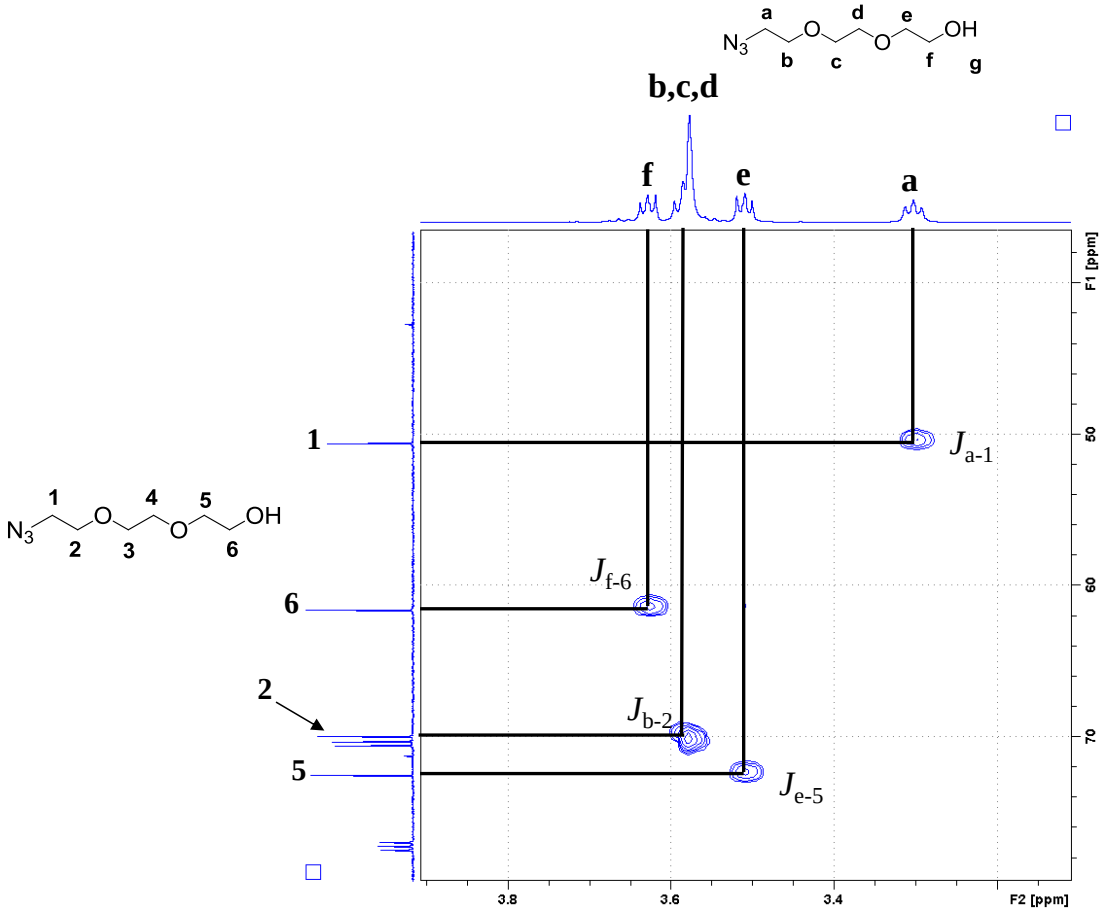

Figure A5.4: 2D-HSQC spectrum (500 MHz) of **2**, recorded in $CDCl_3$ at 298K.

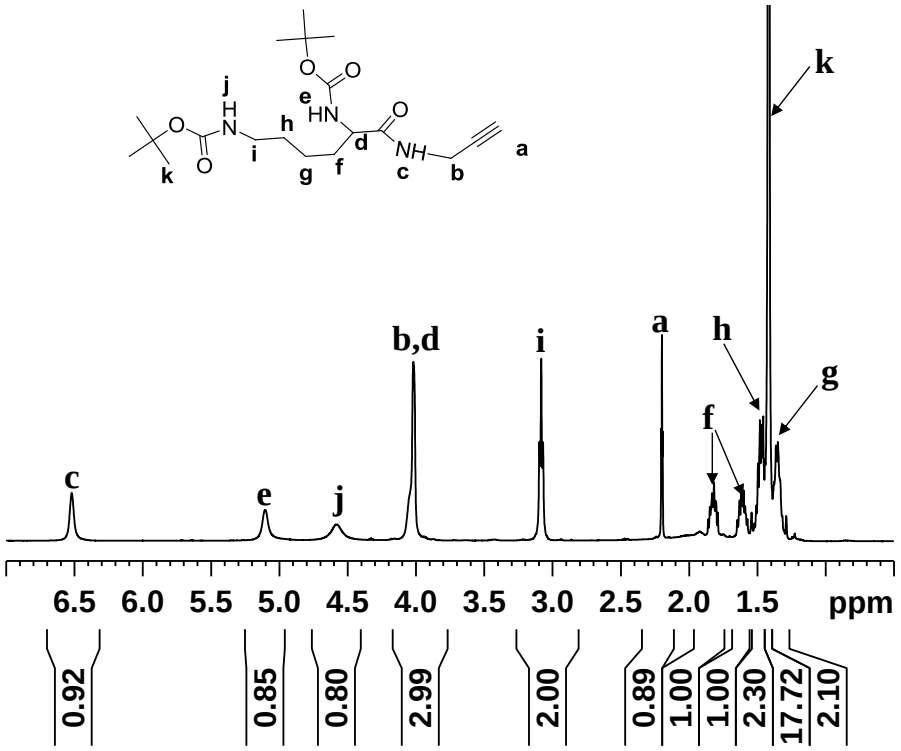

Figure A5.5: ^{1}H NMR of **4**,recorded in $CDCl_3$ at 298 K, 500 M.

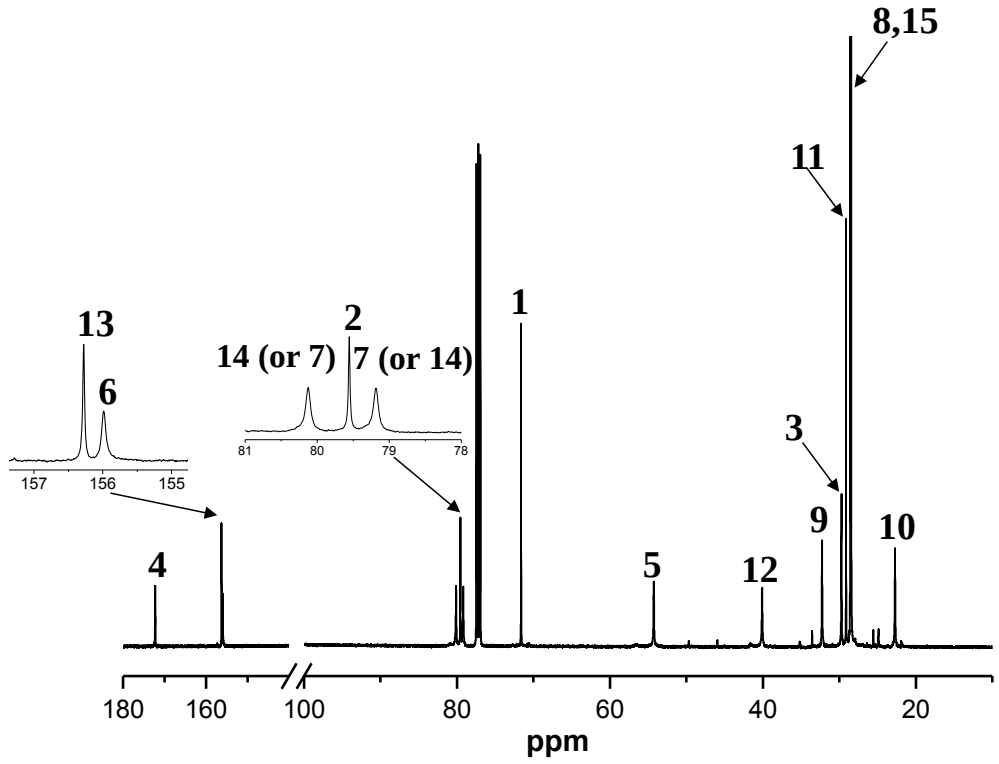

Figure A5.6: 2D-COSY spectrum (500 MHz) of **4**, recorded in $CDCl_3$ at 298K.

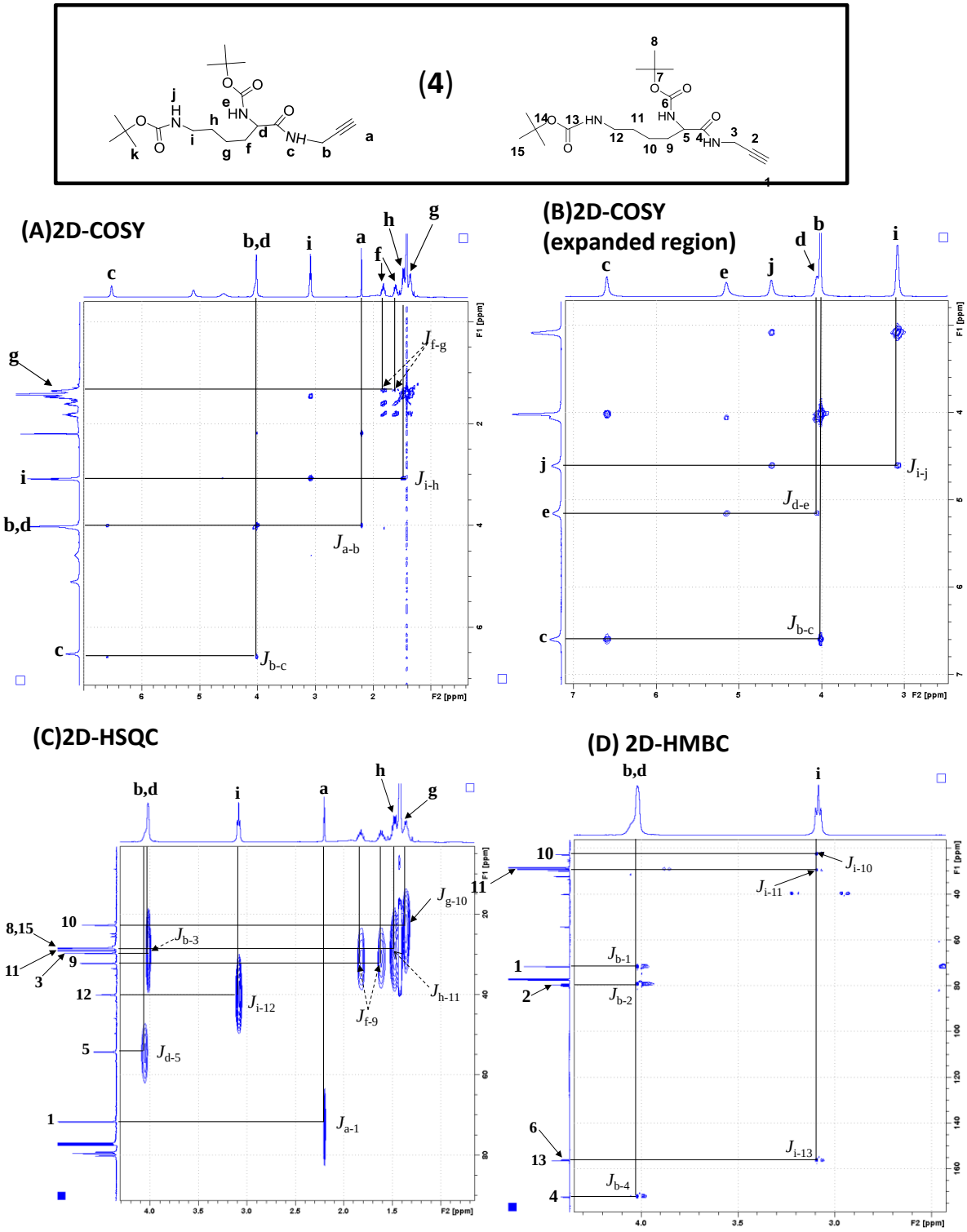

Figure A5.7: NMR of **4** recorded in $CDCl_3$ at 298K, 500MHz.

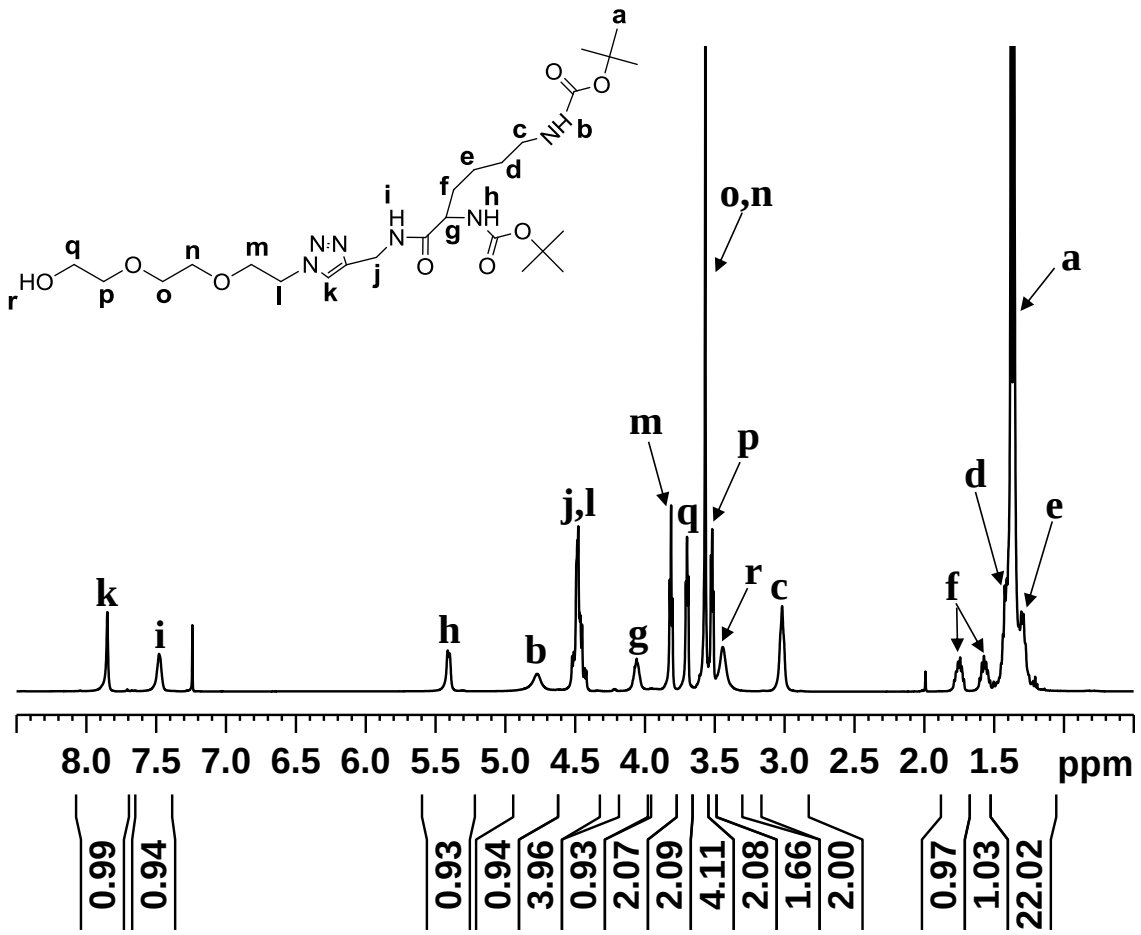

Figure A5.8: ^{1}H NMR spectrum (500 MHz) of **5**, recorded in $CDCl_3$ at 298K.

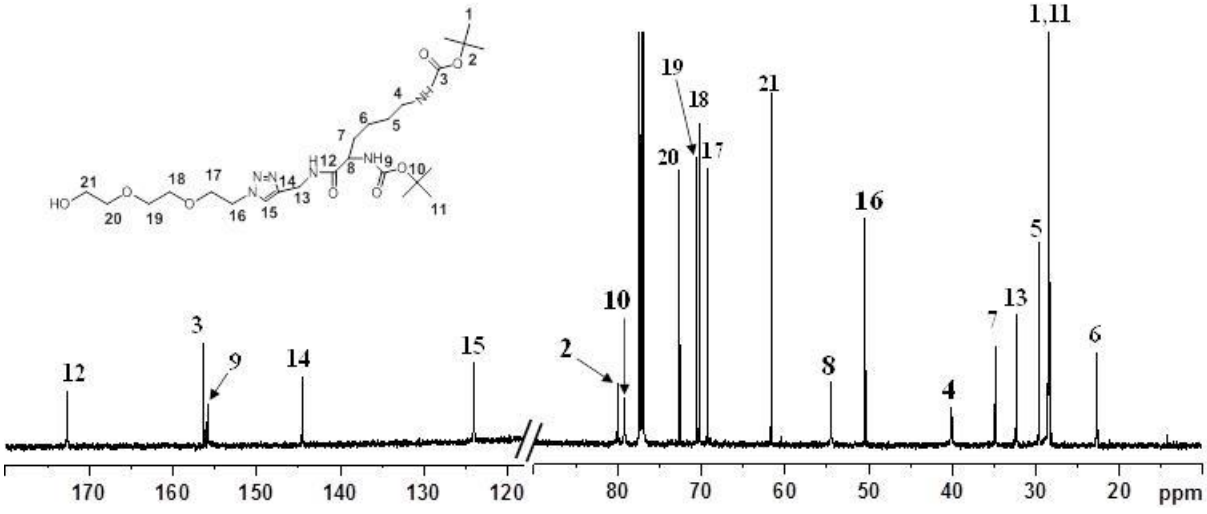

Figure A5.9: ^{13}C NMR spectrum of **5**,recorded in $CDCl_3$ at 298 K, 500 M.

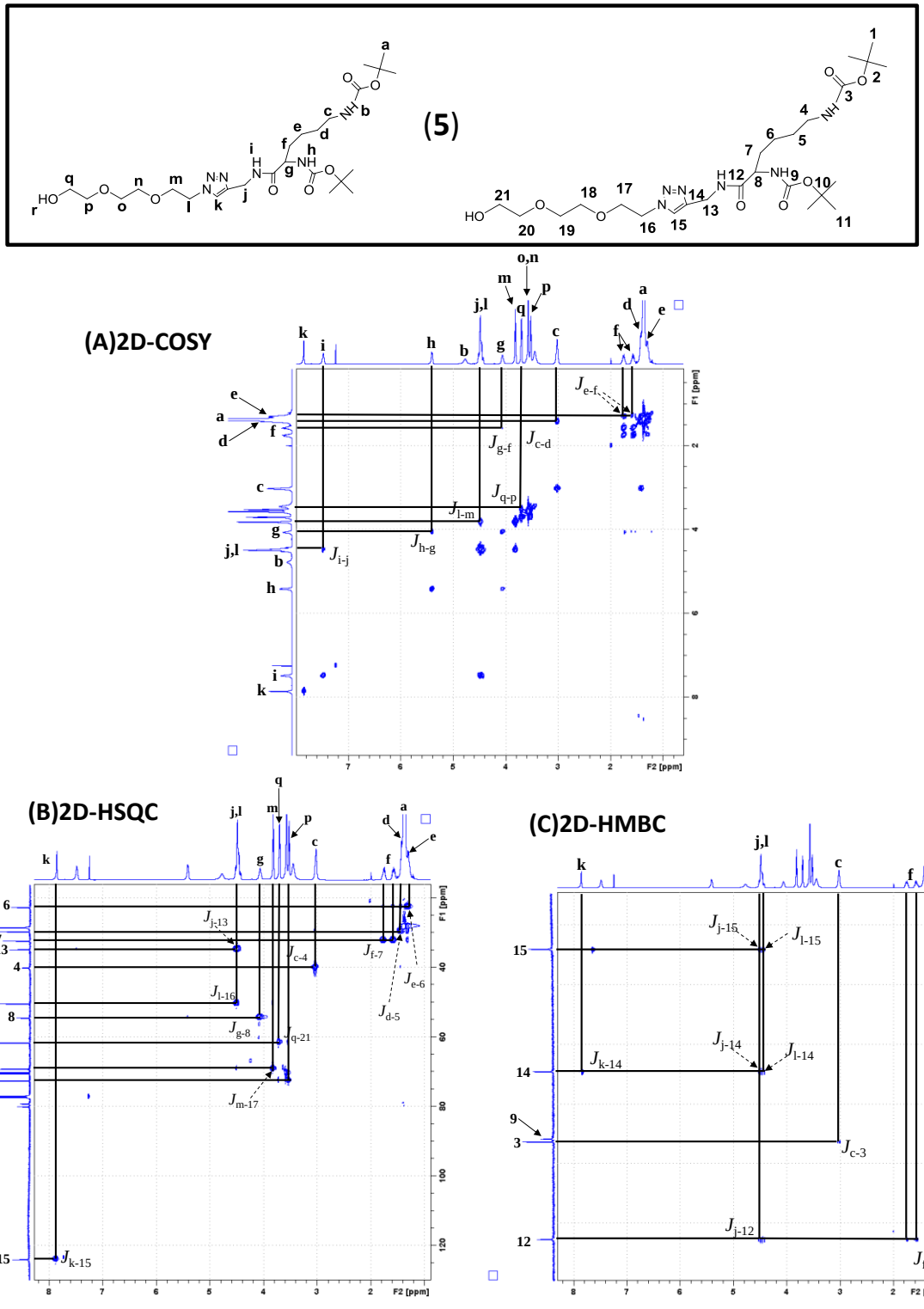

Figure A5.10: NMR of **5** recorded in $CDCl_3$ at 298K, 500MHz.

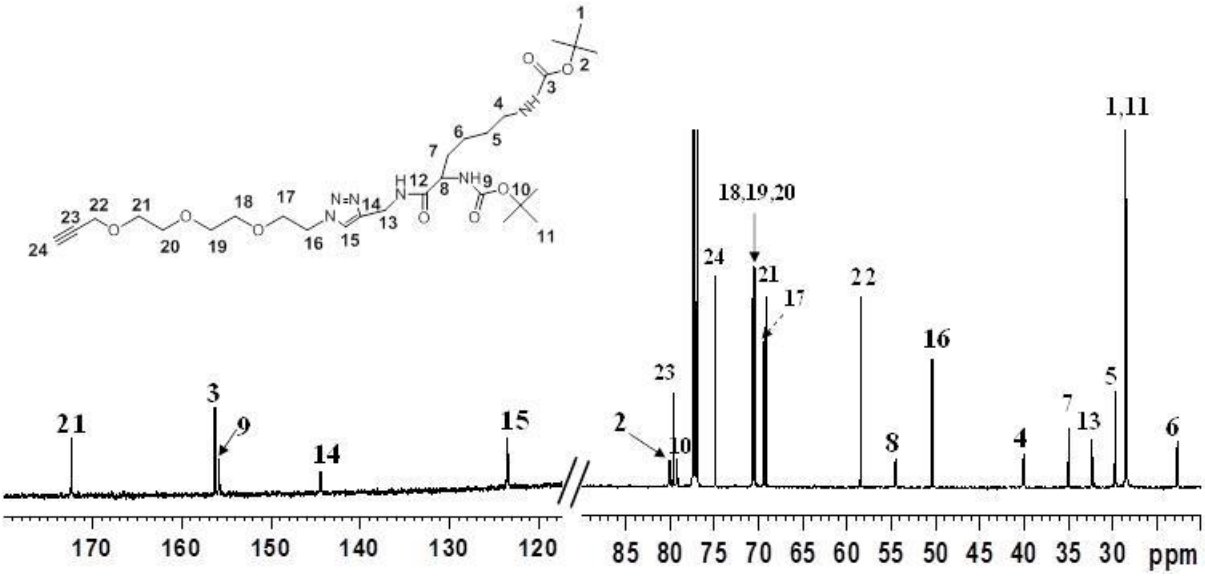

Figure A5.11: ^{13}C NMR spectrum (500 MHz) of **6**, recorded in $CDCl_3$ at 298K.

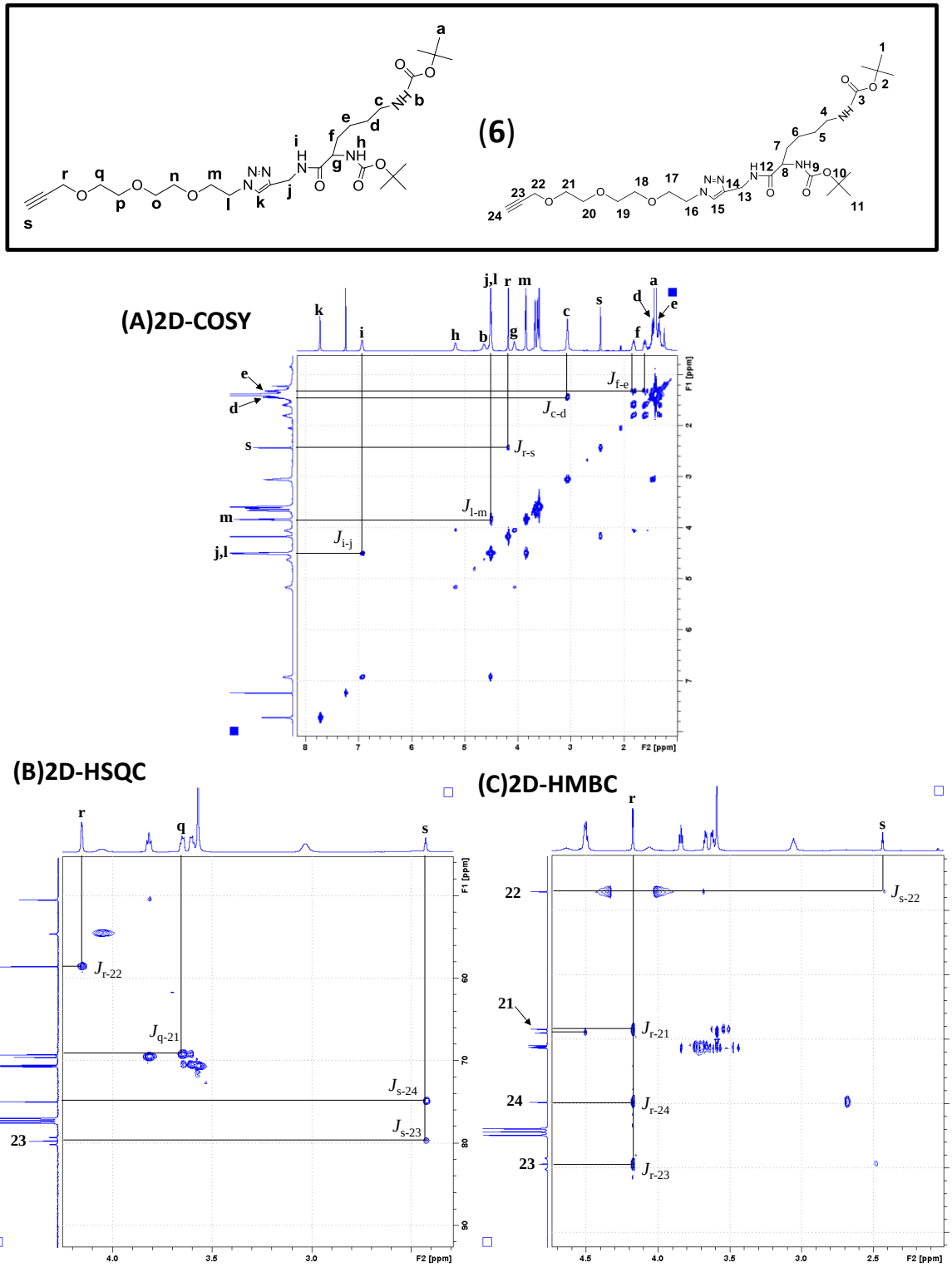

Figure A5.12: NMR of **6** recorded in $CDCl_3$ at 298K, 500MHz.

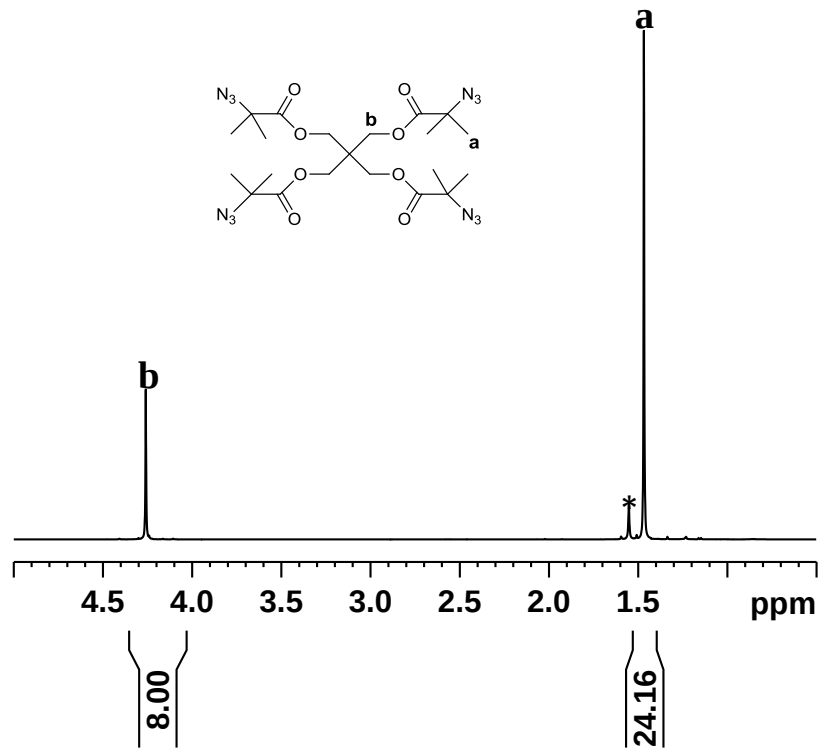

Figure A5.13: ^{1}H NMR spectrum (500 MHz) of **10**, recorded in $CDCl_3$ at 298K, *=H_2O.

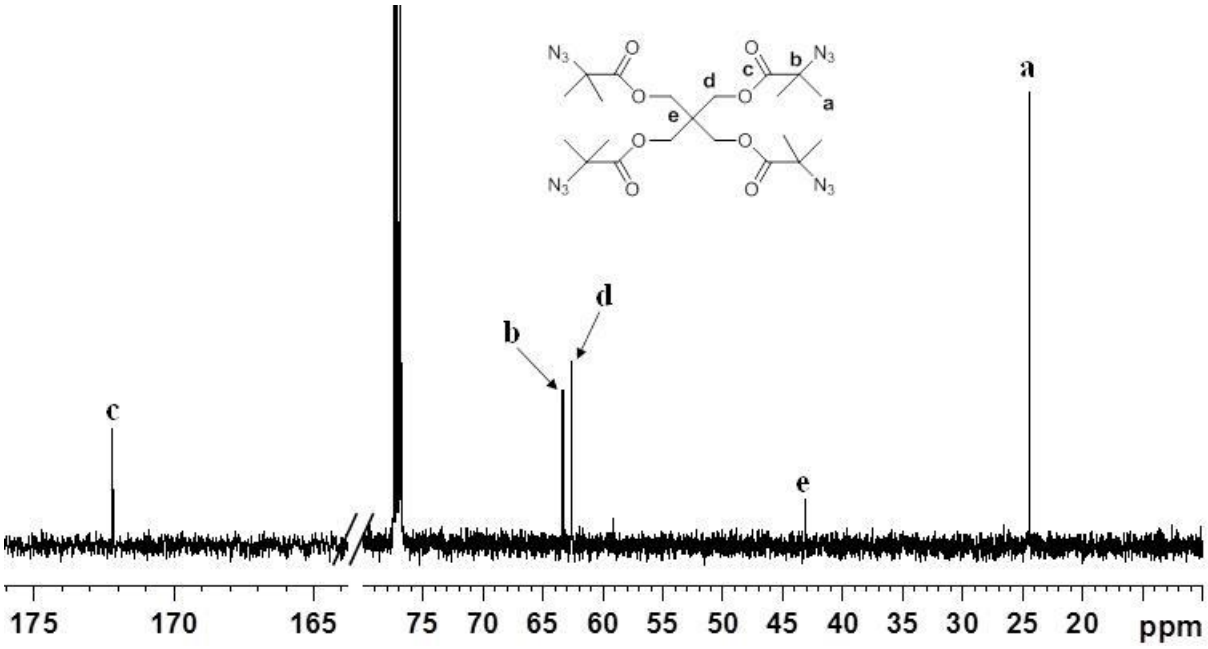

Figure A5.14: ^{13}C NMR spectrum of **10**,recorded in $CDCl_3$ at 298 K, 500 M.

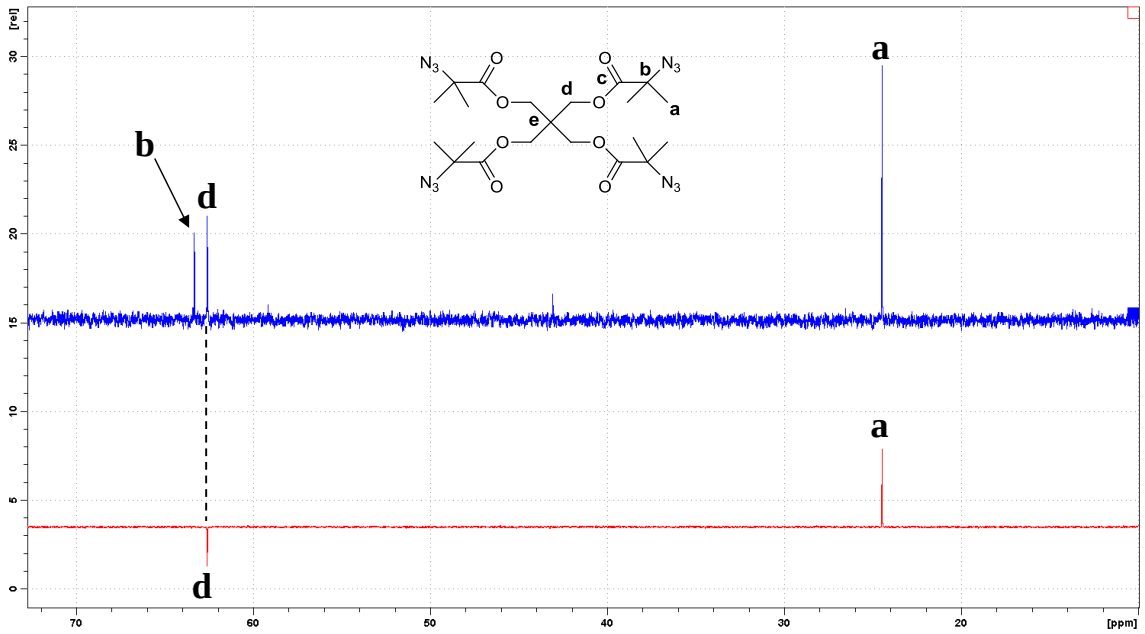

Figure A5.15. NMR spectra of **10** recorded in $CDCl_3$ at 298 K, 500 MHz. (A) ^{13}C NMR, and (B) DEPT-135^{o} NMR.

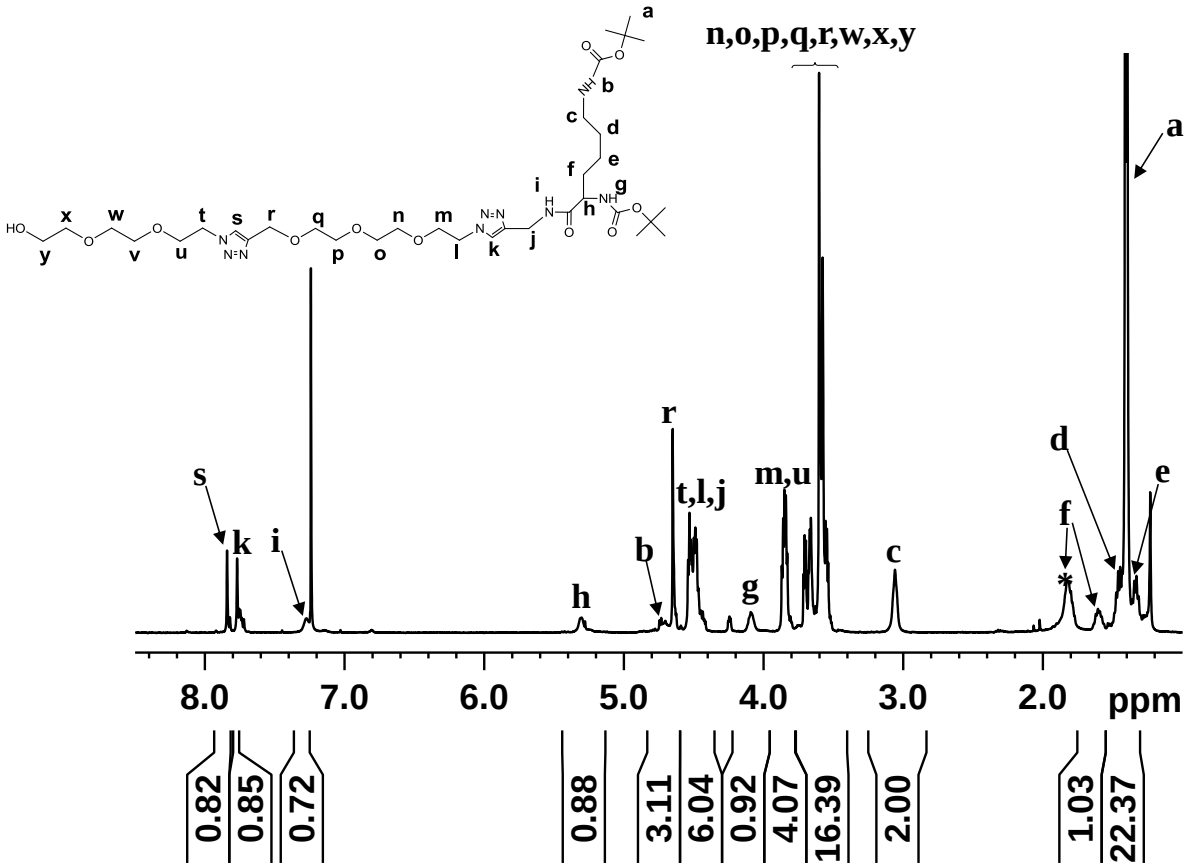

Figure A5.16: ^{1}H NMR spectrum (500 MHz) of **12,** recorded in $CDCl_3$ at 298K,*=H_2O.

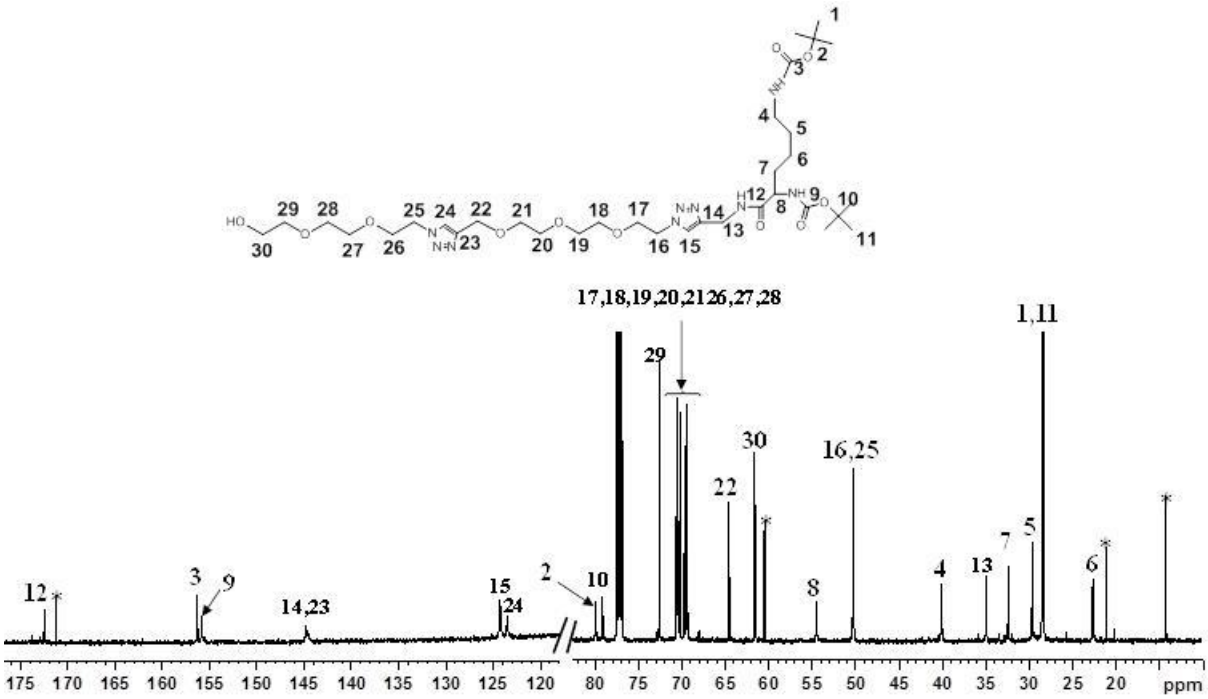

Figure A5.17: ^{13}C NMR spectrum (500 MHz) of **12**, recorded in $CDCl_3$ at 298K, *=EtOAc.

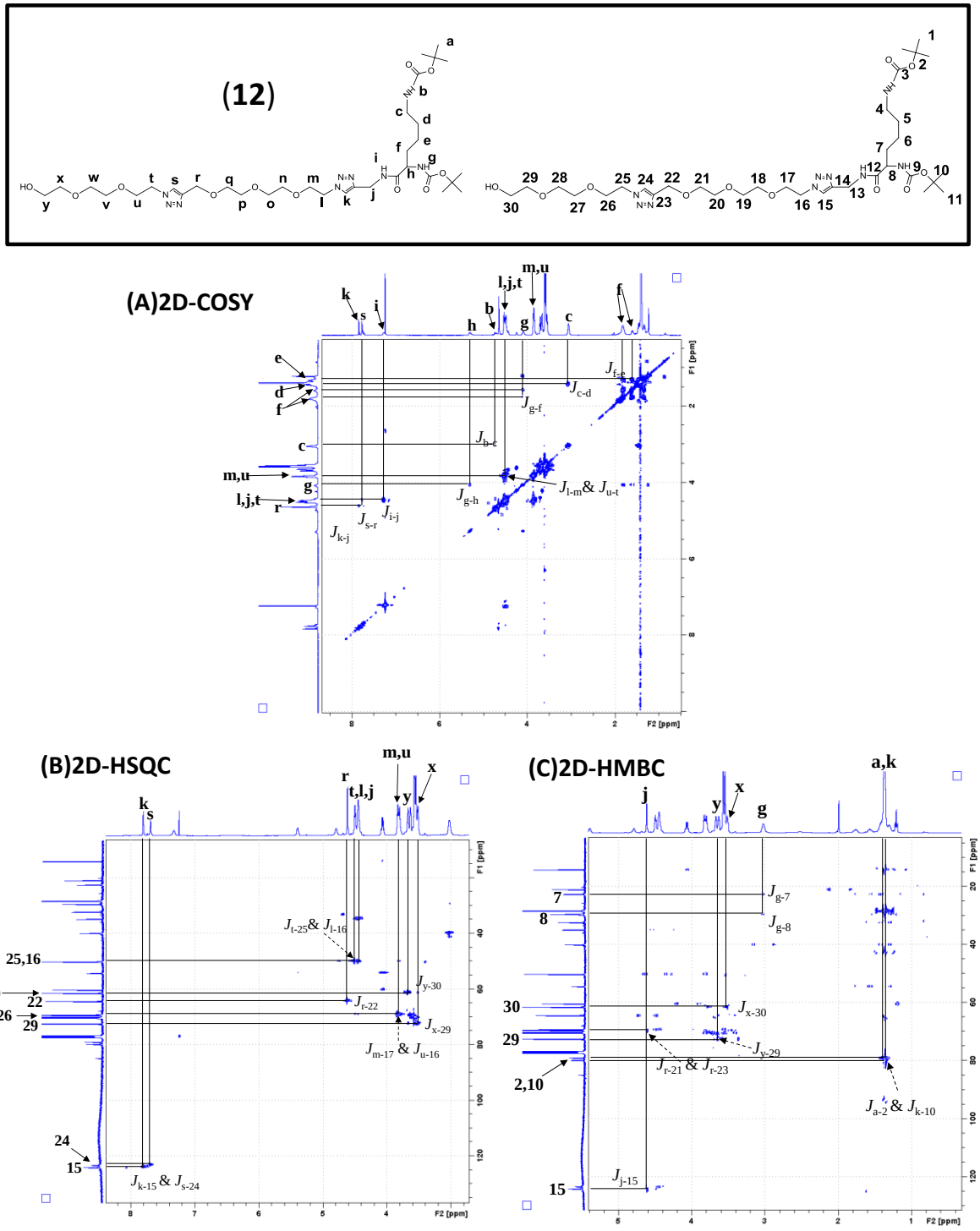

Figure A5.18: NMR of **12** recorded in $CDCl_3$ at 298K, 500MHz.

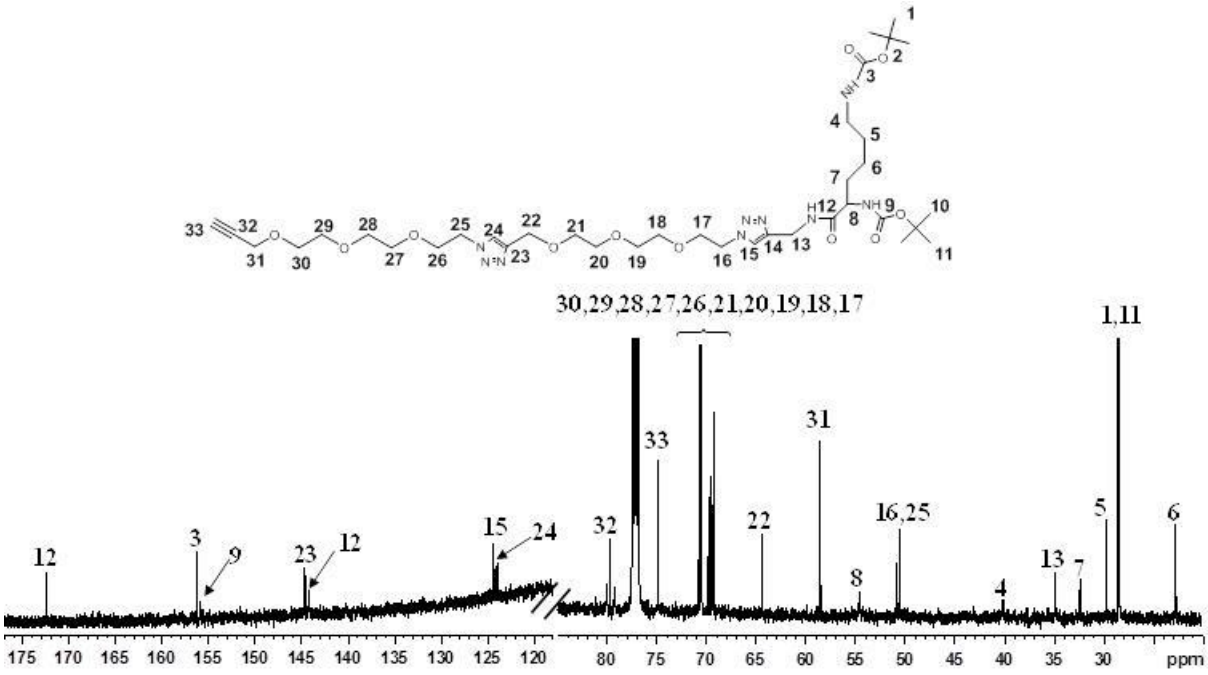

Figure A5.19: ^{13}C NMR spectrum (500 MHz) of **13** recorded in $CDCl_3$ at 298K, *=EtOAc.

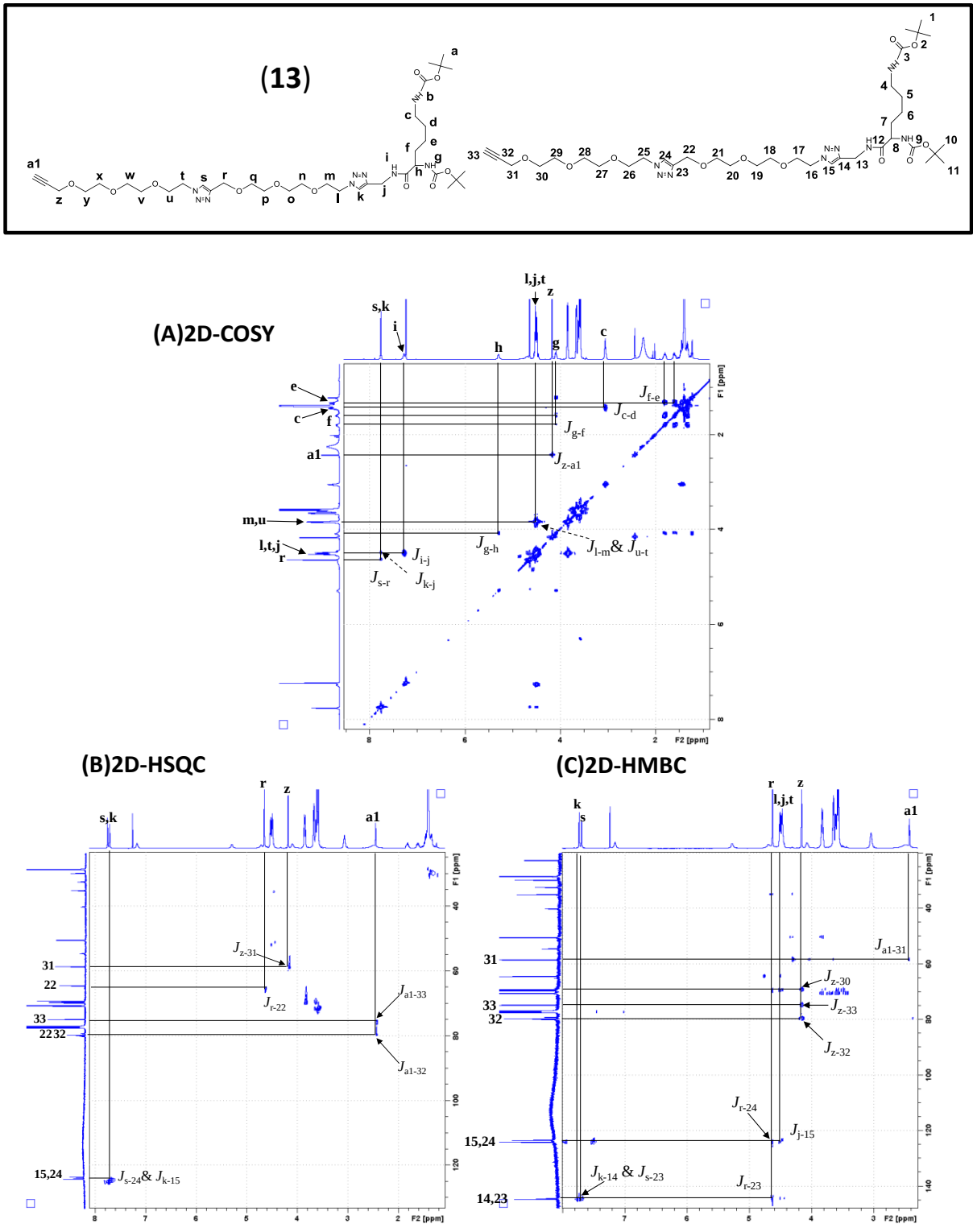

Figure A5.20: NMR of **13** recorded in $CDCl_3$ at 298K, 500MHz.

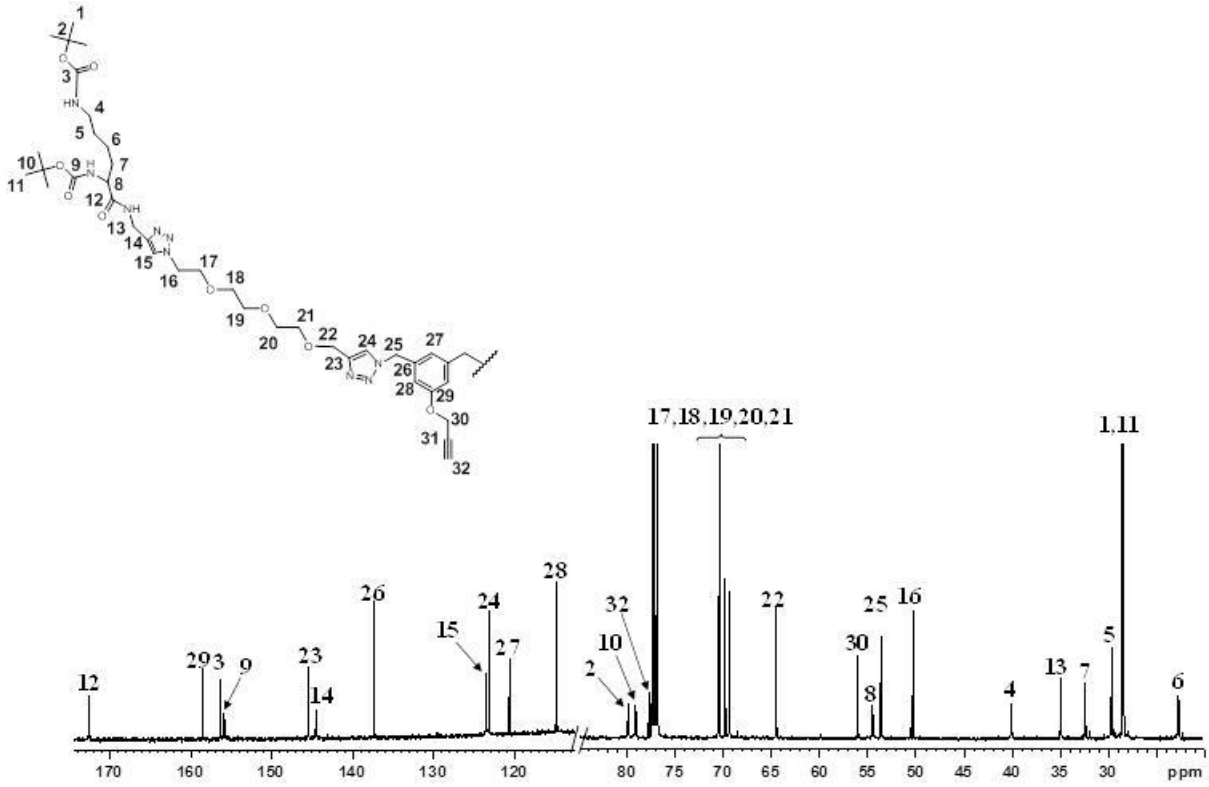

Figure A5.21: ^{13}C NMR spectrum (500 MHz) of **21**, recorded in $CDCl_3$ at 298K.

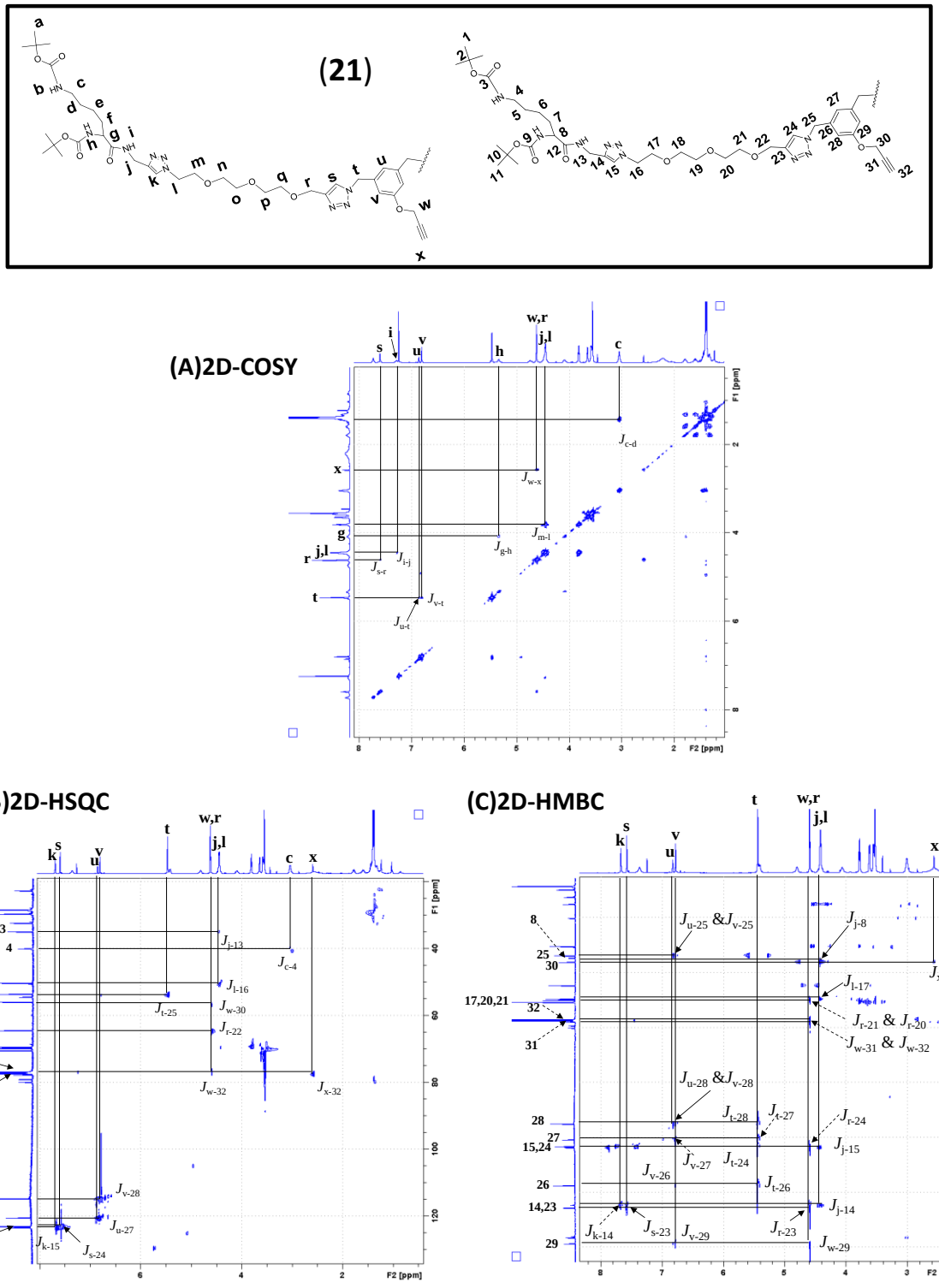

Figure A5.22: NMR spectra of **21**, recorded in CDCl3 at 298K, 500MHz.

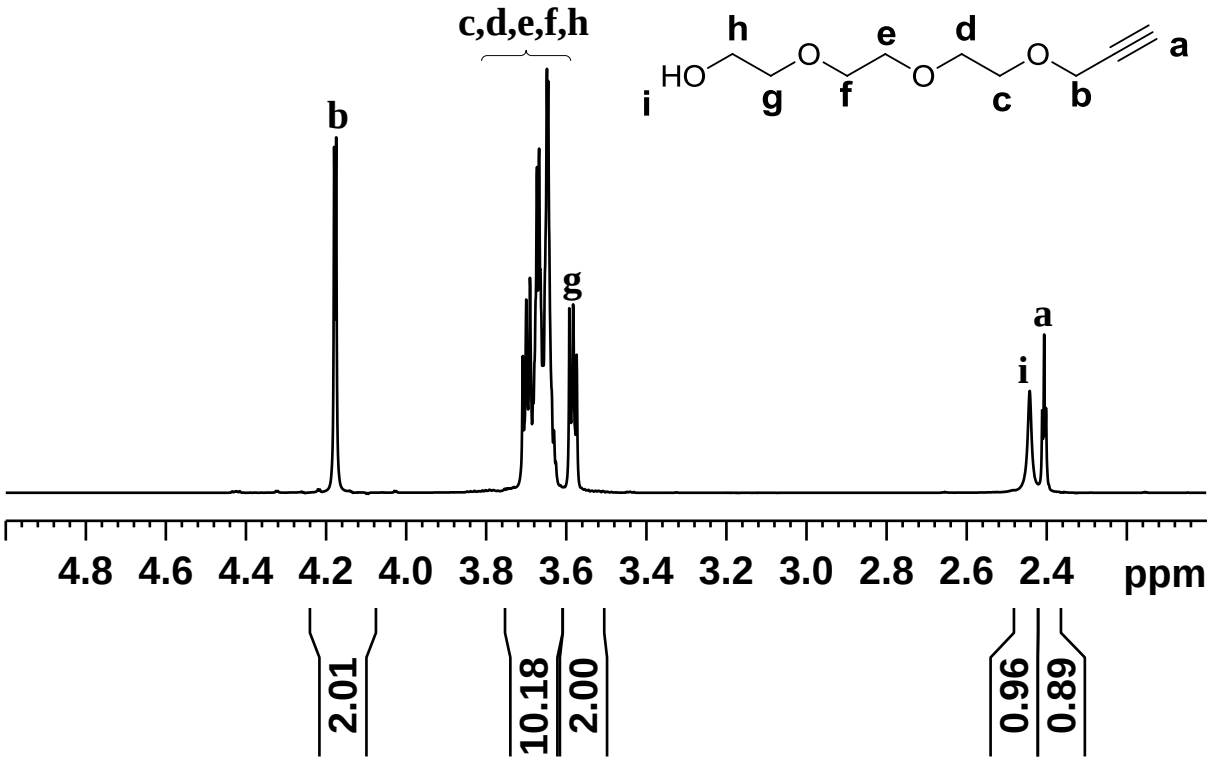

Figure A5.23: ^{1}H NMR spectrum (500 MHz) of **24**, recorded in $CDCl_3$ at 298K.

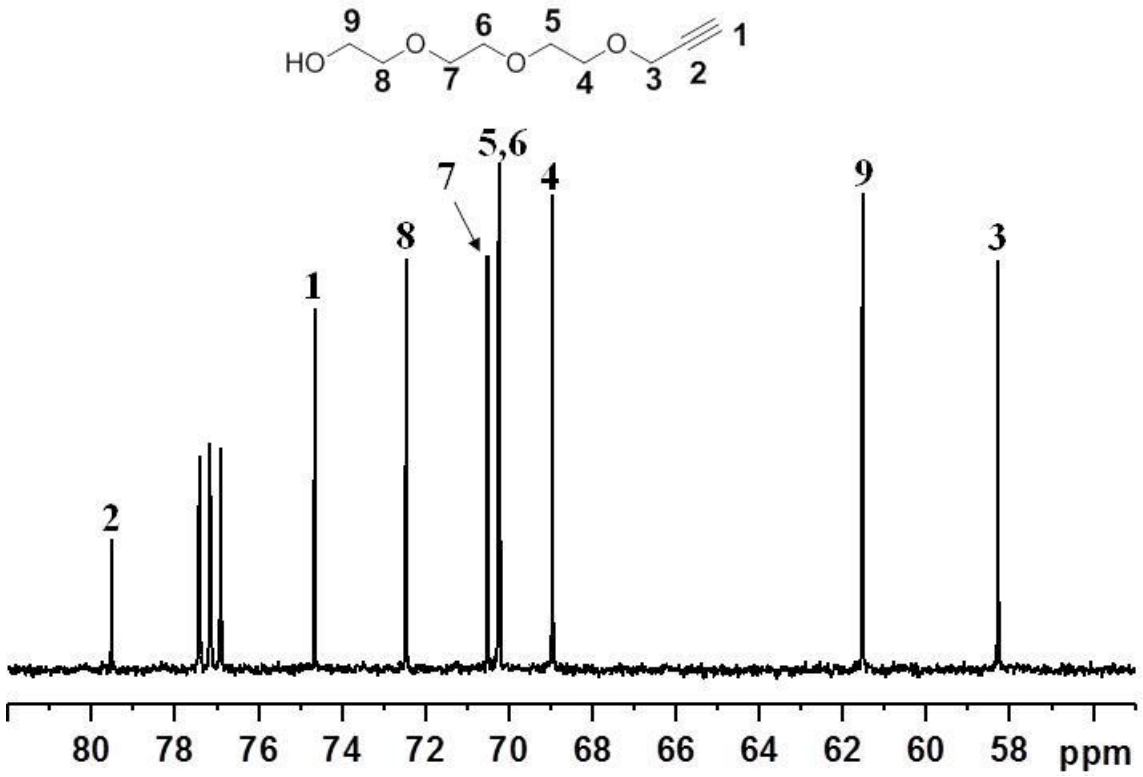

Figure A5.24: ^{13}C NMR spectrum (500 MHz) of **24**, recorded in $CDCl_3$ at 298K.

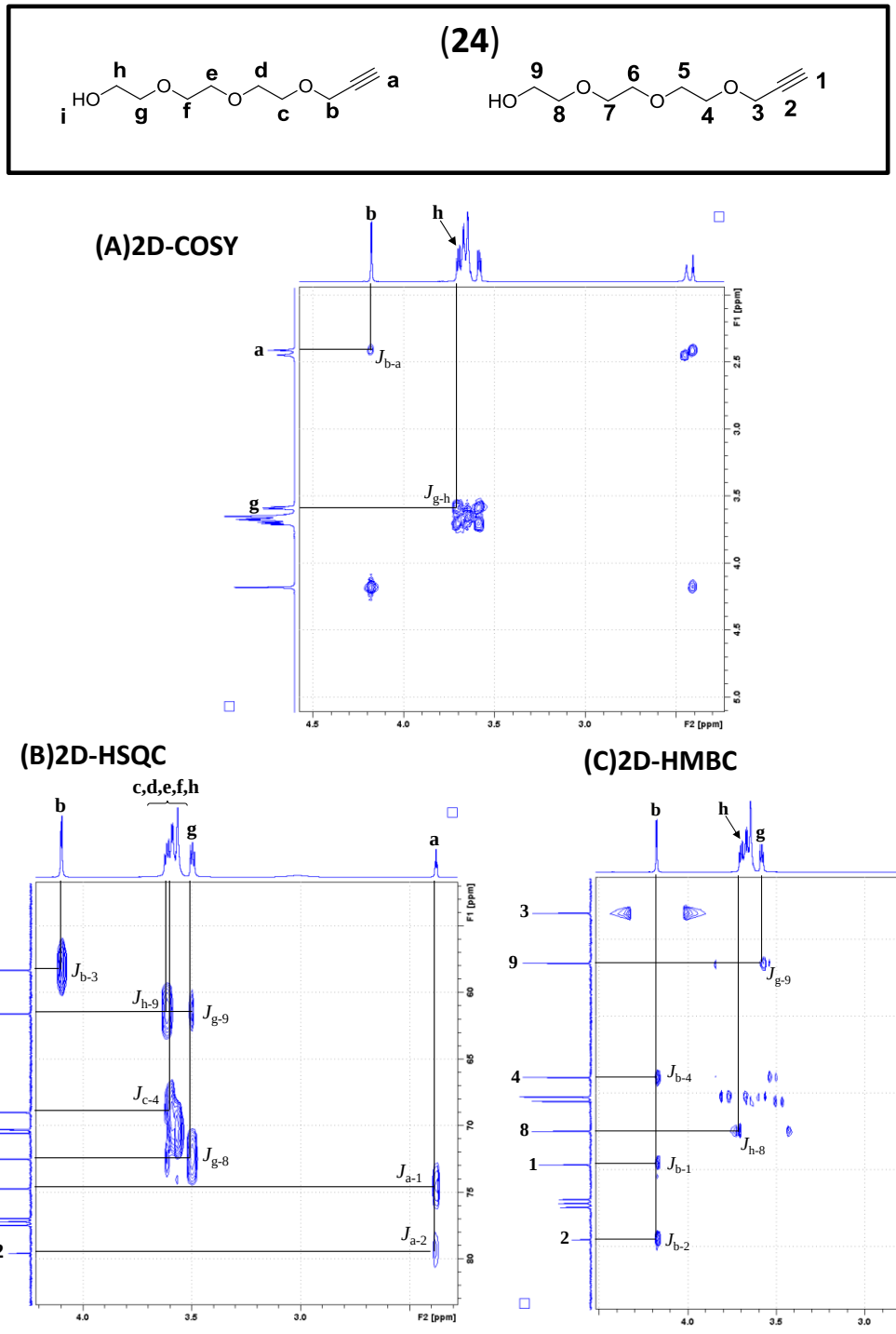

Figure A5.25: NMR spectra of **24**, recorded in CDCl3 at 298K, 500MHz.

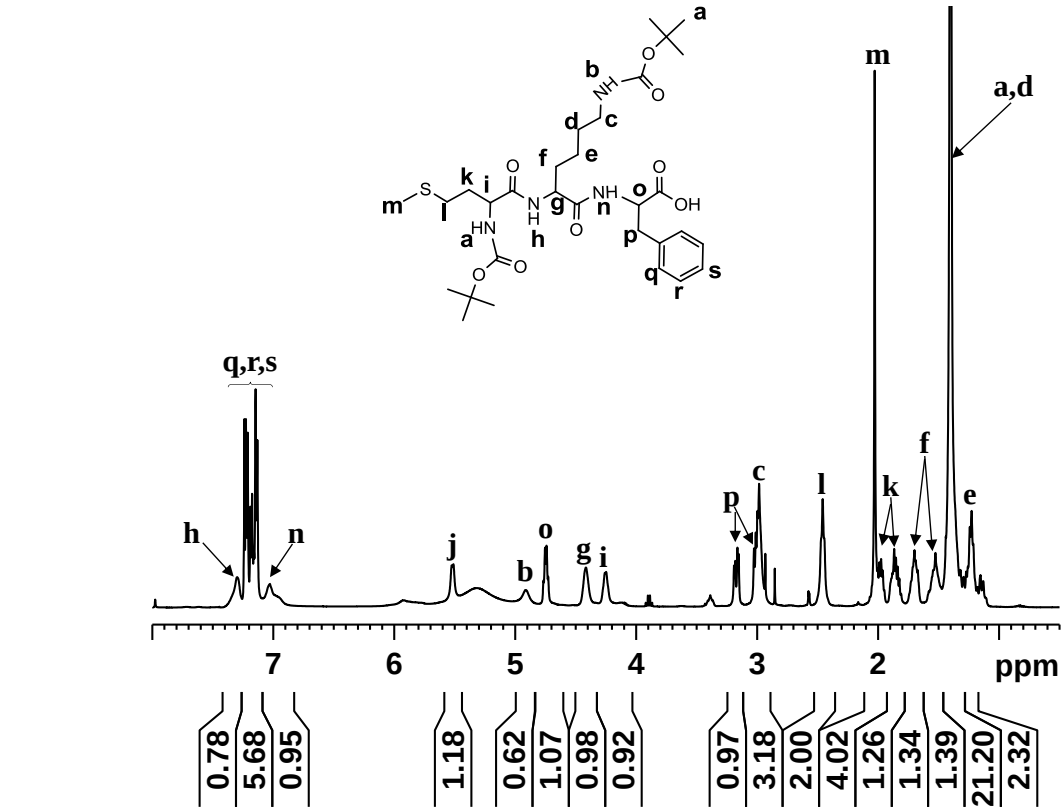

Figure A5.26: ^{1}H NMR spectrum (500 MHz) of **25**, recorded in $CDCl_3$ at 298K.

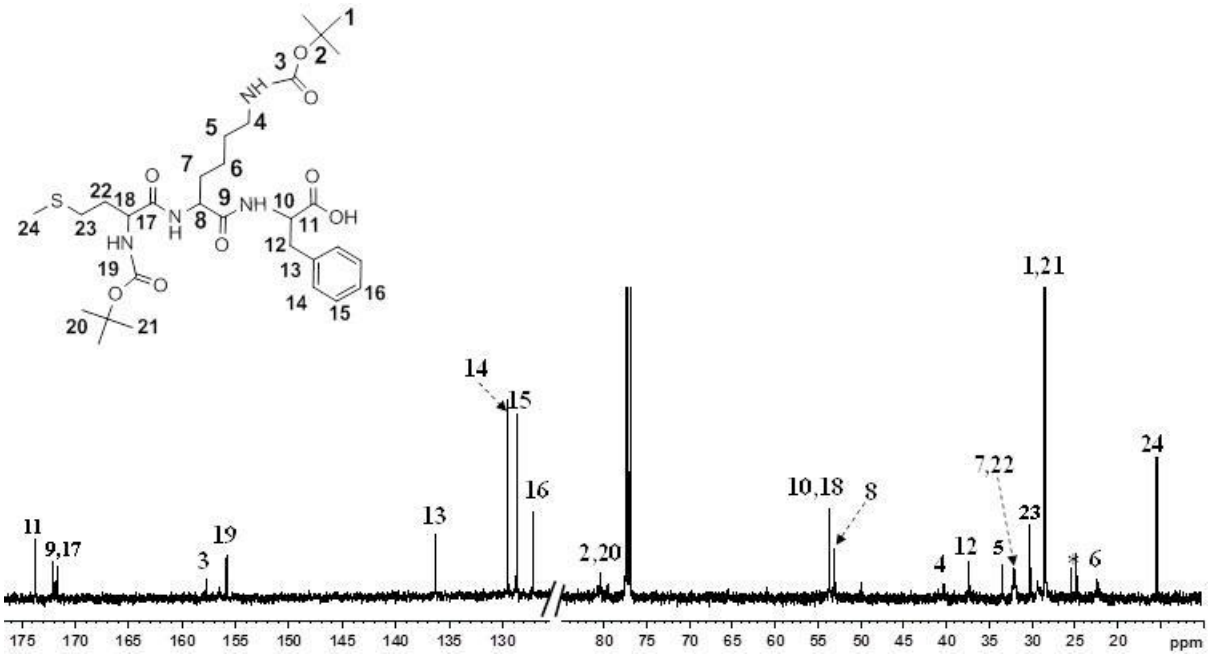

Figure A5.27: ^{13}C NMR spectrum (500 MHz) of **25**, recorded in $CDCl_3$ at 298K, *= unknown impurity.

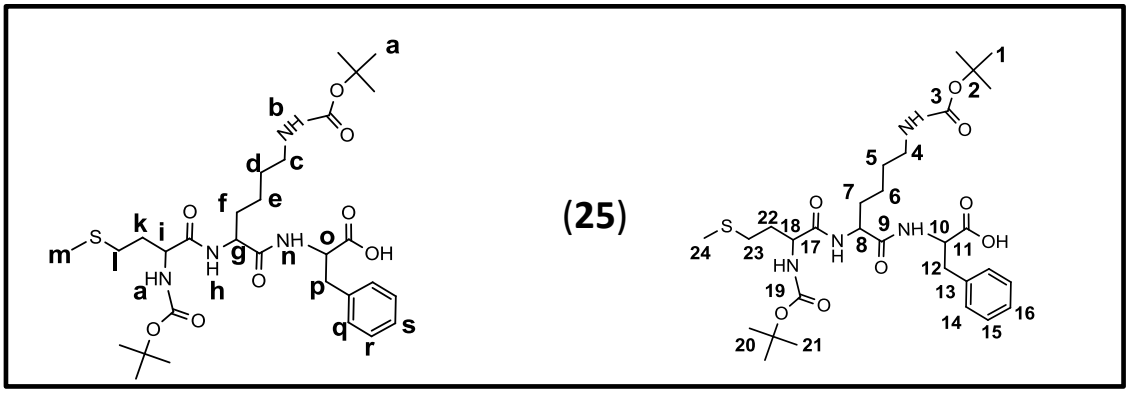

(25)

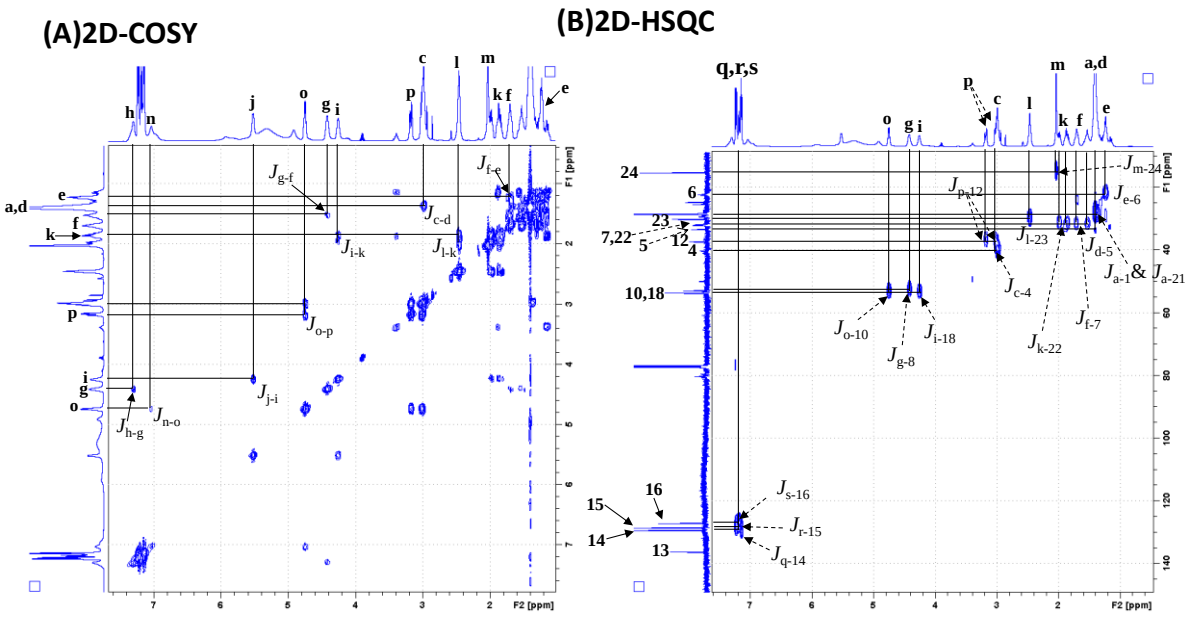

Figure A5.28: NMR spectra of **25**, recorded in CDCl3 at 298K, 500MHz.

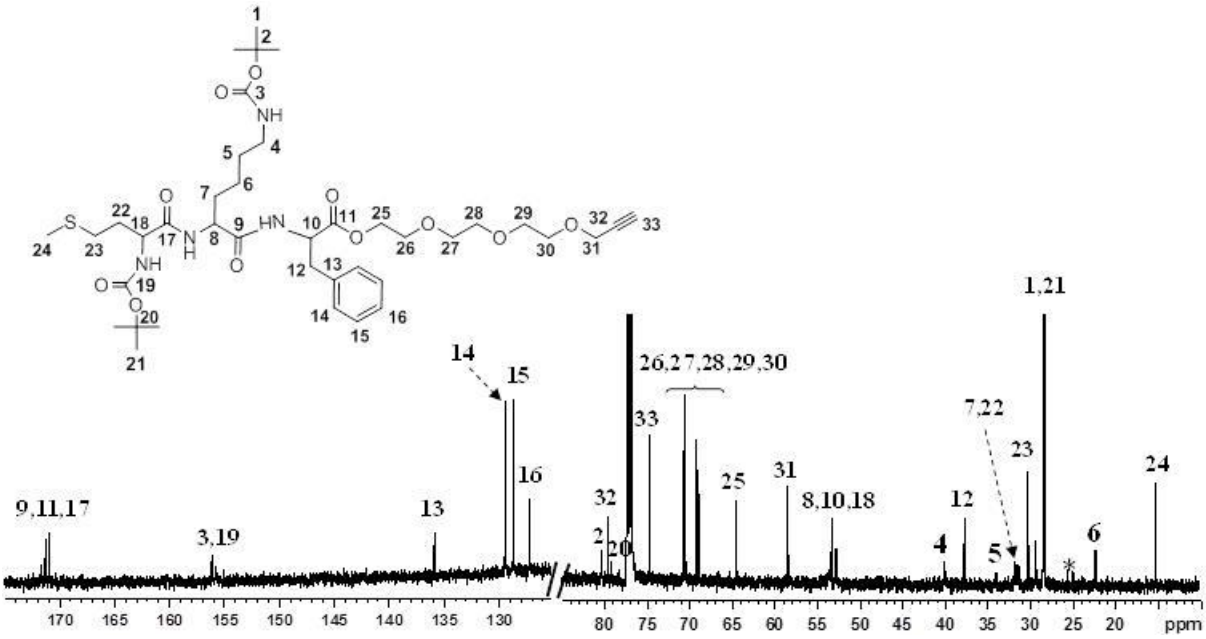

Figure A5.29: ^{13}C NMR spectrum (500 MHz) of **26**, recorded in $CDCl_3$ at 298K, *= unknown impurity.

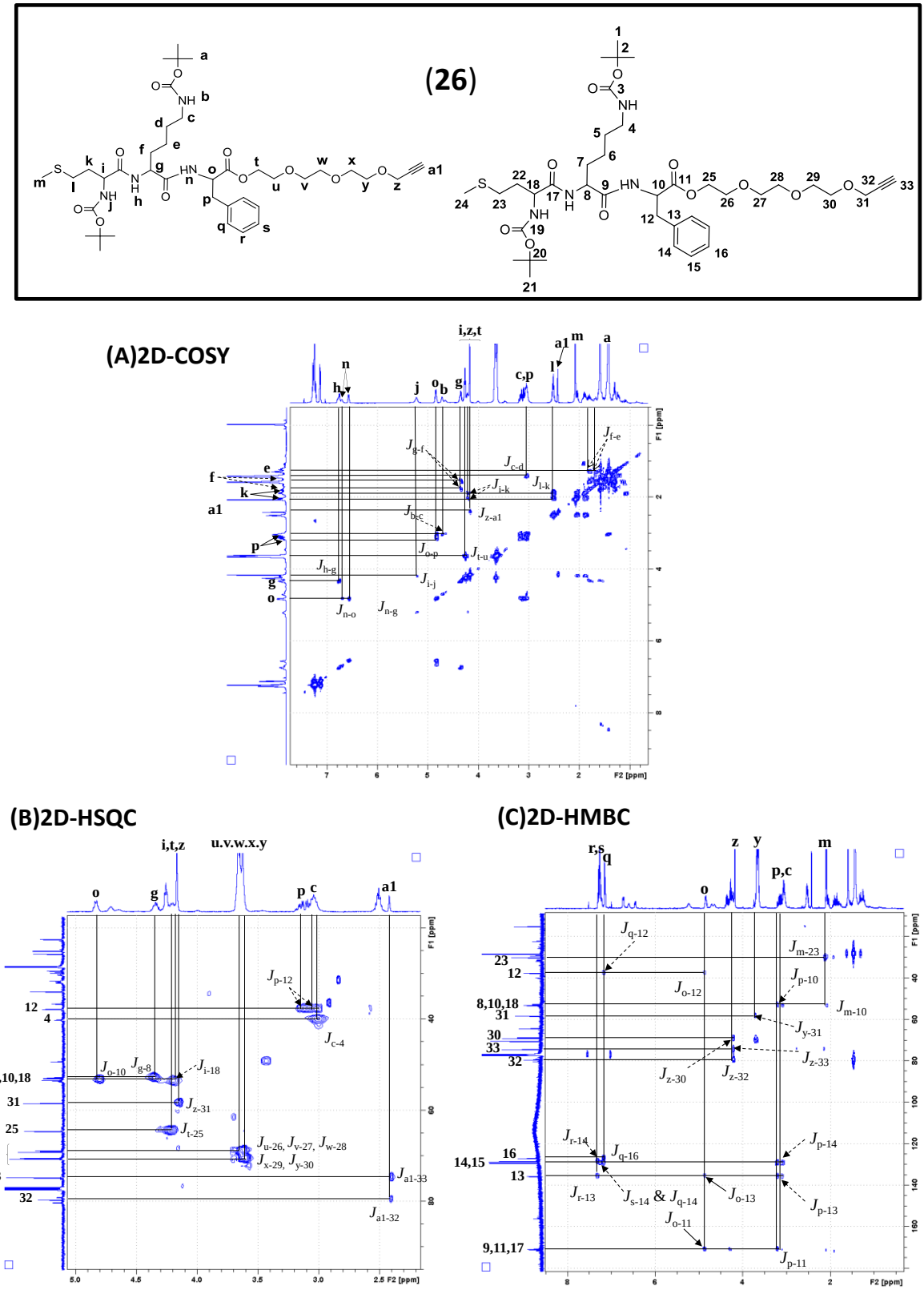

Figure A5.30: NMR spectra of **26**, recorded in CDCl3 at 298K, 500MHz.